



INNOVATIVE THERAPEUTIC AND IMMUNOMODULATORY STRATEGIES FOR PROTOZOAN INFECTIONS

EDITED BY: Jorge Enrique Gomez-Marin and Kamal El Bissati
PUBLISHED IN: *Frontiers in Cellular and Infection Microbiology*



frontiers

Frontiers Copyright Statement

© Copyright 2007-2019 Frontiers Media SA. All rights reserved.

All content included on this site, such as text, graphics, logos, button icons, images, video/audio clips, downloads, data compilations and software, is the property of or is licensed to Frontiers Media SA ("Frontiers") or its licensees and/or subcontractors. The copyright in the text of individual articles is the property of their respective authors, subject to a license granted to Frontiers.

The compilation of articles constituting this e-book, wherever published, as well as the compilation of all other content on this site, is the exclusive property of Frontiers. For the conditions for downloading and copying of e-books from Frontiers' website, please see the Terms for Website Use. If purchasing Frontiers e-books from other websites or sources, the conditions of the website concerned apply.

Images and graphics not forming part of user-contributed materials may not be downloaded or copied without permission.

Individual articles may be downloaded and reproduced in accordance with the principles of the CC-BY licence subject to any copyright or other notices. They may not be re-sold as an e-book.

As author or other contributor you grant a CC-BY licence to others to reproduce your articles, including any graphics and third-party materials supplied by you, in accordance with the Conditions for Website Use and subject to any copyright notices which you include in connection with your articles and materials.

All copyright, and all rights therein, are protected by national and international copyright laws.

The above represents a summary only. For the full conditions see the Conditions for Authors and the Conditions for Website Use.

ISSN 1664-8714

ISBN 978-2-88963-127-8

DOI 10.3389/978-2-88963-127-8

About Frontiers

Frontiers is more than just an open-access publisher of scholarly articles: it is a pioneering approach to the world of academia, radically improving the way scholarly research is managed. The grand vision of Frontiers is a world where all people have an equal opportunity to seek, share and generate knowledge. Frontiers provides immediate and permanent online open access to all its publications, but this alone is not enough to realize our grand goals.

Frontiers Journal Series

The Frontiers Journal Series is a multi-tier and interdisciplinary set of open-access, online journals, promising a paradigm shift from the current review, selection and dissemination processes in academic publishing. All Frontiers journals are driven by researchers for researchers; therefore, they constitute a service to the scholarly community. At the same time, the Frontiers Journal Series operates on a revolutionary invention, the tiered publishing system, initially addressing specific communities of scholars, and gradually climbing up to broader public understanding, thus serving the interests of the lay society, too.

Dedication to Quality

Each Frontiers article is a landmark of the highest quality, thanks to genuinely collaborative interactions between authors and review editors, who include some of the world's best academicians. Research must be certified by peers before entering a stream of knowledge that may eventually reach the public - and shape society; therefore, Frontiers only applies the most rigorous and unbiased reviews.

Frontiers revolutionizes research publishing by freely delivering the most outstanding research, evaluated with no bias from both the academic and social point of view. By applying the most advanced information technologies, Frontiers is catapulting scholarly publishing into a new generation.

What are Frontiers Research Topics?

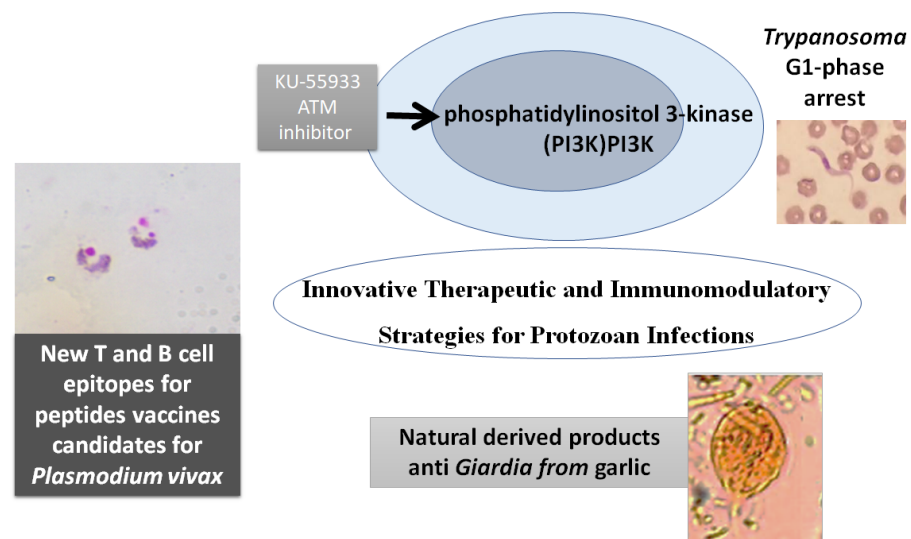
Frontiers Research Topics are very popular trademarks of the Frontiers Journals Series: they are collections of at least ten articles, all centered on a particular subject. With their unique mix of varied contributions from Original Research to Review Articles, Frontiers Research Topics unify the most influential researchers, the latest key findings and historical advances in a hot research area! Find out more on how to host your own Frontiers Research Topic or contribute to one as an author by contacting the Frontiers Editorial Office: researchtopics@frontiersin.org

INNOVATIVE THERAPEUTIC AND IMMUNOMODULATORY STRATEGIES FOR PROTOZOAN INFECTIONS

Topic Editors:

Jorge Enrique Gomez-Marin, Universidad del Quindio, Colombia

Kamal El Bissati, University of Chicago, United States



Examples of innovative therapeutic and immunomodulatory strategies against protozoan infections.
Images by Jorge Gomez Marin under CC-BY.

Human protozoan infections are an important target for development of new vaccines and drugs. No completely efficacious vaccines for human protozoan infections are available and in the case of malaria resistance to the most efficacious antimalarials has become a global challenge. In ocular toxoplasmosis complete eradication of the body is not possible, exposing patients to new reactivations.

The need of treatment or vaccines for and of less toxic drugs for *Leishmania* are urgent tasks for protozoologists research community. New research strategies have appeared that enlarged the possibilities for treatment and vaccine development. Reverse vaccinology, bioinformatic search of second use drug candidates and ex vivo analysis have afforded new fields for development.

Citation: Gomez-Marin, J. E., El Bissati, K, eds. (2019). Innovative Therapeutic and Immunomodulatory Strategies for Protozoan Infections. Lausanne: Frontiers Media. doi: 10.3389/978-2-88963-127-8

Table of Contents

05 Editorial: Innovative Therapeutic and Immunomodulatory Strategies for Protozoan Infections

Jorge Enrique Gómez Marín and Kamal El Bissati

SECTION

NEW ANTI PROTOZOAN DRUG CANDIDATES

08 Cascade Ligand- and Structure-Based Virtual Screening to Identify New Trypanocidal Compounds Inhibiting Putrescine Uptake

Lucas N. Alberca, María L. Sbaraglini, Juan F. Morales, Roque Dietrich, María D. Ruiz, Agustina M. Pino Martínez, Cristian G. Miranda, Laura Fraccaroli, Catalina D. Alba Soto, Carolina Carrillo, Pablo H. Palestro and Alan Talevi

23 A Perspective on Thiazolidinone Scaffold Development as a New Therapeutic Strategy for Toxoplasmosis

Cristian Rocha-Roa, Diego Molina and Néstor Cardona

31 Discovery and Genetic Validation of Chemotherapeutic Targets for Chagas' Disease

Juan Felipe Osorio-Méndez and Ana María Cevallos

47 Evaluation of ATM Kinase Inhibitor KU-55933 as Potential Anti-Toxoplasma gondii Agent

Jonathan Munera López, Agustina Ganuza, Silvina S. Bogado, Daniela Muñoz, Diego M. Ruiz, William J. Sullivan Jr., Laura Vanagas and Sergio O. Angel

58 Novel Synthetic Polyamines Have Potent Antimalarial Activities in vitro and in vivo by Decreasing Intracellular Spermidine and Spermine Concentrations

Kamal El Bissati, Henry Redel, Li-Min Ting, Joseph D. Lykins, Martin J. McPhillie, Rajendra Upadhyay, Patrick M. Woster, Nigel Yarett, Kami Kim and Louis M. Weiss

67 Artemisinin Derivatives and Synthetic Trioxane Trigger Apoptotic Cell Death in Asexual Stages of Plasmodium

Sarika Gunjan, Tanuj Sharma, Kanchan Yadav, Bhavana S. Chauhan, Sunil K. Singh, Mohammad I. Siddiqi and Renu Tripathi

77 CSGID Solves Structures and Identifies Phenotypes for Five Enzymes in Toxoplasma gondii

Joseph D. Lykins, Ekaterina V. Filippova, Andrei S. Halavaty, George Minasov, Ying Zhou, Ievgeniia Dubrovskaya, Kristin J. Flores, Ludmilla A. Shuvalova, Jiapeng Ruan, Kamal El Bissati, Sarah Dovgin, Craig W. Roberts, Stuart Woods, Jon D. Moulton, Hong Moulton, Martin J. McPhillie, Stephen P. Muench, Colin W. G. Fishwick, Elisabetta Sabini, Dhanasekaran Shanmugam, David S. Roos, Rima McLeod, Wayne F. Anderson and Huân M. Ngô

98 Activity of Thioallyl Compounds From Garlic Against *Giardia duodenalis* Trophozoites and in Experimental Giardiasis

Raúl Argüello-García, Mariana de la Vega-Arnaud, Iraís J. Loredó-Rodríguez, Adriana M. Mejía-Corona, Elizabeth Melgarejo-Trejo, Eulogia A. Espinoza-Contreras, Rocío Fonseca-Liñán, Arturo González-Robles, Nury Pérez-Hernández and M. Guadalupe Ortega-Pierres

SECTION

EXPERIMENTAL MODELS FOR IMMUNE RESPONSE EVALUATION AND NEW VACCINES STRATEGIES

116 An Overview of Peripheral Blood Mononuclear Cells as a Model for Immunological Research of *Toxoplasma gondii* and Other Apicomplexan Parasites

John Alejandro Acosta Davila and Alejandro Hernandez De Los Rios

126 Emergence of Leptin in Infection and Immunity: Scope and Challenges in Vaccines Formulation

Dayakar Alti, Chandrasekaran Sambamurthy and Suresh K. Kalangi

144 The in Vitro Antigenicity of *Plasmodium vivax* Rhoptry Neck Protein 2 (PvRON2) B- and T-Epitopes Selected by HLA-DRB1 Binding Profile

Carolina López, Yoelis Yepes-Pérez, Diana Díaz-Arévalo, Manuel E. Patarroyo and Manuel A. Patarroyo

161 Chitosan Microsphere Used as an Effective System to Deliver a Linked Antigenic Peptides Vaccine Protect Mice Against Acute and Chronic Toxoplasmosis

Jingjing Guo, Xiahui Sun, Huiquan Yin, Ting Wang, Yan Li, Chunxue Zhou, Huaiyu Zhou, Shenyi He and Hua Cong



Editorial: Innovative Therapeutic and Immunomodulatory Strategies for Protozoan Infections

Jorge Enrique Gómez Marín^{1*} and Kamal El Bissati²

¹ Grupo GEPAMOL, Centro Investigaciones Biomédicas, Facultad de Ciencias de la Salud, Universidad del Quindío, Armenia, Colombia, ² Institute for Molecular Engineering, University of Chicago Medical Center, Chicago, IL, United States

Keywords: Protozoa (source: MeSH), *Toxoplasma*, *Leishmania*, *Trypanosoma*, *Plasmodium*, immunomodulation, synthetic vaccines, systems biology parasitic sensitivity tests

Editorial on the Research Topic

Innovative Therapeutic and Immunomodulatory Strategies for Protozoan Infections

In this special issue of Frontiers in Cellular and Infection Microbiology, we assembled a collection of 9 original research articles and 3 reviews within the theme “Innovative Therapeutic and Immunomodulatory Strategies for Protozoan Infections.” The intended goal of this Research Topic was to present an updated view of current innovations for intervention strategies against human protozoan infections. No completely efficacious vaccines for human protozoan infections exist. For example, the current vaccines licensed for malaria, or those currently being investigated in clinical trials, are not completely effective and their utility are controversial (Genton, 2008; Thera and Plowe, 2012). This same limitation exists with respect to availability of drugs to treat infected individuals. Often wholly effective medications are lacking, and effective medications are suboptimal. New challenge is posed by artemisinin-based combination therapy (ACT)-resistant strains of *P. falciparum*, making development of new drugs to save malaria patients ever more urgent. In ocular toxoplasmosis, complete eradication of the parasite from the host is not possible, exposing patients to persistent threat of disease reactivation (de la Torre et al., 2009). Pyrimethamine and sulfadiazine, with folinic acid, are the mainstays of treatment for toxoplasmosis, but do not treat the latent bradyzoite life-stage. In the case of South American trypanosomiasis (Chagas disease) only two drugs (benznidazole and nifurtimox) compose the armamentarium of physicians treating patients with this disease (Gomez-Marín, 2010). In light of these challenges, new research strategies have appeared that enhance the possibility of treatment and vaccine development including reverse vaccinology (Cardona et al., 2015), the bioinformatic search of second-use drug candidates (Osorio and García, 2019), and *ex vivo* analysis of immune response (Torres-Morales et al., 2014). This Research Topic evaluates these new possibilities and brings together authorities in this field and experiences that will feed the next wave of drugs and vaccines for this group of infections that have significant human health consequences. In toxoplasmosis, Acosta Davila et al. reviewed and summarize the utility of peripheral blood mononuclear cells (PBMCs) as a model to investigate the immunologic component of host-parasite interaction. It also delineates technical limitations associated with handling and subsequent processing of PBMCs. The authors highlight the importance of variables (e.g., time of collection of PBMC), significant implications for data interpretation and conclusions related to host-parasite interaction, and discuss some controversies related to this model and suggest possible improvements to related protocols. This *ex vivo* model of infection is critical to obtain accurate information about human response to infection, given notable differences in immune response in mice (Gómez-Marín, 2000). Critical to the development of new therapies against *T. gondii*, Rocha-Rao et al. reported the use of a thiazolodione scaffold and its derivatives, all of which

OPEN ACCESS

Edited by:

Nahed Ismail,
University of Illinois at Chicago,
United States

Reviewed by:

Seyed Mahmoud Hashemi,
Shahid Beheshti University of Medical
Sciences, Iran

*Correspondence:

Jorge Enrique Gómez Marín
gepamol2@uniquindio.edu.co

Specialty section:

This article was submitted to
Clinical Microbiology,
a section of the journal
Frontiers in Cellular and Infection
Microbiology

Received: 09 April 2019

Accepted: 30 July 2019

Published: 09 August 2019

Citation:

Gómez Marín JE and El Bissati K
(2019) Editorial: Innovative
Therapeutic and Immunomodulatory
Strategies for Protozoan Infections.
Front. Cell. Infect. Microbiol. 9:293.
doi: 10.3389/fcimb.2019.00293

contain an imidazole ring, and how these compounds may lead, in the future, to improved therapies targeted against the parasite. The authors discuss in their manuscript different scaffolds that they studied and how improvements might be made, especially in terms of *in silico* design. Evaluation of kinase inhibitors represents a novel strategy that may overcome difficulties of cross-inhibition of host kinases. The paper of the Argentinian group, led by López et al., demonstrated interesting compounds that merit further exploration *in vivo*. In this work, proteins involved in DNA replication or repair are proposed as potential therapeutic targets of human pathogens. The authors provide evidence demonstrating the effect of phosphatidylinositol 3-kinase (PI3K) inhibitors (KU-55399), showing that they block *Toxoplasma* tachyzoite replication. They found an abolition of the phosphorylation of H2A.X, proposing that ATM kinase can be a potential drug target for abrogation of *T. gondii* growth. In the same vein, an international interdisciplinary collaborative team including the University of Chicago, the Center for Structural Genomics of Infectious Diseases at Northwestern University, and collaborators across the U.K., provides crystallographic structures of 5 *Toxoplasma* small enzymes function in key metabolic pathways likely to be vital for parasite survival for the international research community to use (Lykins et al.). Moreover, the group demonstrates that target-specific modulation via morpholino inhibited parasite replication *in vitro*. The authors hope that obtaining crystal structures of these enzymes will facilitate discovery of drugs against *Toxoplasma*. Looking for new compounds that block *Toxoplasma* at the bradyzoite stage (responsible for disease reactivation across time) remains a challenging task for scientists. Vaccine development, therefore, represents a reasonable approach to would prevent infection from becoming established. Considerable progress has been made toward identification of vaccine prototypes that are moving closer to clinical studies. This includes recombinant protein that elicits CD8⁺ and CD4⁺ T cells response in HLA transgenic mice (El Bissati et al., 2016); Self Assembling Protein Nanoparticles (SAPN) (El Bissati et al., 2014, 2017). RNA replicons and liposomes, amongst other methods, are other vaccine platforms reported in the literature to improve mouse survival against *Toxoplasma* challenges. One of the most significant challenges in vaccine development is to trigger adequate antigen presentation, requiring not only sufficient quantity of antigen, but also a stable preparation, facilitating a durable immune response. Guo et al. reported use of chitosan microspheres as a system that offers these properties and confers protection to mice against acute and chronic toxoplasmosis. The authors employed bioinformatics to screen predominant peptides that bind to T and B cells epitopes. The ones that elicited IgG were selected to compose a multigenic peptide, emulsified with chitosan and microspheres, allowing assessment for immunogenicity. Similar efforts on antigenic selection was used by Patarroyo's group from Bogota (López et al.). In this work, B- and T-cell epitopes of the *P. vivax* rhoptry neck protein 2 (PvRON2) were predicted *in silico* and then, the binding of predicted epitopes to HLA-DR molecules was experimentally assessed, with four peptides selected to test immunogenicity (i.e.,

T cell proliferation, cytokine production, and IgG production) in cells from *Plasmodium vivax*-exposed individuals from two endemic areas in Colombia. Authors concluded that two T-cell epitopes and one B-cell epitope are promising vaccine candidates. This work illustrates the difficulties to drawing conclusions from immunological assays with human samples. In addition, Alti et al. reviewed current knowledge about the use of leptin as adjuvant. The role of leptin in immune regulation is an interesting topic that should be considered given its implications on the efficacy of vaccines in obese individuals, suggesting this factor should be included in evaluations of vaccine efficacy.

Strategies of treatment against other protozoans were also reported in this Research Topic. In malaria, given the discovery of strains of *Plasmodium* with intrinsic resistance to the very efficacious artemisinin (Aponte et al., 2017), new drugs are urgently needed. El Bissati et al. explored the therapeutic potential of targeting the polyamine pathway in *Plasmodium* and, in particular, spermidine synthase as a target of a new family of inhibitors. The polyamine pathway appears to be a valid target for further exploration and small molecule development, given its essential role in parasite survival, is likely to bear therapeutic fruit. Testing analogs effective against Microsporidia formed the basis of the authors' initial approach toward *P. falciparum* studies. Tetraamines and oligoamines have previously documented efficacy in experimental murine models of microsporidiosis. Surprisingly, these compounds showed no or minimal antimalarial activity. The authors found that addition of cyclohexylmethyl side groups to the tetramine backbone conferred potent inhibitory activity in both chloroquine-resistant (Dd2) and chloroquine-sensitive (3D7) strains at the low nanomolar range. Furthermore, these polyamine analogs decreased levels of spermine in infected cells, suggesting a mechanism involving inhibition of spermidine synthase.

Urban transmission of trypanosomiasis and new foci for Chagas' transmission in South America have increased the interest in development of optimized treatment approaches (Rueda et al., 2014; Bello Corassa et al., 2016). The review by Osorio-Méndez and Cevallos offers perspective regarding how this might be achieved. The authors use current genetic and bioinformatics tools for identifying new molecular targets for chemotherapeutic treatment of *T. cruzi*, the causative agent of Chagas disease, and follow up with in-depth descriptions of possible targets enzymes in three metabolic pathways: synthesis of surface glycoconjugates, ergosterol biosynthesis, and neutralization of reactive oxygen species. Alberca et al. chose to focus their work on an alternative pathway, instead using a virtual ligand and structure-based screening to find polyamine analogs that could bind to the *T. cruzi* polyamine transporter putrescine permease TcPAT12. From the large libraries submitted for docking analysis, the authors found several hits with activities against *T. cruzi* and conclude that virtual screening is effective in finding inhibitors of putrescine uptake in *T. Cruzi*. In another study Gunjan et al., have studied the effect of artemisinin derivatives (α/β artemether, artesunate, and a synthetic 1, 2, 4 trioxane) on apoptotic pathway of malaria parasite and its survival. Finally, the work of the Mexican group on *Giardia*, Argüello-García

et al. and garlics derivatives, is an *excel sum* example about how nature continues offering new possibilities to find anti parasite compounds.

In conclusion, this Research Topic is a good sample of how novel chemoinformatics and bioinformatics strategies are revolutionizing the discovery and identification of new compounds. The new tools such as CRISP arrayed libraries of mutated genes have added recently new possibilities and we have seen recently an explosion of new anti-protozoa compounds. However, there is still the barrier to test such a large number of compounds, the same is occurring with the vaccines candidates

and it is necessary to develop efficacious selective screening methods for new drugs and vaccines. At this respect, the organoids and tissue explant-based models of infection can offer a new strategy to be developed for the evaluation of anti-protozoan drug candidates (Broutier et al., 2017). This could represent a pathway of hope to obtain better drugs and vaccines for these important human diseases.

AUTHOR CONTRIBUTIONS

JG and KE drafted and edited the editorial.

REFERENCES

- Aponte, S., Guerra, Á. P., Álvarez-Larrotta, C., Bernal, S. D., Restrepo, C., González, C., et al. (2017). Baseline *in vivo*, *ex vivo* and molecular responses of *Plasmodium falciparum* to artemether and lumefantrine in three endemic zones for malaria in Colombia. *Trans. R. Soc. Trop. Med. Hyg.* 111, 71–80. doi: 10.1093/trstmh/trx021
- Bello Corassa, R., Aceijas, C., Alves, P. A. B., and Garelick, H. (2016). Evolution of Chagas' disease in Brazil. Epidemiological perspective and challenges for the future: a critical review. *Perspect. Public Health* 137, 289–295. doi: 10.1177/1757913916671160
- Broutier, L., Mastrogiovanni, G., Versteegen, M. M., Francies, H. E., Gavarró, L. M., Bradshaw, C. R., et al. (2017). Human primary liver cancer-derived organoid cultures for disease modeling and drug screening. *Nat. Med.* 23, 1424–1435. doi: 10.1038/nm.4438
- Cardona, N. I. N. I., Moncada, D. M., and Gómez-Marín, J. E. (2015). A rational approach to select immunogenic peptides that induce IFN- γ response against *Toxoplasma gondii* in human leukocytes. *Immunobiology* 220, 1337–1342. doi: 10.1016/j.imbio.2015.07.009
- de la Torre, A., Rios, C., Cardozo, C., and Gomez-Marín, J. (2009). Frequency and factors associated with recurrences of ocular toxoplasmosis in a referral center in Colombia. *Br. J. Ophthalmol.* 93, 1001–1004. doi: 10.1136/bjo.2008.155861
- El Bissati, K., Chentoufi, A. A., Krishack, P. A., Zhou, Y., Woods, S., Dubey, J. P., et al. (2016). Adjuvanted multi-epitope vaccines protect HLA-A*11:01 transgenic mice against *Toxoplasma gondii*. *JCI Insight* 1:e85955. doi: 10.1172/jci.insight.85955
- El Bissati, K., Zhou, Y., Dasgupta, D., Cobb, D., Dubey, J. P., Burkhard, P., et al. (2014). Effectiveness of a novel immunogenic nanoparticle platform for *Toxoplasma* peptide vaccine in HLA transgenic mice. *Vaccine* 32, 3243–3248. doi: 10.1016/j.vaccine.2014.03.092
- El Bissati, K., Zhou, Y., Paulillo, S. M., Raman, S. K., Karch, C. P., Roberts, C. W., et al. (2017). Protein nanovaccine confers robust immunity against *Toxoplasma*. *NPJ Vaccines* 2:24. doi: 10.1038/s41541-017-0024-6
- Genton, B. (2008). Malaria vaccines: a toy for travelers or a tool for eradication? *Expert Rev. Vaccines* 7, 597–611. doi: 10.1586/14760584.7.5597
- Gómez-Marín, J. (2000). No NO production during human *Toxoplasma* infection. *Parasitol. Today* 16, 131. doi: 10.1016/S0169-4758(99)01614-2
- Gomez-Marín, J. E. (2010). *Protozoologia Medica*. First. Bogotá: Manual Moderno.
- Osorio, J. C. C., and García, A. M. G. (2019). Antiparasitic phytotherapy perspectives, scope and current development. *Infection* 23, 189–204. doi: 10.22354/IN.V23I2.777
- Rueda, K., Trujillo, J. E., Carranza, J. C., and Vallejo, G. A. (2014). Transmisión oral de *Trypanosoma cruzi*: un nuevo escenario epidemiológico de la enfermedad de Chagas en Colombia y otros países suramericanos. *Biomédica* 34, 631–641. doi: 10.7705/biomedica.v34i4.2204
- Thera, M. A., and Plowe, C. V. (2012). Vaccines for malaria: how close are we? *Annu. Rev. Med* 63, 345–357. doi: 10.1146/annurev-med-022411-192402
- Torres-Morales, E., Taborda, L., Cardona, N., De-la-Torre, A., Sepulveda-Arias, J. C., Patarroyo, M. A., et al. (2014). Th1 and Th2 immune response to P30 and ROP18 peptides in human toxoplasmosis. *Med. Microbiol. Immunol.* 203, 315–322. doi: 10.1007/s00430-014-0339-0

Conflict of Interest Statement: The authors declare that the research was conducted in the absence of any commercial or financial relationships that could be construed as a potential conflict of interest.

Copyright © 2019 Gómez Marín and El Bissati. This is an open-access article distributed under the terms of the Creative Commons Attribution License (CC BY). The use, distribution or reproduction in other forums is permitted, provided the original author(s) and the copyright owner(s) are credited and that the original publication in this journal is cited, in accordance with accepted academic practice. No use, distribution or reproduction is permitted which does not comply with these terms.



Cascade Ligand- and Structure-Based Virtual Screening to Identify New Trypanocidal Compounds Inhibiting Putrescine Uptake

Lucas N. Alberca¹, María L. Sbaraglini¹, Juan F. Morales¹, Roque Dietrich¹, María D. Ruiz², Agustina M. Pino Martínez³, Cristian G. Miranda³, Laura Fraccaroli², Catalina D. Alba Soto³, Carolina Carrillo², Pablo H. Palestro¹ and Alan Talevi^{1*}

¹ Laboratory of Bioactive Compounds Research and Development (LIDeB), Medicinal Chemistry, Department of Biological Science, Exact Sciences College, National University of La Plata, Buenos Aires, Argentina, ² Institute of Sciences and Technology Dr César Milstein (ICT Milstein), Argentinean National Council of Scientific and Technical Research (CONICET), Buenos Aires, Argentina, ³ Department of Microbiology, Parasitology and Immunology, School of Medicine, Institute of Microbiology and Medical Parasitology (CONICET), University of Buenos Aires, Buenos Aires, Argentina

OPEN ACCESS

Edited by:

Jorge Enrique Gómez Marín,
University of Quindío, Colombia

Reviewed by:

Claudia M. Calvet Alvarez,
University of California, San Diego,
United States
Vishvanath Tiwari,
Central University of Rajasthan, India

*Correspondence:

Alan Talevi
alantalevi@gmail.com

Received: 21 December 2017

Accepted: 04 May 2018

Published: 25 May 2018

Citation:

Alberca LN, Sbaraglini ML, Morales JF, Dietrich R, Ruiz MD, Pino Martínez AM, Miranda CG, Fraccaroli L, Alba Soto CD, Carrillo C, Palestro PH and Talevi A (2018) Cascade Ligand- and Structure-Based Virtual Screening to Identify New Trypanocidal Compounds Inhibiting Putrescine Uptake. *Front. Cell. Infect. Microbiol.* 8:173. doi: 10.3389/fcimb.2018.00173

Chagas disease is a neglected tropical disease endemic to Latin America, though migratory movements have recently spread it to other regions. Here, we have applied a cascade virtual screening campaign combining ligand- and structure-based methods. In order to find novel inhibitors of putrescine uptake in *Trypanosoma cruzi*, an ensemble of linear ligand-based classifiers obtained by has been applied as initial screening filter, followed by docking into a homology model of the putrescine permease TcPAT12. 1,000 individual linear classifiers were inferred from a balanced dataset. Subsequently, different schemes were tested to combine the individual classifiers: MIN operator, average ranking, average score, average voting, with MIN operator leading to the best performance. The homology model was based on the arginine/agmatine antiporter (AdiC) from *Escherichia coli* as template. It showed 64% coverage of the entire query sequence and it was selected based on the normalized Discrete Optimized Protein Energy parameter and the GA341 score. The modeled structure had 96% in the allowed area of Ramachandran's plot, and none of the residues located in non-allowed regions were involved in the active site of the transporter. Positivity Predictive Value surfaces were applied to optimize the score thresholds to be used in the ligand-based virtual screening step: for that purpose Positivity Predictive Value was charted as a function of putative yields of active in the range 0.001–0.010 and the Se/Sp ratio. With a focus on drug repositioning opportunities, DrugBank and Sweetlead databases were subjected to screening. Among 8 hits, cinnarizine, a drug frequently prescribed for motion sickness and balance disorder, was tested against *T. cruzi* epimastigotes and amastigotes, confirming its trypanocidal effects and its inhibitory effects on putrescine uptake. Furthermore, clofazimine, an antibiotic

with already proven trypanocidal effects, also displayed inhibitory effects on putrescine uptake. Two other hits, meclizine and butoconazole, also displayed trypanocidal effects (in the case of meclizine, against both epimastigotes and amastigotes), without inhibiting putrescine uptake.

Keywords: Chagas disease, *Trypanosoma cruzi*, putrescine uptake, drug repositioning, drug repurposing, cinnarizine, virtual screening, positive predictive value

INTRODUCTION

World Health Organization (WHO) describes neglected tropical diseases (NTDs) as a group of tropical diseases which mainly affect people living in poverty, lacking adequate sanitary conditions and in close contact with the infectious vectors (World Health Organization, 2015). One of the most important NTDs—in numerical terms—is Chagas disease, a parasitic disease endemic to Latin-America, caused by the infection by the protozoan *Trypanosoma cruzi*. This parasite can be transmitted to humans and more than 150 domestic and wild mammals, making complete eradication of the parasite practically impossible. The main route of transmission of *T. cruzi* is through the feces of the insect vector, known as *vinchuca*, a bug of the subfamily Triatominae. There are also other transmission routes, as congenital transmission and blood transfusions (Rassi et al., 2010), which are becoming increasingly important in the last years. WHO estimates based on 2010 data indicate that more than 6 million people are infected with *T. cruzi* worldwide, mostly in Latin-American countries (World Health Organization, 2015). However, several reports suggest that the actual number of infected people could be quite higher, reaching 10 million people (Ventura-Garcia et al., 2013; Stanaway and Roth, 2015; Browne et al., 2017).

Chagas disease presents two clinical phases. The initial or acute phase, which lasts between 4 and 8 weeks, is in general asymptomatic or might present as a self-limiting febrile illness. After the acute phase, an indeterminate, latent phase follows, with absence of clinical symptoms. About 60–70% of these people will remain in the indeterminate phase, but the remaining 30–40% will develop the symptomatic chronic phase characterized by damage to specific organs—particularly heart, esophagus, or colon. The chronic phase remains throughout life drastically reducing life expectancy among these patients (Nunes et al., 2013).

The only two approved drugs for the treatment of Chagas disease so far are Benznidazole and Nifurtimox, launched in the early 1970s. Both compounds are well-tolerated in children and effective during the acute phase. However, they present considerable side effects in adults, different susceptibility among *T. cruzi* strains and limited efficacy in adults in chronic phase (Morillo et al., 2015; Bermudez et al., 2016).

Drug repositioning (also known as drug repurposing, indication expansion and indication shift) represents an interesting strategy to approach the development of new medications for NTD (Ekins et al., 2011; Bellera et al., 2015; Ferreira and Andricopulo, 2016; Sbaraglini et al., 2016). It

consists in finding novel medical uses for existing drugs, including approved, experimental, discontinued and shelved drugs. Drug repurposing has several advantages over the search of *de novo* drugs. Since the new indication is built on already available pharmacokinetic and safety data, drug development time and costs can be considerably shortened. Possible manufacturing issues have also been solved. There are several successful cases of repositioned drugs in the field of NTDs: the anticancer drug eflornithine has been approved for the treatment of sleeping sickness and the antifungal drug amphotericin B has been repurposed for treatment of visceral leishmaniasis. To date, however, although there are several reports of drug candidates to be repositioned for the treatment of Chagas disease, none of these has yet been approved (Andrews et al., 2014; Klug et al., 2016; Sbaraglini et al., 2016). While initially drug repurposing stories arose from serendipitous observations, the drug discovery community has progressively adopted more systematic approximations to indication expansion (Ekins et al., 2011; Jin and Wong, 2014; Ferreira and Andricopulo, 2016), including genomic and structural biology tools, *in silico* screening and high-throughput screening platforms.

Polyamines (putrescine, spermidine, spermine) are low molecular weight polycations with crucial physiologic role in all the eukaryotic cells. They take part in fundamental cellular processes such as growth, differentiation, macromolecular biosynthesis and protection against oxidative damage. The polyamine metabolism in *T. cruzi* differs significantly from its human counterpart since the parasite lacks the enzymes arginine decarboxylase and ornithine decarboxylase, which are necessary for the biosynthesis of polyamines (Figure 1; Carrillo et al., 1999, 2003). Thus, *T. cruzi* depends on the incorporation of polyamines from the host cell. These functions are carried out by polyamine transporters such as the high-affinity putrescine permease TcPAT12 (or TcPOT1.1) which does not present homologous in the mammalian lineage (Carrillo et al., 2006). The importance of polyamines for parasites survival, the inability of the parasite to biosynthesize polyamines and the exclusivity of the putrescine transporter in *T. cruzi* makes putrescine uptake an attractive target for the search of new trypanocidal drugs (Hasne et al., 2016).

Back in 2016, we reported the first *in silico* drug repurposing campaign to discover novel inhibitors of polyamine uptake in *T. cruzi* (Alberca et al., 2016); such study applied an ensemble of ligand-based models to screen DrugBank 4.0 and Sweetlead databases and resulted in the identification of three candidates that impaired putrescine transport: paroxetine, triclabendazole

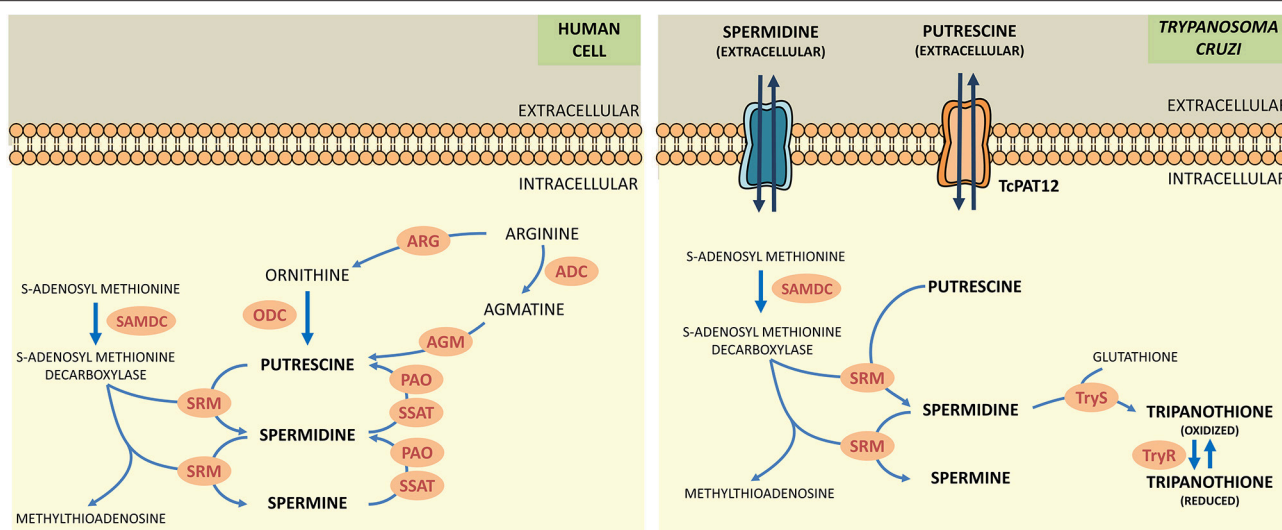


FIGURE 1 | Comparative scheme of polyamine metabolism in human cells and *T. cruzi*. ARG, arginase; ADC, arginine decarboxylase; AGM, agmatinase; ODC, ornithine decarboxylase; SAMDC, s-adenosylmethionine decarboxylase; SRM, spermidine synthase; PAO, polyamine oxidase; SSAT, spermidine acetyltransferase; TryS, trypanothione synthetase; TryR, trypanothione reductase.

and sertaconazole. Here, we have improved our ligand-based computational models and complemented them with molecular docking based on a homology model of TcPAT12; the combined screening has been applied to identify two new TcPAT12 potential inhibitors: clofazimine and cinnarizine. We also report, for the first time, the use of Positivity Predictive Value (PPV) surfaces analysis to select the score threshold that will be used in the virtual screening procedure. The two hits were assayed against *T. cruzi* epimastigotes and trypomastigotes, and the inhibitory effect on putrescine uptake was also determined.

MATERIALS AND METHODS

Ligand-Based Virtual Screening Dataset Collection

Polyamine analogs previously assayed against *T. cruzi* were compiled from literature. 256 polyamine analogs were found and conformed the dataset used here for model calibration and validation. Such dataset was curated using the standardization tool available in Instant JCHEMA v. 17.2.6.0. We have labeled the 256 compounds as ACTIVE or INACTIVE according to their half-maximal effective concentrations (EC₅₀) against *T. cruzi*. The ACTIVE category included compounds with EC₅₀ below 20 μM; the remaining compounds were included in the INACTIVE category. Considering such cut-off, the dataset includes 116 actives and 140 inactives. The molecular diversity of the whole dataset and within each category can be appreciated in the heatmaps displayed in Figure 2, which show, for every compound pair in the database, the Tanimoto distance computed using ECFP₄ molecular fingerprints. The heatmap was built using Gitoools v. 2.3.1 (Perez-Lamas and Lopez-Bigas, 2011) and Tanimoto distances were calculated using ScreenMD—Molecular Descriptor Screening

v. 5.5.0.1 (ChemAxon, 2002–2011). The dataset is included as Supplementary Information.

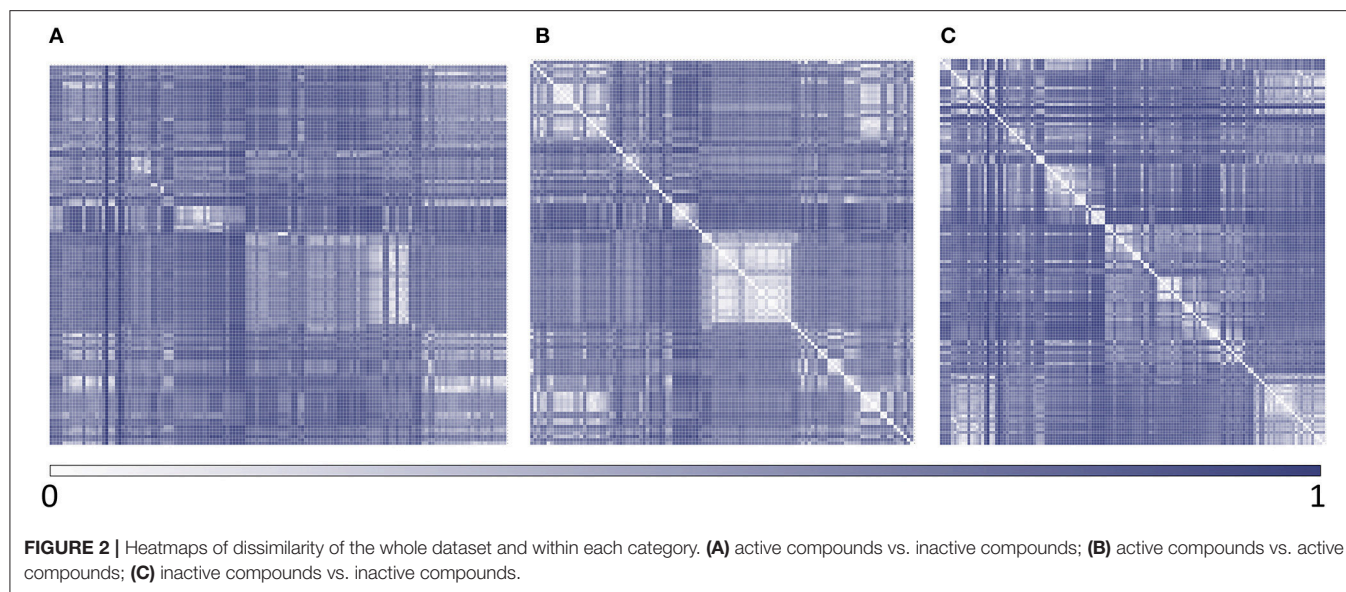
Dataset Splitting

The resulting dataset of 256 polyamine analogs was divided into two groups using a representative sampling procedure: (a) training set, that was used to calibrate the models and; (b) test set, that was used to externally validate the models. The representative partition of the dataset resulted from a serial combination of clustering procedures: first, we have used the hierarchical clustering method included in LibraryMCS software (version 17.2.13.0—ChemAxon), which relies on the Maximum Common Substructure (MCS). From the resulting clusters, a compound from each cluster was randomly chosen and used as a seed to perform a non-hierarchical clustering using the k-means algorithm, as implemented in Statistica 10 Cluster Analysis module (Statsoft, 2011). Such procedure was performed in an independent manner for the ACTIVE and INACTIVE categories.

Seventy-five percent of the compounds in each cluster of the ACTIVE category were kept for the training set (totaling 87 compounds); an equal number of compounds were taken from the INACTIVE category clusters (62.14% of each INACTIVE cluster). The remaining 29 active and 53 inactive compounds were assigned to test set. Note that, to obtain the training set, we have under-sampled the INACTIVE category, so that a balanced calibration sample was obtained. In that way, model bias toward predicting a specific category was avoided.

Molecular Descriptor Calculation and Modeling Procedure

Three thousand six hundred sixty-eight conformation-independent descriptors were computed with Dragon 6.0 software. A random subspace-based method was applied to



obtain 1,000 random descriptor subsets of no more than 200 potential independent variables each. In the random subspace approach, the features (independent variables, e.g., molecular descriptors) are randomly sampled and each model (learner) is trained on one subset of the feature space (El Habib Daho and Amine Chikh, 2015; Vyskovsky et al., 2016), which causes individual models not to over-focus on features that display high explanatory power in the training set.

A dummy, binary variable (class label) was used as dependent variable. Such variable was assigned observed values of 1 for compounds within the ACTIVE, and observed values of 0 for compounds in the INACTIVE category.

Using a Forward Stepwise approach and a semi-correlation approach (Toropova and Toropov, 2017), 1,000 linear classifiers were obtained, one from each of the random subsets of features. In order to avoid overfitting, only one molecular descriptor every 10 training instances was allowed into each model, with no more than 12 independent variables per model. No regression coefficient with p -value above 0.05 was allowed into the model.

R language and environment was used for all data analysis. The R package data table (<https://cran.r-project.org/package=data.table>) was used to handle datasets.

The robustness and predictive ability of the models were estimated through randomization and leave-group-out cross-validation tests. In the case of randomization, the class label was randomized across the compounds in the training set. The training set with the randomized dependent variable was then used to train new models from the descriptor selection step. Such procedure was repeated 10 times within each descriptor subset. It is expected that the randomized models will perform poorly compared to the real ones. Regarding the Leave-Group-Out cross-validation, 18-compound subsets were randomly removed from the training set in each cross-validation round and the model was regenerated. The resulting model was used to predict the class label for the 18 removed compounds. The procedure was repeated 10 times, removing each of the training set compounds once.

Ensemble Learning

Classifier ensembles are known to handle complex data and to provide better generalization and accuracy than single model classifiers (El Habib Daho and Amine Chikh, 2015; Carbonneau et al., 2016; Min, 2016; Vyskovsky et al., 2016); they can be particularly useful to prevent overfitting when handling datasets that suffer from small sample size while their dimensionality is large (Vyskovsky et al., 2016), a quite frequent scenario in the drug design field.

The best individual classifiers were selected and combined (selective ensemble learning approach) using the area under the ROC curve metric (AUC ROC) as criterion of performance. Systematic combinations of the 2–100 best performing classifiers were analyzed. Four combination schemes were applied to obtain a combined score: MIN operator (which returns the minimum score among the individual scores of the combined models); Average Score; Average Ranking and Average Voting. Voting was computed according to the equation previously used by Zhang and Muegge (2006). AUC ROCs were obtained with the pROC package (Robin et al., 2011); the Delong method was used to obtain 95% confidence intervals.

Pilot (Retrospective) Screening Campaign

Through simulated ranking experiments, Truchon et al. demonstrated that the AUC ROC metric is dependent on the ratio of actives/inactives, and the standard deviation of the metric converges to a constant value when small yield of actives of the screened library (Y_a , also called ratio of actives or prevalence of activity) are used (ratios of actives below 0.05 seem to provide more robust results). Reasonably small Y_a also ensures that the saturation effect is constant or absent. A high number of decoys (around 1,000 or higher) contribute to a controlled statistical behavior, especially if poorly performing classifiers/methods are applied (Truchon and Bayly, 2007). Accordingly, we have performed pilot (retrospective) VS campaigns for the individual classifiers and classifier ensembles. For that purpose, we have dispersed the active compounds from each test set among a

large number of decoys obtained with the help of the enhanced Directory of Useful Decoys (DUD-E) (Mysinger et al., 2012). Each of the test set active compounds from each dataset was used as a query in the DUD-E website, thus generating paired putative inactive compounds (decoys) for each of those active compounds. As a result, the pilot database contained 29 known active compounds dispersed among 1302 DUD-E decoys and 53 known inactive compounds, adding up a total of 1384 compounds and displaying a Y_a of 0.021.

Building Positivity Predictive Value Surfaces and Choosing an Adequate Score Threshold Value

A practical concern in virtual screening campaigns is to predict the actual probability that a predicted hit will prove truly active when submitted to experimental testing (the PPV). Estimation of such probability is however obstructed due to its dependency on the Y_a of the screened library, which cannot be known *a priori*:

$$PPV = \frac{(Se)(Y_a)}{(Se)(Y_a) + (1 - Sp)(1 - Y_a)} \quad (1)$$

where Se represents the sensitivity associated to a given score cutoff value and Sp represents the specificity. Equation (1) was applied to build PPV surfaces. 3D plots illustrating the interplay between PPV , the Se/Sp ratio and Y_a were built for each individual model and for each model ensemble. Using the corresponding pilot database (as described in previous subsections), Se and Sp were computed in all the range of possible cutoff score values. Note that there is no guarantee that the Se and Sp associated to each score value (and thus, the ratio Se/Sp) will be the same when applying the classifiers to other compound databases, e.g., in the real virtual screening campaign; nevertheless, since controlled statistical behavior is observed for database sizes of about 1000 compounds or more and Y_a below 0.05, we can reasonably assume that the ROC curve and derived metrics will be similar when applying the models to classify other large chemical databases with low Y_a . In order to build the PPV surfaces, and taking into consideration that in real VS applications Y_a is ignored *a priori* but invariably low, Y_a was varied between 0.001 and 0.010. The R package *plotly* (<https://cran.r-project.org/package=plotly>) was used to obtain all the PPV graphs. Visual analysis of the resulting PPV surfaces allowed us to select a score cutoff value with a desired range of PPV .

Virtual Screening

Based on visual inspections of the resulting of PPV graphs, we have applied an 8-model ensemble using the MIN operator to combine individual models for virtual screening, choosing 0.354 as score threshold (above 0.354 compounds from the screened databases have labeled as predicted active compounds). Such threshold corresponds to a Se/Sp ratio of 0.666. It was checked that every hit belonged to the applicability domain of the model from the model ensemble that assigned the minimum score (which, was, according to our combination scheme, the one that ultimately decided if a compound was or was not labeled as an active). The leverage approach was used to assess if a hit belongs to the applicability domain, using $3d/n$ as cutoff value, where d is

the number of descriptors in the correspondent model and n is the number of compounds in the training set.

We have used the 8-model ensemble to screen two databases: (a) DrugBank 4.0, an online database containing extensive information about the US Food and Drug Administration (FDA) approved, experimental, nutraceutical, illicit and investigational drugs (Law et al., 2014); (b) Sweetlead, a curated database of drugs approved by other international regulatory agencies, compounds isolated from traditional medicinal herbs, and regulated chemicals (Novick et al., 2013). These two databases were curated using Standardizer 16.10.10.0 (ChemAxon). We have applied the following actions to generate homogeneous representations of the molecular structure for the virtual screening: (1) Strip salts; (2) Remove Solvents; (3) Clear Stereo; (4) Remove Absolute Stereo; (5) Aromatize; (6) Neutralize; (7) Add Explicit Hydrogens; and (8) Clean 2D. Additionally, duplicate structures were removed using Instant JCHEM v. 17.2.6.0. Based in the results obtained and considering the most direct candidates for repositioning, two compounds were selected for experimental evaluation. Hits submitted to experimental testing were acquired from Sigma-Aldrich.

Structure-Based Virtual Screening

The 24 best solutions from ligand based virtual screening were submitted to molecular docking calculations. To this end we employed as target our 3D model of the putrescine permease TcPAT12 previously constructed (Dietrich et al., 2018). This model was based on the arginine/agmatine antiporter (AdiC) from *E. coli* as template (Protein data bank accession code: 3L1L, Feng et al., 2000), which was identified through Blast sequence search and showed 23% of sequence identity and 64% coverage of the entire query sequence. The model of TcPAT12 architecture was achieved by Modeller Software (Webb and Sali, 2016). The best model has been selected based on the normalized Discrete Optimized Protein Energy parameter (z -DOPE) (Shen and Sali, 2006) and the GA341 score (which analyze the reliability of a model based on statistical potentials) (Melo and Sali, 2007). This structure had the highest number of residues in allowed area (96%) on Ramachandran plot, and none of the residues located in non-allowed regions were involved in the active site of the transporter.

The docking conditions were defined according to our previous studies, which pointed to Autodock4.2 (rigid mode) as the best software to discriminate known inhibitors from non-inhibitors of TcPAT12 through the docking score (Dietrich et al., 2018). The “docking active site” was set according to previous research of Soysa et al. (2013). They proposed the location of the putrescine-binding pocket in a region that includes Gly69, Cys66, Trp241, Ala244, Asn145, Cys396, Asn245, Tyr148, Tyr400 amino acids. Autodock4.2 calculations were computed in a grid with the default spacing (0.375 Å) between the $44 \times 58 \times 40$ grid points in x, y, z directions respectively. Additionally, we performed the standard estimation for all the variables such as Marsilli-Gasteiger partial charges. We computed 100 docking runs for each compound, with a rigid target and flexible ligands (allowing the rotation of all non-ring torsion angles of the candidates).

Experimental Assays

Biological Activity Against Different *T. cruzi* Stages

For all assays, stock and working solutions of the candidate drugs were prepared using DMSO as solvent and test or control conditions were tested in triplicate.

Epimastigotes of the Y strain of *T. cruzi* were cultured at 28°C in BHT medium supplemented with 20 µg/ml haemin, 10% heat-inactivated fetal bovine serum (FBS), 100 µg/ml streptomycin and 100 U/ml penicillin. The antiproliferative activity of the candidates was tested at concentrations from 1 to 100 µM in cultures initiated at 10⁷ cells/ml. After 4 and 8 days, the number of viable parasites were counted using a hemocytometer chamber under the light microscope (Bellera et al., 2013). Controls were performed under the same culture conditions with equal concentrations of DMSO as for candidate drugs. The EC₅₀ values were determined from dose response curves fitted to a sigmoidal equation (Boltzmann model) or extrapolated from linear fitting plots (Fernández et al., 2013).

T. cruzi trypomastigotes were purified at the parasitemia peak from peripheral blood of mice infected with the RA strain. Trypomastigotes (1 × 10⁴ per well) were cultured in a 96 well-plate (final volume 200 µl) in RPMI medium supplemented with 10% FBS at 37°C in 5% CO₂ atmosphere. After 24 hours motile parasites were counted in hemocytometer chamber under the light microscope (Miranda et al., 2015). Results were expressed as % viability of trypomastigotes at 20 µM of the hits. Controls were performed under the same culture conditions with equal concentrations of DMSO as for candidate drugs. The negative control was cultured with PBS and the positive control was cultured with Benznidazole (20 µM).

In vitro evaluation of drug activity against intracellular amastigotes. J774 cells infected with bloodstream trypomastigotes of RA strain were cultured at 37°C in humidified incubator with 5% CO₂ in 24-well plates (1.5 × 10⁵ cells per well; final volume of 500 µl in duplicate). After 24 h of incubation, increasing doses of freshly prepared dilutions of benznidazole, meclizine dihydrochloride, cinnarizine, or butoconazole were added at final concentrations of 5, 20, and 50 µM for meclizine, and cinnarizine and 1, 5, and 20 µM for butoconazole nitrate. Seventy-two hours later, medium was drained and cells were fixed for 10 min in ice-cold methanol and stained with 10% v/v of Giemsa solution for 15 min. The number of amastigotes per 100 host cells was recorded. Control cultures were incubated in medium alone or with equal DMSO concentrations. Cytotoxicity was analyzed in trypsinized cell suspensions, after addition of Propidium iodide (PI) (Sigma, St. Louis, USA) (5 µg/ml) 10 min prior to analysis by fluorescence and light microscopy of the number of viable and dead cells.

Aminoacid/Polyamine Transport Assay

Aliquots of *T. cruzi* epimastigotes (3 × 10⁷ parasites) starved for 3 h in 2% glucose—phosphate-buffered saline (PBS) were collected, centrifuged at 1,500 g for 10 min and washed three times with PBS. Cells were then resuspended in 2 ml of PBS containing 5 µM (¹⁴C)-putrescine, or (¹⁴C) arginine, and candidates at a final concentration of 50 µM previously solubilized in DMSO. Aliquots were taken at different time

points, centrifuged and washed three times with 1 ml of ice cold 10 mM solution of unlabeled putrescine/arginine in PBS. Pellets were resuspended and radioactivity determined in UltimaGold XR (Díaz et al., 2014). All experiments were performed in triplicate.

The effect of the candidate on parasite viability under uptake assay conditions was evaluated through the tetrazolium salt (MTT) reduction assay (Mosmann, 1983). Briefly, 10 µl of 5 mg/ml MTT dye (3[4,5-dimethylthiazol-2-yl]-2,5-diphenyltetrazolium bromide) was added to the eppendorf tubes containing 10⁶ parasites in 100 µl of BHT and the drug candidates at 50 µM solubilized in DMSO. After incubation for 3 h at 28°C, the tubes were spin-dried (3,000 rpm) and the pellet with the formazan crystals were dissolved with 100 µl of DMSO. The optical density (OD) was determined using a microplate reader (LabSystems Multiskan MS, Finland) at 570/695 nm. Under such conditions, the OD is proportional to the viable cell number in each well. All experiments were performed in triplicate.

RESULTS

Model Development and Validation and Virtual Screening

Two serial virtual screening methods were applied to find out putative *TcPAT12* inhibitors. First, we resorted to a computationally inexpensive ligand-based approach. For that purpose, 1,000 individual linear classifiers were obtained by applying a random subspace approximation. The individual models were externally validated by using an independent test set and, for a more challenging and realistic simulation, by retrospective screening of a simulated library where a small proportion of active compounds was dispersed among a high number of (mostly putative) decoys. 82, 57, and 25% of the individual classifiers displayed AUC ROCs above 0.8 for the training set, the test set and the simulated DUD-E database, in that order. This suggests some degree of overfitting and corroborates that the pilot (retrospective) screening campaign against the DUD-E database is the more challenging task for the classifiers. **Table 1** shows the eight individual classifiers that showed the best performance on the training and test sets, and also on the DUD-E database.

The best individual model included the following features:

Model 348: Class = 3.12777 + 0.03474 * F06[C-C] + 0.20805 * S-107 - 0.04291 * F05[N-N] + 0.39611 * C-039 - 0.34582 * SM5_B(s) + 6.25705 * Eta_epsi_A + 0.53013 * nSO2OH - 1.28338 * SpMax_H2 + 0.44827 * Eig04_AEA(ri) - 1.73390 * ATSC1e + 0.05975 * CATS2D_09_PL + 0.02805 * SaaO
Wilks' Lambda: 0.59
 $F_{(12, 161)} = 9.23$
 $p < 0.0000$

Dragon's nomenclature for the molecular descriptors has been kept in the previous expression. F06[C-C] refers to the count of C-C at a topological distance of 6; S-107 represents the count of R2S/RS-SR groups; F05[N-N] stands for the frequency of

TABLE 1 | Values of the AUROC metric for the best eight individual models and the best 8-model ensemble.

Model	Training set	Test set	DUD-E database
8-MODEL ENSEMBLE (MIN)	0.851 (±0.0281)	0.885 (±0.0367)	0.976*** (±0.0085)
8-MODEL ENSEMBLE (RANKING)	0.886 (±0.0239)	0.878 (±0.0375)	0.976*** (±0.0082)
8-MODEL ENSEMBLE (AVERAGE)	0.891 (±0.0234)	0.887 (±0.0357)	0.970*** (±0.0096)
8-MODEL ENSEMBLE (VOTING)	0.833 (±0.0283)	0.810 (±0.0516)	0.959* (±0.0173)
348	0.882 (±0.0250)	0.885 (±0.0360)	0.934 (±0.0123)
706	0.809* (±0.0319)	0.736** (±0.0565)	0.924 (±0.0205)
981	0.843 (±0.0298)	0.837 (±0.0467)	0.922 (±0.0254)
557	0.778** (±0.0343)	0.818 (±0.0482)	0.919 (±0.0203)
123	0.850 (±0.0285)	0.882 (±0.0382)	0.918 (±0.0185)
693	0.860 (±0.0280)	0.828* (±0.0459)	0.913* (±0.0171)
560	0.775** (±0.0348)	0.779* (±0.0525)	0.911* (±0.0185)
746	0.844 (±0.0288)	0.820 (±0.0456)	0.910 (±0.0195)

AUROC values statistically different from the correspondent column for the best individual model (model 348). * $p < 0.05$, ** $p < 0.01$, and *** $p < 0.001$. The highest AUC for an individual model is indicated in bold.

N - N at a topological distance of 5; C-039 refers to Ar-C(=X)-R groups; SM5_B(s) corresponds to the spectral moment of order 5 from the Burden matrix weighted by I-State; Eta_epsi_A is the eta average electronegativity measure; nSO2OH stands for the number of sulfonic (thio-/dithio-) acids; SpMax_H2 is the leading eigenvalue from reciprocal squared distance matrix; Eig04_AEA(ri) denotes the fourth eigenvalue from augmented edge adjacency matrix weighted by resonance integral; ATSC1e corresponds to the Centred Broto-Moreau autocorrelation of lag 1 weighted by Sanderson electronegativity; CATS2D_09_PL is the CATS2D Positive-Positive at lag 09 and; SaaO corresponds to the sum of aaO E-states.

Whereas the performance of the best individual classifiers was quite satisfactory, we resorted to ensemble learning to obtain meta-classifiers with improved accuracy and a more robust behavior. The expectations on the model combination approach were confirmed statistically: no matter which combination scheme is applied, the model ensembles show a statistically similar behavior to the best individual model when classifying the training and test set compounds, while statistically outperforming the individual models when considering the DUD-E database ($p < 0.05$ in all cases). The MIN, RANKING and AVERAGE combination schemes led to the best results (Table 1), with p -values below 0.001. When considering the influence of the number of combined models on the AUROC metric, it was observed that although the ensemble learning approach always seems to improve the results in comparison with the individual classifiers, combinations above 10 models tend to poorer behavior in terms of AUROC values but also regarding the standard deviation of the mean, which increases with the number of models included in the ensemble (Figure 3).

Since all the model combination approaches exhibited similar behavior against the test set and the DUD-E database for relatively low number (below 10) of combined classifiers, we chose to move to the real virtual screening campaign with the combination scheme based on the MIN. In our experience, this is the most conservative approach which tends to display the smallest false positive rate. This was confirmed when comparing

Sp and Se of the 8-model meta-classifier with those of the best performing individual models, where a substantial improvement in Sp was observed (Figure 4). This is a particularly good result in our context (small academic group from a mid-income country, with limited resources to invest in hit experimental validation); we often prefer to reduce the false positive rate even if this means losing sensitivity and sacrificing some active scaffolds. However, in this particular case we have chosen to refine the former criteria (prioritizing Sp) by resorting to what we have called PPV surfaces. With the help of these surfaces, the evolution of the most relevant metric for our purposes, the PPV value, can be visually (or, eventually, mathematically) optimized as a function of the Se/Sp ratio across a range of Ya values. For this analysis, we have used the association between Se/Sp and score values that have been observed in the pilot screening campaign. The strongest assumption of our approach is that the Se/Sp value observed for a given score during the pilot screening campaign against the DUD-E database will hold when screening other databases (e.g., the ones screened in real virtual screening applications). This is of course not necessarily true. However, since the AUROC values obtained for the DUD-E database are unequivocally high (always above 0.9 for the individual models and very close to the perfect value of 1 for the ensembles) while on the other hand the DUD-E database Ya ratio (quite below 0.05) and size (>1,000 compounds) speak of a controlled statistical behavior, we believe it is a reasonable assumption in the present setting.

When analyzing the PPV surface for the 8-model combination based on the MIN operator, it was observed that in the current scenario favoring Sp over Se has a positive impact on the PPV, thus resulting in higher probabilities of confirming *in silico* hits submitted to experimental validation (Figure 5). It should be emphasized that such behavior is not general: other situations linked to different PPV surface shapes might lead to an entirely different conclusion (that is, the need to prioritize Se over Sp to enhance PPV). The selection of the best cutoff value should be based in the specific PPV surface obtained in each particular modeling situation.

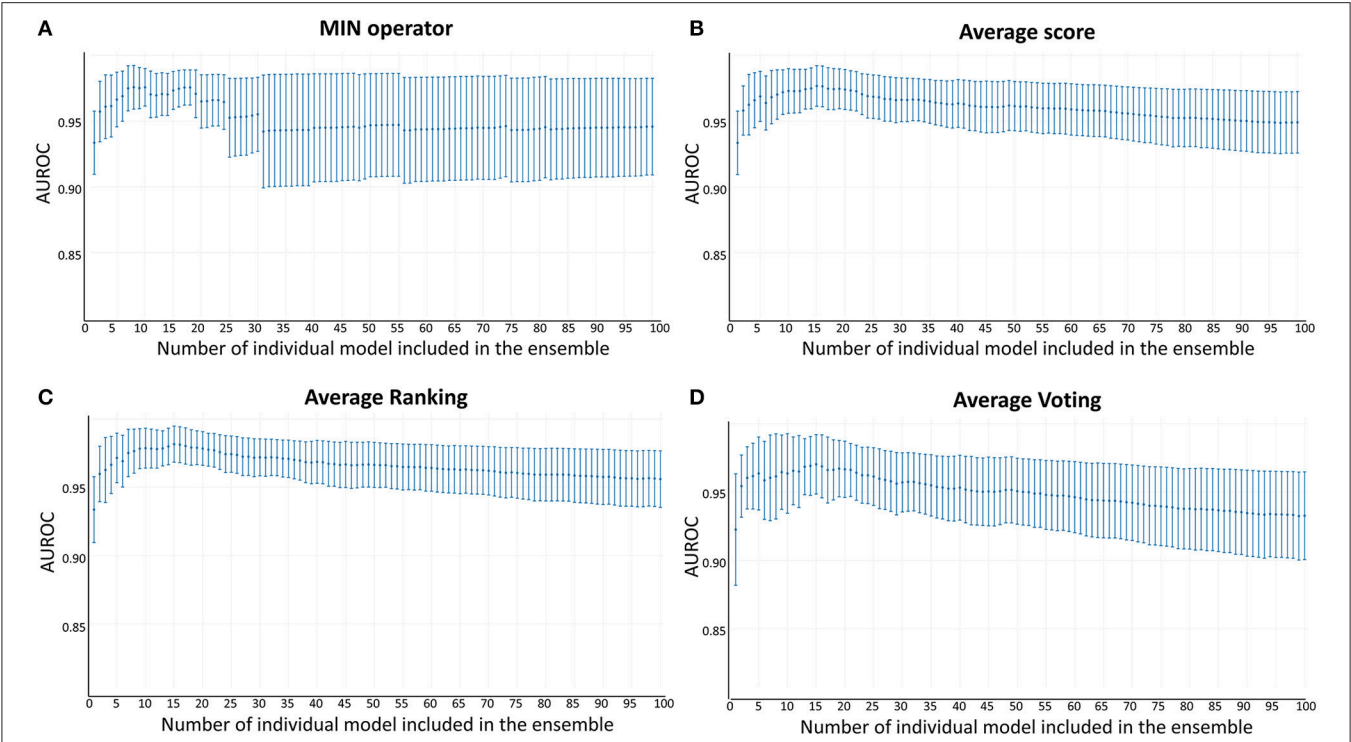


FIGURE 3 | AUROC metric vs. the number of combined models in the DUD-E database **(A)** MIN operator; **(B)** Average score; **(C)** Average Ranking; **(D)** Average Voting.

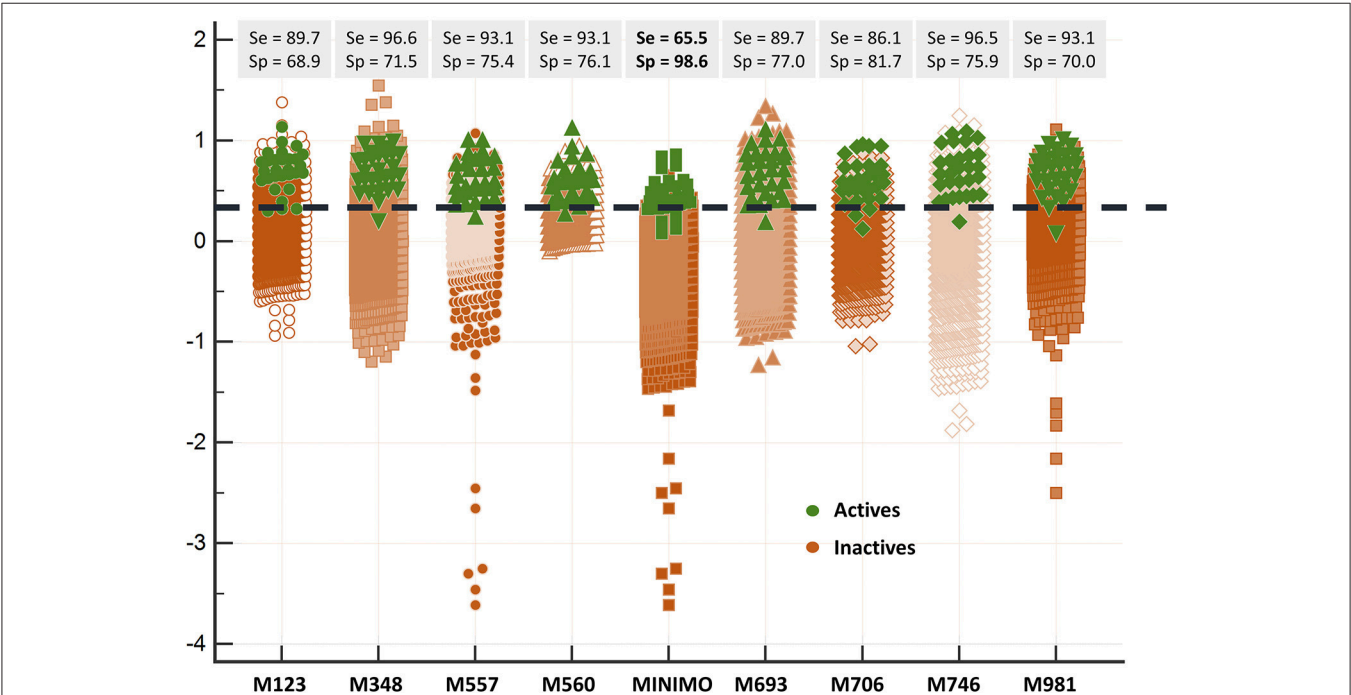
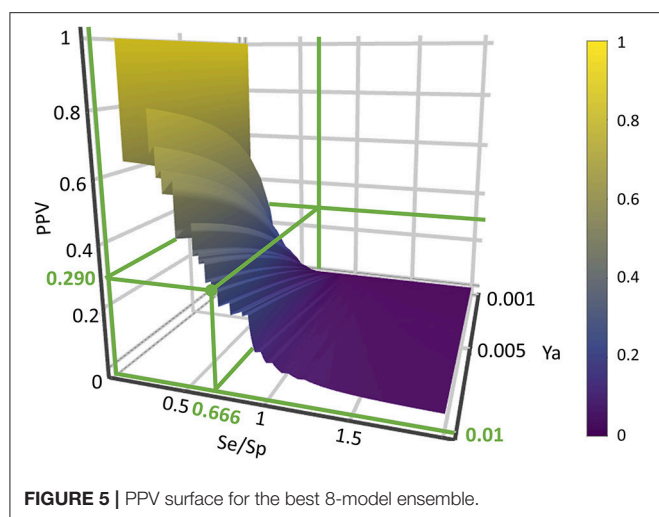


FIGURE 4 | Discriminating abilities of the individual models and the best model ensemble against the DUD-E database. The MIN combination scheme clearly improves Sp (note the enhanced separation of the inactives from the actives in comparison with individual models).



Using the PPV surface, we chose 0.354 as score threshold to be used in our real virtual screening campaign; such score is associated to a Se/Sp ratio of 0.666 for the 8-model ensemble based on the MIN operator. Whereas higher scores linked to lower Se/Sp ratio would, according to the PPV surface, result in improved PPVs, the resulting number of hits would also be substantially diminished, leaving very few choices for subsequent acquisition and experimental testing (the ligand-based screen using the 0.354 cutoff score resulted in only 24 hits, with just 15 of them being approved drugs, the most straightforward candidates to drug repurposing).

The 24 hits emerging from the ligand-based screening stage were submitted to the structure-based screening (docking into the *Tc*PAT12 homology model), with 17 of them surviving the docking stage and only 9 of them having achieved approved status. **Table 2** shows the hits selected through the combined ligand- and target-based approach, including the PPV range for the correspondent score value of the 8-model ensemble between *Ya* values of 0.001 and 0.010. Note that 3 of the hits, namely clomifene, oxiconazole and clofazimine have previously been assayed against *T. cruzi*, with positive results (Sykes and Avery, 2013; Bellera et al., 2015; Kaiser et al., 2015). Most of the compounds have a docking score lower than the value found for the natural ligand putrescine (-6.0), which was calculated previously in the same docking conditions. The results justify the selection of the structures as promising candidates. The exception was clofazimine, with a docking score of -1.58 . In this particular case, the drug has been identified as trypanocidal agent within our research group, during an *in silico* screening to detect novel cruzipain inhibitors. The drug later confirmed its potential both in acute and chronic rodent models of Chagas disease (Bellera et al., 2015; Sbaraglini et al., 2016). In that occasion, though, it was observed that the potency of the drug against the parasite was higher than the inhibitory potency against cruzipain, suggesting multiple mechanisms of action besides cruzipain inhibition.

Based on access to the chosen compounds, we decided to test clofazimine, cinnarizine, meclizine dihydrochloride, and butoconazole nitrate (Sigma Aldrich) effects on putrescine uptake in *T. cruzi*. Cinnarizine, meclizine, and butoconazole

were also tested against *T. cruzi* epimastigotes, trypomastigotes, and amastigotes. The latter assays were omitted for clofazimine, since as already discussed, this drug had previously been tested against the different *T. cruzi* stages, with positive results. Before acquisition, it was verified if the compounds obeyed different druglikeness rules. All compounds satisfy Lipinski's rules (they satisfy three out of four of the Lipinski's proposition, only violating the proposition linked to *clogP*), Veber's rule and the druglikeness criteria adopted by Monge et al. in previous studies (Lipinski et al., 2001; Veber et al., 2002; Monge et al., 2006). All in all, these analysis suggest that they have high probabilities of displaying good oral bioavailability (Lipinski's and Veber's rules) while also excluding some undesirable properties such as highly reactive chemical groups and possible toxicophores (Monge's criteria). This is not a surprising result since all the hits submitted to experimental validation are approved drugs. A summary of the screening workflow and the number of hits surviving each step is presented in **Figure 6**.

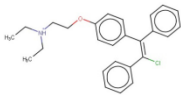
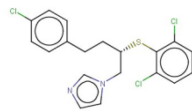
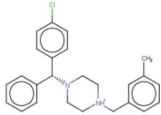
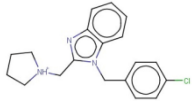
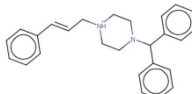
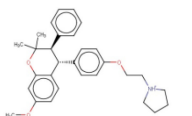
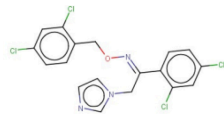
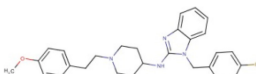
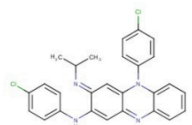
Experimental Testing

The effect of different concentrations of cinnarizine, meclizine and butoconazole against *T. cruzi* epimastigotes was tested (**Figure 7**) and the correspondent EC_{50} was calculated. The three drugs showed a clear inhibition in a dose-dependent manner on the proliferation of epimastigotes, with a EC_{50} (at day 4) of $6.05 \mu\text{M}$, $8.39 \mu\text{M}$ and $3.08 \mu\text{M}$, respectively. The reference drug benznidazole displayed a EC_{50} of $2.56 \mu\text{M}$ against epimastigotes. When tested against trypomastigotes at $20 \mu\text{M}$, cinnarizine displayed a slight inhibition in viability (30%). No inhibition was observed for the other two hits tested. When testing its effects against amastigotes, butoconazole showed a considerable cytotoxicity against J774 cells at all the assayed concentrations (100.0%; $57.5 \pm 0.6\%$; $48.3 \pm 6.3\%$ at $50 \mu\text{M}$; 20 and $5 \mu\text{M}$ respectively), and it was therefore disregarded for future investigations. Meclizine showed cytotoxicity against J774 cells at $50 \mu\text{M}$ ($13.9 \pm 2.0\%$), though no toxic effects were observed at lower concentrations. Cinnarizine showed no toxicity at any of the tested concentrations. Meclizine significantly reduced the number of amastigotes per 100 cells at the three assayed concentrations. Cinnarizine showed a weak effect against amastigotes, displaying almost a 50% inhibition at $50 \mu\text{M}$ (**Figure 8**).

To determine if the mechanism of action of the candidates correlates with that predicted by our models, the inhibition of putrescine uptake by *T. cruzi* epimastigotes was determined (**Figure 9A**). A 10-fold molar excess of the candidate drugs were tested. Cinnarizine and clofazimine showed a clear effect on putrescine uptake with a significant initial velocity reduction to 52.56 ± 4.84 and $30.85 \pm 2.74\%$ respectively, compared with transport in control conditions. In contrast, meclizine and butoconazole did not display any inhibitory effect on putrescine uptake, which suggests that their trypanocidal effect is related to other mechanisms of action. Meclizine has previously been shown to inhibit cruzipain at low μM concentrations (Doak et al., 2010).

The specificity of the putrescine uptake inhibition by cinnarizine and clofazimine was checked by testing the effect of both active hits on other transporter of the same family

TABLE 2 | Candidates selected through the combined ligand- and target-based approach.

Name	MIN Score	PPV% (Ya = 0.001)	PPV% (Ya = 0.01)	Structure	Score docking	Current therapeutic indication
Clomifene	0.4837	14.64	63.38		−9.37	Used mainly in female infertility due to anovulation
Butoconazole	0.4768	14.64	63.38		−9.87	Local treatment of vulvovaginal candidiasis
Meclizine	0.4546	12.30	58.61		−8.95, −6.64 ^a	Motion sickness and vertigo
Clemizole hydrochloride	0.4544	12.30	58.61		−8.91	Allergies
Cinnarizine	0.4273	9.20	50.56		−7.43	Motion sickness and vertigo
Centchroman	0.3798	5.67	37.76		−6.31	Primarily used as a contraceptive
Oxiconazole	0.3751	5.00	34.68		−10.44	Dermal fungal infections.
Astemizole	0.3666	4.25	30.96		−6.45	Allergies
Clofazimine	0.3605	4.06	29.92		−1.58	Leprosy

^aThe docking scores of both isomers were calculated.

(Figure 9B). The MTT assay indicated that under the uptake conditions (with 50 μ M of the drug and 1% DMSO), neither cinnarizine nor clofazimine presented a cytotoxic effect on the parasites (not shown).

DISCUSSION

Comparison With Previous Studies

Whereas studies to exploit polyamine transporters as molecular drug targets for the development of new trypanocidal agents

are at an early stage, some interesting considerations may be outlined from the considering the present study and the few previous reports describing the screening of new inhibitors of *T. cruzi* putrescine uptake. First, some of the hits identified in earlier studies have shown to be more effective against *T. cruzi* trypomastigotes than against other stages of the parasite (Reigada et al., 2017, 2018). For instance, the reported IC₅₀ of isotretinoin against trypomastigotes (130 nM) is about 230-fold lower than the one against epimastigotes (Reigada et al., 2017). The opposite was observed in this study for cinnarizine, since epimastigotes

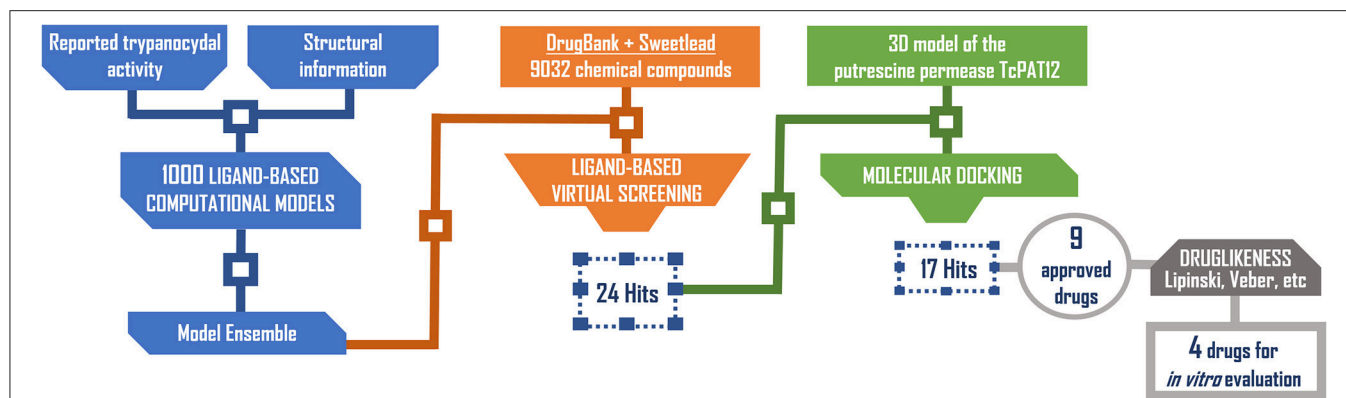


FIGURE 6 | Screening workflow used in the present study. The number of compounds retained at each step for further studies is shown.

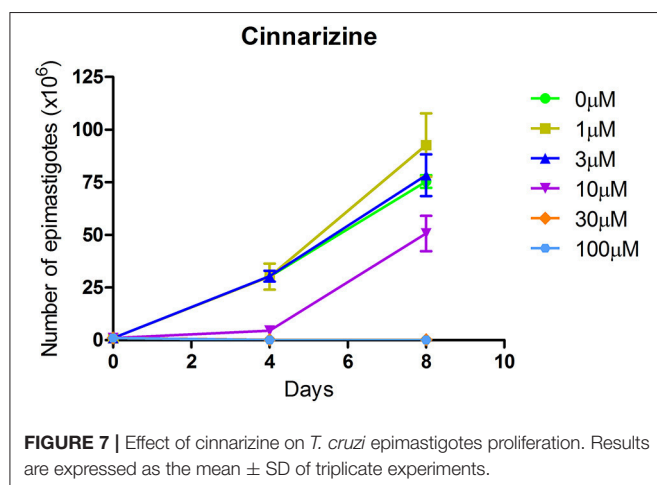


FIGURE 7 | Effect of cinnarizine on *T. cruzi* epimastigotes proliferation. Results are expressed as the mean \pm SD of triplicate experiments.

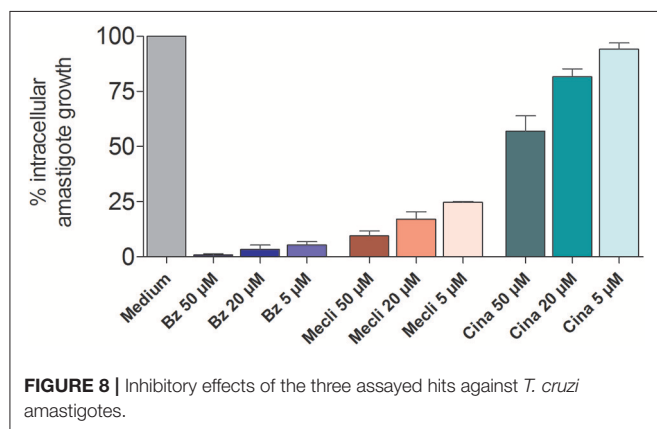


FIGURE 8 | Inhibitory effects of the three assayed hits against *T. cruzi* amastigotes.

were more sensitive to the drug than trypomastigotes. There are some possible explanations to these varying degrees of sensitivity to putrescine uptake inhibition across *T. cruzi* stages. It is possible that different forms of the parasite resort to different primary transport mechanisms of polyamines (each of them with different drug specificities) (Seguel et al., 2016). A similar possibility has been suggested in *Leishmania*, where it has been observed

that amastigotes and promastigotes use different transporters for polyamine uptake (Müller et al., 2001; Colotti and Ilari, 2011).

The comparison of the present study with previous *in silico*-guided drug repurposing campaigns targeting *T. cruzi* polyamine uptake is hindered by the fact that very few earlier studies exist and that different virtual screening approaches have been applied in them. The first report of a virtual screening application to identify putrescine uptake inhibitors came from Alberca et al. who back in 2016 used an ensemble of six linear classifiers and identified three novel confirmed hits (out of five hits submitted to experimental screening): sertaconazole, triclabendazole, and paroxetine (Alberca et al., 2016). The same 6-model ensemble was later applied in parallel with a similarity-based screen and in sequence with target-based screening, with one out of four hits validating their predicted activity *in vitro* (Dietrich et al., 2018). For their part, Reigada et al. used a combination of similarity-based virtual screening and molecular docking, obtaining two experimentally confirmed hits (isotretinoin and acitretin) out of a total of three tested compounds (Reigada et al., 2017). The statistical comparison of the true PPV (confirmed hits over total number of hits tested) in the aforementioned virtual screening campaigns has no point due to the small number of hits tested in each occasion. Nevertheless, such PPV was in all cases, including the current study, well above the median value of hit rate in virtual screening studies (13%), as reported in a critical literature analysis of virtual screening results published between 2007 and 2011 (Zhu et al., 2013).

From a visual comparison of the (theoretic) PPV surfaces of the 6-model ensemble reported by Alberca et al. (2016) and the currently reported 8-model ensemble, it is clear that the 8-model ensemble reported here shows a more robust and predictable behavior in the *Se/Sp* range that goes from 0.3 to 1.0. (Figure 10).

The Power of Ensemble Learning

The DUD-E database used as a validation tool in our retrospective virtual screening campaign confirmed that retrospective screening is the most challenging task (besides prospective screening) for a model conceived for *in silico* screening applications, as in the case of individual classifiers, the

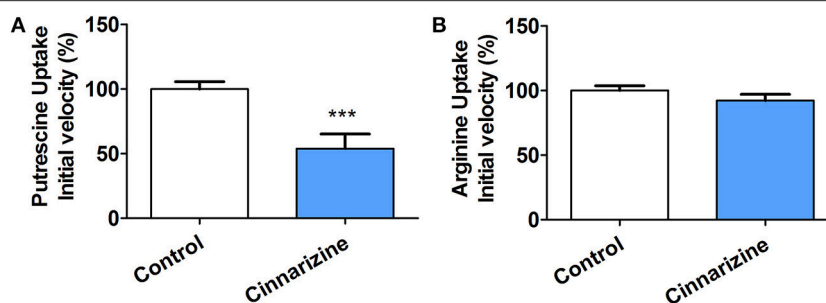


FIGURE 9 | Effect of 50 μ M cinnarizine and clofazimine on putrescine (A) and arginine (B) uptake in *T. cruzi* epimastigotes. Values are expressed as % mean \pm SD in comparison with control. Statistical analysis was performed by one-way ANOVA test followed by a *post-hoc* Dunnett's multiple comparison test ($***p < 0.005$).

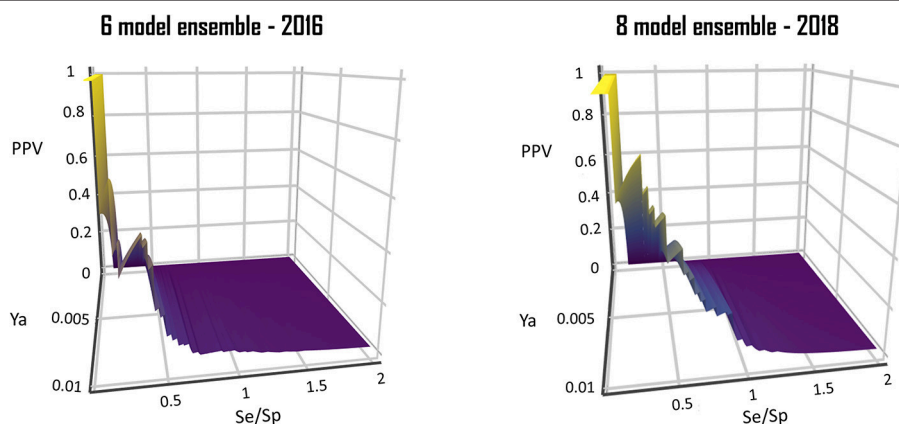


FIGURE 10 | Comparison of the PPV surface of the 8-model ensemble of classifiers reported here with that of the 6-model ensemble reported back in 2016.

AUROC tends to fall sharply when progressing from the training set to the DUD-E database. In fact, whereas an astonishing 82% of the individual models achieved remarkable AUROCs (above 0.8) when confronted to the training set, the percentage of individual models that obtains such achievement against the DUD-E falls to only 25%.

Echoing previous studies, though, the ensemble learning approximation led to more robust results, improving accuracy in the predictions and generalization (which, in our case, is reflected by an improved behavior on the test set and the DUD-E database).

Do We Have Good Repurposed Candidates?

Despite two out of four hits did not confirm inhibitory effects on putrescine uptake, all of them did confirm their trypanocidal effects using concentrations in the low μ M range. However, does this mean that they are good candidates for drug repurposing?

Not necessarily. Cinnarizine, meclizine, and butoconazole all belong to therapeutic classes that have shown potential as antichagasic therapies in the past: calcium channel blockers (Engel et al., 2010; Benaim and Paniz Mondolfi, 2012; Planer et al., 2014), antihistaminic drugs (Engel et al., 2010; Planer et al., 2014; Lara-Ramirez et al., 2017) and antifungals (Lepesheva et al., 2011).

Butoconazole, however, is not a straightforward candidate for repositioning, since it is only used topically as antifungal. Accordingly, most of the advantages of drug repurposing will be lost if the second indication (in this case, Chagas' disease chemotherapy) requires systemic administration (Oprea and Overington, 2015). Furthermore, our experimental evidence of cytotoxic activity discourages further investigation. The advantages of drug repositioning will also be mostly lost if the dose required for the second indication is above the dose range clinically used for the original one (Oprea and Overington, 2015), as would probably be the case for cinnarizine and meclizine, which are currently administered in low daily doses. This is especially true in the case of cinnarizine, which showed only weak activity against the clinically relevant forms of *T. cruzi*. The scenario is further complicated by the fact that free drug exposure will be diminished by plasma protein binding: in the case of cinnarizine, for instance, around 90% of the drug in plasma is bound to plasma proteins.

The previous analysis does not imply that is impossible to efficaciously repurpose meclizine (which showed a very interesting effect against amastigotes, inhibiting 75% growth at only 5 μ M concentration) or that both cinnarizine and meclizine are not useful as starting points for hit-to-lead programs but, in any case, many of the advantages of the strategy (i.e., bypassing some preclinical and clinical studies) will probably be lost.

CONCLUSIONS

A cascade virtual screening approach comprising an ensemble of ligand-based classifiers and structure-based screening has been applied, identifying two new inhibitors of putrescine uptake in *T. cruzi* and reporting, for the first time, the trypanocidal effects of butoconazole (and antifungal) and cinnarizine and meclizine, two antihistaminic agents of the diphenylmethylpiperazine group commonly used to treat motion sickness and balance disorders. Interestingly, neither cinnarizine nor clofazimine modified arginine uptake by another member of the putative amino acid transporter (TcPAT) family.

This is, to our knowledge, the first report implementing PPV surface analysis to select the score value to be applied in a virtual screening campaign.

ETHICS STATEMENT

All animal procedures were approved by institutional regulations of the Committee for the Care and Use of Laboratory Animals of the Universidad de Buenos Aires (Buenos Aires, Argentina) in accordance with government regulations [SENASA, resolution No. RS617/2002, Argentina]. All procedures were performed in accordance with institutional safety procedures.

AUTHOR CONTRIBUTIONS

LA and JM have built and validated (*in silico*) ligand-based models and model ensembles to identify putrescine uptake inhibitors, under the supervision of AT. They later performed the first *in silico* screening step and data analysis related to ligand-based VS. RD and PP have applied structure-based filters

(molecular docking) in the virtual screening campaign. MS, MR, LF, AP, and CM have performed the *in vitro* assays against the different *Trypanosoma cruzi* stages. LA and MR have performed the transport assays. They work in CA and CC labs, under their supervision. LA, MS, CC, CA, PP, and AT have also been actively engaged in manuscript preparation and discussion. All authors took part in the result discussion for the revised version.

FUNDING

Authors thank ANPCyT (PICT 2013-0520) and UNLP (Incentivos X785) for funding their research. All authors hold either permanent positions or fellowships at the Argentinean National Council of Science and Technological Research (CONICET).

ACKNOWLEDGMENTS

All authors but MS hold fellowships or permanent positions at CONICET. Support was received from the National University of La Plata (UNLP) [grant X785], the Agencia Nacional de Promoción Científica y Tecnológica (ANPCyT) [grant PICT2013-0520].

SUPPLEMENTARY MATERIAL

The Supplementary Material for this article can be found online at: <https://www.frontiersin.org/articles/10.3389/fcimb.2018.00173/full#supplementary-material>

Data Sheet S1 | Inactive dataset compounds.

Data Sheet S2 | Active dataset compounds.

REFERENCES

- Alberca, L. N., Sbaraglini, M. L., Balcazar, D., Fraccaroli, L., Carrillo, C., Medeiros, A., et al. (2016). Discovery of novel polyamine analogs with anti-protozoal activity by computer guided drug repositioning. *J. Comput. Aided Mol. Des.* 30, 305–321. doi: 10.1007/s10822-016-9903-6
- Andrews, K. T., Fisher, G., and Skinner-Adams, T. S. (2014). Drug repurposing and human parasitic protozoan diseases. *Int. J. Parasitol. Drugs Drug. Resist.* 4, 95–111. doi: 10.1016/j.ijpddr.2014.02.002
- Bellera, C. L., Balcazar, D. E., Alberca, L., Labriola, C. A., Talevi, A., and Carrillo, C. (2013). Application of computer-aided drug repurposing in the search of new cruzipain inhibitors: discovery of amiodarone and bromocriptine inhibitory effects. *J. Chem. Inf. Model.* 53, 2402–2408. doi: 10.1021/ci400284v
- Bellera, C. L., Sbaraglini, M. L., Balcazar, D. E., Fraccaroli, L., Vanrell, M. C., Casassa, A. F., et al. (2015). High throughput drug repositioning for the discovery of new treatments for Chagas disease. *Mini. Rev. Med. Chem.* 15, 182–193. doi: 10.2174/138955751503150312120208
- Benaim, G., and Paniz Mondolfi, A. E. (2012). The emerging role of amiodarone and dronedarone in Chagas disease. *Nat. Rev. Cardiol.* 9, 605–609. doi: 10.1038/nrcardio.2012.108
- Bermudez, J., Davies, C., Simonazzi, A., Real, J. P., and Palma, S. (2016). Current drug therapy and pharmaceutical challenges for Chagas disease. *Acta Trop.* 156, 1–16. doi: 10.1016/j.actatropica.2015.12.017
- Browne, A. J., Guerra, C. A., Alves, R. V., da Costa, V. M., Wilson, A. L., Pigott, D. M., et al. (2017). The contemporary distribution of *Trypanosoma cruzi* infection in humans, alternative hosts and vectors. *Sci. Data.* 4:170050. doi: 10.1038/sdata.2017.50
- Carbonneau, M. A., Granger, E., Raymond, A. J., and Gagnon, G. (2016). Robust multiple-instance learning ensembles using random subspace instance selection. *Pattern Recogn.* 58, 83–99. doi: 10.1016/j.patcog.2016.03.035
- Carrillo, C., Canepa, G. E., Algranati, I. D., and Pereira, C. A. (2006). Molecular and functional characterization of a spermidine transporter (TcPAT12) from *Trypanosoma cruzi*. *Biochem. Biophys. Res. Commun.* 344, 936–940. doi: 10.1016/j.bbrc.2006.03.215
- Carrillo, C., Cejas, S., González, N. S., and Algranati, I. D. (1999). *Trypanosoma cruzi* epimastigotes lack ornithine decarboxylase but can express a foreign gene encoding this enzyme. *FEBS Lett.* 454, 192–196. doi: 10.1016/S0014-5793(99)00804-2
- Carrillo, C., Cejas, S., Huber, A., González, N. S., and Algranati, I. D. (2003). Lack of arginine decarboxylase in *Trypanosoma cruzi* epimastigotes. *J. Eukaryot. Microbiol.* 50, 312–316. doi: 10.1111/j.1550-7408.2003.tb00141.x
- Colotti, G., and Ilari, A. (2011). Polyamine metabolism in Leishmania: from arginine to trypanothione. *Amino acids* 40, 269–285. doi: 10.1007/s00726-010-0630-3
- Díaz, M. V., Miranda, M. R., Campos-Estrada, C., Reigada, C., Maya, J. D., Pereira, C. A., et al. (2014). Pentamidine exerts *in vitro* and *in vivo* anti *Trypanosoma cruzi* activity and inhibits the polyamine transport in *Trypanosoma cruzi*. *Acta Trop.* 134, 1–9. doi: 10.1016/j.actatropica.2014.02.012
- Dietrich, R. C., Alberca, L. N., Ruiz, D. M., Palestro, P. H., Carrillo, C., and Talevi, A., et al (2018). Identification of cisapride as new inhibitor of putrescine

- uptake in *Trypanosoma cruzi* by combined ligand- and structure-based virtual screening. *Eur. J. Med. Chem.* 149, 22–29. doi: 10.1016/j.ejmech.2018.02.006
- Doak, A. K., Wille, H., Prusiner, S. B., and Shoichet, B. K. (2010). Colloid formation by drugs in simulated intestinal fluid. *J. Med. Chem.* 53, 4259–4265. doi: 10.1021/jm100254w
- Ekins, S., Williams, A. J., Krasowski, M. D., and Freundlich, J. S. (2011). In silico repositioning of approved drugs for rare and neglected diseases. *Drug Discov. Today* 16, 298–310. doi: 10.1016/j.drudis.2011.02.016
- El Habib Daho, M., and Amine Chikh, M. (2015). Combining bootstrapping samples, random subspaces and random forests to build classifiers. *J. Med. Imaging Health Inf.* 5, 539–544. doi: 10.1166/jmihi.2015.1423
- Engel, J., Ang, K. K., Chen, S., Arkin, M. R., McKerrow, J. H., and Doyle, P. S. (2010). Image-based high-throughput drug screening targeting the intracellular stage of *Trypanosoma cruzi*, the agent of Chagas' disease. *Antimicrob. Agents Chemother.* 54, 3326–3334. doi: 10.1128/AAC.01777-09
- Feng, Z., Gilliland, G., Bhat, T. N., Weissig, H., Shindyalov, I. N., Bourne, P. E., et al. (2000). The protein data bank. *Nucleic Acid Res.* 28, 235–242. doi: 10.1093/nar/28.1.235
- Fernández, M., Becco, L., Correia, I., Benítez, J., Piro, O. E., Echeverría, G. A., et al. (2013). Oxidovanadium(IV) and dioxidovanadium(V) complexes of tridentate salicylaldehyde semicarbazones: searching for prospective antitrypanosomal agents. *J. Inorg. Biochem.* 127, 150–160. doi: 10.1016/j.jinorgbio.2013.02.010
- Ferreira, L. G., and Andricopulo, A. D. (2016). Drug repositioning approaches to parasitic diseases: a medicinal chemistry perspective. *Drug Discov. Today* 21, 1699–1710. doi: 10.1016/j.drudis.2016.06.021
- Hasne, M. P., Soysa, R., and Ullman, B. (2016). The *Trypanosoma cruzi* diamine transporter is essential for robust infection of mammalian cells. *PLoS ONE* 11:e0152715. doi: 10.1371/journal.pone.0152715
- World Health Organization (2015). Chagas disease in Latin America: an epidemiological update based on 2010 estimates. *Wkly. Epidemiol.* 90, 33–44.
- Jin, G., and Wong, S. T. (2014). Toward better drug repositioning: prioritizing and integrating existing methods into efficient pipelines. *Drug Discov. Today* 19, 637–644. doi: 10.1016/j.drudis.2013.11.005
- Kaiser, M., Mäser, P., Tadoori, L. P., Ioset, J.-R., and Brun, R. (2015). Antiparasitic activity profiling of approved drugs: a starting point toward drug repositioning. *PLoS ONE* 10:e0135556. doi: 10.1371/journal.pone.0135556
- Klug, D. M., Gelb, M. H., and Pollastri, M. P. (2016). Repurposing strategies for tropical disease drug discovery. *Bioorg. Med. Chem. Lett.* 1, 2569–2576. doi: 10.1016/j.bmcl.2016.03.103
- Lara-Ramírez, E. E., López-Cedillo, J. C., Noguera-Torres, B., Kashif, M., García-Pérez, C., Bocanegra-García, V., et al. (2017). An *in vitro* and *in vivo* evaluation of new potential trans-sialidase inhibitors of *Trypanosoma cruzi* predicted by a computational drug repositioning method. *Eur. J. Med. Chem.* 132, 249–261. doi: 10.1016/j.ejmech.2017.03.063
- Law, V., Knox, C., Djoumbou, Y., Jewison, T., Guo, A. C., Liu, Y., et al. (2014). DrugBank 4.0: shedding new light on drug metabolism. *Nucleic Acids Res.* 42, D1091–1097. doi: 10.1093/nar/gkt1068
- Lepesheva, G. I., Villalta, F., and Waterman, M. R. (2011). Targeting *Trypanosoma cruzi* Sterol 14 α -Demethylase (CYP51). *Adv. Parasitol.* 75, 65–87. doi: 10.1016/B978-0-12-385863-4.00004-6
- Lipinski, C. A., Lombardo, F., Dominy, B. W., and Feeney, P. J. (2001). Experimental and computational approaches to estimate solubility and permeability in drug discovery and development settings. *Adv. Drug. Deliv. Rev.* 46, 3–26. doi: 10.1016/S0169-409X(00)00129-0
- Melo, F., and Sali, A. (2007). Fold assessment for comparative protein structure modeling. *Protein Sci.* 16, 2412–2426. doi: 10.1110/ps.072895107
- Min, S. H. (2016). A genetic algorithm-based heterogeneous random subspace ensemble model for bankruptcy prediction. *Int. J. Appl. Eng. Res.* 11, 2937–2931.
- Miranda, C. G., Solana, M. E., Curto Mde, L., Lammel, E. M., Schijman, A. G., and Alba Soto, C.D. (2015). A flow cytometer-based method to simultaneously assess activity and selectivity of compounds against the intracellular forms of *Trypanosoma cruzi*. *Acta Trop.* 152, 8–16. doi: 10.1016/j.actatropica.2015.08.004
- Monge, A., Arrault, A., Marot, C., and Morin-Allory, L. (2006). Managing, profiling and analyzing a library of 2.6 million compounds gathered from 32 chemical providers. *Mol. Divers.* 10, 389–403. doi: 10.1007/s11030-006-9033-5
- Morillo, C. A., Marin-Neto, J. A., Avezum, A., Sosa-Estani, S., Rassi, A. Jr., Rosas, F., et al. (2015). BENEFIT Investigators. Randomized trial of benznidazole for chronic Chagas' cardiomyopathy. *N. Engl. J. Med.* 373, 1295–1306. doi: 10.1056/NEJMoa1507574
- Mosmann, T. (1983). Rapid colorimetric assay for cellular growth and survival: application to proliferation and cytotoxicity assays. *J. Immunol. Methods* 65, 55–63. doi: 10.1016/0022-1759(83)90303-4
- Müller, S., Coombs, G. H., and Walter, R. D. (2001). Targeting polyamines of parasitic protozoa in chemotherapy. *Trends Parasitol.* 17, 242–249. doi: 10.1016/S1471-4922(01)01908-0
- Mysinger, M. M., Carchia, M., Irwin, J. J., and Shoichet, B. K. (2012). Directory of useful decoys, enhanced (DUD-E): better ligands and decoys for better benchmarking. *J. Med. Chem.* 55, 6582–6594. doi: 10.1021/jm300687e
- Novick, P. A., Ortiz, O. F., Poelman, J., Abdulhay, A. Y., and Pande, V. S. (2013). SWEETLEAD: an *in silico* database of approved drugs, regulated chemicals, and herbal isolates for computer-aided drug discovery. *PLoS ONE* 8:e79568. doi: 10.1371/journal.pone.0079568
- Nunes, M. C., Dones, W., Morillo, C. A., Encina, J. J., and Ribeiro, A. L. (2013). Council on chagas disease of the interamerican society of cardiology. Chagas disease. An overview of clinical and epidemiological aspects. *J. Am. Coll. Cardiol.* 62, 767–776. doi: 10.1016/j.jacc.2013.05.046
- Oprea, T. I., and Overington, J. P. (2015). Computational and practical aspects of drug repositioning. *Drug Repurp. Rescue Reposit.* 1, 28–35. doi: 10.1089/drrr.2014.0009
- Perez-Lamas, C., and Lopez-Bigas, N. (2011). Gitoools: analysis and visualization of genomic data using interactive heat-maps. *PLoS ONE* 6:e19541. doi: 10.1371/journal.pone.0019541
- Planer, J. D., Hulverson, M. A., Arif, J. A., Ranade, R. M., Don, R., and Buckner, F. S. (2014). Synergy testing of FDA-approved drugs identifies potent drug combinations against *Trypanosoma cruzi*. *PLoS Negl. Trop. Dis.* 8:e2977. doi: 10.1371/journal.pntd.0002977
- Rassi, A. Jr., Rassi, A., and Marin-Neto, J. A. (2010). Chagas disease. *Lancet* 375, 1388–1402. doi: 10.1016/S0140-6736(10)60061-X
- Reigada, C., Phanstiel, O., Miranda, M. R., and Pereira, C. A. (2018). Targeting polyamine transport in *Trypanosoma cruzi*. *Eur. J. Med. Chem.* 147, 1–6. doi: 10.1016/j.ejmech.2018.01.083
- Reigada, C., Valera-Vera, E. A., Sayé, M., Errasti, A. E., Avila, C. C., Miranda, M. R., et al. (2017). Trypanocidal effect of isotretinoin through the inhibition of polyamine and amino acid transporters in *Trypanosoma cruzi*. *PLoS Negl. Trop. Dis.* 11:e0005472. doi: 10.1371/journal.pntd.0005472
- Robin, X., Turck, N., Hainard, A., Tiberti, N., Lisacek, F., Sanchez, J. C., et al. (2011). pROC: an open-source package for R and S+ to analyze and compare ROC curves. *BMC Bioinformatics* 12:77. doi: 10.1186/1471-2105-12-77
- Sbaraglini, M. L., Vanrell, M. C., Bellera, C. L., Benaim, G., Carrillo, C., Talevi, A., et al. (2016). Neglected tropical protozoan diseases: drug repositioning as a rational option. *Curr. Top. Med. Chem.* 16, 2201–2222. doi: 10.2174/1568026616666160216154309
- Seguel, V., Castro, L., Reigada, C., Cortes, L., Díaz, M. V., Miranda, M. R., et al. (2016). Pentamidine antagonizes the benznidazole's effect *in vitro*, and lacks of synergy *in vivo*: Implications about the polyamine transport as an anti-*Trypanosoma cruzi* target. *Exp. Parasitol.* 171, 23–32. doi: 10.1016/j.exppara.2016.10.007
- Shen, M. Y., and Sali, A. (2006). Statistical potential for assessment and prediction of protein structures. *Protein Sci.* 15, 2507–2524. doi: 10.1110/ps.062416606
- Soysa, R., Venselaar, H., Poston, J., Ullman, B., and Hasne, M. P. (2013). Structural model of a putrescine-cadaverine permease from *Trypanosoma cruzi* predicts residues vital for transport and ligand binding. *Biochem. J.* 452, 423–432. doi: 10.1042/BJ20130350
- Stanaway, J. D., and Roth, G. (2015). The burden of chagas disease. *Estim. Chall. Glob. Heart.* 10, 139–144. doi: 10.1016/j.jgheart.2015.06.001
- Sykes, M. L., and Avery, V. M. (2013). Approaches to protozoan drug discovery: phenotypic screening. *J. Med. Chem.* 56, 7727–7740. doi: 10.1021/jm4004279
- Toropova, A. P., and Toropov, A. A. (2017). CORAL: binary classifications (active/inactive) for drug-induced liver injury. *Toxicol. Lett.* 268, 51–57. doi: 10.1016/j.toxlet.2017.01.011
- Truchon, J. F., and Bayly, C. L. (2007). Evaluating virtual screening methods: good and bad metrics for the “early recognition” problem. *J. Chem. Inf. Model.* 47, 488–508. doi: 10.1021/ci600426e

- Veber, D. F., Johnson, S. R., Cheng, H. Y., Smith, B. R., Ward, K. W., and Kopple, K. D. (2002). Molecular properties that influence the oral bioavailability of drug candidates. *J. Med. Chem.* 45, 2615–2623. doi: 10.1021/jm020017n
- Ventura-Garcia, L., Roura, M., Pell, C., Posada, E., Gascón, J., Aldasoro, E., et al. (2013). Socio-cultural aspects of chagas disease: a systematic review of qualitative research. *PLoS Negl. Trop. Dis.* 7:e2410. doi: 10.1371/journal.pntd.0002410
- Vyskovsky, R., Schwarz, D., Janousova, E., and Kasperek, T. (2016). “Random subspace ensemble artificial neural networks for first-episode Schizophrenia classification,” in *Proceedings of the 2016 Federated Conference on Computer Science and Information Systems* (Gdansk: FedCSIS), 317–321.
- Webb, B., and Sali, A. (2016). Comparative protein structure modeling using MODELLER. *Curr. Protoc. Bioinform.* 54, 5.6.1–5.6.0. doi: 10.1002/0471250953.bi0506s15
- Zhang, Q., and Muegge, I. (2006). Scaffold hopping through virtual screening using 2D and 3D similarity descriptors: ranking, voting, and consensus scoring. *J. Med. Chem.* 49, 1536–1548. doi: 10.1021/jm050468i
- Zhu, T., Cao, S., Su, P. C., Patel, R., Shah, D., Chokshi, H. B., et al. (2013). Hit identification and optimization in virtual screening: practical recommendations based upon a critical literature analysis. *J. Med. Chem.* 56, 6560–6572. doi: 10.1021/jm301916b

Conflict of Interest Statement: The authors declare that the research was conducted in the absence of any commercial or financial relationships that could be construed as a potential conflict of interest.

Copyright © 2018 Alberca, Sbaraglini, Morales, Dietrich, Ruiz, Pino Martínez, Miranda, Fraccaroli, Alba Soto, Carrillo, Palestro and Talevi. This is an open-access article distributed under the terms of the Creative Commons Attribution License (CC BY). The use, distribution or reproduction in other forums is permitted, provided the original author(s) and the copyright owner are credited and that the original publication in this journal is cited, in accordance with accepted academic practice. No use, distribution or reproduction is permitted which does not comply with these terms.



A Perspective on Thiazolidinone Scaffold Development as a New Therapeutic Strategy for Toxoplasmosis

Cristian Rocha-Roa¹, Diego Molina¹ and Néstor Cardona^{1,2*}

¹ Centre for Biomedical Research CIBM, University of Quindío, Armenia, Colombia, ² Dentistry Faculty, University Antonio Nariño, Armenia, Colombia

OPEN ACCESS

Edited by:

Kamal El Bissati,
University of Chicago, United States

Reviewed by:

Bo Shiun Lai,
The Johns Hopkins University School
of Medicine, United States
Stephen Paul Muench,
University of Leeds, United Kingdom

*Correspondence:

Néstor Cardona
nicardona@uniquindio.edu.co;
nestorcardonape@uniquindio.edu.co

Received: 29 June 2018

Accepted: 26 September 2018

Published: 16 October 2018

Citation:

Rocha-Roa C, Molina D and
Cardona N (2018) A Perspective on
Thiazolidinone Scaffold Development
as a New Therapeutic Strategy for
Toxoplasmosis.
Front. Cell. Infect. Microbiol. 8:360.
doi: 10.3389/fcimb.2018.00360

Toxoplasma gondii is one of the most successful parasites due to its ability to infect a wide variety of warm-blooded animals. It is estimated that one-third of the world's population is latently infected. The generic therapy for toxoplasmosis has been a combination of antifolates such as pyrimethamine or trimethoprim with either sulfadiazine or antibiotics such as clindamycin with a combination with leucovorin to prevent hematologic toxicity. This therapy shows limitations such as drug intolerance, low bioavailability or drug resistance by the parasite. There is a need for the development of new molecules with the capacity to block any stage of the parasite's life cycle in humans or in a different type of hosts. Heterocyclic compounds are promissory drugs due to its reported biological activity; for this reason, thiazolidinone and its derivatives are presented as a new alternative not only for its inhibitory activity against the parasite but also for its high selectivity-level with high therapeutic index. Thiazolidinones are an important scaffold known to be associated with anticancer, antibacterial, antifungal, antiviral, antioxidant, and antidiabetic activities. The molecule possesses an imidazole ring that has been described as an antiprotozoal agent with antiparasitic properties and less toxicity. Thiazolidinone derivatives have been reportedly as building blocks in organic chemistry and as scaffolds for drug discovery. Here we present a perspective of how structural modifications of the thiazolidinone core could generate new compounds with high anti-parasitic effect and less toxic results.

Keywords: Thiazolidinone scaffold, new drug, *Toxoplasma gondii*, toxoplasmosis, *in silico*

INTRODUCTION

To date, pyrimethamine and sulfadiazine with corticosteroids continue to be the gold standard in treating toxoplasmosis (Jasper et al., 2013); this therapy has presented reported cytotoxicity that is minimized using leucovorin, nevertheless, hematologic toxicity is still a problem to overcome. Literature reports show that in encephalitis caused by *Toxoplasma*, 62% of patients presented toxicity and severe side effects (Porter and Sande, 1992), or discontinuation of pyrimethamine-sulfadiazine in a group of patients (Dannemann et al., 1992; Katlama et al., 1996). When cases of allergy to sulfa drugs appear, a replacement with clindamycin can be applied but the efficacy is lower and the toxicity is similar (Katlama et al., 1996). As an alternative, trimethoprim-sulfamethoxazole shows similar effect to pyrimethamine-sulfadiazine (Alday and Doggett, 2017).

For ocular toxoplasmosis, for example, the most frequent chemotherapeutic regime consists of pyrimethamine-sulfadiazine plus corticosteroids; this classical approach may have some risks that depend on patient susceptibility to drug toxicity or allergic reactions (Park and Nam, 2013). Other alternative therapy options are based on the use of atovaquone or azithromycin in combination with pyrimethamine or sulfadiazine but supported by less clinical data and similar rates of patient intolerance (Alday and Doggett, 2017). In general terms, evidence supports the idea that the actual drug regimen used to treat toxoplasmosis could be improved, and the fact that toxicity is the major problem reported strengthens the idea that exploring new pharmaceutical alternatives that would improve the care of patients is feasible.

TOXOPLASMA AND TOXOPLASMOSIS

Toxoplasma gondii is an obligate intracellular protozoan parasite that belongs to the phylum Apicomplexa, it has the ability to infect blood all warmed animals all around the world. Other Apicomplexans medically important such as *Cryptosporidium*, *Babesia*, and *Plasmodium* share biological similarities that make them susceptible to antifolate drugs i.e., pyrimethamine and sulfonamides (Alday and Doggett, 2017). It is estimated that about one-third of the world's population is latently infected with *T. gondii*. The seroprevalence of infection with *T. gondii* is influenced by cultural, hygienic, and nutritional habits, and by climate and environmental conditions (Sroka et al., 2010); with prevalence rates of infection among healthy people ranging from 7.5 to 80% worldwide (Peng et al., 2015).

Toxoplasma gondii presents a complex life cycle with a variety of intermediate hosts. The parasite enters the human mainly by four routes of infection: (i) by consumption of raw or undercooked meat containing viable tissue cysts, (ii) eating food products or drinking water contaminated with oocysts, (iii) transmission of tachyzoites to the fetus through the placenta and (iv) organ transplantation (Peng et al., 2015) or blood transfusion (Alvarado-Esquivel et al., 2018). When acquired via oral, bradyzoites and sporozoites are released from cysts and oocysts invading intestinal cells, thereafter, tachyzoites are differentiated which is the parasite-disseminated form that travels via the blood or lymphatic system to different anatomic regions inducing an acute or chronic infection (Wohlfert et al., 2017).

Host cell invasion is an important event in which three parasite's organelles are mainly involved: micronemes, rhoptries (composed by two different substructures: rhoptry neck and rhoptry bulb) and dense granules. Proteins secreted by these three organelles are crucial in host cell attachment, penetration, and in the formation of the parasitophorous vacuole. Micronemes proteins (MICs) are involved in attachment to the host's membrane receptors. Rhoptries neck proteins (RONs) are released following micronemes to form the moving junction, this structure is important to form the parasitophorous vacuole membrane (PVM) using the host's membrane but without proteins. Then, rhoptries bulb proteins (ROPs) are released within vacuoles to the cytosolic face of PVM. Finally, dense

granules proteins (GRAs) are released into the PVM after invasion (for a complete understanding of MICs, RONs, ROPs, and GRAs function please review J. Laliberté and V. B. Carruthers) (Laliberté and Carruthers, 2008). There are reports that show the importance of proteins involved like ROP18, ROP5, ROP16, and GRA15 in immune modulation depending on the strain type, such as prolonged STAT3/6 activation, reduced IL-12 production, and avoidance of parasite clearance which are related to high virulence in type I strains; non-sustained STAT3/6 activation, high levels of IL-12 and enhanced parasite clearance related to intermediate virulence in type II strains; and prolonged STAT3/6 activation, reduced IL-12 production and enhanced parasite clearance related to low virulence in type III strains (Hunter and Sibley, 2012).

The importance of knowing the bulk of proteins that plays a role as virulence factors or implicated in the host cell invasion process is to have a broad panorama to select potential new drug targets.

Infection with *T. gondii* brings clinical complications such as ocular, neurological and systemic disease mainly in immunocompromised patients and those infected congenitally. Ocular toxoplasmosis is one of the most common causes of posterior uveitis in 20–60% of cases and, in some countries it is one of the most important causes of visual impairment (de-la-Torre et al., 2014). Neurological complications are characteristic of an acquired immunodeficiency syndrome (AIDS) and are one of the causes of CNS mass lesions in AIDS. Cerebral toxoplasmosis is also associated with high mortality and morbidity in patients with states of immunocompromised (Patil et al., 2011). In congenital toxoplasmosis, the infection is acquired during pregnancy and can have devastating consequences in the fetus; in some cases, the infection develops an ocular form that can reactivate depending on different factors (Wallon and Peyron, 2018).

THIAZOLIDINONES CORE ON TOXOPLASMA GONDII AND DRUG ALTERNATIVES

Due to the biological properties of thiazolidinones, this pharmacologic core appears as a good alternative against toxoplasmosis. One of the forms for obtaining the thiazolidinone core arises after the combination of two precursors of which important biological activities are known, hydroxyurea and thiosemicarbazone (Tenório et al., 2005). Hydroxyurea have shown a strong effect on the intracellular elimination of protozoa such as *T. gondii*, *T. cruzi*, and *L. amazonensis* (de Melo et al., 2000). On the other hand, it has been reported that thiosemicarbazones are potential inhibitors of the ribonucleotide reductase enzyme, which is responsible of deoxyribonucleotides synthesis (Liu et al., 1992). The activity of thiosemicarbazones is related to the capacity to chelate metal atoms that are important for the survival of the parasite; this characteristic is also shared with the group arylhydrazones, moiety that has been used for the improvement of the biological activity of the thiazolidinone core (Walcourt et al., 2004). From another point of view, it

could be thought that the fact of gathering structural cores with important biological activities is one of the factors that give the thiazolidinone compounds a broad spectrum of pharmacological activity; for this reason, thiazolidinone core derivatives have become object of study due to its numerous biological activities, becoming a promissory scaffold with pharmaceutical potential and with anti-*Toxoplasma* effects (Kaur Manjal et al., 2017).

The first study to link thiazolidinone compounds with anti-*Toxoplasma* activity was reported by Tenório et al. (2005), who designed a series of substituted thiosemicarbazone compounds in the arylhydrazone moiety with nitro substituents in the *ortho*, *meta* and *para* positions; they also designed a series of thiazolidinones substituted on the nitrogen atom of the 3-position with phenyl, methyl, ethyl and hydrogen groups, in addition, nitrobenzene groups were substituted on the moiety arylhydrazone that is attached to the carbon of the 2-position (Tenório et al., 2005). The 2-position has been described for a long time as one of the most studied and promising positions for the design of drugs based on the thiazolidinone heterocycle (Hamama et al., 2008). In addition, reports of a substitution of the carbon at 5-position for an acetic acid group in the thiazolidinone heterocycle have been made. After *in vitro* experiments, it has been shown that the thiazolidinone derivatives were more efficient on the intracellular elimination of *T. gondii* than the thiosemicarbazone derivatives and hydroxyurea (reference drug), resulting in a lower percentage of infected host cells; the treatment with thiazolidinones resulted in up to 4 intracellular parasites, whereas thiosemicarbazones and hydroxyurea treatment resulted in up to 72 and 186 intracellular parasites, respectively (Tenório et al., 2005). In 2008, de Aquino et al. (2008) continued with the scaffold designed by Tenório et al. (2005); they kept the phenyl group on 3-position, the arylhydrazone group on 2-position and the acetic acid group on 5-position of the thiazolidinone heterocycle. At the same time, they evaluated compounds resulting from the addition of phenyl groups on positions 3 and 4 of the thiosemicarbazone core on the aromatic rings of the arylhydrazone moieties of thiazolidinones and thiosemicarbazones; additions of electron-withdrawing or electron-donating radicals were also evaluated. These modifications resulted in thiazolidinone derivatives that had an effective action on intracellular parasite multiplication, as a consequence, the mean number of normal tachyzoites decreased. The concentration ≤ 0.1 mM of some thiazolidinone derivatives resulted in a 50% inhibition of parasite growth; this concentration is represented in a range of 12.5–30 $\mu\text{g/mL}$. In contrast, effective sulfadiazine concentration in the same *in vitro* conditions was 3 mM. In conclusion, some thiazolidinones reported in this work resulted to be more effective than hydroxyurea at 0.5 mM concentration (de Aquino et al., 2008).

More data of a new series of thiazolidinones and thiosemicarbazones was reported by Carvalho et al. (2010). They kept the arylhydrazone group on the thiosemicarbazones and thiazolidinones and they did not retain the aromatic ring on 3-position of the thiazolidinone core. On the phenyl group of the moiety arylhydrazone they made additions of hydrogen, chlorine, and nitro in the *para* position. The best molecule derivatives were able to drastically decrease the average

number of intracellular parasites, effects that are very promising compared to the pharmacological treatments currently used. In addition, these authors suggest some morphologically effects caused to the intracellular parasites, including the development of a process of vesiculation in the cytoplasm of the *T. gondii* ending up in altering the parasite's cell cycle. This is a first approach to the possible effects of this type of compounds on *T. gondii* (Carvalho et al., 2010).

On the other hand, compounds such as benzinidazole, miconazole, ketoconazole, metronidazole, and others, are currently widely used as therapeutic agents; these have in common the presence of a heterocyclic imidazole ring in its structure, adding up to an extensive list of studies of derivatives with powerful biological activity (Zhang et al., 2014). For this reason, Liesen et al. (2010) mixed the imidazole ring with the core thiosemicarbazide, thiazolidinone, and thiadiazole. In the case of thiazolidinones, the imidazole ring was bound by the region of the hydrazone group. These new compounds were evaluated in Vero cells infected with tachyzoites of *T. gondii*, showing elimination of parasites; the most active compounds were thiosemicarbazide and thiadiazole derivatives at 0.1 mM concentration, while thiazolidinone derivatives showed anti-*Toxoplasma* activity only at 1 mM concentration. Although, the compounds that showed activity on the elimination of intracellular parasites with concentrations of 1 mM are not the best, they can be taken as starting point for further studies in order to improve their activity and reach effective concentrations in the scale of μM and even nM. In this study the majority of the compounds presented high toxicity, and all the compounds evaluated showed drastic changes in the morphology of the parasite as the incubation time passed and also a better activity in comparison with the standard drugs sulfadiazine and hydroxyurea at 10 mM concentration (Liesen et al., 2010).

In another work, Aquino et al. (2011) evaluated the addition of 4-nitrobenzylidene as a new group located in the carbon of 5-position of the thiazolidinone heterocycle and retained the moiety arylhydrazone, in which some substitutions were made in order to explore new pharmacological alternatives with promising anti-proliferative effect of *T. gondii* cultivated *in vitro*; resulting in new thiazolidinone derivatives that showed elimination of parasites in Vero cells at 0.02–0.7 mM concentration and a Mean Lethal Dose (LD_{50}) at >10 mM. These derivatives were most effective compared with the reference drugs hydroxyurea and sulfadiazine, which showed LD_{50} at 1 mM and 8 mM, respectively. Authors report that after drug treatment the tachyzoites showed big morphologic damages prior to complete elimination (Aquino et al., 2011). Alternatively, D'Ascenzio et al. reported a different evaluation in 2014. They evaluated two series of molecules with a total of 74 new thiazolidinone derivatives. The synthesis consisted of the addition of linear, branched, cyclic and heterocyclic carbonyl groups on the hydrazonic nitrogen-1 (moiety coupled to the thiazolidinone core at 2-position). The main difference between the two series was a substitution for a benzyl ring on the nitrogen at 3-position of the thiazolidinone core. The data reported by D'Ascenzio shows therapeutic index values (TI) for thiazolidinone derivatives against *T. gondii*; each compound

was tested for anti-*Toxoplasma* as well as for cytotoxic activity in HFF (human foreskin fibroblast) resulting in compounds with effective concentrations in the micromolar scale ($\leq 10 \mu\text{M}$), equalling and even overcoming the effect and cytotoxicity levels of the control drug trimethoprim. In addition, some of these compounds were able to decrease the attachment and invasion of tachyzoites to the host cells, suggesting an extracellular effect with potent anti-parasitic activity (D'Ascenzio et al., 2014).

In an effort to find new compounds with better effect against *T. gondii* using computational tools, Asadollahi and Mani in 2015 performed a predictive model of Quantitative-Structure-Activity-Relationship (QSAR) using 68 of the molecules reported by D'Ascenzio et al. (2014). The obtained QSAR model was successfully trained for the prediction of therapeutic index values for the new thiazolidinone derivatives used against *T. gondii*. The authors suggest that this model can be used as a complementary tool in the search for new therapeutic agents with anti-*Toxoplasma* activity (Asadollahi-Baboli and Mani-Varnosfaderani, 2015).

Carradori et al. (2017) synthesized and evaluated a series of 33 new compounds derivatives, in which they kept the thiazolidinone core and only different substituent groups varied on the lactate nitrogen of the heterocycle and nitrogen-1 of the moiety hydrazone. These compounds showed better effects compared against sulfadiazine *in vitro* in terms of inhibition of growth, invasion, and replication of *T. gondii*. Carradori et al. suggest that a substitution with a ferrocene group on nitrogen-1 of the moiety hydrazone could be a candidate modification to enhance the effect of the thiazolidinone core since the compounds that presented this group showed high effectiveness against the host cell invasion and the replication of the parasite, also low cytotoxicity; reaching effective concentrations in the micromolar scale. Some compounds showed better values of Median Toxicity (TD_{50}) at $\geq 320 \mu\text{M}$, compared with TD_{50} at $281 \mu\text{M}$ of the reference drug sulfadiazine. The thiazolidinone derivatives reached lower values of IC_{50} at $5 \mu\text{M}$, while the control drug sulfadiazine showed an IC_{50} value of $43 \mu\text{M}$. In addition, these new compounds had a promising effect over attached extracellular *T. gondii* tachyzoites to host cell, as well as the compounds described by D'Ascenzio et al. (2014), converting them into encouraging compounds for an alternative therapy against *Toxoplasma* (Carradori et al., 2017). **Figure 1** summarizes a timeline of all the modifications reported up to 2017 on the thiazolidinone core against *T. gondii*.

Finally, it has been noted that the thiazolidinone core has become a key candidate for the development of drugs with anti-*Toxoplasma* activity. It was also observed that moiety hydrazone was preserved in all studies, which suggests that this moiety is also part of a possible promising scaffold with antiparasitic activity, and recent studies suggest that the presence of moiety hydrazone on the drug would be potentiating its biological activity (Leite et al., 2017; Vargas et al., 2018). It is worth to mention that there are also numerous studies in which the use thiazolidinone-like structural core against *T. gondii* are reported, for example the thiazole core, for which a broad spectrum of biological activity, including anti-*Toxoplasma*, has also been documented (Chimenti et al., 2009; Hencken et al., 2010; McFarland et al., 2016).

IN SILICO APPROACHES FOR RATIONAL DESIGN AND DEVELOPMENT OF DRUGS AGAINST *TOXOPLASMA GONDII*

A good start point to describe the mode of binding of drug-like molecules is to analyze structural crystallizations that present derivatives of the thiazolidinone core in complex with proteins of parasitic origin. For instance, in *Plasmodium malariae* crystallographic reports with thiazolidine derivatives includes the crystal structure of an aspartic protease (PDB:2ANL) (Clemente et al., 2006); in *P. falciparum*, 3 crystallized proteins of the plasmepsin family (PDB: 3QS1, 3FNU, and 3QVI) (Bhaumik et al., 2009, 2011a,b); these aspartic proteases have been described as important for the life cycle of the parasite and also as a strategy to decrease the survival and proliferation of *T. gondii* (Li et al., 2012; Zhao et al., 2017). Another example is *Leishmania major* with a N-myristoyltransferase protein (PDB:5AG4) (Spinks et al., 2015). N-myristoyltransferase as well as palmitoyltransferase, which cause post-translational changes, has been described as keys for invasion, motility, cell morphology, and with a possible role in the formation of daughter cells in *T. gondii* (Foe et al., 2015; Caballero et al., 2016; Brown et al., 2017). However, it should be mentioned that by means of X-ray crystallography and NMR spectroscopy, molecular-targets of drug-like molecules could not be identified. For thiazolidinones target identification in parasites techniques such as enzymatic inhibition assay using recombinant proteins and scintillation proximity assay (Xia et al., 2016) has been used; these type of techniques are part of the so-called direct biochemical methods, since they contemplate the direct interaction between the drug and the purified protein. There are also other methodologies such as genetic interaction manipulation, which are based on the suppression or enhanced expression of the gene of the molecular-target in the cell, which allow generating target hypotheses of drug treatment. Finally, there are computational approaches that are of great help in obtaining a robust understanding of ligand-receptor interactions. These three alternatives are complementary to each other and can give an insight of possible pharmacological targets of thiazolidinones compounds against *T. gondii* (Schenone et al., 2013). Regarding computational approaches, some investigations have explored the possible pharmacodynamics of thiazolidinone derivatives in intracellular parasites, for example, the work by Kumar et al. (2010) and Kaushik et al. (2015) in which they studied proteins such as Lactate dehydrogenase and Enoyl-ACP reductase of *P. falciparum*, respectively, and Cruzain of *Trypanosoma cruzi* (Moreira et al., 2014) using molecular docking techniques to elucidate the energy of interaction of ligand-receptor. In *T. gondii*, such proteins could have homologs that are worth the effort to analyze, as the case of Cruzain that have a functional protein, the cysteine protease Cathepsin L (Huang et al., 2009).

It is worth to mention that the discussed above proteins or those implicated in attachment or invasion to the host cell, like ROPs, RONs, MICs, or GRAs may become candidates for new drug-targets in *T. gondii*, even opening the possibility of a multi-target and multistage effect on the parasite, being this a good approximation of the possible pharmacodynamics and

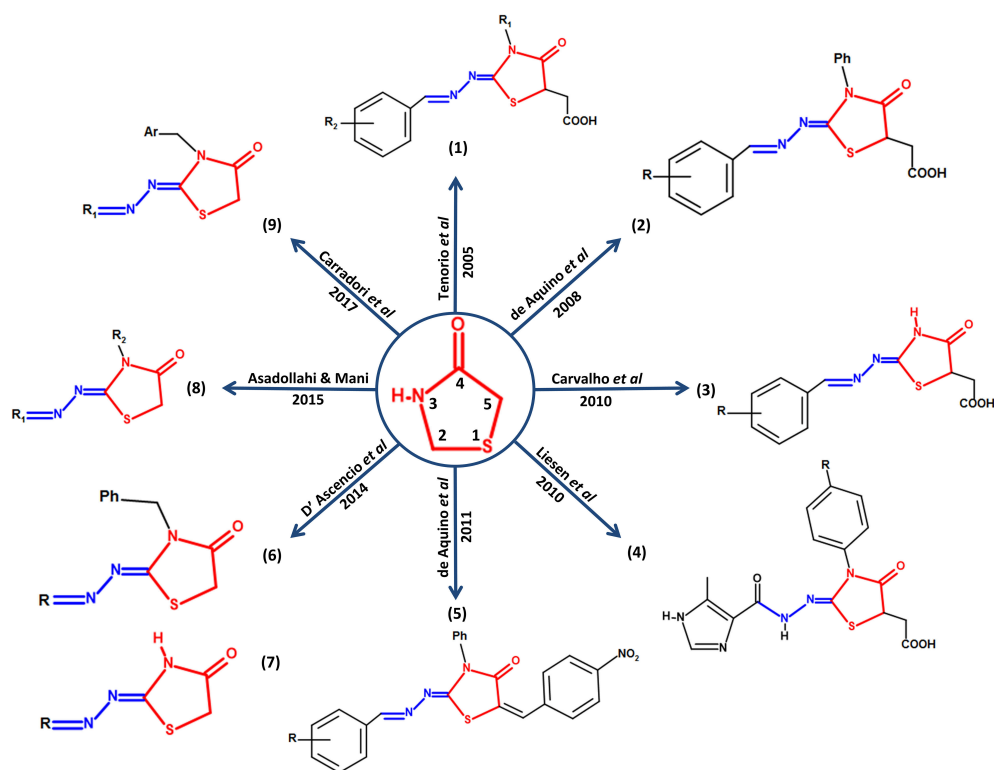


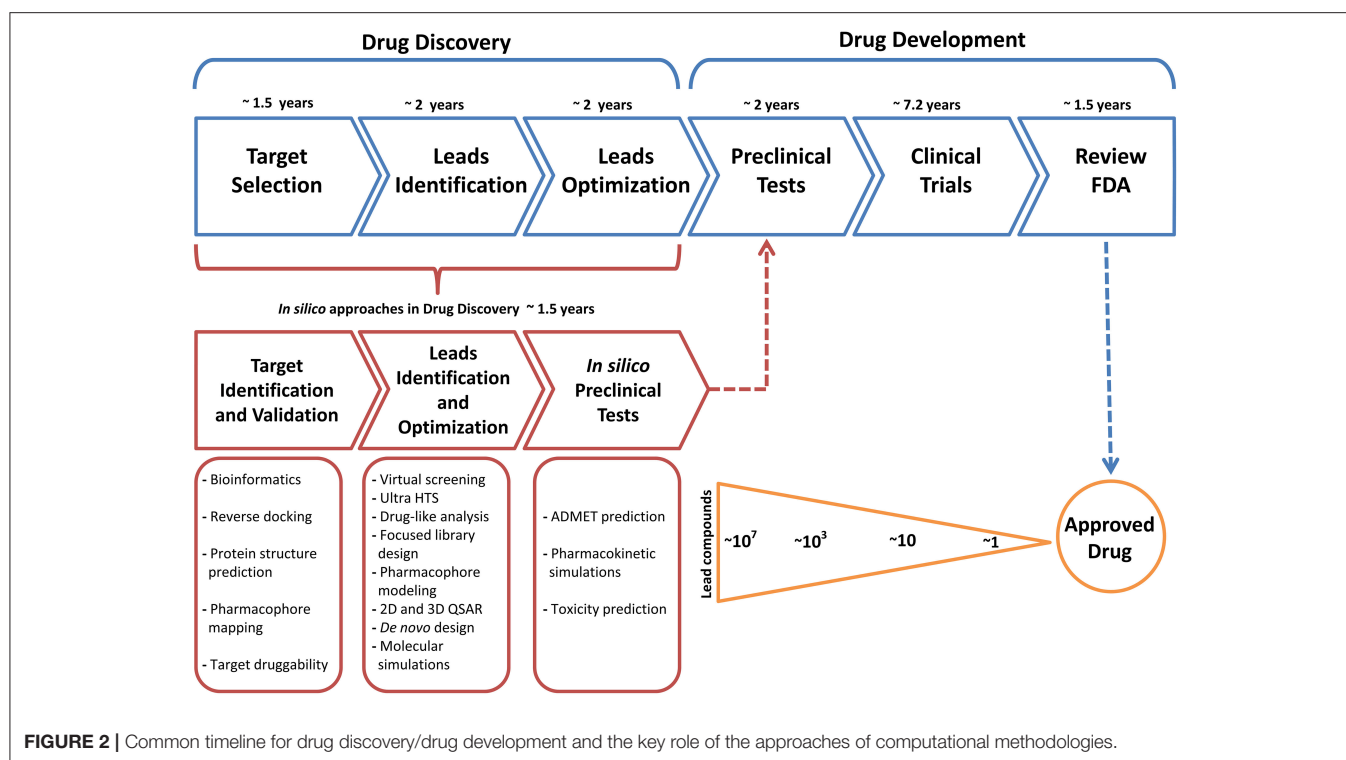
FIGURE 1 | Structural modifications performed on the thiazolidinone core as an alternative for the search of new drugs with possible anti-*Toxoplasma* activity. In the center of the figure, the thiazolidinone core is shown in red with its respective numbering and its conservation around it in all the studies in which they report activity of thiazolidinone derivatives against *T. gondii*. In addition, the structure of moiety hydrazone conserved in position 2 of the heterocyclic thiazolidinone ring is highlighted in blue.

one of the explanations of the potent biological activity of thiazolidinone compounds on *T. gondii*. Traditionally, drugs have been designed and directed to interact with a single target, giving them specificity, but due to current incurable pathologies and drug resistance, it has been clearly seen that in some cases a single target is not an effective treatment, to overcome this, a multi-target effect within the same pathogen is a promising alternative to enhance a pharmacological effect (Ramsay et al., 2018; Sestito et al., 2018).

Recent work in our research group using computational experiments as a first approximation of the pharmacodynamics of thiazolidinone compounds reported by other authors on *T. gondii* (D'Ascenzio et al., 2014; Carradori et al., 2017), suggests a possible preference of these derivatives for kinase proteins, such as TgCDPK1 and especially TgROP18, which has been described as unique and crucial for virulence of the parasite; the compounds caused drastic conformational changes increasing the distance between the catalytic residues, suggesting an inactivation of the kinase activity caused by such changes, these analyses were performed using molecular docking and molecular dynamics simulations (unpublished data).

In general terms, the development path for new molecular and biological entities approved by the FDA requires in average 7 years or more from the start of the clinical trials to

regulatory approval (Kaitin, 2010); additionally, the process of drug discovery before the drug development takes up to 5 years (Figure 2), this initial process can be time improved in terms of time using computational methods as a complementary tools. In recent years, computational methods have played an important role in efforts to obtain effective compounds that can overcome the limitations of current pharmacological treatments for various diseases. Obtaining these bioactive compounds is based on a rational design, where bioinformatics tools are used to provide crucial information to identify and describe a suitable target. A large number of computational tools available provide support to surpass different kinds of problems, for example, if the structure of a target biomolecule such proteins, DNA or RNA are unknown, it can be obtained through molecular modeling techniques like Homology Modeling, which constructs a three-dimensional model by combining the input information and the experimental structures resolved previously (Khan et al., 2016), generally recorded in the Protein Data Bank (<https://www.rcsb.org/>) (Berman et al., 2000). It should be mentioned that in some cases the drug discovery follows two routes: (i) drug design based on the structure (when the structural specific site of the target is known) and (ii) drug design based on the ligand (when starting from a compound lead with known effect and the structure of the receptor is unknown). Both routes generally start with an



extensive number of lead compounds in order to reduce it to a small group of molecules with the desired effect.

Methodologies such as molecular docking simulations accompanied by a High Throughput Screening, QSAR models are usually used. As the number of compounds decreases, more precise and robust tools have to be used, like Quantum Mechanics (QM) simulations, Molecular Mechanics simulations and Hybrid or multi-scale simulations, as Quantum Mechanics/Molecular Mechanics simulations; these techniques allow us to obtain information in greater detail about the mode of interaction of a ligand or about the general behavior of a biological ligand-receptor complex; for example, QM/MM simulations allow the study of enzyme reaction mechanisms, as well as the understanding of electron and structural features that control the reactivity of the molecules. Another type of simulations are so-called Coarse Grained because its main characteristic is the reduction of the number of particles, allowing to simulate bigger biological systems for much longer times, even in the millisecond scale, unlike All Atom simulations (MM simulations) which usually is in the nanosecond and microsecond scale. For more related information about the Multiscale simulations please review the work of Dans et al. (2016). It should be mentioned that the simulated time scale is directly related to the biological phenomenon of interest, for example, protein folding or unfolding, conformational changes by ligand-receptor interaction or protein attachment to plasmatic membranes, etc. (Ou-Yang et al., 2012; Sliwoski et al., 2013; Mohd Hassan et al., 2014).

Based on all the above, a good option to find effective drugs against *Toxoplasma*, would be to identify one of the many

molecular targets of thiazolidinone in *T. gondii* and to use *in silico* approaches to adapt a more specific thiazolidinone derivative that is highly selective for a molecular-target of interest, as in the same mechanism as many kinase inhibitors that work in a specific way despite the similarity among kinases (Ferguson and Gray, 2018).

CONCLUSION

The thiazolidinone scaffold has been showed as a promising drug-like compound against *T. gondii* due to its demonstrated biological effects and the experimental information reported by several authors; these type of data facilitates to propose studies with rational design approaches that can result in new pharmacological alternatives using specific molecular targets from the parasite; in addition, a bulk of evidence show that *in silico* approaches linked with experimental work can result in new workflow schemes that favor the process of design and development of new drugs. The tools of modern drug discovery using experimental and *in silico* techniques have the power to analyze millions of compounds to determine their potential association with a single or multiple target would contribute to improve the activity of obsolete compounds or the generation of new ones, allowing for substantially reduced time and costs for the development and discovery of new drugs. Finally, the better understanding of the mechanism of action of the drug can lead to its improvement, granting specificity to the compound and therefore increasing its effectiveness. These methodologies respond to the call of the rational design of drugs against toxoplasmosis and other pathologies.

AUTHOR CONTRIBUTIONS

DM and NC conceived the idea for the publication; DM, CR-R, and NC prepared the manuscript. All authors read and approved the final manuscript.

REFERENCES

- Alday, P. H., and Doggett, J. S. (2017). Drugs in development for toxoplasmosis: advances, challenges, and current status. *Drug Des. Dev. Ther.* 11, 273–293. doi: 10.2147/DDDT.S60973
- Alvarado-Esquivel, C., Sánchez-Anguiano, L. F., Hernández-Tinoco, J., Ramos-Nevarez, A., Estrada-Martínez, S., Cerrillo-Soto, S. M., et al. (2018). Association between *Toxoplasma gondii* infection and history of blood transfusion: a case-control seroprevalence study. *J. Int. Med. Res.* 46, 1626–1633. doi: 10.1177/0300060518757928
- Aquino, T. M., Nascimento, A. A. P. L., Spacov, I. C. G., Carvalho, C. S., Lima, V. T., Alves, A. Q., et al. (2011). Synthesis, anti-toxoplasma gondii and antimicrobial activities of 2-hydrazolyl-3-phenyl-5-(4-nitrobenzylidene)-4-thiazolidinone substituted derivatives. *Am. J. Pharm.* 30, 1567–1573. Available online at: <https://www3.ufpe.br/posact/images/PDF/1.%20synthesis%20anti-toxoplasma%20gondii%20and%20antimicrobial%20activities%20of%202-hydrazolyl-3-phenyl-5-4-nitrobenzylidene-4-thiazolidinone.pdf>
- Asadollahi-Baboli, M., and Mani-Varnosfaderani, A. (2015). Therapeutic index modeling and predictive QSAR of novel thiazolidin-4-one analogs against *Toxoplasma gondii*. *Eur. J. Pharm. Sci.* 70, 117–124. doi: 10.1016/j.ejps.2015.01.014
- Berman, H. M., Westbrook, J., Feng, Z., Gilliland, G., Bhat, T. N., Weissig, H., et al. (2000). The protein data bank. *Nucleic Acids Res.* 28, 235–242. doi: 10.1093/nar/28.1.235
- Bhaumik, P., Horimoto, Y., Xiao, H., Miura, T., Hidaka, K., Kiso, Y., et al. (2011a). Crystal structures of the free and inhibited forms of plasmepsin I (PMI) from *Plasmodium falciparum*. *J. Struct. Biol.* 175, 73–84. doi: 10.1016/j.jsb.2011.04.009
- Bhaumik, P., Xiao, H., Hidaka, K., Gustchina, A., Kiso, Y., Yada, R. Y., et al. (2011b). Structural insights into the activation and inhibition of histoprotease from *Plasmodium falciparum*. *Biochemistry* 50, 8862–8879. doi: 10.1021/bi201118z
- Bhaumik, P., Xiao, H., Parr, C. L., Kiso, Y., Gustchina, A., Yada, R. Y., et al. (2009). Crystal Structures of the Histo-Aspartic Protease (HAP) from *Plasmodium falciparum*. *J. Mol. Biol.* 388, 520–540. doi: 10.1016/j.jmb.2009.03.011
- Brown, R. W., Sharma, A. I., and Engman, D. M. (2017). Dynamic protein S-palmitoylation mediates parasite life cycle progression and diverse mechanisms of virulence. *Crit. Rev. Biochem. Mol. Biol.* 52, 145–162. doi: 10.1080/10409238.2017.1287161
- Caballero, M. C., Alonso, A. M., Deng, B., Attias, M., de Souza, W., and Corvi, M. M. (2016). Identification of new palmitoylated proteins in *Toxoplasma gondii*. *Biochim. Biophys. Acta* 1864, 400–408. doi: 10.1016/j.bbapap.2016.01.010
- Carradori, S., Secci, D., Bizzarri, B., Chimenti, P., De Monte, C., Guglielmi, P., et al. (2017). Synthesis and biological evaluation of anti- *Toxoplasma gondii* activity of a novel scaffold of thiazolidinone derivatives. *J. Enzyme Inhib. Med. Chem.* 32, 746–758. doi: 10.1080/14756366.2017.1316494
- Carvalho, C. S., Melo E. J., Tenório, R. P., and Góes, A. J. (2010). Anti-parasitic action and elimination of intracellular *Toxoplasma gondii* in the presence of novel thiosemicarbazone and its 4-thiazolidinone derivatives. *Braz. J. Med. Biol. Res.* 43, 139–149. doi: 10.1590/S0100-879X2009005000038
- Chimenti, F., Bizzarri, B., Bolasco, A., Secci, D., Chimenti, P., Carradori, S., et al. (2009). Synthesis and evaluation of 4-acyl-2-thiazolylhydrazones derivatives for anti-*Toxoplasma* efficacy *in vitro*. *J. Med. Chem.* 52, 4574–4577. doi: 10.1021/jm9005862
- Clemente, J. C., Govindasamy, L., Madabushi, A., Fisher, S. Z., Moose, R. E., Yowell, C. A., et al. (2006). Structure of the aspartic protease plasmepsin 4 from the malarial parasite *Plasmodium malariae* bound to an allophenylborstatine-based inhibitor. *Acta Crystallogr. Sect. D Biol. Crystallogr.* 62, 246–252. doi: 10.1107/S0907444905041260
- Dannemann, B., McCutchan, J. A., Israelski, D., Antoniskis, D., Leport, C., Luft, B., et al. (1992). Treatment of toxoplasmic encephalitis in patients with AIDS: a randomized trial comparing pyrimethamine plus clindamycin to pyrimethamine plus sulfadiazine. *Ann. Intern. Med.* 116, 33–43. doi: 10.7326/0003-4819-116-1-33
- Dans, P. D., Walther, J., Gómez, H., and Orozco, M. (2016). Multiscale simulation of DNA. *Curr. Opin. Struct. Biol.* 37, 29–45. doi: 10.1016/j.sbi.2015.11.011
- D'Ascenzio, M., Bizzarri, B., De Monte, C., Carradori, S., Bolasco, A., Secci, D., et al. (2014). Design, synthesis and biological characterization of thiazolidin-4-one derivatives as promising inhibitors of *Toxoplasma gondii*. *Eur. J. Med. Chem.* 86, 17–30. doi: 10.1016/j.ejmech.2014.08.046
- de Aquino, T. M., Liesen, A. P., da Silva, R. E., Lima, V. T., Carvalho, C. S., de Faria, A. R., et al. (2008). Synthesis, anti-*Toxoplasma gondii* and antimicrobial activities of benzaldehyde 4-phenyl-3-thiosemicarbazones and 2-[(phenylmethylene)hydrazono]-4-oxo-3-phenyl-5-thiazolidineacetic acids. *Bioorg. Med. Chem.* 16, 446–456. doi: 10.1016/j.bmc.2007.09.025
- de Melo, E. J., Mayerhoffer, R. O., and de Souza, W. (2000). Hydroxyurea inhibits intracellular *Toxoplasma gondii* multiplication. *FEMS Microbiol. Lett.* 185, 79–82. doi: 10.1111/j.1574-6968.2000.tb09043.x
- de-la-Torre, A., Pfaff, A. W., Grigg, M. E., Villard, O., Candolfi, E., and Gomez-Marin, J. E. (2014). Ocular cytokinome is linked to clinical characteristics in ocular toxoplasmosis. *Cytokine* 68, 23–31. doi: 10.1016/j.cyto.2014.03.005
- Ferguson, F. M., and Gray, N. S. (2018). Kinase inhibitors: the road ahead. *Nat. Rev. Drug Discov.* 17, 353–377. doi: 10.1038/nrd.2018.21
- Foe, I. T., Child, M. A., Majmudar, J. D., Krishnamurthy, S., van der Linden, W. A., Ward, G. E., et al. (2015). Global analysis of palmitoylated proteins in *Toxoplasma gondii*. *Cell Host Microbe* 18, 501–511. doi: 10.1016/j.chom.2015.09.006
- Hamama, W. S., Ismail, M. A., Shaaban, S., and Zoorob, H. H. (2008). Progress in the chemistry of 4- thiazolidinones. *J. Heterocycl. Chem.* 45, 939–956. doi: 10.1002/jhet.5570450401
- Hencken, C. P., Jones-Brando, L., Bordón, C., Stohler, R., Mott, B. T., Yolken, R., et al. (2010). Thiazole, oxadiazole, and carboxamide derivatives of artemisinin are highly selective and potent inhibitors of *Toxoplasma gondii*. *J. Med. Chem.* 53, 3594–3601. doi: 10.1021/jm901857d
- Huang, R., Que, X., Hirata, K., Brinen, L. S., Lee, J. H., Hansell, E., et al. (2009). The cathepsin L of *Toxoplasma gondii* (TgCPL) and its endogenous macromolecular inhibitor, toxostatin. *Mol. Biochem. Parasitol.* 164, 86–94. doi: 10.1016/j.molbiopara.2008.11.012
- Hunter, C. A., and Sibley, L. D. (2012). Modulation of innate immunity by *Toxoplasma gondii* virulence effectors. *Nat. Rev. Microbiol.* 10, 766–778. doi: 10.1038/nrmicro2858
- Jasper, S., Vedula, S. S., John, S. S., Horo, S., Sepah, Y. J., and Nguyen, Q. D. (2013). Corticosteroids as adjuvant therapy for ocular toxoplasmosis. *Cochrane Database Syst. Rev.* 4:CD007417. doi: 10.1002/14651858.CD007417.pub2
- Kaitin, K. I. (2010). Deconstructing the drug development process: the new face of innovation. *Clin. Pharmacol. Ther.* 87, 356–361. doi: 10.1038/clpt.2009.293
- Katlama, C., De Wit, S., O'Doherty, E., Van Glabeke, M., and Clumeck, N. (1996). Pyrimethamine-clindamycin vs. pyrimethamine-sulfadiazine as acute and long-term therapy for toxoplasmic encephalitis in patients with AIDS. *Clin. Infect. Dis.* 22, 268–275.
- Kaur Manjal, S., Kaur, R., Bhatia, R., Kumar, K., Singh, V., Shankar, R., et al. (2017). Synthetic and medicinal perspective of thiazolidinones: a review. *Bioorg. Chem.* 75, 406–423. doi: 10.1016/j.bioorg.2017.10.014
- Kaushik, D., Paliwal, D., and Kumar, A. (2015). 2D QSAR and Molecular docking studies of chloroquine-thiazolidinone derivatives as potential pLDH inhibitors of *Plasmodium falciparum*. *Int. J. Pharmacol. Pharm. Sci.* 2, 42–53.

FUNDING

This work was supported by Colciencias grant 111377757104.

- Available online at: <http://citeseerx.ist.psu.edu/viewdoc/download?doi=10.1.1.736.3692&rep=rep1&type=pdf>
- Khan, F. I., Wei, D. Q., Gu, K. R., Hassan, M. I., and Tabrez, S. (2016). Current updates on computer aided protein modeling and designing. *Int. J. Biol. Macromol.* 85, 48–62. doi: 10.1016/j.ijbiomac.2015.12.072
- Kumar, G., Banerjee, T., Kapoor, N., Surolia, N., and Surolia, A. (2010). SAR and pharmacophore models for the rhodanine inhibitors of *Plasmodium falciparum* enoyl-acyl carrier protein reductase. *IUBMB Life* 62, 204–213. doi: 10.1002/iub.306
- Laliberté, J., and Carruthers, V. B. (2008). Host cell manipulation by the human pathogen *Toxoplasma gondii*. *Cell. Mol. Life Sci.* 65, 1900–1915. doi: 10.1007/s00018-008-7556-x
- Leite, A. C. L., Espíndola, J. W. P., de Oliveira Cardoso, M. V., and de Oliveira Filho, G. B. (2017). Privileged structures in the design of potential drug candidates for neglected diseases. *Curr. Med. Chem.* doi: 10.2174/0929867324666171023163752. [Epub ahead of print]
- Li, H., Child, M. A., and Bogoy, M. (2012). Proteases as regulators of pathogenesis: examples from the Apicomplexa. *Biochim. Biophys. Acta* 1824, 177–185. doi: 10.1016/j.bbapap.2011.06.002
- Liesen, A. P., de Aquino, T. M., Carvalho, C. S., Lima, V. T., de Araújo, J. M., de Lima, J. G., et al. (2010). Synthesis and evaluation of anti-*Toxoplasma gondii* and antimicrobial activities of thiosemicarbazides, 4-thiazolidinones and 1,3,4-thiadiazoles. *Eur. J. Med. Chem.* 45, 3685–3691. doi: 10.1016/j.ejmech.2010.05.017
- Liu, M. C., Lin, T. S., and Sartorelli, A. C. (1992). Synthesis and antitumor activity of amino derivatives of pyridine-2-carboxaldehyde thiosemicarbazone. *J. Med. Chem.* 35, 3672–3677. doi: 10.1021/jm00098a012
- McFarland, M. M., Zach, S. J., Wang, X., Potluri, L. P., Neville, A. J., Vennerstrom, J. L., et al. (2016). Review of experimental compounds demonstrating anti-toxoplasma activity. *Antimicrob. Agents Chemother.* 60, 7017–7034. doi: 10.1128/AAC.01176-16
- Mohd Hassan, K. A., Ahmad, K., Adil, M., Khan, Z. A., Khan, M. I., Lohani, M., et al. (2014). Drug discovery and *in silico* techniques: a mini-review. *Enzym. Eng.* 4, 1–3. doi: 10.4172/2329-6674.1000123
- Moreira, D. R., Leite, A. C., Cardoso, M. V., Srivastava, R. M., Hernandez, M. Z., Rabello, M. M., et al. (2014). Structural design, synthesis and structure-activity relationships of thiazolidinones with enhanced anti-*Trypanosoma cruzi* activity. *ChemMedChem* 9, 177–188. doi: 10.1002/cmdc.2013.00354
- Ou-Yang, S. S., Lu, J. Y., Kong, X. Q., Liang, Z. J., Luo, C., and Jiang, H. (2012). Computational drug discovery. *Acta Pharmacol. Sin.* 33, 1131–1140. doi: 10.1038/aps.2012.109
- Park, Y. H., and Nam, H. W. (2013). Clinical features and treatment of ocular toxoplasmosis. *Korean J. Parasitol.* 51, 393–399. doi: 10.3347/kjp.2013.51.4.393
- Patil, H. V., Patil, V. C., Rajmane, V., and Raje, V. (2011). Successful treatment of cerebral toxoplasmosis with cotrimoxazole. *Indian J. Sex. Transm. Dis.* 32, 44–46. doi: 10.4103/0253-7184.81255
- Peng, H.-J., Tan, F., and Lindsay, D. S. (2015). “Pathogenesis of *Toxoplasma gondii* in Humans,” in *Human Emerging and Re-emerging Infections*, ed. S. K. Singh (Hoboken, NJ: John Wiley & Sons, Inc.), 303–317.
- Porter, S. B., and Sande, M. A. (1992). Toxoplasmosis of the central nervous system in the acquired immunodeficiency syndrome. *N. Engl. J. Med.* 327, 1643–1648. doi: 10.1056/NEJM199212033272306
- Ramsay, R. R., Popovic-Nikolic, M. R., Nikolic, K., Uliassi, E., and Bolognesi, M. L. (2018). A perspective on multi-target drug discovery and design for complex diseases. *Clin. Transl. Med.* 7:3. doi: 10.1186/s40169-017-0181-2
- Schenone, M., Dancik, V., Wagner, B. K., and Clemons, P. A. (2013). Target identification and mechanism of action in chemical biology and drug discovery. *Nat. Chem. Biol.* 9, 232–240. doi: 10.1038/nchembio.1199
- Sestito, S., Runfola, M., Tonelli, M., Chiellini, G., and Rapposelli, S. (2018). New multitarget approaches in the war against glioblastoma: a mini-perspective. *Front. Pharmacol.* 9:874. doi: 10.3389/fphar.2018.00874
- Sliwowski, G., Kothiwale, S., Meiler, J., and Lowe, E. W. (2013). Computational methods in drug discovery. *Pharmacol. Rev.* 66, 334–395. doi: 10.1124/pr.112.007336
- Spinks, D., Smith, V., Thompson, S., Robinson, D. A., Luksch, T., Smith, A., et al. (2015). Development of small-molecule *Trypanosoma brucei* N-Myristoyltransferase inhibitors: discovery and optimisation of a novel binding mode. *ChemMedChem* 10, 1821–1836. doi: 10.1002/cmdc.201500301
- Sroka, S., Bartelheimer, N., Winter, A., Heukelbach, J., Ariza, L., Ribeiro, H., et al. (2010). Prevalence and risk factors of toxoplasmosis among pregnant women in Fortaleza, Northeastern Brazil. *Am. J. Trop. Med. Hyg.* 83, 528–533. doi: 10.4269/ajtmh.2010.10-0082
- Tenório, R. P., Carvalho, C. S., Pessanha, C. S., de Lima, J. G., de Faria, A. R., Alves, A. J., et al. (2005). Synthesis of thiosemicarbazone and 4-thiazolidinone derivatives and their *in vitro* anti-*Toxoplasma gondii* activity. *Bioorg. Med. Chem. Lett.* 15, 2575–2578. doi: 10.1016/j.bmcl.2005.03.048
- Vargas, E., Echeverri, F., Upegui, Y. A., Robledo, S. M., and Quiñones, W. (2018). Hydrazone derivatives enhance antileishmanial activity of thiochroman-4-ones. *Molecules* 23:E70. doi: 10.3390/molecules23010070
- Walcourt, A., Loyevsky, M., Lovejoy, D. B., Gordeuk, V. R., and Richardson, D. R. (2004). Novel aroylhydrazone and thiosemicarbazone iron chelators with anti-malarial activity against chloroquine-resistant and -sensitive parasites. *Int. J. Biochem. Cell Biol.* 36, 401–407. doi: 10.1016/S1357-2725(03)00248-6
- Wallon, M., and Peyron, F. (2018). Congenital toxoplasmosis: a plea for a neglected disease. *Pathogens* 7:25. doi: 10.3390/pathogens7010025
- Wohlfert, E. A., Blader, I. J., and Wilson, E. H. (2017). Brains and brawn: toxoplasma infections of the central nervous system and skeletal muscle. *Trends Parasitol.* 33, 519–531. doi: 10.1016/j.pt.2017.04.001
- Xia, L., de Vries, H., IJzerman, A. P., and Heitman, L. H. (2016). Scintillation proximity assay (SPA) as a new approach to determine a ligand's kinetic profile. A case in point for the adenosine A1 receptor. *Purinergic Signal.* 12, 115–126. doi: 10.1007/s11302-015-9485-0
- Zhang, L., Peng, X. M., Damu, G. L., Geng, R. X., and Zhou, C. H. (2014). Comprehensive review in current developments of imidazole-based medicinal chemistry. *Med. Res. Rev.* 34, 340–437. doi: 10.1002/med.21290
- Zhao, G., Song, X., Kong, X., Zhang, N., Qu, S., Zhu, W., et al. (2017). Immunization with *Toxoplasma gondii* aspartic protease 3 increases survival time of infected mice. *Acta Trop.* 171, 17–23. doi: 10.1016/j.actatropica.2017.02.030

Conflict of Interest Statement: The authors declare that the research was conducted in the absence of any commercial or financial relationships that could be construed as a potential conflict of interest.

Copyright © 2018 Rocha-Roa, Molina and Cardona. This is an open-access article distributed under the terms of the Creative Commons Attribution License (CC BY). The use, distribution or reproduction in other forums is permitted, provided the original author(s) and the copyright owner(s) are credited and that the original publication in this journal is cited, in accordance with accepted academic practice. No use, distribution or reproduction is permitted which does not comply with these terms.



Discovery and Genetic Validation of Chemotherapeutic Targets for Chagas' Disease

Juan Felipe Osorio-Méndez^{1,2*} and Ana María Cevallos^{3†}

¹ Laboratorio de Microbiología y Biología Molecular, Programa de Medicina, Corporación Universitaria Empresarial Alexander von Humboldt, Armenia, Colombia, ² Grupo de Estudio en Parasitología Molecular, Centro de Investigaciones Biomédicas, Universidad del Quindío, Armenia, Colombia, ³ Departamento de Biología Molecular y Biotecnología, Instituto de Investigaciones Biomédicas, Universidad Nacional Autónoma de México, Mexico City, Mexico

OPEN ACCESS

Edited by:

Kamal El Bissati,
University of Chicago, United States

Reviewed by:

Amanda J. Brinkworth,
Washington State University,
United States
Eva Gluenz,
University of Oxford, United Kingdom

*Correspondence:

Juan Felipe Osorio-Méndez
juanfelipe84@gmail.com

†These authors have contributed
equally to this work

Specialty section:

This article was submitted to
Clinical Microbiology,
a section of the journal
Frontiers in Cellular and Infection
Microbiology

Received: 01 July 2018

Accepted: 10 December 2018

Published: 07 January 2019

Citation:

Osorio-Méndez JF and Cevallos AM
(2019) Discovery and Genetic
Validation of Chemotherapeutic
Targets for Chagas' Disease.
Front. Cell. Infect. Microbiol. 8:439.
doi: 10.3389/fcimb.2018.00439

There is an urgent need to develop new treatments for Chagas' disease. To identify drug targets, it is important to understand the basic biology of *Trypanosoma cruzi*, in particular with respect to the biological pathways or proteins that are essential for its survival within the host. This review provides a streamlined approach for identifying drug targets using freely available chemogenetic databases and outlines the relevant characteristics of an ideal chemotherapeutic target. Among those are their essentiality, druggability, availability of structural information, and selectivity. At the moment only 16 genes have been found as essential by gene disruption in *T. cruzi*. At the TDR Targets database, a chemogenomics resource for neglected diseases, information about published structures for these genes was only found for three of these genes, and annotation of validated inhibitors was found in two. These inhibitors have activity against the parasitic stages present in the host. We then analyzed three of the pathways that are considered promising in the search for new targets: (1) Ergosterol biosynthesis, (2) Resistance to oxidative stress, (3) Synthesis of surface glycoconjugates. We have annotated all the genes that participate in them, identified those that are considered as druggable, and incorporated evidence from either *Trypanosoma brucei*, and *Leishmania* spp. that supports the hypothesis that these pathways are essential for *T. cruzi* survival.

Keywords: *Trypanosoma cruzi*, chagas disease, chemotherapeutics, drug discovery, drug validation

INTRODUCTION

Chagas' disease, leishmaniasis, and human African trypanosomiasis are the three main parasitic diseases caused by flagellated protists of the order Kinetoplastida. Chagas' disease is caused by *Trypanosoma cruzi*, and is considered as one of the most prevalent parasitic diseases worldwide. Chagas' disease is present mainly in rural and peri-urban areas of Latin America, although migration has expanded its distribution to non-endemic countries. *T. cruzi* is a parasite that infect multiple species of triatomine hematophagous bugs and several mammalian hosts, including humans. At least four stages have been recognized during the *T. cruzi* life cycle: epimastigotes, amastigotes and metacyclic, and bloodstream trypomastigotes (Tyler and Engman, 2001). Epimastigotes replicate extracellularly in the gut of the insect vector, where they differentiate into non-replicative and highly infective metacyclic trypomastigotes. Parasites at this stage are delivered by the feces of triatomines during a blood meal from a mammalian host, and reach the

mucosa or the bloodstream through a vulnerable region of the skin. There, the parasite invades nucleated cells and differentiates into the amastigote stage, which replicates inside the cytoplasm of the host cell. Then, the parasite egress from the host cells as bloodstream trypomastigotes that may invade additional cells to proliferate to other tissues or be transmitted to a new triatomine vector. Other modes of transmission to the human include congenital and oral infection, and blood transfusion or organ transplantation from infected donors. In humans, the infection starts with an acute phase that lasts 4–8 weeks. The host's immune response typically control the parasite replication, but is not capable of clearing the infection. This leads to the chronic phase of the disease, in which the parasite persists intracellularly mainly in the heart, skeletal muscles, and gastrointestinal tissues. Around 30% of the chronically infected people develop serious cardiac alterations, and up to 10% suffer neurological, digestive, or mixed disorders (Nagajyothi et al., 2012). The mechanisms involved in parasite persistence are not known. However, recently it has been suggested that a form of “dormant” amastigotes may be involved (Sánchez-Valdéz et al., 2018).

The efficacy of the two chemotherapeutic agents of current use (nifurtimox and benznidazole) for the treatment of Chagas' disease is highly variable and often limited, especially during the chronic phase of the infection (Urbina, 2010). Both drugs require long periods of administration and have significant side effects that frequently force the physician to stop treatment (Castro et al., 2006). Furthermore, resistant strains have also been reported (Filardi and Brener, 1987; Bern, 2011). Most significantly, the recently identified dormant forms of the parasite were resistant to extended drug treatment *in vivo* and *in vitro* and remain able to re-establish infection after as many as 30 days of drug exposure (Sánchez-Valdéz et al., 2018). Thus, there is an urgent need to develop new treatments that are safe and of low cost. In this work, we discuss the characteristics required for a drug target to be useful and review the candidate genes and pathways that have been genetically or pharmacologically validated as essential and druggable in *T. cruzi* and incorporate the data that is available from *T. brucei* and *Leishmania* spp.

IDENTIFICATION OF NEW TREATMENTS FOR CHAGAS' DISEASE

The first stage for the discovery or repurposing of antimicrobial agents is target identification. It usually involves the screening of collections of compounds against a molecular target, typically an enzyme (target-based screening), or against whole organisms (cell-based or phenotypic screening). All candidates must then be refined through a cyclic process of structure modifications, until they achieve significant activity, typically in an animal model of infection. Subsequently, the biological activity, pharmacokinetics, and safety profile of the series are optimized by a process that leads to the selection of candidate drugs. Selected drugs are then submitted to a process of regulatory toxicology and scale-up that enables their evaluation in human studies (De Rycker et al., 2018). Unfortunately, the probability of a drug entering the clinical testing phase and its

eventual approval is only about 12%, with an estimated out-of-pocket cost per approved new compound of US \$ 1,395 million (DiMasi et al., 2016). Because of the cost of development of new drugs, the relatively limited target population and the economic power of the countries where Chagas' disease is endemic, the majority of pharmaceutical companies have shown little interest in the development of new drugs for the treatment of parasitic diseases (Tarleton, 2016). In the absence of adequate funding it is vital to design research projects that take advantage of available biological, bioinformatic, structural, and chemical data that is being incorporated in large publicly available databases.

It has been recognized that to obtain a successful new treatment it is important to understand, from the outset, the essential attributes (target product profile) required for a specific drug to be a clinically successful product and substantially better than the existing therapies (Wyatt et al., 2011). The ideal target product profile for Chagas' disease was defined as a drug that is effective in both acute and chronic disease, that it is active against all strains and at all ages, with a clinical efficacy superior to benznidazole (Chatelain, 2015). It should be administered orally (once a day for 30 days) and require no clinical evaluation, laboratory testing nor need for electrocardiograms during treatment. It should not have any contraindications or interactions with other drugs and lack genotoxicity, teratogenicity, inotropic effect, and proarrhythmic potential. There are many challenges to achieve such goals, including the selection of the chemical compounds and the suitability of the chosen target. To help in this goal, criteria for the selection of suitable targets have been suggested (Wyatt et al., 2011). Among them are essentiality, druggability, available structural information, and selectivity over the host's orthologs. Here, we discuss bioinformatic and experimental strategies to identify and validate chemotherapeutic targets based on them.

Essentiality

Essentiality refers to genetic and chemical evidence that the target is indispensable for growth or survival. Ideally, proteins that are essential for survival in the parasite stages present in the host should be selected. To validate them is necessary to demonstrate that the disruption or deletion of such genes causes cell death. In trypanosomatids, studies on the essential role of genes for cell viability are usually conducted in *T. brucei*. This species have a RNA interference (RNAi) system that is widely used to generate gene knock-downs in an inducible manner. The induction of the RNAi against an essential gene product leads to cell death, and thus to a rapid inhibition of cell proliferation. In *T. brucei* this strategy is so efficient that has even been used for a genome-scale screening for essential genes (Alsford et al., 2011). *T. cruzi* lacks a functional RNAi pathway (Kolev et al., 2011), so it cannot be used. An alternative would be extrapolate the huge amount of information obtained in *T. brucei* to *T. cruzi*. However, this is not possible when a given gene of *T. cruzi* has not an orthologous counterpart in *T. brucei*. Also, essentiality may depend on the species or on the developmental stage of the parasite. As an example, in *T. brucei*, a highly conserved protein such as actin is essential in the vertebrate

bloodstream stage but not in the insect procyclic stage (García-Salcedo et al., 2004). Thus, essentiality must be evaluated for each species and at the relevant developmental stages of the parasite. In *T. cruzi*, this has only been accomplished by gene knock-out in epimastigotes, the insect stage of the parasite (see Burle-Caldas et al., 2015 for a review). In this strategy, the endogenous copy of the gene is replaced by a selectable marker using homologous recombination. To evaluate other parasite stages it is necessary to differentiate transgenic epimastigotes or infect cells or animal models with the transformed parasites. There are several limitations with this approach. When there is more than one copy of the gene, several replacements are required to obtain null-mutants. Thus, the essentiality of multicopy genes or those within multigenic families is difficult to evaluate. On the other hand, deletion of essential genes often leads to unviable cells, so null-mutants cannot be selected to analyze the resulting phenotypes. *T. cruzi* is a diploid organism, and in some circumstances only a single copy of an essential gene may be needed (haplosufficiency), with the heterozygote displaying an instructive phenotype. However, when this is intolerable, an inducible, or transient copy of the gene has to be introduced before the gene replacement (Jones et al., 2018). As a reflection of these difficulties, only 16 *T. cruzi* genes have been shown to be essential in reverse genetic experiments (Table 1). An alternative to the mentioned traditional methods to evaluate essentiality is the use of inducible approaches such as Di-Cre or the DHFR degradation domain, or genome edition tools such as CRISPR-Cas9 or Zinc-finger endonucleases. These systems have been adapted to *T. cruzi* in the last 5 years (Kangussu-Marcolino et al., 2014; Peng et al., 2014; Lander et al., 2015; Ma et al., 2015; Burle-Caldas et al., 2017), although recent work has focused on the optimization of different CRISPR-Cas9 configurations (e.g., Beneke et al., 2017; Lander et al., 2017; Soares Medeiros et al., 2017; Burle-Caldas et al., 2018; Costa et al., 2018). The future widespread use of CRISPR-Cas9 will help overcome the current technical limitations for the genetic manipulation of *T. cruzi*. It will allow the rapid evaluation of phenotypes resulting from the disruption of essential genes in different stages of the parasite, including those expressed as multicopy genes and within multigenic families.

Selectivity

Selectivity depends on the target not being either present in the host, or being highly modified or not essential for its survival. High affinity and selectivity are two of the characteristics of a drug for its target that are routinely sought in the search of new therapies. Selectivity can be difficult to achieve, especially for targets that belong to large families of structurally and functionally related proteins. Therefore, targets that are present in the parasite and not in the host would be preferred. If a homolog is present in humans, targets that differ the most would be favored. In general, selectivity can be improved during drug optimization by modifying the compound improving its affinity toward the parasite target to a higher extent than it does to the human homolog (Kawasaki and Freire, 2011). To achieve this, it is necessary to have structural information of both parasitic and human proteins. At October 2018 there are 286 *T. cruzi*

structures deposited at the Protein Data Bank (<https://www.rcsb.org/>). Nearly half of them correspond to only six proteins that are considered as promising drug targets: 58 of Dihydroorotate dehydrogenase, 26 of Cruzain, 21 of Lanosterol 14- α -demethylase, 10 of Dihydrofolate reductase-thymidylate, 15 of Farnesyl diphosphate synthase, and 6 of Squalene synthase. Thus, structural information of other *T. cruzi* proteins is urgently needed.

Druggability

Druggability describes the ability of a protein to bind a drug-like molecule, which in turn modulates its function in a desired way. Druggable proteins should have a well-defined pocket with suitable physicochemical attributes to allow drug binding-sites prediction (Sosa et al., 2018). The druggability of a target is usually estimated by comparing it with homologs in other organisms that have been successfully targeted with specific drugs. Another way to assess druggability is by the development of mathematical algorithms that use structural information about a protein's binding site to estimate its potential as a target. Several databases that contain such information are freely available. Two of the databases that estimate the druggability for *T. cruzi* proteins are: TDR Targets (Magariños et al., 2012, <http://tdrtargets.org/>) and Target-Pathogen database (Sosa et al., 2018, <http://target.sbg.qb.fcen.uba.ar/patho/>). TDR stands for Tropical Disease Research, and it is part of a special program within the World Health Organization that include several tropical pathogens. The database gathers information from multiple sources and published studies including essentiality, functional, and structural information, pathway classification, and information of compounds used to target them. Target-Pathogen database was designed and developed to integrate and give specific weight to protein information (e.g., function, metabolic role, druggability, and essentiality) to facilitate not only the identification of candidate drug targets in pathogens, but also its prioritization. The algorithms employed by both databases are different and therefore discrepancies in the results are likely. The druggability index in both databases is measured in a scale that goes from 0 to 1 and divided into four categories: non druggable (≤ 0.2), poorly druggable (0.2–0.5), druggable (0.5–0.7), and highly druggable (> 0.7) (Sosa et al., 2018).

TRITRYPDB AS A TOOL FOR TARGET SELECTION

TriTrypDB (<http://tritrypdb.org>) is an integrated genomic and functional genomic database for pathogens of the family Trypanosomatidae, including organisms in both *Leishmania* and *Trypanosoma* genera. TriTrypDB is the result of continuous collaborative efforts between EuPathDB, GeneDB, and the Seattle Biomedical Research Institute (Aurrecoechea et al., 2017; Warrenfeltz et al., 2018). EuPathDB release 40 (<https://eupathdb.org/eupathdb/>) contains information about 330 genomes of 321 species that include eukaryotic parasites, relevant free-living non-parasitic organisms and selected pathogen hosts. The current version of the *T. cruzi* CL Brener genome, that was the first

TABLE 1 | List of published essential *T. cruzi* genes as identified by Jones et al. (2018).

Criteria of essentiality ^a	Gene	Protein	Biological process	Druggability score		Structure TDR	Inhibitors TDR
				TP ^d	TDR ^d		
Failed 2KO recombination	TcCLB.503527.40	<i>GPI10</i>	GPI alpha-mannosyltransferase III			✗	✗
	TcCLB.511481.40	<i>GPI12</i>	N-Acetyl-D-glucosaminylphosphatidylinositol de-N-acetylase	0.302	N.D.	✗	✗
	TcCLB.503419.30	<i>TC52</i>	Thioredoxin-glutaredoxin like	0.881	N.D.	✗	✗
	TcCLB.507091.40	<i>DHOD</i>	Dihydroorotate dehydrogenase	0.758	N.D.	✗	✗
	TcCLB.506811.190	<i>GALE</i>	UDP-glucose 4'-epimerase	0.238	0.1	✗	✗
	TcCLB.509153.90	<i>DHFR-TS</i>	Dihydrofolate reductase—thymidylate synthase	0.715	0.8	✓ ^e	✓ ^f
	TcCLB.507547.40	<i>ECH1</i>	Enoyl-coenzyme A (CoA) hydratase 1	0.459	N.D.	✗	✗
	TcCLB.508319.40	<i>SUB2</i> ^b	RNA helicase DEAD-box protein	0.270	N.D.	✗	✗
	TcCLB.511277.450	<i>GPI8</i>	Cysteine peptidase, Clan CD, family C13, putative	Not found	N.D.	✗	✓ ^f
	TcCLB.509011.40	<i>CRT</i>	Calreticulin	0.000	N.D.	✓ ^e	✗
	TcCLB.509461.90	<i>IP3R</i> ^b	Inositol 1,4,5-trisphosphate receptors	0.875	0.7	✗	✗
	TcCLB.510821.50	<i>RPA2</i>	Replication protein A	Not found	N.D.	✗	✗
	TcCLB.509757.30	<i>STI1</i>	Stress-inducible protein 1	0.719	N.D.	✗	✗
	TcCLB.511283.90	<i>NMT</i>	N-myristoyltransferase	0.753	0.6	✗	✗
2KO recombination + episomal copy							
Failed 2KO CRISPR-CAS9	TcCLB.511353.30	? ^c	Triose-phosphate transporter	0.727	N.D.	✗	✗
1KO CRISPR-CAS9 + Posaconazole S	TcCLB.510101.50	<i>CYP51</i>	Lanosterol 14-alpha-demethylase	0.968	0.8	✓ ^e	✓ ^f

^aCriteria of essentiality: Failed 2KO recombination, double knock out were not obtained by targeted disruption by homologous recombination. 2KO recombination + copy, double knock out was obtained but only in the presence of an episomal copy of the gene; Failed 2KO, the double knock out was not obtained using CRISPR-Cas9, 1 KO CRISPR-Cas9 a single knockout was obtained with increased sensitivity to the specific inhibitor posaconazole.

^bThe Gene ID identified in the Jones et al. (2018) study correspond to an allele for which the complete sequence is not available. The Gene ID for the corresponding haplotype (with complete sequence) is used instead.

^cTcCLB.510821.50 is essential but its characterization as *GALF* is not. *TcGalf* is annotated as UDP-galactopyranose mutase (Oppenheimer et al., 2011), the targeted gene is a putative transporter that has not been characterized.

^dDruggability score: TP-found in the Target-Pathogen Database, TDR-found in the Tropical Disease Research Database. Green numbers indicate proteins classified as highly druggable and red numbers those classified within other categories.

^eStructures identified at the TDR database.

^fInhibitors identified at the TDR database.

N.D. indicates genes are included in the database but are not scored. Not found indicates that the gene has not been included in the database.

sequenced parasite strain (El-Sayed et al., 2005), identifies 21,702 genes. Of them, 13,325 (61%) have a deduced function from its similarity to known genes, and 8,377 (39%) are hypothetical and

are therefore of unknown function. Basic research is needed to understand the function and structure of these genes as they may be essential and druggable. Unfortunately, because at least 50% of

the *T. cruzi* genome corresponds to repetitive sequences, there are DNA sequence fragments that have not been assembled. Because this lack of sequence disrupts bioinformatics algorithms used to identify open reading frames, many genes are annotated as two or more independent open reading frames (863 genes are annotated as fragments). EuPathDB makes it easy to search for biological questions relating to issues such as stage-specific expression, and to compile lists of genes that share multiple characteristics. As the database includes information about the presence of orthologs and paralogues, it can be easily compared not only across data sets but also across organisms.

CANDIDATE GENES THAT HAVE BEEN GENETICALLY VALIDATED AS ESSENTIAL IN *T. CRUZI*

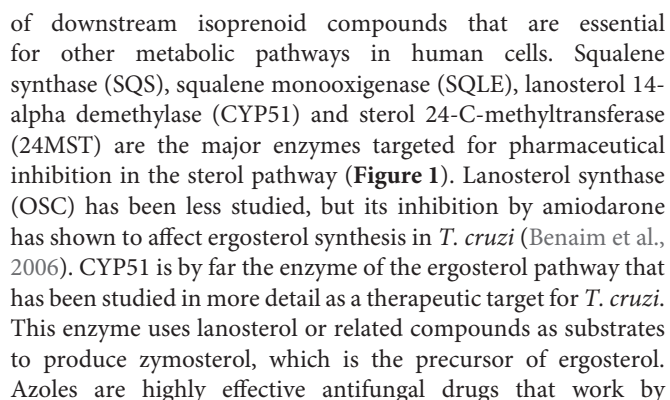
Ideal drug targets should be essential at least in the parasite stages that are present in the host. However, the number of *T. cruzi* genes that have been successfully deleted or disrupted is very small. In a recent review Jones et al. (2018) were able to identify reports where the double knockouts of 20 genes were obtained, demonstrating that these genes were not essential. They also identified papers where the double knockout were not possible to obtain suggesting that the 16 genes studied are essential for epimastigotes (Table 1). We reviewed the available information about these genes to evaluate their potential as drug targets. Based on transcriptomics data available from the TriTrypDB, we found evidence that support the expression of the 16 genes in all stages of the parasite (Li et al., 2016; **Supplementary Figure 1**). Druggability scores were identified in 13 of the 16 genes, with eight of them scored as highly druggable (score >0.7) and five as poorly or non-druggable (score <0.5) (Table 1). Only three of the encoded proteins have available structures. We then selected three biological pathways known to be important for parasite survival: (1) Ergosterol biosynthesis, (2) Resistance to oxidative stress, and (3) Synthesis of surface glyconjugates. We describe the genetic evidence for the essential role for each gene in the pathway in *T. cruzi* or in other trypanosomatid species. We also compare the pathway with its human counterpart in order to identify enzymes whose inhibition might be selective for the parasite. Finally, we describe the chemotherapeutic agents that target each pathway. This information would help identify other points of these pathways that may be chosen for further study. Other aspects of discovery of new treatments for Chagas disease have been recently reviewed in Field et al. (2017); Francisco et al. (2017); Chatelain and Ioset (2018) and Scarim et al. (2018).

Ergosterol Biosynthesis

Sterols are lipids produced by all eukaryotic cells that are essential for several processes, including the organization and function of cell membranes. The sterols being synthesized by an organism may vary according to the taxonomic group (Bloch, 1983). In trypanosomes, the main sterol component of the parasite is ergosterol (reviewed in de Souza and Rodrigues, 2009). In *T. cruzi*, endogenously produced ergosterol is a vital resource for the parasite as it cannot be replaced by sterols

scavenged from the host. Additionally, one of the clinically relevant forms of the parasite (i.e., amastigotes) is particularly sensitive to the pharmacological inhibition of this lipid (Urbina et al., 1996; Liendo et al., 1999). Ergosterol is synthesized through a biosynthetic pathway that is divided into two stages (**Figure 1**): the isoprenoid pathway (from Acetyl-CoA to farnesyl diphosphate) and the sterol pathway (from farnesyl-diphosphate to sterols). Farnesyl diphosphate, which is the last product of the first stage, is also the substrate for enzymes catalyzing the production of ubiquinones (such as Coenzyme Q10), dolichols, heme A, and prenylated proteins. The first committed step for sterol biosynthesis begins with the head-to-head condensation of two molecules of farnesyl diphosphate to produce squalene, a two-step reaction catalyzed by squalene synthase. The complete set of genes encoding for the enzymes involved in both stages have been identified in the *T. cruzi* genome (**Figure 1**). There is only one gene of this pathway whose requirement for the parasite viability has been evaluated in this species (Table 1). In contrast, it has been tested for four of the orthologous genes encoded by *T. brucei*. As expected, silencing of the two first enzymes of the sterol pathway (*TbSQS* and *TbSQLE*) resulted in the depletion of cellular sterol intermediates and end products in procyclic cells (Pérez-Moreno et al., 2012). This was associated with impaired cell growth, aberrant cell morphologies, DNA fragmentation and a profound modification of mitochondrial structure and function. Similarly, silencing of the next enzyme on the pathway (*TbCYP51*) completely stopped growth in procyclic and trypomastigote forms of the parasite (Haubrich et al., 2015; Dauchy et al., 2016). Furthermore, parasites with decreased expression of the enzyme were less virulent for mice (Dauchy et al., 2016). There is also evidence for the importance of CYP51 in the viability of *T. cruzi* and *Leishmania*. In *T. cruzi*, a combination of CRISPR-Cas9 gene edition and pharmacological inhibition of the enzyme produced a concentration-dependent growth decrease in epimastigotes (Soares Medeiros et al., 2017), suggesting that the function CYP51 is essential for the parasite. In *L. donovani*, genes encoding for this enzyme could only be knocked out in the presence of episomal complementation (McCall et al., 2015). *L. major* CYP51-null mutants were viable but had defects in their growth and had hypersensitivity to heat stress (Xu et al., 2014). Finally, inhibition of the last enzyme of the pathway in *T. brucei* (*TbSMT*) showed contradictory evidence regarding its role on parasite growth, as in one study it did decreased it and in the other not (García-Salcedo et al., 2004; Haubrich et al., 2015). The reason for this difference has not been clarified, but it is possibly related with the presence of sterols in the used experimental media that might be used for the parasite to spark cell proliferation.

In contrast with trypanosomes and fungi, human cells produce cholesterol instead ergosterol. For this reason, enzymes from the ergosterol biosynthetic pathway are common targets of inhibitors used to treat fungal infections (**Figure 1**), and some of them have also been tested in trypanosomes. Within the isoprenoid pathway, the HMG-CoA synthase and the farnesyl pyrophosphate synthase are inhibited by statins and biphosphonates, respectively. However, the intervention on this pathway have the disadvantage of affecting the synthesis



inhibiting the activity of CYP51. Several azoles have shown strong anti-*T. cruzi* activity *in vitro* and *in vivo* (Lepesheva et al., 2011), so they have been considered a priority for drug development. The mechanism of action of these compounds against the *T. cruzi* CYP51 has been studied at the structural level (Chen et al., 2010; Lepesheva et al., 2010; Hoekstra et al., 2016). Also, the specificity of inhibition of *T. cruzi*'s CYP51 by posaconazole, a strong anti-fungal azole, has been evaluated using a CRISPR-Cas9 mediated gene edition, which resulted in a 10-fold increase in sensitivity for the drug compared with the wild-type strain (Soares Medeiros et al., 2017). Unfortunately, clinical trials showed that two promising azoles are ineffective to treat chronic Chagas disease in humans. The CHAGASAZOL trial used posaconazole and

ravuconazole monotherapy and failed to obtain a sustained parasite clearance after treatment (Chatelain, 2015). Similarly, the STOP-CHAGAS study showed that benznidazole was superior to posaconazole, either as monotherapy or combined, in obtaining a sustained serological response at 6 months in individuals with asymptomatic *T. cruzi* infection (Morillo et al., 2017). Based on these results, it has been suggested that CYP51 inhibition should no longer be considered as a priority for drug development against *T. cruzi* (Sykes and Avery, 2018). However, azoles such as VNI, VNV, and VT-1161 may not be discarded as feasible candidates as they showed to be safe, and highly efficient, and selective to eradicate *T. cruzi* infections from murine models (Villalta et al., 2013; Lepesheva et al., 2015; Hoekstra et al., 2016; Guedes-da-Silva et al., 2017). A relatively unexplored and promising strategy is the inhibition of the last enzyme of the ergosterol synthesis (*Tc24SMT*) by azasterols (Figure 1). In contrast to other enzymes of the pathway, *Tc24SMT* is absent in humans. *T. cruzi* parasites treated with the 24SMT inhibitors 22,26-azasterol (AZA) and 24(R,S) 25-epiminolanosterol (EIL) showed not detectable levels of 24-alkyl sterols and strongly inhibited parasite growth (Urbina et al., 1996). Interestingly, amastigotes were more susceptible than epimastigotes to these compounds and synergistic antiparasitic effects of AZA and CYP51 inhibitors were observed *in vitro* and in a murine model of acute Chagas disease. Other 24SMT inhibitors have shown effects on epimastigote growth accompanied by severe ultrastructural alterations (Braga et al., 2005).

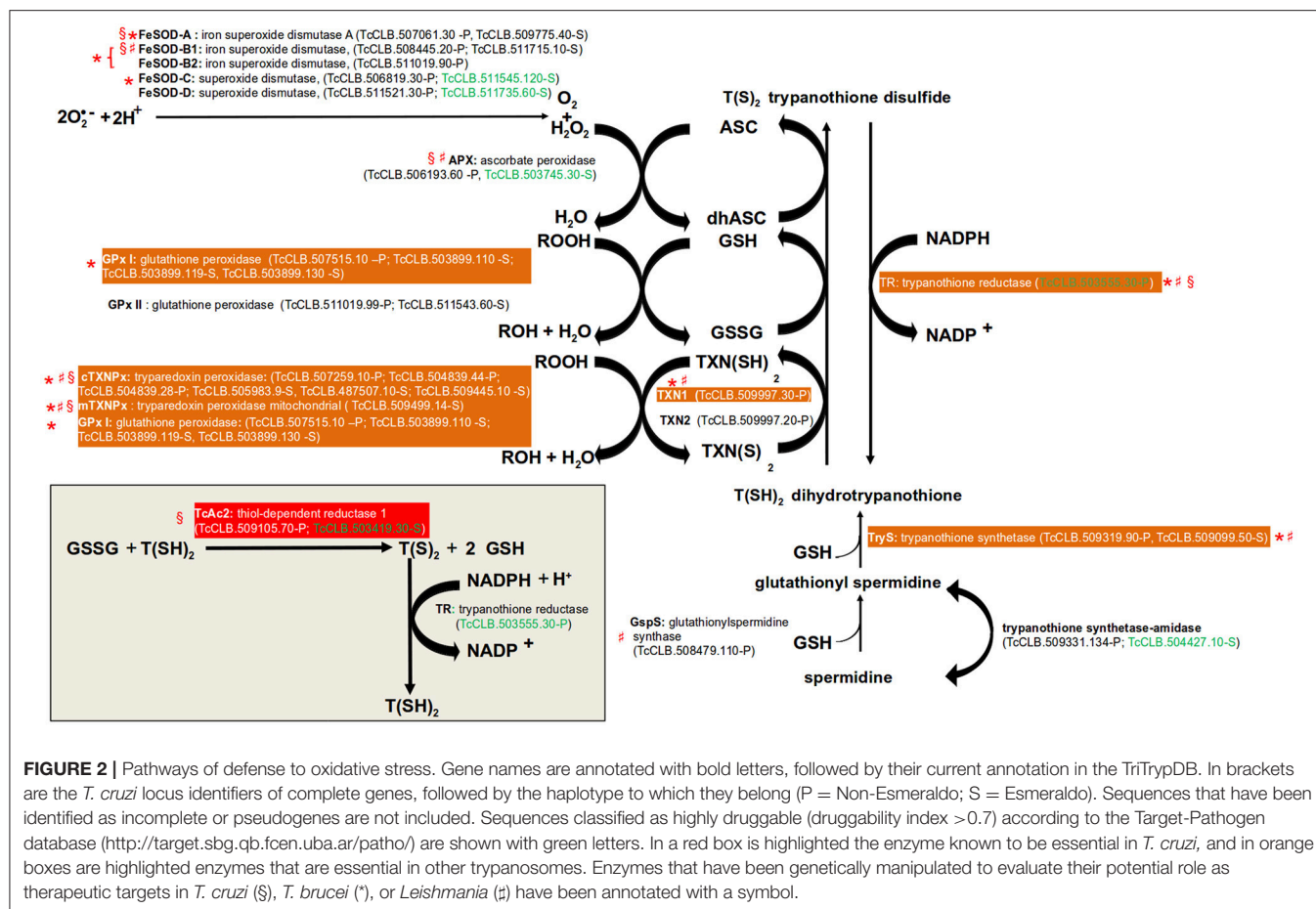
In conclusion, enzymes from the ergosterol pathway are common targets of effective inhibitory compounds to treat fungal infections. Ergosterol is endogenously produced and essential for *T. cruzi*, so these molecules have also been considered promising anti-Chagasic drugs. Most studies in this direction have been focused on the inhibition of CYP51 by azoles. Evidence from these works suggested that these compounds were efficient to combat the infection using *in vitro* and murine models. However, they failed when tested in clinical trials. Despite these results, other azoles and inhibitors of distinct enzymes of the pathway, specially *Tc24SMT*, remain as plausible candidates as anti-*T. cruzi* drugs that deserve further exploration.

Resistance to Oxidative Stress

In all organisms, molecular species with high redox potential have important physiological roles (Sies et al., 2017), especially in signal transduction. However, an excessive exposure to them may lead to oxidative stress, which is detrimental to the cells. Therefore, there are antioxidant mechanisms to deal with these situations. Two major forms of them have been described: (1) Enzymatic protection, (2) Low-molecular weight compounds containing thiol groups (R-SH). The first is comprised by enzymes that directly catalyze the reduction of these molecules. In the second category, the thiol group acts as the reducing agent. Within them, the most ubiquitous is glutathione (GSH), a tripeptide composed by Glu, Cys, and Gly. Others include α -tocopherol (vitamin E) and ascorbate (vitamin C) (Poole, 2015). *T. cruzi* is exposed to toxic oxygen and nitrogen species derived from its aerobic metabolism and from the host immune response. To overcome this, the parasite possess an antioxidant

system based on enzymatic protection, GSH, and the GSH-containing molecule trypanothione (Turrens, 2004; reviewed in Krauth-Siegel and Comini, 2008; Figure 2). The major enzymatic mechanism expressed by *T. cruzi* are five iron superoxide dismutases (FeSOD, two mitochondrial and three cytosolic) that remove superoxide anions (O_2^-) by converting them into hydrogen peroxide (H_2O_2) and molecular oxygen (O_2). The H_2O_2 produced by the FeSODs, and from other sources, can then be reduced in the endoplasmic reticulum (ER) to water by the ascorbate peroxidase (Apx) (Wilkinson et al., 2002). This leads to the conversion of ascorbate (ASC) into dehydroascorbate (dhASC). On the other hand, highly reactive hydroperoxides (ROOH) can be reduced by two sets of enzymes: glutathione peroxidases (cytosolic GPx I and the ER located GPx II) and trypanothione peroxidases (cytosolic cTXNPx and mitochondrial mTXNPx). Glutathione peroxidases oxidize two molecules of GSH to glutathione disulfide (GSSG). Instead of using GSH, trypanothione peroxidases uses the thiol groups of its cysteine residues. Trypanothione [$T(SH)_2$] is composed by two GSH molecules bound by a polyamine named spermidine. $T(SH)_2$ has a key role in the described trypanosomatid antioxidant mechanism because it non-enzymatically reduces the generated dhASC, GSSG, and $TXN(S)_2$. This replenish the parasite with molecules with the potential to keep the system working. The process is assisted by two enzymes that catalyze the reduction of GSSG (Thiol-dependent reductase, *TcAc2*) (Figure 2, inset) and $TXN(S)_2$ (trypanothione, *TXN1* and *2*). The oxidized form of trypanothione [$T(S)_2$] is returned back to $T(SH)_2$ by the enzyme trypanothione reductase, a reaction that requires NADPH.

The essential role of several of these enzymes has been evaluated in *T. cruzi* and other trypanosomatids. Regarding the FeSODs, there are studies for four of the five isoforms encoded by the parasite genome (FeSOD-A, FeSOD-B1 and FeSOD-B2, FeSOD-C) in *T. brucei* and *Leishmania* (Beltrame-Botelho et al., 2016; Figure 2). In *L. chagasi*, a single-allele knockout of FeSOD-B1 resulted in a decrease of growth when exposed to the O_2^- generating agent paraquat (Plewes et al., 2003), suggesting an important role for this enzyme. The mutant parasites also showed a reduced level of survival within macrophages. RNAi studies in the bloodstream forms (BSFs) of *T. brucei* showed that the RNAi mediated knockdown of FeSOD-B1/2, but not for FeSOD-A and FeSOD-C, resulted in a significant reduction in parasite growth (Wilkinson et al., 2006). However, in the presence of paraquat, RNAi inhibition of FeSOD-A resulted in decreased growth (Wilkinson et al., 2006). Apx is an antioxidant enzyme that is absent from the mammalian host, but unfortunately it has been shown to be dispensable for the parasite. *T. cruzi* null mutants for the enzyme had no defects on cell growth and were able to complete their life cycle *in vivo* (Taylor et al., 2015). In *L. major*, Apx null mutants even shown hypervirulence after infection in macrophages and inoculation into mice (Pal et al., 2010). With the exception of GPx II, all tested glutathione and trypanothione peroxidases have shown to be essential for *T. brucei* or *Leishmania* (Figure 2). In *T. brucei*, a knockdown of the GPx I genes was lethal to BSFs (Wilkinson et al., 2003). A similar result was observed for the cytosolic cTXNPx, but not for the mitochondrial mTXNPx (Wilkinson et al., 2003).



However, gene replacement studies showed that this last enzyme is essential in *L. infantum* (Castro et al., 2011). As mentioned above, the reduction of GSSG to GSH is thought to be largely dependent on the oxidation of T(SH)₂. However, in *T. cruzi* TcAc2 is able to catalyze this reaction (Moutiez et al., 1995). Interestingly, this activity seems to be essential for epimastigotes as it was not possible to obtain null mutants for the encoding gene (Allaoui et al., 1999). Trypanothione (TXNs) are oxidoreductases found exclusively in trypanosomatids. There are two TXNs in *T. cruzi*, one cytosolic (TXN1) and the other associated with endomembranes (TXN2) (Arias et al., 2013). The essential role of neither of them have been tested in *T. cruzi*, but in *T. brucei* the knock-down of TXN1 reduced the growth BSF and procyclics and in *L. infantum* it was required for cell survival (Wilkinson et al., 2003; Comini et al., 2007; Romao et al., 2009). Given its central role in the antioxidant system and its absence in human cells, trypanothione reductase is considered an attractive drug target (Figure 2). Additionally, RNAi and knockout studies demonstrated that it is an essential gene in *T. brucei*, *L. donovani*, and *L. major*. Additionally, in *Leishmania* a single allele knockout of the gene resulted in reduced infectivity and capacity to survive within macrophages (Dumas et al., 1997; Tovar et al., 1998; Krieger et al., 2000). Although not directly involved in the antioxidant system, we also search data on the essentiality of the two enzymes required for the production T(SH)₂ (Figure 2).

In BSF of *T. brucei*, knockdown of TryS resulted in growth arrest and led to depletion of both T(SH)₂ and its precursor glutathionylspermidine (Comini et al., 2004). In *L. infantum*, both promastigotes and amastigotes with deletion of GspS were viable. In contrast, elimination of both TryS alleles was only possible when parasites were previously complemented with an episomal copy of the gene (Sousa et al., 2014).

Drugs of current use for the treatment of diseases caused by *T. cruzi* and other trypanosomatids seems to have several modes of action (Field et al., 2017). There is some evidence that one of them is the induction of oxidative stress within the parasite, as pharmacological and genetic inhibition of its antioxidant defense mechanism have effects on the susceptibility to the drugs. For example, treatment of different *T. cruzi* stages with buthionine sulfoximine, an inhibitor of the synthesis of an indispensable precursor of glutathione, increase the antiparasitic effects of nifurtimox and benznidazole (Faundez et al., 2005). However, the molecular targets of these drugs have not been elucidated, as overexpression of some of antioxidant enzymes do not have an effect on drug sensitivity (Wilkinson et al., 2000). Similar to *T. cruzi*, some of the drugs currently used to treat leishmaniasis may also target the antioxidant system. The levels of expression of cTXNPx have been associated with drug resistance to antimonials and amphotericin B in several species of *Leishmania* (Suman et al., 2016; Das et al., 2017). Promastigotes of *L. donovani*, *L.*

tarentolae, and *L. braziliensis*, but not *L. infantum*, overexpressing cTXNPx increased their resistance to antimonials (Iyer et al., 2008; Wyllie et al., 2008; Andrade and Murta, 2014; Das et al., 2017). On the other hand, there have also been efforts to discover and design drugs against enzymes of the antioxidant system, particularly for those involved in the trypanothione synthesis and recycling (Wyllie et al., 2009; Patterson et al., 2011; Spinks et al., 2012).

The components of antioxidant system of *T. cruzi* are attractive drug targets against the parasite, as many of them are essential and absent in mammals. Also, they apparently lack functional redundancy (Krauth-Siegel and Comini, 2008), making them highly selective. Additionally, drugs currently used to treat the diseases caused by trypanosomatids may act, at least in part, by interfering in the antioxidant system of the parasite. Identifying the precise molecular targets within this pathway may open the possibility of designing more potent and selective drugs.

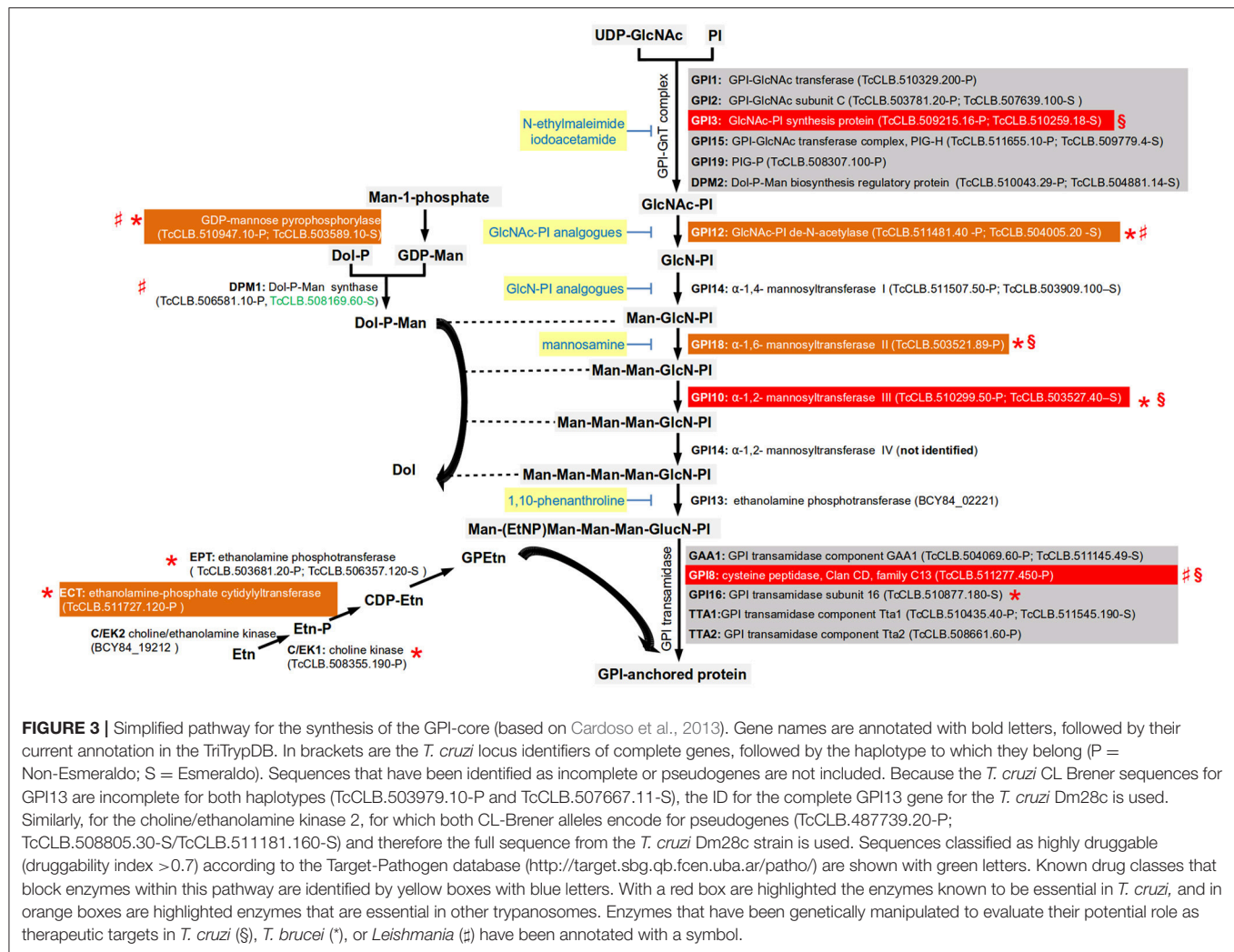
Synthesis of Surface Glycoconjugates

The GPI anchor is a glycolipid structure formed at the parasite endoplasmic reticulum (ER). This moiety has a conserved core of phosphatidylinositol (PI), linked to a trimannosyl-non-acetylated glucosamine. This sugar core is linked to an ethanolamine (Etn) phosphate that is attached to the C-terminus of the protein via an amide bond. The two fatty acids within the hydrophobic PI group anchor the protein to the cell membrane (Cheung et al., 2014). There can be a wide variety of substituents in the mannoside, inositol, or lipid moieties depending on the particular protein, organism, or developmental stage of an organism (Hong and Kinoshita, 2009). The GPI anchor is synthesized by a variety of enzymes, which sequentially transfer sugars and Etn to the PI. After synthesis, the GPI anchor is attached to the protein by GPI transamidase before being transported to the cell surface. The first two steps of the synthesis of GPI anchors that result in the production of the N-glucosaminyl-phosphatidylinositol (GlcNAc-PI) occur at the outside face of the ER membrane and then it is flipped to the inside. Similarly, dolichol-phosphate mannose (Dol-P-Man), the donor molecule for the mannoses within the GPI core, is synthesized in the outside face of the ER membrane, and then flipped inside. The rest of the synthesis of the GPI core occurs inside the ER.

All the enzymes involved in the *T. cruzi* GPI biosynthetic pathway have been identified, with the exception of the enzyme required for the addition a fourth mannose into the GPI core (Cardoso et al., 2013; **Figure 3**). Several differences between the mammalian and trypanosomatid pathways were identified. The mammalian GPI-N-acetylglucosaminyltransferase complex (GPI-GnT) has an element known as PIG-Y that is not present in trypanosomatids (Murakami et al., 2005). There are also differences in the composition of GPI transamidase, the enzymatic complex in charge of adding and processing the protein to the GPI core. The parasitic and the mammalian enzymes have 5 elements, but only three are shared in both complexes (GAA1, GPI8, and PIG-T) and the two others are specific of the mammalian host (PIG-S and PIG-U) or of the parasite (trypanosomatid transamidase 1 and 2) (Nagamune

et al., 2003). Also, mammalian cells require the acylation of the inositol ring prior to the addition of the first mannose to the non-N-acetylated glucosaminyl (GlcN)-PI by the enzyme PIG-W. This acylation group is removed after the addition of the sugar residue to the core and the attachment of the GPI anchor to the protein (Cardoso et al., 2013). No orthologs of PIG-W were identified in either *T. cruzi* or *T. brucei*. However, orthologs involved in inositol deacylation are present in the *T. cruzi* genome (**Figure 3**), as well as in *T. brucei* and *Leishmania*. Mammalian GPI has extra ethanolamine phosphate groups (Etn-P) in other residues, reactions that are catalyzed by different enzymes. The enzymatic pathway that synthesize the donor for ethanolamine group have been identified in *T. brucei* and their orthologs can be identified (Gibellini et al., 2008). Reverse genetics have been used to assess the potential of this biosynthetic pathway as a therapeutic target identifying some differences between species that deserve further study. In *T. brucei*, RNAi studies have demonstrated that GPI8 (Lillico et al., 2003), GPI10 (Nagamune et al., 2000), and GPI12 (Chang et al., 2002) are essential for the bloodstream form (BSF) of the parasite. In contrast, in procyclic cells these enzymes are not essential for growth *in vitro* and therefore knockouts of both alleles have been achieved. GPI8, GPI10, and GPI12 procyclic knockouts have an abnormal surface glycocalyx that do not allow these cells to colonize the tsetse midgut (Nagamune et al., 2000; Güther et al., 2006). The knockout of GPI16 (the ortholog of the human PIG-T) in procyclic cells had normal morphology but reduced growth rate (Hong et al., 2006). In *Leishmania major*, the GPI12 knockout has been obtained in the promastigote stage. Although viable, the knockout had decreased ability to infect and multiply into murine macrophages (Almani et al., 2016). In *L. mexicana*, GPI8 null mutants were obtained that grew normally in liquid culture, and were able to successfully infect macrophages *in vitro* and mice (Hilley et al., 2000). In *T. cruzi* epimastigotes, it was not possible to obtain null mutants for GPI3, GPI8, and GPI10 by homologous recombination suggesting that these enzymes are essential. Interestingly, it was not even possible to obtain a single allele knockout of GPI3 and GPI10 suggesting the need for both functional alleles of the genes (Cardoso et al., 2013).

The pathways involved in the synthesis of mannose and Etn donors for GPI synthesis are also required for parasite survival (**Figure 3**). For the synthesis of Dol-P-Man, the GDP-mannose pyrophosphorylase was found to be essential for the BSFs of *T. brucei* (Denton et al., 2010). In *L. mexicana* procyclic forms, knockouts of either GDP-mannose pyrophosphorylase, or Dol-P-Man synthase were viable but demonstrated decreased virulence (Garami and Ilg, 2001; Garami et al., 2001; Stewart et al., 2005). With respect to glycerophosphoethanolamine (GPEtn) synthesis, the locus annotated as encoding for the enzyme involved in the first step of the pathway (the choline/ethanolamine kinase, C/EK) contains only pseudogenes in the *T. cruzi* CL-Brener genome (**Figure 3**). Interestingly, analysis of synteny of the orthologs in other *T. cruzi* strains reveals the presence of full length open reading frames. The absence of a complete gene in one strain could suggest that the enzyme is not essential for the parasite. However, in *T. brucei* two choline/ethanolamine

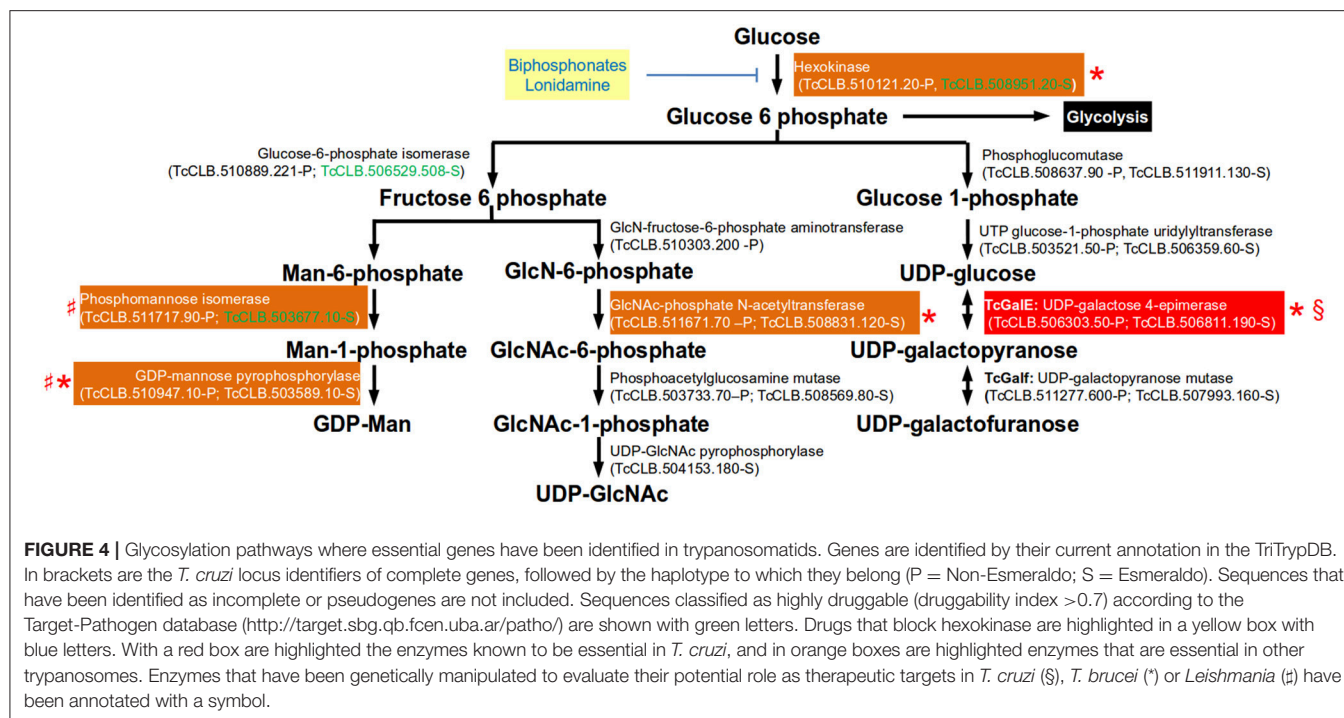


genes are present, being initially named C/EK1 and C/EK2 (Gibellini et al., 2008). *In vitro* characterization of their catalytic activities demonstrated that C/EK1 metabolize Etn but not choline, and therefore they rename it TbEK1. In contrast, TbC/EK2 metabolized both substrates. In the *T. cruzi* CL-Brener genome there is only a functional ortholog for TbEK1, with the locus encoding for the putative TbC/EK2 being a pseudogene. Thus, it is important to characterize the catalytic abilities of the ortholog to TbEK1. In *T. brucei* the three enzymes involved in the synthesis of GPEtn have been evaluated in the procyclic form by reverse genetics (Gibellini et al., 2008, 2009; Signorell et al., 2009). RNAi of the three enzymes resulted in viable organisms. However, in the case ethanolamine-phosphate cytidyltransferase (ECT), depletion of the enzyme was associated with abnormal mitochondrial morphology, and with the accumulation of multinucleated cells (Signorell et al., 2009). A TbECT conditional null mutant of the BSF was obtained by homologous recombination associated with the expression of an ectopic copy of the gene demonstrated that this gene is essential (Gibellini et al., 2009).

Several inhibitors of the GPI synthesis have been shown to kill trypanosomatids. Analogs of the biosynthetic pathway frequently inhibit both parasite and mammalian enzymes. However, different type of substitutions have been evaluated to obtain greater specificity for the trypanosomatid enzymes. Inhibitors that affect GPI synthesis in trypanosomatids without affecting the mammalian enzymes need to be found.

Glycosylation Steps Evaluated as Potential Drug Targets

The specific type of glycoconjugates present in *Trypanosoma cruzi*, *T. brucei*, and *Leishmania major*, are fundamentally different, reflecting their disparate life cycles, modes of infection, and disease pathologies (Turnock and Ferguson, 2007). The addition of sugar moieties to their targets occurs in the lumen of the ER and Golgi apparatus through the action of glycosyltransferases using nucleotide sugars as substrates. Translocation of the sugar nucleotide from the cytosol into the Golgi lumen is mediated by a transporter specific for each nucleotide sugar. Ten different sugar nucleotides have been identified in trypanosomatids, but the repertoire present



in each parasite is species-specific (Turnock and Ferguson, 2007). Five nucleotide sugars are common to the three species [GDP- α -D-mannose, UDP- α -D-N-acetylglucosamine, UDP- α -D-glucose, UDP- α -galactopyranose (UDP-Galp), and GDP- β -L-fucose], three are identified only in *T. cruzi* (UDP- β -L-rhamnopyranose, UDP- α -D-xylose, and UDP- α -D-glucuronic acid), GDP- α -D-arabinopyranose is found only in *L. major*, and UDP- α -D-galactofuranose (UDP-Galf) is present in *T. cruzi* and in *L. major* (Turnock and Ferguson, 2007). Mammalian cells do not synthesize UDP- α -D-galactofuranose and therefore its biosynthetic pathway is an attractive target for new drugs.

To act as glycosyl donors, the monosaccharides must be conjugated with a nucleotide. In trypanosomatids the biosynthesis of all nucleotide sugars initiate with glucose-6-phosphate, with the exception of GDP-arabinose (present only in *Leishmania* spp.) which is thought to be synthesized from glucose by an unknown mechanism (Turnock and Ferguson, 2007). The synthesis of glucose-6-phosphate from glucose is therefore not only important in glycolysis, but also for the synthesis of sugar nucleotides in *T. cruzi* (Figure 4). Hexokinase catalyzes the conversion of the glucose that has entered the cell into glucose-6-phosphate. The regulation of *T. cruzi* hexokinase differs from the mammalian enzyme in that it is not inhibited by glucose-6-phosphate, fructose-1,6-diphosphate, phosphoenol pyruvate, malate, or citrate. Instead, the parasite enzyme, but not the human, is inhibited by non-hydrolyzable analogs of inorganic pyrophosphate (biphosphonates). Biphosphonate inhibitors of the *T. cruzi* enzyme that are not toxic to human cell lines have been identified (Hudock et al., 2006). It was proposed that the lack of toxicity depends of the specificity of the analogs which are highly specific of the hexokinase and poor inhibitors

of farnesyl diphosphate synthase (enzyme that is involved in the Ergosterol synthesis pathway, see Figure 1). Lonidamine is another inhibitor that reduces viability of *T. cruzi*, *T. brucei*, and *Leishmania* (Chambers et al., 2008).

In *T. cruzi*, the major surface glycoproteins are mucin-like proteins which are heavily O-glycosylated. A distinctive property of this type of glycosylation in this organism is that the sugar attached to the hydroxyl group of serine or threonine residues is GlcNAc, whereas both *T. brucei* and *Leishmania* attach GalNAc. The *T. cruzi* and *T. brucei* hexose transporters do not transport D-galactose and therefore their only source of galactose is through the epimerisation of UDP-Glc to UDP-Gal by the UDP-glucose 4'epimerase (GalE) (Roper and Ferguson, 2003; Figure 4). Unlike the mammalian enzyme, the parasitic enzyme is unable to interconvert UDP-GlcNAc and UDP-GalNAc. Therefore, GalE is essential for the synthesis of UDP-Galp and UDP-Galf abundant residues in the *T. cruzi* mucins. The conversion of UDP-Galp to Galf depends on the activity of UDP-Galp mutase, and this enzyme present only in *T. cruzi* and *Leishmania* but not in mammals, which makes it an interesting therapeutic target (Oppenheimer et al., 2011). The attachment of mucins to the plasma membrane is through a GPI-anchor and therefore synthesis of UDP-Man is essential.

Terminal β -Galp residues of *T. cruzi* mucins are sialylated by a GPI-anchored trans-sialidase that catalyzes the transfer of the host's sialic acid to the parasite's proteins. Sialylation of mucins is important for the survival for *T. cruzi*. In epimastigotes it has been implicated adhesion of the parasites to the epithelial cells in the rectal ampoule of the insect. In trypomastigotes, the terminal sialic acids mask parasite antigenic determinants, thus protecting the parasite from host attack

by anti-galactosyl antibodies and by complement (Giorgi and de Lederkremer, 2011). Inhibitors of the trans-sialidase are being developed as potential therapeutic agents. Reverse genetics studies have demonstrated the importance of these pathways *in vivo* (Figure 4). In *T. brucei* there are two hexokinase genes in tandem encoding for proteins with hexokinase that are 98% identical. Experiments with RNAi and ectopic expression of the enzyme demonstrated that hexokinase activity is essential for *T. brucei* procyclic and BSFs (Albert et al., 2005; Chambers et al., 2008). Within the biosynthetic pathway for UDP-Galp, tetracycline-inducible conditional *GalE* null mutants of *T. brucei* procyclic and BSFs were found to be essential (Roper et al., 2002, 2005). This also seems to be the case for *T. cruzi* epimastigotes as it was not possible to obtain the double allele knockout (MacRae et al., 2006). Unlike *T. cruzi* and *T. brucei*, *Leishmania* can obtain galactose from extracellular sources, and therefore *GalE* is not essential in these parasites (Oppenheimer et al., 2011). In *L. major*, double knockout of UDP-galactopyranose mutase (*Galf*) has been obtained. The null mutants were viable but had decreased virulence in mice (Kleczka et al., 2007). In *T. cruzi*, the targeting of two alleles encoding a conserved hypothetical protein (TcCLB.511301.50-P;TcCLB.511353.30-S) that was considered a possible triose-phosphate or UDP-galactofuranose transporter (*Galf*-transporter) was found to be essential (Soares Medeiros et al., 2017). However, although the encoded protein could correspond to a sugar nucleotide transporter, there is no evidence that the transported sugar-nucleotide is indeed *Galf*. As this gene proved to be essential it would be important to do a full characterization of the encoded protein. The role in viability of all enzymes involved in the synthesis of UDP-Man in *Leishmania* have been studied. Promastigote mutants null for phosphomannose isomerase, phosphomannose mutase, and GDP-Man pyrophosphorylase are all viable, and with the exception of the phosphomannose isomerase, the mutants lost their ability to infect macrophages and mice (Turnock and Ferguson, 2007). As previously mentioned, the GDP-mannose pyrophosphorylase is essential in *T. brucei* (Denton et al., 2010). Reverse genetics in the pathway of UDP-GlcNAc synthesis has only been determined for the glucosamine 6-phosphate *n*-acetyltransferase of *T. brucei*. In BSFs of *T. brucei* the conditional null mutant was unable to sustain growth under non-permissive conditions, demonstrating that there are no metabolic, or nutritional routes to UDP-GlcNAc other than via GlcNAc-6-phosphate (Mariño et al., 2011).

REFERENCES

- Albert, M.-A., Haanstra, J. R., Hannaert, V., Van Roy, J., Opperdoes, F. R., Bakker, B. M., et al. (2005). Experimental and *in silico* analyses of glycolytic flux control in bloodstream form *Trypanosoma brucei*. *J. Biol. Chem.* 280, 28306–28315. doi: 10.1074/jbc.M502403200
- Allaoui, A., François, C., Zemzoumi, K., Guilvard, E., and Ouassii, A. (1999). Intracellular growth and metacyclogenesis defects in *Trypanosoma cruzi* carrying a targeted deletion of a Tc52 protein-encoding allele. *Mol. Microbiol.* 32, 1273–1286. doi: 10.1046/j.1365-2958.1999.01440.x

CONCLUSIONS AND PERSPECTIVES

New treatments for Chagas' disease are required. More information is needed not only of the molecular mechanisms involved in the establishment of infection, but also about those involved in parasite survival and persistence. The screening of chemical libraries will undoubtedly identify new potential targets, but they will also need to be individually curated and validated. Unfortunately, it is still difficult to prove the essentiality of a gene in *T. cruzi*, although the CRISPR-Cas9 technology appears to be more efficient for gene disruption than the knockouts by homologous recombination. Improved strategies for the regulated expression of ectopic genes needs to be developed. In the meantime, it is always useful to assess the information available for other trypanosomatids. Public databases such as TriTrypDB or TDR Targets present a great opportunity for data mining and contain a wealth of information that can be easily searched and analyzed. However, the genome sequence of the parasite genome still contain gaps and some errors, so integrity of the selected genes should always be assessed. Although molecular modeling of *T. cruzi* proteins can be done from structural information from orthologs of other species, to develop highly selective inhibitors to target proteins it is necessary to obtain crystal structures of the specific proteins. There is no doubt that identifying and developing new treatments requires a large team of specialists in multiple areas such as chemistry, biology, engineering, informatics, and medicine. Ideally, several teams should be assembled and organized so that every aspect of drug development is met and, hopefully, each team should concentrate in different potential targets.

AUTHOR CONTRIBUTIONS

JO-M and AC contributed equally in this work.

SUPPLEMENTARY MATERIAL

The Supplementary Material for this article can be found online at: <https://www.frontiersin.org/articles/10.3389/fcimb.2018.00439/full#supplementary-material>

Supplementary Figure 1 | Expression profile of selected genes obtained by RNA-seq during experimental infection of fibroblasts with *T. cruzi* (Li et al., 2016). Data was downloaded from the expression section of the TriTrypDB. Data is expressed as transcript levels of fragments per kilobase of exon model per million mapped reads (FPKM). Red boxes represent unique transcript, gray boxes represent reads of sequences shared with other genes.

- Almani, P. G. N., Sharifi, I., Kazemi, B., Babaei, Z., Bandehpour, M., Salari, S., et al. (2016). The role of GlcNAc-PI-de-N-acetylase gene by gene knockout through homologous recombination and its consequences on survival, growth and infectivity of *Leishmania major* in *in vitro* and *in vivo* conditions. *Acta Trop.* 154, 63–72. doi: 10.1016/j.actatropica.2015.10.025
- Alsford, S., Turner, D. J., Obado, S. O., Sanchez-Flores, A., Glover, L., Berriman, M., et al. (2011). High-throughput phenotyping using parallel sequencing of RNA interference targets in the African trypanosome. *Genome Res.* 21, 915–924. doi: 10.1101/gr.115089.110
- Andrade, J. M., and Murta, S. M. F. (2014). Functional analysis of cytosolic trypanodioxin peroxidase in antimony-resistant and -susceptible *Leishmania*

- braziliensis* and *Leishmania infantum* lines. *Parasit. Vectors* 7:406. doi: 10.1186/1756-3305-7-406
- Arias, D. G., Marquez, V. E., Chiribao, M. L., Gadelha, F. R., Robello, C., Iglesias, A. A., et al. (2013). Redox metabolism in *Trypanosoma cruzi*: functional characterization of tryparedoxins revisited. *Free Radic. Biol. Med.* 63, 65–77. doi: 10.1016/j.freeradbiomed.2013.04.036
- Aurrecoechea, C., Barreto, A., Basenko, E. Y., Brestelli, J., Brunk, B. P., Cade, S., et al. (2017). EuPathDB: the eukaryotic pathogen genomics database resource. *Nucleic Acids Res.* 45, D581–D591. doi: 10.1093/nar/gkw1105
- Beltrame-Botelho, I. T., Talavera-López, C., Andersson, B., Grisard, E. C., and Stoco, P. H. (2016). A comparative *in silico* study of the antioxidant defense gene repertoire of distinct lifestyle trypanosomatid species. *Evol. Bioinforma. Online* 12, 263–275. doi: 10.4137/EBO.S40648
- Benaim, G., Sanders, J. M., García-Marchán, Y., Colina, C., Lira, R., Caldera, A. R., et al. (2006). Amiodarone has intrinsic anti-*Trypanosoma cruzi* activity and acts synergistically with posaconazole. *J. Med. Chem.* 49, 892–899. doi: 10.1021/jm050691f
- Beneke, T., Madden, R., Makin, L., Valli, J., Sunter, J., and Gluenz, E. (2017). A CRISPR Cas9 high-throughput genome editing toolkit for kinetoplasts. *R. Soc. Open Sci.* 4:170095. doi: 10.1098/rsos.170095
- Bern, C. (2011). Antitrypanosomal therapy for chronic Chagas' disease. *N. Engl. J. Med.* 364, 2527–2534. doi: 10.1056/NEJMct1014204
- Bloch, K. E. (1983). Sterol structure and membrane function. *CRC Crit. Rev. Biochem.* 14, 47–92. doi: 10.3109/10409238309102790
- Braga, M. V., Magaraci, F., Lorente, S. O., Gilbert, I., and de Souza, W. (2005). Effects of inhibitors of Delta24(25)-sterol methyl transferase on the ultrastructure of epimastigotes of *Trypanosoma cruzi*. *Microsc. Microanal.* 11, 506–515. doi: 10.1017/S143192760505035X
- Burle-Caldas, G., de, A., Grazielle-Silva, V., Laibida, L. A., DaRocha, W. D., and Teixeira, S. M. R. (2015). Expanding the tool box for genetic manipulation of *Trypanosoma cruzi*. *Mol. Biochem. Parasitol.* 203, 25–33. doi: 10.1016/j.molbiopara.2015.10.004
- Burle-Caldas, G. A., Grazielle-Silva, V., Soares-Simões, M., Schumann Burkard, G., Roditi, I., DaRocha, W. D., et al. (2017). Editing the *Trypanosoma cruzi* genome with zinc finger nucleases. *Mol. Biochem. Parasitol.* 212, 28–32. doi: 10.1016/j.molbiopara.2017.01.002
- Burle-Caldas, G. A., Soares-Simões, M., Lemos-Pechnicki, L., DaRocha, W. D., and Teixeira, S. M. R. (2018). Assessment of two CRISPR-Cas9 genome editing protocols for rapid generation of *Trypanosoma cruzi* gene knockout mutants. *Int. J. Parasitol.* 48, 591–596. doi: 10.1016/j.ijpara.2018.02.002
- Cardoso, M. S., Junqueira, C., Trigueiro, R. C., Shams-Eldin, H., Macedo, C. S., Araújo, P. R., et al. (2013). Identification and functional analysis of *Trypanosoma cruzi* genes that encode proteins of the glycosylphosphatidylinositol biosynthetic pathway. *PLoS Negl. Trop. Dis.* 7:e2369. doi: 10.1371/journal.pntd.0002369
- Castro, H., Teixeira, F., Romão, S., Santos, M., Cruz, T., Flórido, M., et al. (2011). *Leishmania* mitochondrial peroxiredoxin plays a crucial peroxidase-unrelated role during infection: insight into its novel chaperone activity. *PLoS Pathog.* 7:e1002325. doi: 10.1371/journal.ppat.1002325
- Castro, J. A., de Mecca, M. M., and Bartel, L. C. (2006). Toxic side effects of drugs used to treat Chagas' disease (American trypanosomiasis). *Hum. Exp. Toxicol.* 25, 471–479. doi: 10.1191/0960327106het653oa
- Chambers, J. W., Fowler, M. L., Morris, M. T., and Morris, J. C. (2008). The anti-trypanosomal agent lonidamine inhibits *Trypanosoma brucei* hexokinase 1. *Mol. Biochem. Parasitol.* 158, 202–207. doi: 10.1016/j.molbiopara.2007.12.013
- Chang, T., Milne, K. G., Güther, M. L. S., Smith, T. K., and Ferguson, M. A. J. (2002). Cloning of *Trypanosoma brucei* and *Leishmania major* genes encoding the GlcNAc-phosphatidylinositol de-N-acetylase of glycosylphosphatidylinositol biosynthesis that is essential to the African sleeping sickness parasite. *J. Biol. Chem.* 277, 50176–50182. doi: 10.1074/jbc.M208374200
- Chatelain, E. (2015). Chagas disease drug discovery: toward a new era. *J. Biomol. Screen.* 20, 22–35. doi: 10.1177/1087057114550585
- Chatelain, E., and Ioset, J.-R. (2018). Phenotypic screening approaches for Chagas disease drug discovery. *Expert Opin. Drug Discov.* 13, 141–153. doi: 10.1080/17460441.2018.1417380
- Chen, C.-K., Leung, S. S. F., Guilbert, C., Jacobson, M. P., McKerrow, J. H., and Podust, L. M. (2010). Structural characterization of CYP51 from *Trypanosoma cruzi* and *Trypanosoma brucei* bound to the antifungal drugs posaconazole and fluconazole. *PLoS Negl. Trop. Dis.* 4:e651. doi: 10.1371/journal.pntd.0000651
- Cheung, A. Y., Li, C., Zou, Y., and Wu, H.-M. (2014). Glycosylphosphatidylinositol anchoring: control through modification. *Plant Physiol.* 166, 748–750. doi: 10.1104/pp.114.246926
- Comini, M. A., Guerrero, S. A., Haile, S., Menge, U., Lünsdorf, H., and Flohé, L. (2004). Validation of *Trypanosoma brucei* trypanothione synthetase as drug target. *Free Radic. Biol. Med.* 36, 1289–1302. doi: 10.1016/j.freeradbiomed.2004.02.008
- Comini, M. A., Krauth-Siegel, R. L., and Flohé, L. (2007). Depletion of the thioredoxin homologue tryparedoxin impairs antioxidative defence in African trypanosomes. *Biochem. J.* 402, 43–49. doi: 10.1042/BJ20061341
- Costa, F. C., Francisco, A. F., Jayawardhana, S., Calderano, S. G., Lewis, M. D., Olmo, F., et al. (2018). Expanding the toolbox for *Trypanosoma cruzi*: a parasite line incorporating a bioluminescence-fluorescence dual reporter and streamlined CRISPR/Cas9 functionality for rapid *in vivo* localisation and phenotyping. *PLoS Negl. Trop. Dis.* 12:e0006388. doi: 10.1371/journal.pntd.0006388
- Das, S., Lemgruber, L., Tay, C. L., Baum, J., and Meissner, M. (2017). Multiple essential functions of *Plasmodium falciparum* actin-1 during malaria blood-stage development. *BMC Biol.* 15:70. doi: 10.1186/s12915-017-0406-2
- Dauchy, F.-A., Bonhivers, M., Landrein, N., Dacheux, D., Courtois, P., Lauruol, F., et al. (2016). *Trypanosoma brucei* CYP51: essentiality and targeting therapy in an experimental model. *PLoS Negl. Trop. Dis.* 10:e0005125. doi: 10.1371/journal.pntd.0005125
- De Rycker, M., Baragaña, B., Duce, S. L., and Gilbert, I. H. (2018). Challenges and recent progress in drug discovery for tropical diseases. *Nature* 559, 498–506. doi: 10.1038/s41586-018-0327-4
- de Souza, W., and Rodrigues, J. C. F. (2009). Sterol biosynthesis pathway as target for anti-trypanosomatid drugs. *Interdiscip. Perspect. Infect. Dis.* 2009:642502. doi: 10.1155/2009/642502
- Denton, H., Fyffe, S., and Smith, T. K. (2010). GDP-mannose pyrophosphorylase is essential in the bloodstream form of *Trypanosoma brucei*. *Biochem. J.* 425, 603–614. doi: 10.1042/BJ20090896
- DiMasi, J. A., Grabowski, H. G., and Hansen, R. W. (2016). Innovation in the pharmaceutical industry: new estimates of R&D costs. *J. Health Econ.* 47, 20–33. doi: 10.1016/j.jhealeco.2016.01.012
- Dumas, C., Ouellette, M., Tovar, J., Cunningham, M. L., Fairlamb, A. H., Tamar, S., et al. (1997). Disruption of the trypanothione reductase gene of *Leishmania* decreases its ability to survive oxidative stress in macrophages. *EMBO J.* 16, 2590–2598. doi: 10.1093/emboj/16.10.2590
- El-Sayed, N. M., Myler, P. J., Bartholomeu, D. C., Nilsson, D., Aggarwal, G., Tran, A.-N., et al. (2005). The genome sequence of *Trypanosoma cruzi*, etiologic agent of Chagas disease. *Science* 309, 409–415. doi: 10.1126/science.1112631
- Faundez, M., Pino, L., Letelier, P., Ortiz, C., López, R., Seguel, C., et al. (2005). Buthionine sulfoximine increases the toxicity of nifurtimox and benznidazole to *Trypanosoma cruzi*. *Antimicrob. Agents Chemother.* 49, 126–130. doi: 10.1128/AAC.49.1.126-130.2005
- Field, M. C., Horn, D., Fairlamb, A. H., Ferguson, M. A. J., Gray, D. W., Read, K. D., et al. (2017). Anti-trypanosomatid drug discovery: an ongoing challenge and a continuing need. *Nat. Rev. Microbiol.* 15:447. doi: 10.1038/nrmicro.2017.69
- Filardi, L. S., and Brenner, Z. (1987). Susceptibility and natural resistance of *Trypanosoma cruzi* strains to drugs used clinically in Chagas disease. *Trans. R. Soc. Trop. Med. Hyg.* 81, 755–759. doi: 10.1016/0035-9203(87)90020-4
- Francisco, A. F., Jayawardhana, S., Lewis, M. D., Taylor, M. C., and Kelly, J. M. (2017). Biological factors that impinge on Chagas disease drug development. *Parasitology* 144, 1871–1880. doi: 10.1017/S0031182017001469
- Garami, A., and Ilg, T. (2001). Disruption of mannose activation in *Leishmania mexicana*: GDP-mannose pyrophosphorylase is required for virulence, but not for viability. *EMBO J.* 20, 3657–3666. doi: 10.1093/emboj/20.14.3657
- Garami, A., Mehler, A., and Ilg, T. (2001). Glycosylation defects and virulence phenotypes of *Leishmania mexicana* phosphomannomutase and dolicholphosphate-mannose synthase gene deletion mutants. *Mol. Cell. Biol.* 21, 8168–8183. doi: 10.1128/MCB.21.23.8168-8183.2001
- García-Salcedo, J. A., Pérez-Morga, D., Gijón, P., Dilbeck, V., Pays, E., and Nolan, D. P. (2004). A differential role for actin during the life cycle of *Trypanosoma brucei*. *EMBO J.* 23, 780–789. doi: 10.1038/sj.emboj.7600094

- Gibellini, F., Hunter, W. N., and Smith, T. K. (2008). Biochemical characterization of the initial steps of the Kennedy pathway in *Trypanosoma brucei*: the ethanolamine and choline kinases. *Biochem. J.* 415, 135–144. doi: 10.1042/BJ20080435
- Gibellini, F., Hunter, W. N., and Smith, T. K. (2009). The ethanolamine branch of the Kennedy pathway is essential in the bloodstream form of *Trypanosoma brucei*. *Mol. Microbiol.* 73, 826–843. doi: 10.1111/j.1365-2958.2009.06764.x
- Giorgi, M. E., and de Lederkremer, R. M. (2011). Trans-sialidase and mucins of *Trypanosoma cruzi*: an important interplay for the parasite. *Carbohydr. Res.* 346, 1389–1393. doi: 10.1016/j.carres.2011.04.006
- Guedes-da-Silva, F. H., Batista, D. G. J., Da Silva, C. F., De Araújo, J. S., Pávão, B. P., Simões-Silva, M. R., et al. (2017). Antitrypanosomal activity of sterol 14 α -demethylase (CYP51) inhibitors VNI and VFV in the Swiss mouse models of chagas disease induced by the *Trypanosoma cruzi* Y strain. *Antimicrob. Agents Chemother.* 61:e02098-16. doi: 10.1128/AAC.02098-16
- Güther, M. L. S., Lee, S., Tetley, L., Acosta-Serrano, A., and Ferguson, M. A. J. (2006). GPI-anchored proteins and free GPI glycolipids of procyclic form *Trypanosoma brucei* are non-essential for growth, are required for colonization of the tsetse fly, and are not the only components of the surface coat. *Mol. Biol. Cell* 17, 5265–5274. doi: 10.1091/mbc.e06-08-0702
- Haubrich, B. A., Singha, U. K., Miller, M. B., Nes, C. R., Anyatonwu, H., Lecordier, L., et al. (2015). Discovery of an ergosterol-signaling factor that regulates *Trypanosoma brucei* growth. *J. Lipid Res.* 56, 331–341. doi: 10.1194/jlr.M054643
- Hilley, J. D., Zawadzki, J. L., McConville, M. J., Coombs, G. H., and Mottram, J. C. (2000). *Leishmania mexicana* mutants lacking glycosylphosphatidylinositol (GPI):protein transamidase provide insights into the biosynthesis and functions of GPI-anchored proteins. *Mol. Biol. Cell* 11, 1183–1195. doi: 10.1091/mbc.11.4.1183
- Hoekstra, W. J., Hargrove, T. Y., Wawrzak, Z., da Gama Jaen Batista, D., da Silva, C. F., Nefertiti, A. S. G., et al. (2016). Clinical candidate VT-1161's antiparasitic effect *in vitro*, activity in a murine model of chagas disease, and structural characterization in complex with the target enzyme CYP51 from *Trypanosoma cruzi*. *Antimicrob. Agents Chemother.* 60, 1058–1066. doi: 10.1128/AAC.02287-15
- Hong, Y., and Kinoshita, T. (2009). Trypanosome glycosylphosphatidylinositol biosynthesis. *Korean J. Parasitol.* 47, 197–204. doi: 10.3347/kjp.2009.47.3.197
- Hong, Y., Nagamune, K., Ohishi, K., Morita, Y. S., Ashida, H., Maeda, Y., et al. (2006). TbGPI16 is an essential component of GPI transamidase in *Trypanosoma brucei*. *FEBS Lett.* 580, 603–606. doi: 10.1016/j.febslet.2005.12.075
- Hudock, M. P., Sanz-Rodríguez, C. E., Song, Y., Chan, J. M. W., Zhang, Y., Odeh, S., et al. (2006). Inhibition of *Trypanosoma cruzi* hexokinase by bisphosphonates. *J. Med. Chem.* 49, 215–223. doi: 10.1021/jm0582625
- Iyer, J. P., Kaprakkaden, A., Choudhary, M. L., and Shaha, C. (2008). Crucial role of cytosolic trypanothione peroxidase in *Leishmania donovani* survival, drug response, and virulence. *Mol. Microbiol.* 68, 372–391. doi: 10.1111/j.1365-2958.2008.06154.x
- Jones, N. G., Catta-Preta, C. M. C., Lima, A. P. C. A., and Mottram, J. C. (2018). Genetically Validated drug targets in *leishmania*: current knowledge and future prospects. *ACS Infect. Dis.* 4, 467–477. doi: 10.1021/acsinfecdis.7b00244
- Kangussu-Marcolino, M. M., Cunha, A. P., Avila, A. R., Herman, J.-P., and DaRocha, W. D. (2014). Conditional removal of selectable markers in *Trypanosoma cruzi* using a site-specific recombination tool: proof of concept. *Mol. Biochem. Parasitol.* 198, 71–74. doi: 10.1016/j.molbiopara.2015.01.001
- Kawasaki, Y., and Freire, E. (2011). Finding a better path to drug selectivity. *Drug Discov. Today* 16, 985–990. doi: 10.1016/j.drudis.2011.07.010
- Klecza, B., Lamerz, A.-C., van Zandbergen, G., Wenzel, A., Gerardy-Schahn, R., Wiese, M., et al. (2007). Targeted gene deletion of *Leishmania* major UDP-galactopyranose mutase leads to attenuated virulence. *J. Biol. Chem.* 282, 10498–10505. doi: 10.1074/jbc.M700023200
- Kolev, N. G., Tschudi, C., and Ullu, E. (2011). RNA interference in protozoan parasites: achievements and challenges. *Eukaryot. Cell* 10, 1156–1163. doi: 10.1128/EC.05114-11
- Krauth-Siegel, R. L., and Comini, M. A. (2008). Redox control in trypanosomatids, parasitic protozoa with trypanothione-based thiol metabolism. *Biochim. Biophys. Acta* 1780, 1236–1248. doi: 10.1016/j.bbagen.2008.03.006
- Krieger, S., Schwarz, W., Ariyanayagam, M. R., Fairlamb, A. H., Krauth-Siegel, R. L., and Clayton, C. (2000). Trypanosomes lacking trypanothione reductase are avirulent and show increased sensitivity to oxidative stress. *Mol. Microbiol.* 35, 542–552. doi: 10.1046/j.1365-2958.2000.01721.x
- Lander, N., Chiurillo, M. A., Vercesi, A. E., and Docampo, R. (2017). Endogenous C-terminal Tagging by CRISPR/Cas9 in *Trypanosoma cruzi*. *Bio-Protoc.* 7:e2299. doi: 10.21769/BioProtoc.2299
- Lander, N., Li, Z.-H., Niyogi, S., and Docampo, R. (2015). CRISPR/Cas9-induced disruption of paraflagellar rod protein 1 and 2 genes in *Trypanosoma cruzi* reveals their role in flagellar attachment. *mBio* 6:e01012. doi: 10.1128/mBio.01012-15
- Lepesheva, G. I., Hargrove, T. Y., Anderson, S., Kleshchenko, Y., Furtak, V., Wawrzak, Z., et al. (2010). Structural insights into inhibition of sterol 14 α -demethylase in the human pathogen *Trypanosoma cruzi*. *J. Biol. Chem.* 285, 25582–25590. doi: 10.1074/jbc.M110.133215
- Lepesheva, G. I., Hargrove, T. Y., Rachakonda, G., Wawrzak, Z., Pomel, S., Cojean, S., et al. (2015). VFV as a new effective CYP51 structure-derived drug candidate for chagas disease and visceral leishmaniasis. *J. Infect. Dis.* 212, 1439–1448. doi: 10.1093/infdis/jiv228
- Lepesheva, G. I., Villalta, F., and Waterman, M. R. (2011). Targeting *Trypanosoma cruzi* sterol 14 α -demethylase (CYP51). *Adv. Parasitol.* 75, 65–87. doi: 10.1016/B978-0-12-385863-4.00004-6
- Li, Y., Shah-Simpson, S., Okrah, K., Belew, A. T., Choi, J., Caradonna, K. L., et al. (2016). Transcriptome remodeling in *Trypanosoma cruzi* and human cells during intracellular infection. *PLoS Pathog.* 12:e1005511. doi: 10.1371/journal.ppat.1005511
- Liendo, A., Visbal, G., Piras, M. M., Piras, R., and Urbina, J. A. (1999). Sterol composition and biosynthesis in *Trypanosoma cruzi* amastigotes. *Mol. Biochem. Parasitol.* 104, 81–91. doi: 10.1016/S0166-6851(99)00129-2
- Lillico, S., Field, M. C., Blundell, P., Coombs, G. H., and Mottram, J. C. (2003). Essential roles for GPI-anchored proteins in African trypanosomes revealed using mutants deficient in GPI8. *Mol. Biol. Cell* 14, 1182–1194. doi: 10.1091/mbc.e02-03-0167
- Ma, Y., Weiss, L. M., and Huang, H. (2015). Inducible suicide vector systems for *Trypanosoma cruzi*. *Microbes Infect.* 17, 440–450. doi: 10.1016/j.micinf.2015.04.003
- MacRae, J. I., Obado, S. O., Turnock, D. C., Roper, J. R., Kierans, M., Kelly, J. M., et al. (2006). The suppression of galactose metabolism in *Trypanosoma cruzi* epimastigotes causes changes in cell surface molecular architecture and cell morphology. *Mol. Biochem. Parasitol.* 147, 126–136. doi: 10.1016/j.molbiopara.2006.02.011
- Magariños, M. P., Carmona, S. J., Crowther, G. J., Ralph, S. A., Roos, D. S., Shanmugam, D., et al. (2012). TDR Targets: a chemogenomics resource for neglected diseases. *Nucleic Acids Res.* 40, D1118–D1127. doi: 10.1093/nar/gkr1053
- Mariño, K., Güther, M. L. S., Wernimont, A. K., Qiu, W., Hui, R., and Ferguson, M. A. J. (2011). Characterization, localization, essentiality, and high-resolution crystal structure of glucosamine 6-phosphate N-acetyltransferase from *Trypanosoma brucei*. *Eukaryot. Cell* 10, 985–997. doi: 10.1128/EC.05025-11
- McCall, L.-I., El Aroussi, A., Choi, J. Y., Vieira, D. F., De Muylder, G., Johnston, J. B., et al. (2015). Targeting Ergosterol biosynthesis in *Leishmania donovani*: essentiality of sterol 14 α -demethylase. *PLoS Negl. Trop. Dis.* 9:e0003588. doi: 10.1371/journal.pntd.0003588
- Morillo, C. A., Waskin, H., Sosa-Estani, S., Del Carmen Bangher, M., Cuneo, C., Milesi, R., et al. (2017). Benznidazole and posaconazole in eliminating parasites in asymptomatic *T. cruzi* carriers: the stop-CHAGAS trial. *J. Am. Coll. Cardiol.* 69, 939–947. doi: 10.1016/j.jacc.2016.12.023
- Moutiez, S., Aumercier, M., Schöneck, R., Meziane-Cherif, D., Lucas, V., Aumercier, P., et al. (1995). Purification and characterization of a trypanothione-glutathione thioltransferase from *Trypanosoma cruzi*. *Biochem. J.* 310 (Pt 2), 433–437. doi: 10.1042/bj3100433
- Murakami, Y., Siripanyaphinyo, U., Hong, Y., Tashima, Y., Maeda, Y., and Kinoshita, T. (2005). The initial enzyme for glycosylphosphatidylinositol biosynthesis requires PIG-Y, a seventh component. *Mol. Biol. Cell* 16, 5236–5246. doi: 10.1091/mbc.e05-08-0743
- Nagajyothi, F., Machado, F. S., Burleigh, B. A., Jelicks, L. A., Scherer, P. E., Mukherjee, S., et al. (2012). Mechanisms of *Trypanosoma cruzi* persistence in Chagas disease. *Cell. Microbiol.* 14, 634–643. doi: 10.1111/j.1462-5822.2012.01764.x

- Nagamune, K., Nozaki, T., Maeda, Y., Ohishi, K., Fukuma, T., Hara, T., et al. (2000). Critical roles of glycosylphosphatidylinositol for *Trypanosoma brucei*. *Proc. Natl. Acad. Sci. U.S.A.* 97, 10336–10341. doi: 10.1073/pnas.180230697
- Nagamune, K., Ohishi, K., Ashida, H., Hong, Y., Hino, J., Kangawa, K., et al. (2003). GPI transamidase of *Trypanosoma brucei* has two previously uncharacterized (trypanosomatid transamidase 1 and 2) and three common subunits. *Proc. Natl. Acad. Sci. U.S.A.* 100, 10682–10687. doi: 10.1073/pnas.1833260100
- Oppenheimer, M., Valenciano, A. L., and Sobrado, P. (2011). Biosynthesis of galactofuranose in kinetoplastids: novel therapeutic targets for treating leishmaniasis and chagas' disease. *Enzyme Res.* 2011:415976. doi: 10.4061/2011/415976
- Pal, S., Dolai, S., Yadav, R. K., and Adak, S. (2010). Ascorbate peroxidase from *Leishmania major* controls the virulence of infective stage of promastigotes by regulating oxidative stress. *PLoS ONE* 5:e11271. doi: 10.1371/journal.pone.0011271
- Patterson, S., Alphey, M. S., Jones, D. C., Shanks, E. J., Street, I. P., Frearson, J. A., et al. (2011). Dihydroquinazolines as a novel class of *Trypanosoma brucei* trypanothione reductase inhibitors: discovery, synthesis, and characterization of their binding mode by protein crystallography. *J. Med. Chem.* 54, 6514–6530. doi: 10.1021/jm200312v
- Peng, D., Kurup, S. P., Yao, P. Y., Minning, T. A., and Tarleton, R. L. (2014). CRISPR-Cas9-mediated single-gene and gene family disruption in *Trypanosoma cruzi*. *mBio* 6, e02097–02014. doi: 10.1128/mBio.02097-14
- Pérez-Moreno, G., Sealey-Cardona, M., Rodrigues-Poveda, C., Gelb, M. H., Ruiz-Pérez, L. M., Castillo-Acosta, V., et al. (2012). Endogenous sterol biosynthesis is important for mitochondrial function and cell morphology in procyclic forms of *Trypanosoma brucei*. *Int. J. Parasitol.* 42, 975–989. doi: 10.1016/j.ijpara.2012.07.012
- Plewes, K. A., Barr, S. D., and Gedamu, L. (2003). Iron superoxide dismutases targeted to the glycosomes of *Leishmania chagasi* are important for survival. *Infect. Immun.* 71, 5910–5920. doi: 10.1128/IAI.71.10.5910-5920.2003
- Poole, L. B. (2015). The basics of thiols and cysteines in redox biology and chemistry. *Free Radic. Biol. Med.* 80, 148–157. doi: 10.1016/j.freeradbiomed.2014.11.013
- Romao, S., Castro, H., Sousa, C., Carvalho, S., and Tomás, A. M. (2009). The cytosolic trypanoredoxin of *Leishmania infantum* is essential for parasite survival. *Int. J. Parasitol.* 39, 703–711. doi: 10.1016/j.ijpara.2008.11.009
- Roper, J. R., and Ferguson, M. A. J. (2003). Cloning and characterisation of the UDP-glucose 4'-epimerase of *Trypanosoma cruzi*. *Mol. Biochem. Parasitol.* 132, 47–53. doi: 10.1016/j.molbiopara.2003.07.002
- Roper, J. R., Güther, M. L. S., Macrae, J. I., Prescott, A. R., Hallyburton, I., Acosta-Serrano, A., et al. (2005). The suppression of galactose metabolism in procyclic form *Trypanosoma brucei* causes cessation of cell growth and alters procyclin glycoprotein structure and copy number. *J. Biol. Chem.* 280, 19728–19736. doi: 10.1074/jbc.M502370200
- Roper, J. R., Güther, M. L. S., Milne, K. G., and Ferguson, M. A. J. (2002). Galactose metabolism is essential for the African sleeping sickness parasite *Trypanosoma brucei*. *Proc. Natl. Acad. Sci. U.S.A.* 99, 5884–5889. doi: 10.1073/pnas.092669999
- Sánchez-Valdéz, F. J., Padilla, A., Wang, W., Orr, D., and Tarleton, R. L. (2018). Spontaneous dormancy protects *Trypanosoma cruzi* during extended drug exposure. *eLife* 7:e34039. doi: 10.7554/eLife.34039
- Scarim, C. B., Jornada, D. H., Chelucci, R. C., de Almeida, L., Dos Santos, J. L., and Chung, M. C. (2018). Current advances in drug discovery for Chagas disease. *Eur. J. Med. Chem.* 155, 824–838. doi: 10.1016/j.ejmech.2018.06.040
- Sies, H., Berndt, C., and Jones, D. P. (2017). Oxidative Stress. *Annu. Rev. Biochem.* 86, 715–748. doi: 10.1146/annurev-biochem-061516-045037
- Signorell, A., Gluenz, E., Rettig, J., Schneider, A., Shaw, M. K., Gull, K., et al. (2009). Perturbation of phosphatidylethanolamine synthesis affects mitochondrial morphology and cell-cycle progression in procyclic-form *Trypanosoma brucei*. *Mol. Microbiol.* 72, 1068–1079. doi: 10.1111/j.1365-2958.2009.06713.x
- Soares Medeiros, L. C., South, L., Peng, D., Bustamante, J. M., Wang, W., Bunkofski, M., et al. (2017). Rapid, selection-free, high-efficiency genome editing in protozoan parasites using CRISPR-Cas9 ribonucleoproteins. *mBio* 8:e01788-17. doi: 10.1128/mBio.01788-17
- Sosa, E. J., Burguener, G., Lanzarotti, E., Defelipe, L., Radusky, L., Pardo, A. M., et al. (2018). Target-Pathogen: a structural bioinformatic approach to prioritize drug targets in pathogens. *Nucleic Acids Res.* 46, D413–D418. doi: 10.1093/nar/gkx1015
- Sousa, A. F., Gomes-Alves, A. G., Benítez, D., Comini, M. A., Flohé, L., Jaeger, T., et al. (2014). Genetic and chemical analyses reveal that trypanothione synthetase but not glutathionylspermidine synthetase is essential for *Leishmania infantum*. *Free Radic. Biol. Med.* 73, 229–238. doi: 10.1016/j.freeradbiomed.2014.05.007
- Spinks, D., Torrie, L. S., Thompson, S., Harrison, J. R., Frearson, J. A., Read, K. D., et al. (2012). Design, synthesis, and biological evaluation of *Trypanosoma brucei* trypanothione synthetase inhibitors. *ChemMedChem* 7, 95–106. doi: 10.1002/cmdc.201100420
- Stewart, J., Curtis, J., Spurck, T. P., Ilg, T., Garami, A., Baldwin, T., et al. (2005). Characterisation of a *Leishmania mexicana* knockout lacking guanosine diphosphate-mannose pyrophosphorylase. *Int. J. Parasitol.* 35, 861–873. doi: 10.1016/j.ijpara.2005.03.008
- Suman, S. S., Equbal, A., Zaidi, A., Ansari, M. Y., Singh, K. P., Singh, K., et al. (2016). Up-regulation of cytosolic trypanoredoxin in Amp B resistant isolates of *Leishmania donovani* and its interaction with cytosolic trypanoredoxin peroxidase. *Biochimie* 121, 312–325. doi: 10.1016/j.biochi.2015.12.017
- Sykes, M. L., and Avery, V. M. (2018). 3-pyridyl inhibitors with novel activity against *Trypanosoma cruzi* reveal *in vitro* profiles can aid prediction of putative cytochrome P450 inhibition. *Sci. Rep.* 8:4901. doi: 10.1038/s41598-018-22043-z
- Tarleton, R. L. (2016). Chagas disease: a solvable problem, ignored. *Trends Mol. Med.* 22, 835–838. doi: 10.1016/j.molmed.2016.07.008
- Taylor, M. C., Lewis, M. D., Fortes Francisco, A., Wilkinson, S. R., and Kelly, J. M. (2015). The *Trypanosoma cruzi* vitamin C dependent peroxidase confers protection against oxidative stress but is not a determinant of virulence. *PLoS Negl. Trop. Dis.* 9:e0003707. doi: 10.1371/journal.pntd.0003707
- Tovar, J., Wilkinson, S., Mottram, J. C., and Fairlamb, A. H. (1998). Evidence that trypanothione reductase is an essential enzyme in *Leishmania* by targeted replacement of the tryA gene locus. *Mol. Microbiol.* 29, 653–660. doi: 10.1046/j.1365-2958.1998.00968.x
- Turnock, D. C., and Ferguson, M. A. J. (2007). Sugar nucleotide pools of *Trypanosoma brucei*, *Trypanosoma cruzi*, and *Leishmania major*. *Eukaryot. Cell* 6, 1450–1463. doi: 10.1128/EC.00175-07
- Turrens, J. F. (2004). Oxidative stress and antioxidant defenses: a target for the treatment of diseases caused by parasitic protozoa. *Mol. Aspects Med.* 25, 211–220. doi: 10.1016/j.mam.2004.02.021
- Tyler, K. M., and Engman, D. M. (2001). The life cycle of *Trypanosoma cruzi* revisited. *Int. J. Parasitol.* 31, 472–481. doi: 10.1016/S0020-7519(01)00153-9
- Urbina, J. A. (2010). Specific chemotherapy of Chagas disease: relevance, current limitations, and new approaches. *Acta Trop.* 115, 55–68. doi: 10.1016/j.actatropica.2009.10.023
- Urbina, J. A., Vivas, J., Lazard, K., Molina, J., Payares, G., Piras, M. M., et al. (1996). Antiproliferative effects of delta 24(25) sterol methyl transferase inhibitors on *Trypanosoma (Schizotrypanum) cruzi*: *in vitro* and *in vivo* studies. *Chemotherapy* 42, 294–307. doi: 10.1159/000239458
- Villalta, F., Dobish, M. C., Nde, P. N., Kleshchenko, Y. Y., Hargrove, T. Y., Johnson, C. A., et al. (2013). VNI cures acute and chronic experimental Chagas disease. *J. Infect. Dis.* 208, 504–511. doi: 10.1093/infdis/jit042
- Warrenfeltz, S., Basenko, E. Y., Crouch, K., Harb, O. S., Kissinger, J. C., Roos, D. S., et al. (2018). EuPathDB: the eukaryotic pathogen genomics database resource. *Methods Mol. Biol.* 1757, 69–113. doi: 10.1007/978-1-4939-7737-6_5
- Wilkinson, S. R., Horn, D., Prathalingam, S. R., and Kelly, J. M. (2003). RNA interference identifies two hydroperoxide metabolizing enzymes that are essential to the bloodstream form of the african trypanosome. *J. Biol. Chem.* 278, 31640–31646. doi: 10.1074/jbc.M303035200
- Wilkinson, S. R., Obado, S. O., Mauricio, I. L., and Kelly, J. M. (2002). *Trypanosoma cruzi* expresses a plant-like ascorbate-dependent hemoperoxidase localized to the endoplasmic reticulum. *Proc. Natl. Acad. Sci. U.S.A.* 99, 13453–13458. doi: 10.1073/pnas.202422899
- Wilkinson, S. R., Prathalingam, S. R., Taylor, M. C., Ahmed, A., Horn, D., and Kelly, J. M. (2006). Functional characterisation of the iron superoxide dismutase gene repertoire in *Trypanosoma brucei*. *Free Radic. Biol. Med.* 40, 198–209. doi: 10.1016/j.freeradbiomed.2005.06.022
- Wilkinson, S. R., Temperton, N. J., Mondragon, A., and Kelly, J. M. (2000). Distinct mitochondrial and cytosolic enzymes mediate trypanothione-dependent

- peroxide metabolism in *Trypanosoma cruzi*. *J. Biol. Chem.* 275, 8220–8225. doi: 10.1074/jbc.275.11.8220
- Wyatt, P. G., Gilbert, I. H., Read, K. D., and Fairlamb, A. H. (2011). Target validation: linking target and chemical properties to desired product profile. *Curr. Top. Med. Chem.* 11, 1275–1283. doi: 10.2174/156802611795429185
- Wyllie, S., Oza, S. L., Patterson, S., Spinks, D., Thompson, S., and Fairlamb, A. H. (2009). Dissecting the essentiality of the bifunctional trypanothione synthetase-amidase in *Trypanosoma brucei* using chemical and genetic methods. *Mol. Microbiol.* 74, 529–540. doi: 10.1111/j.1365-2958.2009.06761.x
- Wyllie, S., Vickers, T. J., and Fairlamb, A. H. (2008). Roles of trypanothione S-transferase and trypanothione peroxidase in resistance to antimonials. *Antimicrob. Agents Chemother.* 52, 1359–1365. doi: 10.1128/AAC.01563-07
- Xu, W., Hsu, F.-F., Baykal, E., Huang, J., and Zhang, K. (2014). Sterol biosynthesis is required for heat resistance but not extracellular survival in *Leishmania*. *PLoS Pathog.* 10:e1004427. doi: 10.1371/journal.ppat.1004427
- Conflict of Interest Statement:** The authors declare that the research was conducted in the absence of any commercial or financial relationships that could be construed as a potential conflict of interest.

Copyright © 2019 Osorio-Méndez and Cevallos. This is an open-access article distributed under the terms of the Creative Commons Attribution License (CC BY). The use, distribution or reproduction in other forums is permitted, provided the original author(s) and the copyright owner(s) are credited and that the original publication in this journal is cited, in accordance with accepted academic practice. No use, distribution or reproduction is permitted which does not comply with these terms.



Evaluation of ATM Kinase Inhibitor KU-55933 as Potential Anti-*Toxoplasma gondii* Agent

Jonathan Munera López^{1†}, Agustina Ganuza^{1†}, Silvina S. Bogado¹, Daniela Muñoz¹, Diego M. Ruiz¹, William J. Sullivan Jr.^{2,3}, Laura Vanagas^{1*} and Sergio O. Angel^{1*}

¹ Laboratorio de Parasitología Molecular, IIB-INTECH, Consejo Nacional de Investigaciones Científicas (CONICET)-Universidad Nacional General San Martín (UNSAM), Chascomús, Argentina, ² Pharmacology and Toxicology, Indiana University School of Medicine, Indianapolis, IN, United States, ³ Microbiology and Immunology, Indiana University School of Medicine, Indianapolis, IN, United States

OPEN ACCESS

Edited by:

Kamal El Bissati,
University of Chicago, United States

Reviewed by:

Ying Zhou,
University of Chicago, United States
Elisa Azuara-Liceaga,
Universidad Autónoma de la Ciudad
de México, Mexico

*Correspondence:

Laura Vanagas
lauravanagas@gmail.com
Sergio O. Angel
sangel@intech.gov.ar

[†]These authors have contributed
equally to this work

Specialty section:

This article was submitted to
Parasite and Host,
a section of the journal
Frontiers in Cellular and Infection
Microbiology

Received: 09 October 2018

Accepted: 25 January 2019

Published: 13 February 2019

Citation:

Munera López J, Ganuza A, Bogado SS, Muñoz D, Ruiz DM, Sullivan WJ Jr, Vanagas L and Angel SO (2019) Evaluation of ATM Kinase Inhibitor KU-55933 as Potential Anti-*Toxoplasma gondii* Agent. *Front. Cell. Infect. Microbiol.* 9:26. doi: 10.3389/fcimb.2019.00026

Toxoplasma gondii is an apicomplexan protozoan parasite with a complex life cycle composed of multiple stages that infect mammals and birds. Tachyzoites rapidly replicate within host cells to produce acute infection during which the parasite disseminates to tissues and organs. Highly replicative cells are subject to Double Strand Breaks (DSBs) by replication fork collapse and ATM, a member of the phosphatidylinositol 3-kinase (PI3K) family, is a key factor that initiates DNA repair and activates cell cycle checkpoints. Here we demonstrate that the treatment of intracellular tachyzoites with the PI3K inhibitor caffeine or ATM kinase-inhibitor KU-55933 affects parasite replication rate in a dose-dependent manner. KU-55933 affects intracellular tachyzoite growth and induces G1-phase arrest. Addition of KU-55933 to extracellular tachyzoites also leads to a significant reduction of tachyzoite replication upon infection of host cells. ATM kinase phosphorylates H2A.X (γ H2AX) to promote DSB damage repair. The level of γ H2AX increases in tachyzoites treated with camptothecin (CPT), a drug that generates fork collapse, but this increase was not observed when co-administered with KU-55933. These findings support that KU-55933 is affecting the *Toxoplasma* ATM-like kinase (TgATM). The combination of KU-55933 and other DNA damaging agents such as methyl methane sulfonate (MMS) and CPT produce a synergic effect, suggesting that TgATM kinase inhibition sensitizes the parasite to damaged DNA. By contrast, hydroxyurea (HU) did not further inhibit tachyzoite replication when combined with KU-55933.

Keywords: *Toxoplasma gondii*, DNA repair, cell cycle, fork collapse, antiparasitic drugs

INTRODUCTION

Toxoplasma gondii is a widespread protozoan parasite that infects humans and warm-blooded animals. Although the course of toxoplasmic infection is usually asymptomatic, severe problems, and even death can occur in immunocompromised individuals (e.g., AIDS, transplantation) or as a result of congenital infection. In HIV patients, reactivation of the infection can cause neurological defects, encephalitis, and chorioretinitis; congenital toxoplasmosis is responsible for neurological defects, chorioretinitis, and in some cases abortion (Luft and Remington, 1992; Moncada and Montoya, 2012). The life cycle of *Toxoplasma* includes the sexual stage (sporozoite), which occurs only in the definitive host (felines), and asexual stages (tachyzoite and bradyzoite), both occurring

in all mammals and birds (Dubey, 1994). It is generally accepted that the highly replicative tachyzoites produce clinical symptoms whereas the bradyzoites (which reside within intracellular tissue cysts) cause the asymptomatic latent infection with the ability to reconvert into tachyzoites. However, recent associations have been made between chronic *Toxoplasma* infection and neurological disorders, such as schizophrenia (Torrey et al., 2012; Sutherland et al., 2015; Flegr and Horacek, 2017; Fuglewicz et al., 2017; Yolken et al., 2017).

The frontline treatment for toxoplasmosis includes anti-folate drugs, which are only effective against the tachyzoite stage and produce serious adverse effects and allergic reactions (Luft and Remington, 1992; Carlier et al., 2012). There is no effective treatment for chronic toxoplasmosis as no drug is known to eliminate tissue cysts. Newer, safer drugs effective in treating toxoplasmosis are urgently needed.

Rapidly replicating cells such as tachyzoites must contend with DNA damage. *Toxoplasma* tachyzoites cultured *in vitro* show detectable basal levels of γ H2A.X, a marker of DNA damage, as revealed by Western blot and mass spectrometry analysis (Dalmasso et al., 2009; Nardelli et al., 2013). Histone H2A.X is a H2A variant with a SQE C-terminal motif that can be modified by a kinase, generating the phosphorylated form γ H2A.X. The spreading of γ H2A.X at both sides of a double strand break (DSB) is one of the earliest events involved in the DNA damage response (DDR) to different genotoxic stresses and occupies megabase chromatin domains (Rogakou et al., 1998, 1999; Redon et al., 2002; Martin et al., 2003). H2A.X phosphorylation is mediated by members of phosphatidylinositol 3-kinase family (PI3K) such as Ataxia telangiectasia mutated (ATM) kinase, ATM Rad-3-related (ATR), and DNA dependent protein kinase (DNA-PK). ATM kinase and DNA-PK are involved mainly in DSB repair whereas ATR is associated with single strand DNA (ssDNA) and stalled replication forks (Branzei and Foiani, 2008). ATM is the key kinase for H2A.X phosphorylation after DSB, and also phosphorylates other cell cycle and DDR proteins, allowing the γ H2A.X foci generation and DDR either by non-homologous end joining (NHEJ) or homologous recombination repair (HRR) (Bakkenist and Kastan, 2003). DNA-PK is activated through its interaction with Ku and is associated with the NHEJ pathway (Pannunzio et al., 2017), however, DNA-PK and ATM kinase have overlapping functions to phosphorylate H2A.X after ionizing radiation DNA damage (Stiff et al., 2004; Wang et al., 2005). ATM kinase also phosphorylates H2A.X and DNA-PK in response to DSB produced by the topoisomerase I inhibitor camptothecin (CPT) or topoisomerase II inhibitor mitoxantrone (Kurose et al., 2005; Cristini et al., 2016). Various cellular mechanisms work to ensure the integrity of the genome during DNA replication, but sometimes fork stalling occurs and generates ssDNA. In the event that the lesion cannot be repaired, the forks collapse, generating one-end DSB that requires DDR. Among factors that are recruited to one-end DSB are the Mre11-Rad50-Nbs1/Xrs2 complex and ATM kinase (Lee and Paull, 2005). DSBs produced by fork collapse generated by topoisomerase I inhibitor topotecan require ATM kinase for the completion of HRR (Kurose et al., 2005; Tanaka et al., 2006; Kocher et al., 2013). γ H2A.X can

also appear by chemical and environmental agents that do not induce DSBs, such as benz[a]pyrene, which leads to formation of covalent DNA adducts. In this case, H2A.X phosphorylation has shown to be induced by ATM, ATR, or DNA-PK kinases (Yan et al., 2011). Hyperthermia and heat shock can also cause ATM-dependent γ H2A.X induction (Hunt et al., 2007; Takahashi et al., 2010). Among targets of ATM kinase is Hsp90a; phosphorylation of Hsp90a at threonine 5 and 7 correlates with an increase in γ H2A.X (Elaimy et al., 2016).

The *Toxoplasma* ATM (TgATM) kinase (Vonlaufen et al., 2010) seems to be essential as observed by a CRISPR-screen assay (Sidik et al., 2016), along with other PI3Ks (Table 1). These findings suggest an important biological role for such kinases under normal growth conditions. There are several compounds (caffeine, KU-55933 and derivatives) that have shown inhibitory effects against PI3K kinases and were studied as promising candidates for cancer therapy (Bode and Dong, 2007; Kuroda et al., 2012; Batey et al., 2013; Teng et al., 2015). Caffeine is a non-specific PI3K inhibitor whose targets include ATM kinase at IC₅₀ of 0.2 mM, ATR kinase at IC₅₀ of 1.1 mM, DNA-PK at IC₅₀ between 0.2 and 0.6 mM (Block et al., 2004), and other targets (Bode and Dong, 2007). By contrast, KU-55933 is a potent and selective ATP-competitor of ATM kinase at IC₅₀ of 12.9 nM (Hickson et al., 2004).

DNA replication and repair pathways are promising drug targets for the development of novel antiparasitic. In the present study, we analyzed the effect of the ATM kinase inhibitors caffeine and KU-55399 on tachyzoites *in vitro*. We observed that both inhibitors impair *T. gondii* replication. The presence of KU-55933 also inhibits H2A.X phosphorylation in intracellular tachyzoites cultured in presence of camptothecin (CPT), a topoisomerase I venom (Hickson et al., 2004; Tomicic and Kaina, 2013; Botella and Rivero-Buceta, 2017). The combination of KU-55933 and DNA damaging agents such as CPT or methyl methane sulfonate (MMS) showed a synergic effect in slowing parasite growth. The impact of our findings in light of the discovery of future drug targets in toxoplasmosis is discussed.

MATERIALS AND METHODS

Parasite Culture

Wild-type RH strain parasites and RH RFP, which express red fluorescent protein (van Dooren et al., 2008), were cultured in standard tachyzoite conditions *in vitro*: human foreskin fibroblast (HFF) monolayers were infected with tachyzoites and incubated in Dulbecco's modified Eagle medium (DMEM, GIBCO) supplemented with 10% fetal bovine serum, penicillin (100 UI/ml; GIBCO), and streptomycin (100 μ g/ml; GIBCO) at 37°C and 5% CO₂.

Chemicals and Antibodies

Camptothecin (CPT, Sigma-Aldrich Argentina, catalog number C9911) was dissolved in DMSO at a concentration of 1 mM and stored at -20°C as stock solution. Caffeine (Sigma-Aldrich Argentina, catalog number C0750) was dissolved in water at a concentration of 100 mM and stored at -20°C as stock solution. KU-55933 (Calbiochem catalog number 118500) was dissolved in

TABLE 1 | Domain structure of *T. gondii* phosphatidylinositol 3- and 4-kinase (PIKK) domain-containing proteins.

Gene ID (e.g., TGME49)	NLS	FAT	PRD	FATC	MW (kDa)	Blastp	Phenotype Score ^a
_248530	2	NO	ND	1	246	HuATM	−2.71
_266010	1	NO	ND	1	964	DNA-PK	−3.15
_268370	2	1	1	1	904	HuTRRAP	−3.56
_283702	NO	NO	1	1	647	HuATR	−2.68
_316430	2	1	1	1	543	mTOR	0.21

These PI3,4K putative proteins were retrieved from www.toxodb.org based on Blast analysis by using Human ATM (AAB65827), ATR (CAA70298), and DNA-PK (AAB39925) aminoacidic sequences. Domains and motifs were searched by using motifscan (<http://hits.isb-sib.ch/cgi-bin/PFSCAN>). FAT, FRAP (FKBP12-rapamycin-associated protein)-ATM-TRRAP (Transformation/transcription domain-associated protein) domain; PRD, PIKK regulatory domain; FATC, FAT-C-terminal domain. HuTRRAP, transformation/transcription domain-associated protein, isoform CRA_e (EAW76697). mTOR: mammalian Target Of Rapamycin (NP_004949). mRNA sequence is obtained by exon/intron prediction on genome sequence. For this reason, the gene, ORF, and protein sequences are subjected to future modifications.

ND: not detected

^a"Genome-wide loss of function screen (CRISPR) that measures each gene's contribution to *Toxoplasma gondii* fitness during infection of human fibroblasts. Phenotype score = \log_2 (sgRNA of infected cultures/sgRNA composition of original library)" (www.toxodb.org). Negative score, fitness conferring; positive score, dispensable.

DMSO at a concentration of 10 mM and stored at -20°C as stock solution. Hydroxyurea (HU, Sigma-Aldrich Argentina, catalog number H8627-5G) was dissolved in water at a concentration of 50 mg/ml as stock solution and disposed after use. Methyl methane sulfonate (MMS, Sigma-Aldrich Argentina, catalog number 129925-5G, liquid, 11,8 M) was dissolved in DMEM at the concentrations indicated for each assay and disposed after use.

Anti- γH2AX antibody was obtained from Merck Argentina (JBW301). Rabbit anti-*Toxoplasma* H2A.X and Hsp90 were previously produced in our laboratory (Echeverria et al., 2005; Dalmaso et al., 2009). Anti-actin antibody was kindly provided by Jean F. Dubremetz (Université de Montpellier, Montpellier, France). Murine anti-SAG1 antibody was kindly provided by Marina Clemente (Albarracín et al., 2015). Mouse monoclonal anti-H3 antibody was purchased from Abcam (10799). Alexa fluor goat antibodies anti-mouse 594 (A-11032), anti-rabbit 594 (A-11037), anti-mouse 488 (A-11001), and anti-rabbit 488 (A-11034) were purchased from Invitrogen.

Replication Assay

The replication rate was determined in infected monolayers, treated or untreated with different doses of caffeine, KU-55933 or CPT. Coverslips with confluent HFFs were infected with 1×10^4 parasites (MOI: 0.1 Tachyzoites/host cell). After 1 h of incubation, cells were washed three times with PBS and incubated 12–48 h in DMEM plus treatment, then cells were analyzed by indirect immunofluorescence (IFA) to facilitate counting. Briefly, they were fixed with 4% (v/v) paraformaldehyde and blocked with 1% BSA. Primary antibodies anti-SAG1 diluted 1:100 with 0.5% BSA or anti-*T. gondii* Hsp90 1:2,000 were incubated at room temperature for 1 h. After several washes with PBS, they were incubated with secondary antibodies Alexa fluor goat anti-mouse 594 or Alexa fluor goat anti-mouse 488 (Invitrogen). Cover slips were washed three times and mounted in Fluoromont G (Southern Biotechnology Associates) and viewed using a Nikon Model Eclipse E600 (magnification 100X, numerical aperture 1,40 at 24°C). Green or red fluorescence were recorded separately and the images were analyzed by Image-Pro Plus version 5.1.0.20 and merged using Adobe Photoshop. Parasites

in 100 randomly chosen parasitophorous vacuoles (PV) were counted in triplicate. Data are presented as the average number of tachyzoites per PV. IC_{50} was obtained by GraphPad Prism 6: data were normalized with 0 as the smallest value and transformed to semi-logarithmic scale [$x = \log(x)$]. After that, they were analyzed as a nonlinear regression parameter-Dose-response inhibition- $\log(\text{inhibitor})$ vs. normalized response-variable slope.

RH RFP Fluorescence Assay

Fluorescence assay was carried out using an RH strain parasite clone engineered to express Red Fluorescent Protein (RFP), kindly provided by Silvia Moreno (University of Georgia, Athens, Georgia). RH RFP tachyzoites were used to infect HFF monolayer in a 96-well plate with or without the indicated drugs. Fluorescence values were measured 4 days post-infection and both excitation (544 nm) and emission (590 nm) were read from the bottom of the plates in a microplate reader (Synergy H1). Data were plotted and analyzed using GraphPad Prism 6 software.

Cell Cycle

HFF cells were grown to confluence in 6 well plates then infected with 1×10^6 RH tachyzoites per well and treated with 60 μM pyrrolidine dithiocarbamate (PDTS) for 6 h in DMEM (Conde de Felipe et al., 2008). Plates were then washed with PBS and incubated with 5 μM KU-55933, 4 mM HU, or 0.1%v/v DMSO for 7 h. Plates were washed with PBS and the cells were harvested with trypsin, passed through different sizes of needles to lyse the host cells and finally the parasites were filtered using a 3 μm filter. Purified parasites were centrifuged at 2,000 RPM for 10 min and washed with PBS, then fixed with 70% ethanol, and incubated 24 h at -20°C . Afterwards, samples were centrifuged and washed with PBS supplemented at 2% with FBS. After centrifugation again, they were resuspended in 1 ml of supplemented PBS + 180 μg / ml RNase and incubated for 10 min at 37°C . Finally, they were incubated with Propidium Iodide (0.5mg / ml) for 10 min before carrying out the measurement in the BD FACS Calibur flow cytometer and analyzed by FlowJo 7.6.

Immunoblotting

Proteins from purified parasites were resolved by SDS-PAGE and transferred onto a nitrocellulose membrane. Non-specific binding sites were blocked with 5% non-fat-dried milk in PBS containing 0.05% Tween-20 (PBS-T) and the membranes were then incubated (1 h at room temperature) with primary antibodies. The antibodies and dilutions used in this study were: murine anti- γ H2AX (1:1000) from Millipore (05-636), anti-actin (1:500), anti-H3 (1:1,000), and antibodies produced by our laboratory: rabbit anti-H2A.X (1:5,000) (Dalmasso et al., 2009). The membranes were washed several times with TBS-T prior to incubation with alkaline phosphatase-conjugated anti-rabbit or anti-mouse secondary antibodies, diluted 1:10,000 (Santa Cruz Biotechnology). Immunoreactive protein bands were visualized by the NBT-BCIP method (Sigma-Aldrich™ Argentina S.A). Intensities of bands were quantified from scanned images using ImageJ software.

RESULTS

Effect of Caffeine PI3K Inhibitor on Tachyzoite Replication and Growth

The inhibition of PI3K kinases such as ATM and ATR can block the correct DDR at DSB (Figure 1). There is evidence of putative homologs of ATM, ATR, and DNA-PK PI3K kinases in *Toxoplasma* [Table 1 and (Vonlaufen et al., 2010)]. Based on human ATM domain organization (Stracker et al., 2013), the most similar regions among ATM/Tel1 kinases involve the PI3K domain (Figure S1). In order to test whether PI3K inhibitors affect tachyzoite replication, infected monolayers were treated with different doses of caffeine, which is a broad-spectrum kinase inhibitor with known activity against ATM, and ATR kinases (Sarkaria, 2003; Bode and Dong, 2007). Intracellular tachyzoites were incubated with caffeine for 48 h and then the number of parasites per parasitophorous vacuole (PV) was counted. Caffeine significantly slowed the tachyzoite replication rate in a dose-dependent manner with an $IC_{50} = 370 \mu M$ (Figure 2A). In addition, the effect of caffeine on tachyzoite growth was also determined. Figure 2B shows that doses higher than $200 \mu M$ significantly affect tachyzoite growth and completely abolished it at $800 \mu M$. MTT (3-(4,5-dimethylthiazol-2-yl)-2,5-diphenyl-tetrazolium bromide) assay did not evidence impact of caffeine on HFF metabolism (Figure S2). In addition, caffeine did not disturb neither shape nor “rosette” organization of tachyzoites within PV (Figure 2C).

Effect of ATM Kinase Inhibitor KU-55933 in *Toxoplasma* Cell Cycle and Growth

As caffeine likely has multiple PI3K targets that could adversely affect parasite replication, we sought to test whether KU-55933, an established and selective ATM kinase inhibitor, had an effect on tachyzoite growth *in vitro*. Our findings show that *Toxoplasma* replication was affected by KU-55933 in a dose dependent manner with an $IC_{50} = 2.15 \mu M$ (Figure 3A).

In order to study how KU-55933 affects the tachyzoite cell cycle, intracellular parasites were grown in presence of

PDTs to synchronize the tachyzoites in G1. After releasing of PDTs treatment intracellular tachyzoites were grown for 7 h in the presence of DMSO, $5 \mu M$ KU-55933, or 4 mM HU. Following treatment with KU-55933, parasites show a significant enrichment in DNA content compatible with G1-phase in comparison with the observed in the control and similar to the observed with HU and tachyzoites arrested in G1 (DMEM group) (Figure 3B).

To confirm the effect observed in tachyzoites treated with KU-55933, RFP expressing tachyzoites were cultured in presence of KU-55933 or DMSO, showing a significant reduction of tachyzoite growth in a dose-dependent manner and with $IC_{50} = 2.49 \mu M$ (Figure 3C).

The presence of KU-55933 at these concentrations did not induce alterations in uninfected HFF monolayer morphology and MTT assay did not evidence impact of KU-55933 on HFF metabolism (Figure S2). In addition, KU-55933 did not disturb neither shape nor “rosette” organization of tachyzoites within PV (Figure 3D).

These results indicate that KU-55933 has a detrimental effect on intracellular tachyzoite replication. However, the indirect effect of PI3K inhibitors on tachyzoite replication due to HFF alterations, specifically at high doses, cannot be ruled out. To investigate if KU-55933 can have an effect directly on *Toxoplasma*, extracellular tachyzoites were incubated 4 h in presence of different doses of KU-55933 at room temperature. After that HFF monolayers were infected and incubated in absence of the drug for 12 h. Figure 3E shows a significant reduction in tachyzoite replication from $2.5 \mu M$, suggesting that KU-55933 has a direct impact on *Toxoplasma*.

KU-55933 Inhibits *Toxoplasma* H2A.X Phosphorylation at Serine 132 Under Fork Collapse

During cell replication DNA is duplicated in the S-phase, and replication forks remain stable until completion of DNA duplication. However, replication forks are subject to a variety of insults (dNTP depletion, DNA damage, DNA secondary structures, among others) that lead to fork stalling. The presence of several ssDNA and/or regressed forks (a structure also named “chickenfoot” in which complementary daughter ssDNAs regress and pair between them) promotes the collapse of forks and DSB (Postow et al., 2001; Alexander and Orr-Weaver, 2016). Camptothecin (CPT) is a topoisomerase I inhibitor that generates fork collapse, producing DSB and therefore γ H2A.X, and induction of the HRR pathway (Chanoux et al., 2009; Xu et al., 2015; Rybak et al., 2016). We used CPT to further analyze KU-55933 activity, using the generation of γ H2A.X in *Toxoplasma* as a marker of DSB in genomic DNA of tachyzoites. As it is known, ATM is able to phosphorylate SQ/TQ motif (Weber and Ryan, 2015) which is present in *T. gondii* H2A.X (SQEF) and detected by commercial γ H2A.X (Dalmasso et al., 2009; Vonlaufen et al., 2010). Despite we purified *T. gondii* tachyzoites through $3 \mu m$ nitrocellulose filters before Western blot analysis, we tested the possibility to detect any contamination of HFF host cell. As observed in Figure S3, in our conditions anti- γ H2A.X only

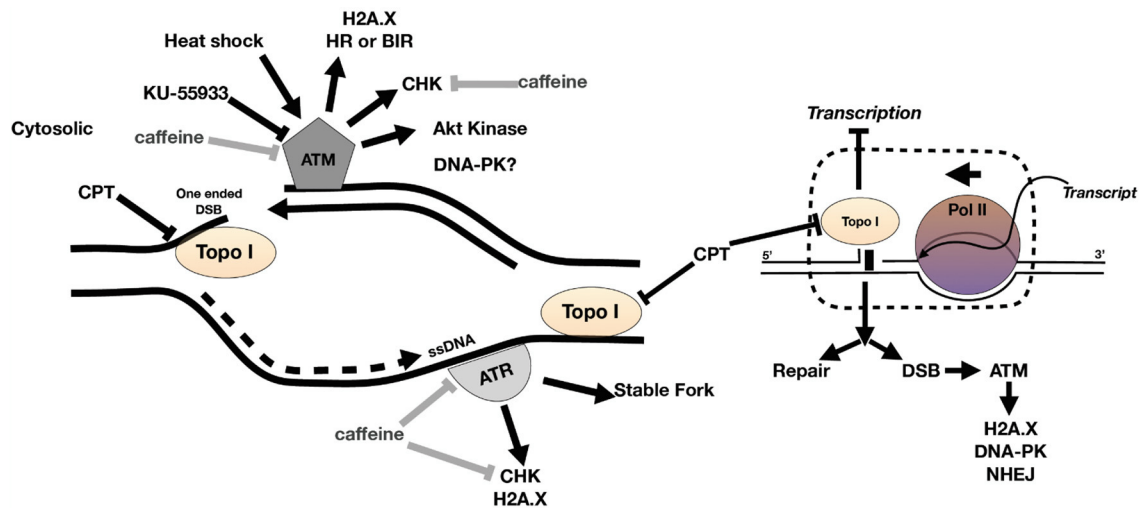


FIGURE 1 | Model of DNA damage at fork during replication. ATR binds to ssDNA at a stalled fork to stabilize the fork. ATM kinase binds to one-ended DSB at collapsed fork. DNA damage activates ATM and ATR to phosphorylate DNA damage response (DDR) proteins such as H2A.X and checkpoint kinases, the latter blocking the cell cycle until DNA is repaired (or apoptosis commences). The collision of replication fork and transcription fork can also generate DSB and recruitment of DDR factors including ATM kinase. CPT is a topoisomerase I (topo I) venom and can cause fork collapse and DSB during DNA replication. Caffeine inhibits ATM and ATR kinase activity and KU-55933 inhibits ATM kinase.

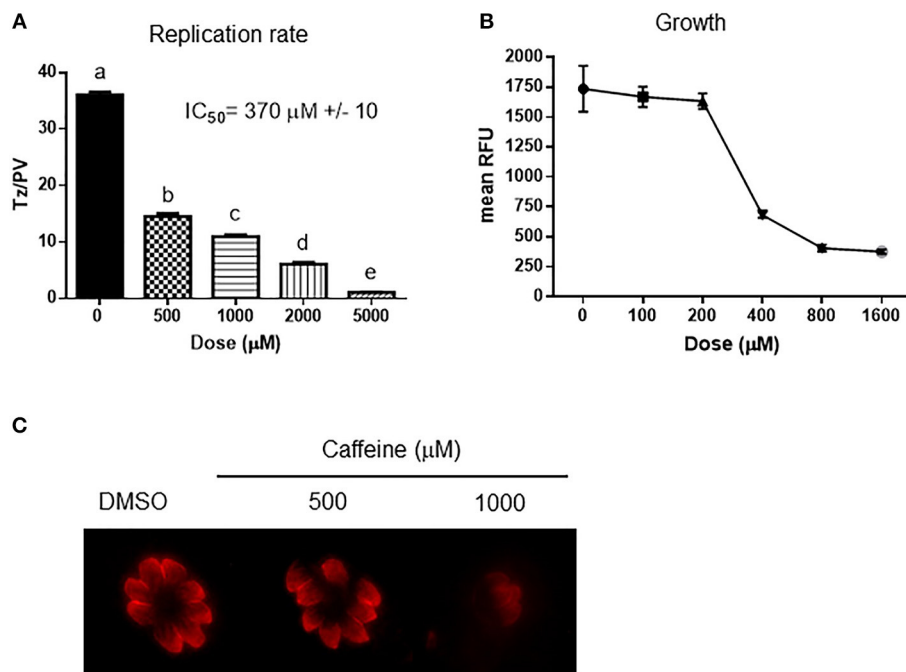


FIGURE 2 | Effect of caffeine on *Toxoplasma* replication and growth. **(A)** Intracellular tachyzoites were grown in culture with DMSO or different doses of caffeine during 48 h. After that, they were fixed and stained with anti-tubulin. Tachyzoites per parasitophorous vacuole (Tz/PV) were counted in 100 randomly chosen vacuoles. Statistical analysis was performed by one-way ANOVA and Tukey's Multiple Comparison Test. Results are the mean of three replicates plus SD. Different letters indicate statistically significant differences between columns ($p \leq 0.05$), according to one-way ANOVA, and Tukey's multiple comparison test. Details: $p \leq 0.001$: a vs. b, c, d, and e; $p \leq 0.001$: b vs. c, d, and e; $p \leq 0.001$: c vs. d and e; $p \leq 0.001$: d vs. e. The graph is representative of three independent experiments with similar results. **(B)** Intracellular tachyzoites from RH RFP strain were treated with Caffeine at different doses during 96 h and their growth analyzed at 544 nm. Results were plotted by GraphPad Prism 6. Results are mean of three replicates plus SD. **(C)** Arrangement of tachyzoites inside PV is visualized at different doses of caffeine. In presence of DMSO, or caffeine up to 1,000 μM the typical rosette organization could be observed. PV with similar number of tachyzoites were selected to compare.

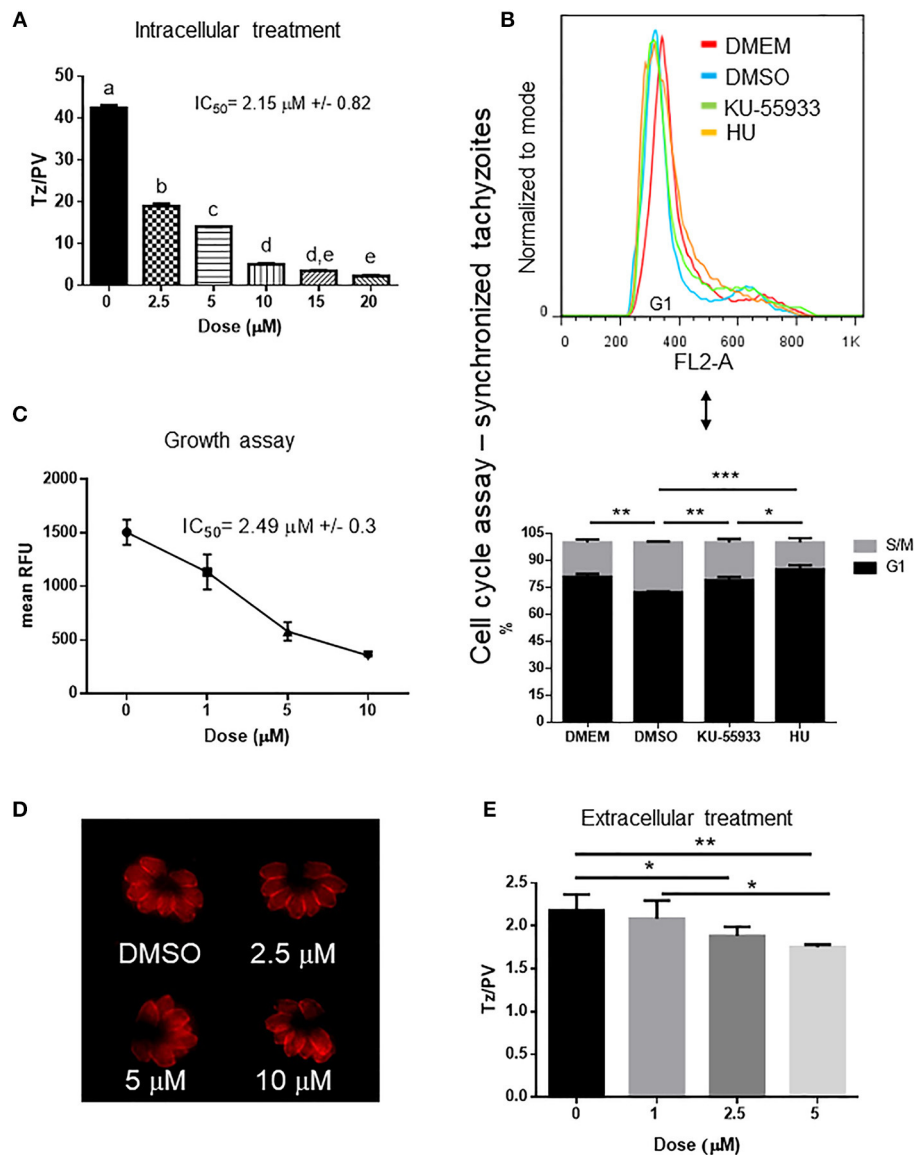


FIGURE 3 | Effect of ATM kinase inhibitor KU-55933 on *Toxoplasma* replication and growth. Intracellular tachyzoites were grown in culture with DMSO or different doses of KU-55933 during 48 h. After that, they were fixed and stained with anti-tubulin. **(A)** Tachyzoites per PV (Tz/PV) were counted in 100 PV. Statistical analysis was performed by one-way ANOVA and Tukey's Multiple Comparison Test. Results are mean of three replicates plus SD. Same letters above the column indicate no significant differences; different letters indicate statistically significant differences between columns ($p \leq 0.05$), according to one-way ANOVA, and Tukey's multiple comparison test. Details: $p \leq 0.0001$: a vs. b, c, d, and e; $p \leq 0.0001$: b vs. c, d, and e; $p \leq 0.0001$: c vs. d and e; $p \leq 0.01$: d vs. e. The graph is representative of three independent experiments with similar results. **(B)** Tachyzoites were added to confluent HFF host cells during 16 h and treated with PDTs for 6 h. Plates were then washed with PBS and incubated with 5 μ M KU-55933, 4 mM HU or 0.1%v/v DMSO for 7 h and propidium iodide used to stain DNA. The tachyzoites were analyzed by FACS and DNA content was determined (G1: 1N). Statistical analysis was performed with one-way ANOVA and Tukey's multiple comparison test ($*p \leq 0.05$; $**p \leq 0.01$, and $***p \leq 0.001$). **(C)** Intracellular tachyzoites (RH RFP strain) were cultured in presence of DMSO or different doses of μ M KU-55933 in 96-well plates for 4 days and then read at 544 nm (bottom of the plate) in a microplate reader. Results are means of six replicates plus SD. The graph is representative of three independent experiments with similar results. **(D)** Arrangement of tachyzoites inside PV is visualized at different doses of KU-55933. In presence of DMSO or the drug the typical rosette organization could be observed. PV with similar number of tachyzoites were selected to compare. **(E)** Extracellular tachyzoites were incubated for 4 h with DMSO or different doses of KU-55933. After that, they were added to HFF monolayers and incubated for 12 h in normal conditions. Replication rate was analyzed as in **(A)**. Statistical analysis was performed with one-way ANOVA and Tukey's multiple comparison test ($*p \leq 0.05$; $**p \leq 0.01$). Results are mean of three replicates plus SD.

detected a band in *T. gondii* lysate but not in HFF (Figure S3), suggesting that the experiment avoids putative false results due to the presence of HFF γ H2A.X. The treatment with CPT increases the presence of γ H2A.X in *Toxoplasma* as analyzed by Western

blot (Figure 4A). The treatment of intracellular tachyzoites with KU-55933 did not block basal levels of γ H2A.X, but the presence of KU-55933 in combination with CPT reduced γ H2A.X levels compared parasites treated with CPT (Figure 4A).

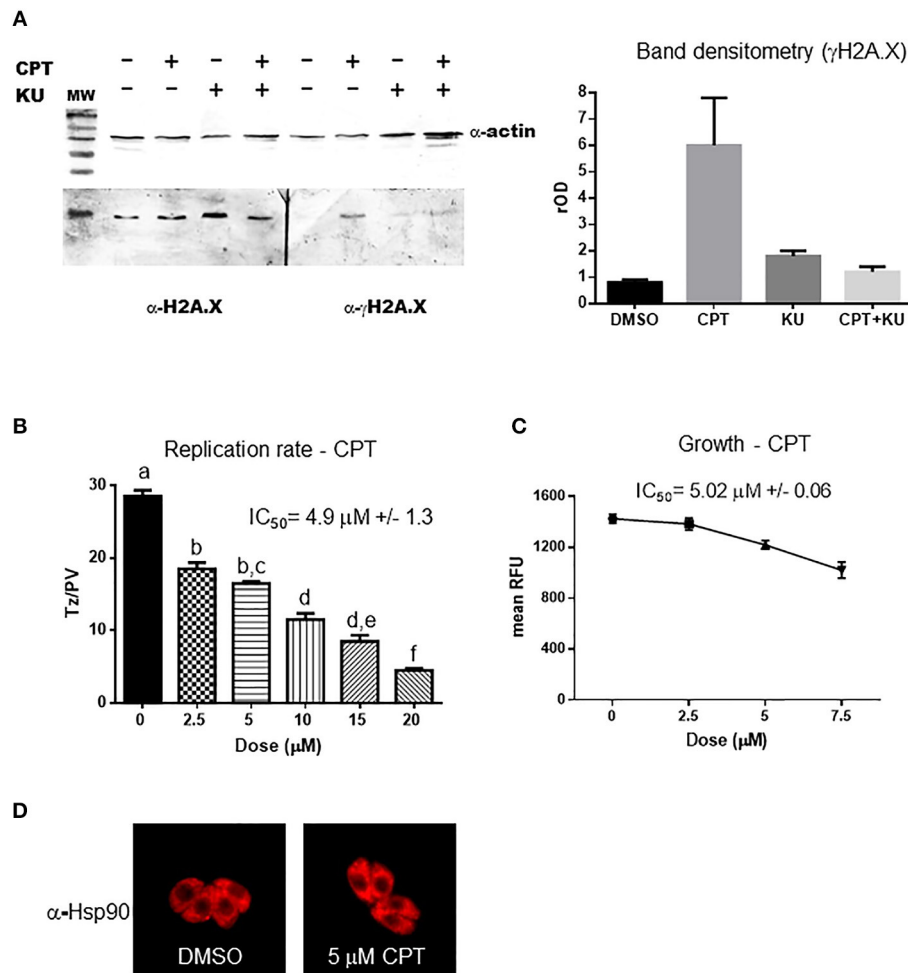


FIGURE 4 | Campthothecin effect on H2A.X phosphorylation and tachyzoite replication. **(A)** Extracts of intracellular tachyzoite treated with 5 μ M CPT, 5 μ M KU-55933, both or DMSO for 24 h were analyzed by Western blot with anti- γ H2AX antibody (α - γ H2AX) and anti-*Toxoplasma* H2A.X. Anti-actin (α -actin) antibody was used as control of loaded protein. Band density was measured and relativized to DMSO (rOD). The graph is representative of three independent experiments with similar results. **(B)** Tachyzoites per PV (Tz/PV) were counted in 100 PV. Statistical analysis was performed by one-way ANOVA and Tukey's Multiple Comparison Test. Results are mean of three replicates plus SD. Same letters above the column indicate no significant differences; different letters indicate statistically significant differences between columns ($p \leq 0.05$), according to one-way ANOVA and Tukey's multiple comparison test. Details: $p \leq 0.0001$: a vs. b, c, d, e, and f; $p \leq 0.001$: b vs. d; $p \leq 0.0001$: b vs. e and f; $p \leq 0.01$: c vs. d; $p \leq 0.0001$: c vs. e and f; $p \leq 0.001$: d vs. f; $p \leq 0.05$: e vs. f. The graph is representative of three independent experiments with similar results. **(C)** Intracellular tachyzoites (RH RFP strain) were cultured in presence of DMSO or different doses of CPT in 96-well plates for 4 days and then read at 544 nm (bottom of the plate) in a microplate reader. Results are means of six replicates plus SD. **(D)** Arrangement of tachyzoites inside PV is visualized at 5 μ M CPT. In presence of DMSO or the drug the typical rosette organization could be observed. PV with similar number of tachyzoites were selected to compare.

CPT treatment of infected HFF showed an inhibition of parasite replication rate and growth in a dose-dependent manner with $IC_{50} = 4.9$ and $5.02 \mu M$, respectively, (Figures 4B,C). CPT at these concentrations did not induce morphological alterations in uninfected HFF monolayers but a strong reduction of HFF metabolism was observed by MTT assay from 2.5 μ M (Figure S2). However, the addition of 5 μ M CPT did not disturb neither shape nor "rosette" organization of tachyzoites within PV (Figure 4D).

Our findings show that CPT generates DSB in the *Toxoplasma* genome, as evidenced by the increase in γ H2A.X. The fact that this phosphorylation event could be abolished by the inhibitor

KU-55933 during DNA damage suggests that it is mediated by TgATM kinase.

Effect of CPT, Methyl Methane Sulfonate (MMS) and Hydroxyurea (HU) in Combination With KU-55933 on Tachyzoites

In order to test the effect of other DNA damaging agents on *Toxoplasma* replication, we analyzed methyl methane sulfonate (MMS) and hydroxyurea (HU) (de Melo et al., 2000; Vonlaufen et al., 2010) using *Toxoplasma* RFP parasites, treated alone or

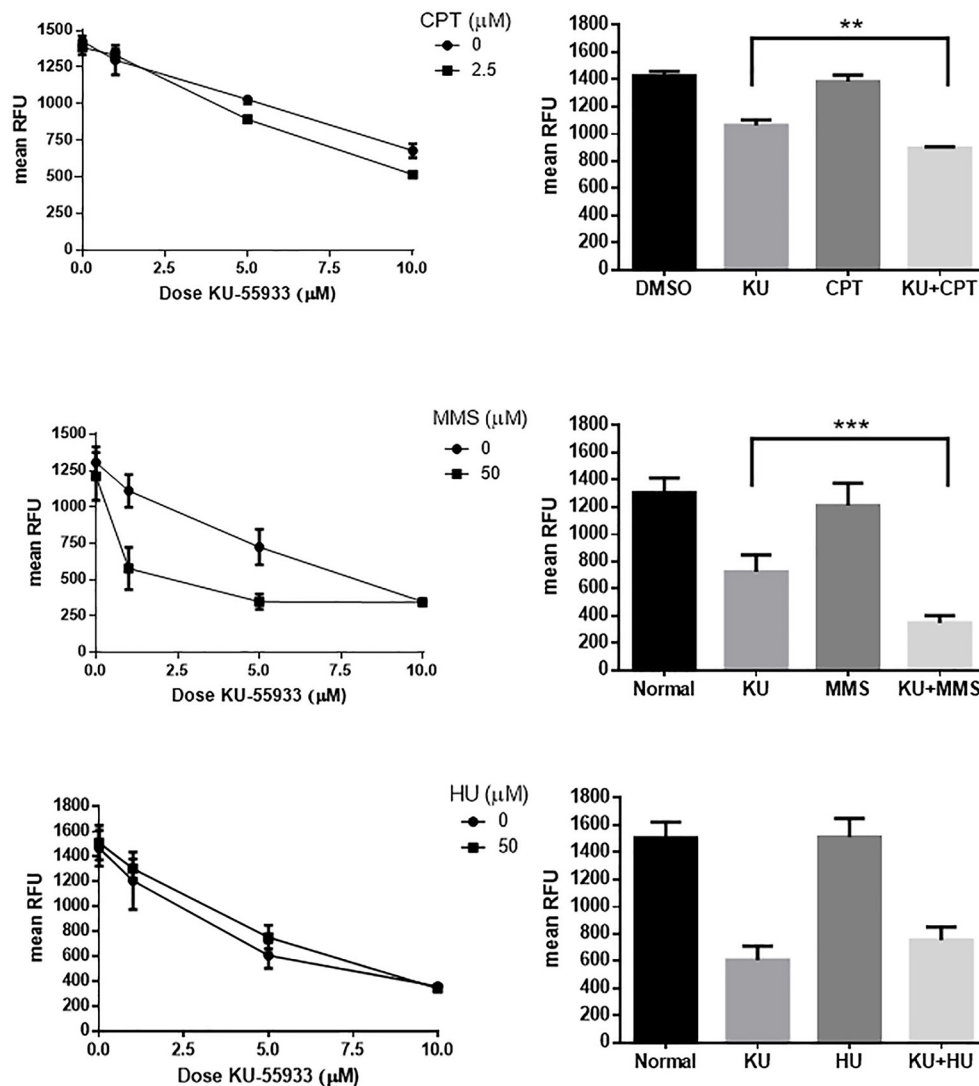


FIGURE 5 | Effect on *Toxoplasma* ATM kinase with different DNA damaging agents. Intracellular tachyzoites (RH RFP strain) were treated with 2.5 μ M CPT, 50 μ M MMS, or 50 μ M HU alone or in combination with KU-55933 at different doses during 96 h and their growth analyzed at 544 nm. As control DMSO (CPT) or PBS (MMS and HU) were used. Results were plotted by GraphPad Prism 6 (left panels). Combination of 5 μ M KU-55933 and 2.5 μ M CPT, 50 μ M MMS, and 50 μ M HU, and controls, were plotted as bar graphs (right panels). Statistical analysis was performed by one-way ANOVA and Tukey's Multiple Comparison Test. Results are mean of three replicates plus SD. There were not significant differences between DMSO and CPT, normal and MMS or normal and HU. Only differences between KU-55933 and combination is shown. ** $p \leq 0.01$; *** $p \leq 0.001$, according to one-way ANOVA and Tukey's multiple comparison test. The graph is representative of three independent experiments with similar results.

in combination with KU-55933. A dose of 2.5 μ M CPT in combination with KU-55933 was also analyzed. HU and MMS both block tachyzoite replication at concentrations higher than 50 μ M (Figure S4). KU-55933 treatment administered with CPT or MMS increased the inhibitory effect of KU-55933 whereas HU in combination with KU-55933 presented no synergistic effect (Figure 5).

DISCUSSION

In this study, we demonstrated that PI3K inhibitors such as caffeine and KU-55933 are able to block *Toxoplasma* tachyzoite

replication. A previous study has shown that caffeine, as an agonist of ryanodine-responsive calcium-release channels, increased the level of intracellular Ca^{2+} in *Toxoplasma* (Chini et al., 2005). In our study, we found that caffeine also produces a strong effect on intracellular tachyzoite replication. CGK 733, an ATM/ATR kinases inhibitor, has been shown to block *Toxoplasma* tachyzoite growth in a recent small molecule screen (Dittmar et al., 2016). These collective studies suggest that PI3 kinases, including ATM/ATR kinases, are important modulators for parasite growth and replication, and thus serve as attractive drug targets.

Whereas, caffeine targets a broad range of kinases and phosphatases (Velic et al., 2015), KU-55933 is specific for human

ATM kinase ($IC_{50} = 12.9 \text{ nM}$) being able to inhibit DNA-PK and ATR at $IC_{50} = 2.5$ and $16.6 \mu\text{M}$, respectively (Hickson et al., 2004). KU-55933 blocks tachyzoite replication and generates G1-phase arrest, suggesting that TgATM kinase may have a role along *Toxoplasma* cell cycle. ATM kinase has a large number of substrates associated with the DDR, especially those involved in DSB repair (Matsuoka et al., 2007). Interestingly, the effect of KU-55933 on tachyzoite replication and growth was observed without any exogenous DNA damage treatment, suggesting that ATM kinase is required during tachyzoite cell cycle. Since ATM kinase is a key kinase that triggers the DDR during checkpoints when DSBs are present in DNA, it is possible that the demands of rapid tachyzoite replication create DNA replication stress and fork collapse generating one-ended DSB, similar to what is observed in cancer cells (Hickson et al., 2004; Alexander and Orr-Weaver, 2016; Zhang et al., 2016). Recently, it was observed that DDR associated with ATM kinase and histone ubiquitination is required for proper DNA replication in cells without S-phase perturbation (Schmid et al., 2018). The presence of basal $\gamma\text{H2A.X}$ is consistent with this conclusion.

When studying the effects of drugs on intracellular parasites, it is hard to rule out their potential effect on the host cells. One way to address this issue is to treat extracellular parasites with the drugs prior to infecting host cells. For example, the treatment of human retinal pigment epithelial cells, ARPE-19 with different PI3K inhibitors such as LY294002, wortmannin, GDC-0941, and ZSTK474, during 1 h prior to *T. gondii* infection blocked tachyzoite replication by reducing activation of host AKT (Zhou et al., 2013). We found that pre-incubation of extracellular tachyzoite with KU-55933 led to a significant reduction of tachyzoite replication following infection of HFFs. This result suggests KU-55933 can act directly on TgATM kinase and impede its ability to function during infection. Since extracellular tachyzoite is not a replicative stage, the effect of KU-55933 at this stage is intriguing. One explanation could be that KU-55933 is affecting the fitness of extracellular tachyzoites that need to recover after invasion. In this sense, ATM kinase has also been described to have a role in peroxisomes activating some proteins in response to reactive oxygen species (ROS), among them TORC1 (Alexander et al., 2010; Ditch and Paull, 2012; Zhang et al., 2015). Another explanation may be that treated tachyzoites contains residual traces of KU-55933 after host cell entry, requiring a time for ATM kinase recovery, and its participation in DNA replication process. Further analysis should be done to shed light on this question.

Recently, Dittmar et al. (2016) screened 1,120 compounds for an effect against *Toxoplasma* growth; in their study, KU-55933 at $5 \mu\text{M}$ showed no inhibitory effect, contrasting with our results. We found that the IC_{50} for KU-55933 against *Toxoplasma* was $2.15 \mu\text{M}$, a concentration below the usual dose ($10 \mu\text{M}$) that produces an effect on mammalian cells (Teng et al., 2015; Tian et al., 2015). As ATM kinase is a known target of KU-55933, our results are in agreement with a genome-wide CRISPR screen suggesting that TgATM kinase is essential for tachyzoite viability (Sidik et al., 2016). Importantly, treatment

of tachyzoites with KU-55933 impairs H2A.X phosphorylation, indicating that TgATM kinase is sensitive to KU-55933 during DDR.

Our observations indicate that CPT is able to generate DSB damage on parasite DNA, probably during tachyzoite replication, since it induces an increase of $\gamma\text{H2A.X}$. Our findings lend support to the idea that DNA topoisomerases may also be promising drug targets in Apicomplexan and trypanosomatid parasites (Garcia-Estrada et al., 2010; D'Annessa et al., 2015). However, in our conditions CPT induced a decay in HFF metabolism as measured by MTT assay, suggesting certain toxic effect on host cell. Interestingly, this toxicity did not impair tachyzoite replication inside the host cell, but could affect our interpretation of data relative to blocking *T. gondii* replication. Recently, a novel plasmodial topoisomerase I venom was designed on CPT derivative topotecan structure (Cortopassi et al., 2014). They demonstrated that a compound named LQB223 has a high selectivity for *P. falciparum* topoisomerase I in comparison with human counterpart and reduced *Plasmodium berghei* parasitemia in mice. In the future, a selective *T. gondii* topoisomerase I venom should be analyzed to confirm the value of this therapeutic strategy.

Interestingly, here we demonstrate in a first approach that KU-55933 could have a synergic effect when used in combination with DNA damaging agents such as MMS and CPT, even at low doses. This could be due to the effect of these compounds generating DSB combined with the inhibition of DSB repair by KU-55933. This strategy, opens the possibility to investigate the value of druggable HRR and DNA replication factors. As mentioned above, in the future, a similar strategy could be used but using a *Toxoplasma* specific topoisomerase I venom, possibly LQB223, which could be used in combination with KU-55933, analogs or HRR inhibitors (e.g., Mre11 targets) that are being tested in human.

HU is known to generate fork stalling and activate DDR via ATR kinase rather than ATM kinase (Abraham, 2001), which may explain lack of synergy when combining it with KU-55933. In fact, it was observed that at low doses ($50 \mu\text{M}$), HU cannot present synergic effect with KU-55933 as observed at high doses (e.g., 1 mM) in mammalian cells, in which a ATM-associated G1/S-phase arrest is occurring (Snyder et al., 2009).

In summary, we identified drugs effective in producing DSB in the parasite, and others that affect the mechanisms of DDR. Our findings imply that the mechanisms of DSB repair, for example the HRR pathway that repairs DSBs during DNA replication, could be replete with novel therapeutic targets to combat toxoplasmosis.

AUTHOR CONTRIBUTIONS

JM and AG accomplished most of the assays and the analysis, equally. SB contributed with the standarization of the caffeine, CPT, and KU-55933 experiments. DM performed experiments about *Toxoplasma* cell cycle analysis. DR contributed with the citotoxicity analysis. WS, LV, and SA contributed with the direction, analysis of the data, and writing the manuscript.

ACKNOWLEDGMENTS

SA (Researcher), SB (Fellow), JM (Fellow), LV (Researcher), and DR (Researcher) are members of Consejo Nacional de Investigaciones Científicas y Técnicas (CONICET). A. Ganuza (Technician) is member of Consejo de Investigaciones Científicas (CIC). SA (Full Professor) and LV (Assistant Professor) are also members of Universidad Nacional de San Martín. DM is a Student (Universidad Nacional de San Martín). This work was supported by ANPCyT PICT 1288 (to SA), NIH AI129807

REFERENCES

- Abraham, R. T. (2001). Cell cycle checkpoint signaling through the ATM and ATR kinases. *Genes Dev.* 15, 2177–2196. doi: 10.1101/gad.914401
- Albarracín, R. M., Becher, M. L., Farran, I., Sander, V. A., Corigliano, M. G., Yacono, M. L., et al. (2015). The fusion of *Toxoplasma gondii* SAG1 vaccine candidate to *Leishmania infantum* heat shock protein 83-kDa improves expression levels in tobacco chloroplasts. *Biotechnol. J.* 10, 748–759. doi: 10.1002/biot.201400742
- Alexander, A., Cai, S. L., Kim, J., Nanez, A., Sahin, M., MacLean, K. H., et al. (2010). ATM signals to TSC2 in the cytoplasm to regulate mTORC1 in response to ROS. *Proc Natl Acad Sci USA*. 107, 4153–4158. doi: 10.1073/pnas.0913860107
- Alexander, J. L., and Orr-Weaver, T. L. (2016). Replication fork instability and the consequences of fork collisions from rereplication. *Genes Dev.* 30, 2241–2252. doi: 10.1101/gad.288142.116
- Bakkenist, C. J., and Kastan, M. B. (2003). DNA damage activates ATM through intermolecular autophosphorylation and dimer dissociation. *Nature* 421, 499–506. doi: 10.1038/nature01368
- Batey, M. A., Zhao, Y., Kyle, S., Richardson, C., Slade, A., Martin, N. M., et al. (2013). Preclinical evaluation of a novel ATM inhibitor, KU59403, *in vitro* and *in vivo* in p53 functional and dysfunctional models of human cancer. *Mol. Cancer Ther.* 12, 959–967. doi: 10.1158/1535-7163.MCT-12-0707
- Block, W. D., Merkle, D., Meek, K., and Lees-Miller, S. P. (2004). Selective inhibition of the DNA-dependent protein kinase (DNA-PK) by the radiosensitizing agent caffeine. *Nucleic Acids Res.* 32, 1967–1972. doi: 10.1093/nar/gkh508
- Bode, A. M., and Dong, Z. (2007). The enigmatic effects of caffeine in cell cycle and cancer. *Cancer Lett.* 247, 26–39. doi: 10.1016/j.canlet.2006.03.032
- Botella, P., and Rivero-Buceta, E. (2017). Safe approaches for camptothecin delivery: structural analogues and nanomedicines. *J. Control Release* 247, 28–54. doi: 10.1016/j.jconrel.2016.12.023
- Branzei, D., and Foiani, M. (2008). Regulation of DNA repair throughout the cell cycle. *Nat. Rev. Mol. Cell Biol.* 9, 297–308. doi: 10.1038/nrm2351
- Carlier, Y., Truysens, C., Deloron, P., and Peyron, F. (2012). Congenital parasitic infections: a review. *Acta Trop.* 121, 55–70. doi: 10.1016/j.actatropica.2011.10.018
- Chanoux, R. A., Yin, B., Urtishak, K. A., Asare, A., Bassing, C. H., and Brown, E. J. (2009). ATR and H2AX cooperate in maintaining genome stability under replication stress. *J. Biol. Chem.* 284, 5994–6003. doi: 10.1074/jbc.M806739200
- Chini, E. N., Nagamune, K., Wetzel, D. M., and Sibley, L. D. (2005). Evidence that the cADPR signalling pathway controls calcium-mediated microneme secretion in *Toxoplasma gondii*. *Biochem. J.* 389 (Pt 2), 269–277. doi: 10.1042/BJ20041971
- Conde de Felipe, M. M., Lehmann, M. M., Jerome, M. E., and White, M. W. (2008). Inhibition of *Toxoplasma gondii* growth by pyrrolidine dithiocarbamate is cell cycle specific and leads to population synchronization. *Mol. Biochem. Parasitol.* 157, 22–31. doi: 10.1016/j.molbiopara.2007.09.003
- Cortopassi, W. A., Penna-Coutinho, J., Aguiar, A. C., Pimentel, A. S., Buarque, C. D., Costa, P. R., et al. (2014). Theoretical and experimental studies of new modified isoflavonoids as potential inhibitors of topoisomerase I from *Plasmodium falciparum*. *PLoS ONE* 9:e91191. doi: 10.1371/journal.pone.0091191
- Cristini, A., Park, J. H., Capranico, G., Legube, G., Favre, G., and Sordet, O. (2016). DNA-PK triggers histone ubiquitination and signaling in response

(to SA and WS), and PIP-CONICET 11220150100145CO (to SA). We thank Dr. Jean F. Dubremetz and Dr. Silvia Moreno for gently giving us anti-actin antibody and RH RFP tachyzoites, respectively.

SUPPLEMENTARY MATERIAL

The Supplementary Material for this article can be found online at: <https://www.frontiersin.org/articles/10.3389/fcimb.2019.00026/full#supplementary-material>

- to DNA double-strand breaks produced during the repair of transcription-blocking topoisomerase I lesions. *Nucleic Acids Res.* 44, 1161–1178. doi: 10.1093/nar/gkv1196
- Dalmasso, M. C., Onyango, D. O., Naguleswaran, A., Sullivan, W. J. Jr., and Angel, S. O. (2009). *Toxoplasma* H2A variants reveal novel insights into nucleosome composition and functions for this histone family. *J. Mol. Biol.* 392, 33–47. doi: 10.1016/j.jmb.2009.07.017
- D'Annese, I., Castelli, S., and Desideri, A. (2015). Topoisomerase 1B as a target against leishmaniasis. *Mini. Rev. Med. Chem.* 15, 203–210. doi: 10.2174/138955751503150312120912
- de Melo, E. J., Mayerhoffer, R. O., and de Souza, W. (2000). Hydroxyurea inhibits intracellular *Toxoplasma gondii* multiplication. *FEMS Microbiol. Lett.* 185, 79–82. doi: 10.1111/j.1574-6968.2000.tb09043.x
- Ditch, S., and Paull, T. T. (2012). The ATM protein kinase and cellular redox signaling: beyond the DNA damage response. *Trends Biochem. Sci.* 37, 15–22. doi: 10.1016/j.tibs.2011.10.002
- Dittmar, A. J., Drozda, A. A., and Blader, I. J. (2016). Drug repurposing screening identifies novel compounds that effectively inhibit *Toxoplasma gondii* Growth. *mSphere* 1:e00042-15. doi: 10.1128/mSphere.00042-15
- Dubey, J. P. (1994). Toxoplasmosis. *J. Am. Vet. Med. Assoc.* 205, 1593–1598
- Echeverria, P. C., Matrajt, M., Harb, O. S., Zappia, M. P., Costas, M. A., Roos, D. S., et al. (2005). *Toxoplasma gondii* Hsp90 is a potential drug target whose expression and subcellular localization are developmentally regulated. *J. Mol. Biol.* 350, 723–734. doi: 10.1016/j.jmb.2005.05.031
- Elaimy, A. L., Ahsan, A., Marsh, K., Pratt, W. B., Ray, D., Lawrence, T. S., et al. (2016). ATM is the primary kinase responsible for phosphorylation of Hsp90alpha after ionizing radiation. *Oncotarget* 7, 82450–82457. doi: 10.18632/oncotarget.12557
- Fleg, J., and Horacek, J. (2017). *Toxoplasma*-infected subjects report an obsessive-compulsive disorder diagnosis more often and score higher in obsessive-compulsive inventory. *Eur. Psychiatry* 40, 82–87. doi: 10.1016/j.eurpsy.2016.09.001
- Fuglewicz, A. J., Piotrowski, P., and Stodolak, A. (2017). Relationship between toxoplasmosis and schizophrenia: a review. *Adv. Clin. Exp. Med.* 26, 1031–1036. doi: 10.17219/acem/61435
- Garcia-Estrada, C., Prada, C. F., Fernandez-Rubio, C., Rojo-Vazquez, F., and Balana-Fouce, R. (2010). DNA topoisomerases in apicomplexan parasites: promising targets for drug discovery. *Proc. Biol. Sci.* 277, 1777–1787. doi: 10.1098/rspb.2009.2176
- Hickson, I., Zhao, Y., Richardson, C. J., Green, S. J., Martin, N. M., Orr, A. I., et al. (2004). Identification and characterization of a novel and specific inhibitor of the ataxia-telangiectasia mutated kinase ATM. *Cancer Res.* 64, 9152–9159. doi: 10.1158/0008-5472.CAN-04-2727
- Hunt, C. R., Pandita, R. K., Laszlo, A., Higashikubo, R., Agarwal, M., Kitamura, T., et al. (2007). Hyperthermia activates a subset of ataxia-telangiectasia mutated effectors independent of DNA strand breaks and heat shock protein 70 status. *Cancer Res.* 67, 3010–3017. doi: 10.1158/0008-5472.CAN-06-4328
- Kocher, S., Spies-Naumann, A., Krieger, M., Dahm-Daphi, J., and Dornreiter, I. (2013). ATM is required for the repair of Topotecan-induced replication-associated double-strand breaks. *Radiother. Oncol.* 108, 409–414. doi: 10.1016/j.radonc.2013.06.024
- Kuroda, S., Urata, Y., and Fujiwara, T. (2012). Ataxia-telangiectasia mutated and the Mre11-Rad50-NBS1 complex: promising targets for radiosensitization. *Acta Med. Okayama* 66, 83–92. doi: 10.18926/AMO/48258

- Kurose, A., Tanaka, T., Huang, X., Halicka, H. D., Traganos, F., Dai, W., et al. (2005). Assessment of ATM phosphorylation on Ser-1981 induced by DNA topoisomerase I and II inhibitors in relation to Ser-139-histone H2AX phosphorylation, cell cycle phase, and apoptosis. *Cytometry A* 68, 1–9. doi: 10.1002/cyto.a.20186
- Lee, J. H., and Paull, T. T. (2005). ATM activation by DNA double-strand breaks through the Mre11-Rad50-Nbs1 complex. *Science* 308, 551–554. doi: 10.1126/science.1108297
- Luft, B. J., and Remington, J. S. (1992). Toxoplasmic encephalitis in AIDS. *Clin. Infect. Dis.* 15, 211–222
- Martin, O. A., Pilch, D. R., Redon, C., and Bonner, W. M. (2003). Involvement of H2AX in the DNA damage and repair response. *Cancer Biol. Ther.* 2, 233–235. doi: 10.4161/cbt.2.3.373
- Matsuoka, S., Ballif, B. A., Smogorzewska, A., McDonald, E. R. III, Hurov, K. E., Luo, J., et al. (2007). ATM and ATR substrate analysis reveals extensive protein networks responsive to DNA damage. *Science* 316, 1160–1166. doi: 10.1126/science.1140321
- Moncada, P. A., and Montoya, J. G. (2012). Toxoplasmosis in the fetus and newborn: an update on prevalence, diagnosis and treatment. *Expert Rev. Anti. Infect. Ther.* 10, 815–828. doi: 10.1586/eri.12.58
- Nardelli, S. C., Che, F. Y., Silmon de Monerri, N. C., Xiao, H., Nieves, E., Madrid-Aliste, C., et al. (2013). The histone code of *Toxoplasma gondii* comprises conserved and unique posttranslational modifications. *MBio* 4, e00922–e00913. doi: 10.1128/mBio.00922-13
- Pannunzio, N. R., Watanabe, G., and Lieber, M. R. (2017). Nonhomologous DNA end joining for repair of DNA double-strand breaks. *J. Biol. Chem.* 293, 10512–10523. doi: 10.1074/jbc.TM117.000374
- Postow, L., Crisano, N. J., Peter, B. J., Hardy, C. D., and Cozzarelli, N. R. (2001). Topological challenges to DNA replication: conformations at the fork. *Proc. Natl. Acad. Sci. U.S.A.* 98, 8219–8226. doi: 10.1073/pnas.111006998
- Redon, C., Pilch, D., Rogakou, E., Sedelnikova, O., Newrock, K., and Bonner, W. (2002). Histone H2A variants H2AX and H2AZ. *Curr Opin Genet Dev* 12, 162–169. doi: 10.1016/S0959-437X(02)00282-4
- Rogakou, E. P., Boon, C., Redon, C., and Bonner, W. M. (1999). Megabase chromatin domains involved in DNA double-strand breaks *in vivo*. *J. Cell Biol.* 146, 905–916
- Rogakou, E. P., Pilch, D. R., Orr, A. H., Ivanova, V. S., and Bonner, W. M. (1998). DNA double-stranded breaks induce histone H2AX phosphorylation on serine 139. *J. Biol. Chem.* 273, 5858–5868
- Rybak, P., Hoang, A., Bujnowicz, L., Bernas, T., Berniak, K., Zarebski, M., et al. (2016). Low level phosphorylation of histone H2AX on serine 139 (gammaH2AX) is not associated with DNA double-strand breaks. *Oncotarget* 7, 49574–49587. doi: 10.18632/oncotarget.10411
- Sarkaria, J. N. (2003). Identifying inhibitors of ATM and ATR kinase activities. *Methods Mol. Med.* 85, 49–56. doi: 10.1385/1-59259-380-1:49
- Schmid, J. A., Berti, M., Walser, F., Raso, M. C., Schmid, F., Krietsch, J., et al. (2018). Histone ubiquitination by the DNA damage response is required for efficient DNA replication in unperturbed S phase. *Mol. Cell.* 71, 897–910.e8. doi: 10.1016/j.molcel.2018.07.011
- Sidik, S. M., Huet, D., Ganesan, S. M., Huynh, M. H., Wang, T., Nasamu, A. S., et al. (2016). A genome-wide CRISPR screen in toxoplasma identifies essential apicomplexan genes. *Cell* 166, 1423–1435.e1412. doi: 10.1016/j.cell.2016.08.019
- Snyder, A. R., Zhou, J., Deng, Z., and Lieberman, P. M. (2009). Therapeutic doses of hydroxyurea cause telomere dysfunction and reduce TRF2 binding to telomeres. *Cancer Biol. Ther.* 8, 1136–1145. doi: 10.4161/cbt.8.12.8446
- Stiff, T., O'Driscoll, M., Rief, N., Iwabuchi, K., Lobrich, M., and Jeggo, P. A. (2004). ATM and DNA-PK function redundantly to phosphorylate H2AX after exposure to ionizing radiation. *Cancer Res* 64, 2390–2396. doi: 10.1158/0008-5472.CAN-03-3207
- Stracker, T. H., Roig, I., Knobel, P. A., and Marjanovic, M. (2013). The ATM signaling network in development and disease. *Front. Genet.* 4:37. doi: 10.3389/fgene.2013.00037
- Sutterland, A. L., Fond, G., Kuin, A., Koeter, M. W., Lutter, R., van Gool, T., et al. (2015). Beyond the association. *Toxoplasma gondii* in schizophrenia, bipolar disorder, and addiction: systematic review and meta-analysis. *Acta Psychiatr. Scand.* 132, 161–179. doi: 10.1111/acps.12423
- Takahashi, A., Mori, E., Su, X., Nakagawa, Y., Okamoto, N., Uemura, H., et al. (2010). ATM is the predominant kinase involved in the phosphorylation of histone H2AX after heating. *J. Radiat. Res.* 51, 417–422. doi: 10.1269/jrr.10015
- Tanaka, T., Kurose, A., Huang, X., Dai, W., and Darzynkiewicz, Z. (2006). ATM activation and histone H2AX phosphorylation as indicators of DNA damage by DNA topoisomerase I inhibitor topotecan and during apoptosis. *Cell Prolif.* 39, 49–60. doi: 10.1111/j.1365-2184.2006.00364.x
- Teng, P. N., Bateman, N. W., Darcy, K. M., Hamilton, C. A., Maxwell, G. L., Bakkenist, C. J., et al. (2015). Pharmacologic inhibition of ATR and ATM offers clinically important distinctions to enhancing platinum or radiation response in ovarian, endometrial, and cervical cancer cells. *Gynecol. Oncol.* 136, 554–561. doi: 10.1016/j.ygyno.2014.12.035
- Tian, X., Lara, H., Wagner, K. T., Saripalli, S., Hyder, S. N., Foote, M., et al. (2015). Improving DNA double-strand repair inhibitor KU55933 therapeutic index in cancer radiotherapy using nanoparticle drug delivery. *Nanoscale* 7, 20211–20219. doi: 10.1039/c5nr05869d
- Tomicic, M. T., and Kaina, B. (2013). Topoisomerase degradation, DSB repair, p53 and IAPs in cancer cell resistance to camptothecin-like topoisomerase I inhibitors. *Biochim. Biophys. Acta* 1835, 11–27. doi: 10.1016/j.bbcan.2012.09.002
- Torrey, E. F., Bartko, J. J., and Yolken, R. H. (2012). *Toxoplasma gondii* and other risk factors for schizophrenia: an update. *Schizophr. Bull.* 38, 642–647. doi: 10.1093/schbul/sbs043
- van Dooren, G. G., Tomova, C., Agrawal, S., Humbel, B. M., and Striepen, B. (2008). *Toxoplasma gondii* Tic20 is essential for apicoplast protein import. *Proc. Natl. Acad. Sci. U.S.A.* 105, 13574–13579. doi: 10.1073/pnas.0803862105
- Velic, D., Couturier, A. M., Ferreira, M. T., Rodrigue, A., Poirier, G. G., Fleury, F., et al. (2015). DNA damage signalling and repair inhibitors: the long-sought-after Achilles' heel of cancer. *Biomolecules* 5, 3204–3259. doi: 10.3390/biom5043204
- Vonlaufen, N., Naguleswaran, A., Coppens, I., and Sullivan, W. J. Jr. (2010). MYST family lysine acetyltransferase facilitates ataxia telangiectasia mutated (ATM) kinase-mediated DNA damage response in *Toxoplasma gondii*. *J. Biol. Chem.* 285, 11154–11161. doi: 10.1074/jbc.M109.066134
- Wang, H., Wang, M., Wang, H., Bocker, W., and Iliakis, G. (2005). Complex H2AX phosphorylation patterns by multiple kinases including ATM and DNA-PK in human cells exposed to ionizing radiation and treated with kinase inhibitors. *J. Cell Physiol.* 202, 492–502. doi: 10.1002/jcp.20141
- Weber, A. M., and Ryan, A. J. (2015). ATM and ATR as therapeutic targets in cancer. *Pharmacol. Ther.* 149, 124–138. doi: 10.1016/j.pharmthera.2014.12.001
- Xu, Y., Wu, X., and Her, C. (2015). hMSh5 facilitates the repair of camptothecin-induced double-strand breaks through an interaction with FANCD1. *J. Biol. Chem.* 290, 18545–18558. doi: 10.1074/jbc.M115.642884
- Yan, C., Lu, J., Zhang, G., Gan, T., Zeng, Q., Shao, Z., et al. (2011). Benzo[a]pyrene induces complex H2AX phosphorylation patterns by multiple kinases including ATM, ATR, and DNA-PK. *Toxicol. in vitro* 25, 91–99. doi: 10.1016/j.tiv.2010.09.012
- Yolken, R., Torrey, E. F., and Dickerson, F. (2017). Evidence of increased exposure to *Toxoplasma gondii* in individuals with recent onset psychosis but not with established schizophrenia. *PLoS Negl. Trop. Dis.* 11:e0006040. doi: 10.1371/journal.pntd.0006040
- Zhang, J., Dai, Q., Park, D., and Deng, X. (2016). Targeting DNA replication stress for cancer therapy. *Genes* 7:51. doi: 10.3390/genes7080051
- Zhang, J., Tripathi, D. N., Jing, J., Alexander, A., Kim, J., Powell, R. T., et al. (2015). ATM functions at the peroxisome to induce pexophagy in response to ROS. *Nat. Cell Biol.* 17, 1259–1269. doi: 10.1038/ncb3230
- Zhou, W., Quan, J. H., Lee, Y. H., Shin, D. W., and Cha, G. H. (2013). *Toxoplasma gondii* proliferation require down-regulation of host Nox4 expression via activation of PI3 kinase/akt signaling pathway. *PLoS ONE* 8:e66306. doi: 10.1371/journal.pone.0066306

Conflict of Interest Statement: The authors declare that the research was conducted in the absence of any commercial or financial relationships that could be construed as a potential conflict of interest.

Copyright © 2019 Munera López, Ganuza, Bogado, Muñoz, Ruiz, Sullivan, Vanagas and Angel. This is an open-access article distributed under the terms of the Creative Commons Attribution License (CC BY). The use, distribution or reproduction in other forums is permitted, provided the original author(s) and the copyright owner(s) are credited and that the original publication in this journal is cited, in accordance with accepted academic practice. No use, distribution or reproduction is permitted which does not comply with these terms.



OPEN ACCESS

Edited by:

Alexis Kaushansky,
Seattle Children's Research Institute,
United States

Reviewed by:

Paras Jain,
Intellectual Ventures, United States
Rapatbhorn Patrapuvich,
Mahidol University, Thailand

***Correspondence:**

Kamal El Bissati
kelbissati@uchicago.edu
Kami Kim
kamikim@health.usf.edu
Louis M. Weiss
louis.weiss@einstein.yu.edu

† Present Address:

Henry Redel,
Rutgers Robert Wood Johnson
Medical School, Department of
Medicine, East Brunswick, NJ,
United States;
NYU School of Medicine,
Department of Medicine, New York,
NY, United States
Kami Kim,
Department of Internal Medicine,
Morsani College of Medicine,
University of South Florida, Tampa,
FL, United States

Specialty section:

This article was submitted to
Clinical Microbiology,
a section of the journal
Frontiers in Cellular and Infection
Microbiology

Received: 20 June 2018

Accepted: 14 January 2019

Published: 14 February 2019

Citation:

El Bissati K, Redel H, Ting L-M,
Lykins JD, McPhillie MJ, Upadhy R,
Woster PM, Yarlett N, Kim K and
Weiss LM (2019) Novel Synthetic
Polyamines Have Potent Antimalarial
Activities *in vitro* and *in vivo* by
Decreasing Intracellular Spermidine
and Spermine Concentrations.
Front. Cell. Infect. Microbiol. 9:9.
doi: 10.3389/fcimb.2019.00009

Novel Synthetic Polyamines Have Potent Antimalarial Activities *in vitro* and *in vivo* by Decreasing Intracellular Spermidine and Spermine Concentrations

Kamal El Bissati^{1*}, Henry Redel^{2†}, Li-Min Ting², Joseph D. Lykins³, Martin J. McPhillie⁴, Rajendra Upadhy², Patrick M. Woster⁵, Nigel Yarlett⁶, Kami Kim^{2,7*†} and Louis M. Weiss^{2,7*}

¹ Department of Ophthalmology and Visual Science, The University of Chicago, Chicago, IL, United States, ² Department of Medicine, Albert Einstein College of Medicine and Montefiore Medical Center, Bronx, NY, United States, ³ Department of Internal Medicine and Department of Emergency Medicine, Virginia Commonwealth University Health System, Richmond, VA, United States, ⁴ School of Chemistry, University of Leeds, Leeds, United Kingdom, ⁵ Department of Drug Discovery and Biomedical Sciences, Medical University of South Carolina, Charleston, SC, United States, ⁶ Haskins Laboratories, Department of Chemistry and Physical Sciences, Pace University, New York, NY, United States, ⁷ Department of Pathology, Albert Einstein College of Medicine and Montefiore Medical Center, Bronx, NY, United States

Twenty-two compounds belonging to several classes of polyamine analogs have been examined for their ability to inhibit the growth of the human malaria parasite *Plasmodium falciparum* *in vitro* and *in vivo*. Four lead compounds from the thiourea sub-series and one compound from the urea-based analogs were found to be potent inhibitors of both chloroquine-resistant (Dd2) and chloroquine-sensitive (3D7) strains of *Plasmodium* with IC₅₀ values ranging from 150 to 460 nM. In addition, the compound RHW, N1,N7-bis (3-(cyclohexylmethylamino) propyl) heptane-1,7-diamine tetrabromide was found to inhibit Dd2 with an IC₅₀ of 200 nM. When RHW was administered to *P. yoelii*-infected mice at 35 mg/kg for 4 days, it significantly reduced parasitemia. RHW was also assayed in combination with the ornithine decarboxylase inhibitor difluoromethylornithine, and the two drugs were found not to have synergistic antimalarial activity. Furthermore, these inhibitors led to decreased cellular spermidine and spermine levels in *P. falciparum*, suggesting that they exert their antimalarial activities by inhibition of spermidine synthase.

Keywords: polyamine, *Plasmodium*, malaria, spermidine, spermine, spermidine synthase, thiourea

INTRODUCTION

Malaria is a global health threat, especially in the developing world. *Plasmodium falciparum* causes the most lethal form of the disease. It is responsible for a high number of clinical cases and deaths annually. About 3.2 billion people remain at risk of malaria. In 2015 alone, there was an estimated 214 million new cases of malaria and 438,000 deaths (World Health Organization, 2015). The number of malaria cases fell from an estimated 262 million in 2000 to 214 million in 2015 (World Health Organization, 2015), due to employment of artemisinin and drug-impregnated bed nets (White et al., 2014; World Health Organization, 2015). Artemisinin-based combination therapies ACTs have become widely adopted as

first-line treatment in almost all countries where malaria is endemic (White, 2008). However, recent studies report decreases in parasite clearance rates following artesunate monotherapy or artesunate-mefloquine combination therapy in Thailand and Cambodia, suggesting increasing resistance to this therapeutic approach (Dondorp et al., 2009; Amaratunga et al., 2012; Phyo et al., 2012; Ferreira et al., 2013). In light of the challenge posed by resistant strains of *P. falciparum*, development of new drugs to combat this infection is increasingly necessary and will save lives.

The intraerythrocytic life cycle of *P. falciparum* is dynamic, with the parasite undergoing numerous morphological and physiological transformations throughout the course of infection. Whilst actively dividing, the parasite is capable of generating 36 daughter parasites within 2 days. Innumerable parasitic cellular processes offer diverse chemotherapeutic targets for the inhibition of parasite replication and, thereby, abrogation of disease. Among these targets, is the biosynthesis of polyamines. There is a 10 to 20-fold increase in polyamine levels when the parasite transitions from ring stage to schizonts in infected erythrocytes and there is evidence of parasitic dependence on the polyamine pathway for intraerythrocytic development (Assaraf et al., 1984; Gupta et al., 2005). Moreover, inhibitors of this pathway cause decreased polyamine levels, which, in turn, results in transcriptional arrest (van Brummelen et al., 2009). Consequently, the polyamine pathway appears to be a valid target for further exploration and small molecular development, given its essential role in parasite survival. Polyamines, which include putrescine, spermidine, spermine, and cadaverine (an analog of putrescine), are amine-containing, cationic, low molecular mass compounds, and ubiquitous in eukaryotes and prokaryotes. These polycation compounds interact electrostatically with anionic macromolecules like RNA, DNA, ATP, proteins, and phospholipids (Igarashi and Kashiwagi, 2000; Wallace et al., 2003). These interactions regulate replication, transcription, membrane biogenesis, maintenance of chromatin conformation, specific gene expression, ion channels, and confer protection of nucleic acids against oxidative stress (Igarashi and Kashiwagi, 2000; Wallace et al., 2003). Synthesis of polyamines in most cells is initiated by the production of putrescine from ornithine through the activity of ornithine decarboxylase (ODC). The addition of either one or two aminopropyl groups to the terminal amino groups of putrescine form spermidine and spermine, respectively via S-adenosylmethionine (AdoMet) decarboxylase. Most animal and yeast cells can take up polyamines and convert them back to spermidine and putrescine via spermidine/spermine-N-acetyltransferase and polyamine oxidase (Pegg and McCann, 1982; Marton and Pegg, 1995). *P. falciparum* lacks the capacity for polyamine interconversion, and the parasite controls polyamine levels exclusively through *de novo* spermidine synthase, which determines levels of spermidine (Müller et al., 2001; Clark et al., 2010). This enzyme has the additional unique function of producing low levels of spermine (Haider et al., 2005).

Many inhibitors of both ODC and AdoMetDC have been synthesized, with the goal of interfering with polyamine metabolism in tumor cells as anti-cancer therapy and prevention (Marton and Pegg, 1995; Casero and Marton,

2007). DFMO (alpha-difluoromethylornithine) was successfully exploited against West African human sleeping sickness (*Trypanosoma brucei gambiense*) (Bacchi et al., 1980; Burri and Brun, 2003). Interestingly, the functions of AdoMetDC and ODC are combined into a single unique bi-functional protein (*PfAdoMet/ODC*) in *P. falciparum* (Müller et al., 2000). This enzyme has formed the basis of multiple studies assessing polyamine metabolism as a chemotherapeutic target in this organism. Inhibitors of this enzyme, however, have only cytostatic effects *in vitro* with cure achieved only with co-administration with polyamine analogs in murine malaria models (Bitonti et al., 1989).

Other polyamine analogs interfering with polyamine functions and metabolism have been synthesized and tested in different organisms. The tetraamines, homologs of spermine in which the external aminopropyl groups present in spermine were replaced by aminobutyl groups, are shown along with oligoamines to be effective in the treatment of microsporidiosis, an opportunistic infection associated with severe HIV infection (Bacchi et al., 2002). Spermine analogs were found to condense DNA and are indeed powerful inhibitors of human cell proliferation (Osland and Kleppe, 1977).

Based on these findings, we tested the oligoamines (SL-11158 and SL-11144) and the tetraamine SL-11093, with demonstrated efficacy against microsporidia, for their activities against malaria parasites. Here we report the identification of four lead compounds from the thiourea sub-series and one compound from the urea-based analogs from the list of twenty-two polyamine analogs effective against chloroquine-sensitive and -resistant parasites, at nanomolar levels. Moreover, these compounds were tested *in vivo* in a murine model with *Plasmodium yoelii* and found to significantly reduce levels of parasitemia. These effects are correlated with an observed decrease in spermidine and spermine levels and highlight the importance of this polyamine to the parasite.

METHODS

Strains

The *P. falciparum* strains 3D7 and Dd2 used in this study were obtained from the Malaria Research and Reference Reagent Resource Center (MR4). *P. yoelii* clones were obtained from the WHO Registry Standard Malaria Parasites, University of Edinburgh.

Chemicals

Hypoxanthine radiolabelled chemicals were purchased from NEN Life Science Products. Compounds SL-11144, SL-11158, SL-11091, and SL-11093 were synthesized by the Frydman group as described elsewhere (Reddy et al., 1998; Valasinas et al., 2003). All of the remaining compounds were synthesized by Dr. Patrick M. Woster, Medical University of South Carolina, as previously described (Zou et al., 2001; Bi et al., 2006; Verlinden et al., 2011; Verlinden et al., 2015).

Cell Culture and Materials

P. falciparum was cultured *in vitro* with erythrocytes using a gas mixture of 3% O₂, 3% CO₂, and 94% N₂ as described by the method of Trager and Jensen (1976). Briefly, we used RPMI medium 1,640 supplemented with 30 mg/liter hypoxanthine (Sigma), 25 mM Hepes (Sigma), 0.225% NaHCO₃ (Sigma), 0.5% Albumax I (Life Technologies, Grand Island, NY) and 10 µg/ml of gentamycin (Life Technologies) for the parasite growth. Synchronization of the parasites was obtained by incubation with 5% sorbitol treatments (Lambros and Vanderberg, 1979). The stage of the parasite was confirmed by fixed smears of the infected erythrocytes using Giemsa staining and observation by bright-field microscopy.

Hypoxanthine Incorporation Assay

The susceptibility of parasites to different compounds was assessed by tritiated hypoxanthine uptake as described by Desjardins et al. (1979). Briefly, infected erythrocytes with 3% at the ring stages were incubated with the compounds from the list of twenty-two polyamine analogs at 0, 0.01, 0.05, 0.1, 1, 5, 10, 50, 100, 250, 500, and 750 µM in a medium free of hypoxanthine for 48 h. Two hundred microliter of the mixture was then added to a 96-well plate with 3H-hypoxanthine at a concentration of 0.5 µCi/well. The cells were incubated for 24 h, washed on an ultrafilter and radioactivity was counted using a scintillation counter. IC₅₀ values are calculated from the sigmoidal inhibition curves using Prism and are represented in nM. Values are means of three independent experiments each performed in triplicate.

Infection of Mice With Blood-Stage Parasites and Drug Treatments

Naive 8-weeks-old female Swiss Webster mice were intravenously infected with 2×10^5 infected red blood cells (iRBCs) of *P. yoelii* YM parasites; 3 mice were included in each infection group. Two groups per treatment were performed. Drugs were dissolved in dimethyl sulfoxide (DMSO). For example, to inject 35 mg/kg, we first dissolved 35 mg of the drug in 1 mL of DMSO and then diluted it in 0.05% Tween 80 H₂O, for a total of 10 mL. We then injected 200 µL of this solution into mice with a body weight of 20 g. The polyamine compounds and pyrimethamine were administered intraperitoneally. All mice were treated for 4 days. Parasitemia was monitored by Giemsa staining of blood smears obtained after the 4 days of treatment and on a daily basis. Parasites were harvested by collecting blood samples from the tail vein of infected mice. The mice tolerated (without observable toxicity) up to 35 mg/kg when the schedule described above was used. All mice studies were performed with the Institutional Animal Care and Use Committee at the Albert Einstein College of Medicine approval and oversight.

Polyamine Quantification

Polyamine content was quantified as described previously (Bacchi et al., 2004). Briefly, *P. falciparum* Dd2 strain infected red blood cells were treated in the late schizont stage (42 h post invasion) with 1 µM of RHW (IC₅₀ = 200 nM), 750 nM of compound 13 (IC₅₀ = 150 nM), and with 5 mM DFMO (IC₅₀ =

1 mM), to ensure complete parasite arrest. Treated and untreated cultures, at 10% parasitemia, were harvested at trophozoite phase (18–24 h). Polyamine interconversion was assayed by incubation infected red blood cells to 0.25 µCi (2.1 nmol) [1-¹⁴C]spermine as described previously by Bacchi et al. (2001). After incubation, mixtures were centrifuged and the supernatant was discarded. Pellets were extracted with 10% TCA overnight and frozen. Separation of polyamines was performed by HPLC equipped with a 5 µm C-18 reversed-phase column, samples and standards were detected by a UV detector (Perkin Elmer), and signals were integrated using a β-ram (IN/US Systems) Version 3.1 software package.

Molecular Modeling

The graphical user interface Maestro (version 10.3, Schrodinger LLC, New York, NY, 2018) was used to visualize the PfSpdS protein (PDB IDs: 2I7C and 4CWA), which was prepared using the Protein Preparation Wizard. Only chain A was used in both crystal structures for further modeling. The ligand RHW was prepared using the Maestro user interface. MacroModel force-field based molecular modeling (MacroModel v10.3, Schrodinger LLC, New York, NY, 2018) was used to predict the binding pose of the ligand RHW (Harder et al., 2015). The obtained molecular conformations were visualized using PyMOL (The PyMOL Molecular Graphics System, Version 1.8 Schrödinger, LLC).

RESULTS

Effects of Polyamine Analogs on Growth of 3D7 and Dd2 of *P. falciparum* Strains

Previous studies have shown that polyamine analogs with a backbone of repeating *N*-butyl subunits, such as pentamines, oligoamines or bis-(aryl)-substituted 3-7-3 analogs (Figure 1A), sterilized *Encephalitozoon cuniculi*-infected monolayer cells and cured two murine model infections (Bacchi et al., 2002). The IC₅₀ of SL-11158 and SL-11144 against microsporidia was 8.2 and 0.62 µM (Bacchi et al., 2002). In order to examine the antimalarial activity of polyamine analogs, we have tested the effect of increasing concentrations of these compounds on the intraerythrocytic life cycle of *P. falciparum* in culture, by following the incorporation of radiolabeled hypoxanthine into parasite nucleic acids. We then determined the 50% inhibitory concentration (IC₅₀) that blocks the replication of *P. falciparum* inside the red cells. The study was performed with two strains of *P. falciparum* (3D7 and Dd2) with different levels of sensitivity to the antimalarial drugs pyrimethamine and chloroquine (Figure 2 and Table 1). As a control, we confirmed the IC₅₀ of chloroquine in the two strains. As expected, the strain 3D7 was sensitive to chloroquine with IC₅₀ of 5 ± 0.2 nM and Dd2 was highly resistant to chloroquine (IC₅₀ 300 ± 21 nM) (Supplementary Figure 1).

As shown in Table 1 and Supplementary Figure 1, RHW exhibited antimalarial activity, with an IC₅₀ of 2.6 µM against 3D7 and 0.2 µM against Dd2 parasite strains. This prompted the testing of a variety of polyamine analogs for antiparasitic effects. We tested 17 compounds belonging to three different classes, namely ureas, thioureas, and amidines (Figures 1C–E). The polyamines of the thiourea group were found to be the most

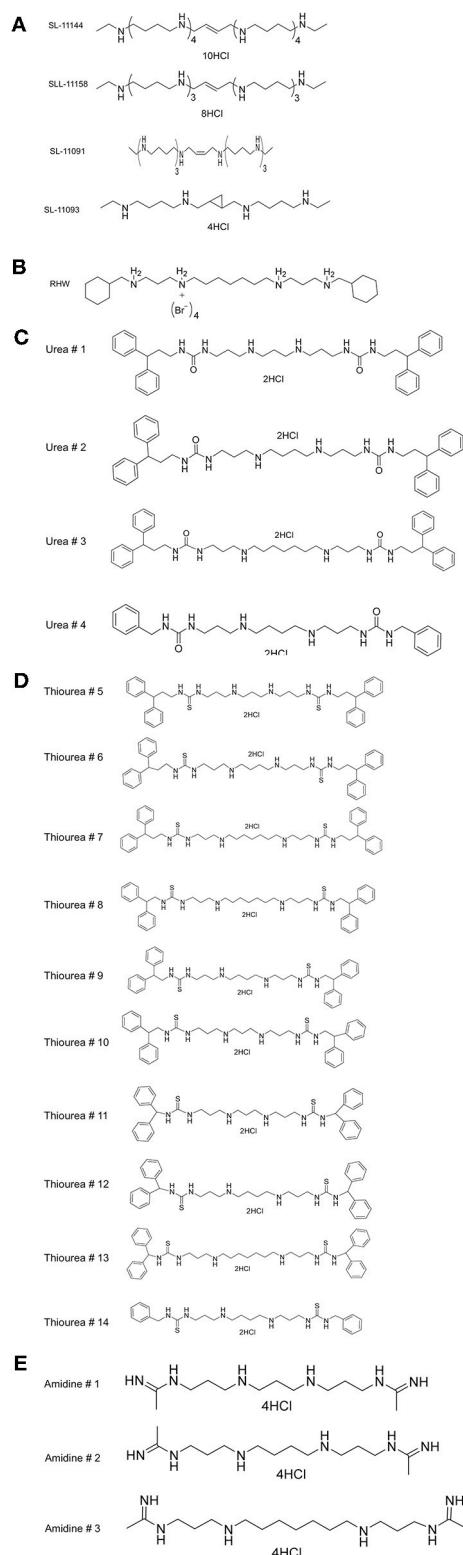


FIGURE 1 | Structures of **(A)** various oligoamine and tetraamine analogs of polyamines, **(B)** N1, N7-bis (3-(cyclohexylmethylamino) propyl) heptane-1,7-diamine tetrabromide (RHW), **(C)** Urea, **(D)** Thiourea, **(E)** Amidine.

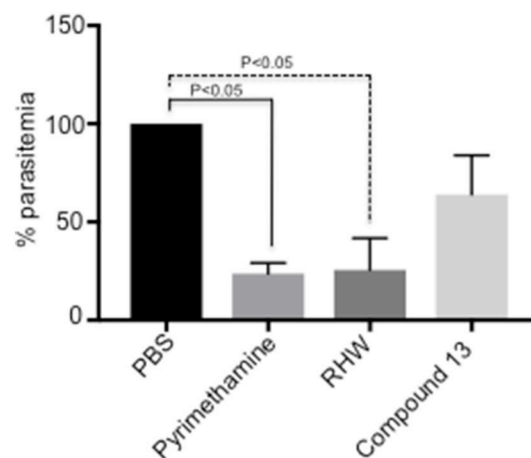


FIGURE 2 | *In vivo* study of the effect on *P. yoelii*-infected mice ($n = 3$ animals per group) of polyamine analogs administered ip at 35 mg/kg/day as indicated in Methods. Pyrimethamine was administered ip as a positive control at 10 mg/kg/day. A control untreated group received PBS. Activity was determined by percentage of parasitemia at day 6-post infection relative to untreated control. The results are shown as the means of three independent experiments \pm standard deviation. Significant differences relative to untreated control are determined by student's *t*-test.

potent in inhibiting parasite growth, with IC_{50} ranging from 160 to 3,200 nM for 3D7 strain and 150 to 3,600 nM for Dd2 strain (**Table 1**). Compound 13 was found to be more effective in inhibiting parasitic growth of both 3D7 and Dd2 strains with IC_{50} values of 160 nM and 150 nM, respectively. Both 3D7 and Dd2 parasite strains exhibited varied sensitivity toward the urea class of polyamine analogs, with compound 2 exhibiting the strongest growth inhibition of the class, with an IC_{50} of 370 nM for 3D7 and 440 nM for Dd2 strains (**Table 1**). The amidine class of analogs showed the least effect on growth of both strains of *P. falciparum* with an $IC_{50} > 100 \mu M$ (**Table 1**). To further confirm the inhibitory effects of these classes of polyamine analogs on *P. falciparum* growth, we employed the pLDH colorimetric assay (data not shown), which measures parasite-specific lactate dehydrogenase activity (Makler and Hinrichs, 1993; Makler et al., 1993).

Efficacies of Polyamine Analogs *in vivo*

We tested the efficacy of the most potent compounds on the growth inhibitory potential of *Plasmodium* employing a murine model. We infected mice with *P. yoelii*, as described in materials and methods, and the infected mice were treated with RHW and compound 13, the compounds with the most efficacy *in vitro*. PBS infected mice served as control and pyrimethamine drug treated animals were used as a positive control group. As shown in **Figure 2**, treatment of animals with RHW resulted in a significant ($p < 0.05$) decrease in parasitemia compared to the untreated control. Even though compound 13 decreased parasitemia *in vivo*, the level of inhibition was not significantly different ($p > 0.05$) to the PBS control group (**Figure 2** and **Supplementary Figure 2**). In conclusion, these *in vivo* results

TABLE 1 | Structure of various analogs of polyamines and their effect on the growth of 3D7 and Dd2 strains of *P. falciparum* under *in vitro* conditions.

Compounds	No.	IC ₅₀ (nM)*	
		3D7 strains	Dd2 strains
SL-11144		>250,000	>250,000
SL-11158		>250,000	>250,000
SL-11091		>250,000	>250,000
SL-11093		>250,000	>250,000
RHW		2,600 ± 135	200 ± 12
Urea	1	1,700 ± 95	800 ± 23
Urea	2	370 ± 4.8	440 ± 3.2
Urea	3	530 ± 7.2	630 ± 11
Urea	4	2,900 ± 37	700 ± 21
Thiourea	5	3,200 ± 19	3,600 ± 7.9
Thiourea	6	590 ± 53	510 ± 4.8
Thiourea	7	220 ± 2	350 ± 6.1
Thiourea	8	170 ± 10.5	160 ± 8
Thiourea	9	560 ± 2.3	690 ± 1.9
Thiourea	10	570 ± 6.0	850 ± 10.5
Thiourea	11	650 ± 29	1,950 ± 18
Thiourea	12	240 ± 6.8	460 ± 3.7
Thiourea	13	160 ± 10.4	150 ± 24
Thiourea	14	1,200 ± 8	1,720 ± 125
Amidine	15	>100,000	>100,000
Amidine	16	>100,000	>100,000
Amidine	17	>100,000	>100,000

*IC₅₀: The half maximal inhibitory concentration. IC₅₀ values are calculated from the sigmoidal inhibition curves using Prism. IC₅₀ values are an average of three independent experiments, each carried out in triplicate with ± standard deviations.

show the efficacy of RHW on the inhibition of parasitemia in the murine model.

Polyamine Quantification

We examined the effects of polyamine analogs on overall uptake of arginine and putrescine, and production of spermidine and spermine. **Table 2** shows the results of polyamine contents in red blood cells [experiment was performed twice, each in five replicate experiments, where the polyamine content of *Plasmodium* infected red blood cells was compared to treated cells with RHW, compound 13, and ornithine decarboxylase inhibitor difluoromethylornithine (DFMO) as a control]. We monitored the intracellular content of arginine, putrescine, spermidine, and spermine. Data show that DFMO substantially decreases the amount of spermidine. However, spermine levels were similar for both untreated and DFMO treated. These results were in concordance with previous data that show the same effect of DFMO (Sugiura et al., 1984). In contrast, infected red blood cells treated with RHW showed a significant decrease in spermidine ($p < 0.05$) and spermine levels ($p < 0.01$). These data suggest an effect of RHW on polyamine metabolism in *Plasmodium*, including an effect on enzymes involved on spermidine and spermine synthesis. In addition, when RHW or compound 13 was assayed in combination with DFMO in both

TABLE 2 | Effect of treatment of RHW and compound 13 on the polyamine contents of *Plasmodium falciparum*.

Sample	Amount (nmoles/ml)			
	Arginine	Putrescine	Spermidine	Spermine
Infected untreated RBC	11.5 ± 3.9	8.0 ± 1.1	52.5 ± 1.9	13.0 ± 3.1
DFMO	32.5 ± 11	11.0 ± 2.4	32.0 ± 0.9	15.0 ± 2.9
Compound 13	12.0 ± 1.2	5.9 ± 1.7	50 ± 2.8	14.5 ± 1.7
RHW	41.0 ± 12.9	6.0 ± 2.1	41 ± 1.3	2.0 ± 0.8

Plasmodium falciparum Dd2 strain infected red blood cells were treated in the late schizont stage with 1 μM of RHW (IC₅₀ = 200 nM), 750 nM of compound 13 (IC₅₀ = 150 nM), and with 5 mM DFMO (IC₅₀ = 1 mM, as a positive control). The treated parasites were then extracted and monitored for intracellular polyamine levels. The results are presented as mean ± SD for 2 separate experiments, each performed in 5 replicates. Significant differences relative to untreated control are determined by student's t-test.

Dd2 and 3D7 strains, the two drugs were found not to have synergistic antimalarial activity (**Figure 3**).

Molecular Modeling of Compound RHW

In order to understand the putative binding conformations of RHW to *P. falciparum* spermidine synthase (PfSpdS) and the observed biological activity, we utilized *in silico* molecular modeling. Sprenger et al. proposed three areas of the active site: the distal aminopropyl cavity, the putrescine site and the larger dcAdoMet site (composed of the central aminopropyl cavity and the MTA cavity) within PfSpdS (Sprenger et al., 2016). Because RHW showed potent activity *in vitro* and *in vivo*, all our molecular modeling was performed with this inhibitor. RHW is a long linear molecule consisting of 20 rotatable bonds (**Figure 1B**). Attempts to dock and predict the binding mode of RHW using Schrodinger Glide XP mode were unsuccessful. Instead, we modified an existing ligand (5-(1H-benzimidazol-2-yl) pentan-1-amine) within the PfSpdS active site of PBD ID: 4CWA (Sprenger et al., 2015), and subjected it to MacroModel minimization using force-field OPLS_2005, keeping the protein backbone rigid (locked) and allowing the side chains to move and generate a lower energy ligand:protein complex (**Figure 4**). RHW is predicted to bind across all three areas of the active site (**Figure 4A**), and when overlaid with inhibitor AdoDATO from crystal structure 2I7C (Dufe et al., 2007), RHW showed a similar mode of binding (**Figure 4B**). Some movement of the amino acid side chains (W234, C266, I235, H236, E231, M50, W51, and D178) was observed to accommodate the terminal cyclohexylmethyl groups. Of these, only H236 and D178 displayed significant movement (2.0 Å) of their side chain positions.

DISCUSSION

Multiple polyamine analogs in this study have demonstrated potent antimalarial properties, with IC₅₀ at the nanomolar range for *P. falciparum* strains, both sensitive and resistant to chloroquine. Drug-resistance continues to present challenges in treating *P. falciparum* infection, and medications

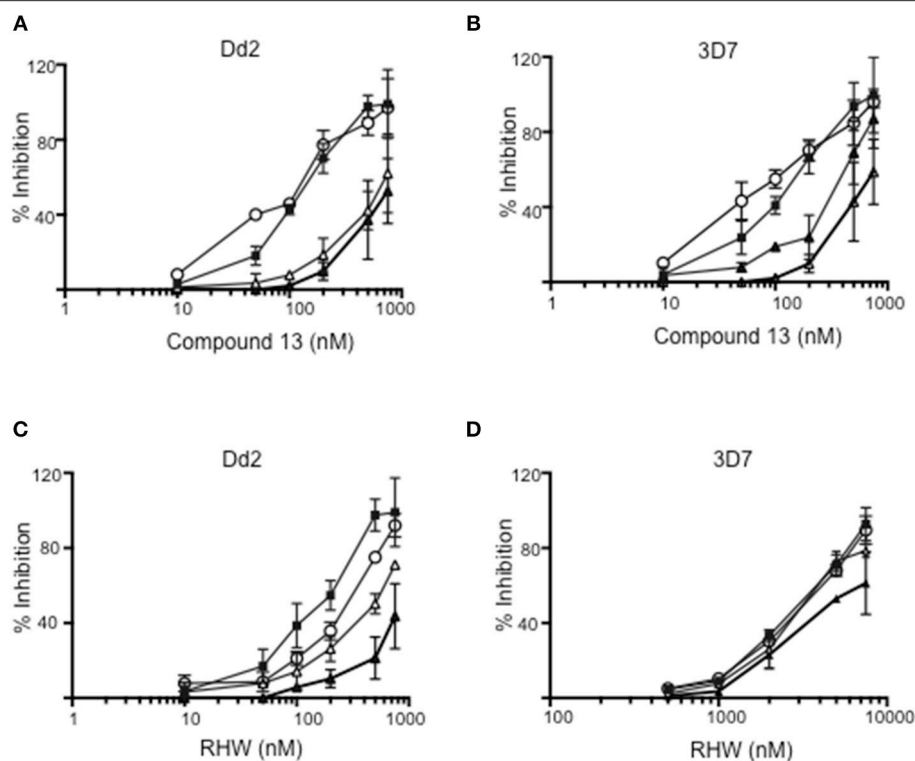


FIGURE 3 | Inhibition of Dd2 and 3D7 strains by different concentrations of compound 13 (A,B) and RHW (C,D) in the absence of DFMO (closed squares), or in presence of 500 mM (open triangles), 1 mM (open circles), and 3 mM (closed triangles) of DFMO.

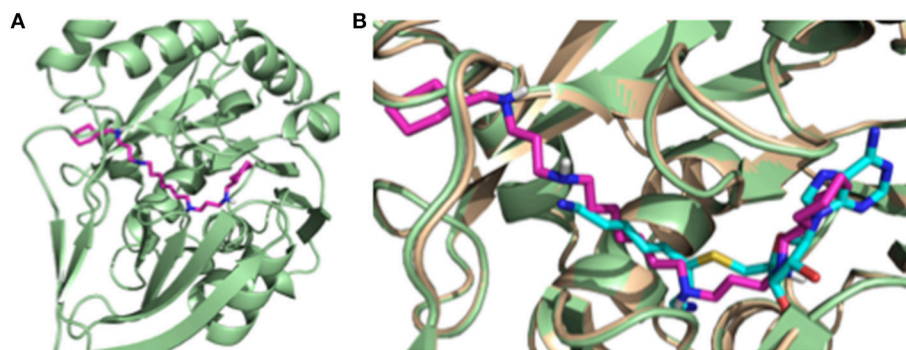


FIGURE 4 | (A) Putative binding conformation of RHW (pink) in PfSpdS (green) traversing the three areas of the active site. (B) Overlay of RHW modeled conformation (pink) with 217C (wheat) and its co-crystal inhibitor AdoDATO (sky blue).

previously useful for treating drug-resistant isolates are increasingly inadequate, as illustrated by the emergence of artemisinin-resistance.

The utilization of polyamine analogs to treat infection has been previously demonstrated in experimental murine models of microsporidiosis, with several of the analogs demonstrating significant efficacy (Bacchi et al., 2004). The compounds with the most efficacies were shown to be tetraamines and oligoamines. These tetraamine compounds, which are structural homologs of spermine, have been studied extensively, and have been shown to

interrupt and modify DNA conformational structure, inducing bends and kinks in the double helix (Hsieh et al., 1994). The oligoamine compounds have been demonstrated previously to contribute to the collapse of DNA, promoting condensation of DNA. These compounds have also documented anti-tumor activity (Frydman et al., 2003; Huang et al., 2003).

Given the importance of polyamine metabolism for transcriptional activity and cellular replication microsporidia and *Plasmodium*, testing analogs effective against microsporidia formed the basis of our initial approach toward *P. falciparum*.

Surprisingly, these compounds showed no or minimal antimalarial activity. The lack of effect of the tetraamine compounds on *P. falciparum* prompted further synthetic efforts.

The addition of cyclohexylmethyl side groups to the tetraamine backbone resulted in the compound abbreviated as RHW. This compound showed substantial promise, with efficacy at the nanomolar range against chloroquine-resistant *P. falciparum*, and further medicinal chemistry allowed for additional modifications to these compounds. Some of these modifications proved beneficial, enhancing antimalarial activity, such as the urea and thiourea examples, while others were detrimental (amidine analogs). It has also been noted previously (Verlinden et al., 2011) that the compounds with aromatic rings demonstrated enhanced efficacy when compared to matched-pair compounds without these groups. The length of the carbon chain between the two central amines appears to also be important (see compounds 1–3). While the exact, mechanistic underpinning of this difference requires further exploration, this observation should inform any medicinal chemistry efforts with these polyamine analogs. We present a putative model of RHW bound to *P. falciparum* spermidine synthase (*PfSpdS*) (**Figure 4**).

The observed differences in responsiveness to these compounds between microsporidia and *P. falciparum* highlight differences in the metabolic handling of polyamines by these two pathogens. It has been noted previously that microsporidia, including *E. cuniculi*, have an operative polyamine synthesis and interconversion pathway, the latter of which is lacking in *Plasmodium* (Müller et al., 2001). This difference in capacity could, in part, explain the differences observed in response to the tetraamine compounds. An alternative explanation could be structural differences in particular enzymes targeted by these compounds. The data presented here demonstrate decreased levels of spermine in infected cells and argue in favor of the polyamine analogs inhibiting spermidine synthase. While functional studies demonstrating this relationship are still needed, this seems a probable hypothesis for the mechanism by which the action of these compounds is exerted. Another potential target to inhibit polyamine synthesis is through blocking the transport of these molecules. Polyamine

transporters have not yet been identified in the *P. falciparum* genome, but a drug combination selectively inhibiting both polyamine biosynthesis and transport may provide a promising anti-malarial strategy (van Brummelen et al., 2009).

The polyamine analogs investigated in this study have been demonstrated to hold promise as antimalarial agents and should be further characterized with respect to kinetics and impact on spermidine synthase. Moreover, following optimization, future studies with respect to efficacy, toxicity, and delivery to infected patients will be of value. Malaria is an enormous threat to the health of populations globally, responsible for millions of deaths annually. Novel therapeutic strategies are desperately needed in the continued fight against *Plasmodium*, and these polyamine analogs have the potential to represent one of these strategies, with the goal of more effectively treating infections and preventing the severe morbidity and mortality caused by this parasite worldwide.

AUTHOR CONTRIBUTIONS

KE, LW, and KK designed research. KE, HR, L-MT, RU, and NY performed research. KE, HR, L-MT, RU, NY, PW, JL, MM, LW, and KK analyzed data. KE, JL, KK, and LW wrote the paper. All authors read and approved the final manuscript version.

ACKNOWLEDGMENTS

We are grateful to Dr. Rima McLeod and Dr. Gang Cheng for critical reading of the manuscript. This research was supported by grants R01AI087625 (KK), RC4AI092801 (KK), R01AI031788 (LW) from the National Institute of Allergy and Infectious Disease and RO1 CA149095 (PW). This work was also supported by Knights Templar Eye Foundation (to KE).

SUPPLEMENTARY MATERIAL

The Supplementary Material for this article can be found online at: <https://www.frontiersin.org/articles/10.3389/fcimb.2019.00009/full#supplementary-material>

REFERENCES

- Amaratunga, C., Sreng, S., Suon, S., Phelps, E. S., Stepniewska, K., Lim, P., et al. (2012). Artemisinin-resistant *Plasmodium falciparum* in Pursat province, Western Cambodia: a parasite clearance rate study. *Lancet Infect. Dis.* 12, 851–858. doi: 10.1016/S1473-3099(12)70181-0
- Assaraf, Y. G., Golenser, J., Spira, D. T., and Bachrach, U. (1984). Polyamine levels and the activity of their biosynthetic enzymes in human erythrocytes infected with the malarial parasite, *Plasmodium falciparum*. *Biochem. J.* 222, 815–819. doi: 10.1042/bj2220815
- Bacchi, C. J., Lane, S., Weiss, L. M., Yarlett, N., Takvorian, P., and Wittner, M. (2001). Polyamine synthesis and interconversion by the microsporidian *Encephalitozoon cuniculi*. *J. Eukaryot. Microbiol.* 48, 374–381. doi: 10.1111/j.1550-7408.2001.tb00327.x
- Bacchi, C. J., Nathan, H. C., Hutner, S. H., McCann, P. P., and Sjoerdsma, A. (1980). Polyamine metabolism: a potential therapeutic target in trypanosomes. *Science* 210, 332–334. doi: 10.1126/science.6775372
- Bacchi, C. J., Rattendi, D., Faciane, E., Yarlett, N., Weiss, L. M., Frydman, B., et al. (2004). Polyamine metabolism in a member of the phylum *Microspora* (*Encephalitozoon cuniculi*): effects of polyamine analogues. *Microbiology* 150, 1215–1224. doi: 10.1099/mic.0.26889-0
- Bacchi, C. J., Weiss, L. M., Lane, S., Frydman, B., Valasinas, A., Reddy, V., et al. (2002). Novel synthetic polyamines are effective in the treatment of experimental microsporidiosis, an opportunistic AIDS-associated infection. *Antimicrob. Agents Chemother.* 46, 55–61. doi: 10.1128/AAC.46.1.55-61.2002
- Bi, X., Lopez, C., Bacchi, C. J., Rattendi, D., and Woster, P. M. (2006). Novel alkylpolyaminoguanidines and alkylpolyaminobiguanides with potent antitrypanosomal activity. *Bioorg. Med. Chem. Lett.* 16, 3229–3232. doi: 10.1016/j.bmcl.2006.03.048

- Bitonti, A. J., Dumont, J. A., Bush, T. L., Edwards, M. L., Stermerick, D. M., McCann, P. P., et al. (1989). Bis(benzyl)polyamine analogs inhibit the growth of chloroquine-resistant human malaria parasites (*Plasmodium falciparum*) *in vitro* and in combination with alpha-difluoromethylornithine cure murine malaria. *Proc. Natl. Acad. Sci. U.S.A.* 86, 651–655. doi: 10.1073/pnas.86.2.651
- Burri, C., and Brun, R. (2003). Eflornithine for the treatment of human African trypanosomiasis. *Parasitol. Res.* 90, S49–S52. doi: 10.1007/s00436-002-0766-5
- Casero, R. A., and Marton, L. J. (2007). Targeting polyamine metabolism and function in cancer and other hyperproliferative diseases. *Nat. Rev. Drug Discov.* 6, 373–390. doi: 10.1038/nrd2243
- Clark, K., Niemand, J., Reeksting, S., Smit, S., van Brummelen, A. C., Williams, M., et al. (2010). Functional consequences of perturbing polyamine metabolism in the malaria parasite, *Plasmodium falciparum*. *Amino Acids* 38, 633–644. doi: 10.1007/s00726-009-0424-7
- Desjardins, R. E., Canfield, C. J., Haynes, J. D., and Chulay, J. D. (1979). Quantitative assessment of antimalarial activity *in vitro* by a semiautomated microdilution technique. *Antimicrob. Agents Chemother.* 16, 710–718. doi: 10.1128/AAC.16.6.710
- Dondorp, A. M., Nosten, F., Yi, P., Das, D., Phyto, A. P., Tarning, J., et al. (2009). Artemisinin resistance in *Plasmodium falciparum* malaria. *N. Engl. J. Med.* 361, 455–467. doi: 10.1056/NEJMoa0808859
- Dufe, V. T., Qiu, W., Müller, I. B., Hui, R., Walter, R. D., and Al-Karadaghi, S. (2007). Crystal structure of *Plasmodium falciparum* spermidine synthase in complex with the Substrate decarboxylated S-adenosylmethionine and the potent inhibitors 4MCHA and AdoDATO. *J. Mol. Biol.* 373, 167–177. doi: 10.1016/j.jmb.2007.07.053
- Ferreira, P. E., Culleton, R., Gil, J. P., and Meshnick, S. R. (2013). Artemisinin resistance in *Plasmodium falciparum*: what is it really? *Trends Parasitol.* 29, 318–320. doi: 10.1016/j.pt.2013.05.002
- Frydman, B., Blokhin, A. V., Brummel, S., Wilding, G., Maxuitenko, Y., Sarkar, A., et al. (2003). Cyclopropane-containing polyamine analogues are efficient growth inhibitors of a human prostate tumor xenograft in nude mice. *J. Med. Chem.* 46, 4586–4600. doi: 10.1021/jm030175u
- Gupta, R. D., Krause-Ihle, T., Bergmann, B., Müller, I. B., Khomutov, A. R., Müller, S., et al. (2005). 3-Aminoxy-1-Aminopropane and derivatives have an antiproliferative effect on cultured *Plasmodium falciparum* by decreasing intracellular polyamine concentrations. *Antimicrob. Agents Chemother.* 49, 2857–2864. doi: 10.1128/AAC.49.7.2857-2864.2005
- Haider, N., Eschbach, M.-L., Dias, S., de, S., Gilberger, T.-W., Walter, R. D., et al. (2005). The spermidine synthase of the malaria parasite *Plasmodium falciparum*: molecular and biochemical characterisation of the polyamine synthesis enzyme. *Mol. Biochem. Parasitol.* 142, 224–236. doi: 10.1016/j.molbiopara.2005.04.004
- Harder, E., Damm, W., Maple, J., Wu, C., Reboul, M., Xiang, J. Y., et al. (2015). OPLS3: a force field providing broad coverage of drug-like small molecules and proteins. *J. Chem. Theory Comput.* 12:281–96. doi: 10.1021/acs.jctc.5b00864
- Hsieh, H.-P., Muller, J. G., and Burrows, C. J. (1994). Structural effects in novel steroidal polyamine-DNA binding. *J. Am. Chem. Soc.* 116, 12077–12078. doi: 10.1021/ja00105a068
- Huang, Y., Hager, E. R., Phillips, D. L., Dunn, V. R., Hacker, A., Frydman, B., et al. (2003). A novel polyamine analog inhibits growth and induces apoptosis in human breast cancer cells. *Clin. Cancer Res.* 9, 2769–2777. doi: 10.3389/fmicb.2019.00009
- Igarashi, K., and Kashiwagi, K. (2000). Polyamines: mysterious modulators of cellular functions. *Biochem. Biophys. Res. Commun.* 271, 559–564. doi: 10.1006/bbrc.2000.2601
- Lambros, C., and Vanderberg, J. P. (1979). Synchronization of *Plasmodium falciparum* erythrocytic stages in culture. *J. Parasitol.* 65, 418–420. doi: 10.2307/3280287
- Makler, M. T., and Hinrichs, D. J. (1993). Measurement of the lactate dehydrogenase activity of *Plasmodium falciparum* as an assessment of parasitemia. *Am. J. Trop. Med. Hyg.* 48, 205–210. doi: 10.4269/ajtmh.1993.48.205
- Makler, M. T., Ries, J. M., Williams, J. A., Bancroft, J. E., Piper, R. C., Gibbins, B. L., et al. (1993). Parasite lactate dehydrogenase as an assay for *Plasmodium falciparum* drug sensitivity. *Am. J. Trop. Med. Hyg.* 48, 739–741. doi: 10.4269/ajtmh.1993.48.739
- Marton, L. J., and Pegg, A. E. (1995). Polyamines as targets for therapeutic intervention. *Annu. Rev. Pharmacol. Toxicol.* 35, 55–91. doi: 10.1146/annurev.pa.35.040195.00415
- Müller, S., Coombs, G. H., and Walter, R. D. (2001). Targeting polyamines of parasitic protozoa in chemotherapy. *Trends Parasitol.* 17, 242–249. doi: 10.1016/S1471-4922(01)01908-0
- Müller, S., Da'dara, A., Lüersen, K., Wrenger, C., Gupta, R. D., Madhubala, R., et al. (2000). In the human malaria parasite *Plasmodium falciparum*, polyamines are synthesized by a bifunctional ornithine decarboxylase, S-adenosylmethionine decarboxylase. *J. Biol. Chem.* 275, 8097–8102. doi: 10.1074/jbc.275.11.8097
- Osland, A., and Kleppe, K. (1977). Polyamine induced aggregation of DNA. *Nucleic Acids Res.* 4, 685–695. doi: 10.1093/nar/4.3.685
- Pegg, A. E., and McCann, P. P. (1982). Polyamine metabolism and function. *Am. J. Physiol. Cell Physiol.* 243, C212–C221. doi: 10.1152/ajpcell.1982.243.5.C212
- Phyo, A. P., Nkhoma, S., Stepniewska, K., Ashley, E. A., Nair, S., McGready, R., et al. (2012). Emergence of artemisinin-resistant malaria on the western border of Thailand: a longitudinal study. *Lancet Lond. Engl.* 379, 1960–1966. doi: 10.1016/S0140-6736(12)60484-X
- Reddy, V. K., Valasinas, A., Sarkar, A., Basu, H. S., Marton, L. J., and Frydman, B. (1998). Conformationally restricted analogues of 1N,12N-bisethylspermine: synthesis and growth inhibitory effects on human tumor cell lines. *J. Med. Chem.* 41, 4723–4732. doi: 10.1021/jm980172v
- Sprenger, J., Carey, J., Svensson, B., Wengel, V., and Persson, L. (2016). Binding and inhibition of spermidine synthase from *Plasmodium falciparum* and implications for *in vitro* inhibitor testing. *PLoS ONE* 11:e0163442. doi: 10.1371/journal.pone.0163442
- Sprenger, J., Svensson, B., Hålander, J., Carey, J., Persson, L., and Al-Karadaghi, S. (2015). Three-dimensional structures of *Plasmodium falciparum* spermidine synthase with bound inhibitors suggest new strategies for drug design. *Acta Crystallogr. D Biol. Crystallogr.* 71, 484–493. doi: 10.1107/S1399004714027011
- Sugiura, M., Shafman, T., and Kufe, D. (1984). Effects of polyamine depletion on proliferation and differentiation of murine erythroleukemia cells. *Cancer Res.* 44, 1440–1444.
- Trager, W., and Jensen, J. B. (1976). Human malaria parasites in continuous culture. *Science* 193, 673–675. doi: 10.1126/science.781840
- Valasinas, A., Reddy, V. K., Blokhin, A. V., Basu, H. S., Bhattacharya, S., Sarkar, A., et al. (2003). Long-chain polyamines (oligoamines) exhibit strong cytotoxicities against human prostate cancer cells. *Bioorg. Med. Chem.* 11, 4121–4131. doi: 10.1016/S0968-0896(03)00453-X
- van Brummelen, A. C., Olszewski, K. L., Wilinski, D., Llinás, M., Louw, A. I., and Birkholtz, L.-M. (2009). Co-inhibition of *Plasmodium falciparum* S-adenosylmethionine decarboxylase/ornithine decarboxylase reveals perturbation-specific compensatory mechanisms by transcriptome, proteome, and metabolome analyses. *J. Biol. Chem.* 284, 4635–4646. doi: 10.1074/jbc.M807085200
- Verlinden, B. K., de Beer, M., Pachaiyappan, B., Besaans, E., Andayi, W. A., Reader, J., et al. (2015). Interrogating alkyl and arylalkylpolyamino (bis)urea and (bis)thiourea isosteres as potent antimalarial chemotypes against multiple lifecycle forms of *Plasmodium falciparum* parasites. *Bioorg. Med. Chem.* 23, 5131–5143. doi: 10.1016/j.bmc.2015.01.036
- Verlinden, B. K., Niemand, J., Snyman, J., Sharma, S. K., Beattie, R. J., Woster, P. M., et al. (2011). Discovery of novel alkylated (bis)urea and (bis)thiourea

- polyamine analogues with potent antimalarial activities. *J. Med. Chem.* 54, 6624–6633. doi: 10.1021/jm200463z
- Wallace, H. M., Fraser, A. V., and Hughes, A. (2003). A perspective of polyamine metabolism. *Biochem. J.* 376, 1–14. doi: 10.1042/bj20031327
- White, N. J. (2008). Qinghaosu (artemisinin): the price of success. *Science* 320, 330–334. doi: 10.1126/science.1155165
- White, N. J., Pukrittayakamee, S., Hien, T. T., Faiz, M. A., Mokuou, O. A., and Dondorp, A. M. (2014). Malaria. *Lancet* 383, 22–28. doi: 10.1016/B.978-0-7020-5101-2.00044-3
- World Health Organization (2015) *World Health Organization Malaria Report*. Geneva: World Health Organization.
- Zou, Y., Wu, Z., Sirisoma, N., Woster, P. M., Casero, R. A., Weiss, L. M., et al. (2001). Novel alkylpolyamine analogues that possess both antitrypanosomal and antimicrosporidial activity. *Bioorg.*

Med. Chem. Lett. 11, 1613–1617. doi: 10.1016/S0960-894X(01)00315-8

Conflict of Interest Statement: The authors declare that the research was conducted in the absence of any commercial or financial relationships that could be construed as a potential conflict of interest.

Copyright © 2019 El Bissati, Redel, Ting, Lykins, McPhillie, Upadhyay, Woster, Yarlett, Kim and Weiss. This is an open-access article distributed under the terms of the Creative Commons Attribution License (CC BY). The use, distribution or reproduction in other forums is permitted, provided the original author(s) and the copyright owner(s) are credited and that the original publication in this journal is cited, in accordance with accepted academic practice. No use, distribution or reproduction is permitted which does not comply with these terms.



Artemisinin Derivatives and Synthetic Trioxane Trigger Apoptotic Cell Death in Asexual Stages of *Plasmodium*

Sarika Gunjan^{1,2}, Tanuj Sharma^{1,3}, Kanchan Yadav², Bhavana S. Chauhan^{1,2}, Sunil K. Singh², Mohammad I. Siddiqi^{1,3} and Renu Tripathi^{1,2*}

¹ Academy of Scientific and Innovative Research, New Delhi, India, ² Division of Parasitology, Central Drug Research Institute (CDRI), Council of Scientific and Industrial Research (CSIR), Lucknow, India, ³ Division of Molecular & Structural Biology, Central Drug Research Institute (CDRI), Council of Scientific and Industrial Research (CSIR), Lucknow, India

Although over the last 15 years, prevalence of malaria became reduced by over half but developing resistance against artemisinin derivatives and its combinations, which are only ray of hope to treat resistant malaria set back the control efforts and the key hinderence to achieve the goal of malaria elimination till 2030. In spite these artemisinins are precious antimalarials, their action mechanism is yet to be fully understood. Reactive oxygen species (ROS) produces by cleavage of endoperoxide bridge of artemisinin derivatives are known to be its antimalarial efficacy. Since ROS could induce apoptosis, here we had explored the effect of artemisinin derivatives on apoptotic machinery of malaria parasite, *Plasmodium falciparum* and its survival. We have studied the effect of α/β arteether, artesunate and a synthetic 1, 2, 4 trioxane on mitochondria, caspase activity and DNA during asexual blood stages of *Plasmodium falciparum* 3D7. Results have shown that cleavage of peroxide bridge of artemisinin derivatives and 1,2,4 trioxane generate reactive oxygen species which depolarize mitochondrial membrane potential and make it permeable which further followed by activation of caspase like enzyme and DNA fragmentation, which are hallmark of apoptotic cell death. These findings suggest that artemisinin derivatives and synthetic trioxane induce apoptosis like phenomena in erythrocytic stage of malaria parasite; *Plasmodium falciparum*.

Keywords: arteether, artesunate, CDRI-97/78, apoptosis, *Plasmodium*

OPEN ACCESS

Edited by:

Kamal El Bissati,
University of Chicago, United States

Reviewed by:

Larance Ronsard,
Ragon Institute of MGH, MIT and
Harvard, United States
Sabrina Absalon,
Boston Children's Hospital, Harvard
University, United States

*Correspondence:

Renu Tripathi
renu1113@rediffmail.com

Received: 20 March 2018

Accepted: 04 July 2018

Published: 26 July 2018

Citation:

Gunjan S, Sharma T, Yadav K, Chauhan BS, Singh SK, Siddiqi MI and Tripathi R (2018) Artemisinin Derivatives and Synthetic Trioxane Trigger Apoptotic Cell Death in Asexual Stages of *Plasmodium*. *Front. Cell. Infect. Microbiol.* 8:256. doi: 10.3389/fcimb.2018.00256

INTRODUCTION

Lots of efforts are carrying out to control the deadly disease, malaria but it is still a burden to human health and ~3.2 billion people are at risk of malaria world wide. According to WHO 445,000 deaths and 216 million malaria cases were reported in 2015 but due to employment of artemisinin and drug impregnated bed nets, 30% decrease in malaria cases and 47% in mortality rate was observed since 2000 (White et al., 2014; WHO, 2014, 2015). In spite of having these magic drugs, the decreasing clinical efficacy and emerging resistance to artemisinin derivatives in Thailand and Cambodia have raised an alarming situation about future treatment options (Price et al., 1996; Amaratunga et al., 2012; Phyo et al., 2012; Ferreira et al., 2013). Peroxide bridge linkage of artemisinin, a sesquiterpene trioxane lactone, is known to be responsible for its anti-malarial activity (Butler, 1992). Since artemisinin is poorly soluble in water as well as in oil, it becomes reduced into dihydroartemisinin (DHA) and its derivatives such as the water-soluble artesunate and oil-soluble artemether and arteether. Due to limited availability of artemisinins, continued efforts led

to the development of synthetic trioxanes. A novel trioxane 97/78, developed by CSIR-Central Drug Research Institute (CDRI), India, has shown promising antimalarial activity and is currently under clinical trials (Singh et al., 2011). CDRI-97/78 contains 1, 2, 4-trioxane nucleus similar to endoperoxide lactone of artemisinin. It emerged as lead compound with excellent pharmacological antimalarial activity (Singh et al., 2004, 2011; Griesbeck et al., 2005). Although, at the present time artemisinin derivatives are the main stay of malaria therapy, its mode of action is a topic of debate. Considering its importance, here we explored the action mechanisms of artemisinin derivatives (ART, ARS) and a CDRI compound- 97/78 during erythrocytic cycle of parasites via apoptotic markers as apoptosis found to be a novel cell death pathway in *Plasmodium* and multiple markers of apoptosis have been observed in different stages of *Plasmodium* life cycle that occur in vector and the host (Al-Olayan et al., 2002; Meslin et al., 2007; Ch'ng et al., 2010; Gunjan et al., 2016).

MATERIALS AND METHODS

In-Vitro Cultivation of *P. falciparum*

In vitro culture of chloroquine sensitive strain (Pf3D7) of *P. falciparum* was carried out in fresh human erythrocytes at 5% hematocrit in complete RPMI-1640 (HEPES modified) medium (Sigma) supplemented with 0.5% AlbuMaxII, 0.2% glucose, 0.2% NaHCO₃ and 15 μ M hypoxanthine and incubated at 37°C in CO₂ incubator (Trager and Jensen, 1976). Parasite growth rate and stage was determined by the examination of Giemsa's stained thin blood smears of infected erythrocytes.

Evaluation of *in Vitro* Antimalarial Profile of Drugs

To evaluate antimalarial activity of drugs on erythrocytic stages of the *P. falciparum* 3D7, SYBRGreen I fluorometric assay was carried out with some modifications (Johnson et al., 2007). Briefly, two fold serial dilutions of drugs were prepared in 96 well plates and then 50 μ l asynchronous culture (~95% ring) of infected erythrocytes with 0.8–1% parasitaemia and 1% hematocrit was added to each well (100 μ l-final volume). Eight wells were treated as positive control (without drug) and 4 wells as negative controls (without parasite and drug). Further culture were incubated at 37°C for 72 h in CO₂ incubator. After 72 h, 100 μ l of lytic buffer containing 1X SYBR Green was added to each well and incubated for 2 h at room temperature in dark. Fluorescence of SYBR Green was recorded using fluorescence reader at Ex. 485 nm, Em. 535 nm. IC₅₀ was calculated on the basis of DNA content of the parasite by using MS-Excel template.

Computational Studies

Considering that the metacaspase protein (PLASMODB id - PF3D7_1354800) may be potential drug target, we attempted 3D-structural investigation on sequenced protein of *P. falciparum*. Modeled protein was selected using methodology described previously from our lab (Gunjan et al., 2016). Structure of arteether, artesunate and parent compound CDRI 97/78 used for docking studies were built and minimized using Gaussian version

09 (Dennington et al., 2009; Frisch et al., 2009). Computational studies were performed on the metacaspase protein model to get the molecular insights of how the drugs were bound to its target protein. Binding site was generated using the SiteMap module of Schrodinger package (Halgren, 2009). Further, the grid around binding sites identified by SiteMap were generated using Grid generating module of Schrodinger software package (Schrödinger, 2016b). Van der Waals radius used for scaling was 1.0 Å and default settings were used for other parameters. Both protein and ligands (arteether, artesunate, compound CDRI 97/78) were prepared using the Ligand and Protein preparation modules of Schrodinger software package (Schrödinger, 2016a,c). Prepared ligands were then docked with Ubiquitin Proteasome using Glide-7.1 module (Friesner et al., 2006). Docking was performed using Extra precision mode and default setting were used for docking. Ligand receptor interaction images were generated using the “Ligand interaction” module of Schrodinger software package. Poses for interaction studies were selected from largest cluster. The interactions which were analyzed in this module were “Hydrogen Bonding, Pi-Pi interaction, Pi-Cation interaction, Salt Bridges” at cut-off radius of 2.50 Å. Coulomb surface for model and ribbon view were generated using UCSF-Chimera version 1.10 (Pettersen et al., 2004).

Caspase Assay

To measure the caspase-like protease activity during erythrocytic stage in drug treated and untreated parasites EnzChek® Caspase-3 Assay Kit (Molecular probe) was used and assay was performed according to the manufacturer's instructions with some modification. In brief, infected erythrocytes (iRBCs) having 8–10% parasitaemia were exposed with 10 nM of ART/ARS and 100 nM of CDRI-97/78 for 24 h. Cell free parasites were prepared by saponin lysis of drug treated and untreated iRBCs. Parasite lysate were prepared by mild sonication and 2X reaction buffer containing caspase substrate Z-DEVD-R110 was added into 1:1 ratio followed by incubation at room (25°C) temperature for 30 min. in dark (Gunjan et al., 2016). Increase in fluorescence caused by cleavage of the Z-DEVD-R110 substrate was measured at excitation and emission wavelengths of 485/20 and 530/20 nm, respectively using micro plate reader (Synergy HT Biotek). In a parallel set of reactions, the caspase inhibitor Ac-DEVD-CHO was added to the reaction mixture before the addition of parasite lysate. All the experiments were performed in duplicate.

Mitochondrial Membrane Potential ($\Delta\psi$ m)

To determine the effect of ART, ARS, and CDRI-97/78 on the mitochondria of erythrocytic stages of *P. falciparum*, iRBCs were exposed with these drugs for 6 and 24 h and further mature stage enriched parasitized red blood cells were stained with 6 μ M JC-1 dye (Sigma-Aldrich) for 20 min. in dark at 37°C. Cells were washed twice and resuspend in 0.5 ml assay buffer for acquiring the fluorescence using flow cytometer.

Acquisition was carried out using FACS-CELLQUEST software on FACS Calibur (BD Biosciences) and analysis of flow cytometric data was performed using Flow Jo software (Tree star Inc., Ashland, OR). Dissipation in $\Delta\psi$ m was measured by

calculating the ratio between red and green fluorescence (i.e., 590/530 nm) (Gunjan et al., 2016).

In Situ Detection of DNA Fragmentation by Terminal Deoxynucleotidyl Transferase (TdT)-Mediated dUTP Nick End Labeling (TUNEL)

DNA fragmentation in malaria parasite during erythrocytic cycle was analyzed using an *in situ* cell death detection kit (Promega). Briefly, asexual stages of *P. falciparum* were treated with ART (10 nM), ARS (10 nM), and CDRI-97/78 (100 nM) for 24 h followed by saponin enrichment to isolate cell free parasite. Parasites were fixed with 1% paraformaldehyde for 1 h at 4°C followed by permeabilization with a solution of 0.2% Triton X-100. Fixed and permeabilized parasites were labeled with the TUNEL solution for 1 h at 37°C. Reactions were terminated by adding 20 nM EDTA. Finally cells were resuspended in PBS and analyzed by LSRII flow cytometer (BD Biosciences) equipped with 488 nm argon laser (Gunjan et al., 2016). Percentage of TUNEL positive cells were calculated using Flow Jo analysis software.

Measurement of ROS Level in Blood Stages of *P. falciparum*

Intracellular ROS levels were measured in treated and untreated cells as described previously (Gunjan et al., 2016). In Brief, iRBCs having 8–10% parasitaemia were exposed with 10 nM

ART and ARS, 100 nM of CDRI-97/78 for 24 and 48 h. Further cells were incubated with 10 μ M concentration of dichlorodihydrofluorescein diacetate (H₂DCFDA) (Sigma) and incubated in CO₂ incubator at 37°C for 30 min in dark. Samples were washed twice with 1X PBS and cell free parasites were isolated by saponin lysis of iRBCs (Gunjan et al., 2016) and resuspended in PBS for acquiring fluorescence of DCF. Acquisitions were done on FACS caliber flow cytometer and data were analyzed using FlowJo 8.1.0 software (Tree Star Inc., USA).

Statistical Analysis

The statistical analyses of the antimalarial effect of drugs on the asexual stages of *P. falciparum* were performed using Student's *t*-test. The statistical analyses of other apoptotic markers were performed using analysis of variance (ANOVA) and the Tukey *post hoc* test.

RESULTS

In Vitro Antimalarial Profile of α/β Arteether (ART), Artesunate (ARS) and CDRI-97/78

In vitro growth of *P. falciparum* 3D7 was inhibited by ART, ARS and CDRI-97/78 in a dose dependent manner. The IC₅₀ values of ART, ARS and CDRI-97/78 were found to be 2.19 ± 0.9 nM, 4.79 ± 0.7 nM and 49 ± 2.8 nM (Figure 1). For further studies to check the effect of these drugs on apoptotic markers;

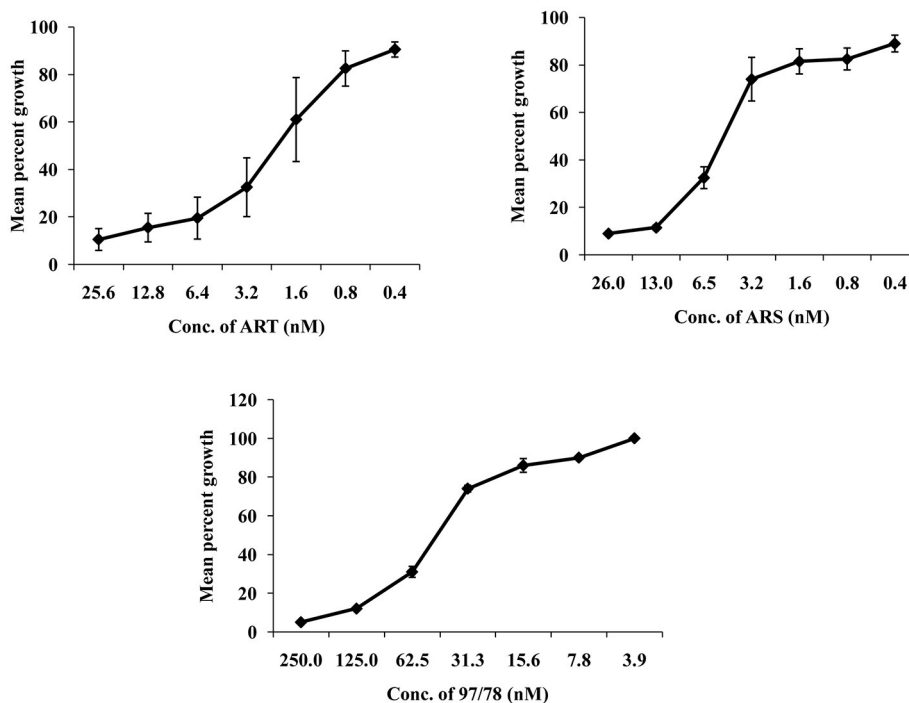


FIGURE 1 | Typical dose response of ART, ARS, and CDRI-97/78 on growth of CQ sensitive strain of *P. falciparum*. **(A)** Graph showing ~90 and 50% inhibition in parasite growth at 25.6 and 2.19 nM conc. of ART respectively. **(B)** ~90 and 50% parasite growth inhibition is shown at 26 and 4.79 nM of ARS respectively. **(C)** CDRI synthetic compound 97/78 inhibits ~90 and 50% growth of *Plasmodium* at 125 and 49 nM.

mitochondrial outer membrane potential, caspase like activity and DNA fragmentation \sim IC₉₀ concentration of drugs was used.

Computational Studies

Homology models were generated using structure of the yeast metacaspase (YCA1) having PDB id - 4F6O (Wong et al., 2012). Since, for our protein MCA-1 in *P. falciparum* we were unable to retrieve any template having higher identity more than 50%. Literature review does suggest that template structure having identity greater than 30% can be utilized for homology modeling (Xiang, 2006). Thus, homology modeling was performed using template having 42% identity, 62% similarity. Ramachandran plot analysis of best model indicated 82.8% residues in favored region, 16.2% region in addition allowed region and 1.0% residues in disallowed region. Modeled protein indicated presence of binding sites, as predicted by SiteMap (Figure 2A). Of these, top 3 binding sites were used for generating grid and docking was performed around it using GLIDE-7.1. Best pose of ART, ARS, CDRI-97/98 parent compound indicated Glide Score of -6.29 , -4.02 , -5.36 Kcal/mol respectively. These scores were in agreement with the wet lab experimental data on Metacaspase assay. For Arteether, protein residues found important for interaction were Q249, N253, H273, K275, Q276, H277, S278, K289, F290, N291, N314 (Figure 2B). Of these most prominent interaction was hydrogen bonding of 2.02 Å with Ser278. Similarly for Artesunate, residues important for interaction were Q249, N253, H273, N279, K289, F290, and N314 (Figure 2C) residues important for interaction were Asn253 having hydrogen bond of 2.8 Å and Asn279 having hydrogen bond of 2.9 Å. For compound 97/78, important residues for interaction were P239, G240, T245, V248, Q249, K252, S278, N279, K289, F290, N291, N314 (Figure 2D). Residues important for interaction were Phe290 having 4.9 Å Pi-Pi stacking interaction, Gln249 having 2.7 Å hydrogen bond, Gly240 having 2.41 Å hydrogen bond, Lys289 having 2.35 Å hydrogen bond and Asn314 having 2.00 Å hydrogen bond (Table S1). For arteether and artesunate the binding of cyclo-hexadecane group was having same orientation but variation in binding energies was observed owing to the different ethoxy- and butanoic acid- side chains respectively. This group was mimicked by the phenoxy-propoxy moiety in compound 97/78. Residues namely Gln249, Ser278, Lys289, Phe290, and Asn314 were found to be important for interaction with compounds. Of these Gln249, His273, and Lys289 have been previously characterized for interaction with the metacaspase protein (Gunjan et al., 2016). They can be further utilized for the rational design and synthesis of anti-malarial compounds.

Artemisinin Derivatives Activate Caspase Like Enzyme in Malaria Parasites

DEVD-specific protease activities (Caspase-3) in drug treated and untreated parasites was measured using rhodamine 110 bis-N-CBZ-L-aspartyl-L-glutamyl-L-valyl-L-aspartic acid amide—(Z-DEVD-R110). Upon enzymatic cleavage, the non-fluorescent bisamide substrate is converted to fluorescent monoamide Cytosolic fraction of artemisinin derivatives and synthesized 1,2,4 trioxane treated parasites has showed increased caspase 3 activity as compared to control viz. 164, 56, and 121% after

24 h treatment of 10 nM ART, 10 nM ARS, and 100 nM CDRI-97/78 respectively (Figure 3). Moreover, the activity of caspase-3 was significantly inhibited in the presence of Ac-DEVD-CHO, a potent inhibitor of caspase-3, indicating that *P. falciparum* contains a protease having caspase-3-like activity.

Artemisinin Derivatives Reduces Mitochondrial Membrane Potential of Malaria Parasite

Mitochondrial membrane potential ($\Delta\psi_m$), which is an index of mitochondrial function, was also examined to evaluate the effect of artemisinin derivatives and 1,2,4 trioxane (CDRI-97/78) on mitochondria of asexual blood stages of Plasmodium. The detection of mitochondrial membrane potential in drug treated/untreated parasites was done using JC-1, cationic probe which aggregate in mitochondria due to electronegative environment inside the mitochondria and give red color fluorescence but at depolarization of mitochondrial membrane (low mitochondrial membrane potential) JC-1 remains in monomeric form and give green color fluorescence.

Dot plot analysis showed that after 6 h treatment there is no significant changes in green fluorescence intensity in comparison to untreated parasites whereas after 24 h treatment, percentage of JC-1 monomer were increased significantly.

In dot plot analysis, green fluorescence of JC-1 monomer was measured in R2 gate (low mitochondrial membrane potential). In untreated parasite, R2 gate contained 76% cells whereas ART, ARS and 97/78 treated parasite have shown 90, 81, and 85% cells respectively in R2 gate (Figure 4).

Red/Green ratios were obtained to determine the extent of mitochondrial dysregulation. In untreated cells red: green ratio is 0.33 ± 0.01 while it is found to be decreased to 0.11 ± 0.005 , 0.20 ± 0.01 and 0.18 ± 0.004 after 24 h treatment of ART, ARS and 97/78 respectively (Figure 4).

Increase in *in Situ* DNA Fragmentation in Erythrocytic Stage of Plasmodium Under Artemisinin Derivatives Treatment

To evaluate the effect of artemisinin derivatives on DNA fragmentation in Plasmodium, parasites were exposed to 10 nM conc. of ART/ARS and 100 nM of 97/78 for 24 h. Before TUNEL staining, parasites were isolated by saponin lysis of iRBCs so that fluorescence of the parasite itself could be clearly recorded. Dot plot analysis has showed increase DNA fragmentation in these artemisinin derivatives and CDRI-97/78 treated parasites as compared to untreated (Figure 5).

Assessment of ROS Generation in Artemisinin Derivative and CDRI-97/78 Treated/Untreated Parasites

Intracellular ROS production was measured by staining with DCFDA in treated and untreated parasites. Results showed 12.5, 37.5, and 54.1% increase in reactive oxygen species in ART, ARS, and 97/78 treated parasite respectively as compared to untreated parasites (Figure 6).

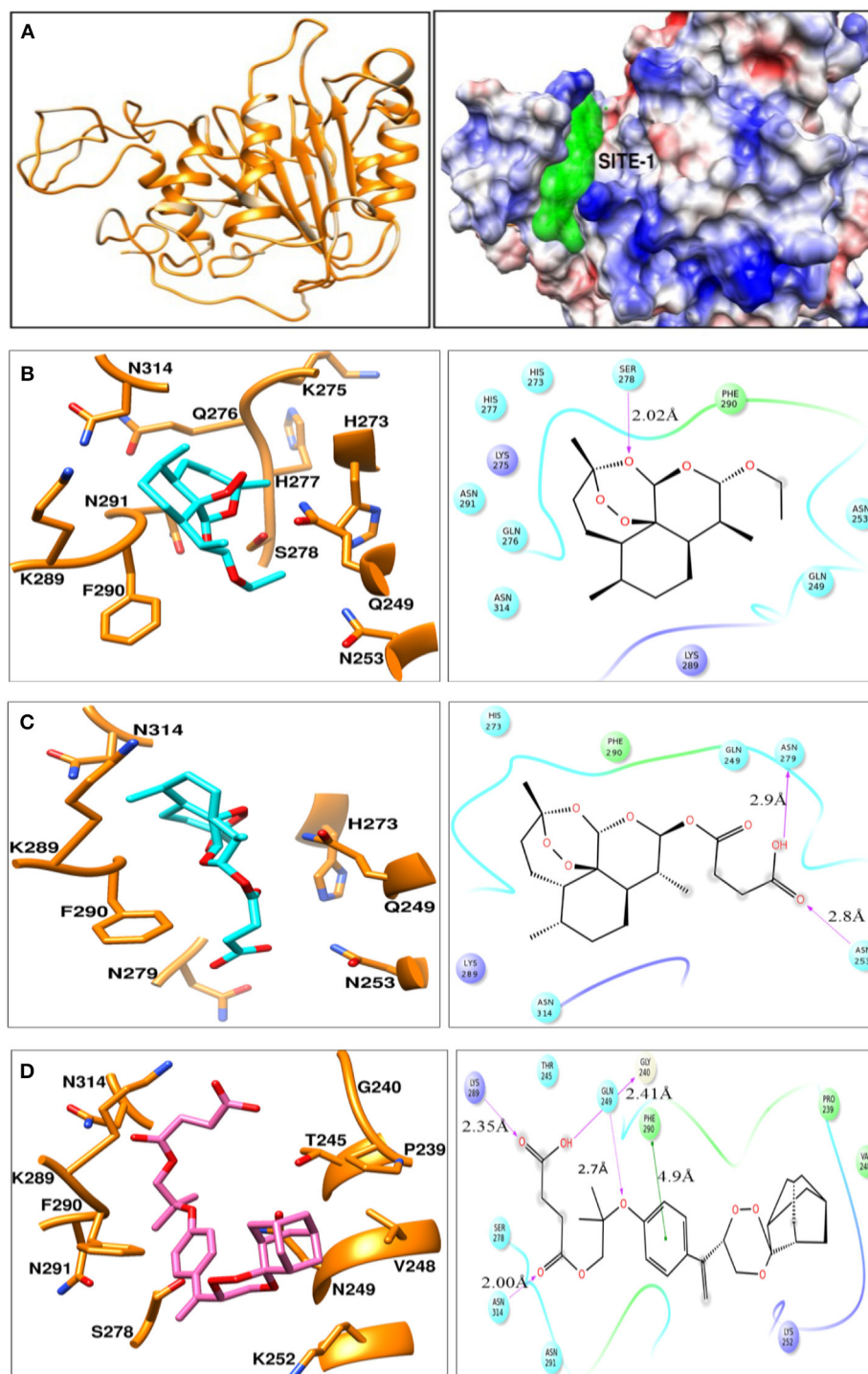


FIGURE 2 | (A) Ribbon view model of metacaspase modeled protein. Indicates coulomb surface model of receptor along with the best predicted binding site (green color) by SiteMap module of Schrodinger version 2016-2. **(B–D)** indicates the ligand-interaction plots of ART, ARS, and compound CDRI- 97/78 respectively along with interacting residues of Metacaspase protein identified using ligand interaction module of Schrodinger-2016-2. The color code of various interacting residues indicates their physiochemical property. Blue stands for polar, red for charged negative, purple for charged positive, green for hydrophobic. Light shadows indicate solvent exposed region.

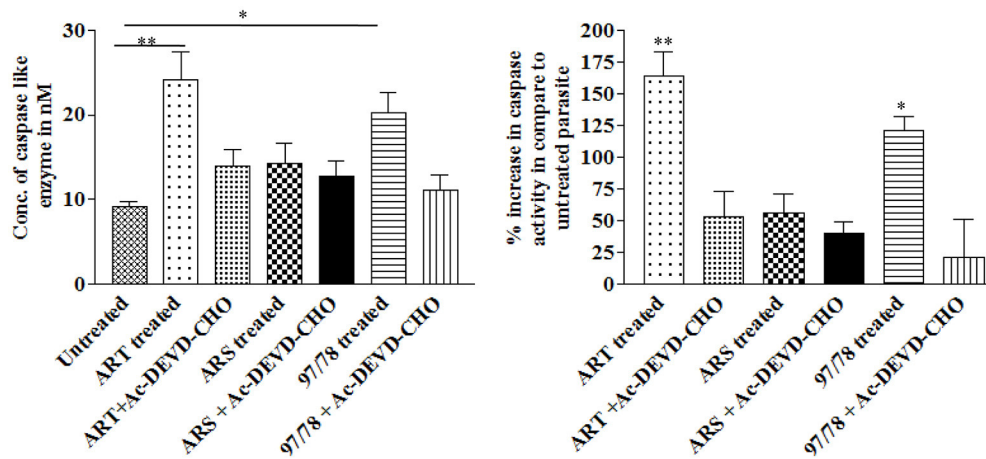


FIGURE 3 | Effect of artemisinin derivatives and CDRI-97/78 on caspase like activity. Caspase-3-like activity was measured in the cytosolic fraction (100 μ g protein) from untreated and drug treated parasites. * $p < 0.05$; ** $p < 0.01$.

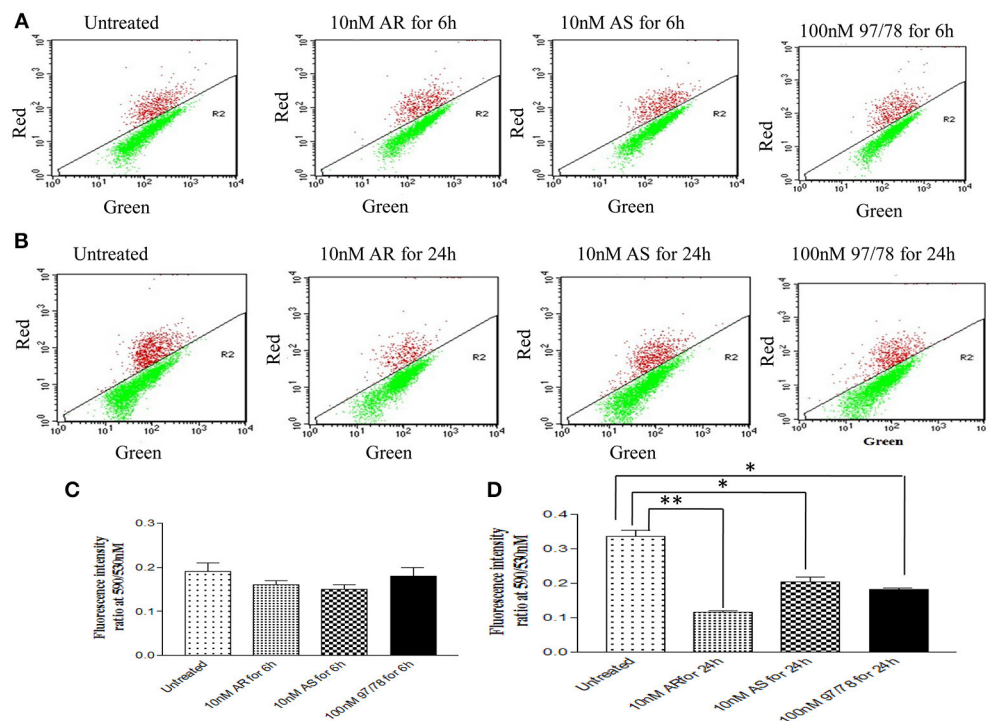


FIGURE 4 | JC-1 staining of iRBCs shows reduction in mitochondrial membrane potential ($\Delta\psi_m$) in *Plasmodium falciparum* parasites treated with drugs. Flow cytometry dot plot showing the gating of JC1 (red)-aggregates and JC1 (green)-monomer populations. Ratio of which represents the JC1-positive population. (A,C) Parasites were treated with drugs for 6 h (B,D) parasites were treated with drugs for 24 h. * $p < 0.05$; ** $p < 0.01$.

DISCUSSION

Artemisinin derivatives are known to be effective against both erythrocytic stages; asexual schizontocidal as well as sexual gametocytocidal and showing promise as antimalarial drugs with transmission-blocking potential (Kumar and Zheng, 1990; Price et al., 1996; Haynes and Krishna, 2004). Understanding the

mode of action for artemisinin derivatives is very important to select their partner drugs and to overcome the problem of resistance toward these drugs. Even though many cellular targets have been identified, the mechanism of action of artemisinin derivatives still remains vague. No single mechanism exists for artemisinins' action and it was suggested that it functions through multiple modes (Pandey and Pandey-Rai, 2016).

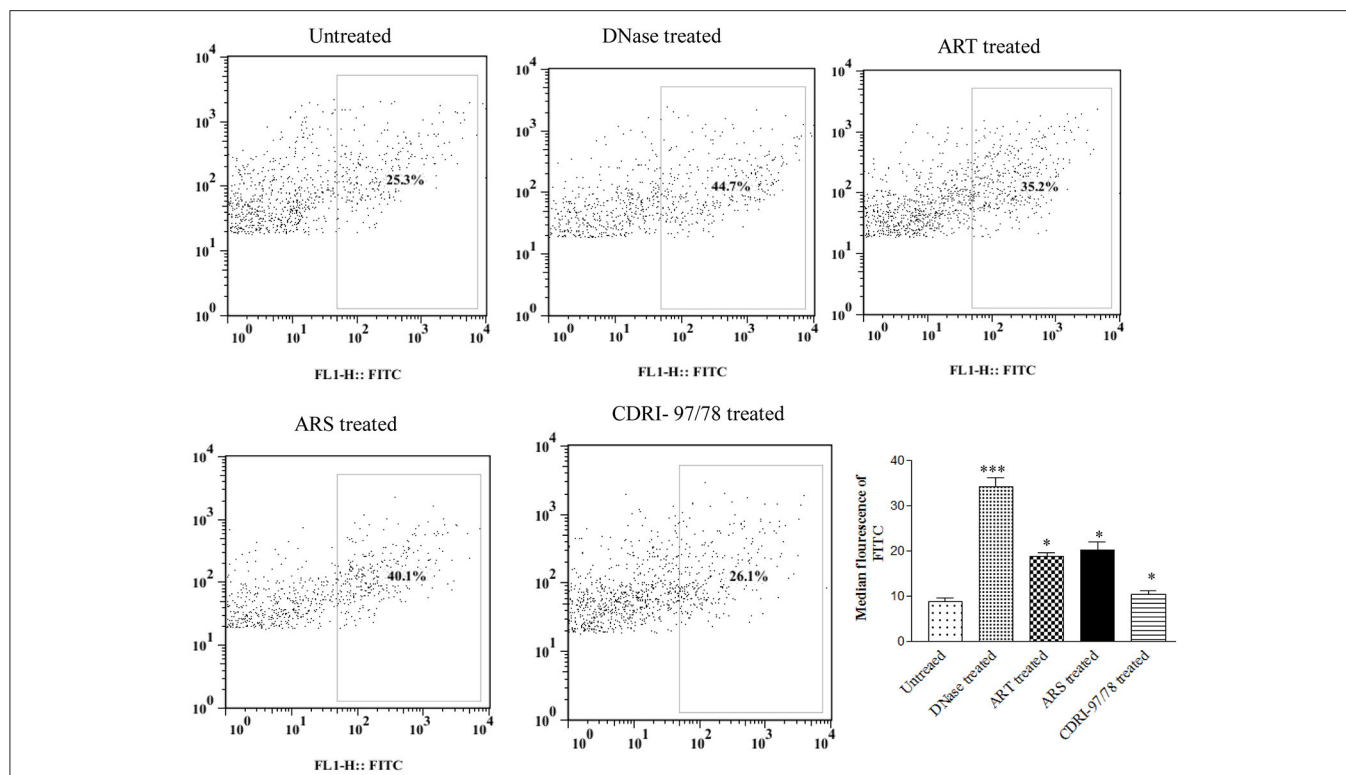


FIGURE 5 | Evaluation of DNA fragmentation using TUNEL assay. Flow cytometry dot plot showing shifting of population toward FITC channel (R2 gated), and percent increase in DNA fragmentation after treatment of ART, ARS and 97/78 treated cells. Data is representative of duplicate sample of two separate experiments. p -value is <0.001 for untreated vs. DNase, for ARS treated parasites, p -value is <0.01 whereas for ART and 97/78 treated parasites p -value is <0.05 . * $p < 0.05$; *** $p < 0.001$.

A decade ago, *PfATP6*, the *P. falciparum* sarco-endoplasmic reticulum calcium ATPase (SERCA) was identified as potential target for artemisinin (Friesner et al., 2006). It has been proposed that the endoperoxide bridge is responsible for antimalarial activity as it generates free radical which alkylates the different parasitic protein resulting in death of parasite (Pettersen et al., 2004). Artemisinin are activated by binding of Fe^{2+} of heme/non-heme and generate carbon centered free radicals or reactive oxygen species which cause damage to cellular targets in their vicinity through alkylation (Cui and Su, 2009). Recently, Hartwig et al. have demonstrated that artemisinin accumulates in neutral lipid of parasite membrane and damage it (Price et al., 1996) which was also advocated by Wang et al. who studied that artemisinin depolarize the mitochondrial membrane via ROS generation which lead to the mitochondria malfunctioning and parasite cell death (Amaratunga et al., 2012). On the other hand Gopalakrishnan and his group has revealed that artesunate induces DNA double-strand breaks in *P. falciparum* with simultaneous increase in intercellular ROS level in the parasite ultimately causing parasite death (Phyo et al., 2012). DNA damage caused by ROS generation in ARS treated mice and impaired function of mitochondria in parasite due to artemisinin treatment providing the premise for our hypothesis that in addition to the above-mentioned effects, the antimalarial action

of artemisinin derivatives involves apoptotic cell death in parasite.

Before going to check the apoptotic markers, first we have studied the interaction of these artemisinin derivatives; ART/ARS and 97/78 with metacaspase enzyme by *in silico* study and results of docking studies have shown that these drugs effectively bind with the metacaspase enzyme which was further confirmed by *in vitro* studies. Although the *P. falciparum* genome contain metacaspase instead of classical caspase-3 (PlasmoDB, 2013), the cytosolic fraction of artemisinin derivatives and synthesized 1,2,4 trioxane treated parasites significantly cleaved the caspase-3 substrate, Z-DEVD-R110 whereas the same fraction of control parasites (untreated) showed very little activity (Figure 3). Moreover in the presence of caspase-3 inhibitor, caspase activity found to be decreased. Finding of *in silico* and *in vitro* studies indicate that parasite's metacaspase has caspase 3 like properties. Except the caspase activation, other markers of apoptotic cell death; mitochondrial membrane potential and DNA fragmentation were also studied to evaluate the apoptotic cell death phenomena in asexual stages of malaria parasite. Depolarization of mitochondrial membrane potential is the characteristic feature observed in cells that are undergoing programmed cell death. In the cells, which are going to apoptotic cell death, mitochondrial membrane potential found to be low which allow release of cytochrome c in cytoplasm. Cytoplasm

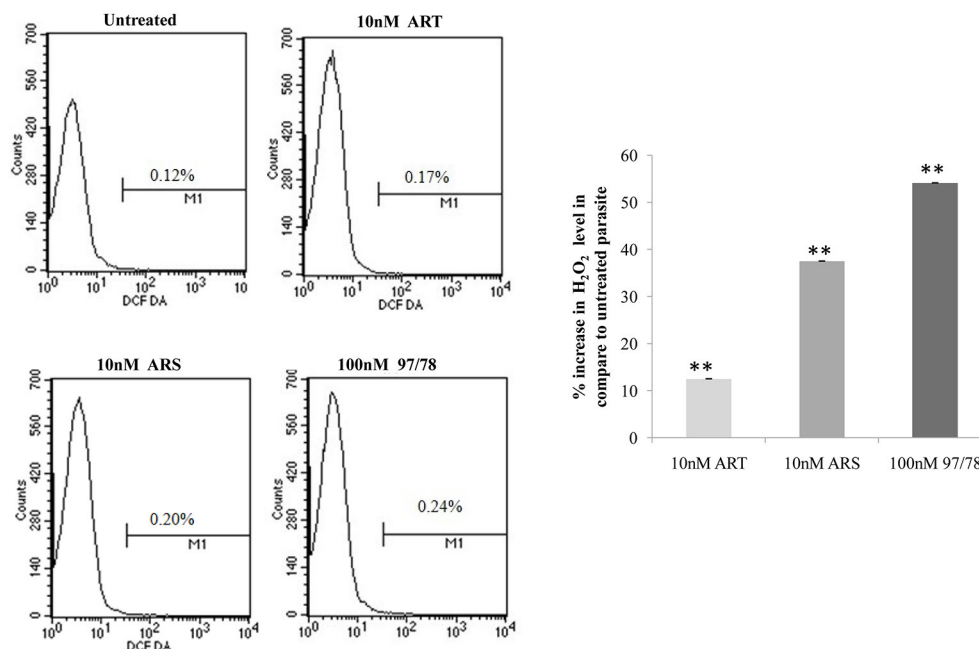
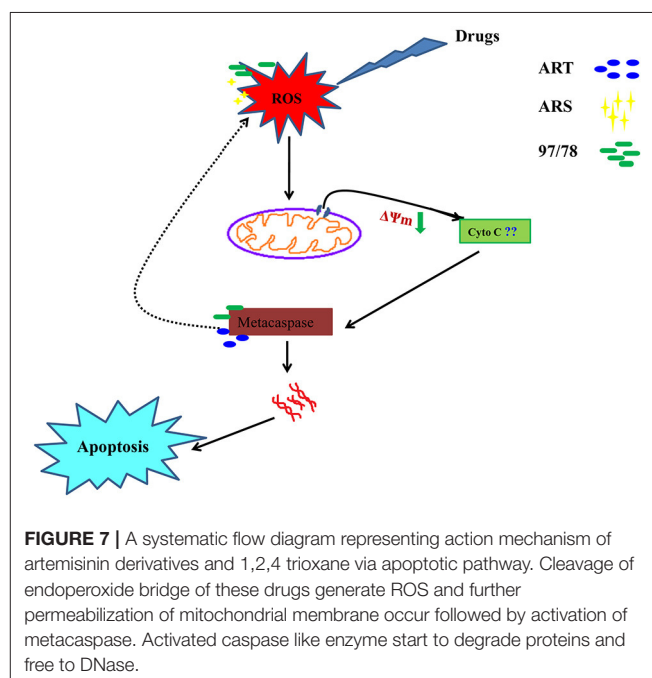


FIGURE 6 | Flow cytometric analysis of ROS generation in *P. falciparum* 3D7. Parasites isolated from all groups by saponin enrichment and loaded with DCFDA probe to evaluate ROS generation. Flow cytometry histograms showing increase in DCF positive cells after treatment with 10 nM concentrations of ART/ARS and 100 nM of CDRI-97/78 compound. Bar graph is showing percent increase of H₂O₂ level in drug treated parasite as compared to untreated. The experiments were performed twice ($n = 2$) and data expressed as mean values \pm SEM. ** $P \leq 0.01$ vs. control; Tukey's test.

activate caspases followed by apoptosome formation and cell death (Gottlieb et al., 2003). Here we observed that mitochondrial membrane potential of malaria parasites was getting reduced in the presence of artemisinin derivatives and CDRI 97/78. Our results showed a significant decrease in JC-1 positive cells which indicate the low mitochondrial membrane potential in drug treated parasites as compared to untreated parasites which advocate the findings of Wang and his coauthors (Wang et al., 2010) and also indicate that mitochondrial machinery of *Plasmodium* could be the target of artemisinin derivatives and synthetic trioxane. Next, DNA fragmentation was quantified from fixed and isolated parasites by the flow cytometric TUNEL assay as fragmentation in genomic DNA is considered as the hall-mark of apoptotic cell death. Here we observed increased number of fragmented DNA in drug treated parasites as compare to untreated parasite, which resemble with the finding of A.M Rama Gopalkrishna who had suggested that artesunate induce ROS dependent DNA fragmentation in malaria parasite (Gopalakrishnan and Kumar, 2014; **Figure 5**). These findings for arteether/CDRI 97/78 are reported for the first time. Since the mechanism of PCD induction usually includes an increase in the levels of reactive oxygen species (ROS). Monitoring of oxidative burst revealed significant increase in generation of reactive oxygen species (ROS) in ART, ARS, and 97/78 treated parasites after 24 h ($P < 0.01$) (**Figure 6**). These findings indicate that artemisinin derivatives induce free radicals mediated apoptotic cell death in asexual stages of malaria parasite.

In the present study we have concluded that these drugs generate ROS due to the cleavage of endoperoxide



bridge which cause depolarization of mitochondrial outer membrane and lead to its permeabilization. Further caspase like enzyme get activated and start degradation of different proteins and free to DNase. In higher eukaryotes, cytochrome c (Cyt C) release from mitochondria and

induce the activation of caspases but in *Plasmodium*, role of cytochrome c in apoptosis is still unknown so here we have hypothesized that may be Cyt C or Cyt C like any other protein could be involved in the activation of metacaspase (Figure 7).

AUTHOR CONTRIBUTIONS

SG has helped in designing experiments and analyzing the results of experiments, performed most of the experiments and wrote the manuscript. TS has performed *in silico* experiments of this study. KY has done the experiment to measure the oxidative burst after treatment of drugs. BSC and SKS have helped in doing the experiments to find out antimalarial activity of artesunate, artesunate and synthetic trioxane CDRI-97/78. MIS designed the *in silico* experiments and analyzed the results of computational studies. RT has designed the whole study as well as objectives and analyzed all results/outcomes of each experiment and also helped in writing manuscript.

REFERENCES

- Al-Olayan, E. M., Williams, G. T., and Hurd, H. (2002). Apoptosis in the malaria protozoan, *Plasmodium berghei*: a possible mechanism for limiting intensity of infection in the mosquito. *Int. J. Parasitol.* 32, 1133–1143. doi: 10.1016/S0020-7519(02)00087-5
- Amaratunga, C., Sreng, S., Suon, S., Phelps, E. S., Stepniewska, K., Lim, P., et al. (2012). Artemisinin-resistant *Plasmodium falciparum* in Pursat province, western Cambodia: a parasite clearance rate study. *Lancet Infect. Dis.* 12, 851–858. doi: 10.1016/S1473-3099(12)70181-0
- Butler, A. R. (1992). Traditional Chinese herbal medicine. *Rep. Proc. Scott. Soc. Hist. Med.* 3, 8–16.
- Ch'ng, J. H., Kotturi, S. R., Chong, A. G., Lear, M. J., and Tan, K. S. (2010). A programmed cell death pathway in the malaria parasite *Plasmodium falciparum* has general features of mammalian apoptosis but is mediated by clan CA cysteine proteases. *Cell Death Dis.* 1:e26. doi: 10.1038/cddis.2010.2
- Cui, L., and Su, X. Z. (2009). Discovery, mechanisms of action and combination therapy of artemisinin. *Expert Rev. Anti Infect. Ther.* 7, 999–1013. doi: 10.1586/eri.09.68
- Dennington R., Keith, T., and Millam, J. (2009). *GaussView, Version 5*. Shawnee Mission, KS: Semichem Inc.
- Ferreira, P. E., Culleton, R., Gil, J. P., and Meshnick, S. R. (2013). Artemisinin resistance in *Plasmodium falciparum*: what is it really? *Trends Parasitol.* 29, 318–320. doi: 10.1016/j.pt.2013.05.002
- Friesner, R. A., Murphy, R. B., Repasky, M. P., Frye, L. L., Greenwood, J. R., Halgren, T. A., et al. (2006). Extra precision glide: docking and scoring incorporating a model of hydrophobic enclosure for protein-ligand complexes. *J. Med. Chem.* 49, 6177–6196. doi: 10.1021/jm051256o
- Frisch, M. J., Trucks, G. W., Schlegel, H. B., Scuseria, G. E., Robb, M. A., Cheeseman, J. R., et al. (2009). *Gaussian 09, Revision E.01*. Wallingford, CT: Gaussian, Inc.
- Gopalakrishnan, A. M., and Kumar, N. (2014). Antimalarial action of artesunate involves DNA damage mediated by reactive oxygen species. *Antimicrob. Agents Chemother.* 59, 317–325. doi: 10.1128/AAC.03663-14
- Gottlieb, E., Armour, S. M., Harris, M. H., and Thompson, C. B. (2003). Mitochondrial membrane potential regulates matrix configuration and cytochrome c release during apoptosis. *Cell Death Differ.* 10, 709–717. doi: 10.1038/sj.cdd.4401231
- Griesbeck, A. G., El-Idreesy, T. T., Hoinck, L. O., Lex, J., and Brun, R. (2005). Novel spiroanellated 1,2,4-trioxanes with high *in vitro* antimalarial activities. *Bioorg. Med. Chem. Lett.* 15, 595–597. doi: 10.1016/j.bmcl.2004.11.043

FUNDING

Study was funded by Network project BSC0104.

ACKNOWLEDGMENTS

We are thankful to Council of Scientific and Industrial Research Center (CSIR), India for funding to perform this study. The authors also thank to the Director CDRI, for extending all the necessary facilities. Funding received from SPLENIDID CSIR Project is also acknowledged. We are also thankful to Mr. A. L. Vishwakarma for helping in FACS studies.

CDRI communication no. 9717.

SUPPLEMENTARY MATERIAL

The Supplementary Material for this article can be found online at: <https://www.frontiersin.org/articles/10.3389/fcimb.2018.00256/full#supplementary-material>

- Gunjan, S., Singh, S. K., Sharma, T., Dwivedi, H., Chauhan, B. S., Imran Siddiqi, M., et al. (2016). Mefloquine induces ROS mediated programmed cell death in malaria parasite: *plasmodium*. *Apoptosis* 21, 955–964. doi: 10.1007/s10495-016-1265-y
- Halgren, T. A. (2009). Identifying and characterizing binding sites and assessing druggability. *J. Chem. Inf. Model.* 49, 377–389. doi: 10.1021/ci800324m
- Haynes, R. K., and Krishna, S. (2004). Artemisinins: activities and actions. *Microb. Infect.* 6, 1339–1346. doi: 10.1016/j.micinf.2004.09.002
- Johnson, J. D., Denu, R. A., Gerena, L., Lopez-Sanchez, M., Roncal, N. E., and Waters, N. C. (2007). Assessment and continued validation of the malaria SYBR green I-based fluorescence assay for use in malaria drug screening. *Antimicrob. Agents Chemother.* 51, 1926–1933. doi: 10.1128/AAC.01607-06
- Kumar, N., and Zheng, H. (1990). Stage-specific gametocytocidal effect *in vitro* of the antimalarial drug qinghaosu on *Plasmodium falciparum*. *Parasitol. Res.* 76, 214–218. doi: 10.1007/BF.00930817
- Meslin, B., Barnadas, C., Boni, V., Latour, C., De Monbrison, F., Kaiser, K., et al. (2007). Features of apoptosis in *Plasmodium falciparum* erythrocytic stage through a putative role of PfMCA1 metacaspase-like protein. *J. Infect. Dis.* 195, 1852–1859. doi: 10.1086/518253
- Pandey, N., and Pandey-Rai, S. (2016). Updates on artemisinin: an insight to mode of actions and strategies for enhanced global production. *Protoplasma* 253, 15–30. doi: 10.1007/s00709-015-0805-6
- Pettersen, E. F., Goddard, T. D., Huang, C. C., Couch, G. S., Greenblatt, D. M., Meng, E. C., et al. (2004). UCSF Chimera—a visualization system for exploratory research and analysis. *J. Comput. Chem.* 25, 1605–1612. doi: 10.1002/jcc.20084
- Phyo, A. P., Nkhoma, S., Stepniewska, K., Ashley, E. A., Nair, S., McGready, R., et al. (2012). Emergence of artemisinin-resistant malaria on the western border of Thailand: a longitudinal study. *Lancet* 379, 1960–1966. doi: 10.1016/S0140-6736(12)60484-X
- PlasmoDB (2013). *PlasmoDB: The Plasmodium Genomics Resource*. Available online at: www.plasmodb.org
- Price, R. N., Nosten, F., Luxemburger, C., Ter Kuile, F. O., Paiphun, L., Chongsuphajaisiddhi, T., et al. (1996). Effects of artemisinin derivatives on malaria transmissibility. *Lancet* 347, 1654–1658. doi: 10.1016/S0140-6736(96)91488-9
- Schrödinger, L. (2016a). *Schrödinger Release 2016-2: LigPrep*, Version 3.8. New York, NY.
- Schrödinger, L. (2016b). *Schrödinger Release 2016-2: Maestro*, Version 10.6. New York, NY.
- Schrödinger, L. (2016c). *Schrödinger Release 2016-2: Schrödinger Suite 2016-2 Protein Preparation Wizard: Epik*, Version 3.6. New York, NY.

- Singh, C., Srivastav, N. C., and Puri, S. K. (2004). Synthesis and antimalarial activity of 6-cycloalkylvinyl substituted 1,2,4-trioxanes. *Bioorg. Med. Chem.* 12, 5745–5752. doi: 10.1016/j.bmc.2004.08.042
- Singh, R. P., Sabarinath, S., Gautam, N., Gupta, R. C., and Singh, S. K. (2011). Pharmacokinetic study of the novel, synthetic trioxane antimalarial compound 97-78 in rats using an LC-MS/MS method for quantification. *Arzneimittelforschung* 61, 120–125. doi: 10.1055/s-0031-1296177
- Trager, W., and Jensen, J. B. (1976). Human malaria parasites in continuous culture. *Science* 193, 673–675. doi: 10.1126/science.781840
- Wang, J., Huang, L., Li, J., Fan, Q., Long, Y., Li, Y., et al. (2010). Artemisinin directly targets malarial mitochondria through its specific mitochondrial activation. *PLoS ONE* 5:e9582. doi: 10.1371/journal.pone.0009582
- White, N. J., Pukrittayakamee, S., Hien, T. T., Faiz, M. A., Mokuolu, O. A., and Dondorp, A. M. (2014). Malaria *Lancet* 383, 22–28. doi: 10.1016/B978-0-7020-5101-2.00044-3
- WHO (2014). *World Malaria Report 2014*. Geneva: World Health Organization.
- WHO (2015). *World Malaria Report*. Geneva: World Health Organization.
- Wong, A. H., Yan, C., and Shi, Y. (2012). Crystal structure of the yeast metacaspase Yca1. *J. Biol. Chem.* 287, 29251–29259. doi: 10.1074/jbc.M112.381806
- Xiang, Z. (2006). Advances in homology protein structure modeling. *Curr. Protein Pept. Sci.* 7, 217–227. doi: 10.2174/138920306777452312
- Conflict of Interest Statement:** The authors declare that the research was conducted in the absence of any commercial or financial relationships that could be construed as a potential conflict of interest.

Copyright © 2018 Gunjan, Sharma, Yadav, Chauhan, Singh, Siddiqi and Tripathi. This is an open-access article distributed under the terms of the Creative Commons Attribution License (CC BY). The use, distribution or reproduction in other forums is permitted, provided the original author(s) and the copyright owner(s) are credited and that the original publication in this journal is cited, in accordance with accepted academic practice. No use, distribution or reproduction is permitted which does not comply with these terms.



OPEN ACCESS

Edited by:

Nicolas Blanchard,
INSERM U1043 Centre de
Physiopathologie de Toulouse Purpan,
France

Reviewed by:

Qian Han,
Hainan University, China
Andrés Palencia,
INSERM U1209 Institut pour
l'Avancée des Biosciences (IAB),
France

*Correspondence:

Rima McLeod
rmcleod@bsd.uchicago.edu
Wayne F. Anderson
wf-anderson@northwestern.edu
Huân M. Ngô
dr.huan.ngo@gmail.com

†These authors have contributed
equally to this work

*Present Address:

Joseph Lykins,
Department of Internal Medicine and
Department of Emergency Medicine,
Virginia Commonwealth University
Health System, Richmond, VA,
United States

Ekaterina V. Filippova,
Department of Biochemistry and
Molecular Biology, Knapp Center for
Biomedical Discovery, University of
Chicago, IL, United States

Jiapeng Ruan,
Department of Internal Medicine, Yale
University School of Medicine, New
Haven, CT, United States

Sarah Dovgin,
Case Western Reserve University,
Cleveland, OH, United States

Martin McPhillie,
School of Chemistry and Astbury
Centre for Structural Molecular
Biology, University of Leeds, Leeds,
United Kingdom

Specialty section:

This article was submitted to
Parasite and Host,
a section of the journal
Frontiers in Cellular and Infection
Microbiology

Received: 30 July 2018

Accepted: 14 September 2018

Published: 05 October 2018

CSGID Solves Structures and Identifies Phenotypes for Five Enzymes in *Toxoplasma gondii*

Joseph D. Lykins^{1†}, Ekaterina V. Filippova^{2†}, Andrei S. Halavaty^{2†}, George Minasov^{2†}, Ying Zhou^{3†}, Ievgeniia Dubrovskaya², Kristin J. Flores², Ludmilla A. Shuvalova², Jiapeng Ruan^{2†}, Kamal El Bissati³, Sarah Dovgin^{4†}, Craig W. Roberts⁵, Stuart Woods⁵, Jon D. Moulton⁶, Hong Moulton⁷, Martin J. McPhillie^{8†}, Stephen P. Muench⁹, Colin W. G. Fishwick¹⁰, Elisabetta Sabini², Dhanasekaran Shanmugam¹¹, David S. Roos¹², Rima McLeod^{3,13*}, Wayne F. Anderson^{2*} and Huân M. Ngô^{2,14*}

¹ Pritzker School of Medicine, University of Chicago, Chicago, IL, United States, ² Center for Structural Genomics of Infectious Diseases and the Department of Biochemistry and Molecular Genetics, Feinberg School of Medicine, Northwestern University, Chicago, IL, United States, ³ Department of Ophthalmology and Visual Sciences, University of Chicago, Chicago, IL, United States, ⁴ Illinois Math and Science Academy, Aurora, IL, United States, ⁵ Strathclyde Institute of Pharmacy and Biomedical Sciences, University of Strathclyde, Glasgow, United Kingdom, ⁶ Gene Tools, LLC, Philomath, OR, United States, ⁷ Department of Biomedical Sciences, College of Veterinary Medicine, Oregon State University, Corvallis, OR, United States, ⁸ Department of Molecular Biology and Biotechnology, University of Sheffield, Sheffield, United Kingdom, ⁹ School of Biomedical Sciences, Faculty of Biological Sciences, and Astbury Centre for Structural Molecular Biology, University of Leeds, Leeds, United Kingdom, ¹⁰ School of Chemistry and Astbury Centre for Structural Molecular Biology, University of Leeds, Leeds, United Kingdom, ¹¹ Biochemical Sciences Division, CSIR National Chemical Laboratory, Pune, India, ¹² Department of Biology, University of Pennsylvania, Philadelphia, PA, United States, ¹³ Department of Pediatrics (Infectious Diseases), Institute of Genomics, Genetics, and Systems Biology, Global Health Center, Toxoplasmosis Center, CHeSS, The College, University of Chicago, Chicago, IL, United States, ¹⁴ BrainMicro LLC, New Haven, CT, United States

Toxoplasma gondii, an Apicomplexan parasite, causes significant morbidity and mortality, including severe disease in immunocompromised hosts and devastating congenital disease, with no effective treatment for the bradyzoite stage. To address this, we used the Tropical Disease Research database, crystallography, molecular modeling, and antisense to identify and characterize a range of potential therapeutic targets for toxoplasmosis. Phosphoglycerate mutase II (PGMII), nucleoside diphosphate kinase (NDK), ribulose phosphate 3-epimerase (RPE), ribose-5-phosphate isomerase (RPI), and ornithine aminotransferase (OAT) were structurally characterized. Crystallography revealed insights into the overall structure, protein oligomeric states and molecular details of active sites important for ligand recognition. Literature and molecular modeling suggested potential inhibitors and druggability. The targets were further studied with vivoPMO to interrupt enzyme synthesis, identifying the targets as potentially important to parasitic replication and, therefore, of therapeutic interest. Targeted vivoPMO resulted in statistically significant perturbation of parasite replication without concomitant host cell toxicity, consistent with a previous CRISPR/Cas9 screen showing PGM, RPE, and RPI contribute to parasite fitness. PGM, RPE, and RPI have the greatest promise for affecting replication in tachyzoites. These targets are shared between other medically important parasites and may have wider therapeutic potential.

Keywords: *Toxoplasma gondii*, PPMO, phosphoglycerate mutase, nucleoside diphosphate kinase, ribulose-3-phosphate epimerase, ribose-5-phosphate isomerase, ornithine aminotransferase, crystallography

INTRODUCTION

Toxoplasma gondii is one of the most significant parasites that impacts human health, with estimates that as many as one third to one half of the human population are infected (Montoya and Liesenfeld, 2004; Furtado et al., 2011; Torgerson and Mastroiacovo, 2013; Flegr et al., 2014; McLeod et al., 2014; Lykins et al., 2016). A relative of the parasite that causes malaria, *T. gondii* is an intracellular parasite that has two major life stages in humans, tachyzoites and bradyzoites. Tachyzoites cause acute infection, while bradyzoites are the encysted, dormant life stage responsible for reactivation disease. While treatment is available for the acute infection, there is currently no effective medication for the bradyzoite stage (McLeod et al., 2014). Additionally, parasites can be passed to a fetus *in utero* when a pregnant woman is acutely infected during gestation. This can cause chorioretinitis and neurological complications in the fetus (McLeod et al., 2012). Moreover, there is increasing understanding of the potential long-term sequelae of chronic infection with *T. gondii* on risk of neurodegenerative disease and malignancy (Ngô et al., 2017). Treatment for active infection exists but is limited by toxicity and hypersensitivity. Thus, new therapeutic targets and medicines are needed, with several potential solutions in development (Zhou et al., 2014; McPhillie et al., 2016; Sidik et al., 2016).

At the Center for Structural Genomics of Infectious Diseases (CSGID), the first *Toxoplasma* Structural Genomics Pipeline was established. Subsequently, CSGID began selecting parasite proteins for structural characterization using established approaches capable of successful identification of potential drug targets, coupled with the Tropical Diseases Research (TDR) Database (Anderson, 2009; Crowther et al., 2010; Magariños et al., 2012). Herein, 5 soluble enzymes were selected for further study. This process was made possible due to the integration of large amounts of genomic, biochemical, and pharmacological data by the TDR Database, which provides evidence collectively generated by the scientific community concerning potential molecular targets and inhibitory compounds that have properties consistent with Lipinski's rules for orally available drugs (Lipinski, 2004). The targets studied herein were crystallized and their structures characterized, as structural studies have potential to inform molecular targeting and medicinal chemistry can facilitate development of novel anti-parasitic compounds.

We further hypothesized that using phosphorodiamidate morpholino oligomers linked to a cellular delivery moiety, such as either an octaguanidinium dendrimer [Vivo-Morpholinos (vivoPMOs)], or arginine-rich peptide, we would decrease expression of these enzymes, identified as potential drug targets by the *Toxoplasma* Structural Genomic Pipeline, in YFP-expressing *T. gondii* tachyzoites, and that down-regulation of these enzymes would result in decreased replication as quantified by fluorescent intensity. The approach of using morpholinos to target specific parasitic enzymes has been successful in previous studies (Lai et al., 2012; McPhillie et al., 2016). VivoPMOs are typically used to decrease gene expression by one of two different mechanisms, namely mechanical disruption of interactions between RNA and snRNP, thereby preventing splicing of introns, resulting in nonsense-mediated decay of the transcript and/or

defective protein upon translation, and through direct prevention of translation by blocking interactions between mature mRNA and the ribosome. In preventing effective protein expression, we could determine whether a particular enzyme contributed to parasite replication, suggesting its potential as a therapeutic target.

Molecular transporters can deliver PMOs and small inhibitory molecules of therapeutic value. Transductive peptides or octaguanidinium dendrimer of a Vivo-Morpholino (Gene Tools, Philomath, Oregon) deliver PMOs or other molecules across cell membranes. Octaarginine can carry small molecules into the retina (McLeod et al., 2013). Similar arginine-rich cell-penetrating peptides can access other places where medication transport is problematic; for example, rabies virus glycoprotein-tagged small molecules are capable of passing through the blood-brain barrier and octaarginine-conjugated small molecules, for example, cross into encysted bradyzoites (Samuel et al., 2003; Liu et al., 2009).

The enzymes selected from the TDR database as small and tractable for expression and crystallization included: phosphoglycerate mutase II (hereafter referred to as PGM), nucleotide diphosphate kinase (NDK), ribulose phosphate 3-epimerase (RPE), ribose-5-phosphate isomerase (RPI), and ornithine aminotransferase (OAT). Information about candidate inhibitors of these apicomplexan enzymes is summarized in Table 1.

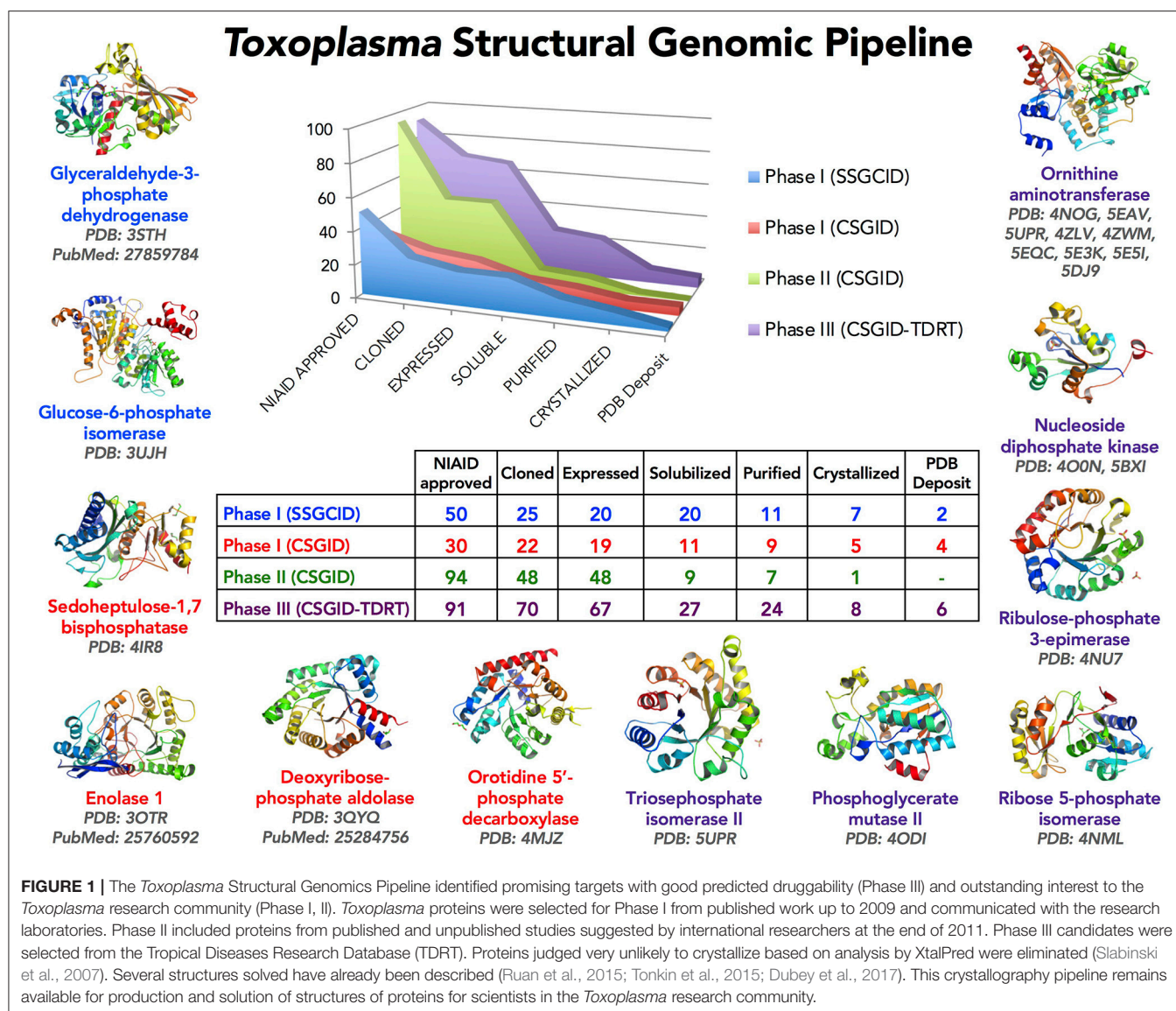
METHODS

Cloning, Expression, and Purification

Five genes from *T. gondii* ME49 (GI: 237843677, 237844373, 237835673, 237834547, and 237832613) corresponding to a putative phosphoglycerate mutase II (TgPGM; residues 1–265 of the original CSGID entry; this entry was modified in 2012; see original NCBI Reference Sequence: XP_002371136.1), a putative nucleoside diphosphate kinase (TgNDK) (residues 1–155), ribulose phosphate 3-epimerase (TgRPE) (residues 1–230), a putative ribose 5-phosphate isomerase (TgRPI) (residues 1–259), and a putative ornithine aminotransferase (TgOAT) (residues 17–441), respectively, were cloned into the ligation-independent-cloning (Aslanidis and de Jong, 1990) isopropyl β -D-1-thiogalactopyranoside (IPTG)-inducible pMCSG28 vector for recombinant bacterial expression in BL21(DE3)/pMagic *Escherichia coli* (*E. coli*). All clones were obtained from J. Craig Venter Institute, a CSGID partner, and submitted into the CSGID protein production pipeline (Figure 1) as IDP92076 (TgPGM), IDP92074 (TgNDK), IDP92047 (TgRPE), IDP92040 (TgRPI), and IDP92102 (TgOAT). The pMCSG28 vector possesses a purification tag including 6 \times His affinity sequence and a Tobacco Etch Virus (TEV) protease cleavage site. The *E. coli* cells were induced with 1 mM IPTG at 25°C after the optical density of cells in culture flasks reached 0.6 at 600 nm under 37°C and constant aeration at 200 rpm. Terrific Broth (TB) (PGM, NDK, and RPE) and the Se-Met MCSG-M9 (Medicilon Inc.) (RPI) medium was used. Overnight induction was completed by collecting cells at 6,000 rpm, 4°C for 10 min. Cells' paste was resuspended in chilled Lysis Buffer [43 mM Na₂HPO₄, 3.25 mM citric acid, 250 mM NaCl, 100 mM ammonium sulfate, 5% glycerol, 5 mM imidazole,

TABLE 1 | Target enzyme characterization and candidate inhibitors.

Target enzyme	Function	Pathogens in which it has been studied	Phenotypes/ Means of assay	Candidate inhibitors	References
Phosphoglycerate Mutase	Catalyzes transition from 3-phosphoglycerate to 2-phosphoglycerate; important for glycolysis	<i>Trypanosoma</i> spp. <i>Toxoplasma gondii</i>	replication	Inositol hexakisphosphate, benzene hexacarboxylate, 2-hydroxy-4-phosphonobutanoate, epigallocatechin-3-gallate Xanthone derivatives	McAleese et al., 1985; Rigden et al., 1999; Chevallier et al., 2000; Opperdoes and Michels, 2001; Dijkeng et al., 2007; Singh et al., 2013; Li et al., 2017; Wang et al., 2018
Nucleoside Diphosphate Kinase	Catalyzes movement of phosphate from nucleoside triphosphate to nucleoside diphosphate (GTP + ADP -> GDP + ATP)	<i>Plasmodium falciparum</i> <i>Leishmania amazonensis</i>	Stress response in RPS-13; replication	Adenosine-3-phosphate-5-phosphosulfate SU11652	Reyes et al., 1982; Schneider et al., 1998; Kolli et al., 2008; Motomura et al., 2014; Vieira et al., 2015
Ribulose Phosphate 3-Epimerase	Converts ribulose-5-phosphate into xylulose-5-phosphate (part of Calvin cycle in plants)	<i>Trypanosoma cruzi</i> <i>Plasmodium falciparum</i>	Involved in pentose-phosphate pathway and the generation of nucleotides; replication; in same pathway as the R5PI; implications for plastid	D-2-Deoxyribose 5-phosphate	Wood, 1979; Caruthers et al., 2005; Igoillo-Esteve et al., 2007
Ribose-5-Phosphate Isomerase	Catalyzes transition from ribose-5-phosphate to ribulose-5-phosphate (upstream of above enzyme)	<i>Trypanosoma cruzi</i>	important in growth phase; cell invasion; implications for plasticity; cell death/ replication potentially (observed in Arabidopsis)	4-phosphoerythronate	Igoillo-Esteve et al., 2007
Ornithine Aminotransferase	Forms first intermediate in pathway to proline from ornithine (is reversible); been implicated in eye disease	<i>Plasmodium falciparum</i>	Replication	L-canaline, 5-fluoromethylornithine	Kito et al., 1978; Storici et al., 1999; Müller et al., 2009; Sturm et al., 2009; Kronenberger et al., 2014



1.5 mM magnesium acetate, 1 mM CaCl₂, 0.08% n-Dodecyl β-D-maltoside (DDM), 5 mM β-mercaptoethanol (BME)] pH 7.8 followed by sonication on ice. Crude sonication mixture was centrifuged at 19,000 rpm, 4°C for 40 min to obtain soluble fraction containing target protein, which was applied onto a 5-ml Ni-NTA column (GE Healthcare, Piscataway, NJ) for purification. The column was washed with buffer containing 10 mM Tris-HCl pH 8.3, 500 mM NaCl, 25 mM imidazole and 5 mM BME to remove non-specifically bound *E. coli* proteins, followed by elution of target protein with 500 mM imidazole in the 10 mM Tris-HCl buffer pH 8.3 containing 500 mM NaCl and 5 mM BME (buffer A). A HiLoad™ 26/60 Superdex™ 200 column (GE Healthcare, Piscataway, NJ) was used to further purify target protein in the buffer A. Purity of all proteins was analyzed by SDS-PAGE. Pooled fractions were concentrated and stored at -80°C for further use or used in screening crystallization conditions.

Crystallization, X-Ray Data Collection, and Structure Determination

Each target protein was crystallized by the vapor-diffusion sitting-drop method mixing 1 μL of the protein in buffer A and 1 μL of a crystallization screen solution at 22°C. Single crystals were soaked in a crystallization condition for cryoprotection and flash frozen in liquid nitrogen for monochromatic X-ray data collection. Data were collected at 100 K from a single frozen crystal at the LS-CAT beamline 21-ID-F (λ = 0.97872 Å) at the Argonne National Laboratory (ANL), Advanced Photon Source (APS). Diffraction images were collected in oscillation mode and processed with HKL-3000 (Minor et al., 2006). Crystal structures of TgPGM, TgNDK, TgRPE, and TgOAT were determined by molecular replacement using Phaser (McCoy et al., 2007) from CCP4 suite (Winn et al., 2011). Initial molecular replacement solutions were rebuilt with ARP/wARP (Morris et al., 2003). Crystal structure of TgRPI was determined by single-wavelength

anomalous dispersion (SAD) method in *HKL-3000* (Minor et al., 2006). Non-Crystallographic Symmetry (NCS) restraints and Translation-Libration-Screw (TLS) groups refinement in *REFMAC* v.5.7 (Murshudov et al., 2011) were used to improve the quality of the structures. *Coot* (Emsley and Cowtan, 2004; Emsley et al., 2010) was used to manually check structures after each cycle of refinement in *REFMAC* and correct for side chain rotamers and fitting. The final models were validated with the Protein Data Bank (PDB) validation server (*ADIT* validation server; <https://validate-rcsb-2 wwplib.org/>) and *MolProbity* (<http://molprobity.biochem.duke.edu/>) (Davis et al., 2007; Chen et al., 2010). Figures presenting crystal structures were prepared in the graphical program *PyMol* (The PyMOL Molecular Graphics System, Version 2.0 Schrödinger, LLC). Crystallization conditions, data-collection, structure determination and refinement statistics are summarized in **Table 2**. Crystal structures are described in **Figures 2–6**.

Data Accessibility

Coordinates and structure factors of the determined crystal structures were deposited to Protein Data Bank (www.rcsb.org) (Berman et al., 2000). Diffraction images for the deposited crystal structures can be found at the CSGID website (<http://www.csgrid.org/csgrid/pages/home>).

Crystal Structure Data Analysis

We used CATH/Gene3D v4.1 (<http://www.cathdb.info/>) (Sillitoe et al., 2015; Lam et al., 2016) to assess domain composition of studied proteins. Oligomeric state of the proteins and buried surface area (BSA) of multimers were estimated from crystal structure coordinates using PISA (<http://www.ebi.ac.uk/pdbe/pisa/pistart.html>) (Krissinel and Henrick, 2005, 2007; Krissinel, 2009). The number of intermolecular bonds that may contribute to protein quaternary structure was estimated from the structure coordinates using PDBsum (<http://www.ebi.ac.uk/thornton-srv/databases/cgi-bin/pdbsum/GetPage.pl?pdbcode=index.html>) (de Beer et al., 2014). Assessment of metal binding sites was done with help of the CheckMyMetal server (http://csgrid.org/csgrid/metal_sites) (Zheng et al., 2017). Protein structure comparison service PDBeFold at European Bioinformatics Institute (<http://www.ebi.ac.uk/msd-srv/ssm>) was used to identify structural homologs (Krissinel and Henrick, 2004). Pair-wise structural alignments were performed with DaliLite v.3 (<https://www.ebi.ac.uk/Tools/structure/dalilite/>) (Hasegawa and Holm, 2009).

Molecular Modeling

Schrödinger 2015-3, maestro v10.3 was used for binding site identification (SiteMap) on the five enzymes, and therefore, predict “druggability” by small molecules (Schrödinger Release 2015-3, 2018). A SiteScore threshold of 0.80 (with > 0.80 suggesting druggability) is used in this regard (Halgren, 2007).

Cell Culture

Human foreskin fibroblasts (HFF) were maintained in Iscove's Modified Dulbecco's Medium (IMDM) supplemented with 10% fetal bovine serum (FBS) and PENSTRA (penicillin and streptomycin). Cells were maintained at 37°C and 5% CO₂.

VivoPMO Design

The vivoPMOs were designed using genomic DNA sequences obtained from ToxoDB (accession numbers for genomic DNA sequences: PGM-TGME49_297060, NDK-TGME49_295350, RPE-TGME49_047670, RPI-TGME49_039310, OAT-TGME49_069110) with exon/intron junctions identified. One of these junctions was identified in each target gene and a vivoPMO was designed to be complementary to nucleotides on both sides of said junction. A diagrammatic representation of vivoPMO structure and RNA binding is in **Figure 7A**. The sequences of these morpholinos can be found in **Figure 7B**.

VivoPMO Efficacy Assay

HFFs were grown in black, flat-bottomed 96-well microplates. HFFs were infected with 3,200 Type I RH parasites expressing yellow fluorescent protein (YFP). This allowed quantification of parasites *in vitro* post-treatment with vivoPMO. The parasites were incubated with the cells for 1 h, to allow sufficient time for invasion of HFFs, and were then treated with vivoPMO. Control triplicates with only fibroblasts and with pyrimethamine and sulfadiazine (the current standard of treatment for *T. gondii* infection) were also conducted. A concentration gradient of YFP parasites was also established, allowing quantification of knockdown. Several replicates of this efficacy assay were completed applying different concentrations of vivoPMO (2.5, 5, 10, and 20 μM). The cells and parasites were then incubated at 37°C for 72 h. This timing was previously established in other work. Fluorescence was measured using a Bio-Tek Synergy™ H4 Hybrid Multi-Mode Microplate Reader. This methodology was consistent with previous work using morpholinos in *T. gondii* (Lai et al., 2012).

VivoPMO Toxicity Assay

HFFs were grown in 96-well microplates, as in the efficacy assay. A gradient of dimethyl sulfoxide (DMSO) was used to quantify the amount of cell death caused by the vivoPMO *in vitro*. Different concentrations of vivoPMO (3.5, 5, 10, and 20 μM) were used to identify the level at which toxicity occurred. Following 72 h of incubation at 37°C, each well was treated with 10 μL WST-1, which reacts in metabolically active, viable cells through a complex set of chemical reactions dependent upon glycolytic NADPH production to form formazan dyes, which can be detected via a colorimeter. This method is also consistent with previous work (Lai et al., 2012).

Data Analysis of Knockdown With VivoPMO

Knockdown was analyzed statistically using student *T*-test comparing parasite fluorescence between enzyme-specific vivoPMO and off-target vivoPMO. Additionally, the enzyme-specific vivoPMOs were compared to the levels of fluorescence at the standardized parasite load (2000 YFP-expressing parasites per well). Student *T*-test was also used to analyze toxicity data, comparing levels of optical density at 420 nm for untreated fibroblasts to treated cells. Statistical analysis was performed using STATA. Results were considered significant with $p < 0.05$.

TABLE 2 | Crystallization conditions, data-collection, structure determination and refinement statistics of *T. gondii* proteins.

Protein name	PGM	NDK data set I	NDK data set II	RPE	RPI	OAT
CRYSTALLIZATION CONDITIONS						
Screen conditions	0.2 M MgCl ₂ , 0.1 M HEPES pH 7.5, 25% PEG3350	0.2 M ammonium sulfate, 0.1 M Bis-Tris pH 5.5, 25% PEG3350	0.2 M MgCl ₂ , 0.1 M MES, 20% PEG6000	2 M ammonium sulfate, 0.1 M citric acid pH 3.5	2.1 M DL-Malic acid pH 7.0	0.2 M ammonium acetate, 0.1 M Bis-Tris pH 6.5, 25% PEG3350
Protein concentration (mg/ml)	7.5	7.5	6	7.4	7.1	22.8
DATA COLLECTION						
Space group	<i>P</i> 2 ₁ 2 ₁ 2	<i>P</i> 2 ₁ 2 ₁ 2 ₁	<i>C</i> 2	<i>H</i> 32	<i>P</i> 4 ₁ 22	<i>P</i> 1
Unit cell parameters (Å; °)	<i>a</i> = 97.2, <i>b</i> = 149.5, <i>c</i> = 72.1; $\alpha = \beta = \gamma = 90.0$	<i>a</i> = 73.4, <i>b</i> = 121.6, <i>c</i> = 212.3; $\alpha = \beta = \gamma = 90.0$	<i>a</i> = 236.8, <i>b</i> = 73.4, <i>c</i> = 122.7; $\alpha = \gamma$ = 90.0, β = 116.8	<i>a</i> = <i>b</i> = 138.5, <i>c</i> = 349.3; $\alpha = \beta = 90.0$, γ = 120.0	<i>a</i> = <i>b</i> = 95.6, <i>c</i> = 112.7; $\alpha = \beta = \gamma = 90.0$	<i>a</i> = 56.2, <i>b</i> = 61.3, <i>c</i> = 63.7; α = 100.6, β = 93.2, γ = 107.7
Resolution range (Å)	30.00–2.60 (2.64–2.60)	30.00–2.40 (2.44–2.40)	30.00–1.70 (1.73–1.70)	30.00–2.05 (2.09–2.05)	30.00–2.60 (2.64–2.60)	62.10–1.20 (1.22–1.20)
No. of reflections	33,033 (1,604)	75,092 (3,725)	202,729 (10,203)	81,012 (3,999)	16,774 (818)	224,574 (11,241)
<i>R</i> _{merge} (%)	10.6 (64.5)	8.4 (52.3)	5.9 (48.2)	7.2 (61.5)	9.4 (61.6)	4.3 (37.0)
Completeness (%)	100.0 (100.0)	99.6 (99.8)	98.5 (99.9)	100.0 (100.0)	100.0 (100.0)	91.0 (91.0)
$\langle I/\sigma(I) \rangle$	18.3 (3.3)	18.2 (3.2)	22 (3.2)	20.1 (2.4)	44.9 (5.4)	11.2 (2.0)
Multiplicity	7.3 (7.4)	5.7 (5.8)	4.9 (4.9)	4.5 (4.5)	14.2 (14.7)	2.0 (2.0)
Wilson <i>B</i> factor	52.0	51.0	28.0	32.6	61.4	14.4
STRUCTURE DETERMINATION						
MR initial model (PDB ID)	1xq9	1ndl		3qc3	-	3lg0
REFINEMENT						
Resolution range (Å)	29.72–2.60 (2.67–2.60)	29.49–2.40 (2.46–2.40)	29.98–1.7 (1.74–1.7)	29.88–2.05 (2.10–2.05)	29.53–2.60 (2.67–2.60)	62.1–1.2 (1.23–1.20)
Completeness (%)	99.8 (98.2)	99.5 (99.7)	98.2 (97.04)	99.9 (99.9)	99.8 (99.8)	90.8 (90.0)
No. of reflections	31,317 (2,253)	71,019 (5,181)	192,440 (13,960)	76,865 (5,594)	15,802 (1,134)	213,305 (15,538)
<i>R</i> _{work} / <i>R</i> _{free} (%)	19.7/23.9 (25.9/27.7)	19.2/23.8 (26.1/34.3)	15.4/19.2 (20.8/24.6)	14.9/18.7 (21.9/26.8)	16.4/20.5 (25.8/34.4)	13.3/16.5 (20.9/23.8)
Protein molecules/atoms	2/6,560	12/14,699	12/14,647	4/6,761	1/1,866	2/6,560
Solvent atoms	1,041	548	1854	513	71	1,041
Mean temperature factor (Å ²)	56.3	48.7	33.4	39.9	56.8	18.4
COORDINATE DEVIATIONS						
R.m.s.d. bonds (Å)	0.011	0.007	0.010	0.010	0.012	0.021
R.m.s.d. angles (°)	1.626	1.219	1.398	1.434	1.711	1.927
RAMACHANDRAN PLOT†						
Most favored (%)	90.2	92.8	95.0	91.8	95.4	90.2
Allowed (%)	9.0	6.4	5.0	8.2	4.1	9.0
Generously allowed (%)	0.3	0.8	0.0	0.0	0.5	0.3
Outside allowed (%)	0.5	0.0	0.0	0.0	0.0	0.5
PDB Accession Code	4odi	4o0n	5bxi	4nu7	4nml	4nog

Values in parentheses are for the highest resolution shell.

† Statistics are based on PROCHECK (Laskowski et al., 1993).

Antibody Production

Antibodies were raised in mice at the University of Strathclyde (CR, SW). Briefly, mice were given two injections of formulated protein with NISV (non-ionic surfactant vesicle). The vesicles were made by melting mono-palmitoyl glycerol, cholesterol and dicetyl-phosphate (All from Sigma, UK) in a molar ratio of 5:4:1. 10 days after the final injection, serum was collected and tested by Western Blot using recombinant protein and *Toxoplasma* lysate.

Immunofluorescence Assay (IFA)

HFF cells were grown to confluence on sterilized coverslips in 24-well plates. Cells were fixed in 3% paraformaldehyde ~20–24 h after infection with Type I RH-strain tachyzoites and permeabilized in 0.25% Triton X-100. Serum from immunized mice, coupled with another primary antibody, RPS13, was applied at 1:500 dilution in PBS 1x/3% BSA/Triton-X-100 and detected using either Texas Red-conjugated goat

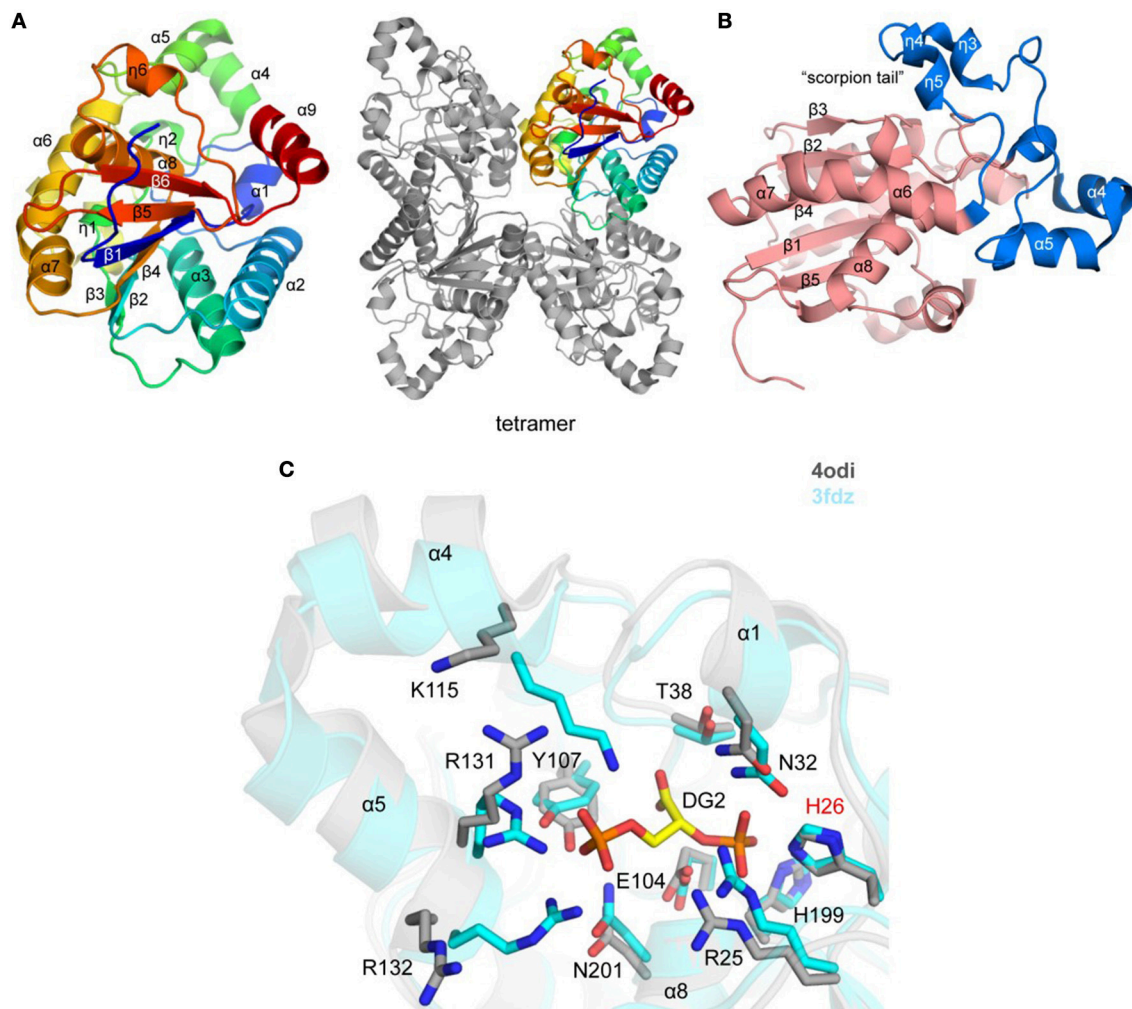


FIGURE 2 | Crystal structure of *TgPGM* (A). Ribbon representation of *TgPGM* monomer (left side) colored blue (N-terminus) to red (C-terminus) and tetramer of *TgPGM* (right side) (B). Domain structure of *TgPGM* [red—an $\alpha/\beta/\alpha$ -sandwich domain (residues 12–107 and 169–257) and blue—a domain without any defined folding motif (residues 108–168)] (C). Pairwise structural alignment of *TgPGM* (gray) and *BpPGM* (cyan) showing active site with residues of *TgPGM* shown in sticks and labeled in one-letter code. Equivalent residues of *BpPGM* are displayed. *BpPGM* binds (2R)-2,3-diphosphoglyceric acid, DG2, in the active site.

anti-mouse antibody, or Alexa-488-conjugated goat anti-rabbit antibody. DAPI was used to stain for DNA. Coverslips were mounted with Antifade (Molecular Probes, Eugene, OR), and images were analyzed by high-resolution fluorescence using deconvolution protocols. Microscopy was performed with an inverted microscope (IX81; Olympus).

Comparison to Predicted Essentiality via Literature CRISPR/Cas9 Screen

As an approach to identify whether target enzymes might be essential to parasite viability and fitness, a survey was done of phenotypic scores previously published in a genome-wide CRISPR/Cas9 screen (Sidik et al., 2016). Gene IDs were used and the average of the three available scores was taken. Negative scores were considered likely to be significant contributors to parasite fitness. Data of the genome-wide CRISPR/Cas9

screen are subsequently annotated in ToxoDB (<http://toxodb.org/toxo/>), including these gene IDs: *TgPGM*: TGME49_297060, *TgNDK*: TGME49_295350, *TgRPE*: TGME49_247670, *TgRPI*: TGME49_239310, *TgOAT*: TGME49_269110.

RESULTS

Structural Genomic Pipeline for *Toxoplasma*

The NIAID Structural Genomics Centers selected 265 proteins for the *Toxoplasma* Structural Genomic Pipeline in three phases (Figure 1). Phase I and II were a collaborative effort between CSGID and the *Toxoplasma* research community. Proteins were selected from published and unpublished work up to 2011. Selection was based on the mechanisms and pathways that are important for parasite infection and survival in human and

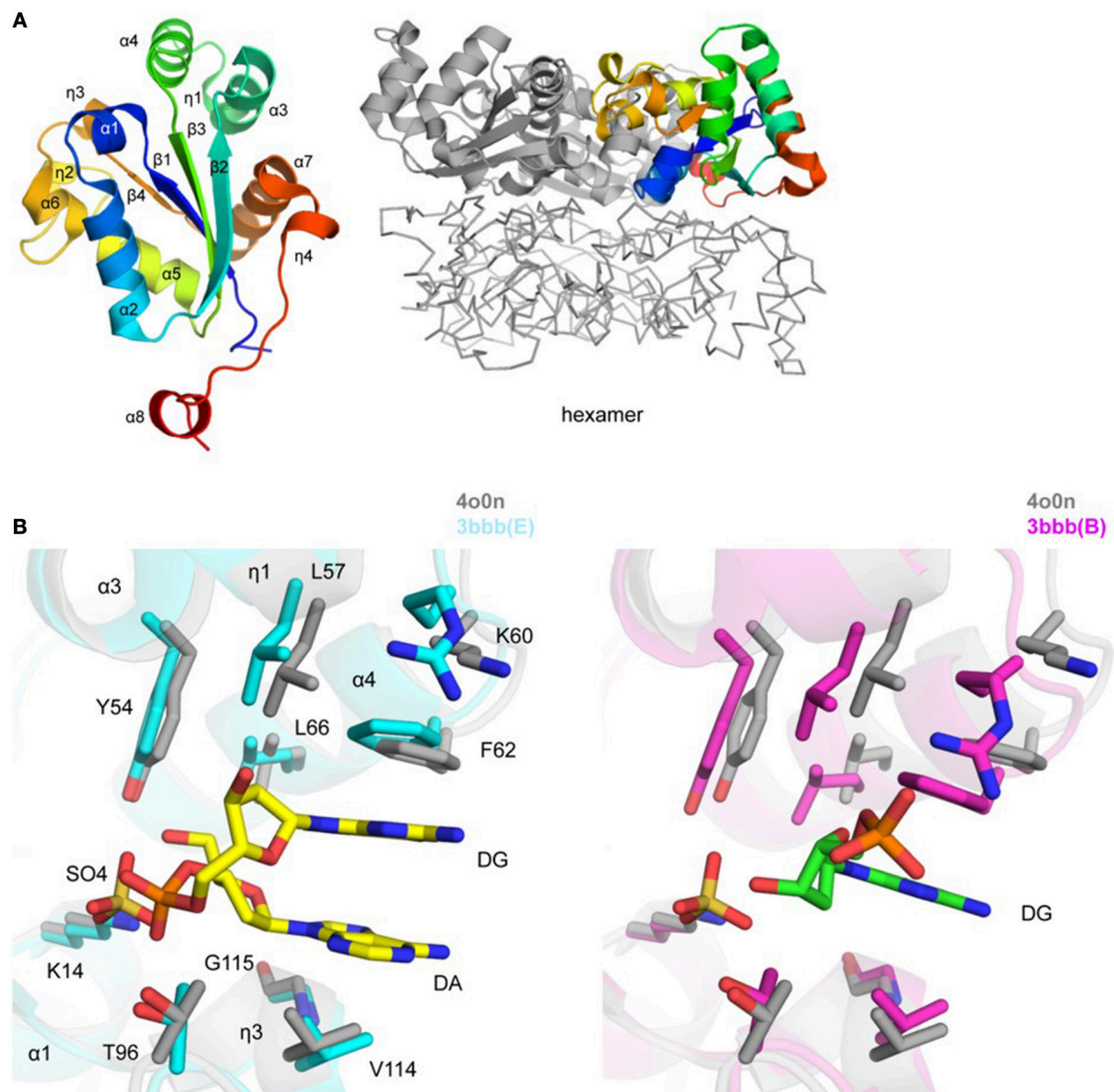


FIGURE 3 | Crystal structure of *TgNDK* (A). Ribbon representation of *TgNDK* monomer (left side) colored blue (N-terminus) to red (C-terminus) and trimeric and hexameric assemblies of *TgNDK* (middle and right side) (B). Pairwise structural alignment of *TgPDM* (gray; SO4 is shown in sticks) and human NM23-H2 transcription factor [cyan (chain E with bound 2'-deoxyguanosine-5'-monophosphate (DG) and 2'-deoxyadenosine-5'-monophosphate (DA)) and magenta [chain B with bound 2'-deoxyguanosine-5'-monophosphate (DG)] showing active site with residues of *TgNDK* shown in sticks and labeled in one-letter code. Equivalent residues of human NM23-H2 transcription factor are displayed.

animal hosts. Protein sequences were analyzed by XtalPred and final selection was also based on their crystallization feasibility (Slabinski et al., 2007).

Phase III utilized the TDR Database (Anderson, 2009; Crowther et al., 2010; Magariños et al., 2012). TDR integrated and weighed candidate drug targets based on extensive genetic, biochemical, pharmacologic, compound desirability and computationally-predicted druggability characteristics. Herein, 5 soluble enzymes were selected for further study. The genes encoding these enzymes were cloned, proteins expressed and purified, crystallized, and crystal structures were determined (Figures 2–6). The crystal structures have been deposited in the PDB database in accordance with CSGID

and NIH policies. PDB codes can be found in Figure 1 and Table 2.

Phosphoglycerate Mutase II (PGM)

The crystal structure of a putative *TgPDM1* was determined and refined to 2.6 Å resolution (PDB 4odi) (Table 2 and Figure 2A). The $P2_12_12$ asymmetric unit comprises four PGM chains [~ 0.4 Å root-mean-square-deviation (r.m.s.d.) over 240 C α atoms] assembled in two dimers with BSA of $\sim 1,900$ Å², while four chains bury a surface area of $\sim 6,800$ Å² (Figure 2A). Eleven salt bridges, 15 hydrogen-bonded and 236 van der Waals interactions hold the tetramer in place. A sodium ion-binding site (e.g., NA 301/A) was identified during structure refinement. Tyr155,

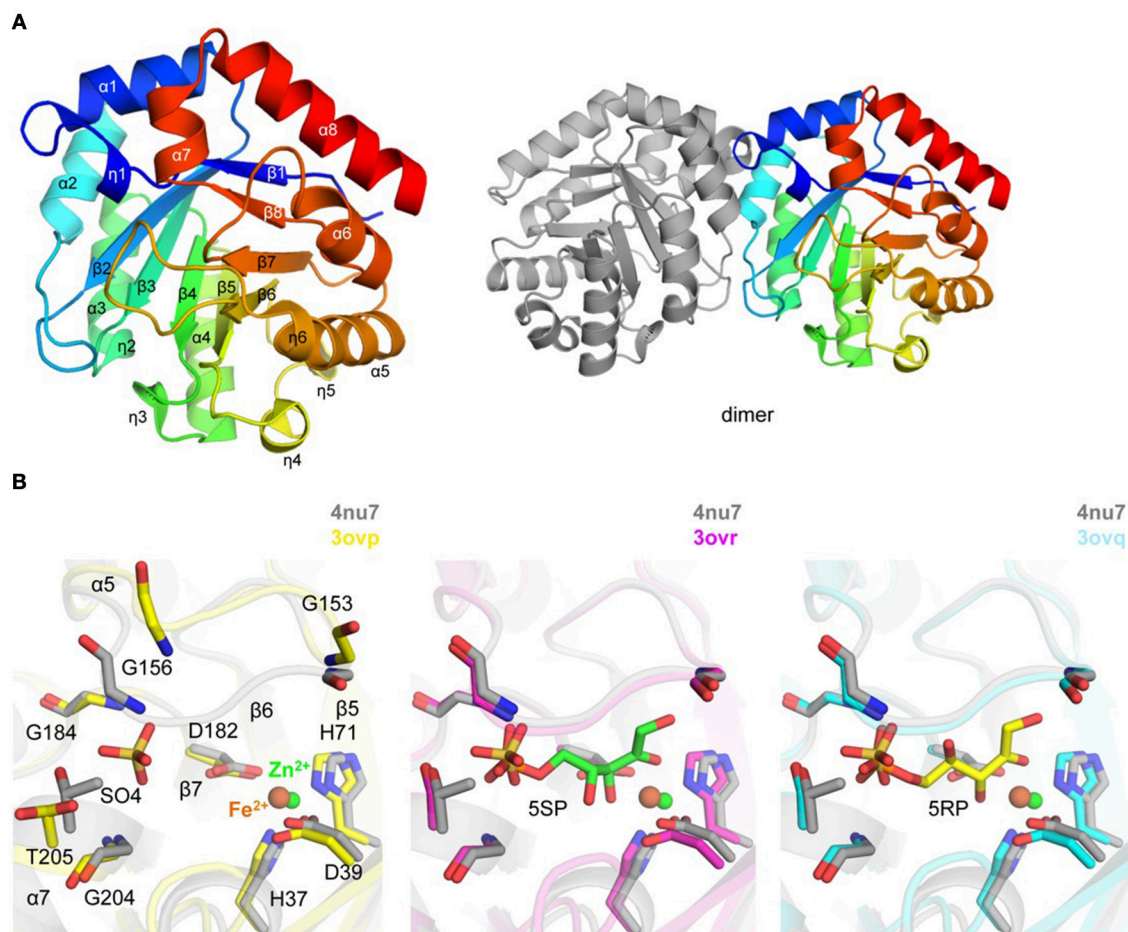


FIGURE 4 | Crystal structure of *TgRPE* (A). Ribbon representation of *TgRPE* monomer (left side) colored blue (N-terminus) to red (C-terminus) and *TgRPE* dimer (right side) (B). Pairwise structural alignment of *TgRPE* (gray; SO4 is shown in sticks and Zn^{2+} as green sphere) and human RPE with bound Fe^{2+} (yellow ribbon), 5-O-phosphono-D-xylulose (5SR; magenta ribbon), and ribulose-5-phosphate (5RP; cyan ribbon) showing active site with residues of *TgRPE* are shown in sticks and labeled in one-letter code. Equivalent residues of human RPE are displayed.

Val158, and Asn160 coordinate NA 301/A. Residues 12–257 (chain A), 15–259 (chain B), 15–257 (chain C), and 17–248 (chain D) are present in the deposited structure.

TgPGM has an $\alpha/\beta/\alpha$ -sandwich domain that comprises residues 12–107 and 169–257 (Figure 2A). The domain has a six-stranded central β -sheet flanked by helices $\alpha 1$, $\alpha 2$, $\alpha 3$, $\alpha 6$, $\alpha 7$, $\alpha 8$, and $\alpha 9$, and 3_{10} -helices $\eta 1$ and $\eta 6$. Residues 108–168 (helices $\alpha 4$ and $\alpha 5$, and four 3_{10} helices; $\eta 2$ – $\eta 5$) flank the $\alpha/\beta/\alpha$ domain without any defined folding motif (Figure 2B). Lys115 and Arg132 of this motif comprise a portion of the active site and together with Arg25, His26, Asn32, Thr38, Glu104, Tyr107, His199, and Asn201 of the $\alpha/\beta/\alpha$ domain shape the entrance to the active site (Figure 2C). An interesting feature of the structure is a “scorpion tail” segment (residues 136–168 belonging to 3_{10} -helices $\eta 3$, $\eta 4$, and $\eta 5$) that lies on top of the $\alpha/\beta/\alpha$ domain (Figure 2B). Position of this segment within the crystal lattice suggests that it affects oligomerization and crystal packing. The tip of the tail possesses the sodium ion-binding site.

The structure of the *Plasmodium falciparum* PGM (*PfPGM*; PDB 3kkk; DOI: 10.2210/pdb3KKK/pdb) is the closest homolog of *TgPGM* with estimated 75% sequence identity and ~ 0.6 Å r.m.s.d. over 229 C α atoms. The structure of the homologous bacterial enzyme from *Burkholderia pseudomallei* (PDB 3fdz; 67% sequence identity; r.m.s.d. ~ 1.0 Å over 230 C α atoms) determined in the complex with (2R)-2,3-diphosphoglyceric reveals that *TgPGM* possesses identical active site residues with an essential phospho-acceptor residue His26 (Davies et al., 2011). Preliminary validation of this active site in Schrödinger SiteMap gave a favorable score of 0.98. Structural alignment of *BpPGM* and *TgPGM* demonstrates significant main- and side-chain conformational changes at the protein active site that would most likely take place in *TgPGM* during the interconversion of its substrate 3-phosphoglycerate to 2-phosphoglycerate (Figure 2C). Conformational differences were also observed for residues located on the tip of the scorpion-like tail.

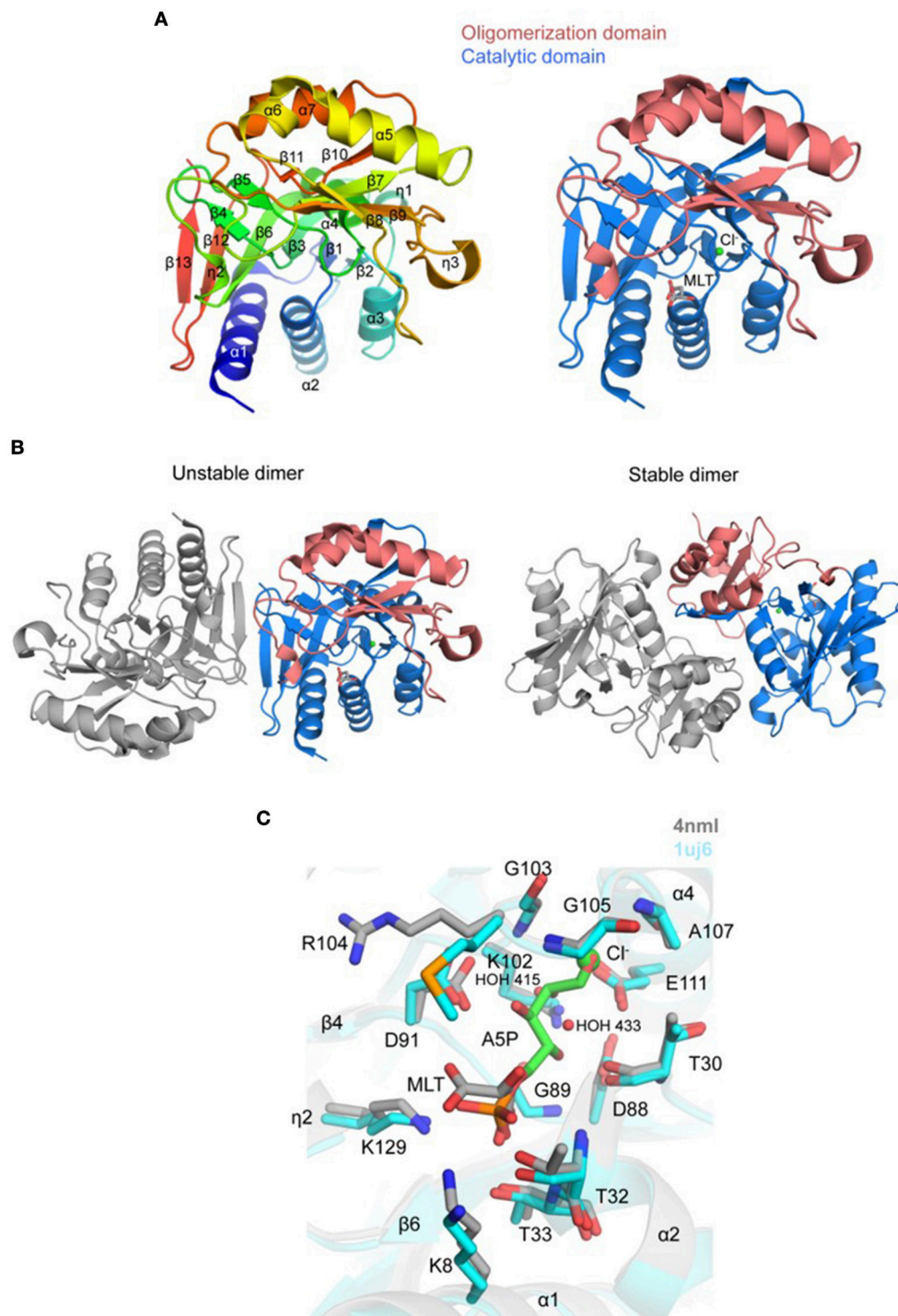
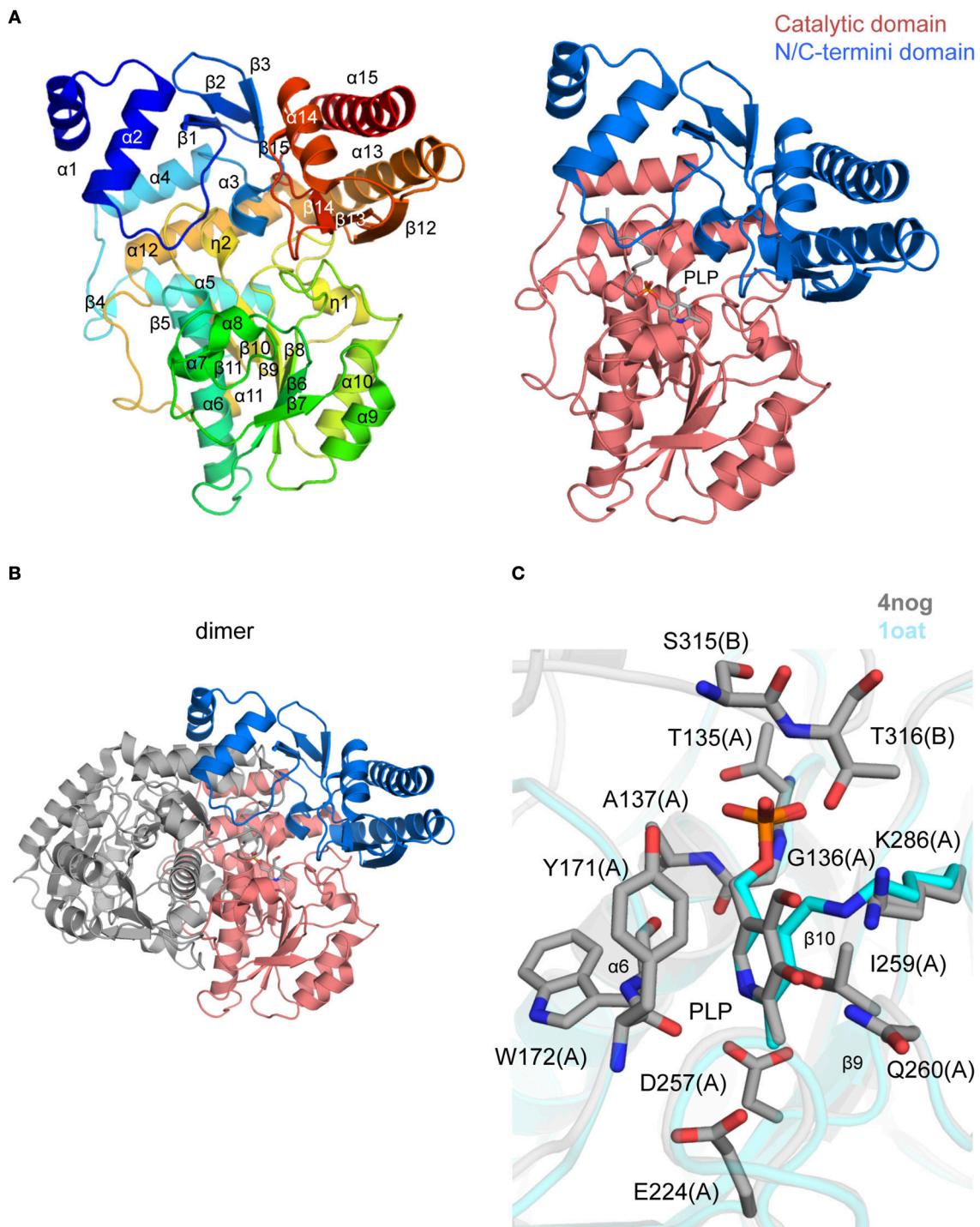


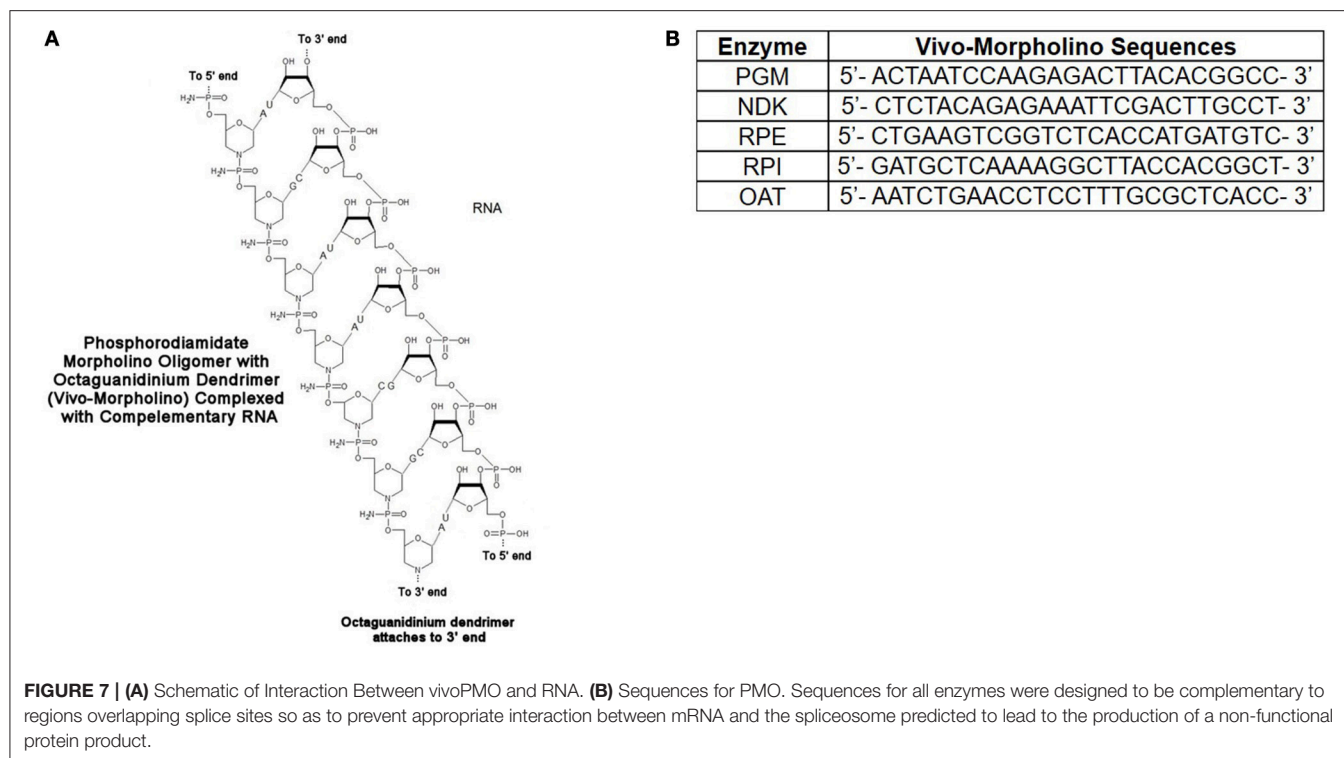
FIGURE 5 | Crystal structure of *TgRPI* (**A**). Ribbon representation of *TgRPI* monomer (left side) colored blue (N-terminus) to red (C-terminus). Catalytic domain and oligomerization domain of *TgRPI* with bound D-malate (MLT; sticks) and chloride ion (Cl^- ; green sphere) are shown on the right. (**B**). Unstable and stable *TgRPI* dimers according to PISA prediction (**C**). Pairwise structural alignment of *TgRPI* (gray; MLT is shown in sticks and Cl^- as green sphere) and *TtRPI* (cyan ribbon) with bound arabinose 5-phosphate (A5P; sticks) showing active site with residues of *TgRPI* are shown in sticks and labeled in one-letter code. Equivalent residues of *TtRPI* are displayed. Water molecules are shown as small red spheres.



Nucleoside Diphosphate Kinase (NDK)

Crystal structures of a putative *TgNDK* were determined and refined to 2.4 Å (PDB 4o0n) and 1.7 Å (PDB 5bxi) resolution

(Figure 3A and Table 2). Monomers in both *TgNDK* structures are superimposed with ~ 0.2 – 0.7 Å r.m.s.d. over 153 C α atoms, while monomers in 4o0n align with ~ 0.2 – 0.7 Å r.m.s.d (153 C α



atoms) and monomers in 5bxi align with $\sim 0.2\text{--}0.6$ Å r.m.s.d (153 C α atoms). In both structures, TgNDK forms a hexamer with an average BSA of $\sim 18,900$ Å² (Figure 3A). Comparison of TgNDK with known crystal structures of homologous proteins suggests that the TgNDK hexamer is likely a biologically functional assembly (Min et al., 2002; Vieira et al., 2015).

Residues 156–160 (GENLY) of the C-terminal tag in chains D and G only of the 5bxi structure were modeled, while they are absent in all chains of the 4o0n structure. These residues protrude to the solvent and make contacts with symmetry-related hexamer. The side chain of Tyr160 is spatially positioned in a nucleotide base-binding pocket of the active site of a symmetry-related molecule (not shown). In addition, residues 56–64 (DLKGKPFPP; chain C of 5bxi) that belong to the C-terminus of helix $\alpha 3$, 3_{10} helix $\eta 1$, $\eta 1\text{--}\alpha 4$ loop, and the N-terminus of helix $\alpha 4$ are disordered. This peptide stretch may constitute a portion of a nucleotide base-binding pocket of the active site. Superposition of all twelve chains in 5bxi and 4o0n structures revealed that this segment has similar secondary structure conformations. Presumably, lack of favorable crystal contacts resulted in its disorder in chain C of the 5bxi structure.

TgNDK adopts an $\alpha/\beta/\alpha$ sandwich fold with four β strands and eight surrounding α helices (Figure 3A). The putative active site of TgNDK was identified based on a pairwise structural alignment with the crystal structure of human NM23-H2 transcription factor in complex with the dinucleotide d(AG) (PDB 3bbb; Dexheimer et al., 2009). The active site comprises residues Lys14, Tyr54, Leu57, Lys60, Phe62, Leu66, Thr96, Val114, and Gly115 (Figure 3B), where analysis by Schrödinger SiteMap revealed a score of 0.99 (using PDB 4o0n), indicating

a “druggable” pocket. Crystals of TgNDK (PDB 4o0n) grew in the presence of ammonium sulfate and, thus, several sulfate ions were identified and modeled during refinement. Superposition of TgNDK with the structure of human NM23-H2 transcription factor ($\sim 67\%$ homology; ~ 0.6 Å r.m.s.d. over 148 C α atoms) revealed that a sulfate ion (e.g., SO4 201/A) binds close to a phosphate-binding pocket of the active site (Figure 3B). A bicarbonate ion (e.g., BCT 201/A) was modeled at a similar location in the 5bxi structure. Similar main- and side-chain rearrangements of residues of the active site as seen in NM23-H2 are expected in TgNDK upon binding its substrate.

Ribulose Phosphate 3-Epimerase (RPE)

Crystal structure of TgRPE was determined and refined to 2.05 Å resolution (PDB 4nu7; Table 2 and Figure 4A). TgRPE adopts an aldolase-type TIM-barrel α/β fold resembling homologous RPEs. Four chains of TgRPE ($\sim 0.3\text{--}0.5$ Å r.m.s.d. over 225 C α atoms) in the H32 asymmetric unit form two dimers (A–C and B–D; Figure 4A) each burying a surface area of $\sim 3,500$ Å². The dimer is similar to one observed for known RPEs (Williamson and Wood, 1966; Jelakovic et al., 2003; Caruthers et al., 2005; Liang et al., 2011). Helices $\alpha 1$ and $\alpha 2$, and the $\beta 2\text{--}\alpha 2$ and $\eta 1\text{--}\alpha 1$ loops of TgRPE comprise the dimer interface with 4 salt bridges, 8 hydrogen-bonded and 130 van der Waals contacts (e.g., between chains A and C). PISA prediction and crystal packing analysis revealed a hexameric assembly of TgRPE (BSA is $\sim 13,300$ Å²; not shown) that has been reported previously for homologous RPEs (Kopp et al., 1999; Wise et al., 2004; Akana et al., 2006).

A Zn²⁺ (e.g., ZN 303/A) ion was modeled per each chain of TgRPE, with His37, Asp39, His71, Asp182 and a water molecule

coordinating the metal (**Figure 4B**). Similar coordination has been reported for D-xylulose 5-phosphate co-crystallized with human RPE enzyme (PDB: 3ovr) (Liang et al., 2011) (**Figure 4B**). PDBeFold identified human RPE as the closest homolog of *TgRPE* (~ 0.9 Å r.m.s.d. over 215 C α atoms; 52% sequence identity). The CheckMyMetal analysis identified that Co²⁺ and Cu²⁺ may also bind in a similar position as zinc in *TgRPE*. It is known that the RPE enzymes can utilize Fe²⁺, Co²⁺, and Mn²⁺ for catalysis (Jelakovic et al., 2003; Wise et al., 2004; Caruthers et al., 2005; Akana et al., 2006; Liang et al., 2011). Residues of the metal binding site are strictly conserved in the RPE enzymes. Structural superposition revealed that Fe²⁺ in ferrous-, substrate- and product-bound human RPE structures is ~ 1.0 Å away from the position of Zn²⁺ in *TgRPE*. We also compared *TgRPE* structure with two other RPEs structures (PDBs 1tqx and 1h1z) (Jelakovic et al., 2003; Caruthers et al., 2005) that have zinc and SO₄²⁻ bound in similar locations as *TgRPE*. Positions of zinc and side chains of the Zn²⁺-coordinating residues are similar in the three compared structures (not shown). Other RPE structures with bound Zn²⁺ and other than SO₄²⁻ ligands (e.g., PDBs 2fli, 3qc3, and 5umf) have similar positions of Zn²⁺ and side chains of the metal-binding residues (Akana et al., 2006; Joint Center for Structural Genomics, 2011; Dranow et al., 2017). Additional experiments are needed to confirm the biological importance of zinc in the *TgRPE*-based catalysis. This metal-binding region was analyzed for “druggability” and scored 1.04 (Schrödinger SiteMap).

Crystals of *TgRPE* grew in the presence of 500 mM NaCl and 2 M ammonium sulfate and, thus multiple sulfate and chloride ions were modeled to interpret additional electron density. Structure comparison analysis revealed that a sulfate ion (e.g., SO₄ 304/A) in *TgRPE* occupies the binding site of a phosphate moiety of substrate or product observed in the structure of the human RPE enzyme (PDBs 3ovq and 3ovr) (**Figure 4B**). In all ligand-bound human RPE structures, a loop (e.g., the $\beta 6$ – $\alpha 5$ loop in *TgRPE*) supports position of a ligand at the active site, i.e., moves from its ligand-free conformation to cap a ligand bound to the enzyme. Thus, similar loop movement is expected for *TgRPE* upon binding of the substrate, i.e., a ligand. Apparently, binding of SO₄²⁻ sufficed the loop repositioning in *TgRPE* (**Figure 4B**).

Ribose 5-Phosphate Isomerase (RPI)

Crystal structure of a putative *TgRPI* was determined and refined to 2.6 Å resolution with one protein molecule per asymmetric unit (PDB 4nml; **Figure 5A** and **Table 2**). *TgRPI* has a larger $\alpha/\beta/\alpha$ sandwich catalytic domain (residues 1–127 and residues 225–259) with the Rossmann topology and a smaller α/β sandwich oligomerization domain (residues 128–224) (**Figure 5A**). Residues 180–186 between strand $\beta 8$ and a 3_{10} -helix ($\eta 3$), Arg258, and Lys259 are absent in the structure due to their disorder. BME was used in buffers during purification and crystallization and is covalently linked to Cys82 in the structure. One D-malate molecule and two chloride ions were modeled to interpret additional electron density (**Figures 5A,C**). Applying crystal symmetry operations PISA predicted that *TgRPI* might exist as unstable dimer (BSA of $\sim 2,430$ Å²) or stable dimer (BSA of $\sim 3,340$ Å²) in the crystal environment (**Figure 5B**).

Visualization of both dimers revealed that the first assembly is held in place primarily by hydrogen-bonded interactions between main-chain atoms of strand $\beta 13$ of each monomer's catalytic domain (**Figure 5B**). The second dimer is stabilized by multiple intramolecular contacts between residues from both *TgRPI* domains. Homologous RPIs form similar stable dimers and, thus stable *TgRPI* dimer may be considered biologically relevant.

PDBeFold identified several homologs of *TgRPI*, and we used the crystal structure of RPI from *Thermus thermophilus* (*TtRPI*; PDB 1uj6) (Hamada et al., 2003) determined in complex with arabinose 5-phosphate to identify the active site of *TgRPI* (**Figure 5C**). Both proteins share 45% sequence homology and are superimposed with ~ 1.0 Å r.m.s.d. over 218 C α atoms. This structural alignment revealed that D-malate and chloride ion (e.g., CL 301/A) in *TgRPI* are bound in the protein's active site, mimicking parts of arabinose 5-phosphate in 1uj6 (**Figure 5C**). D-malate makes hydrogen bonds with side chains of Lys8, Thr32, and Thr33, and several van der Waals contacts with residues of the phosphate-binding pocket of the active site (Schrödinger SiteMap score 0.97). CL 301/A is bound in the oxyanion hole of the active site and coordinated by main-chain nitrogen atoms of Gly105 and Ala107, side chain carboxyl group of Glu111, and two water molecules, HOH 415 and HOH 433 (**Figure 5C**). The second chloride ion (e.g., CL 302/A) in *TgRPI* binds near disordered residues 179–185 and makes bonds with main-chain nitrogen atoms of Phe172 and Ile190, and the ϵ -amino group of Lys154 (not shown).

The catalytic domain of homologous RPIs align well, while the oligomerization domain has some distinct structural differences among various species. For example, a peptide stretch between residues Leu160 and Arg169 of the oligomerization domain of *TgRPI* is longer than the equivalent region in *TtRPI*. In the *TgRPI*, structure this segment is helix $\alpha 6$. We have found that a similar helical element is present in *E. coli* RPI (Zhang et al., 2003) (PDB 1o8b; 45% sequence homology; ~ 1.4 Å r.m.s.d. over 164 C α atoms) and *P. falciparum* RPI (Holmes et al., 2006) (PDB 2f8m; 45% sequence homology; ~ 1.1 Å r.m.s.d. over 233 C α atoms). Another example, strands $\beta 8$ and $\beta 9$ in *TgRPI* are separated by a 3_{10} -helix ($\eta 3$) and disordered residues 179–185, while similar region in *TtRPI*, *EcRPI*, and *PfRPI* is shorter, ordered, and extends toward the N-terminus of helix $\alpha 4$ of the superimposed *TgRPI*. Thus, $\eta 3$ and residues 179–185 seem to be unique to *TgRPI*. Its length, proximity to the phosphate-binding pocket, and potential flexibility suggest that it may participate in the catalysis.

Ornithine Aminotransferase (OAT)

The crystal structure of *TgOAT* in complex with pyridoxal-5'-phosphate (PLP) was determined at 1.2 Å resolution (PDB 4nog; **Figure 6A** and **Table 2**) and contains two protein chains in the asymmetric unit (~ 0.3 Å r.m.s.d. over 422 C α atoms) that form a well-studied functional dimer with BSA of $\sim 5,770$ Å² (Shah et al., 1997; Shen et al., 1998; Markova et al., 2005; Vedadi et al., 2007; Jortzik et al., 2010) (**Figure 6B**). Each monomer has a mixed α/β structural fold and consists of the cofactor PLP-binding domain (residues 87–336), an N-terminal domain (residues 17–86), and a C-terminal domain (residues 337–441) (**Figure 6A**). The

PLP-binding domain comprises the eight-stranded central β -sheet linked to 10 α -helices and 4 short α -helical segments. The N- and C-terminal domain comprises three α -helices bounded to a β -sheet of three and four β strands, respectively. The difference between *TgOAT* monomers is observed at the position of N-terminal α -helix and is likely affected by crystal packing. BME used in the protein buffer solutions forms a covalent bond to Cys353 in both *TgOAT* monomers. One 1,3,5-*Tris*(4-carboxyphenyl)benzene (BTB), polyethylene glycol (PEG) and acetate (ACT) molecule were modeled to interpret additional electron density in chain B.

The dimerization interface is primarily formed between residues of the PLP-binding and N-terminal domains of *TgOAT*. The dimer is held by 3 salt bridges, Cys96–Cys96 disulfide bond, 63 hydrogen bonds and 782 van der Waals interactions. The *TgOAT* dimer bears structural similarities to homologous enzymes from the aminotransferase class-III protein family (Christen and Metzler, 1985; Mehta et al., 1993) and, thus, may be considered biologically relevant. The list of homologous structures with sequence identity >40% encloses structure of OAT from human (r.m.s.d. ~ 0.9 Å over 404 C α atoms) (Shah et al., 1997; Storici et al., 1999), OAT from *P. falciparum* (r.m.s.d. ~ 1.2 Å over 384 C α atoms) (Vedadi et al., 2007; Jortzik et al., 2010) and OAT from *P. yoelii* (r.m.s.d. ~ 1.0 Å over 369 C α atoms) (Vedadi et al., 2007). Among structures with similar secondary structure fold and high r.m.s.d. value (~ 1.9 Å over 395 C α atoms) is the structure of GABA-OAT from *E. coli* with sequence identity 31%. Recent reports indicate that *TgOAT* shows a dual N-acetyl-ornithine (AcOrn) and γ -aminobutyric acid (GABA) transaminase activity and may function in both arginine and GABA metabolism (Astegno et al., 2017).

The cofactor-binding domain of *TgOAT* non-covalently binds PLP molecule, i.e., PLP does not form the Schiff base with conserve Lys286 (Figures 6A,C). Similarly to homologous OAT structures obtained in complex with the cofactor (Shah et al., 1997; Shen et al., 1998; Storici et al., 1999; Vedadi et al., 2007; Jortzik et al., 2010), PLP interacts with Thr135, Gly136, Ala137, Tyr171, Trp172, Glu224, Asp257, Ile259, Gln260, Lys286, Ser315, and Thr316 (Figure 6C). Most of these residues are highly conserved among *TgOAT* homologs and represent a viable, “druggable” pocket (SiteMap score 1.03).

In vitro Studies of Targeted VivoPMO on *T. gondii* Replication

HFFs were infected with YFP-expressing *T. gondii* tachyzoites and treated with vivoPMOs targeted against all five enzymes of interest. When treated at 10 μ M concentrations, each morpholino resulted in approximately 50% reduction in fluorescence *in vitro* (between 44% for PGM-targeted vivoPMO to 56% reduction for OAT-targeted vivoPMO). This was compared to the off-target, control morpholino, which resulted in <10% fluorescence reduction. When compared statistically using student *T*-test, levels of fluorescence *in vitro* were statistically decreased ($p < 0.05$) when treating with targeted vivoPMO relative to untreated fibroblasts infected with 2000 YFP-expressing tachyzoites as well as when compared to infected cells treated with off-target morpholino. A representative experiment showing these findings is in Figure 8A. Data

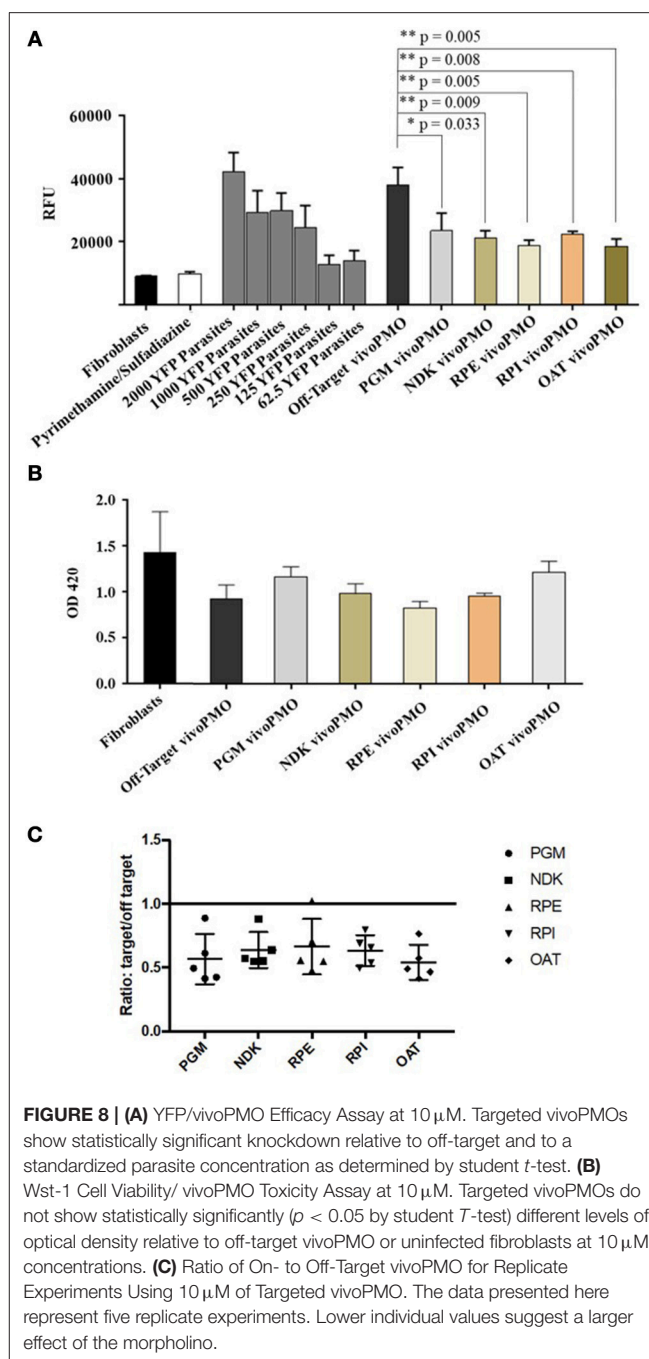


FIGURE 8 | (A) YFP/vivoPMO Efficacy Assay at 10 μ M. Targeted vivoPMOs show statistically significant knockdown relative to off-target and to a standardized parasite concentration as determined by student *t*-test. **(B)** WST-1 Cell Viability/ vivoPMO Toxicity Assay at 10 μ M. Targeted vivoPMOs do not show statistically significantly ($p < 0.05$ by student *T*-test) different levels of optical density relative to off-target vivoPMO or uninfected fibroblasts at 10 μ M concentrations. **(C)** Ratio of On- to Off-Target vivoPMO for Replicate Experiments Using 10 μ M of Targeted vivoPMO. The data presented here represent five replicate experiments. Lower individual values suggest a larger effect of the morpholino.

from all replicate experiments of the morpholino efficacy assays, as well as statistical calculations and ratios reflecting efficacy of targeted morpholino to off-target can be found in **Supplementary Table 1**.

To confirm that these findings of decreased fluorescence *in vitro* was not secondary to host-cell toxicity from the vivoPMOs, a WST-1 assay was used. HFFs treated with 10 μ M concentrations of enzyme-targeted vivoPMOs were statistically indistinguishable ($p > 0.05$) from untreated cells by Student *T*-test. Toxicity was demonstrated at higher vivoPMO concentrations of 20 μ M. A representative experiment

demonstrating the absence of host-cell toxicity with vivoPMO treatment at 10 μ M is in **Figure 8B**.

The ratio of targeted to off-target vivoPMO are displayed in **Figure 8C**. This is shown for five replicate experiments (**Supplementary Table 1**). This demonstrates that, in cultures treated with on-target vivoPMO, parasitic replication was reduced.

These findings were compared with the effect on tachyzoites in a previously published full genome screen using CRISPR/Cas9 (Sidik et al., 2016). Three of the target proteins (*Tg*PGM, *Tg*RPE, and *Tg*RPI) that had a significantly reduced replication phenotype in tachyzoites caused by vivoPMO knockdown were found to contribute to parasite fitness when studied using CRISPR/Cas9. The CRISPR/Cas9 data was annotated and graphically presented in ToxoTB (<http://toxodb.org/toxo>). *Tg*PGM, *Tg*RPE, and *Tg*RPI show negative phenotypic/fitness scores (−4.45, −0.31, −1.92, respectively) suggesting essentiality. *Tg*OAT appeared dispensable (fitness score of +1.2) in the tachyzoite CRISPR/Cas9 assays consistent with *Tg*OAT appeared to be expressed predominantly in the oocyst stage (ToxoDB). *Tg*NDK (+2.45) also appeared to be dispensable in tachyzoites.

Immunofluorescence Assay

Recombinant protein for the five targets was also used to produce antibodies in mice, which were used for immunostaining to determine expression patterns within the parasite. Immunolocalization was not successful with tachyzoites of *Toxoplasma* for four of the five enzymes. For NDK, enzyme was present in a granular pattern in the cytoplasm of tachyzoites, located around the perimeter of the parasite and the posterior part of the parasite. This can be seen in **Figure 9**.

DISCUSSION

The work characterized herein presents a detailed characterization of enzyme structure that can be used for modeling inhibitors of these targets and also presents approaches for studying target phenotype with vivoPMO and CRISPR/Cas9 which in combination develops a system to move forward candidate targets (**Figure 10**). The targeted vivoPMOs demonstrated statistically significant perturbation of parasitic replication when compared to off-target morpholinos, without concomitant host-cell toxicity, confirmed for some of these with CRISPR/CAS9 screen. Inhibition of target enzymatic function via small molecules or anti-sense might be a novel therapeutic modality, should such small molecules exist. Given the current limitations of anti-parasitic medicines for the treatment of toxoplasmosis, new pharmacotherapy is of significant interest. The multi-step approach, detailed here, of *in vitro* inhibition through anti-sense techniques accompanied by detailed structural characterization to identify possible exploitable differences between host and parasite enzymes. Confirmation by referring to a recently published CRISPR/Cas9-based analysis, can also help to suggest importance of targets in *T. gondii* tachyzoites (Sidik et al., 2016). This provides another level of evidence that particular targets may be important for the parasites replication. This approach was performed for each of five enzymes identified as having potential biologic

importance and with favorable predicted druggability using the TDR methodology. This favorable druggability was also confirmed with *in silico* modeling using Schrödinger SiteMap, which indicated each target demonstrated “druggable” pockets. Each enzyme will be considered sequentially hereafter.

Phosphoglycerate mutase II, an enzyme at the core of the glycolytic pathway, catalyzes the transition from 3-phosphoglycerate to 2-phosphoglycerate, an important preparatory step upstream of enolase and pyruvate kinase. Although little work had been done on this Apicomplexan enzyme as a potential drug target, we inferred that interrupting glycolysis would prevent the production of pyruvate by glycolysis, and thereby reduce input into the Krebs Cycle. This, in turn, will reduce the number of electron carrying compounds (NADH, FADH₂), which would markedly reduce ATP production. Interestingly, glycolysis has been targeted successfully in other parasites, and also has been demonstrated to have importance to host cell egress, as well as maintenance of energy reserves when the parasite is found outside of host cells (Ananvoranich et al., 2006; Fleige et al., 2007; Pomel et al., 2008; Lin et al., 2011; Singh et al., 2013). These observations, coupled with our own, are consistent with the observed effect on parasite replication. It appears that putative inhibitors could make this a robust tachyzoite molecular target with a compound easily available to test. With the present crystal structure, further structure-based molecular design approaches (such as virtual screening) is possible given the favorable SiteMap score (0.98).

Nucleotide diphosphate kinase catalyzes the movement of phosphate from a nucleoside triphosphate to a nucleoside diphosphate (e.g., GTP + ADP → GDP + ATP). Naturally, disruption of this process could have an impact on the energy economy within the parasite, as ATP would not be available for important cellular tasks related to DNA replication and the production of more parasites. Additionally, this is a stress kinase, and thus its impact on the stressed organism (through a tetracycline-dependent gene expression construct, RPS-13) would be useful to explore. An immunofluorescence assay revealed peripheral and posterior concentration of staining. Interestingly, another intracellular pathogen, *Leishmania amazonensis*, has been shown to secrete NDK to prevent host-cell autolysis (Kolli et al., 2008). It would be of interest to determine whether this enzyme plays a similar role in Apicomplexans like *T. gondii*. Of note, NDK inhibition by candidate compounds has been demonstrated to have efficacy against certain species of *Leishmania in vitro* (Vieira et al., 2015; Mishra et al., 2017). Crystal structure of *Tg*NDK suggests that the protein forms a hexamer with conserved nucleotide binding sites. Pairwise structural alignment revealed that active site of *Tg*NDK may undergo similar conformational changes as its closest homolog, human NM23-H2 transcription factor (**Figure 3B**). High structural homology to human transcription factor (NM23-H2) in the residues in the catalytic site indicate that selective inhibitors that do not act on human NM23-H2 will be needed. Possible strategies that will facilitate such selectivity include antisense, CRISPR, aptamer-based approaches where the DNA/RNA sequences are divergent, among others. When the dinucleotide is present in the active site, the residues in both *Tg* and Hs structures have similar side chain orientations

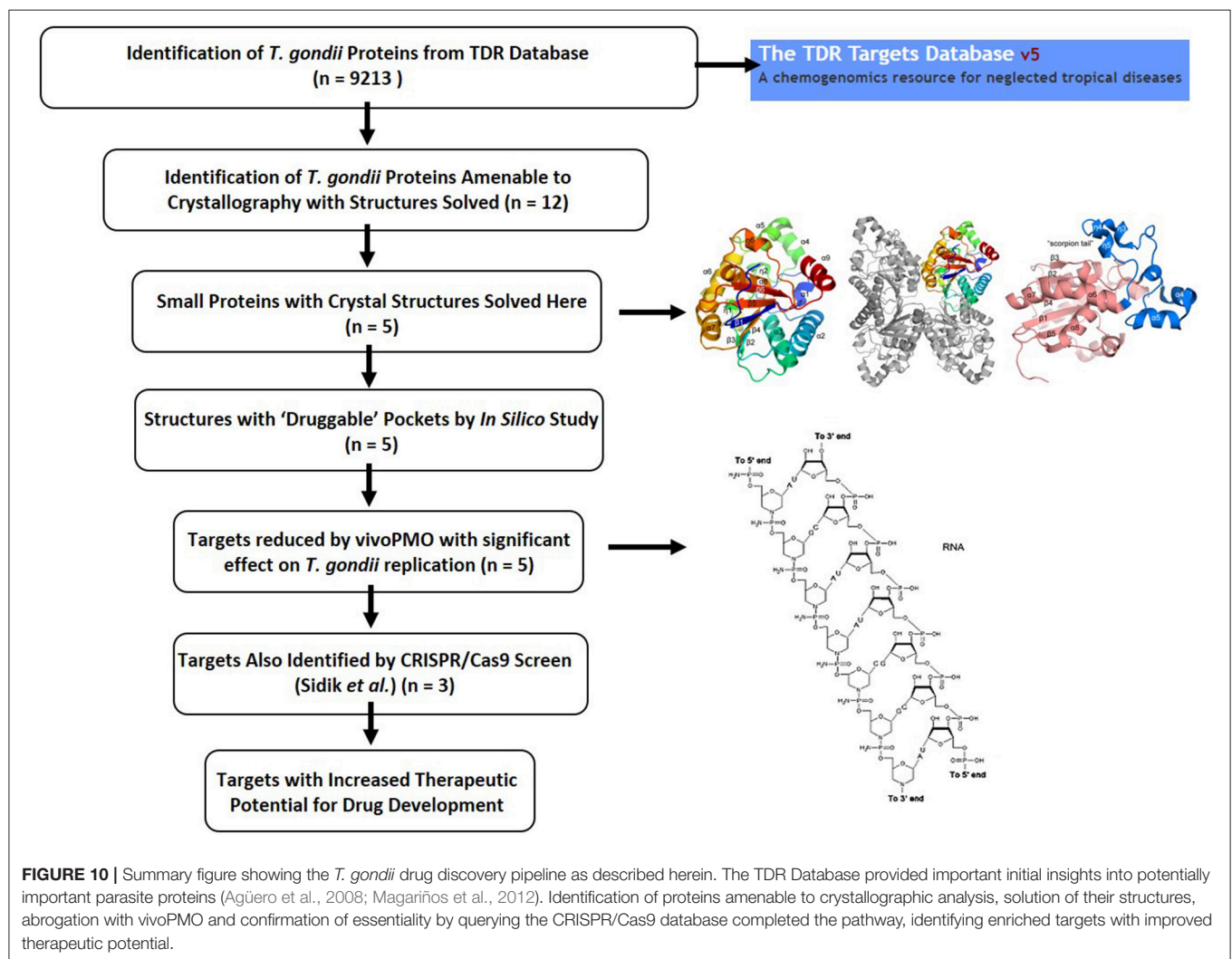
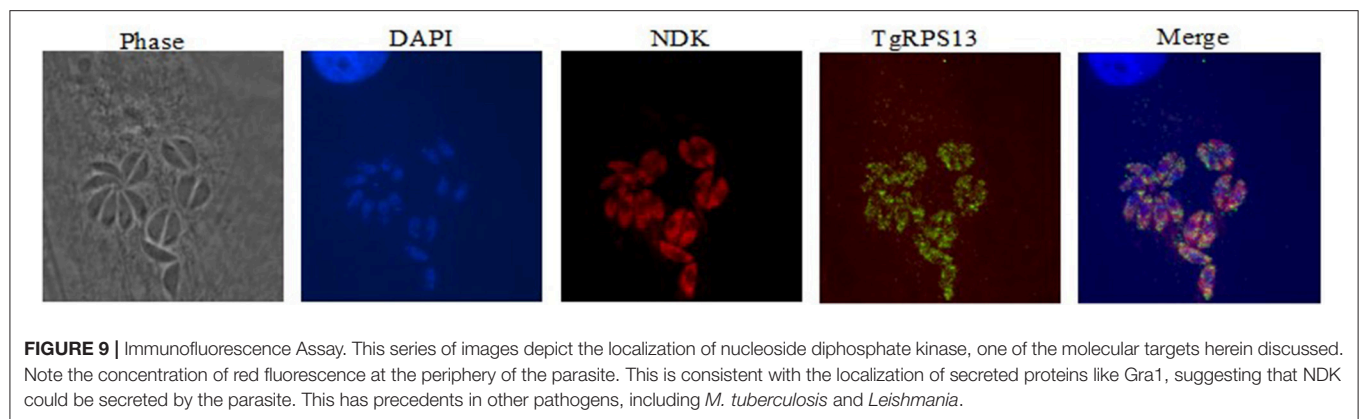


(Figure 3B), suggesting inhibitor selectivity between the species might be difficult to achieve. On the other hand, when the dinucleotide is absent, the active site loop comprising of residues G59–F62 (*Tg* numbering) is shifted significantly (3–4 Å) between species. Additionally, *Tg*NDK residue K60 is residue R58 in the human ortholog, offering different hydrogen-bond capacities to putative ligands. These observations suggest

opportunities for the selective design of *Tg*NDK inhibitors using structure-based molecular modeling techniques. Wang et al. reported selective NM23-H2 (human ortholog) inhibitors based on an isaindigotone scaffold (Wang et al., 2017). These compounds were subjected to molecular docking studies and were predicted to bind to the dinucleotide pocket. More so, they offer an obvious starting point for biological evaluation in

in vitro parasite models and the subsequent design of selective TgNDK chemical probes/ligands.

The next two enzymes, due to their sequential placement within the pentose-phosphate pathway, should be considered together. Ribulose phosphate 3-epimerase functions in the conversion of ribulose-5-phosphate into xylulose-5-phosphate, which is a reaction in the Calvin cycle. It is just downstream of the next target enzyme, ribose-5-phosphate isomerase, and is important for the development of a pool of NADPH, as well as in the pentose phosphate pathway that can convert monosaccharides like glucose into nucleotide precursor pentose sugars. This pathway has been of interest in targeting various organisms, including *P. falciparum* and *Trypanosoma cruzi* (Barrett, 1997; Bozdech and Ginsburg, 2005; Igoillo-Esteve et al., 2007). The biology of RPE has proven to be of particular interest in *T. cruzi* (Gonzalez et al., 2017). Indeed, the structure of RPE had already been characterized in *P. falciparum* (Caruthers et al., 2005). Determined crystal structure of TgRPE revealed that Zn²⁺ binds in a putative active site. In addition, the presence of SO₄²⁻ in the active site induces the β6–α5 loop to move from its presumed apo conformation in the absence of ligand, as seen in the human RPE homolog, to holo conformation in the ligand bound state (Figure 4B). Ribose-5-phosphate isomerase is the enzyme in the pentose phosphate pathway just upstream of ribulose phosphate 3-epimerase, and it has similar functions, though it catalyzes the transition from ribose-5-phosphate to ribulose-5-phosphate. It has been identified as a potential drug target in *P. falciparum*, one of the causative agents of malaria, due to its necessity in creating nucleotide precursors for DNA synthesis and for maintaining a large pool of NADPH for rapid replication and the metabolism necessary for the maintenance thereof (Holmes et al., 2006). It has also been of interest and targeted in *Mycobacterium tuberculosis* where inhibitors have been identified (Roos et al., 2005). Additionally, this pathway has been suggested as a drug target in trypanosomes, with identified compounds and multiple mechanisms of inhibition having been demonstrated, with current patents existing (de V. C. Sinatti et al., 2017). Perhaps the most interesting feature of the determined crystal structure of TgRPI is the disordered region between residues 179–185 that comprises a part of what may appear to be an active site loop. These residues and 3₁₀-helix η3 are unique to TgRPI and might be important for catalysis (Figure 5A).

Ornithine aminotransferase, the final enzyme considered herein, is an enzyme involved in the urea cycle, TCA cycle, polyamine synthesis, and other pathways. It catalyzes a reversible reaction allowing interconversion of intermediates from ornithine to amino acids. Other enzymes which act in this pathway have been suggested as potential drug targets, and it is critical for maintaining proper amounts of free amino acids, so it was a good candidate for further study. Herein we found a modest phenotype on replication but raised antibody did not immunostain tachyzoites. Ornithine aminotransferase will be studied further in the future to resolve some of these questions and attempt to develop effective inhibitors, were it to prove to be essential. Structural analysis reveals that TgOAT shares similar structural folds to known OAT enzymes (Figure 6). We have identified that TgOAT shares a conserved cofactor and

substrate-binding site with its closest homolog human GABA-AT. To gain insights into function of TgOAT, we attempted to crystallize this enzyme with several different inhibitors and inactivators. As a result, three additional crystal structures of TgOAT in complex with gabaculine (a potent inhibitor of human GABA-AT) and (S)-4-amino-5-fluoropentanoic acid have been determined (PDBs 5DJ9, 5E5L, and 5E3K). Therefore, we have performed a full kinetic and structural analysis. The details of the structure, substrate binding site, kinetic mechanism and function of TgOAT will be described in our subsequent works.

Our approach described herein is a productive way to identify molecular targets and could potentially be useful for identifying small molecule inhibitors. *In silico* analysis of each enzyme's surface pockets/active sites suggest "druggable" areas for binding of putative small molecules. The recent discovery that CRISPR/Cas9 has future potential for treating HIV (Yin et al., 2017) also raises the possibility that expression of simply validated molecular targets can be eliminated by CRISPR/Cas9. SiRNA is another possible therapeutic modality, and is being studied in several infectious diseases, including Hepatitis C, Ebola, and viral encephalitis, among others (Kumar et al., 2006; Wan et al., 2014; Watanabe et al., 2014; Thi et al., 2015). As our studies suggest, vivoPMO inhibited *T. gondii* replication; antisense PMO is, therefore, another potential therapeutic modality that might effectively treat parasitic infection. The data presented in Figure 8 and CRISPR/Cas9 screen suggest a phenotype for TgPGM, TgRPE, and TgRPI, but do not yet prove the targets are essential. With confirmation in the future, vivoPMO-based therapy with a less toxic molecular transporter has promise. The safety of PMO is well-documented in several clinical trials in treating genetic, cardiovascular, and infectious diseases including Duchenne muscular dystrophy (DMD), restenosis, and Marburg and Ebola hemorrhagic fevers (Kipshidze et al., 2007; Kinali et al., 2009; Cirak et al., 2011; Heald et al., 2014). It has even shown efficacy against a relative of *T. gondii*, the causative agent of malaria, *P. falciparum* (Augagneur et al., 2012). Eteplirsen (ExonDys51) is an FDA-approved PMO drug for treatment of DMD in patients who have confirmed mutation of the DMD gene that is amenable to exon 51 skipping. A clinical trial is underway using a cell-penetrating peptide conjugated eteplirsen (the PPMO technology) to increase intracellular delivery of eteplirsen for greater efficacy, lower dose and less frequent dosing (clinicaltrials.gov: NCT03375255). With the advent of novel modalities, including antisense and small molecule inhibition, for the treatment of both active and latent infection, it may be possible to eradicate human *T. gondii* infection, and the successes achieved by physicians and scientists in combatting smallpox and dracunculiasis might extend to toxoplasmosis as well.

ETHICS STATEMENT

This study was carried out in accordance with the recommendations of The Home Office of the UK Government under the Animals [Scientific Procedures] Act 1986. All work was covered by License PPL60/4568, Treatment and Prevention of Toxoplasmosis with approval by the University of Strathclyde ethical review board.

AUTHOR CONTRIBUTIONS

IJL, HN, and RM: Conceptualization. JL, HN, EF, AH, GM, YZ, ID, KF, LS, JR, KE, SD, CR, SW, MM, SM, CF, ES, RM, and WA: Data curation. JL, EF, AH, GM, YZ, and RM: Formal analysis. CR, RM, and WA: Funding acquisition. JL, HN, EF, AH, GM, YZ, ID, KF, LS, JR, KE, SD, CR, SW, MM, SM, CF, ES, RM, and WA: Investigation. JL, HN, EF, AH, GM, YZ, ID, KF, LS, JR, KE, SD, CR, SW, JM, HM, MM, SM, CF, ES, DS, DR, RM, and WA: Methodology. RM and WA: Project administration. CR, RM, and WA: Resources. RM and WA: Supervision. JL, EF, AH, GM, YZ, RM, and WA: Validation. JL, EF, AH, GM, YZ, and KE: Visualization. JL, EF, AH, GM, and RM: Writing-original draft. JL, HN, EF, AH, GM, YZ, ID, KF, LS, JR, KE, SD, CR, SW, JM, HM, MM, SM, CF, ES, DS, DR, RM, and WA: Writing-review and editing.

ACKNOWLEDGMENTS

This research was supported in part by the NIH NIDDK grant #2T35DK062719-27. The data collection was performed

at the LS-CAT Sector 21 at the Advanced Photon Source supported by the Argonne National Laboratory operated by the University of Chicago Argonne, LLC, for the U.S. Department of Energy, Office of Biological and Environmental Research under contract DE-AC02-06CH11357. The LS-CAT is supported by the Michigan Economic Development Corporation and the Michigan Technology Tri-Corridor (Grant 085P1000817). This work has been funded by NIAID, NIH, Department of HHS, under Contracts No. HHSN 272200700058C, HHSN272201200026C, and HHSN2722017 00060C (WA).

SUPPLEMENTARY MATERIAL

The Supplementary Material for this article can be found online at: <https://www.frontiersin.org/articles/10.3389/fcimb.2018.00352/full#supplementary-material>

Supplementary Table 1 | Data from replicate experiments demonstrate the efficacy of target-specific morpholino on parasite replication *in vitro*. Ratios of target-specific to off-target morpholino for all targets reflect statistically significant perturbation of parasite replication.

REFERENCES

- Agüero, F., Al-Lazikani, B., Aslett, M., Berriman, M., Buckner, F. S., Campbell, R. K., et al. (2008). Genomic-scale prioritization of drug targets: the TDR Targets database. *Nat. Rev. Drug Discov.* 7, 900–907. doi: 10.1038/nrd2684
- Akana, J., Fedorov, A. A., Fedorov, E., Novak, W. R. P., Babbitt, P. C., Almo, S. C., et al. (2006). D-Ribulose 5-phosphate 3-epimerase: functional and structural relationships to members of the ribulose-phosphate binding (beta/alpha)8-barrel superfamily. *Biochemistry* 45, 2493–2503. doi: 10.1021/bi052474m
- Ananvoranich, S., Al Rayes, M., Al Riyahi, A., and Wang, X. (2006). RNA silencing of glycolysis pathway in *Toxoplasma gondii*. *J. Eukaryot. Microbiol.* 53(Suppl. 1), S162–S163. doi: 10.1111/j.1550-7408.2006.00216.x
- Anderson, W. F. (2009). Structural genomics and drug discovery for infectious diseases. *Infect. Disord.* 9, 507–517. doi: 10.2174/187152609789105713
- Aslanidis, C., and de Jong, P. J. (1990). Ligation-independent cloning of PCR products (LIC-PCR). *Nucleic Acids Res.* 18, 6069–6074. doi: 10.1093/nar/18.20.6069
- Astegno, A., Maresi, E., Bertoldi, M., Verde, V. L., Paiardini, A., and Dominici, P. (2017). Unique substrate specificity of ornithine aminotransferase from *Toxoplasma gondii*. *Biochem. J.* 474, 939–955. doi: 10.1042/BCJ20161021
- Augagneur, Y., Wesolowski, D., Tae, H. S., Altman, S., and Mamoun, C. B. (2012). Gene selective mRNA cleavage inhibits the development of *Plasmodium falciparum*. *Proc. Natl. Acad. Sci. U.S.A.* 109, 6235–6240. doi: 10.1073/pnas.1203516109
- Barrett, M. P. (1997). The pentose phosphate pathway and parasitic protozoa. *Parasitol. Today* 13, 11–16. doi: 10.1016/S0169-4758(96)10075-2
- Berman, H. M., Bhat, T. N., Bourne, P. E., Feng, Z., Gilliland, G., Weissig, H., et al. (2000). The protein data bank and the challenge of structural genomics. *Nat. Struct. Mol. Biol.* 7, 957–959. doi: 10.1038/80734
- Bozdech, Z., and Ginsburg, H. (2005). Data mining of the transcriptome of *Plasmodium falciparum*: the pentose phosphate pathway and ancillary processes. *Malar. J.* 4:17. doi: 10.1186/1475-2875-4-17
- Caruthers, J., Bosch, J., Buckner, F., Van Voorhis, W., Myler, P., Worthey, E., et al. (2005). Structure of a ribulose 5-phosphate 3-epimerase from *Plasmodium falciparum*. *Proteins Struct. Funct. Bioinforma.* 62, 338–342. doi: 10.1002/prot.20764
- Chen, V. B., Arendall, W. B., Headd, J. J., Keedy, D. A., Immormino, R. M., Kapral, G. J., et al. (2010). MolProbity: all-atom structure validation for macromolecular crystallography. *Acta Crystallogr. D Biol. Crystallogr.* 66, 12–21. doi: 10.1107/S0907444909042073
- Chevalier, N., Rigden, D. J., Van Roy, J., Opperdoes, F. R., and Michels, P. A. (2000). *Trypanosoma brucei* contains a 2,3-bisphosphoglycerate independent phosphoglycerate mutase. *Eur. J. Biochem. FEBS* 267, 1464–1472. doi: 10.1046/j.1432-1327.2000.01145.x
- Christen, P., and Metzler, D. E. (1985). *Transaminases*. New York, NY: Wiley.
- Cirak, S., Arechavala-Gomez, V., Guglieri, M., Feng, L., Torelli, S., Anthony, K., et al. (2011). Exon skipping and dystrophin restoration in patients with Duchenne muscular dystrophy after systemic phosphorodiamidate morpholino oligomer treatment: an open-label, phase 2, dose-escalation study. *Lancet* 378, 595–605. doi: 10.1016/S0140-6736(11)60756-3
- Crowther, G. J., Shanmugam, D., Carmona, S. J., Doyle, M. A., Hertz-Fowler, C., Berriman, M., et al. (2010). Identification of attractive drug targets in neglected-disease pathogens using an *in silico* approach. *PLoS Negl. Trop. Dis.* 4:e804. doi: 10.1371/journal.pntd.0000804
- Davies, D. R., Staker, B. L., Abendroth, J. A., Edwards, T. E., Hartley, R., Leonard, J., et al. (2011). An ensemble of structures of *Burkholderia pseudomallei* 2,3-bisphosphoglycerate-dependent phosphoglycerate mutase. *Acta Crystallogr. Sect. F Struct. Biol. Cryst. Commun.* 67, 1044–1050. doi: 10.1107/S1744309111030405
- Davis, I. W., Leaver-Fay, A., Chen, V. B., Block, J. N., Kapral, G. J., Wang, X., et al. (2007). MolProbity: all-atom contacts and structure validation for proteins and nucleic acids. *Nucleic Acids Res.* 35, W375–W383. doi: 10.1093/nar/gkm216
- de Beer, T. A., Berka, K., Thornton, J. M., and Laskowski, R. A. (2014). PDBsum additions. *Nucleic Acids Res.* 42, D292–D296. doi: 10.1093/nar/gkt940
- de V. C. Sinatti, V., R Baptista, L. P., Alves-Ferreira, M., Dardenne, L., Hermínio Martins da Silva, J., and Guimarães, A. C. (2017). *In silico* identification of inhibitors of ribose 5-phosphate isomerase from *Trypanosoma cruzi* using ligand and structure based approaches. *J. Mol. Graph. Model.* 77, 168–180. doi: 10.1016/j.jmgm.2017.08.007
- Dexheimer, T. S., Carey, S. S., Zuohe, S., Gokhale, V. M., Hu, X., Murata, L. B., et al. (2009). NM23-H2 may play an indirect role in transcriptional activation of c-myc gene expression but does not cleave the nuclease hypersensitive element III1. *Mol. Cancer Ther.* 8, 1363–1377. doi: 10.2210/pdb3bbb/pdb
- Djikeng, A., Raverdy, S., Foster, J., Bartholomeu, D., Zhang, Y., El-Sayed, N. M., et al. (2007). Cofactor-independent phosphoglycerate mutase is an essential gene in procyclic form *Trypanosoma brucei*. *Parasitol. Res.* 100, 887–892. doi: 10.1007/s00436-006-0332-7

- Dranow, D. M., Conrady, D. G., Lorimer, D. D., and Edwards, T. E. (2017). Crystal Structure of a ribulose-phosphate 3-epimerase from *Neisseria gonorrhoeae* with bound phosphate. *BE Publ.* doi: 10.2210/pdb5umf/pdb
- Dubey, R., Staker, B. L., Foe, I. T., Bogyo, M., Myler, P. J., Ngô, H. M., et al. (2017). Membrane skeletal association and post-translational allosteric regulation of *Toxoplasma gondii* GAPDH1. *Mol. Microbiol.* 103, 618–634. doi: 10.1111/mmi.13577
- Emsley, P., and Cowtan, K. (2004). Coot: model-building tools for molecular graphics. *Acta Crystallogr. D Biol. Crystallogr.* 60, 2126–2132. doi: 10.1107/S0907444904019158
- Emsley, P., Lohkamp, B., Scott, W. G., and Cowtan, K. (2010). Features and development of Coot. *Acta Crystallogr. D Biol. Crystallogr.* 66, 486–501. doi: 10.1107/S0907444910007493
- Flegel, J., Prandota, J., Sovičková, M., and Israili, Z. H. (2014). Toxoplasmosis – A Global Threat. Correlation of latent toxoplasmosis with specific disease burden in a set of 88 countries. *PLoS ONE* 9:e90203. doi: 10.1371/journal.pone.0090203
- Fleige, T., Fischer, K., Ferguson, D. J. P., Gross, U., and Bohn, W. (2007). Carbohydrate metabolism in the *Toxoplasma gondii* apicoplast: localization of three glycolytic isoenzymes, the single pyruvate dehydrogenase complex, and a plastid phosphate translocator. *Eukaryot. Cell* 6, 984–996. doi: 10.1128/EC.00061-07
- Furtado, J. M., Smith, J. R., Belfort, R., Gattay, D., and Winthrop, K. L. (2011). Toxoplasmosis: a global threat. *J. Glob. Infect. Dis.* 3, 281–284. doi: 10.4103/0974-777X.83536
- Gonzalez, S. N., Valsecchi, W. M., Maugeri, D., Delfino, J. M., and Cazzulo, J. J. (2017). Structure, kinetic characterization and subcellular localization of the two ribulose 5-phosphate epimerase isoenzymes from *Trypanosoma cruzi*. *PLoS ONE* 12:e0172405. doi: 10.1371/journal.pone.0172405
- Halgren, T. (2007). New method for fast and accurate binding-site identification and analysis. *Chem. Biol. Drug Des.* 69, 146–148. doi: 10.1111/j.1747-0285.2007.00483.x
- Hamada, K., Ago, H., Sugahara, M., Nodake, Y., Kuramitsu, S., and Miyano, M. (2003). Oxyanion hole-stabilized stereospecific isomerization in ribose-5-phosphate isomerase (Rpi). *J. Biol. Chem.* 278, 49183–49190. doi: 10.1074/jbc.M309272200
- Hasegawa, H., and Holm, L. (2009). Advances and pitfalls of protein structural alignment. *Curr. Opin. Struct. Biol.* 19, 341–348. doi: 10.1016/j.sbi.2009.04.003
- Heald, A. E., Iversen, P. L., Saoud, J. B., Sazani, P., Charleston, J. S., Axtelle, T., et al. (2014). Safety and pharmacokinetic profiles of phosphorodiamidate morpholino oligomers with activity against ebola virus and marburg virus: results of two single ascending dose studies. *Antimicrob. Agents Chemother.* 58, 6639–47. doi: 10.1128/AAC.03442-14
- Holmes, M. A., Buckner, F. S., Van Voorhis, W. C., Verlinde, C. L. M. J., Mehlin, C., Boni, E., et al. (2006). Structure of ribose 5-phosphate isomerase from *Plasmodium falciparum*. *Acta Crystallogr. Sect. F Struct. Biol. Cryst. Commun.* 62, 427–431. doi: 10.1107/S1744309106010876
- Igoillo-Esteve, M., Maugeri, D., Stern, A. L., Beluardi, P., and Cazzulo, J. J. (2007). The pentose phosphate pathway in *Trypanosoma cruzi*: a potential target for the chemotherapy of Chagas disease. *An. Acad. Bras. Ciênc.* 79, 649–663. doi: 10.1590/S0001-37652007000400007
- Jelakovic, S., Kopriva, S., Süß, K.-H., and Schulz, G. E. (2003). Structure and catalytic mechanism of the cytosolic d-ribulose-5-phosphate 3-epimerase from rice. *J. Mol. Biol.* 326, 127–135. doi: 10.1016/S0022-2836(02)01374-8
- Joint Center for Structural Genomics (2011). *Crystal Structure of a D-ribulose-5-phosphate-3-epimerase (NP_954699) from HOMO SAPIENS at 2.20 Å Resolution*. Available online at: <http://www.rcsb.org/pdb/explore.do?structureId=3qc3>
- Jortzik, E., Fritz-Wolf, K., Sturm, N., Hipp, M., Rahlfs, S., and Becker, K. (2010). Redox regulation of *Plasmodium falciparum* ornithine δ-aminotransferase. *J. Mol. Biol.* 402, 445–459. doi: 10.1016/j.jmb.2010.07.039
- Kinali, M., Arechavala-Gomez, V., Feng, L., Cirak, S., Hunt, D., Adkin, C., et al. (2009). Local restoration of dystrophin expression with the morpholino oligomer AVI-4658 in Duchenne muscular dystrophy: a single-blind, placebo-controlled, dose-escalation, proof-of-concept study. *Lancet Neurol.* 8, 918–928. doi: 10.1016/S1474-4422(09)70211-X
- Kipshidze, N., Iversen, P., Overlie, P., Dunlap, T., Titus, B., Lee, D., et al. (2007). First human experience with local delivery of novel antisense AVI-4126 with Infiltrator catheter in de novo native and restenotic coronary arteries: 6-month clinical and angiographic follow-up from AVAIL study. *Cardiovasc. Revasc. Med. Mol. Interv.* 8, 230–235. doi: 10.1016/j.carrev.2007.04.002
- Kito, K., Sanada, Y., and Katunuma, N. (1978). Mode of inhibition of ornithine aminotransferase by L-canaline. *J. Biochem.* 83, 201–206.
- Kolli, B. K., Kostal, J., Zaborina, O., Chakrabarty, A. M., and Chang, K.-P. (2008). Leishmania-released nucleoside diphosphate kinase prevents ATP-mediated cytotoxicity of macrophages. *Mol. Biochem. Parasitol.* 158, 163–175. doi: 10.1016/j.molbiopara.2007.12.010
- Kopp, J., Kopriva, S., Süß, K. H., and Schulz, G. E. (1999). Structure and mechanism of the amphibolic enzyme D-ribulose-5-phosphate 3-epimerase from potato chloroplasts. *J. Mol. Biol.* 287, 761–771. doi: 10.1006/jmbi.1999.2643
- Krissinel, E. (2009). Crystal contacts as nature's docking solutions. *J. Comput. Chem.* 31, 133–143. doi: 10.1002/jcc.21303
- Krissinel, E., and Henrick, K. (2004). Secondary-structure matching (SSM), a new tool for fast protein structure alignment in three dimensions. *Acta Crystallogr. D Biol. Crystallogr.* 60, 2256–2268. doi: 10.1107/S0907444904026460
- Krissinel, E., and Henrick, K. (2005). "Detection of protein assemblies in crystals," in *Computational Life Sciences Lecture Notes in Computer Science*, eds M. R. Berthold, R. C. Glen, K. Diederichs, O. Kohlbacher, and I. Fischer (Berlin; Heidelberg: Springer), 163–174.
- Krissinel, E., and Henrick, K. (2007). Inference of macromolecular assemblies from crystalline state. *J. Mol. Biol.* 372, 774–797. doi: 10.1016/j.jmb.2007.05.022
- Kronenberger, T., Lindner, J., Meissner, K. A., Zimbres, F. M., Coronado, M. A., Sauer, F. M., et al. (2014). Vitamin B6-dependent enzymes in the human malaria parasite *Plasmodium falciparum*: a druggable target? *BioMed Res. Int.* 2014:108516. doi: 10.1155/2014/108516
- Kumar, P., Lee, S. K., Shankar, P., and Manjunath, N. (2006). A single siRNA suppresses fatal encephalitis induced by two different flaviviruses. *PLoS Med.* 3:e96. doi: 10.1371/journal.pmed.0030096
- Lai, B.-S., Witola, W. H., Bissati, K. E., Zhou, Y., Mui, E., Fomovska, A., et al. (2012). Molecular target validation, antimicrobial delivery, and potential treatment of *Toxoplasma gondii* infections. *Proc. Natl. Acad. Sci. U.S.A.* 109, 14182–7. doi: 10.1073/pnas.1208775109
- Lam, S. D., Dawson, N. L., Das, S., Sillitoe, I., Ashford, P., Lee, D., et al. (2016). Gene3D: expanding the utility of domain assignments. *Nucleic Acids Res.* 44, D404–409. doi: 10.1093/nar/gkv1231
- Laskowski, R. A., MacArthur, M. W., Moss, D. S., and Thornton, J. M. (1993). PROCHECK: a program to check the stereochemical quality of protein structures. *J. Appl. Crystallogr.* 26, 283–291.
- Li, X., Tang, S., Wang, Q.-Q., Leung, E. L.-H., Jin, H., Huang, Y., et al. (2017). Identification of epigallocatechin-3-gallate as an inhibitor of phosphoglycerate mutase 1. *Front. Pharmacol.* 8:325. doi: 10.3389/fphar.2017.00325
- Liang, W., Ouyang, S., Shaw, N., Joachimiak, A., Zhang, R., and Liu, Z.-J. (2011). Conversion of D-ribulose 5-phosphate to D-xylulose 5-phosphate: new insights from structural and biochemical studies on human RPE. *FASEB J.* 25, 497–504. doi: 10.1096/fj.10-171207
- Lin, S. S., Blume, M., von Ahsen, N., Gross, U., and Bohn, W. (2011). Extracellular *Toxoplasma gondii* tachyzoites do not require carbon source uptake for ATP maintenance, gliding motility and invasion in the first hour of their extracellular life. *Int. J. Parasitol.* 41, 835–841. doi: 10.1016/j.ijpara.2011.03.005
- Lipinski, C. A. (2004). Lead- and drug-like compounds: the rule-of-five revolution. *Drug Discov. Today Technol.* 1, 337–341. doi: 10.1016/j.ddtec.2004.11.007
- Liu, Y., Huang, R., Han, L., Ke, W., Shao, K., Ye, L., et al. (2009). Brain-targeting gene delivery and cellular internalization mechanisms for modified rabies virus glycoprotein RVG29 nanoparticles. *Biomaterials* 30, 4195–4202. doi: 10.1016/j.biomaterials.2009.02.051
- Lykins, J., Wang, K., Wheeler, K., Clouser, F., Dixon, A., Bissati, K. E., et al. (2016). Understanding toxoplasmosis in the united states through "large data" analyses. *Clin. Infect. Dis.* 63, 468–475. doi: 10.1093/cid/ciw356
- Magariños, M. P., Carmona, S. J., Crowther, G. J., Ralph, S. A., Roos, D. S., Shanmugam, D., et al. (2012). TDR Targets: a chemogenomics resource for neglected diseases. *Nucleic Acids Res.* 40, D1118–D1127. doi: 10.1093/nar/gkr1053
- Markova, M., Peneff, C., Hewlins, M. J. E., Schirmer, T., and John, R. A. (2005). Determinants of substrate specificity in ω-aminotransferases. *J. Biol. Chem.* 280, 36409–36416. doi: 10.1074/jbc.M506977200

- McAleese, S. M., Fothergill-Gilmore, L. A., and Dixon, H. B. (1985). The phosphonomethyl analogue of 3-phosphoglycerate is a potent competitive inhibitor of phosphoglycerate mutases. *Biochem. J.* 230, 535–542.
- McCoy, A. J., Grosse-Kunstleve, R. W., Adams, P. D., Winn, M. D., Storoni, L. C., and Read, R. J. (2007). Phaser crystallographic software. *J. Appl. Crystallogr.* 40, 658–674. doi: 10.1107/S0021889807021206
- McLeod, R., Boyer, K. M., Lee, D., Mui, E., Wroblewski, K., Karrison, T., et al. (2012). Prematurity and severity are associated with *Toxoplasma gondii* alleles (NCCCTS, 1981–2009). *Clin. Infect. Dis.* 54, 1595–1605. doi: 10.1093/cid/cis258
- McLeod, R., Lai, B. S., Witola, W., Bissati, K. E., Mui, E., Moulton, H., et al. (2013). *Conjugate Constructs, Delivery, and Use for Treatment of Disease*. Available online at: <http://www.google.com/patents/US8575126> (Accessed May 8, 2017).
- McLeod, R., Lykins, J., Noble, A. G., Rabiha, P., Swisher, C. N., Heydemann, P. T., et al. (2014). Management of congenital toxoplasmosis. *Curr. Pediatr. Rep.* 2, 166–194. doi: 10.1007/s40124-014-0055-7
- McPhillie, M., Zhou, Y., El Bissatai, K., Dubey, J., Lorenzi, H., Capper, M., et al. (2016). New paradigms for understanding and step changes in treating active and chronic, persistent apicomplexan infections. *Sci. Rep.* 6:29179. doi: 10.1038/srep29179
- Mehta, P. K., Hale, T. I., and Christen, P. (1993). Aminotransferases: demonstration of homology and division into evolutionary subgroups. *Eur. J. Biochem.* 214, 549–561. doi: 10.1111/j.1432-1033.1993.tb17953.x
- Min, K., Song, H. K., Chang, C., Kim, S. Y., Lee, K.-J., and Suh, S. W. (2002). Crystal structure of human nucleoside diphosphate kinase A, a metastasis suppressor. *Proteins Struct. Funct. Bioinform.* 46, 340–342. doi: 10.1002/prot.10038
- Minor, W., Cymborowski, M., Otwinowski, Z., and Chruszcz, M. (2006). HKL-3000: the integration of data reduction and structure solution – from diffraction images to an initial model in minutes. *Acta Crystallogr. D Biol. Crystallogr.* 62, 859–866. doi: 10.1107/S0907444906019949
- Mishra, A. K., Singh, N., Agnihotri, P., Mishra, S., Singh, S. P., Kolli, B. K., et al. (2017). Discovery of novel inhibitors for *Leishmania* nucleoside diphosphatase kinase (NDK) based on its structural and functional characterization. *J. Comput. Aided Mol. Des.* 31, 547–562. doi: 10.1007/s10822-017-0022-9
- Montoya, J. G., and Liesenfeld, O. (2004). Toxoplasmosis. *Lancet* 363, 1965–1976. doi: 10.1016/S0140-6736(04)16412-X
- Morris, R. J., Perrakis, A., and Lamzin, V. S. (2003). “ARP/wARP and automatic interpretation of protein electron density maps,” in *Macromolecular Crystallography, Part D*, ed. B.-M. Enzymology (Academic Press), 229–244. Available online at: <http://www.sciencedirect.com/science/article/pii/S0076687903740117> (Accessed May 5, 2017).
- Motomura, K., Hirota, R., Okada, M., Ikeda, T., Ishida, T., and Kuroda, A. (2014). A new subfamily of polyphosphate kinase 2 (Class III PPK2) catalyzes both nucleoside monophosphate phosphorylation and nucleoside diphosphate phosphorylation. *Appl. Environ. Microbiol.* 80, 2602–2608. doi: 10.1128/AEM.03971-13
- Müller, I. B., Wu, F., Bergmann, B., Knöckel, J., Walter, R. D., Gehring, H., et al. (2009). Poisoning pyridoxal 5-phosphate-dependent enzymes: a new strategy to target the malaria parasite *Plasmodium falciparum*. *PLoS ONE* 4:e4406. doi: 10.1371/journal.pone.0004406
- Murshudov, G. N., Skubák, P., Lebedev, A. A., Pannu, N. S., Steiner, R. A., Nicholls, R. A., et al. (2011). REFMAC5 for the refinement of macromolecular crystal structures. *Acta Crystallogr. D Biol. Crystallogr.* 67, 355–367. doi: 10.1107/S0907444911001314
- Ngô, H. M., Zhou, Y., Lorenzi, H., Wang, K., Kim, T.-K., Zhou, Y., et al. (2017). Toxoplasma modulates signature pathways of human epilepsy, neurodegeneration & cancer. *Sci. Rep.* 7:11496. doi: 10.1038/s41598-017-10675-6
- Opperdoes, F. R., and Michels, P. A. (2001). Enzymes of carbohydrate metabolism as potential drug targets. *Int. J. Parasitol.* 31, 482–490. doi: 10.1016/S0020-7519(01)00155-2
- Pomel, S., Luk, F. C. Y., and Beckers, C. J. M. (2008). Host cell egress and invasion induce marked relocations of glycolytic enzymes in *Toxoplasma gondii* tachyzoites. *PLoS Pathog* 4:e1000188. doi: 10.1371/journal.ppat.1000188
- Reyes, P., Rathod, P. K., Sanchez, D. J., Mrema, J. E., Rieckmann, K. H., and Heidrich, H. G. (1982). Enzymes of purine and pyrimidine metabolism from the human malaria parasite, *Plasmodium falciparum*. *Mol. Biochem. Parasitol.* 5, 275–290.
- Rigden, D. J., Walter, R. A., Phillips, S. E. V., and Fothergill-Gilmore, L. A. (1999). Polyanionic inhibitors of phosphoglycerate mutase: combined structural and biochemical analysis. *J. Mol. Biol.* 289, 691–699. doi: 10.1006/jmbi.1999.2848
- Roos, A. K., Burgos, E., Ericsson, D. J., Salmon, L., and Mowbray, S. L. (2005). Competitive inhibitors of *Mycobacterium tuberculosis* ribose-5-phosphate isomerase B reveal new information about the reaction mechanism. *J. Biol. Chem.* 280, 6416–6422. doi: 10.1074/jbc.M412018200
- Ruan, J., Mouveau, T., Light, S. H., Minasov, G., Anderson, W. F., Tomavo, S., et al. (2015). The structure of bradyzoite-specific enolase from *Toxoplasma gondii* reveals insights into its dual cytoplasmic and nuclear functions. *Acta Crystallogr. D Biol. Crystallogr.* 71, 417–426. doi: 10.1107/S1399004714026479
- Samuel, B. U., Hearn, B., Mack, D., Wender, P., Rothbard, J., Kirisits, M. J., et al. (2003). Delivery of antimicrobials into parasites. *Proc. Natl. Acad. Sci. U.S.A.* 100, 14281–14286. doi: 10.1073/pnas.2436169100
- Schneider, B., Xu, Y. W., Janin, J., Véron, M., and Deville-Bonne, D. (1998). 3'-Phosphorylated nucleotides are tight binding inhibitors of nucleoside diphosphate kinase activity. *J. Biol. Chem.* 273, 28773–28778. doi: 10.1074/jbc.273.44.28773
- Schrödinger Release 2015-3. (2018). *Small-Molecule Drug Discovery Suite 2018-3*. New York, NY: Schrödinger, LLC.
- Shah, S. A., Shen, B. W., and Brünger, A. T. (1997). Human ornithine aminotransferase complexed with L-canaline and gabaculine: structural basis for substrate recognition. *Structure* 5, 1067–1075. doi: 10.1016/S0969-2126(97)00258-X
- Shen, B. W., Hennig, M., Hohenester, E., Jansonius, J. N., and Schirmer, T. (1998). Crystal structure of human recombinant ornithine aminotransferase. *J. Mol. Biol.* 277, 81–102. doi: 10.1006/jmbi.1997.1583
- Sidik, S. M., Huet, D., Ganesan, S. M., Huynh, M.-H., Wang, T., Nasamu, A. S., et al. (2016). A genome-wide CRISPR screen in toxoplasma identifies essential apicomplexan genes. *Cell* 166, 1423–1435.e12. doi: 10.1016/j.cell.2016.08.019
- Sillitoe, I., Lewis, T. E., Cuff, A., Das, S., Ashford, P., Dawson, N. L., et al. (2015). CATH: comprehensive structural and functional annotations for genome sequences. *Nucleic Acids Res.* 43, D376–D381. doi: 10.1093/nar/gku947
- Singh, P. K., Kushwaha, S., Mohd, S., Pathak, M., and Misra-Bhattacharya, S. (2013). *in vitro* gene silencing of independent phosphoglycerate mutase (iPGM) in the filarial parasite *Brugia malayi*. *Infect. Dis. Poverty* 2:5. doi: 10.1186/2049-9957-2-5
- Slabinski, L., Jaroszewski, L., Rychlewski, L., Wilson, I. A., Lesley, S. A., and Godzik, A. (2007). XtalPred: a web server for prediction of protein crystallizability. *Bioinform. Oxf. Engl.* 23, 3403–3405. doi: 10.1093/bioinformatics/btm477
- Storici, P., Capitani, G., Müller, R., Schirmer, T., and Jansonius, J. N. (1999). Crystal structure of human ornithine aminotransferase complexed with the highly specific and potent inhibitor 5-fluoromethylornithine11. *J. Mol. Biol.* 285, 297–309. doi: 10.1006/jmbi.1998.2289
- Sturm, N., Jortzik, E., Mailu, B. M., Koncarevic, S., Deponte, M., Forchhammer, K., et al. (2009). Identification of proteins targeted by the thioredoxin superfamily in *Plasmodium falciparum*. *PLoS Pathog.* 5:e1000383. doi: 10.1371/journal.ppat.1000383
- Thi, E. P., Mire, C. E., Lee, A. C. H., Geisbert, J. B., Zhou, J. Z., Agans, K. N., et al. (2015). Lipid nanoparticle siRNA treatment of Ebola-virus-Makona-infected nonhuman primates. *Nature* 521, 362–365. doi: 10.1038/nature14442
- Tonkin, M. L., Halavaty, A. S., Ramaswamy, R., Ruan, J., Igarashi, M., Ngô, H. M., et al. (2015). Structural and functional divergence of the aldolase fold in *Toxoplasma gondii*. *J. Mol. Biol.* 427, 840–852. doi: 10.1016/j.jmb.2014.09.019
- Torgerson, P. R., and Mastroiacovo, P. (2013). The global burden of congenital toxoplasmosis: a systematic review. *Bull. World Health Organ.* 91, 501–508. doi: 10.2471/BLT.12.111732
- Vedadi, M., Lew, J., Artz, J., Amani, M., Zhao, Y., Dong, A., et al. (2007). Genome-scale protein expression and structural biology of *Plasmodium falciparum* and related Apicomplexan organisms. *Mol. Biochem. Parasitol.* 151, 100–110. doi: 10.1016/j.molbiopara.2006.10.011
- Vieira, P. S., de Giuseppe, P. O., Murakami, M. T., and de Oliveira, A. H. C. (2015). Crystal structure and biophysical characterization of the nucleoside diphosphate kinase from *Leishmania braziliensis*. *BMC Struct. Biol.* 15:2. doi: 10.1186/s12900-015-0030-8
- Wan, C., Allen, T. M., and Cullis, P. R. (2014). Lipid nanoparticle delivery systems for siRNA-based therapeutics. *Drug Deliv. Transl. Res.* 4, 74–83. doi: 10.1007/s13346-013-0161-z

- Wang, P., Jiang, L., Cao, Y., Zhang, X., Chen, B., Zhang, S., et al. (2018). Xanthone derivatives as phosphoglycerate mutase 1 inhibitors: design, synthesis, and biological evaluation. *Bioorg. Med. Chem.* 26, 1961–1970. doi: 10.1016/j.bmc.2018.02.044
- Wang, Y.-Q., Huang, Z.-L., Chen, S.-B., Wang, C.-X., Shan, C., Yin, Q.-K., et al. (2017). Design, synthesis, and evaluation of new selective NM23-H2 binders as c-MYC transcription inhibitors via disruption of the NM23-H2/G-quadruplex interaction. *J. Med. Chem.* 60, 6924–6941. doi: 10.1021/acs.jmedchem.7b00421
- Watanabe, T., Hatakeyama, H., Matsuda-Yasui, C., Sato, Y., Sudoh, M., Takagi, A., et al. (2014). *in vivo* therapeutic potential of Dicer-hunting siRNAs targeting infectious hepatitis C virus. *Sci. Rep.* 4:4750. doi: 10.1038/srep04750
- Williamson, W. T., and Wood, W. A. (1966). “[108] d-Ribulose 5-phosphate 3-epimerase,” in *Methods in Enzymology Carbohydrate Metabolism*, ed W. Wood (East Lansing: Academic Press), 605–608. Available online at: <http://www.sciencedirect.com/science/article/pii/0076687966091225>
- Winn, M. D., Ballard, C. C., Cowtan, K. D., Dodson, E. J., Emsley, P., Evans, P. R., et al. (2011). Overview of the CCP4 suite and current developments. *Acta Crystallogr. D Biol. Crystallogr.* 67, 235–242. doi: 10.1107/S0907444910045749
- Wise, E. L., Akana, J., Gerlt, J. A., and Rayment, I. (2004). Structure of d-ribulose 5-phosphate 3-epimerase from *Synechocystis* to 1.6 Å resolution. *Acta Crystallogr. D Biol. Crystallogr.* 60, 1687–1690. doi: 10.1107/S0907444904015896
- Wood, T. (1979). Purification and properties of d-ribulose-5-phosphate 3-epimerase from calf liver. *Biochim. Biophys. Acta* 570, 352–362. doi: 10.1016/0005-2744(79)90155-4
- Yin, C., Zhang, T., Qu, X., Zhang, Y., Putatunda, R., Xiao, X., et al. (2017). *in vivo* excision of HIV-1 provirus by saCas9 and Multiplex Single-Guide RNAs in animal models. *Mol. Ther.* 25, 1168–1186. doi: 10.1016/j.ymthe.2017.03.012
- Zhang, R., Andersson, C. E., Savchenko, A., Skarina, T., Evdokimova, E., Beasley, S., et al. (2003). Structure of *Escherichia coli* Ribose-5-phosphate isomerase: a ubiquitous enzyme of the pentose phosphate pathway and the calvin cycle. *Struct. Lond. Engl.* 11, 31–42. doi: 10.1016/S0969-2126(02)00933-4
- Zheng, H., Cooper, D. R., Porebski, P. J., Shabalin, I. G., Handing, K. B., and Minor, W. (2017). CheckMyMetal: a macromolecular metal-binding validation tool. *Acta Crystallogr. Sect. Struct. Biol.* 73, 223–233. doi: 10.1107/S2059798317001061
- Zhou, Y., Fomovska, A., Muench, S., Lai, B.-S., Mui, E., McLeod, R. (2014). Spiroindolone that inhibits PfATPase4 Is a potent, cidal inhibitor of *Toxoplasma gondii* Tachyzoites *in vitro* and *in vivo*. *Antimicrob. Agent Chemother.* 58, 1789–92. doi: 10.1128/AAC.02225-13

Conflict of Interest Statement: RM, KE, HM, and JM are inventors on a U.S. patent (US8575126B2) that is focused on delivery of morpholino oligomers as a treatment for *Toxoplasma gondii* infection. JM is employed by Gene Tools, LLC, the company that manufactured the vivoPMO for this study. However, he took no part in data collection or analysis. RM has completed an unrelated literature review for Sanofi-Pasteur.

The remaining authors declare that the research was conducted in the absence of any commercial or financial relationships that could be construed as a potential conflict of interest.

Citation: Lykins JD, Filippova EV, Halavaty AS, Minasov G, Zhou Y, Dubrovskaya I, Flores KJ, Shuvalova LA, Ruan J, El Bissati K, Dovgin S, Roberts CW, Woods S, Moulton JD, Moulton H, McPhillie MJ, Muench SP, Fishwick CWG, Sabini E, Shanmugam D, Roos DS, McLeod R, Anderson WF and Ngô HM (2018) CSGID Solves Structures and Identifies Phenotypes for Five Enzymes in *Toxoplasma gondii*. *Front. Cell. Infect. Microbiol.* 8:352. doi: 10.3389/fcimb.2018.00352

Copyright © 2018 Lykins, Filippova, Halavaty, Minasov, Zhou, Dubrovskaya, Flores, Shuvalova, Ruan, El Bissati, Dovgin, Roberts, Woods, Moulton, Moulton, McPhillie, Muench, Fishwick, Sabini, Shanmugam, Roos, McLeod, Anderson and Ngô. This is an open-access article distributed under the terms of the Creative Commons Attribution License (CC BY). The use, distribution or reproduction in other forums is permitted, provided the original author(s) and the copyright owner(s) are credited and that the original publication in this journal is cited, in accordance with accepted academic practice. No use, distribution or reproduction is permitted which does not comply with these terms.



Activity of Thioallyl Compounds From Garlic Against *Giardia duodenalis* Trophozoites and in Experimental Giardiasis

Raúl Argüello-García¹, Mariana de la Vega-Arnaud¹, Irais J. Loredó-Rodríguez¹, Adriana M. Mejía-Corona¹, Elizabeth Melgarejo-Trejo¹, Eulogia A. Espinoza-Contreras¹, Rocío Fonseca-Liñán¹, Arturo González-Robles², Nury Pérez-Hernández³ and M. Guadalupe Ortega-Pierres^{1*}

OPEN ACCESS

Edited by:

Jorge Enrique Gómez Marín,
University of Quindío, Colombia

Reviewed by:

Elisa Azuara-Liceaga,
Universidad Autónoma de la Ciudad
de México, Mexico
César López-Camarillo,
Universidad Autónoma de la Ciudad
de México, Mexico

*Correspondence:

M. Guadalupe Ortega-Pierres
gortega@cinvestav.mx

Specialty section:

This article was submitted to
Parasite and Host,
a section of the journal
Frontiers in Cellular and Infection
Microbiology

Received: 12 May 2018

Accepted: 18 September 2018

Published: 15 October 2018

Citation:

Argüello-García R, de la Vega-Arnaud M, Loredó-Rodríguez IJ, Mejía-Corona AM, Melgarejo-Trejo E, Espinoza-Contreras EA, Fonseca-Liñán R, González-Robles A, Pérez-Hernández N and Ortega-Pierres MG (2018) Activity of Thioallyl Compounds From Garlic Against *Giardia duodenalis* Trophozoites and in Experimental Giardiasis. *Front. Cell. Infect. Microbiol.* 8:353. doi: 10.3389/fcimb.2018.00353

¹ Departamento de Genética y Biología Molecular, Centro de Investigación y de Estudios Avanzados del Instituto Politécnico Nacional, Mexico City, Mexico, ² Departamento de Infectómica y Patogénesis Experimental, Centro de Investigación y de Estudios Avanzados del Instituto Politécnico Nacional, Mexico City, Mexico, ³ Escuela Nacional de Medicina y Homeopatía, Instituto Politécnico Nacional, Mexico City, Mexico

Fresh aqueous extracts (AGEs) and several thioallyl compounds (TACs) from garlic have an important antimicrobial activity that likely involves their interaction with exposed thiol groups at single aminoacids or target proteins. Since these groups are present in *Giardia duodenalis* trophozoites, in this work we evaluated the anti-giardial activity of AGE and several garlic's TACs. *In vitro* susceptibility assays showed that AGE affected trophozoite viability initially by a mechanism impairing cell integrity and oxidoreductase activities while diesterase activities were abrogated at higher AGE concentrations. The giardicidal activities of seven TACs were related to the molecular descriptor HOMO (Highest Occupied Molecular Orbital) energy and with their capacity to modify the –SH groups exposed in giardial proteins. Interestingly, the activity of several cysteine proteases in trophozoite lysates was inhibited by representative TACs as well as the cytopathic effect of the virulence factor giardipain-1. Of these, allicin showed the highest anti-giardial activity, the lower HOMO value, the highest thiol-modifying activity and the greatest inhibition of cysteine proteases. Allicin had a cytolytic mechanism in trophozoites with subsequent impairment of diesterase and oxidoreductase activities in a similar way to AGE. In addition, by electron microscopy a marked destruction of plasma membrane and endomembranes was observed in allicin-treated trophozoites while cytoskeletal elements were not affected. In further flow cytometry analyses pro-apoptotic effects of allicin concomitant to partial cell cycle arrest at G2 phase with the absence of oxidative stress were observed. In experimental infections of gerbils, the intragastric administration of AGE or allicin decreased parasite numbers and eliminated trophozoites in experimentally infected animals, respectively. These data suggest a potential use of TACs from garlic against *G. duodenalis* and in the treatment of giardiasis along with their additional benefits in the host's health.

Keywords: *Giardia duodenalis*, trophozoite damage, garlic, thioallyl compounds, allicin, giardiasis

INTRODUCTION

Giardiasis is the intestinal parasitosis of highest incidence in developed countries with a global distribution of 280 million cases per year. Nearly 200 million people with symptomatic infections have been reported in Asia, Africa and Latin America where some 500,000 new cases per year are reported (Adam, 2001; Lane and Lloyd, 2002; WHO, 2006). Infection initiates when a vertebrate host consumes water or food containing infective cysts of *Giardia duodenalis* (syn. *Giardia lamblia*, *Giardia intestinalis*) and in the acidic gastric environment excystation is induced releasing excystozoites that divide to form trophozoites. These latter adhere to duodenum and jejunum epithelia triggering the pathogenic onset associated to giardiasis. At jejunum-ileum lumen trophozoites are exposed to high bile and low cholesterol concentrations at a slightly alkaline pH conditions that induce encystation. Cysts are shed in feces where they mature and remain viable for long periods of time until these are ingested by a new host. This infection may be symptomatic with acute signals characterized by diarrhea and abdominal complaints that may lead to malabsorption syndrome eventually associated to chronic outcomes. However, asymptomatic carriers have been found as a major group in hyperendemic areas (Redlinger et al., 2002).

The main strategy for the control of infections caused by *G. duodenalis*, comprises the use of a variety of antimicrobial drugs including acridines, (quinacrine), aminoglycosides (paromomycin) and most commonly drugs uses are 5-nitroheterocyclic compounds [metronidazole (MTZ), furazolidone, and nitazoxanide] and benzimidazoles [albendazole (ABZ) and mebendazole]. Most of these drugs have mild-to-severe secondary effects (revised by Gardner and Hill, 2001). Further, the use of sublethal concentrations of anti-giardial drugs *in vitro* or suboptimal therapy regimes, which include single-dose regimes of benzimidazoles given in communitarian programs to deworm children in endemic localities, may derive into selection of drug resistant parasites and increased incidences of giardiasis (Northrop-Clewes et al., 2001; Argüello-García et al., 2004). Thereby a better knowledge of therapeutic targets in *Giardia* is needed to develop more effective drugs for the treatment of giardiasis. In this context, compounds derived from natural products such as garlic (*Allium sativum* L.), may be considered as promising and alternative perspective for treatment of giardiasis (Anthony et al., 2005).

Garlic, a perennial crop common in the human diet, has been used since ancient times in folk medicine of different cultures as a panacea. Likewise aqueous and oil extracts of garlic bulbs provide benefits in the prevention and treatment of gastrointestinal disorders including carcinogenesis and some infections (Ankri and Mirelman, 1999; Anthony et al., 2005; Bhagyalakshmi et al., 2007), however the basis of its effectiveness have not yet been completely unraveled. In this context, there are reports on the anti-tumoral activities of a number of organosulfur compounds contained or derived from garlic. This is most likely due to the modulatory activity of these compounds on carcinogen metabolizing enzymes combined with the pro-apoptotic, antioxidant and radical scavenging properties

(Milner, 2001; Yang et al., 2001; Argüello-García et al., 2010; De Gianni and Fimognari, 2015). Also, garlic compounds were reported to have a direct activity against bacterial, protozoan, fungal and viral pathogens (reviewed by Bhagyalakshmi et al., 2007). Although this broad antimicrobial activity is not readily explained by the aforementioned activities, there is accumulating evidence that organosulfur compounds are able to interact with highly reactive or unshielded thiol moieties of target proteins or aminoacids (e.g., enzymes or cysteine, respectively) forming the corresponding thioallyl adducts ($R-SCH_2CHCH_2$), an event potentially life threatening for the cell. Components from garlic that may be involved on these thiol-disulphide exchange reactions are the thioallyl compounds (TACs) that include S-allyl cysteine (obtained by long-time organic fermentation of whole bulbs in ethanolic solutions), allyl thiosulfonates (e.g., allicin, obtained by crushing or macerating bulbs in water) and some products of allicin decomposition (allyl sulfides and ajoenes) (Lawson and Wang, 1993; Rabinkov et al., 1998; Gallwitz et al., 1999; Gupta and Porter, 2001; Pinto et al., 2006).

Garlic has been shown to have an effect in children suffering from giardiasis when used at 1:20 dilutions of aqueous extract in 2 doses per day for 3 days (Soffar and Mokhtar, 1991) and *in vitro* studies have shown that whole garlic extract and allyl alcohol have an effect on the physiology of *Giardia* trophozoites. These include cell surface rigidity, adhesion, flagellar activity, cytoskeletal components, and endomembrane elements (vesicles and vacuoles) while allyl mercaptan (AM, a TAC) preferentially induced vesicle distension and cell swelling, possibly related to a primary effect on membrane osmoregulation (Harris et al., 2000). Based on these observations it is likely that several garlic components do have different electivity in *G. duodenalis* trophozoites, however the mechanisms involved in their giardicidal activity are still undefined. Although this microaerophilic protozoan is devoid of glutathione as major non-protein thiol, *Giardia* possesses a plethora of cysteine-rich surface proteins, cysteine-type proteinases and other sulfur-containing intracellular proteins (Ali and Nozaki, 2007) that may be targets of TACs. In this work, we carried out an analysis on the structure-activity relationship (SAR), mode of action and efficacy in experimental giardiasis of representative TACs from garlic.

MATERIALS AND METHODS

Parasites

G. duodenalis trophozoites from the WB strain (ATCC # 30957) were axenically cultured in modified Diamond's TYI-S-33 medium (Keister, 1983) without bile at 37°C. Cell harvests were carried out by chilling flasks at the log phase of growth reached after 72–96 h routine subcultures. Detached trophozoites were either directly counted in a haemocytometer or washed 3 times with phosphate buffer saline (PBS) prior to counting and the cell number was adjusted as required in the assays.

Garlic Extracts and Compounds

Fresh, aqueous garlic extract (AGE) was prepared by crushing peeled, chopped and weighed garlic bulbs (*A. sativum* L.) in distilled water (0.1 g/mL) at pH 6.5 using a mortar. After

resting for 10 min, homogenate was filtered through a 0.45 μM pore size MilliporeTM membrane. The filtrate was recovered and used at the required concentrations. Regarding the garlic components the following compounds were used: alliin (S-allyl cysteine sulphoxide, ALI), diallyl sulfide (DAS) and dipropyl sulfide (DPS) from Fluka Chemika AG (Buchs, Switzerland); diallyl disulphide (DADS), dipropyl disulphide (DPDS), allyl methyl sulfide (AMS) and allyl mercaptan (AM) from Aldrich Chem. Co. (Milwaukee, WI, USA); methyl methanethiosulfonate (MMTS) and sodium p-hydroxymercuribenzoate (pHMB) from Sigma Chem. Co. (St. Louis, MO, USA); S-allyl-L-cysteine (SAC) from TCI (Tokyo Kasei Kogyo Co., Tokyo, Japan) and diallyl trisulfide (DATS) from MP Biomedicals Inc. (Solon, OH, USA). Allicin (diallyl thiosulfinate, ALC) was obtained by oxidation of DADS using the protocol originally reported by Lawson (Lawson, 1996; Argüello-García et al., 2010). In this, 1 g DADS was dissolved in 5 mL acetic acid under stirring on an ice bath. Hydrogen peroxide (1.5 mL, 30% v/v) was added stepwise and the reaction was allowed to proceed for 30 min. Then, the reaction was kept at 13°C for 20 min then it was placed on an ice bath for 5 h to minimize the content of remaining DADS. Reaction was stopped by adding 15 mL distilled water at pH 6.5 and it was extracted with 30 mL dichloromethane. Acetic acid was removed by 5 extractions with 5% (w/v) sodium bicarbonate (20 mL each) then by 3 extractions with distilled water (20 mL each). The solvent was left to evaporate until yellowish oil (ALC, yield of ~600–800 μL per assay) was obtained. For stabilization and storage of ALC, the oily product was resuspended in water at 1.5% (w/v) and kept in 1 mL aliquots at –70°C until analyzed and used. Under these conditions, ALC retained its full activity for up to 6 months. The identification of ALC was performed by Nuclear Magnetic Resonance (¹³C- and ¹H-spectra) using a Jeol EclipseTM spectrometer with deuterated carbon trichloride (CDCl₃) as solvent and tetramethylsilane as reference solution. Chemical shifts were recorded in ppm at 300 MHz in a Bruker system. Purity of ALC was determined by High Performance Liquid Chromatography (Waters model 996 coupled to a pump Waters model 600) using 4.6 \times 250 mm SpherisorbTM columns (10 μM particle size), mobile phase 30% methanol:70% water, flow rate 0.4 mL/min and UV detection at 254 nm, rendering an average time retention of 3.61 min and a mean purity of 90–92% for synthetic allicin.

In vitro Susceptibility Assays

When complete TYI-S-33 medium (final cysteine concentration = 12.4 mM) was used, it was no older than 10 days to avoid cysteine oxidation. In these assays, 1×10^6 trophozoites were exposed to increasing concentrations of AGE or TACs for 24 h at 37°C in 4.5 mL screw-capped vials. Positive controls included trophozoites treated with metronidazole at 3.0 and 5.9 μM (corresponding to its IC₅₀ and MLC; Argüello-García et al., 2004) and as a negative control for the vehicle, 20 μL distilled water, pH 6.5 were included in all experiments to discard significant variabilities in standard drug susceptibility of the WB strain used in this study. Parasites were harvested and counted and trophozoite's viability was determined by physiological methods to determine the growth capacity of trophozoites

after drug exposure (subculture in liquid medium SCLM)] or trophozoite and membrane integrity [direct cell count (DCC) and trypan blue exclusion (TBE), respectively]. Also, enzyme activity-based methods were used and these included fluorescein diacetate-propidium iodide staining (FDA-PI) that relies on the ability of cellular esterases in living cells to hydrolyse FDA into fluorescein while PI form complexes with nucleic acids of dead cells (Breeuwer et al., 1995); the 3-(4,5-dimethyl-2-thiazolyl)-2,5-diphenyl-2-H-tetrazolium bromide (MTT) reduction assay that is based on the crystallization of the formazan derivative of MTT in living cells by the action of cellular oxidoreductases (NAD(P)H-dependent dehydrogenases, reductases) (Liu et al., 1997). All these protocols have been described elsewhere (Argüello-García et al., 2004) except that DCC values were calculated from total cell numbers of compound-exposed trophozoites divided by the initial trophozoites' inoculum (1×10^6) and TBE was performed by incubating PBS-washed parasites in a trypan blue solution (0.4% [w/v] final concentration) for 5 min at room temperature followed by microscopic count of "stained" (non-viable) parasites. As reference, the "gold standard" method (SCLM) consisted in the back growth of 1×10^5 parasites for 48 h at 37°C after exposure to compounds and the interpolation of cell counts into a standard growth curve run in parallel using increasing number of parasites (5,000–250,000) non exposed to any drug.

In each method, the inhibitory concentration at 50% (IC₅₀) and the minimal lethal concentration (MLC) corresponding to the lower concentration of compound that caused mortality in all cells were calculated using the concentration-viability curves in which the minimal-square method was used. Statistical significance between the data obtained in two or more experiments was determined by paired, two-tailed *t*-Student's test (Microsoft ExcelTM).

Electron Microscopy Studies

Trophozoites were exposed to TACs in two ways: under long (24 h, standard toxicity) and short (3 h, acute toxicity) incubations at 37°C using concentrations corresponding to the experimental MLC (as determined at 24 h) and twofold the MLC, respectively. For scanning electron microscopy, PBS-washed parasites were fixed with 2.5% glutaraldehyde in 0.1 M sodium cacodylate buffer, pH 7.2, dehydrated under increasing concentrations of ethanol, critical-point dried using a Samdri apparatus, gold coated in an ion sputtering device (JEOL-JFC-1100), and examined with a JEOL 35-C scanning electron microscope. In transmission electron microscopy (TEM) studies, washed cells were fixed with 2.5% glutaraldehyde and post-fixed with 1% osmium tetroxide in cacodylate buffer. Following sequential dehydration in ethanol, samples were embedded with epoxy resins. Thin sections were observed in a JEOL 100-SX transmission electron microscope.

SAR Analyses

The values of four electronic and two molecular transport (absorption prediction) descriptors have been previously determined for most TAC used herein (see Table 2 in Argüello-García et al., 2010). Briefly, the chemical structures of the

ten compounds were constructed using Chemdraw Ultra 8.0 software (Cambridge soft Corp. Cambridge, MA, USA) and imported into SPARTAN'04 package (Wave function Inc. Irvine, CA, USA). The *ab initio* approach was used in this software to minimize structures and obtain equilibrium geometry *in vacuo* using the semi-empirical AM1 module. Thus, the minimal energy conformations (Boltzmann conformers) of each compound were obtained by default parameters in order to determine values for electronic properties that included HOMO (highest occupied molecular orbital, E_{HOMO}) and LUMO (lowest unoccupied molecular orbital, E_{LUMO}) eigen values, dipole moment (Debye) and total energy (E_{TOTAL}). Regarding the two descriptors related to absorption prediction, the octanol/water partition coefficient ($\log P_{oct}$) values were retrieved from other studies while the molecular polar surface area (PSA) was calculated following the fragment-based contribution procedure. The relationship between the values of each of these molecular descriptors and the giardicidal activity (expressed as MLC values) were determined by multiple regression analysis (MLR) using the 16.0.18 version of Statgraphics Centurion XVI software.

Thiol-Modifying Activity of TACs

The technique reported by Lawson and Wang (1993) was followed. In these assays trophozoites were collected from 60 mL flasks, washed 3 times with PBS and resuspended in 500 μ L PBS containing a 1:12.5 dilution of a commercial mixture of protease inhibitors (CompleteTM, Roche Diagnostics GmbH, Indianapolis, IN, USA) and lysed by sonication at 12 microns/60% amplitude (Ultrasonic apparatus Sonic UVX1130PB). Soluble proteins were recovered by centrifugation at $15,400 \times g$ for 30 min at 4°C and protein concentration was determined by the Bradford technique. These samples were adjusted to a concentration of 1 mg/mL. Reactions were carried out in 1.5 mL microcentrifuge tubes with a mixture of 100 μ g protein (100 μ L) and NaH_2PO_4 45 mM pH 7.0 mM (800 μ L) to which increasing volumes of TACs stocks or a positive control with the thiol derivatizing agent MMTS prepared at 50 mM in the same buffer, were added and total volume was adjusted to 1 mL. After incubation for 10 min at 37°C, 100 μ L of 1.5 mM dithionitrobenzoic acid (DTNB, Ellman's reagent) were added to each tube and following incubation for 10 min at room temperature the absorbances (yellow solutions) were recorded at 412 nm (Smart Spec 3000TM, Bio-Rad, Hercules, CA, USA). A calibration curve was obtained using increasing volumes (0–100 μ L) of 15.5 mM cysteine instead protein extracts and the maximal blocking concentration (MBC) corresponding to a complete absence of thiol-DTNB complexes produced by TACs were calculated using the least-square method (Microsoft ExcelTM).

Proteolytic Activity Assays

Trophozoite lysates were prepared as mentioned above except that cell lysis was carried out by sonication in 1.5 mL microcentrifuge tubes under ice bath using eight 15-s pulses at 80% amplitude with resting periods of 30 s (Ultrasonic Processor mod. CV19). Protein concentration was adjusted to 2 mg/mL and aliquoted in 25 μ L fractions that were incubated

for 30 min room temperature with 2–5 μ L stock solutions of representative TACs (ALC, DADS, and AM). The reaction mixtures were diluted in Laemmli's sample buffer, loaded in wells of 10% acrylamide-0.2% gelatin slab gels and these were electrophoretically analyzed using 80 V/4°C. After this, gels were incubated in a solution of triton X-100 2.5% (v/v) in water for 1 h and washed 3 times with distilled water. Bands with proteolytic activity were detected as follows: gels were incubated in acetate buffer pH 5.5 with 1 mM DTT for 16 h at 37°C under constant stirring, washed 3 times with distilled water and stained with Coomassie blue (BioRad) for 2 h at 37°C under constant stirring. Finally, gels were washed with distilled water and incubated with a solution of 5% acetic acid/40% methanol (v/v). Gel images were documented with a UVP High Performance Ultraviolet Transilluminator and software Launch DocItLS.

Effect of Representative TACs as Possible Inhibitors of the Cytolytic Effect of Giardipain-1 on IEC6 Cell Monolayers

Based on the inhibitory concentrations of TACs over the activity displayed by the ≈ 25 -kDa sized band containing giardipain-1 in zymograms, this protease purified by affinity chromatography from trophozoite lysates at a cytotoxic concentration (16 μ g/mL; Ortega-Pierres et al., 2018) was pre-incubated for 30 min at room temperature in 200 μ L DMEM medium alone or containing ALC (5.3 mM), DADS (275 mM), AM (514 mM), or E64 (20 μ M). Additional assays were carried out using the MLCs of TACs (without giardipain-1) previously obtained in trophozoite cultures to monitor their toxicity. These solutions were added to monolayers of the intestinal cell line IEC6 grown in 1 cm^2 -microwells and incubated for 100 min at 37°C. After incubation, supernatants were discarded and monolayers were fixed with 2% paraformaldehyde in PBS. The effects of TACs and E64 on the cytolytic effect of giardipain-1 were evaluated by light microscopy using Nomarski optics (Axioskop 40, Zeiss).

Flow Cytometry Analyses

The identification and quantitative determinations of trophozoites were carried out as follows: (a) apoptosis or necrosis were determined using anti-annexin V-fluorescein isothiocyanate (FITC) antibodies or PI as respective markers, (b) oxidative stress was determined by formation of reactive oxygen species (ROS) with the fluorescent ROS-complexing agent 5-(and 6)-carboxy 2',7'-dichlorodihydrofluorescein diacetate (H_2DCFDA), and (c) determination of trophozoites cell cycle stages (G1, S, G2, and G2/M) after exposure to ALC or to a control drug (albendazole, ABZ) was carried out as previously described (Martínez-Espinosa et al., 2015). In all these assays 20,000 cells per sample were recorded.

Efficacy of Age and TACs in Experimental Giardiasis

Mongolian gerbils (*Meriones unguiculatus*) used in this study were kept at CINVESTAV's bioterium facilities under regulated conditions of temperature, humidity, and filtered air. Animals

were fed *ad libitum* with rodent pellets (PurinaTM) and water and monitored daily. The management of gerbils was performed according to the Mexican official norm NOM-062-ZOO-1999 for the production, care and use of laboratory animals (UPEAL-CINVESTAV). Eighty male Mongolian gerbils (*M. unguiculatus*) 6–10 weeks old, weighted 45–60 g and sentinel-checked gerbils free of intestinal parasites were kept in individual cages and distributed in 12 groups of 6 animals per treatment and experimental infections were performed as described elsewhere (Argüello-García and Ortega-Pierres, 1997). In brief, animals were inoculated intragastrically with 1×10^6 *G. duodenalis* trophozoites in 500 μ l sterile PBS *per os* using gavage under ether anesthesia. Control animals received 500 μ l sterile PBS each. At day 10 post-infection (p.i.), gerbils were treated with AGE at single doses of 385, 770, 1,155, and 1,550 mg/kg or two doses of 770 mg/kg (days 10 and 11 p.i.) or a selected TAC (here ALC at 35, 70, 138, or 276 mg/kg at single dose). As additional control, one group of animals received MTZ (38.4 mg/kg at single or double dose). Only the higher, single doses of AGE (1.55 g/kg) and ALC (276 mg/kg) caused a noticeable irritation in intestinal epithelium as assessed by surgical examination of treated, non-infected animals ($n = 1$ per single dose). Treatment efficacy was evaluated by determining the presence or absence of trophozoites in intestinal contents of control and treated gerbils at day 13 post-infection. For this, gerbils were euthanized by an intraperitoneal injection of pentobarbital at a dose of 150 mg/kg to minimize stress and to reduce suffering, then a 10 cm-long section of intestine (from stomach ending, equivalent to nearly the entire small intestine) was excised after laparotomy, and it was longitudinally opened and rinsed in 20 mL PBS at 4°C for 20 min under shaking (720 rpm, HeidolphTM rotatory shaker) to determine trophozoites number after parasite detachment from microvilli. Supernatant was collected and centrifuged at $750 \times g$ for 10 min at 4°C, cell pellet was resuspended in 1 mL PBS and trophozoites were counted using a haemocytometer. Gerbils were scored as cured if no trophozoites were recovered from infected animals.

Molecular Modeling and Docking Studies

The three-dimensional protein structure of giardipain-1 was obtained from the sequence of GL50803_14019 deposited in GiardiaDB using the Swiss Model server (<https://swissmodel.expasy.org/>). To predict the ability of garlic TACs (ALC, DADS, and AM) as possible inhibitors of the protease activity of giardipain-1 by interaction with its catalytic moiety, *in silico* approaches of molecular docking were performed using the Swiss Dock web service (<http://swissdock.ch>). This platform delivers a set of 256 *viable* positions between rigid target (mGiardipain-1) and one flexible ligand (TACs) that are input in PDB and MOL2 formats, respectively. Of these predictions, only those involving a likely interaction of inhibitor with the catalytic Cys27 in giardipain-1 were selected and from these, the most favored docking corresponded to the lowest (i.e., negative value) Gibbs free energy (ΔG). In these analyses, the crystal structure of human Cathepsin B (PDB ID: 2PBH) was used as structure of reference. All structures and predictions obtained from Swiss Model, SwissDock and

ZINC archives of TACs ([www:// http://zinc.docking.org/](http://www.zinc.docking.org/)) were visualized and edited using the UCSF chimera package v. 1.10.1

Statistical Analyses

In all experiments involving concentration-response curves the values obtained were adjusted with the least-square method to linearize calibration curves (Microsoft Excel 2010TM) and differences in mean \pm SD values between two or more groups were assessed by the *t*-student test at a significance of $P < 0.05$.

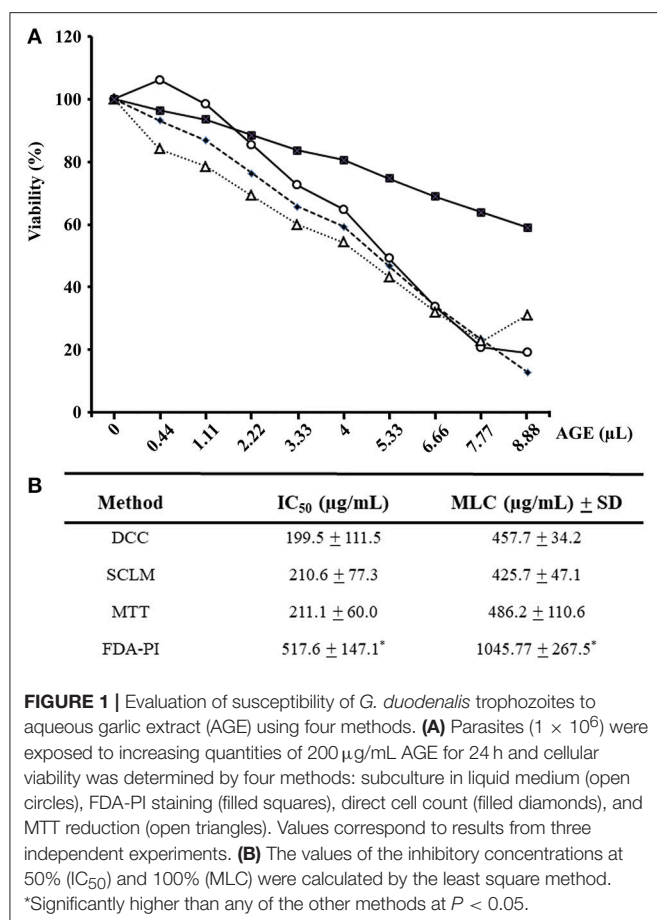
RESULTS

Efficacy and Mode of Action of Age Against *Giardia* Trophozoites

In all drug susceptibility assays, positive controls with 3.0 and 5.9 μ M metronidazole inhibited trophozoite growth by 45–55% and more than 95%, respectively, as expected while distilled water pH 6.5 did not affect parasite's growth. In a first set of experiments, fresh AGEs were prepared and added at increasing concentrations to trophozoite cultures to assess parasite's viability by physiological (SCLM and DCC) and enzyme activity-based (FDA-PI and MTT) methods. It is worth mention that garlic components in the 0–400 μ g/mL range produced a progressive decay (up to >80%) in the number of trophozoites with ability to either re-grow, maintain cellular integrity or reduce MTT; however even at 400 μ g/mL AGE more than 60% of remaining cells were still positive for FDA-PI staining (**Figure 1A**). IC₅₀ and MLC calculations confirmed a similar sensitivity of SCLM, DCC, and MTT assays and a significantly lower sensitivity of the FDA-PI method (**Figure 1B**), indicating that components from garlic extracts induce primary effects on trophozoite integrity concomitant to loss of oxidoreductase activities and a delayed detriment of esterase activities.

SAR of TACs

To evaluate the giardicidal activity of the six garlic's TACs initially included and its relation to the compound structure the SCLM method was chosen considering its aforementioned higher sensitivity and from reports using well-known anti-giardial compounds that include 5-nitroimidazoles and bencimidazoles (Argüello-García et al., 2004, 2009). These TACs have defined modifications in their chemical structure mainly involving increasing hydrocarbon chains with carbon-carbon double bonds and additions of sulfur and/or oxygen atoms or even α -aminoacidic groups thus rendering AM as the simplest and SAC as the most complex TAC evaluated herein. As shown in **Table 1** the thioallyl group displayed in bold in each chemical formula and comparing experimental MLC values, the giardicidal efficacy of AM was drastically lowered (3.06 vs. 74.28 mM) by replacing the sulfur-attached Hydrogen by a methyl group as in AMS; however the replacement of this Hydrogen by an allyl group as in DAS partially recovers the efficacy in one order of magnitude (23.71 mM) below to that of AM. Interestingly the further addition of a second sulfur atom, as in DADS, recovers fully the efficacy to a comparable level of that displayed by AM (2.66 mM). Further the addition of a



sulfur-attached oxygen atom, as displayed in ALC increased the giardicidal activity to sub-milimolar concentrations (0.6 mM) being ALC (allicin or diallyl thiosulfinate) the most effective TACs tested. In contrast, the presence of one α -amino carboxylic group (cysteine) in SAC decreased the efficacy of TACs to similar levels as that of AMS (69.1 vs. 74.28 mM). These assays indicated the importance of the dithiol moiety (-S-S-) to potentiate the activity of TACs against *G. duodenalis* trophozoites.

In further analysis in which the activity of TACs were compared, an *in silico* approach based on MLR was used to determine if some of the four electronic (E_{TOTAL} , E_{HOMO} , E_{LUMO} , dipole) and two molecular transport ($\log P_{\text{OCT}}$, TPSA) descriptors calculated for these compounds (Supplementary Table 1) could be directly related to the giardicidal efficacy observed. In these analyses an additional TAC, diallyl trisulphide (DATS), was included as a “test” compound to evaluate the predictive value of the best structure-activity model raised. After these analyses, the molecular descriptor E_{HOMO} was the unique parameter associated to MLCs of the six TACs used as “drivers” to standardize the regression model. This latter rendered the lower variance ($S = 0.177$) and the highest regression coefficient ($R = 0.9827$) that were useful for this purpose (Figure 2). When the E_{HOMO} value calculated for DATS (-209.33 kcal/mol) was

TABLE 1 | Experimental MLC values of six TACs against *G. duodenalis* trophozoites determined by SCLM.

Thioallyl compound	Chemical formula	IC_{50} (mM) \pm SD	MLC (mM) \pm SD
Allyl Mercaptan (AM)	$\text{H}_2\text{C}=\text{CH}-\text{CH}_2-\text{SH}$	0.83 ± 0.2	3.06 ± 0.7
Allyl Methyl Sulfide (AMS)	$\text{H}_2\text{C}=\text{CH}-\text{CH}_2-\text{S}-\text{CH}_3$	40.3 ± 3.5	74.28 ± 12.3
Diallyl Sulfide (DAS)	$\text{H}_2\text{C}=\text{CH}-\text{CH}_2-\text{S}-\text{CH}_2-\text{CH}=\text{CH}_2$	14.5 ± 2.3	23.71 ± 6.0
Diallyl Disulfide (DADS)	$\text{H}_2\text{C}=\text{CH}-\text{CH}_2-\text{S}-\text{S}-\text{CH}_2-\text{CH}=\text{CH}_2$	1.4 ± 0.6	2.66 ± 0.8
Allicin (ALC)	$\text{H}_2\text{C}=\text{CH}-\text{CH}_2-\text{S}-\text{S}(\text{O})-\text{CH}_2-\text{CH}=\text{CH}_2$	0.32 ± 0.02	0.60 ± 0.1
S-Allyl Cysteine (SAC)	$\text{H}_2\text{C}=\text{CH}-\text{CH}_2-\text{S}-\text{CH}_2(\text{NH}_2)-\text{COOH}$	40.82 ± 6.3	69.10 ± 13.1

interpolated in this model a MLC = 1.41 mM was predicted. This value was closer to the experimental MLC = 1.35 ± 0.18 mM that was determined independently for this compound. Thus based on this approach we concluded that E_{HOMO} is a useful tool to predict the giardicidal activity of garlic's TACs.

Differential Thiol-Disulphide Exchange Capacity of TACs

Since TACs could modify thiol groups exposed in *G. duodenalis* trophozoite proteins into di-(thioallyl) derivatives thus hampering the further derivatization of these groups by DTNB, the blocking capacity of seven TACs was evaluated using parasite's total soluble extracts. The data obtained were in general compatible with their already known giardicidal activity, this is ALC was the most potent thiol-modifying compound tested (MBC = 93.8 mmol/mg protein) followed by DATS and DADS with MECs slightly higher to 200 mmol/mg. DAS had an intermediate efficacy (351.3 mmol/mg) and AMS and SAC exhibited a much lower efficacy (845.9 and 1260.9 mmol/mg, respectively) (Figure 3). Interestingly AM, in spite of its high giardicidal activity, it did not react with parasite extracts as noted by the increasing absorbance when higher concentrations of this compound were added and instead it formed complexes with DTNB. Indeed, the presence of increasing sulfur atoms and sulfur-attached oxygen influenced the higher efficacy of TACs to derivatize thiol groups exposed in giardial proteins.

Differential Inhibition of Trophozoite's Proteolytic Activities by Garlic TACs

Considering the thiol-modifying activity of TACs on trophozoite protein extracts, three representative compounds showing high (ALC), intermediate (DADS), and low (AM) activities were chosen to evaluate their inhibitory effect on cysteine protease activities in trophozoite lysates. Zymogram analysis showed that lysates displayed several bands of proteolysis (mostly between 25 and 110 kDa; Figure 4A) of which bands of 75, 60, and 25

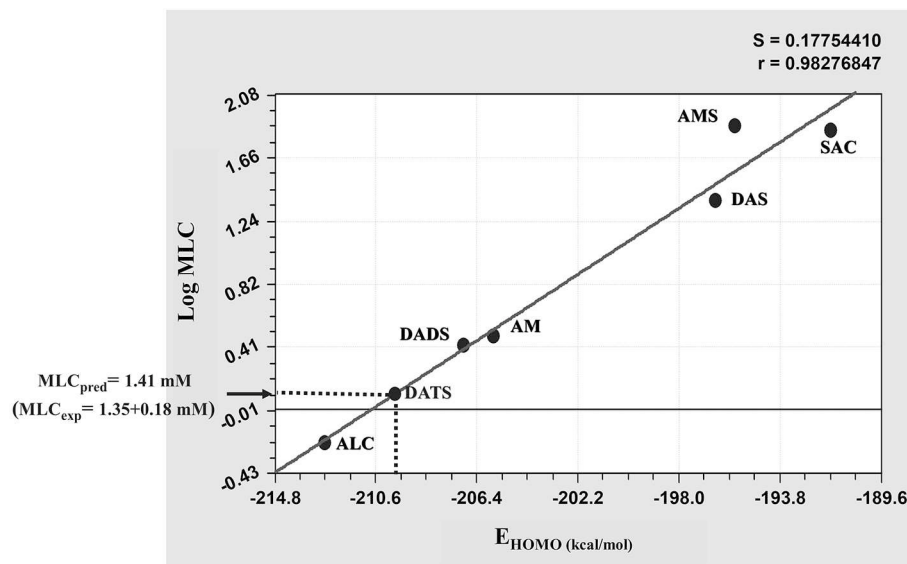


FIGURE 2 | Linear regression model for the MLC- E_{HOMO} relationship of thioallyl compounds (TACs). The values of giardicidal activity (MLC) and the electronic descriptor E_{HOMO} of the six TACs included as “drivers” were processed by multiple linear regression and the value of E_{HOMO} calculated for the “test” compound diallyl trisulfide (DATS) was interpolated in the model (dotted line) to predict the MLC of this compound and to compare it with its experimental MLC. Abbreviations of compound names are as indicated in section Materials and Methods.

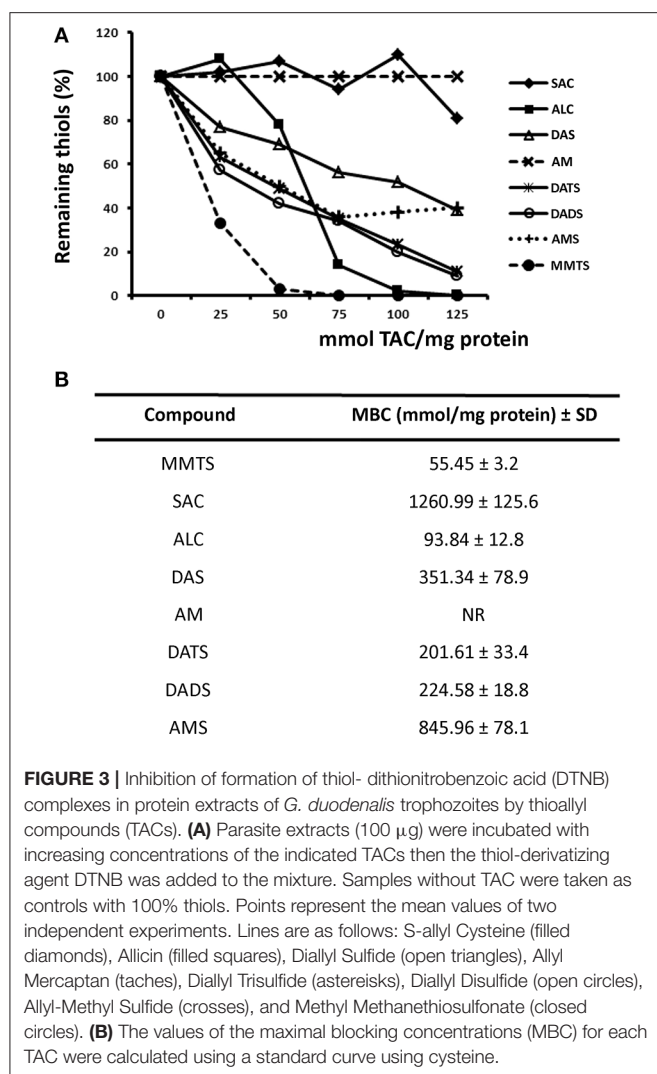
kDa were the most prominent. Some of these activities (110, 60, 75, and 25 kDa) were strongly inhibited by 3.5 mM ALC while DADS at a much higher concentration (275 mM) could diminish similar activities except for the one at 60 kDa. Intriguingly AM produced a significant increase of activity in bands of 75, 60, and 25 kDa though this might reflect its lack of reactivity toward protein -SH groups and its “cooperative” activity with DTT. As expected, a full inhibition of all proteolytic bands was observed with the unspecific thiol-active inhibitor pHMB at 10 mM. On the other hand the typical cathepsin B protease inhibitor E64 displayed a selective inhibition on the 25 kDa band that contains the processed form of the cathepsin B-like protease named as giardipain-1 (Ortega-Pierres et al., 2018). By molecular modeling and docking approaches, the higher inhibitory activity of ALC toward proteases like giardipain-1 could be at least partially explained by the predicted ability of its Oxygen atom to form an electron bridge with the Hydrogen G3 of the catalytic Cys26 (**Figure 4B**) thereby interfering with protease activity. This is reinforced by the similar entropy values predicted for these TACs ($\Delta G_{ALC} = -5.561$ kCal/mol; $\Delta G_{DADS} = -6.093$ kCal/mol; $\Delta G_{AM} = -5.554$ kCal/mol). Taken together, these data are concurrent with the notion that garlic TACs target several types of cysteine proteases in *G. duodenalis* trophozoites.

Inhibition of Cytopathic Effects of mGiardipain-1 by Representative Garlic TACs

Once the concentrations of ALC, DADS and E64 used in zymograms were shown to inhibit a specific cysteine protease

of *G. duodenalis* trophozoites, namely giardipain-1 (≈ 25 kDa), next it was assessed if these compounds could also block the already reported cytopathic effects of giardipain-1 as are shrinkage, detachment from surface, rounding and/or profuse vacuolisation (Ortega-Pierres et al., 2018). As shown in **Figure 5**, giardipain-1 causes a strong destruction of monolayers beginning with cell shrinkage and profuse blebbing (arrows) and the subsequent appearance of zones with absence of cells reflecting extensive destruction (asterisks) that are consistent with the pro-apoptotic damage reported for this secreted cysteine protease (Ortega-Pierres et al., 2018). However, the pre-incubation of giardipain-1 with ALC and AM noticeably blocked these effects while DADS reduced the frequency of cells displaying apoptotic damage. In general, these observations support a correlation between the inhibitory ability of garlic TACs on the proteolytic activity of giardipain-1 and the damage blockade exerted by these compounds. As expected, the potent cathepsin B inhibitor E64 efficiently inhibited the giardipain-1 induced damage in IEC6 cell monolayers. Of interest, with the exception of DADS concentration used in zymography analyses (275 mM) that affected some cells, none concentrations of TACs tested either at protease-inhibiting level or at MLCs that kill trophozoites in culture, were harmful to cell monolayers (**Supplementary Figure 1**). These results suggest that TACs have a pharmacologically favorable and selective toxicity against trophozoites over epithelial cells.

Based on these comparative analyses, ALC was the garlic's derivative with the highest anti-giardial activity, with the lower HOMO value, with the highest thiol-modifying activity and with the higher cysteine protease inhibitory capacity. Due to these



properties, ALC was chosen in further studies to analyse its mechanism of action over trophozoites at different levels.

Allicin Has a Primary Cytolytic Mode of Action Like Age Against *Giardia* Trophozoites

Since AGE had previously showed a detrimental effect on trophozoite's integrity followed by a decreased functionality of metabolic enzymes, we tested if ALC could have an effect as observed with whole garlic extracts. In these assays, the TBE protocol was also included in order to assess whether the integrity of trophozoite's membrane is primarily targeted by ALC. As expected, SCLM was the most sensitive method where cell viability completely decreased at concentrations below 0.8 mM ALC while all other methods still displayed viability rates of >20% (Figure 6A). Thus parasite replication was initially suppressed at 600 μ M ALC; the other two physiological methods (DCC and TBE) showed a concomitant decrease of viability (1.08 and 1.12 mM, respectively) and the two enzyme-based assays

(FDA-PI and MTT) showed the lowest sensitivity (Figure 6B), suggesting that ALC primarily affected the cellular replication by impairing membrane permeability hence cellular integrity, with a secondary effect on the activity of metabolic enzymes as oxidoreductases and diesterases. When compare the AGE with ALC the latter had a primary cytolytic mechanism on trophozoites albeit oxidoreductases (MTT) were affected more lately by ALC.

Electron Microscopy Analyses of the Damage Caused by Allicin on *Giardia* Trophozoites

To further analyse the effect of ALC on trophozoites a standard toxicity (24 h-exposure to 1 MLC) and an acute (3 h-exposure to 2 MLC) procedures were used. By SEM, control trophozoites exhibited the typical half a pear-shaped morphology with four pairs of flagella and a relatively smooth surface at ventral (Figure 7A-A) and dorsal (Figure 7A-B) planes. During standard toxicity, ALC provoked the appearance of multiple "holes" particularly in the so-called *bare area* of the ventral disk, which retained its normal contour (Figure 7A-C, arrow) along to the presence of small protrusions in flagella. The dorsal surface also presented a rough texture that resembled a membrane blebbing process with profuse holes and even nuclear membranes had severe damage (Figure 7A-D, arrows). In other cells the contour of the ventral disk appeared as less rigid and flagella displayed rounded tips (Figures 7A-E,F, asterisks). In parasites under acute ALC toxicity, the bare area showed severe damage in which cell surface presented multiple protrusions (blebbing) and flagella also showed rounded tips (Figure 7A-G, arrow and asterisks) while dorsal surface showed holes with a greater size and damaged areas that allowed the release of cytoplasmic material (Figure 7A-H). Of note, cell shrinkage was not a typical feature because ALC-treated cells did not display a contracted size (compare images Figure 7A and Figure 7B with the corresponding ventral or dorsal views).

At the intracellular level, in control cells the TEM analyses showed integrity of plasma membrane, peripheral vacuoles, nuclei and cytoskeletal elements as ventral disk microtubules and associated microribbons and flagellar axonemes with the typical 9+2 arrangement (Figures 7B-1,3). Regardless of the standard or acute toxicity protocols, ALC treatment leads to a complete loss of electron density of the intracellular elements and the integrity of plasma membrane, a diffuse destruction of cytoplasmic content rendering a granulose appearance and even nuclear envelopes seemed to be compromised (Figures 7B-2,4). In this context, a profuse condensation of chromatin at the inner periphery was seen (Figure 7B-4). As a consequence, a profuse vacuolisation pattern that occurs frequently with anti-giardial drugs was not observed with ALC. Under these conditions, all cytoskeletal elements at ventral disk, cell periphery and flagella remained structurally unaltered and also cell shrinkage was not observed by SEM. These observations reinforced the presence of a cytolytic effect of ALC on *Giardia* trophozoites that promoted alterations at cellular (and even nuclear) membrane(s)'s integrity associated to further destruction of intracellular structures. To

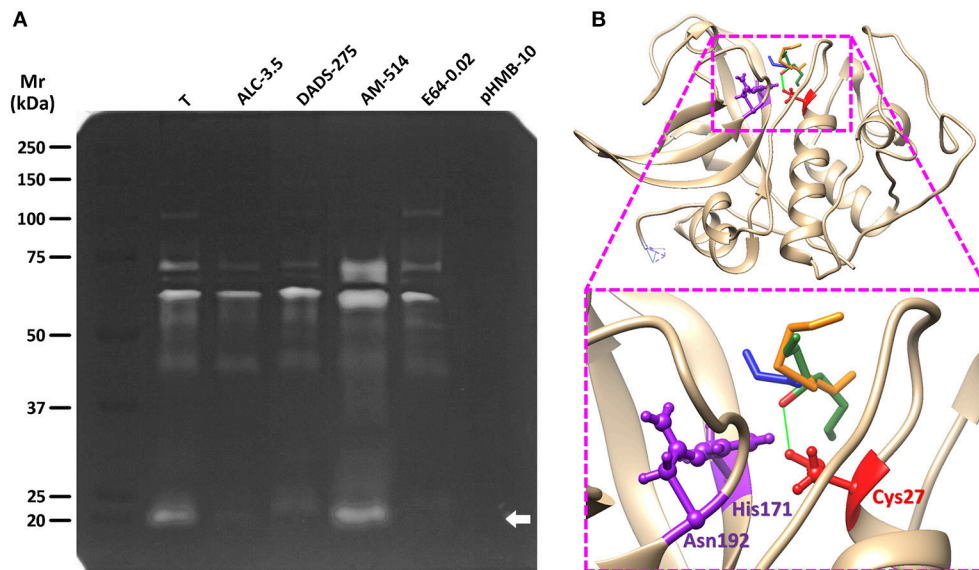


FIGURE 4 | Effect of representative TACs on the proteolytic activity of *G. duodenalis* trophozoite lysates and docking with giardipain-1. **(A)** Trophozoite lysates (50 μ g) were electrophoretically separated in 10% acrylamide-0.2% gelatin gels and cysteine protease activities were developed and detected by DTT treatment at pH 5.5 and Coomassie blue staining. Lanes in which extracts were pre-incubated with the three TACs tested (ALC, DADS, and AM) are indicated along with the concentration values (mM) used in each case. The thiol-active inhibitor pHMB (10 mM) and the cathepsin B-specific inhibitor E64 (20 μ M) were included as controls. Molecular weight standards and its relative mobility (Mr) are as indicated at the left. The arrow points to the band containing the cysteine protease giardipain-1. **(B)** The most favored docking position of representative TACs (in stick conformation, green: ALC, orange: DADS, blue: AM) at the proximity of the catalytic Cys27 of giardipain-1 in which the Oxygen atom of ALC is predicted to form a bridge with the Hydrogen G1 of Cys27 at a distance of 2.425 Å (green line). The three catalytic residues (Cys26, His171, and Asn192) are represented in ball-and-stick conformation.

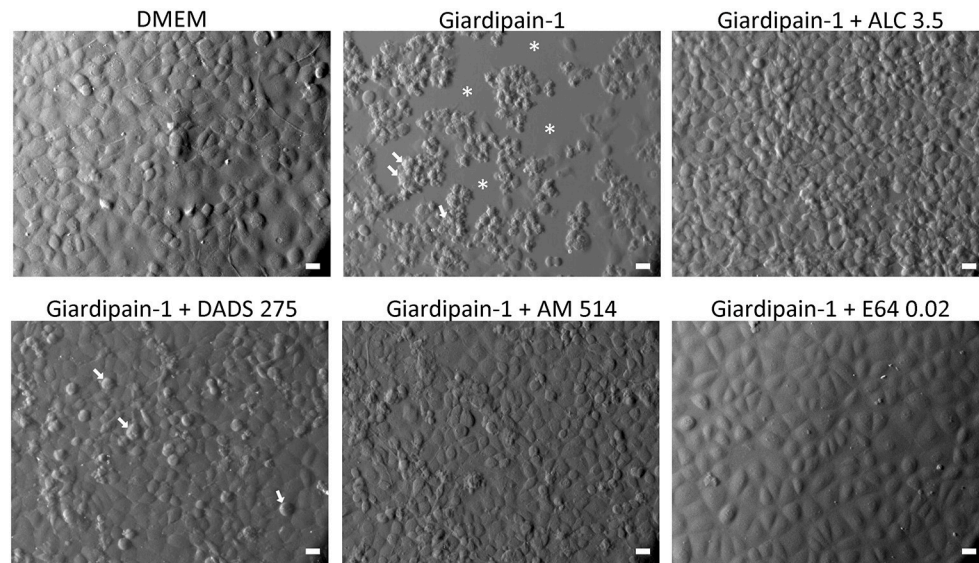


FIGURE 5 | Effect of garlic TACs on the cytolysis caused by giardipain-1 in epithelial IEC6 cell monolayers. Confluent IEC6 cells were exposed for 100 min at 37°C to affinity chromatography-purified giardipain-1 alone or pre-incubated with the concentrations indicated (in mM) of representative TACs that caused inhibition of its protease activity in zymograms and monolayers were observed by Nomarski optics. Asterisks denote zones of monolayer destruction and arrows point to cells undergoing apoptotic death as indicated by membrane blebbing, shrinkage, and shape degeneration. Bars: 20 μ m.

gain more insights on the ALC-mediated damage, we tested whether programmed cell death, oxidative stress and cell cycle arrest could be induced by ALC and then we compared these

data with those obtained using ABZ which effects under similar conditions have been already described (Martínez-Espinosa et al., 2015).

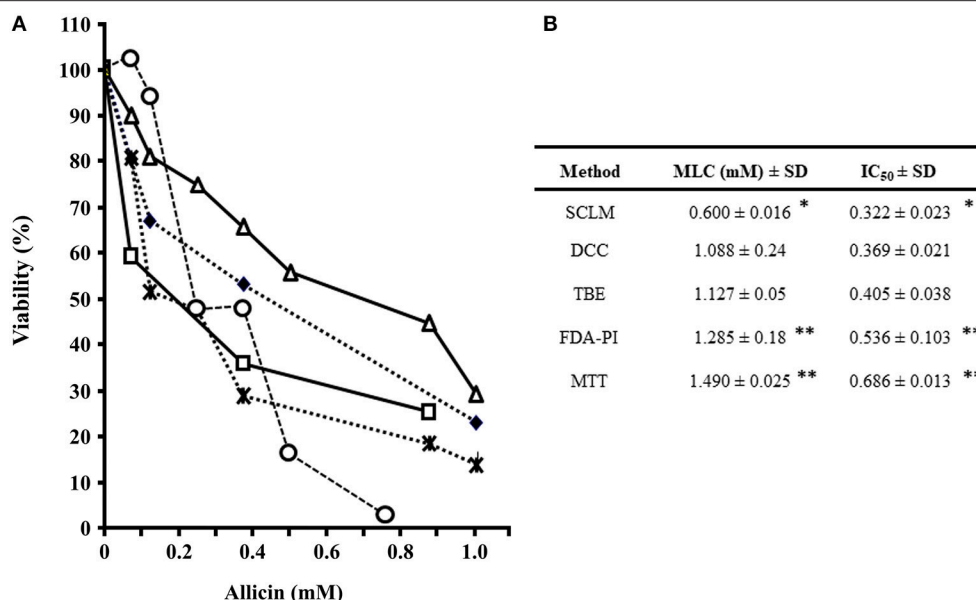


FIGURE 6 | Evaluation of susceptibility of *G. duodenalis* trophozoites to allicin using five methods. **(A)** Parasites (1×10^6) were exposed to increasing quantities of 2.5% ALC for 24 h and cellular viability was determined by several methods as previously described (Argüello-García et al., 2004). Values correspond to results from three independent experiments. Lines are as follows: subculture in liquid medium (open circles), fluorescein diacetate-propidium iodide staining (FDA-PI) staining (filled diamonds), direct cell count (taches), 3-(4,5-dimethyl-2-thiazolyl)-2,5-diphenyl-2-H-tetrazolium bromide (MTT) reduction (open triangles) and trypan blue exclusion (open squares). **(B)** The values of IC₅₀ and MLC were calculated by the least square method. *Significantly lower than any of the other methods at $P < 0.05$. **Significantly higher than SCLM, DCC, and TBE ($P < 0.05$).

Pro-apoptotic, Non-prooxidant and G2-Arresting Effect of Allicin on Trophozoites

Based on the fact that ALC caused cytolysis in *G. duodenalis* trophozoites, it was of interest to determine the way by which parasites were killed by this TAC. To assess if ALC at increasing concentrations induces apoptotic or necrotic cell death in *G. duodenalis* trophozoites, anti-annexin V antibodies coupled to FITC and PI were used as markers of apoptosis and necrosis, respectively. In these assays, ABZ was used as control because of its known ability to induce apoptosis-like death in *G. duodenalis* (Martínez-Espinosa et al., 2015). As can be seen in a representative experiment shown in **Figure 8**, upon exposure to ALC at MLC (0.6 mM) 10.2% of trophozoites were at early apoptosis and 18.6% displayed late apoptosis and by increasing ALC concentration up to twice the MLC (i.e., 1.2 mM) three-times more cells were at apoptosis (46.6% in early and 44.0% in late stage, respectively). In all samples the percentages of cells in necrosis was always <2.5%. Control trophozoites exposed to ABZ even at 1.5 times its MLC (0.48 μ M) only induced 41.0% cells in apoptosis and 5% cells were necrotic. These results indicated that ALC leads to a marked apoptosis-like cell death in trophozoites.

Next, we tested if apoptosis-like death induced by ALC was associated with oxidative stress. In this, ROS were monitored in ALC-exposed trophozoites using the fluorescent tracer H₂DCFDA. **Figure 9** shows representative results in which,

as compared to controls, only 0.75% cells were positive for ROS even using twice the MLC of ALC (1.2 mM) while using the control drug ABZ up to 33.85% of trophozoites displayed ROS formation as previously reported (Martínez-Espinosa et al., 2015). With the well-known ROS inducer tert-butyl hydroperoxide (TBHP) up to 17.1% cells were ROS-positive. These results demonstrated that ALC does not induce oxidative stress in *G. duodenalis* trophozoites as a death-associated mechanism.

Further flow cytometry analyses to determine the point(s) at which ALC interrupts cell cycle progression of vegetative trophozoites (**Figure 10**) showed that in control cells most of these were at G2 phase (53.3%) followed by a subpopulation at S phase (26.2%) whereas a lower proportion of cells were at G1 phase (13.4%) and the boundary G2/M contained 6.9% of cells. When trophozoite cultures were exposed to MLC and twice the MLC of ALC (0.6 mM and 1.2 mM) there were some changes: a marked decrease in G1 subpopulation with both ALC concentrations (7.4 and 2.2%, respectively), a significant decrease in S subpopulation with 1.2 mM ALC (5.7%) and an important increase in cells at G2 phase (61.0 and 75.3%, respectively). Interestingly, cells at G2/M phase did not significantly change (4.4 and 5.7%). As a reference, 1.35 μ M ABZ partially decreased cells S at phase (22.1%) and partially arrested cells at G2 phase (69.9%) as previously reported (Martínez-Espinosa et al., 2015). All these data suggest that cytotoxic ALC concentrations allow an exit of G1 and

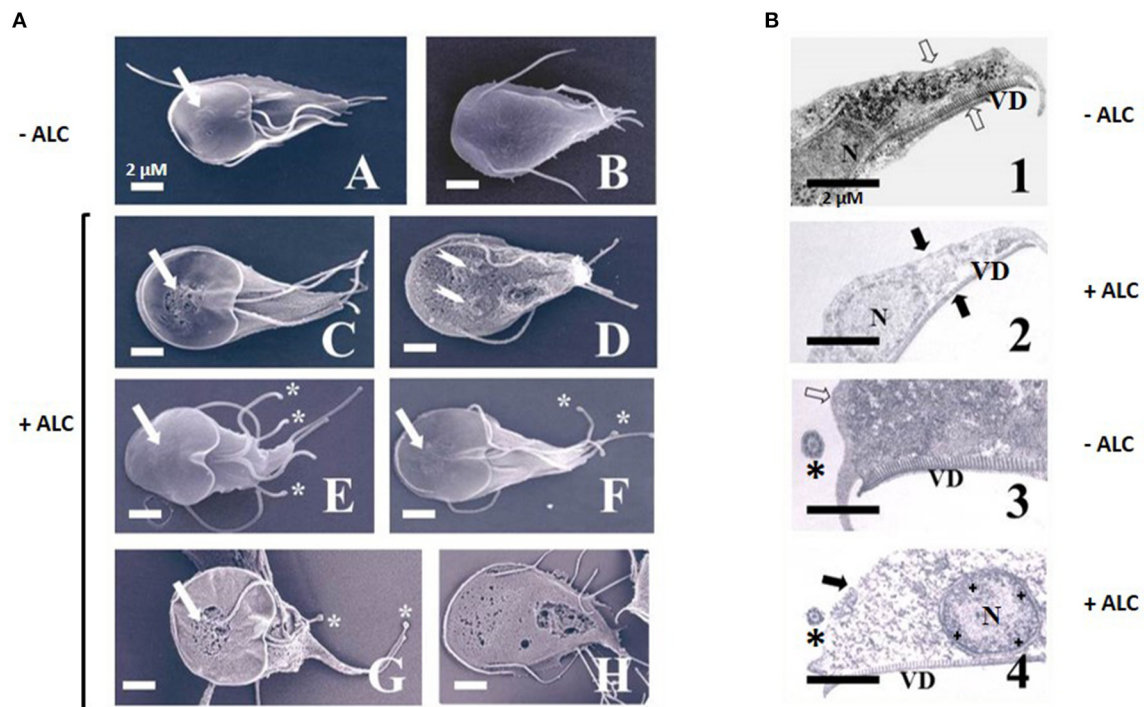


FIGURE 7 | Analysis by scanning (A) and transmission (B) electron microscopy of *G. duodenalis* trophozoites exposed to allicin. (A) Parasites (1×10^6) were either not exposed (A,B) or exposed to 600 μM ALC (C–F) for 24 h or 1.2 mM ALC for 3 h (G,H) at 37°C. Trophozoites are shown in ventral (A,C, E–G) and dorsal (B,D,H) views. The higher roughness of cell surface in images C–H as compared to A,B, except over the ventral disk, are indicative of a degree of membrane blebbing. Arrows denote the so-called “bared area” of the ventral disk and asterisks point to tip rounding at flagella. (B) Parasites not exposed (1, 3) and exposed to 600 μM ALC (2, 4) for 24 h at 37°C. Trophozoites are shown in longitudinal (1, 2) and cross-sections (3, 4). Arrows indicate the plasma membranes, asterisks show flagellar axonemes and crosses show inner peripheral areas of nucleus with chromatin condensation. N, nuclei; VD, ventral disk. Bars correspond to the indicated size.

S phases but most parasites were partially arrested at the G2 phase.

Antiparasitic Efficacy of AGE and ALC in Experimental Giardiasis

The pre-clinic and potential therapeutic effectiveness of AGE and ALC to treat giardiasis was evaluated in this work using the well-established model of experimental infections in Mongolian gerbils (Belosevic et al., 1982; Argüello-García and Ortega-Pierres, 1997). As shown in **Figure 11**, AGE-treated animals exhibited a significant reduction in trophozoite numbers with all doses tested as compared to PBS-treated, control gerbils. However only partial cure rates were obtained with 385 (2 out of 6 gerbils), 770 (3 out of 6), 1,155 (5 out of 6) and 770 mg/kg twice (5 out of 6) while none gerbil was cured with 1,515 mg/kg. Interestingly in ALC-treated animals, a progressive decrease in parasite numbers was observed upon increasing doses and cure rates increased as follows: 3 out of 6 gerbils with 35 mg/kg, 5 out of 6 with 70 mg/kg, 6 out of 6 with 138 mg/kg and 5 out of 6 with 276 mg/kg. These two latter doses were even more effective than the control drug MTZ that cured 3 out of 6 gerbils with 36 mg/kg and 5 out of 6 animals at twice dose.

All these data showed that ALC at increasing single doses had a dose-dependent and consistent giardicidal effect that caused

a complete elimination of trophozoites in infected animals and a partially effective action using AGE. In spite that ALC is a major thiosulfinate in garlic extracts (Lawson, 1996) these differences are likely attributed to a distinct availability of ALC at intestinal lumen of infected animals to reach its targets in resident trophozoites.

DISCUSSION

Garlic has widely proven to be a rich source of nutraceutical compounds (Bhagyalakshmi et al., 2007) that are mostly organosulfur compounds as TACs. Indeed, garlic's TACs have a double benefit, i.e., health promoting and illness fighting, upon dietary or supplementary consumption. In recent years TACs contained in aqueous (e.g., ALC), ethanol (e.g., SAC) or oily (e.g., allyl sulfides as DATS, DADS, DAS, AMS, AM) garlic extracts have been studied in relation to the treatment of infectious diseases because of their direct effects over a plethora of pathogens (Ankri and Mirelman, 1999; D'Souza et al., 2017). In this work, the seven TACs mentioned above were evaluated in *G. duodenalis* trophozoites regarding its cytotoxic mechanism and therapeutic potential in experimental giardiasis.

Our results showed that the AGE's MLC as determined in this work ($425 \pm 47 \mu\text{g/mL}$) is slightly higher than the value

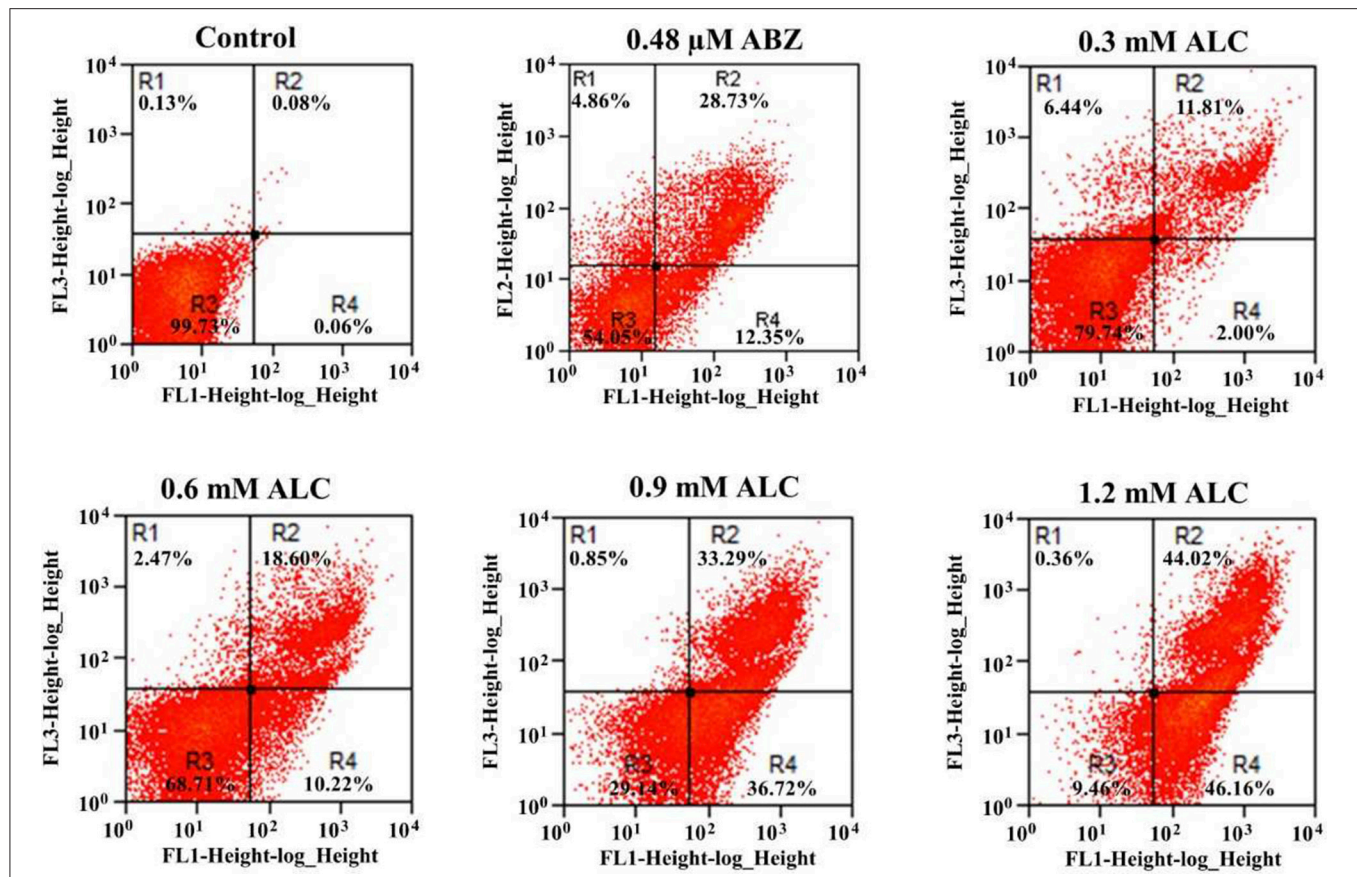


FIGURE 8 | Allicin promotes apoptosis-like death in *G. duodenalis* trophozoites. Parasites (1×10^6) were exposed to 1.0% double distilled water pH 6.5 (Control) or the indicated concentrations of ALC for 24 h at 37°C then stained with annexin V-PI and processed by flow cytometry. Data shown in the figure are as follows: quadrant R1 are cells positive for necrosis (PI+); quadrant R2 are cells positive for late apoptosis (annexin V+/PI+); quadrant R3 are cells negative for both markers and quadrant R4 are cells positive for early apoptosis (annexin V+). As a positive control, trophozoites were exposed to the indicated cytotoxic concentration of albendazole (ABZ). Percentages of total cells are indicated within each quadrant. The dot plots are representative of two independent experiments.

of 300 μ g/mL previously determined (Harris et al., 2000). It is tempting to speculate that the use of two parasite strains (WB vs. Portland-1) along to different garlic sources (fresh cloves macerated in water vs. freeze-dried powder vortexed in culture medium) may account for the differences obtained in both studies. In addition, values of MLCs of four similar TACs used in our study and in another work (AM, AMS, DAS, and DADS) differed quantitatively, albeit AM and DADS were in both cases more active against trophozoites than either DAS or AMS. When its effect was compared to the one observed against other pathogens, AGE had a lower effectivity against enteric bacteria e.g., *Helicobacter pylori* (MLC: from 5 to 25–400 mg/mL) (Cellini et al., 1996; Moghadam et al., 2014) or even anaerobic protozoa as *Trichomonas gallinae* (MLC: 75 mg/mL) (Seddiek et al., 2014) thus highlighting the importance of the conspicuous repertoire of thiol-containing proteins and the dependence on cysteine import and metabolism in *G. duodenalis* (Ali and Nozaki, 2007) concomitant to its higher susceptibility to garlic constituents.

The use of physiological and enzyme activity based protocols were useful to determine that AGE had a cytolytic

mechanism (i.e., TBE and DCC assays displayed high sensitivity) concomitant to an impaired oxidoreductase capacity as assessed by MTT assays and a further impairment of diesterase activity in trophozoites as shown by the lower sensitivity of FDA-PI assays. The effect of garlic components on the integrity of cell membranes were in agreement with a previous report (Harris et al., 2000) that showed a collapse in the electrochemical potential of trophozoite plasma membranes exposed to AGE and allyl alcohol. In this context, the abundance of cysteine (i.e., thiol)-rich proteins in *Giardia* surface proteins (Adam, 2001; Pinto et al., 2006; Ali and Nozaki, 2007) play a direct role as primary targets of garlic constituents, especially organosulfur compounds as TACs. Likewise, it is possible that some enzymes having a rate-limiting role in glucose metabolism of *G. duodenalis* and harboring cysteine residues critical for activity modulation (e.g., triosephosphate isomerase) (Reyes-Vivas et al., 2007) are also affected by garlic components. Further assays using recombinant or purified target molecules may be useful to provide more data on the effects of garlic components on *Giardia* trophozoites.

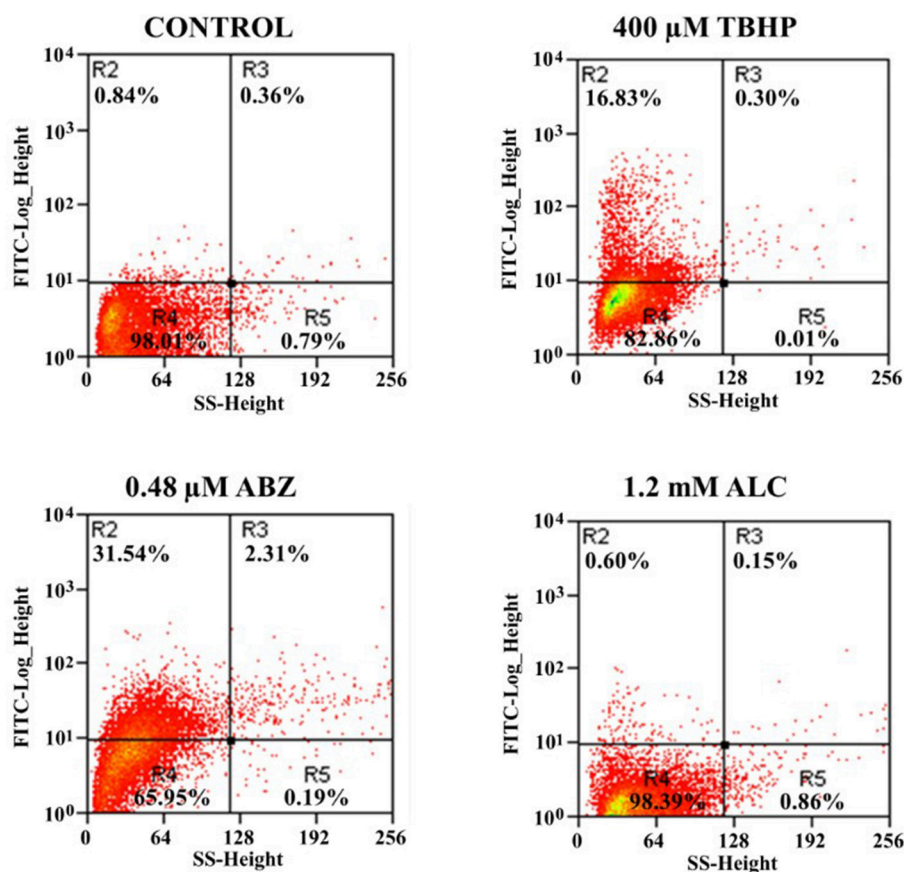
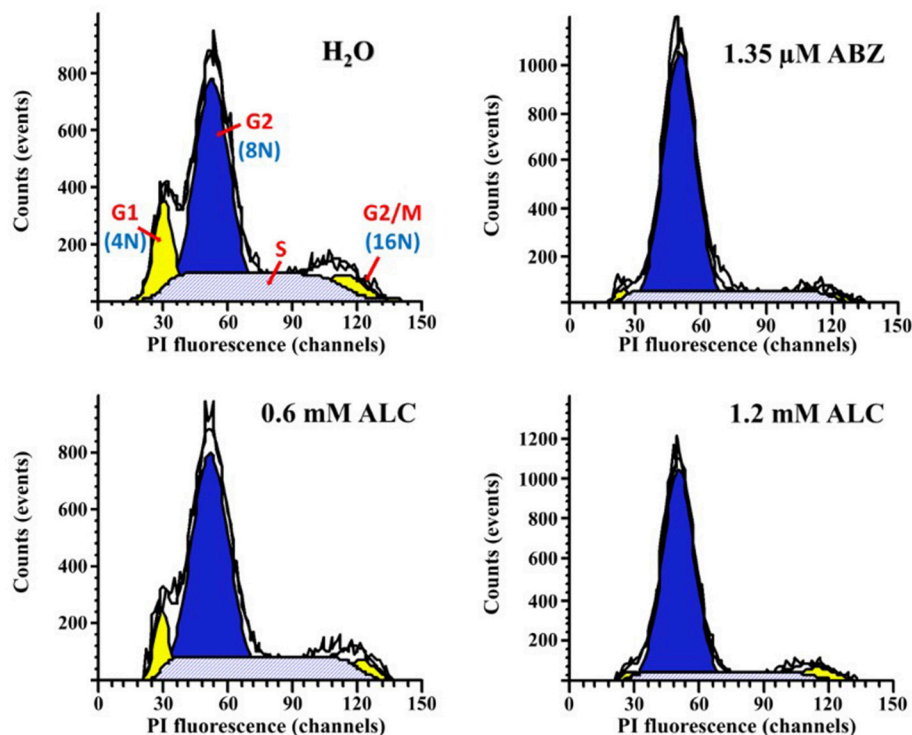


FIGURE 9 | Allicin does not cause reactive oxygen species (ROS) formation in *G. duodenalis* trophozoites. Parasites (1×10^6) were exposed to 1.0% double distilled water pH 6.5 (Control) or the indicated concentrations of ALC, tert-butyl hydroperoxide (TBHP, positive control) or prooxidant ABZ for 24 h at 37°C then incubated with the ROS-monitoring agent H_2DCF_{DH} and processed by flow cytometry. Data shown in the figure are as follows: quadrants R2-R3 are cells positive for ROS and quadrants R4-R5 are cells negative for ROS. Percentages of total cells are indicated within each quadrant. The dot plots are representative of two independent experiments.

The relation between TAC structure and giardicidal activity showed that the increasing numbers of sulfur atoms are important for this effect and remarkably, points out that the presence of the sulfur-attached oxygen atom in ALC accounts for its maximal efficacy. When comparing the relative giardicidal activity of these seven TACs (ALC> DATS> DADS> AM> DAS> SAC> AMS) with its HOCl-scavenging capacity (SAC> DATS> DAS> ALC> DADS> AM>AMS; Argüello-García et al., 2010) it was observed that garlic's TACs have a wide biological mechanisms suggesting that there is a need to choose the best compound for a defined benefit, either therapeutic (e.g., anticancer and antimicrobial) or antioxidant that will finally induce health-promoting activities upon consumption (Capasso, 2013). As examples, AMS could provide low beneficial effects whereas DATS (sell as Dasuansu in China) could give multiple benefits while ALC could also provide several benefits but with a higher efficacy as antimicrobial agent. Nevertheless, it is still necessary to compare these TACs in other systems to obtain compelling data on the effects of TACs. In addition, the molecular descriptor E_{HOMO} was useful to predict the anti-giardial effect of

TACs and interestingly it was a partial contributor for HOCl-scavenging activities of these TACs (Argüello-García et al., 2010). Considering that HOMO are electron orbitals that could act as electron donors and LUMO are electron acceptor orbitals in a given molecule, these data suggest that ALC exhibiting the highest E_{HOMO} value (-211.71 kcal/mol) is a strong electron donor that could hence act as a nucleophile toward parasite's molecules bearing electron-acceptor groups e.g., thiols (R-SH) at a greater extent as compared with all other TACs used leading to trophozoite death.

There is a growing body of information regarding the efficacy of ALC against other protozoan pathogens. For example, in the human intestinal parasite *Entamoeba histolytica* the reported IC_{60} ($500 \mu M$; Ankri et al., 1997) is similar to the IC_{50} value obtained for *G. duodenalis* in this work using the same assay ($686 \mu M$) again reflecting the cysteine-rich content and thiol-dependent metabolism of these mitosome-containing parasites (Ali and Nozaki, 2007). In the also diplomonad but aerotolerant, hydrogenosome-containing fish parasite *Spironucleus vortens* ALC has a higher IC_{50} value (>1.12 mM; Millet et al., 2011) that



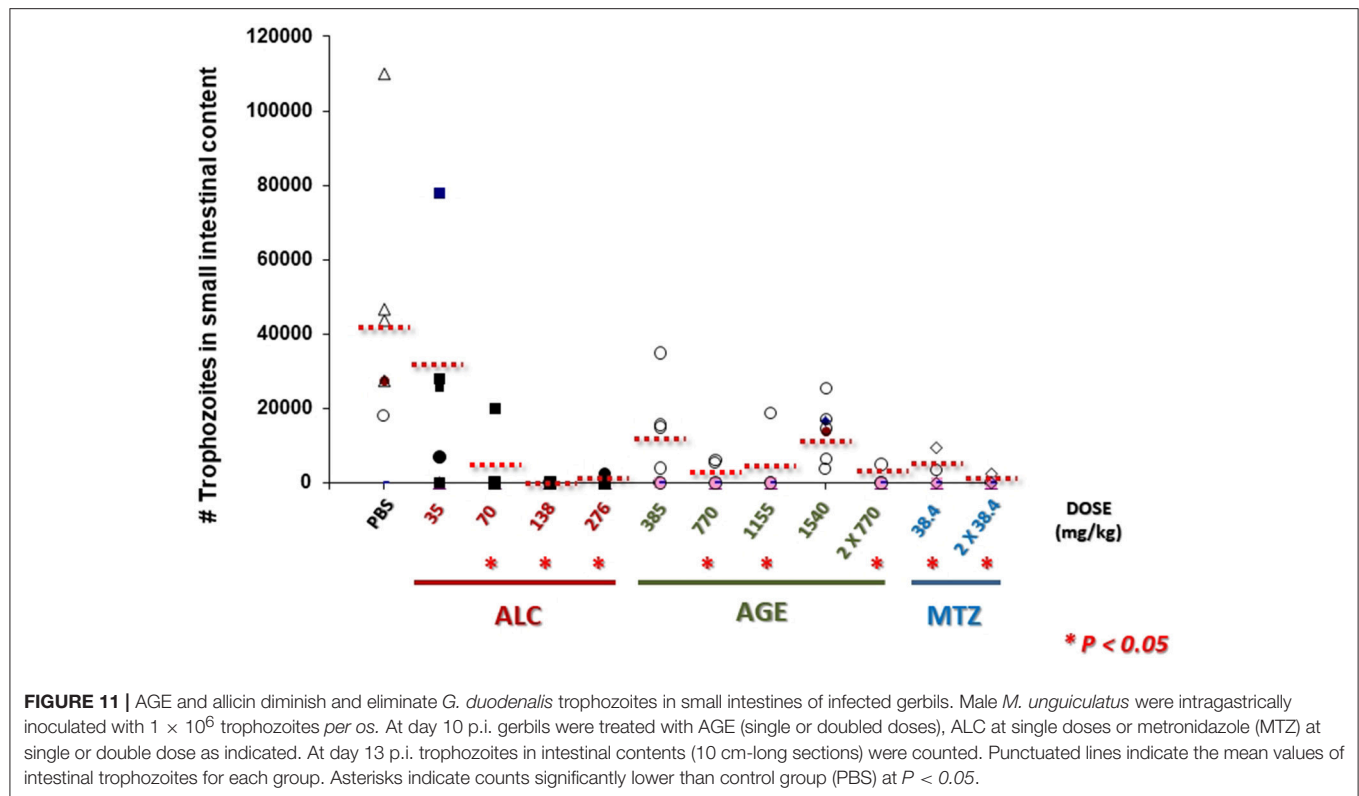
Sample	G1	S	G2	G2/M
Control (H ₂ O)	13.44	26.25	53.34	6.97
0.6 mM ALC	7.43	27.03	61.09	4.44
1.2 mM ALC	2.22	5.72	75.53	5.72

FIGURE 10 | Allicin partially arrests *G. duodenalis* trophozoites at G2 phase. Parasites (1×10^6) were exposed to 1.0% double distilled water pH 6.5 (Control) or the indicated concentrations of ABZ (positive control for cell cycle arrest) or ALC for 24 h at 37°C. Nuclei of permeabilised and RNase A-treated cells were stained with PI and processed by flow cytometry. The areas under curve (AUC) corresponding to G1, S, G2, or G2/M cell cycle phases are indicated in the control histogram. Percentages of cells within each AUC are shown in the table at the bottom of histograms. Data are representative of two independent experiments.

is likely linked to a lower susceptibility of its glutathione-based metabolism (Williams et al., 2014) to this TAC. In contrast, the small intestinal chicken parasite *Eimeria tenella* displays a poor susceptibility to ALC (IC₉₉ = 11.1 mM; Alnassan et al., 2015) due at least in part to its diverse metabolism highlighted by several shunt-off pathways like the mannitol cycle (Schmatz, 1997).

As far as the mechanism of cytotoxic action of ALC is concerned, its cytolytic, membrane-damaging effects were evidenced by the higher sensitivity of physiological methods (DCC and TBE) and electron microscopy analyses. In contrast with AGE, the MTT reduction assay displayed the lowest sensitivity of all methods used, suggesting that cellular oxidoreductases are not primary targets of ALC. Although ALC behaved as AGE did against trophozoite's integrity, it had a thiol-disulfide exchange capacity that correlated to and accounted for its highest giardicidal efficacy as compared to all other TACs

tested. Therefore, the derivatizing reaction mediated by TACs on giardial proteins exposing thiol-groups to form S-allylmereptio adducts ($R-SH \rightarrow R-S-S-CH_2-CH=CH_2$) was proven to be a major mechanism promoting trophozoite's death. However, this general reaction of ALC (Rabinkov et al., 1998) could take place at certain proteins that have important implications for cell viability, proliferation, and differentiation in *G. duodenalis*. Among these are cysteine proteases that intrinsically have the catalytic triad Cys-His-Asn. These constitute a repertoire of around 10 proteins in this parasite, participate in host cell damage and are feasible candidates for new therapeutic strategies in giardiasis (DuBois et al., 2006; Ali and Nozaki, 2007; Ankarklev et al., 2010; Gargantini et al., 2016; Cabrera-Licona et al., 2017; Ortega-Pierres et al., 2018). The zymogram analysis presented in Figure 4 indicates that garlic TACs are effectively inhibitors of several cysteine proteases in trophozoite lysates



with ALC displaying a remarkably higher inhibitory action than DADS in good agreement with their thiol-modifying activities determined herein and in recent reports in other parasite models (Waag et al., 2010). Of particular interest was the marked inhibition of the proteolytic activity of giardipain-1, a secreted virulence factor of *G. duodenalis* trophozoites, observed with ALC, DADS, and E64 in zymograms, Giardipain-1 has recently been reported to exert pro-apoptotic effects in epithelial cells monolayers including membrane blebbing, external phosphatidylserine exposure, loss of barrier function, caspase 3 activation, and altered localization of tight junction proteins as occludin and claudin-1 (Ortega-Pierres et al., 2018). Moreover, representative TACs as are ALC, DADS and AM were not only able to reduce the cytopathic effects of giardipain-1 but to display a much more marked effect in trophozoites' viability over epithelial cell integrity. These facts suggest that ALC is a promising candidate in further studies at preclinical level in giardiasis.

Other likely targets of ALC and remainder TACs in *Giardia* are the variable surface proteins (VSPs) that are a family with over 230 members having 10–12% of cysteine residues in their sequence that are involved in antigenic variation and other functions, the high-cysteine membrane proteins (HCMp) family with role in epithelium-trophozoite interactions and cell differentiation along with the iron-sulfur cluster containing protein family (e.g., ferredoxins) involved in redox metabolism. Studies in our group on these interactions are now under progress.

At the level of cellular processes, ALC induced apoptotic-like cell death and arrest at G2 phase with thiol but not oxidative

stress as shown by flow cytometry studies. When the effects of ABZ, a potent anti-giardial agent currently prescribed, it was observed that ALC also promoted apoptosis-like death as many other anti-giardial agents from synthetic or plant resources; nevertheless ALC did not cause ROS formation suggesting that TACs are not significantly metabolized by trophozoites unlike most of prescribed drugs as ABZ, MTZ, furazolidone or nitazoxanide (Gardner and Hill, 2001). On the other hand, the putative induction of thiol stress in *G. duodenalis* trophozoites caused by ALC and other TACs by modification of thiol groups to S-allylmercapto adducts (Figure 3) is similar to that reported in *Escherichia coli*; however, in these bacteria ALC induced oxidative stress as assessed by the upregulation of antioxidant enzymes such as OxyR, alkyl hydroperoxide reductase and thioredoxins 1 and 2 (Müller et al., 2016). Interestingly ALC also induced oxidative stress with the same probe used here (H_2DCFDA) in the mitochondria-containing protozoan parasite *Leishmania infantum* albeit the absence of phosphatidylserine externalization at cell membrane as assessed by annexin V and positive staining with PI indicated a necrotic process of cell death (Corral et al., 2016). All these studies shed light on the multiplicity of microbicidal effects of ALC regardless of its well-recognized mode of action on cellular thiols.

In the experimental gerbil model of giardiasis ALC demonstrated a potential utility at single doses of 70 (5/6 gerbils cured) and 138 mg/kg (6/6 gerbils cured) while AGE was effective using two doses of 770 mg/kg (5/6 gerbils cured). In our experience ALC by intragastric route shows a lethal dose in gerbils of >400 mg/kg and in other rodents this TAC displays oral lethality at 300 mg/kg (mouse) and 980 mg/kg (rat). In

spite of this apparently narrow margin of therapeutic security for ALC, in further studies splitting into two or more days the treatment could reduce these doses. Some encouraging examples on this regard have been reported with experimental infections of mice by systemic protozoa as *Babesia microti* where 30 mg/kg ALC orally for 5 days significantly reduced parasitemia and with *Plasmodium berghei* in which 4 daily doses of ALC at either 9 mg/kg (orally) or 8 mg/kg (intravenously) markedly reduced mortality (Coppi et al., 2006; Salama et al., 2014). Concurrent to these purposes is the possibility to improve the bioavailability of ALC or AGE components at intestinal milieu using carriers such as nanoparticles (Pinilla et al., 2017; Soumya et al., 2017).

In summary, the results obtained in this study highlight the cytolytic mechanism involved in the cytotoxic activity of AGE and particularly TACs as ALC that also produce thiol stress, apoptosis-like cell death as a consequence of targeting multiple proteins in *G. duodenalis* including cysteine proteinase activities as shown in this work. The identification and characterization of interactions of garlic components/derivatives with giardial biomolecules deserves future studies and indicates that ALC is a promising anti-giardial agent with concomitant benefits for host health.

ETHICS STATEMENT

This study was carried out in accordance with the recommendations of Comité Interno para el Cuidado y Uso de los Animales de Laboratorio (CICUAL) Del Cinvestav, México. According with the Official Mexican Rule (Norma Oficial Mexicana) NOM-062-ZOO-1999. The protocol was approved by the Comité Interno para el Cuidado y Uso de los Animales de Laboratorio (CICUAL) Del Cinvestav, México.

AUTHOR CONTRIBUTIONS

RA-G and MO-P conceived the work, designed the experiments, and analyzed the data. RA-G and NP-H participated in allicin synthesis. NP-H obtained the values of molecular descriptors.

REFERENCES

- Adam, R. D. (2001). Biology of *Giardia lamblia*. *Clin. Microbiol. Rev.* 14, 447–475. doi: 10.1128/CMR.14.3.447-475.2001
- Ali, V., and Nozaki, T. (2007). Current therapeutics, their problems, and sulfur-containing-amino-acid-metabolism as a novel target against infections by “amitochondriate” protozoan parasites. *Clin. Microbiol. Rev.* 20, 164–187. doi: 10.1128/CMR.00019-06
- Alnassan, A. A., Thabet, A., Dausgies, A., and Bangoura, B. (2015). *In vitro* efficacy of allicin on chicken *Eimeria tenella* sporozoites. *Parasitol. Res.* 114, 3913–3915. doi: 10.1007/s00436-015-4637-2
- Ankarklev, J., Jerlström-Hultqvist, J., Ringqvist, E., Troell, K., and Svärd, S. G. (2010). Behind the smile: cell biology and disease mechanisms of *Giardia* species. *Nat. Rev. Microbiol.* 8, 413–422. doi: 10.1038/nrmicro2317
- Ankri, S., and Mirelman, D. (1999). Antimicrobial properties of allicin from garlic. *Microbes Infect.* 1, 125–129. doi: 10.1016/S1286-4579(99)80003-3
- Ankri, S., Miron, T., Rabinkov, A., and Wilchek, M., Mirelman, D. (1997). Allicin from garlic strongly inhibits cysteine proteinases and cytopathic effects of *Entamoeba histolytica*. *Antimicrob. Agents Chemother.* 41, 2286–2288.

MdIV-A performed all techniques of susceptibility assays. IL-R, AM-C, EM-T, and EE-C evaluated extracts and compounds in the gerbil model of giardiasis. RF-L performed the proteolytic activity (zymograms) assays, the co-culture assays to analyzed representative TACs as possible inhibitors of the cytolytic effect of giardipain-1 on IEC6 cell monolayers and to determine the effect of representative TACs on epithelial IEC6 cell monolayers. RA-G did the docking of with giardipain-1. AG-R performed the electron microscopy (scanning and transmission) studies. RA-G carried out flow cytometry studies. RA-G and MO-P wrote and corrected the manuscript.

ACKNOWLEDGMENTS

We are grateful to Dr. José Pedraza Chaverri for critically reading the manuscript. We would like to thank Blanca Herrera Ramírez for technical assistance, Víctor Hugo Rosales García for his expert help in flow cytometry studies and Arturo Pérez-Taylor Reyes for artwork. This work was supported in part by Fondo Secretaria de Educación Pública-Consejo Nacional de Ciencia y Tecnología (SEP-CONACYT) México. Grant number 128426.

SUPPLEMENTARY MATERIAL

The Supplementary Material for this article can be found online at: <https://www.frontiersin.org/articles/10.3389/fcimb.2018.00353/full#supplementary-material>

Supplementary Figure 1 | Determination of the effect of representative TACs on epithelial IEC6 cell monolayers. Confluent IEC6 cells were exposed for 100 min at 37°C to affinity chromatography-purified giardipain-1 alone (control for cell cytotoxic effect) or to concentrations (in mM) of representative TACs causing inhibition of its protease activity in zymograms (center panels) or corresponding to the MLCs in trophozoites (right panels) of representative garlic TACs (ALC, Allicin; DADS, Diallyl disulfide; AM, Allyl mercaptan). Monolayers were analyzed by Nomarski optics. Asterisks denote zones of monolayer destruction and arrows point to cells undergoing apoptotic death as indicated by membrane blebbing, shrinkage and shape degeneration. Bars: 20 µm.

Supplementary Table 1 | Values of electronic and molecular transport descriptors calculated for garlic's TACs used in this study.

- Anthony, J. P., Fyfe, L., and Smith, H. (2005). Plant active components – a resource for antiparasitic agents? *Trends Parasitol.* 21, 462–468. doi: 10.1016/j.pt.2005.08.004
- Argüello-García, R., Cruz-Soto, M., Romero-Montoya, L., and Ortega-Pierres, G. (2004). Variability and variation in drug susceptibility among *Giardia duodenalis* isolates and clones exposed to 5-nitroimidazoles and benzimidazoles *In vitro*. *J. Antimicrob. Chemother.* 54, 711–721. doi: 10.1093/jac/dkh388
- Argüello-García, R., Cruz-Soto, M., Romero-Montoya, L., and Ortega-Pierres, G. (2009). *In vitro* resistance to 5-nitroimidazoles and benzimidazoles in *Giardia duodenalis*: variability and variation in gene expression. *Infect. Genet. Evol.* 9, 1057–1064. doi: 10.1016/j.meegid.2009.05.015
- Argüello-García, R., Medina-Campos, O. N., Pérez-Hernández, N., Pedraza-Chaverri, J., and Ortega-Pierres, G. (2010). Hypochlorous acid scavenging activities of thioallyl compounds from garlic. *J. Agric. Food Chem.* 58, 11226–11233. doi: 10.1021/jf102423w
- Argüello-García, R., and Ortega-Pierres, M. G. (1997). *Giardia duodenalis*: analysis of humoral immune response in experimentally infected gerbils (*Meriones unguiculatus*). *Arch. Med. Res.* 28, 171–178.

- Belosevic, M., Faubert, G. M., MacLean, J. D., Law, C., and Croll, N. A. (1982). *Giardia lamblia* infections in Mongolian gerbils: an animal model. *J. Infect. Dis.* 147, 222–226. doi: 10.1093/infdis/147.2.222
- Bhagyalakshmi, N., Thimmaraju, R., Venkatachalam, L., Chidambaram-Murthy, K. N., and Sreedhar, R. V. (2007). Nutraceuical applications of garlic and the intervention of biotechnology. *Crit. Rev. Food Sci. Nutr.* 45, 607–621. doi: 10.1080/10408390500455508
- Breeuwer, P., Drocourt, J. L., Bunschoten, N., Zwietering, M. H., Rombouts, F. M., and Abee, T. (1995). Characterization of uptake and hydrolysis of fluorescein diacetate and carboxyfluorescein diacetate by intracellular esterases in *Saccharomyces cerevisiae*, which result in accumulation of fluorescent product. *Appl. Environ. Microbiol.* 61, 1614–1619.
- Cabrera-Licon, A., Solano-González, E., Fonseca-Liñán, R., Bazán-Tejeda, M. L., Argüello-García, R., Bermúdez-Cruz, R. M., et al. (2017). Expression and secretion of the *Giardia duodenalis* variant surface protein 9B10A by transfected trophozoites causes damage to epithelial cell monolayers mediated by protease activity. *Exp. Parasitol.* 179, 49–64. doi: 10.1016/j.exppara.2017.06.006
- Capasso, A. (2013). Antioxidant action and therapeutic efficacy of *Allium sativum* L. *Molecules* 18, 690–700. doi: 10.3390/molecules18010690
- Cellini, L., Di Campli, E., Masulli, M., Di Bartolomeo, S., and Allocati, N. (1996). Inhibition of *Helicobacter pylori* by garlic extract (*Allium sativum*). *FEMS Immunol. Med. Microbiol.* 13, 273–277. doi: 10.1111/j.1574-695X.1996.tb00251.x
- Coppi, A., Cabinian, M., Mirelman, D., and Sinnis, P. (2006). Antimalarial activity of allicin, a biologically active compound from garlic cloves. *Antimicrob. Agents Chemother.* 50, 1731–1737. doi: 10.1128/AAC.50.5.1731-1737.2006
- Corral, M. J., Benito-Peña, E., Jiménez-Antón, M. D., Cuevas, L., Moreno-Bondí, M. C., and Alunda, J. M. (2016). Allicin induces calcium and mitochondrial dysregulation causing necrotic death in *Leishmania*. *PLoS Negl. Trop. Dis.* 10:e0004525. doi: 10.1371/journal.pntd.0004525
- De Gianni, E., and Fimognari, C. (2015). Anticancer mechanism of sulfur-containing compounds. *Enzymes* 37, 167–192. doi: 10.1016/bs.enz.2015.05.003
- D'Souza, S. P., Chavannavar, S. V., Kanchanashri, B., and Niveditha, S. B. (2017). Pharmaceutical perspectives of spices and condiments as alternative antimicrobial remedy. *J. Evid. Based Complementary Altern. Med.* 22, 1002–1010. doi: 10.1177/2156587217703214
- DuBois, K. N., Abodeely, M., Sajid, M., Engel, J. C., and McKerrow, J. H. (2006). *Giardia lamblia* cysteine proteases. *Parasitol. Res.* 99, 313–316. doi: 10.1007/s00436-006-0149-4
- Gallwitz, H., Bonse, S., Martínez-Cruz, A., Schlichting, I., Schumacher, K., and Krauth-Siegel, R. L. (1999). Ajoene is an inhibitor and subversive substrate of human glutathione reductase and *Trypanosoma cruzi* trypanothione reductase: crystallographic, kinetic, and spectroscopic studies. *J. Med. Chem.* 42, 363–372. doi: 10.1021/jm980471k
- Gardner, T. B., and Hill, D. R. (2001). Treatment of giardiasis. *Clin. Microbiol. Rev.* 14, 114–128. doi: 10.1128/CMR.14.1.114-128.2001
- Gargantini, P. R., Serradell, M. D. C., Ríos, D. N., Tenaglia, A. H., and Luján, H. D. (2016). Antigenic variation in the intestinal parasite *Giardia lamblia*. *Curr. Opin. Microbiol.* 32, 52–58. doi: 10.1016/j.mib.2016.04.017
- Gupta, N., and Porter, T. D. (2001). Garlic and garlic-derived compounds inhibit human squalene monooxygenase. *J. Nutr.* 131, 1662–1667. doi: 10.1093/jn/131.6.1662
- Harris, J. C., Plummer, S., Turner, M. P., and Lloyd, D. (2000). The microaerophilic flagellate *Giardia intestinalis*: *Allium sativum* (garlic) is an effective anti-giardial. *Microbiology* 12, 3119–3127. doi: 10.1099/00221287-146-12-3119
- Keister, D. B. (1983). Axenic culture of *Giardia lamblia* in TYI-S-33 medium supplemented with bile. *Trans. R. Soc. Trop. Med. Hyg.* 77, 487–488. doi: 10.1016/0035-9203(83)90120-7
- Lane, S., and Lloyd, D. (2002). Current trends in research into the waterborne parasite *Giardia*. *Crit. Rev. Microbiol.* 28, 123–147. doi: 10.1080/1040-840291046713
- Lawson, L. D. (1996). "The composition and chemistry of garlic cloves and processed garlic," in *Garlic: The Science and Therapeutic Applications of Allium sativum L. and Related Species*, eds H. P. Koch and L. D. Lawson (Baltimore, MD: Williams & Wilkins), 57.
- Lawson, L. D., and Wang, Z. G. (1993). Pre-hepatic fate of the organosulfur compounds derived from garlic (*Allium sativum*). *Planta Med.* 59, A688–A689. doi: 10.1055/s-2006-959976
- Liu, Y., Peterson, D. A., Kimura, H., and Schubert, D. (1997). Mechanism of cellular 3-(4,5-dimethylthiazol-2-yl)-2,5-diphenyltetrazolium bromide (MTT) reduction. *J. Neurochem.* 69, 581–593.
- Martínez-Espinosa, R., Argüello-García, R., Saavedra, E., and Ortega-Pierres, G. (2015). Albendazole induces oxidative stress and DNA damage in the parasitic protozoan *Giardia duodenalis*. *Front. Microbiol.* 6:800. doi: 10.3389/fmicb.2015.00800
- Millet, C. O., Lloyd, D., Williams, C., Williams, D., Evans, G., Saunders, R. A., et al. (2011). Effect of garlic and allium-derived products on the growth and metabolism of *Spironucleus vortens*. *Exp. Parasitol.* 127, 490–499. doi: 10.1016/j.exppara.2010.10.001
- Milner, J. A. (2001). Mechanisms by which garlic and allyl sulfur compounds suppress carcinogen activation. *Garlic and carcinogenesis. Adv. Exp. Med. Biol.* 492, 69–81. doi: 10.1007/978-1-4615-1283-7_7
- Moghadam, F. J., Navidifar, T., and Amin, M. (2014). Antibacterial activity of garlic (*Allium sativum* L.) on multi-drug resistant *Helicobacter pylori* isolated from gastric biopsies. *Int. J. Enteric Pathog.* 2:e16749. doi: 10.17795/ijep16749
- Müller, A., Eller, J., Albrecht, F., Prochnow, P., Kuhlmann, K., Bandow, J. E., et al. (2016). Allicin induces thiol stress in bacteria through S-Allylmercapto modification of protein cysteines. *J. Biol. Chem.* 291, 11477–11490. doi: 10.1074/jbc.M115.702308
- Northrop-Clewes, C. A., Rousham, E. K., Mascie-Taylor, C. N., and Lunn, P. G. (2001). Anthelmintic treatment of rural Bangladeshi children: effect on host physiology, growth, and biochemical status. *Am. J. Clin. Nutr.* 73, 53–60. doi: 10.1093/ajcn/73.1.53
- Ortega-Pierres, G., Argüello-García, R., Laredo-Cisneros, M. S., Fonseca-Liñán, R., Gómez-Mondragón, M., Flores-Benítez, D., et al. (2018). Giardipain-1, a protease secreted by *Giardia duodenalis* trophozoites causes junctional, barrier and apoptotic damages in epithelial cell monolayers. *Int. J. Parasitol.* 48, 621–639. doi: 10.1016/j.ijpara.2018.01.006
- Pinilla, C. M., Noreña, C. P., and Brandelli, A. (2017). Development and characterization of phosphatidylcholine nanovesicles, containing garlic extract, with antilisterial activity in milk. *Food Chem.* 220, 470–476. doi: 10.1016/j.foodchem.2016.10.027
- Pinto, J. T., Krasnikov, B. F., and Cooper, A. J. L. (2006). Redox-sensitive proteins are potential targets of garlic-derived mercaptocysteine derivatives. *J. Nutr.* 136, 835S–841S. doi: 10.1093/jn/136.3.835S
- Rabinkov, A., Miron, T., Konstantinovski, L., Wilchek, M., Mirelman, D., and Weiner, L. (1998). The mode of action of allicin: trapping of radicals and interaction with thiol containing proteins. *Biochim. Biophys. Acta* 1379, 233–244. doi: 10.1016/S0304-4165(97)00104-9
- Redlinger, T., Corella-Barud, V., Graham, J., Galindo, A., Avitia, R., and Cárdenas, V. (2002). Hyperendemic *Cryptosporidium* and *Giardia* in households lacking municipal sewer and water on the United States-Mexico border. *Am. J. Trop. Med. Hyg.* 66, 794–798. doi: 10.4269/ajtmh.2002.66.794
- Reyes-Vivas, H., Diaz, A., Peon, J., Mendoza-Hernandez, G., Hernandez-Alcantara, G., De la Mora-De la Mora, I., et al. (2007). Disulfide bridges in the mesophilic triosephosphate isomerase from *Giardia lamblia* are related to oligomerization and activity. *J. Mol. Biol.* 365, 752–763. doi: 10.1016/j.jmb.2006.10.053
- Salama, A. A., AbouLaila, M., Terkawi, M. A., Mousa, A., El-Sify, A., Allaam, M., et al. (2014). Inhibitory effect of allicin on the growth of *Babesia* and *Theileria equi* parasites. *Parasitol. Res.* 113, 275–283. doi: 10.1007/s00436-013-3654-2
- Schmatz, D. M. (1997). The mannitol cycle in *Eimeria*. *Parasitology* 114(Suppl.), S81–S89.
- Seddiek, S. H. A., El-Shorbagy, M. M., Khater, H. F., and Ali, A. M. (2014). The antitrichomonal efficacy of garlic and metronidazole against *Trichomonas gallinae* infecting domestic pigeons. *Parasitol. Res.* 113, 1319–1329. doi: 10.1007/s00436-014-3771-6
- Soffar, S. A., and Mokhtar, G. M. (1991). Evaluation of the antiparasitic effect of aqueous garlic (*Allium sativum*) extract in *Hymenolepis nana* and giardiasis. *J. Egypt Soc. Parasitol.* 21, 497–502.

- Soumya, R. S., Sherin, S., Raghu, K. G., and Abraham, A. (2017). Allicin functionalized locust bean gum nanoparticles for improved therapeutic efficacy: An *in silico*, *In vitro* and *in vivo* approach. *Int. J. Biol. Macromol.* 109, 740–747. doi: 10.1016/j.ijbiomac.2017.11.065
- Waag, T., Gelhaus, C., Rath, J., Stich, A., Leippe, M., and Schirmeister, T. (2010). Allicin and derivatives are cysteine protease inhibitors with antiparasitic activity. *Bioorg. Med. Chem. Lett.* 20, 5541–5543. doi: 10.1016/j.bmcl.2010.07.062
- WHO (2006). *The World Health Report 1996. Fighting Disease Fostering Development*. World Health Organization. Available online at: <http://www.who.int/whr/1996/en/>
- Williams, C. F., Yarett, N., Aon, M. A., and Lloyd, D. (2014). Antioxidant defences of *Spironucleus vortens*: glutathione is the major non-protein thiol. *Mol. Biochem. Parasitol.* 196, 45–52. doi: 10.1016/j.molbiopara.2014.07.010
- Yang, C. S., Chhabra, S. K., Hong, J. Y., and Smith, T. J. (2001). Mechanisms of inhibition of chemical toxicity and carcinogenesis by diallyl sulfide (DAS) and related compounds from garlic. *J. Nutr.* 131, 1041S–1045S. doi: 10.1093/jn/131.3.1041S

Conflict of Interest Statement: The authors declare that the research was conducted in the absence of any commercial or financial relationships that could be construed as a potential conflict of interest.

Copyright © 2018 Argüello-García, de la Vega-Arnaud, Loredó-Rodríguez, Mejía-Corona, Melgarejo-Trejo, Espinoza-Contreras, Fonseca-Liñán, González-Robles, Pérez-Hernández and Ortega-Pierres. This is an open-access article distributed under the terms of the Creative Commons Attribution License (CC BY). The use, distribution or reproduction in other forums is permitted, provided the original author(s) and the copyright owner(s) are credited and that the original publication in this journal is cited, in accordance with accepted academic practice. No use, distribution or reproduction is permitted which does not comply with these terms.



An Overview of Peripheral Blood Mononuclear Cells as a Model for Immunological Research of *Toxoplasma gondii* and Other Apicomplexan Parasites

John Alejandro Acosta Davila* and Alejandro Hernandez De Los Rios

GEPAMOL, Centro de Investigaciones Biomédicas, Universidad del Quindío, Armenia, Colombia

OPEN ACCESS

Edited by:

Kamal El Bissati,
University of Chicago, United States

Reviewed by:

Yang Zhang,
University of Pennsylvania,
United States
Juan Carlos Sepúlveda-Arias,
Technological University of Pereira,
Colombia

*Correspondence:

John Alejandro Acosta Davila
jaacostad@uqvirtual.edu.co

Specialty section:

This article was submitted to
Clinical Microbiology,
a section of the journal
Frontiers in Cellular and Infection
Microbiology

Received: 30 June 2018

Accepted: 22 January 2019

Published: 08 February 2019

Citation:

Acosta Davila JA and Hernandez De
Los Rios A (2019) An Overview of
Peripheral Blood Mononuclear Cells
as a Model for Immunological
Research of *Toxoplasma gondii* and
Other Apicomplexan Parasites.
Front. Cell. Infect. Microbiol. 9:24.
doi: 10.3389/fcimb.2019.00024

In biology, models are experimental systems meant to recreate aspects of diseases or human tissue with the goal of generating inferences and approximations that can contribute to the resolution of specific biological problems. Although there are many models for studying intracellular parasites, their data have produced critical contradictions, especially in immunological assays. Peripheral blood mononuclear cells (PBMCs) represent an attractive tissue source in pharmacogenomics and in molecular and immunologic studies, as these cells are easily collected from patients and can serve as sentinel tissue for monitoring physiological perturbations due to disease. However, these cells are a very sensitive model due to variables such as temperature, type of stimulus and time of collection as part of posterior processes. PBMCs have been used to study *Toxoplasma gondii* and other apicomplexan parasites. For instance, this model is frequently used in new therapies or vaccines that use peptides or recombinant proteins derived from the parasite. The immune response to *T. gondii* is highly variable, so it may be necessary to refine this cellular model. This mini review highlights the major approaches in which PBMCs are used as a model of study for *T. gondii* and other apicomplexan parasites. The variables related to this model have significant implications for data interpretation and conclusions related to host-parasite interaction.

Keywords: PBMCs (peripheral blood mononuclear cells), immunologic research, *toxoplasma gondii*, model of study, apicomplexa

INTRODUCTION

The phylum Apicomplexa consists of approximately 6,000 species of intracellular protozoan parasites, including various important human and animal pathogens such as *Plasmodium*, the causative agent of malaria; *Cryptosporidium*, the causative agent of cryptosporidiosis; *Theileria*, *Babesia* and *Eimeria*, which are important pathogens in cattle and fowl; and *T. gondii*, which is responsible for toxoplasmosis in birds, marsupials and mammals including humans (Tenter et al., 2000; Dubey, 2010). *T. gondii* has emerged as a model system for the study of intracellular parasitism; it is one of the most studied parasites due to its medical and veterinary importance, its wide range of distribution and its suitability as a model of study in pharmacogenomics, cell biology, molecular genetics and immunology. *T. gondii* infections are generally subclinical in

healthy individuals but can be major problems for immunosuppressed adults and fetuses (Dubey, 2008). The severity of such infections can vary greatly, perhaps based on the status of the host immune system (Lahmar et al., 2009), the genotype of the infective parasite strain (Ferreira et al., 2011) and the host's genetic background (Sullivan and Jeffers, 2012). There has been significant progress, but no vaccine is currently available that will prevent *T. gondii* infection; indeed, very few drugs effectively reduce *T. gondii*'s presence in infected individuals (Zhou et al., 2016a). Researchers frequently select models for studying *T. gondii* based on their similarity to humans in terms of genetics, anatomy, and physiology; this includes the cellular models that have been used to study *T. gondii* (Szabo and Finney, 2017). However, many studies make use of mouse models (Alfonzo et al., 2002; Martens et al., 2005; Tanaka et al., 2013; Unno et al., 2013; Dzitko et al., 2015; He et al., 2015). There have been highly controversial results associated with some of these models because they do not completely mimic human toxoplasmosis (Hunter and Sibley, 2012; Nieldelman et al., 2012; Seok et al., 2013). In fact, some scientists have argued that new approaches must be explored; some have even proposed new models for studying *T. gondii* (Cornelissen et al., 2014; Tanaka et al., 2016; Nau et al., 2017).

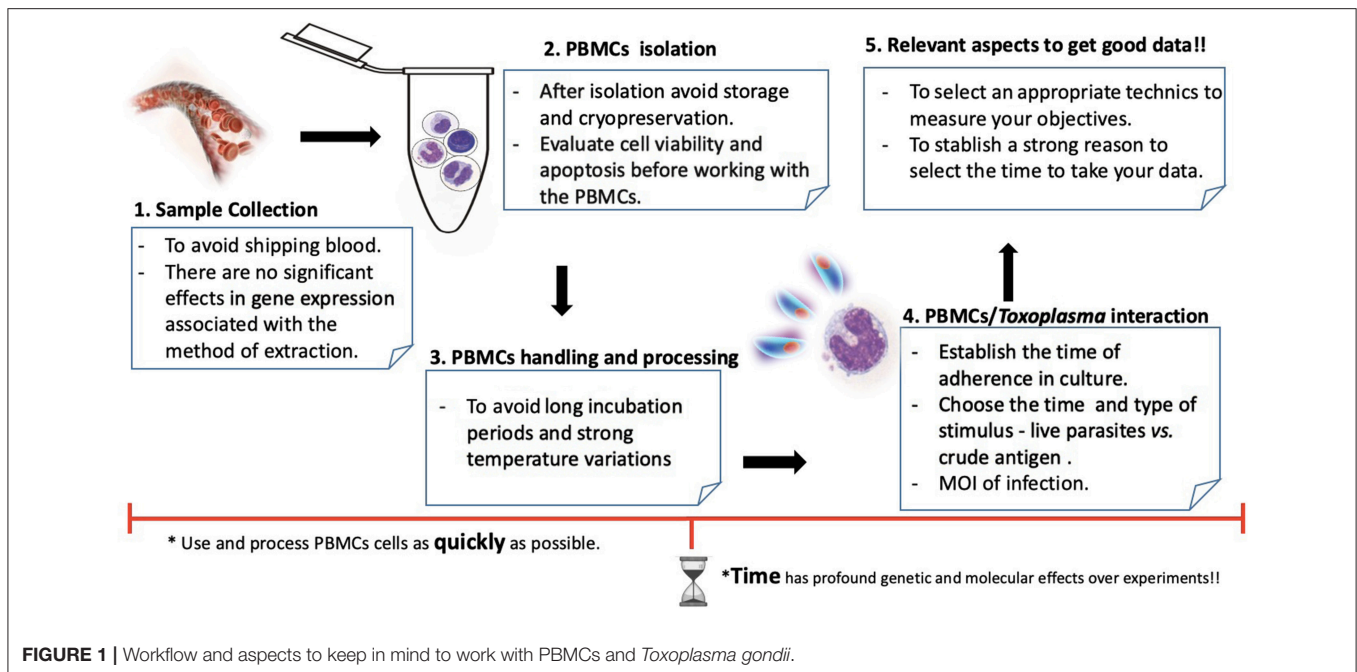
The PBMC cellular model includes T and B cells (~80%), natural killer cells (~10%) and monocytes (~10%) (Autissier et al., 2010). These blood cells play an important role in the immune response that is meant to preserve the host's homeostasis and defend it against parasite infection (Zhou et al., 2016a). Researchers have used PBMC to study *T. gondii* with various goals, but especially to improve diagnostic, drug-screening and immunogenetic approaches (Vendrell et al., 1992; Dzitko et al., 2015). Although PBMCs do not completely mimic an infection *in vivo*, they can be taken directly from affected individuals and can generate certain qualities that when added to the recommendations (Figure 1) discussed below can improve the quality of the experimental data regarding toxoplasmosis. Therefore, understanding and improving models is imperative to the appropriate interpretation and translation of this work into clinical setting (Szabo and Finney, 2017). In this review, we present a summary of how PBMCs have been used to study *T. gondii* and other apicomplexan parasites, discuss some controversies related to this cellular model and then describe possible improvements to the related protocols.

IMMUNE RESPONSE IN PBMCs STIMULATED WITH *T. GONDII*

PBMCs have mainly been used to model *T. gondii* as part of the evaluation of potential new vaccines or drugs, as well as to understand the relationships between the host's immune system and the parasite (see Table 1). The studies using these models have shown that cytokine levels can vary according to the evaluated clinical condition, the type of strain and the culture conditions which can include the type of media culture supplement; the time of data collection; and the temperature variations during storage, shipping and handling (Weinberg

et al., 2010). In chronic asymptomatic individuals, the PBMCs' immune responses against total lysate antigen and against peptides derived from *T. gondii* are predominantly characterized by high levels of interferon gamma (IFN- γ) (Prigione et al., 2006; Bayram Delibaş et al., 2009; Cong et al., 2011; Cardona et al., 2015; Meira et al., 2015); in ocular toxoplasmosis and *Toxoplasma*-seronegative individuals, however, the level of this cytokine is much lower (Alfonzo et al., 2005; Meira et al., 2014; Maia et al., 2017). PBMCs have also been useful in studying the immune response of HIV-infected individuals and of pregnant women with toxoplasmosis. In one study on HIV patients who had been coinfecting with *T. gondii*, researchers measured the IFN- γ expression of stimulated total lysate antigen using PBMCs, both before and after treatment with antiparasitic drugs (sulfadiazine, pyrimethamine, folinic acid, trimethoprim-sulfamethoxazole, and corticosteroids); the infection's evolution was correlated with the restoration of the IFN- γ response and with decreased inflammation (Meira et al., 2015). In another study, researchers showed that, during pregnancy, tumor necrosis factor alpha (TNF- α) and interleukin (IL)-12 had decreased expression when cells were stimulated with live tachyzoites (Rezende-Oliveira et al., 2012). Interestingly, the addition of the prolactin hormone to the cells seemed to restrict the parasite's proliferation (Dzitko et al., 2012). In similar works, researchers have shown the importance of IFN- γ production in the congenital transmission of *T. gondii* through the upregulation of intercellular adhesion molecular 1 (ICAM-1) (Pfaff et al., 2005). Stimulating PBMCs with complete or partial antigens of *T. gondii* seems to reveal important aspects of the host's immune response. However, *T. gondii* and other apicomplexans secrete proteins in a highly regulated manner that is involved in the parasite's immune evasion mechanisms (Tosh et al., 2016). These processes are not seen when parasite antigens are used, so we recommend the use of live parasites to stimulate PBMCs (Figure 1).

On the other hand, the vaccine candidates for *T. gondii* are typically parasite proteins or the peptides that elicit protective immune responses in mice. However, vaccine candidates that are effective in mice are not necessarily effective in humans. PBMCs are potentially very useful tools for identifying and characterizing novel vaccine candidates for *T. gondii*. Cells from individuals with varied genetic and immunological backgrounds can be easily isolated and stimulated with the antigens of interest, thus allowing measurement of the desired cytokine profile or cell response. However, to our knowledge, few researchers have used this strategy (Tan et al., 2010; Cong et al., 2012; Cardona et al., 2015). The studies mentioned above have identified novel parasite derived peptides that induce strong production of IFN- γ in people who express one of the most common human leukocyte antigen (HLA) supertypes (HLA-A02, HLA-B07, and HLA-A11), making those peptides attractive vaccine candidates. PBMCs have also been used to evaluate the efficacy of two phytoecdysteroids (α -ecdysone and 20-hydroxyecdysone) in controlling *T. gondii* infections. These drugs are effective against *Babesia gibsoni* but have no effect on *T. gondii*'s proliferation and do not elicit a Th1 protective immune response against the parasite (Dzitko et al., 2015). Thus, all these studies show that PBMCs may



represent an important and undervalued model for vaccine and drug development.

TECHNICAL ASPECTS TO CONSIDER BEFORE WORKING WITH PBMCs AND *T. GONDII*

To obtain scientifically valid data, the experimental conditions and the study's model must be closely controlled. PBMCs are one of the best sources for assessing the differences or changes associated with diseases or with drug responses and therapies; in addition, these cells are relatively easy to obtain from whole blood through isolation (Burczynski and Dorner, 2006). A major challenge in the monitoring of PBMCs' quality is establishing protocols that define the proper isolation, shipping and storage methods so that they can be tested without changes in cellular functionality. For researchers who work with PBMCs, it is very important to note that many variables affect these cells. This model can be used to study *Toxoplasma* under clinical or non-clinical conditions; however, the whole procedure—from blood withdrawal to experimentation—must be highly standardized. PBMCs are perishable living cells, and some of them begin to die immediately after their isolation from whole blood. Scientists have compared isolation techniques, but they have found no differences with respect to the generally used methods, which include Ficoll-Paque density-gradient centrifugation and BD Vacutainer cell-preparation tubes (Corkum et al., 2015).

However, after isolation of PBMC, early apoptotic events are present in both *in vitro* and *ex vivo* experiments; as a result, it is very important to determine apoptosis before using these cells in the experiments (Wunsch et al., 2015). Various methods

have been used to measure apoptosis, including the YO-PRO-1/7-AAD method, which has been proposed as a good, low-cost alternative for sensitive detection of early apoptosis in PBMCs and >80% of viability is recommended before starting to work (Glisic-Milosavljevic et al., 2005). Working with freshly isolated PBMCs is not always possible; thus, the cells are generally frozen and thawed for processing at later times (see Table 1); this allows for the batched thawing of samples and for direct comparability in assays, thus reducing inter-assay variability and allowing for future analysis of later-emerging issues (Riedhammer et al., 2016). As a consequence, both apoptosis and necrosis happen; this phenomenon has been well documented to occur during cryopreservation (Fowke et al., 2000; Baust, 2002; Cosentino et al., 2007; Mallone et al., 2011). For example, in a recent study on how storage temperature affects PBMCs and cryopreserves PBMCs' viability, recovery and gene expression patterns were all affected, as compared to those of freshly isolated PBMCs (Yang et al., 2016). In a cell infected with *Toxoplasma*, each hour represents a specific differential gene-expression profile (He et al., 2015; Zhou et al., 2016b), which indicates that the best possible method for handling missing data is to prevent the problem by properly planning each study and by collecting the data carefully (Wisniewski et al., 2006). The goal is to eventually have studies with comparable data. Along the same order of ideas, the time variable is important to consider when working with PBMCs, as it can lead to missing data. The problem of missing data is relatively common in most fields of research, and it can significantly affect the conclusions drawn from the data (Little et al., 2012). Accordingly, some medical researchers have focused on handling missing data and related problems using methods that prevent or minimize missing data (O'Neill and Temple, 2012). One of the main problems with using the PBMC model for *T. gondii* is that the majority of studies are

TABLE 1 | Characteristics and use of PBMC as a study model for *T. gondii* and other Apicomplexan parasites during the last 10 years.

Organism	Technical observations	PBMC culture (number of cells/final volume/culture plates)	Main findings	References
Human PBMC and <i>Toxoplasma gondii</i>	Stimulus: RH strain (TLA, 1 μ g/mL) Technic: RT-qPCR Process time: 48 h after collection Cryopreserved: No Supplemented: 10% FCS	1 \times 10 ⁶ /500 μ L/48-well	High levels of TGF- β , IL-6, IL-10 in OT individuals	Maia et al., 2017
	Stimulus: RH strain (TLA, 1 μ g/mL) Technic: RT-qPCR Process time: 48 h after collection Cryopreserved: No Supplemented: 10% FBS	1 \times 10 ⁶ /500 μ L/48-well	TATA box-binding protein (TBP) and ubiquitin C (UBC) are the most stable genes for mRNA analysis in PBMCs	Meira-Strejvitch et al., 2017
	Stimulus: ND Technic: Radioactivity Process time: 168 h in incubation Cryopreserved: No Supplemented: 5% human AB serum	ND	Despite high proliferation, lymphocytes from meth users had a lower proliferative capacity	Massanella et al., 2015
	Stimulus: Peptides from P30 and ROP 18 (10 μ g/mL) Technic: ELISPOT Process time: 24 h in incubation Cryopreserved: Yes Supplemented: No	2 \times 10 ⁵ /100 μ L/96-well	Four peptides induced IFN- γ expression	Cardona et al., 2015
	Stimulus: RH strain (TLA, 1 μ g/mL) Technic: ELISA Process time: 48 h in incubation Cryopreserved: No Supplemented: 10% FBS	1 \times 10 ⁶ /500 μ L/48-well	Restoration of IFN- γ response and a decrease of the inflammatory cytokines TNF- α and IL-10	Meira et al., 2015
	Stimulus: RH strain (Live) Technic: Radioactivity Process time: ND Cryopreserved: ND Supplemented: ND	2.5 \times 10 ⁵ /100 μ L/96-well	Phytoecdysteroids did not inhibit <i>Toxoplasma</i> and did not affect the cytokine response (IFN- γ , IL-12, IL-10)	Dzitko et al., 2015
	Stimulus: TLA (ND) Technic: ELISPOT Process time: 120 h in incubation Cryopreserved: No Supplemented: No	3 \times 10 ⁵ /200 μ L/ND	No association was observed when PBMCs were stimulated with TLA or mitogen	Nogueira et al., 2014
	Stimulus: BK strain (Live) Technic: ELISA Process time: 48 h in incubation Cryopreserved: No Supplemented: 0.1% BSA	2.5 \times 10 ⁶ /ND/ND	Correlation between Prolactine and the level of IL-10, but not with IFN- γ	Dzitko et al., 2012
	Stimulus: RH and ME49 strains (Live) Technic: ELISA Process time: 48 h in incubation Cryopreserved: No Supplemented: No	2 \times 10 ⁶ /ND/24-well	<i>T. gondii</i> -seronegative non-pregnant women produced significantly higher levels of TNF- α and IL-12	Rezende-Oliveira et al., 2012
	Stimulus: <i>T. gondii</i> peptides Technic: ELISPOT Process time: ND Cryopreserved: Yes Supplemented: No	2 \times 10 ⁵ /100 μ L/96-well	Peptides induced significant IFN- γ production by PBMCs from 4 HLA-A*0201 persons infected with <i>T. gondii</i>	Cong et al., 2011
	Stimulus: TRRH strain (TLA, 5 mg/mL) Technic: ELISA Process time: 72 h in incubation Cryopreserved: No Supplemented: 10% FBS	1 \times 10 ⁶ /200 μ L/96-well	IL-5 was higher than IFN- γ in the initial phase of the infection; as the IgG started to rise, IFN- γ increased and suppressed the synthesis of IL-5	Bayram Delibaş et al., 2009

(Continued)

TABLE 1 | Continued

Organism	Technical observations	PBMC culture (number of cells/final volume/culture plates)	Main findings	References
Pigs PBMC and <i>Toxoplasma gondii</i>	Stimulus: IPB-G/LR strain (TLA, 10 μ g/mL) Technic: Flow cytometry Process time: 72 h in incubation Cryopreserved: No Supplemented: 10% FBS	1 \times 10 ⁶ /ND/ND	High levels of IFN- γ	Jennes et al., 2017
	Stimulus: RH strain (TLA) Technic: RNAseq Process time: 8, 24, 48 h in incubation Cryopreserved: No Supplemented: 10% FBS	ND	More than 2,400 differentially expressed genes	Zhou et al., 2016a
Human PBMC and <i>Plasmodium</i> sp.	Stimulus: <i>P. falciparum</i> crude lysate (50 mg) Technic: Flow cytometry and RT-qPCR Process time: 168 h in incubation Cryopreserved: No Supplemented: 10% FCS	1 \times 10 ⁶ /ND/ND	Crude antigens exhibited strong heterogeneity in the cytokine production	Kijogi et al., 2018
	Stimulus: <i>P. falciparum</i> crude lysate (50 mg) Technic: Flow cytometry and RT-qPCR Process time: 10 h in incubation Cryopreserved: No Supplemented: 2% FCS	ND	Decreased parasite growth and expression of PD-1 and IL-10 genes using L-citrulline supplemented media	Awasthi et al., 2017
	Stimulus: Peptide Pooling Scheme Technic: ELISPOT Process time: 18 h in incubation Cryopreserved: ND Supplemented: 10% FCS	1 \times 10 ⁶ /ND/96-well	Highest immunogenicity was identified at 7 days after boosting with 932 SFC compared with 57 SFC among control vaccinees	Mensah et al., 2016
	Stimulus: Recombinant RAMA protein Technic: ELISA Process time: ND Cryopreserved: ND Supplemented: ND	ND	High levels of interferon (IFN)- γ and interleukin (IL)-10 cytokines were detected	Changrob et al., 2016
	Stimulus: Peptides from CSP and AMA1 protein (10 μ g/ml) Technic: ELISPOT Process time: 36 h in incubation Cryopreserved: No Supplemented: No	1 \times 10 ⁶ /100 μ L/96-well	CSP and AMA1 peptides recalled IFN- γ responses from naturally exposed individuals	Ganeshan et al., 2016
	Stimulus: TLR1/2 ligand PAM3CSK4 (20 ng) Technic: ND Process time: 72 h in incubation Cryopreserved: Yes Supplemented: ND	2 \times 10 ⁵ /100 μ L/96-well	IL-1 β and TNF- α were significantly higher in severe malaria cases compared with healthy controls	Manning et al., 2016
	Stimulus: CelTOS (10 ng) or other single (1.25 μ g/ml) peptide pools Technic: ELISPOT Process time: 36 h in incubation Cryopreserved: No Supplemented: No	4 \times 10 ⁵ /100 μ L/96-well	Natural malaria transmission induces CelTOS-specific <i>ex vivo</i> IFN- γ	Anum et al., 2015
	Stimulus: Recombinant <i>C. parvum</i> p23 vaccine antigen Technic: Flow Cytometry Process time: ND Cryopreserved: ND Supplemented: ND	ND	Recombinant p23 vaccine antigen can stimulate a Type-1-like immune response	Wyatt et al., 2005
	Stimulus: Recombinant Eimeria Antigen (rEA) Technic: Flow Cytometry Process time: 72 h in incubation Cryopreserved: ND Supplemented: 5%FCS	25 \times 10 ⁶ /ND/6-well	rEA stimulates human NK cell effector functions including increasing levels of IFN- γ and Granzyme B	Aylsworth et al., 2013

(Continued)

TABLE 1 | Continued

Organism	Technical observations	PBMC culture (number of cells/final volume/culture plates)	Main findings	References
Sheep PBMC and <i>Babesia</i> sp.	Stimulus: BdE or BQ1E (10 µg/well) Technic: ELISA Process time: 120 h in incubation Cryopreserved: No Supplemented: 10% autologous plasma	2 × 10 ⁵ /ND/96-well	Production of IFN-γ and IL10 have key roles in the course of infection by <i>Babesia</i> sp.	Guan et al., 2010
Bovines PBMC and <i>Theileria</i> sp.	Stimulus: Sporozoites in homogenized infected tick Technic: RT-qPCR Process time: 48 h in incubation Cryopreserved: No Supplemented: 40% FBS	4 × 10 ⁶ /ND/6-well	MHC-DQ, SIRPA, PRNP, TLR10, cMAF and MAFB genes showed no change in mRNA expression after <i>T. annulata</i> infection	Panigrahi et al., 2016
	Stimulus: Sporozoites in homogenized infected tick Technic: RT-qPCR Process time: 48 h in incubation Cryopreserved: No Supplemented: 40% FBS	2 × 10 ⁶ /ND/6-well	Up-regulation in SIRPA, PRNP and MHC DQα genes and down-regulation in TLR10, cMAF and MAFB genes in crossbreds as compared to indigenous cattle was observed	Dewangan et al., 2015
	Stimulus: MPSP Peptides Technic: ELISPOT Process time: 42 h in incubation Cryopreserved: Yes Supplemented: No	1 × 10 ⁶ /100 µL/96-well	IFN-γ and IL-10 were detected in infected Holsteins but weak responses were exhibited by infected Angus and Japanese Black cattle	Yamaguchi et al., 2010

TLA, *T. gondii* Lysate Antigen; ND, Not determine; OT, Ocular Toxoplasmosis; NC, Negative Control; FCS, Fetal Calf Serum; MPSP, Major piroplasm surface protein; RAMA, Rhostry-associated membrane antigen; SFC, Spot Forming Cells (SFC)/106; CSP, *Plasmodium falciparum* circum- sporozoite protein; AMA-1, Apical membrane antigen-1.

not comparable, as researchers do not usually consider the time aspect when obtaining data. Most studies have shown that the time spent collecting data from cells after a stimulus varies; for example, no one has argued that a supernatant for cytokine measurement should be performed in an exact period of time. In the bulk of the studies, there are differences in the time accorded to the PBMC culture (varying from 48 h to 7 days) and even in the collection of supernatant for the measurement of IFN-γ after 12, 24 or 48 h (see Table 1). In this sense, the time between the making of the culture and the collection of data should be methodologically explained.

PBMCs IN OTHER APICOMPLEXAN PARASITES

Although apicomplexans comprise a large phylum of parasitic organisms (with more than 5,000 species), only a few have been studied in detail. Most of these studies focus on parasites that produce disease in humans such as *T. gondii*, *Plasmodium* spp. and *Cryptosporidium*. There are fewer studies on parasites that do not affect humans directly (e.g., *Eimeria*, *Babesia*, and *Theileria*). One of the most studied apicomplexan parasites is *Plasmodium*, the pathogen that causes malaria, one of the most important public health problems worldwide. Nearly all studies regarding this parasite that have used PBMCs have focused on the development of vaccine candidates, particularly those using the peptide polling scheme (Anum et al., 2015; Ganeshan et al., 2016; Mensah et al., 2016) or recombinant proteins (Garraud

et al., 2002; Garg et al., 2008; Gitau et al., 2014; Changrob et al., 2016). These studies have shown that, when PBMCs are challenged with molecules derived from *Plasmodium*, the immune response is characterized by Th1 cytokines such as IFN-γ, IL-1β, and TNF-α. The nuclear transcription factor kappa B (NF-κB) is what mainly regulates these proinflammatory cytokines. However, patients with complications of malaria have much lower levels of NF-κB than healthy controls do; as a consequence, these low levels limit the Th1 cell response (Punsawad et al., 2012).

Similarly, low levels of IL-1β and TNF-α have been found in patients with severe malaria. In one study, researchers analyzed 29 single-nucleotide polymorphism (SNPs) in the PBMCs of patients with various clinical conditions and found that only the “toll-like receptor-1” variant could contribute to this reduced cellular phenotype (Manning et al., 2016). Although this and other studies have shown that malaria infections inhibit the immune response, in one recent study, PBMCs from asymptomatic school children showed a strong heterogeneity of cytokine production, which suggests suppress immune responses could be related only with active infections (Kijogi et al., 2018). The donors’ immunological histories could influence this strong heterogeneous response because these PBMCs could present cross-reactivity with other infections such as schistosomiasis, leishmaniasis, toxoplasmosis, and Chagas disease. For this reason, other authors have proposed alternatives to the use of PBMCs in studying the primary immune response; one such alternative are

hematopoietic stem cells (naïve cells), which would reduce the discrepancies in mononuclear cell quality between studies (Chitsanoor et al., 2017).

In a study of *Cryptosporidium parvum* in calves recovering from cryptosporidiosis, scientists used PBMCs to evaluate the immunogenic potential of a specific protein (p23) as a vaccine antigen; in the first step, the researchers infected the calves with the parasite's oocysts, and in the next step, the PBMCs from the calves were stimulated with recombinant p23, showing that this antigen can stimulate a Type-1-like immune response among T cells (Wyatt et al., 2005). A similar response occurred in HIV-positive people infected with *Cryptosporidium*; their PBMCs were used to evaluate the cytokine profile after stimulation with the parasite crude extract, and this showed that INF- γ is one of the most important cytokines in the immune response against this parasite (Gomez Morales et al., 1999). With the help of IL-15, INF- γ eliminates this intracellular parasite by activating natural killer cells (Dann et al., 2005). In the case of *Eimeria*, PBMCs have been used to evaluate the parasite's proteins as adjuvants for vaccines or for immunostimulatory therapeutic agents in the treatment of human cancer (Aylsworth et al., 2013). For *Babesia*, PBMCs have been utilized to evaluate the cytokine profile response in cattle vaccination (East et al., 1997) and to identify the immune mechanisms involved in this parasite's pathogenicity (Guan et al., 2010).

With respect to *Theileria*, researchers have evaluated the mRNA levels of six immunological markers in PBMCs from crossbred, Tharparkar and Buffalo cattle after a parasite challenge. The markers included MHC class II DQ- α (BoLA-DQ), signal-regulatory protein alpha, prion protein, toll-like receptor 10, c-musculoaponeurotic fibrosarcoma oncogene homolog and V-maf avian musculoaponeurotic fibrosarcoma oncogene homolog B. For crossbred and Tharparkar cattle, significant differences occurred in the expression of genes in infected and uninfected cells (Dewangan et al., 2015), whereas the genes in Buffalo cattle did not show significant differences, suggesting that those genes had little effect in the progression of tropical theileriosis in the Buffalo species (Panigrahi et al., 2016). These results indicate that, although PBMCs are a good model for studying immunological phenomena, using them to make inferences or generalize results across species is not advisable, regardless of how evolutionarily close those species are.

The evidence suggests that PBMCs could be a good model for studying the immune response in apicomplexan parasites and for evaluating the efficiency of vaccine candidates, therapeutic agents and immunomodulatory molecules. However, these cells are not the most appropriate model for studying primo-infections (Chitsanoor et al., 2017). Therefore, despite all the benefits of the PBMC model, precautions should be taken related to its limitations and the type of immune response that is being evaluated.

PBMCs, OMICS, AND TOXOPLASMA

Omics techniques are powerful tools in modern biology, as they enable high-throughput measurements of many genes, proteins and metabolites in samples. A limited number of studies with

Toxoplasma have employed PBMCs in global transcriptional profiling, with only one using PBMCs from pigs (Zhou et al., 2016a; see **Table 1**). Some other studies have applied omics in research on *Toxoplasma* and cortical neurons, astrocytes, skeletal muscle cells, fibroblasts, and other cells; almost all of these were derived from murine models (Tanaka et al., 2013; Pittman et al., 2014; He et al., 2016; Zhou et al., 2016b). All these studies show that gene expression—and consequently, protein and metabolite levels—can undergo changes based on physiological conditions. The results of other studies suggest that the gene expression patterns in PBMCs greatly depend on temporal and interindividual variations and also show strong evidence that these cells' gene-expression profiles are very sensitive to long incubation periods (Baechler et al., 2004) in addition to being dramatically affected by cryopreservation (Yang et al., 2016). As yet, no reports in the literature exist regarding the analysis of global transcriptional profiling using human PBMCs stimulated with *T. gondii*. Therefore, omics techniques, including dual RNAseq (Westermann et al., 2017) in PBMCs from healthy individuals and toxoplasmosis sufferers, could provide excellent opportunities to obtain important and relevant data on this infectious disease. Given the number of methodological differences among studies, *ex vivo* assays can be considered a suitable model for the analysis of what occurs during infection with *Toxoplasma* in humans. These assays emerge as a good alternative for these main reasons: (i) an *ex vivo* experiment should usually be done within a 24 h period in order to minimize the effect that stress generates on the cells; (ii) PBMCs' characteristics are very interesting because they are primary cells, are not immortalized and have the genetic backgrounds of real patients; and (iii) *ex vivo* experiments have the advantage of being analyzable very shortly after sampling, which is particularly critical in studies of gene expression, where data can be altered dramatically with the time factor.

CONCLUSION

PBMCs allow for the study of the immune-system response to infections with apicomplexan parasites, the evaluation of vaccine candidates and the development of immunotherapeutic strategies. To obtain reproducible and comparable results, several variables must be optimized when working with this model. The evaluated response of human PBMCs in apicomplexans has also been restricted to a few cytokines, so it is highly advisable to include additional immunological techniques that can comprehensively reflect the host's response to the pathogen.

AUTHOR CONTRIBUTIONS

JA and AH contributed to the conception of the publication and prepared the manuscript. Both authors read and approved the final manuscript.

ACKNOWLEDGMENTS

We acknowledge the funding from the COLCIENCIAS program, project: 1113-744-55-323.

REFERENCES

- Alfonzo, M., Badell, E., Pourcel, C., Dumas, G., Colle, J. H., and Scott-Algara, D. (2005). Cell-mediated and not humoral immune response is responsible for partial protection against toxoplasmosis in SCID mice reconstituted with human PBMC. *Immunologia* 24, 273–282.
- Alfonzo, M., Blanc, D., Troadec, C., Huerre, M., Eliazewicz, M., González, G., et al. (2002). Temporary restoration of immune response against *Toxoplasma gondii* in HIV-infected individuals after HAART, as studied in the hu-PBMC-SCID mouse model. *Clin. Exp. Immunol.* 129, 411–419. doi: 10.1046/j.1365-2249.2002.01941.x
- Anum, D., Kusi, K. A., Ganeshan, H., Hollingdale, M. R., Ofori, M. F., Koram, K. A., et al. (2015). Measuring naturally acquired *ex vivo* IFN- γ responses to *Plasmodium falciparum* cell-traversal protein for ookinets and sporozoites (CelTOS) in Ghanaian adults. *Malar. J.* 14, 1–8. doi: 10.1186/s12936-014-0539-5
- Autissier, P., Soulas, C., Burdo, T. H., and Williams, K. C. (2010). Evaluation of a 12-color flow cytometry panel to study lymphocyte, monocyte, and dendritic cell subsets in humans. *Cytom. Part A* 77, 410–419. doi: 10.1002/cyto.a.20859
- Awasthi, V., Chauhan, R., Chattopadhyay, D., and Das, J. (2017). Effect of L-arginine on the growth of *Plasmodium falciparum* and immune modulation of host cells. *J. Vector Borne Dis.* 54, 139–145.
- Aylsworth, C. F., Aldhamen, Y. A., Seregin, S. S., Godbehere, S., and Amalfitano, A. (2013). Activation of human natural killer cells by the novel innate immune modulator recombinant *Eimeria* antigen. *Hum. Immunol.* 74, 916–926. doi: 10.1016/j.humimm.2013.04.035
- Baechler, E. C., Batliwalla, F. M., Karypis, G., Gaffney, P. M., Moser, K., Ortmann, W. A., et al. (2004). Expression levels for many genes in human peripheral blood cells are highly sensitive to *ex vivo* incubation. *Genes Immun.* 5, 347–353. doi: 10.1038/sj.gene.6364098
- Baust, J. M. (2002). Molecular mechanisms of cellular demise associated with cryopreservation failure. *Cell Preserv. Technol.* 1, 17–31. doi: 10.1089/15383440260073266
- Bayram Delibaş, S., Turgay, N., and Gürüz, A. Y. (2009). The role of cytokines in the immunopathogenesis of toxoplasmosis. *Turkiye Klin. J. Med. Sci.* 29, 1217–1221.
- Burczynski, M. E., and Dorner, A. J. (2006). Transcriptional profiling of peripheral blood cells in clinical pharmacogenomic studies. *Pharmacogenomics* 7, 187–202. doi: 10.2217/14622416.7.2.187
- Cardona, N. I., Moncada, D. M., and Gómez-Marin, J. E. (2015). A rational approach to select immunogenic peptides that induce IFN- γ response against *Toxoplasma gondii* in human leukocytes. *Immunobiology* 220, 1337–1342. doi: 10.1016/j.imbio.2015.07.009
- Changrob, S., Wang, B., Han, J. H., Lee, S. K., Nyunt, M. H., Lim, C. S., et al. (2016). Naturally-acquired immune response against *Plasmodium vivax* rhoptry-associated membrane antigen. *PLoS ONE* 11:e148723. doi: 10.1371/journal.pone.0148723
- Chitsanoor, S., Somsri, S., Panburana, P., Mungthin, M., Ubalee, R., Emyeam, M., et al. (2017). A novel *in vitro* model reveals distinctive modulatory roles of *Plasmodium falciparum* and *Plasmodium vivax* on naïve cell-mediated immunity. *Malar. J.* 16, 1–10. doi: 10.1186/s12936-017-1781-4
- Cong, H., Mui, E. J., Witola, W. H., Sidney, J., Alexander, J., Sette, A., et al. (2011). Towards an immunosense vaccine to prevent toxoplasmosis: protective *Toxoplasma gondii* epitopes restricted by HLA-A*0201. *Vaccine* 29, 754–762. doi: 10.1016/j.vaccine.2010.11.015
- Cong, H., Mui, E. J., Witola, W. H., Sidney, J., Alexander, J., Sette, A., et al. (2012). *Toxoplasma gondii* HLA-B*0702-restricted GRA720-28 peptide with adjuvants and a universal helper T cell epitope elicits CD8⁺ T cells producing interferon- γ and reduces parasite burden in HLA-B*0702 mice. *Hum. Immunol.* 73, 1–10. doi: 10.1016/j.humimm.2011.10.006
- Corkum, C. P., Ings, D. P., Burgess, C., Karwowska, S., Kroll, W., and Michalak, T. I. (2015). Immune cell subsets and their gene expression profiles from human PBMC isolated by Vacutainer Cell Preparation Tube (CPT™) and standard density gradient. *BMC Immunol.* 16, 1–18. doi: 10.1186/s12865-015-0113-0
- Cornelissen, J. B. W. J., van der Giessen, J. W. B., Takumi, K., Teunis, P. F. M., and Wisselink, H. J. (2014). An experimental *Toxoplasma gondii* dose response challenge model to study therapeutic or vaccine efficacy in cats. *PLoS ONE* 9:e104740. doi: 10.1371/journal.pone.0104740
- Cosentino, L. M., Corwin, W., Baust, J. M., Diaz-Mayoral, N., Cooley, H., Shao, W., et al. (2007). Preliminary report: evaluation of storage conditions and cryococktails during peripheral blood mononuclear cell cryopreservation. *Cell Preserv. Technol.* 5, 189–204. doi: 10.1089/cpt.2007.9987
- Dann, S. M., Wang, H., Gambarin, K. J., Actor, J. K., Robinson, P., Lewis, D. E., et al. (2005). Interleukin-15 activates human natural killer cells to clear the intestinal protozoan *Cryptosporidium*. *J. Infect. Dis.* 192, 1294–1302. doi: 10.1086/444393
- Dewangan, P., Panigrahi, M., Kumar, A., Saravanan, B. C., Ghosh, S., Asaf, V. N. M., et al. (2015). The mRNA expression of immune-related genes in crossbred and Tharparkar cattle in response to *in vitro* infection with *Theileria annulata*. *Mol. Biol. Rep.* 42, 1247–1255. doi: 10.1007/s11033-015-3865-y
- Dubey, J. P. (2008). The history of *Toxoplasma gondii* - The first 100 years. *J. Eukaryot. Microbiol.* 55, 467–475. doi: 10.1111/j.1550-7408.2008.00345.x
- Dubey, J. P. (2010). *Toxoplasmosis of Animals and Humans*. Boca Raton, FL: CRC Press.
- Dzitko, K., Grzybowski, M. M., Pawelczyk, J., Dziadek, B., Gatkowska, J., Staczek, P., et al. (2015). Phytoecdysteroids as modulators of the *Toxoplasma gondii* growth rate in human and mouse cells. *Parasit. Vect.* 8:422. doi: 10.1186/s13071-015-1019-7
- Dzitko, K., Ławnicka, H., Gatkowska, J., Dziadek, B., Komorowski, J., and Długowska, H. (2012). Inhibitory effect of prolactin on *Toxoplasma* proliferation in peripheral blood mononuclear cells from patients with hyperprolactinemia. *Parasite Immunol.* 34, 302–311. doi: 10.1111/j.1365-3024.2012.01359.x
- East, I. J., Zakrzewski, H., Gale, K. R., Leatch, G., Dimmock, C. M., Thomas, M. B., et al. (1997). Vaccination against *Babesia bovis*: T cells from protected and unprotected animals show different cytokine profiles. *Int. J. Parasitol.* 27, 1537–1545. doi: 10.1016/S0020-7519(97)00141-0
- Ferreira, I. M. R., Vidal, J. E., de Mattos, C., de, C. B., de Mattos, L. C., Qu, D., et al. (2011). *Toxoplasma gondii* isolates: multilocus RFLP-PCR genotyping from human patients in São Paulo State, Brazil identified distinct genotypes. *Exp. Parasitol.* 29, 190–195. doi: 10.1016/j.exppara.2011.06.002
- Fowke, K. R., Behnke, J., Hanson, C., Shea, K., and Cosentino, L. M. (2000). Apoptosis: A method for evaluating the cryopreservation of whole blood and peripheral blood mononuclear cells. *J. Immunol. Methods* 244, 139–144. doi: 10.1016/S0022-1759(00)00263-5
- Ganeshan, H., Kusi, K. A., Anum, D., Hollingdale, M. R., Peters, B., Kim, Y., et al. (2016). Measurement of *ex vivo* ELISpot interferon-gamma recall responses to *Plasmodium falciparum* AMA1 and CSP in Ghanaian adults with natural exposure to malaria. *Malar. J.* 15, 1–15. doi: 10.1186/s12936-016-1098-8
- Garg, S., Chauhan, S. S., Singh, N., and Sharma, Y. D. (2008). Immunological responses to a 39.8 kDa *Plasmodium vivax* tryptophan-rich antigen (PvTRAg39.8) among humans. *Microbes Infect.* 10, 1097–1105. doi: 10.1016/j.micinf.2008.05.008
- Garraud, O., Perraut, R., Diouf, A., Nambei, W. S., Tall, A., Spiegel, A., et al. (2002). Regulation of antigen-specific immunoglobulin G subclasses in response to conserved and polymorphic *Plasmodium falciparum* antigens in an *in vitro* model. *Infect. Immun.* 70, 2820–2827. doi: 10.1128/IAI.70.6.2820-2827.2002
- Gitau, E. N., Tuju, J., Karanja, H., Stevenson, L., Requena, P., Kimani, E., et al. (2014). CD4⁺ T Cell Responses to the *Plasmodium falciparum* erythrocyte membrane protein 1 in children with mild malaria. *J. Immunol.* 192, 1753–1761. doi: 10.4049/jimmunol.1200547
- Glisic-Milosavljevic, S., Waukau, J., Jana, S., Jaiwala, P., Rovinsky, J., and Ghosh, S. (2005). Comparison of apoptosis and mortality measurements in peripheral blood mononuclear cells (PBMCs) using multiple methods. *Cell Prolif.* 38, 301–311. doi: 10.1111/j.1365-2184.2005.00351.x
- Gomez Morales, M. A., La Rosa, G., Ludovisi, A., Onori, A. M., and Pozio, E. (1999). Cytokine profile induced by *Cryptosporidium* antigen in peripheral blood mononuclear cells from immunocompetent and immunosuppressed persons with cryptosporidiosis. *J. Infect. Dis.* 179, 967–973.
- Guan, G., Chauvin, A., Yin, H., Luo, J., and Moreau, E. (2010). Course of infection by *Babesia* sp. BQ1 (Linton) and *B. divergens* in sheep depends on the production of IFN γ and IL10. *Parasite Immunol.* 32, 143–152. doi: 10.1111/j.1365-3024.2009.01169.x

- He, J.-J., Ma, J., Elsheikha, H. M., Song, H.-Q., Huang, S.-Y., Zhu, X.-Q., et al. (2016). Transcriptomic analysis of mouse liver reveals a potential hepatointerpathogenic mechanism in acute *Toxoplasma gondii* infection. *Parasit. Vectors* 9:427. doi: 10.1186/s13071-016-1716-x
- He, J. A., Ma, J. A. B., Song, H. Q. A., Zhou, D. H. A., Wang, J. L. A., Huang, S. Y. A., et al. (2015). Transcriptomic analysis of global changes in cytokine expression in mouse spleens following acute *Toxoplasma gondii* infection. *Parasitol. Res.* 115, 703–712. doi: 10.1007/s00436-015-4792-5
- Hunter, C. A., and Sibley, L. D. (2012). Modulation of innate immunity by *Toxoplasma gondii* virulence effectors. *Nat. Rev. Microbiol.* 10, 766–778. doi: 10.1038/nrmicro2858
- Jennes, M., De Craeye, S., Devriendt, B., Dierick, K., Dorny, P., and Cox, E. (2017). Strain- and dose-dependent reduction of *Toxoplasma gondii* burden in pigs is associated with interferon-gamma production by CD8⁺ lymphocytes in a heterologous challenge model. *Front. Cell. Infect. Microbiol.* 7:232. doi: 10.3389/fcimb.2017.00232
- Kijogi, C., Kimura, D., Bao, L. Q., Nakamura, R., Chadeka, E. A., Cheruiyot, N. B., et al. (2018). Modulation of immune responses by *Plasmodium falciparum* infection in asymptomatic children living in the endemic region of Mbita, western Kenya. *Parasitol. Int.* 67, 284–293. doi: 10.1016/j.parint.2018.01.001
- Lahmar, I., Abou-Bacar, A., Abdelrahman, T., Guinard, M., Babba, H., Ben Yahia, S., et al. (2009). Cytokine profiles in toxoplasmic and viral uveitis. *J. Infect. Dis.* 199, 1239–1249. doi: 10.1086/597478
- Little, R. J., D'Agostino, R., Cohen, M. L., Dickersin, K., Emerson, S. S., Farrar, J. T., et al. (2012). The prevention and treatment of missing data in clinical trials. *N. Engl. J. Med.* 367, 1355–1360. doi: 10.1056/NEJMs1203730
- Maia, M. M., Meira-Strejevitch, C. S., Pereira-Chioccola, V. L., de Hippólito, D. D. C., Silva, V. O., Brandão de Mattos, C. C., et al. (2017). Evaluation of gene expression levels for cytokines in ocular toxoplasmosis. *Parasite Immunol.* 39:e12462. doi: 10.1111/pim.12462
- Mallone, R., Mannering, S. I., Brooks-Worrell, B. M., Durinovic-Bell, I., Cilio, C. M., Wong, F. S., et al. (2011). Isolation and preservation of peripheral blood mononuclear cells for analysis of islet antigen-reactive T cell responses: position statement of the T-cell workshop committee of the immunology of diabetes society. *Clin. Exp. Immunol.* 163, 33–49. doi: 10.1111/j.1365-2249.2010.04272.x
- Manning, L., Cutts, J., Stanisic, D. I., Laman, M., Carmagnac, A., Allen, S., et al. (2016). A Toll-like receptor-1 variant and its characteristic cellular phenotype is associated with severe malaria in Papua New Guinean children. *Genes Immun.* 17, 52–59. doi: 10.1038/gene.2015.50
- Martens, S., Parvanova, I., Zerrahn, J., Griffiths, G., Schell, G., Reichmann, G., et al. (2005). Disruption of *Toxoplasma gondii* parasitophorous vacuoles by the mouse p47-resistance GTPases. *PLoS Pathog.* 1:e24. doi: 10.1371/journal.ppat.0010024
- Massanella, M., Gianella, S., Schrier, R., Dan, J. M., Pérez-Santiago, J., Oliveira, M. F., et al. (2015). Methamphetamine use in HIV-infected individuals affects T-cell function and viral outcome during suppressive antiretroviral therapy. *Sci. Rep.* 5:13179. doi: 10.1038/srep13179
- Meira, C. S., Pereira-Chioccola, V. L., Vidal, J. E., de Mattos, C. C. B., Motoie, G., Costa-Silva, T. A., et al. (2014). Cerebral and ocular toxoplasmosis related with IFN- γ , TNF- α , and IL-10 levels. *Front. Microbiol.* 5:492. doi: 10.3389/fmicb.2014.00492
- Meira, C. S., Pereira-Chioccola, V. L., Vidal, J. E., Motoie, G., da Costa-Silva, T. A., Gava, R., et al. (2015). Evolution of cytokine profile during the treatment of cerebral toxoplasmosis in HIV-infected patients. *J. Immunol. Methods* 426, 14–18. doi: 10.1016/j.jim.2015.07.005
- Meira-Strejevitch, C. S., Pereira-Chioccola, V. L., Maia, M. M., de Hippólito, D. D. C., Wang, H.-T. L., Motoie, G., et al. (2017). Reference genes for studies in infectious parasitic diseases in five types of human tissues. *Gene Rep.* 7, 98–105. doi: 10.1016/j.genrep.2017.03.002
- Mensah, V. A., Gueye, A., Ndiaye, M., Edwards, N. J., Wright, D., Anagnostou, N. A., et al. (2016). Safety, immunogenicity and efficacy of prime-boost vaccination with chad63 and mva encoding me-trap against *plasmodium falciparum* infection in adults in senegal. *PLoS One* 11:e167951. doi: 10.1371/journal.pone.0167951
- Nau, J., Eller, S. K., Wenning, J., Spekker-Bosker, K. H., Schrotten, H., Schwerk, C., et al. (2017). Experimental porcine *Toxoplasma gondii* infection as a representative model for human toxoplasmosis. *Mediators Inflamm.* 2017:3260289. doi: 10.1155/2017/3260289
- Niedelman, W., Gold, D. A., Rosowski, E. E., Sprockholt, J. K., Lim, D., Arenas, A. F., et al. (2012). The rho-try proteins ROP18 and ROP5 mediate *Toxoplasma gondii* evasion of the Murine, But Not the human, interferon-gamma response. 8:e1002784. doi: 10.1371/journal.ppat.1002784
- Nogueira, R. S., Gomes-Silva, A., Bittar, R. C., Silva Mendonça, D., Amato, V. S., da Silva Mattos, M., et al. (2014). Antigen-triggered interferon- γ and interleukin-10 pattern in cured mucosal leishmaniasis patients is shaped during the active phase of disease. *Clin. Exp. Immunol.* 177, 679–686. doi: 10.1111/cei.12364
- O'Neill, R. T., and Temple, R. (2012). The prevention and treatment of missing data in clinical trials: an FDA perspective on the importance of dealing with it. *Clin. Pharmacol. Ther.* 91, 550–554. doi: 10.1038/clpt.2011.34
- Panigrahi, M., Kumar, A., Bhushan, B., Ghosh, S., Saravanan, B. C., Sulabh, S., et al. (2016). No change in mRNA expression of immune-related genes in peripheral blood mononuclear cells challenged with *Theileria annulata* in Murrah buffalo (*Bubalus bubalis*). *Ticks Tick. Borne. Dis.* 7, 754–758. doi: 10.1016/j.ttbdis.2016.03.006
- Pfaff, A. W., Georges, S., Abou-Bacar, A., Letscher-Bru, V., Klein, J.-P., Mousli, M., et al. (2005). *Toxoplasma gondii* regulates ICAM-1 mediated monocyte adhesion to trophoblasts. *Immunol. Cell Biol.* 83, 483–489. doi: 10.1111/j.1440-1711.2005.01356.x
- Pittman, K. J., Aliota, M. T., and Knoll, L. J. (2014). Dual transcriptional profiling of mice and *Toxoplasma gondii* during acute and chronic infection. *BMC Genomics* 15:806. doi: 10.1186/1471-2164-15-806
- Prigione, I., Chiesa, S., Taverna, P., Ceccarelli, R., Frulio, R., Morandi, F., et al. (2006). T cell mediated immune responses to *Toxoplasma gondii* in pregnant women with primary toxoplasmosis. *Microbes Infect.* 8, 552–560. doi: 10.1016/j.micinf.2005.08.008
- Punsawad, C., Krudsood, S., Maneerat, Y., Chaisri, U., Tangpukdee, N., Pongponratn, E., et al. (2012). Activation of nuclear factor kappa B in peripheral blood mononuclear cells from malaria patients. *Malar. J.* 11:191. doi: 10.1186/1475-2875-11-191
- Rezende-Oliveira, K., Silva, N. M., Mineo, J. R., and Rodrigues Junior, V. (2012). Cytokines and chemokines production by mononuclear cells from parturient women after stimulation with live *Toxoplasma gondii*. *Placenta* 33, 682–687. doi: 10.1016/j.placenta.2012.05.013
- Riedhammer, C., Halbritter, D., and Weissert, R. (2016). Peripheral blood mononuclear cells: isolation, freezing, thawing, and culture christine. *Methods Mol. Biol.* 1304, 53–61. doi: 10.1007/7651_2014_99
- Seok, J., Warren, H. S., Cuenca, A. G., Mindrinos, M. N., Baker, H. V., Xu, W., et al. (2013). Genomic responses in mouse models poorly mimic human inflammatory diseases. *Proc. Natl. Acad. Sci. U.S.A.* 110, 3507–3512. doi: 10.1073/pnas.1222878110
- Sullivan, W. J., and Jeffers, V. (2012). Mechanisms of *Toxoplasma gondii* persistence and latency. *FEMS Microbiol. Rev.* 36, 717–733. doi: 10.1111/j.1574-6976.2011.00305.x
- Szabo, E. K., and Finney, C. A. M. (2017). *Toxoplasma gondii*: one organism, multiple models. *Trends Parasitol.* 33, 113–127. doi: 10.1016/j.pt.2016.11.007
- Tan, T. G., Mui, E., Cong, H., Witola, W. H., Montpetit, A., Muench, S. P., et al. (2010). Identification of *T. gondii* epitopes, adjuvants, and host genetic factors that influence protection of mice and humans. *Vaccine* 28, 3977–3989. doi: 10.1016/j.vaccine.2010.03.028
- Tanaka, N., Ashour, D., Dratz, E., and Halonen, S. (2016). Use of human induced pluripotent stem cell-derived neurons as a model for Cerebral Toxoplasmosis. *Microbes Infect.* 18, 496–504. doi: 10.1016/j.micinf.2016.03.012
- Tanaka, S., Nishimura, M., Ihara, F., Yamagishi, J., Suzuki, Y., and Nishikawa, Y. (2013). Transcriptome analysis of mouse brain infected with *toxoplasma gondii*. *Infect. Immun.* 81, 3609–3619. doi: 10.1128/IAI.00439-13
- Tenter, A. M., Heckeroth, A. R., and Weiss, L. M. (2000). *Toxoplasma gondii*: from animals to humans. *Int. J. Parasitol.* 30, 1217–1258. doi: 10.1016/S0020-7519(00)00124-7
- Tosh, K. W., Mittereder, L., Bonne-Annee, S., Hieny, S., Nutman, T. B., Singer, S. M., et al. (2016). The IL-12 response of primary human dendritic cells and monocytes to *Toxoplasma gondii* is stimulated by phagocytosis of live parasites rather than host cell invasion. *J. Immunol.* 196, 345–356. doi: 10.4049/jimmunol.1501558
- Unno, A., Kachi, S., Batanova, T. A., Ohno, T., Elhawary, N., Kitoh, K., et al. (2013). *Toxoplasma gondii* tachyzoite-infected

- peripheral blood mononuclear cells are enriched in mouse lungs and liver. *Exp. Parasitol.* 134, 160–164. doi: 10.1016/j.exppara.2013.03.006
- Vendrell, J. P., Pratlong, F., Decostert, A., Boulot, P., Conge, A. M., and Darcyt, F. (1992). Secretion of *Toxoplasma gondii*-specific antibody *in vitro* by peripheral blood mononuclear cells as a new marker of acute toxoplasmosis *in vivo*. *Clin. Exp. Immunol.* 89, 126–130.
- Weinberg, A., Song, L. Y., Wilkening, C. L., Fenton, T., Hural, J., Louzaod, R., et al. (2010). Optimization of storage and shipment of cryopreserved peripheral blood mononuclear cells from HIV-infected and uninfected individuals for ELISPOT assays. *J. Immunol. Methods* 363, 42–50. doi: 10.1016/j.jim.2010.09.032
- Westermann, A. J., Barquist, L., and Vogel, J. (2017). Resolving host-pathogen interactions by dual RNA-seq. *PLoS Pathog.* 13:e1006033. doi: 10.1371/journal.ppat.1006033
- Wisniewski, S. R., Leon, A. C., Otto, M. W., and Trivedi, M. H. (2006). Prevention of missing data in clinical research studies. *Biol. Psychiatry* 59, 997–1000. doi: 10.1016/j.biopsych.2006.01.017
- Wunsch, M., Caspell, R., Kuerten, S., Lehmann, P. V., and Sundararaman, S. (2015). Serial measurements of apoptotic cell numbers Provide Better Acceptance Criterion for PBMC quality than a single measurement prior to the T cell assay. *Cells* 4, 40–55. doi: 10.3390/cells4010040
- Wyatt, C. R., Lindahl, S., Austin, K., Kapil, S., and Branch, J. (2005). Response of T lymphocytes from previously infected calves to recombinant *Cryptosporidium parvum* P23 vaccine antigen. *J. Parasitol.* 91, 1239–1242. doi: 10.1645/GE-3446RN.1
- Yamaguchi, T., Yamanaka, M., Ikehara, S., Kida, K., Kuboki, N., Mizuno, D., et al. (2010). Generation of IFN- γ -producing cells that recognize the major piroplasm surface protein in *Theileria orientalis*-infected bovines. *Vet. Parasitol.* 171, 207–215. doi: 10.1016/j.vetpar.2010.03.038
- Yang, J., Diaz, N., Adelsberger, J., Zhou, X., Stevens, R., Rupert, A., et al. (2016). The effects of storage temperature on PBMC gene expression. *BMC Immunol.* 17, 1–15. doi: 10.1186/s12865-016-0144-1
- Zhou, C.-X., Zhou, D.-H., Liu, G.-X., Suo, X., and Zhu, X.-Q. (2016a). Transcriptomic analysis of porcine PBMCs infected with *Toxoplasma gondii* RH strain. *Acta Trop.* 154, 82–88. doi: 10.1016/j.actatropica.2015.11.009
- Zhou, C. X., Elsheikha, H. M., Zhou, D. H., Liu, Q., Zhu, X. Q., and Suo, X. (2016b). Dual identification and analysis of differentially expressed transcripts of porcine PK-15 cells and *Toxoplasma gondii* during *in vitro* infection. *Front. Microbiol.* 7:721. doi: 10.3389/fmicb.2016.00721

Conflict of Interest Statement: The authors declare that the research was conducted in the absence of any commercial or financial relationships that could be construed as a potential conflict of interest.

Copyright © 2019 Acosta Davila and Hernandez De Los Rios. This is an open-access article distributed under the terms of the Creative Commons Attribution License (CC BY). The use, distribution or reproduction in other forums is permitted, provided the original author(s) and the copyright owner(s) are credited and that the original publication in this journal is cited, in accordance with accepted academic practice. No use, distribution or reproduction is permitted which does not comply with these terms.



Emergence of Leptin in Infection and Immunity: Scope and Challenges in Vaccines Formulation

Dayakar Alti^{1*†}, Chandrasekaran Sambamurthy² and Suresh K. Kalangi^{1*†}

¹ School of Life Sciences, University of Hyderabad, Hyderabad, India, ² BIO5 Institute, University of Arizona, Tucson, AZ, United States

OPEN ACCESS

Edited by:

Kamal El. Bissati,
University of Chicago, United States

Reviewed by:

Huafeng Wang,
California Institute for Biomedical
Research, United States
Aziz Alami Chentoufi,
Centre Hospitalier Universitaire
Mohammed VI, Morocco

*Correspondence:

Dayakar Alti
dayakar.pcu@gmail.com
Suresh K. Kalangi
suresh.kalangi@
indrashiluniversity.edu.in

[†]These authors have contributed
equally to this work.

*Present Address:

Suresh K. Kalangi,
Department of Biosciences, School of
Sciences, Indrashil University,
Mehsana, India

Received: 23 December 2017

Accepted: 20 April 2018

Published: 09 May 2018

Citation:

Alti D, Sambamurthy C and
Kalangi SK (2018) Emergence of
Leptin in Infection and Immunity:
Scope and Challenges in Vaccines
Formulation.
Front. Cell. Infect. Microbiol. 8:147.
doi: 10.3389/fcimb.2018.00147

Deficiency of leptin (*ob/ob*) and/or desensitization of leptin signaling (*db/db*) and elevated expression of suppressor of cytokine signaling-3 (SOCS3) reported in obesity are also reported in a variety of pathologies including hypertriglyceridemia, insulin resistance, and malnutrition as the risk factors in host defense system. Viral infections cause the elevated SOCS3 expression, which inhibits leptin signaling. It results in immunosuppression by T-regulatory cells (Tregs). The host immunity becomes incompetent to manage pathogens' attack and invasion, which results in the accelerated infections and diminished vaccine-specific antibody response. Leptin was successfully used as mucosal vaccine adjuvant against *Rhodococcus equi*. Leptin induced the antibody response to *Helicobacter pylori* vaccination in mice. An integral leptin signaling in mucosal gut epithelial cells offered resistance against *Clostridium difficile* and *Entamoeba histolytica* infections. We present in this review, the intervention of leptin in lethal diseases caused by microbial infections and propose the possible scope and challenges of leptin as an adjuvant tool in the development of effective vaccines.

Keywords: leptin, obesity, malnutrition, immunity, infections, vaccination

INTRODUCTION

Leptin and Leptin Receptors

Leptin was discovered as the product of obese (*ob*) gene (Zhang et al., 1994), which is located on the long arm of 7th chromosome at the position 31.3 (7q31.3) of about ~20 Kb length (Considine and Caro, 1997). The nascent non-glycosylated protein has a M.W. 16 kDa, with an NH₂ terminal signal peptide (21-amino acids). Biologically active form of leptin is 146 amino acids peptide. Leptin freely circulates in the blood and exerts its actions via membrane bound leptin receptors (LEPRs) (Ceddia, 2005). Leptin receptor gene (*Ob-R*) comprises four short-isoforms (*Ob-Ra*, *Rc*, *Rd*, and *Rf*), one long-isoform (*Ob-Rb*) and one soluble-isoform (*Ob-Re*) (Tartaglia, 1997). Six isoforms of *Ob-R* are identical to each other and contain 805 amino acids and 1–14 exons present in extracellular domain. *Ob-Rb* isoform consist of long intracellular domain that resembles the type-I cytokine receptor signaling domain and transduces via Janus tyrosine kinase/signal transducer and activator of transcription (JAK/STAT) pathway (Houseknecht and Portocarrero, 1998; Licinio et al., 1998). In fact, most of the biological functions of leptin are exerted by *Ob-Rb*-JAK/STAT signaling cascade, which is present predominantly in hypothalamus but has moderate presence in other tissues. *Ob-Ra* and *Ob-Rc* isoforms regulate the transportation of leptin across the blood-brain barrier (BBB) to hypothalamus and *Ob-Rf* also performs the same function to a lesser extent. *Ob-Re* isoform is a soluble binding protein and lacks the transmembrane and cytoplasmic domains (Figure 1). It

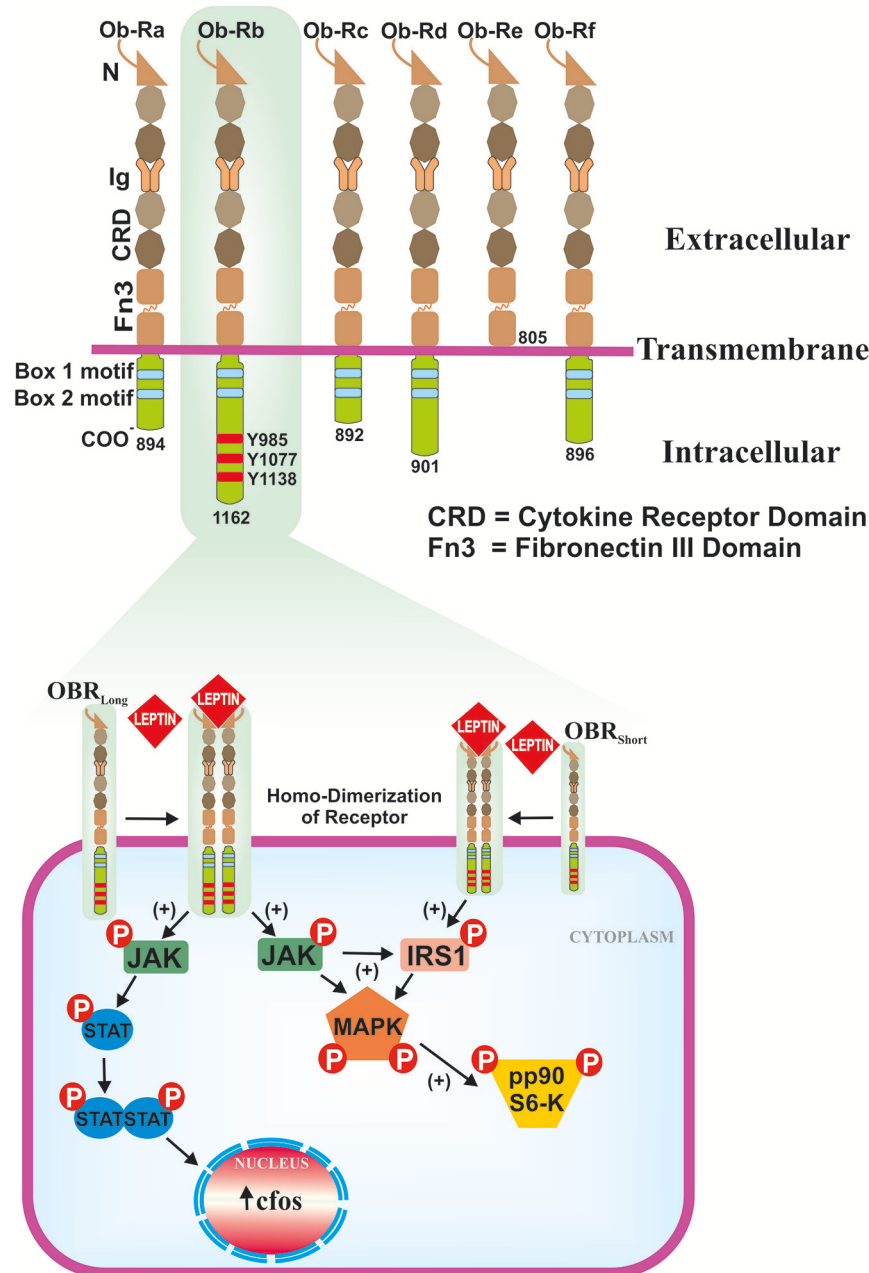


FIGURE 1 | Isoforms of the leptin receptor and ob-Rb signaling pathways. Six isoforms (Ob-Ra to Ob-Rf) of LEPR are existed, all are identical in extracellular ligand binding domains but differ in C-terminus. Out of six isoforms, only Ob-Rb encodes protein motifs involve in the activation of JAK-STAT signaling pathway. Ob-Rb has three tyrosine conserved regions (Y985, Y1077 & Y1138) in cytoplasmic domain. Later, it functions as a docking site for STAT3. Binding of leptin to ob-Rb leads to receptor homodimerization, in turn activates JAK/STAT pathways that result in the activation of c-fos. Ob-Rb also phosphorylates JAK to the activation of insulin receptor substrate-1 (IRS-1) and MAPK.

binds to the plasma leptin and inhibits its glomerular clearance, but it does not interfere with the binding of leptin to Ob-Rb. Ob-Re infusion into *ob/ob* null mice enhances the activity of leptin and its overexpression independent of the adipose leptin expression (Huang et al., 2001).

Functionally, leptin is a hormone derived from adipocytes (La Cava and Matarese, 2004), in response to the food

intake and energy balance. It conveys the signals to the hypothalamus/central nervous system (CNS) and peripheral organs, to maintain the metabolic homeostasis. The systemic leptin concentrations are influenced by the total fat mass (Grinspoon et al., 1996) and body mass index (BMI). They are also influenced by metabolic hormones, sex, and body energy demands. Congenital leptin deficiency in humans is

rare and limited to <5%, reported in obese population in the United States. Diet-induced obesity in humans' results in the increase in systemic leptin levels and its resistance is due to the desensitized LEPRs (Burguera et al., 2000; Morrison, 2008); conversely, the systemic leptin levels are reduced in malnutrition and in starvation. Malnutrition is a burning issue and affects around 826 million people of the world population (Katona and Katona-Apte, 2008). Children, <5 years of age, are the major victims of malnutrition, which accounts for 2.2 million annual deaths globally (Black et al., 2008). Malnutrition affects both innate and acquired immunity (Woodward, 1998; Schaible and Stefan, 2007), and the ratio of CD4+/CD8+ T cells (Chandra, 1992). People with malnutrition are vulnerable to infections because of immunosuppression (Faggioni et al., 2000b) and defective cytokine production (Zhang et al., 1997).

In this article, we discuss in detail about the leptin dependent regulation of immune responses, relation between microbial infections and leptin signaling; and discuss the potential of leptin as vaccine adjuvant.

LEPTIN IN IMMUNE SYSTEM

Leptin bridges a link between nutritional status and immune system of individuals. Human leptin has four α -helices similar to that of long-chain α -helical cytokine family, which includes interleukin (IL)-6, IL-11, IL-12, leukemia inhibitory factor (LIF), granulocyte-colony stimulating factor (G-CSF), ciliary neurotrophic factor (CNTF), and oncostatin (Zhang et al., 1997). LEPRs exhibit homology with the glycoprotein (gp)-130 signal transducing subunit of the IL-6 type cytokine receptor (Tartaglia et al., 1995; Baumann et al., 1996; Lee et al., 1996). Because of the structural similarities with the above-mentioned immune components, leptin acts as a cytokine. It is also called "adipokine" since it is derived from adipose tissue. As an adipokine, leptin regulates the normal development of hematopoiesis, angiogenesis, and innate & adaptive immunity (Loffreda et al., 1998; Santos-Alvarez et al., 1999; Martín-Romero et al., 2000; La Cava and Matarese, 2004; Matarese et al., 2005) (see **Table 1**). In immune cells, leptin and LEPRs predominantly activates JAK2/STAT3 signaling cascade, in which the phosphorylated tyrosine-1138 (pTyr¹¹³⁸) of Ob-Rb intracellular domain acts as a docking site for STAT3 (Papathanassoglou et al., 2006). Beside this, leptin also triggers SH2-containing tyrosine phosphatase (SHP2)-dependent mitogen-activated protein kinase (MAPK) and phosphoinositide 3-kinase/serine/threonine protein kinase/mammalian target of rapamycin (PI3K/Akt/mTOR) pathway in which, the pTyr⁹⁸⁵ residue acts as a docking site for SHP-2 (Fernández-Riejos et al., 2010). Leptin signaling is inhibited by the overexpression of SOCS3 (Krebs and Hilton, 2001), which affects JAK/STAT pathway by binding to the pTyr⁹⁸⁵ of Ob-Rb and induces dephosphorylation of JAK2 (Bjørnbæk et al., 2000). Protein tyrosine phosphatases (PTPs), the phosphatase and tensin homolog (PTEN), receptor-type PTPe (RPTPe), and PTP1B also induce dephosphorylation of JAK2 and inhibit leptin signaling. The expression of PTP1B and T cell PTP (TCPTP) upregulates in high-fat diet and obesity, and

TABLE 1 | Adipokine action of leptin on the cells of both innate and adaptive immunity.

Immune cell type	Observation	References
LEPTIN ACTION ON DIFFERENT CELLS OF INNATE IMMUNITY		
Neutrophils	+ Activation	La Cava and Matarese, 2004
	+ Chemotaxis	Mancuso et al., 2002
	+ Phagocytosis	Fernández-Riejos et al., 2010
	+ H ₂ O ₂ , O ₂ ⁻ production	Caldefie-Chez et al., 2001
Monocytes/Macrophages	+ Proinflammatory cytokines (IL-1, IL-6, TNF) production	Loffreda et al., 1998 Santos-Alvarez et al., 1999
	+ Phagocytosis	Bruno et al., 2005
	+ Leukotrienes B ₄	La Cava and Matarese, 2004
	+ Antigen presentation	
	+ MHC expression	
	+ Acute inflammation	
Natural Killer cells	+ Adhesion molecules	
	+ Cytotoxicity	La Cava and Matarese, 2004
	+ Perforin production	
	+ IL-2 secretion	Tian et al., 2002
Dendritic cells	+ Activation	Spencer and Daynes, 1997
	+ IL-12 secretion	
	+ Th1-priming	Mattioli et al., 2005
LEPTIN ACTION ON DIFFERENT CELLS OF ADAPTIVE IMMUNITY		
Thymic T-cells	+ Proliferation	Matarese et al., 2005
	+ Maturation & Homeostasis	
	+ CD4+CD8+ & CD4+CD8-	Howard et al., 1999
	+ Bcl-2 & Bcl-XL, - Apoptosis	Bruno et al., 2005
Naive T-cells (CD4+CD45RA+)	+ Proliferation	Lord et al., 1998
	+ Activation of MAPK & PI3K	
	+ IL-2 production	
Memory T-cells (CD4+CD45RO+)	- Proliferation	Lord et al., 1998
Th1-cells	+ Stimulation	Martin-Romero et al., 2000
	+ IFN- γ & TNF production	
	+ DTH response	Napoleone et al., 2007
	+ IgG2a switching by B-cells	
Th2-cells or Tregs	+ Inhibition	Martin-Romero et al., 2000
	+ IL-4 & IL-10	
	- IgG1 switching by B-cells	Napoleone et al., 2007
Cytotoxic T-cells	+ Activation & proliferation	
	+ Granzyme production	Dayakar et al., 2017
	- PD-1, CTLA-4 expression	

inhibits leptin-mediated STAT3 phosphorylation (St-Pierre and Tremblay, 2012). The PTP1B mediated endoplasmic reticulum (ER) stress induces leptin resistance (Hosoi et al., 2008; Ozcan et al., 2009), possibly by inhibiting STAT3 phosphorylation.

In innate immunity, leptin modulates the activity and function of neutrophils by increasing chemotaxis and secretion of oxygen radicals such as hydrogen peroxide (H₂O₂) and superoxide (O₂⁻). In mice, directly acts on neutrophils, whereas, in humans, its action is mediated by tumor-necrosis factor (TNF) secreted from monocytes. The stimulation of human monocytes by leptin induces the production of TNF- α and IL-6 (Santos-Alvarez et al.,

1999). Leptin enhances phagocytosis by macrophages, secretion of pro-inflammatory mediators of acute-phase response, and expression of adhesion molecules. In natural killer (NK) cells, it increases cytotoxic ability and secretion of perforin and IL-2. In adaptive immunity, leptin promotes the generation, maturation, and survival of thymic T cells, Leptin inhibits the apoptosis of thymocytes by inducing tyrosine phosphorylation of sam68 and insulin receptor substrate (IRS)-1, which associates with p85 regulatory subunit of SH2-domain, and PI3K signaling (Sung et al., 1994; Sánchez-Margalet and Najib, 1999). In naive T cells, leptin increases proliferation and IL-2 secretion via the activation of MAPK and PI3K pathways. In memory T cells, leptin triggers Th1 polarization by increasing interferon (IFN)- γ and TNF- α secretion. It also promotes delayed type hypersensitivity (DTH) response and immunoglobulin class-switching to produce IgG2a. This process sustained by an autocrine loop of leptin secretion by Th1 cells. Leptin has anti-apoptotic effects on mature T cells and hematopoietic precursors (La Cava and Matarese, 2004).

Studies on *ob/ob* mice revealed that they produce low amount of IL-2, IFN- γ , and IL-18, and large amount of Th2 cytokines (IL-4 and IL-10). Leptin regulates thymic homeostasis and induces Th1 response by increasing the production of IFN- γ and TNF- α , which in turn activates monocyte or macrophages and dendritic cells (DCs) (Zhang et al., 1997; Loffreda et al., 1998; Santos-Alvarez et al., 1999; Martín-Romero et al., 2000; Matarese et al., 2005; Mattioli et al., 2005). Leptin induces granulocyte-macrophage colony stimulating factor (GM-CSF) and G-CSF production from murine peritoneal macrophages (Gainsford et al., 1996) and leptin-deficient mice exhibit phenotypic abnormalities in macrophages (Lee et al., 1999). Leptin signaling in immature DCs upregulates surface expression of chemokine receptor CCR7 and induces structural changes by facilitating the remodeling of actin microfilaments in the cytoskeleton and in turn migratory potential of DCs (Mattioli et al., 2008). Leptin directly activates DCs to secrete IL-12, which is a key cytokine that facilitates the shifting of T cells toward Th1 phenotype (Spencer and Daynes, 1997). The *ob/ob* mice have shown impaired function of DCs and their altered steady-state number (Macia et al., 2006) and *db/db* mice have shown obese diabetic phenotype with increased number and suppressive function of Tregs (Taleb et al., 2007). Leptin stimulates the expression of toll-like receptor (TLR)-2 on primary human monocytes in hyperleptinemia to potentiate innate immunity and inflammation but had no effect on TLR-4. Leptin induces CD14 expression on THP-1 monocytes but not on primary human monocytes to potentiate lipopolysaccharide (LPS) mediated proinflammatory cytokine response (Jaedicke et al., 2013). An impaired cytotoxic activity of NK cells, lymphopenia, increased number of blood monocytes, reduced antigen-specific T cell proliferation, and thymic atrophy are common features to both *ob/ob* and *db/db* mice (Fernández-Riejos et al., 2010). These findings are consistent in human patients with congenital leptin-deficiency (Farooqi et al., 2007). On the other hand, malnutrition induces anti-inflammatory cytokines IL-4 and IL-10 and impairs pro-inflammatory cytokines IL-2 and IFN- γ production from CD4+ and CD8+ T cells in children. However, leptin administration in these children substantially reversed the above

effects and induces the expression of CD25 and CD69 activation markers on peripheral blood T cells (Rodríguez et al., 2007). A drastic fall in systemic leptin levels during starvation for 48 h increases susceptibility to LPS and TNF-induced toxicity in mice. However, leptin replacement therapy markedly reverses these deleterious effects and protects the mice from fasting-induced lymphopenia (Faggioni et al., 2000b). Both malnutrition and fasting are associated with nutrients insufficiency, which limits the availability and uptake of glucose by effector T cells to fuel their maintenance and activity results in immunosuppression and incompetency to produce inflammatory cytokines. In fasting animals, an intraperitoneal injection of leptin induces the activated T cell's glucose-uptake by upregulating the expression of glucose transporter-1 (Glut1) and intrinsic glucose metabolism through glycolysis and mitochondrial respiration, which results in activated T cell proliferation and inflammatory cytokines production. However, such a metabolic regulation in naive T cells and Tregs did not require the leptin action. On the other hand, at sufficient nutritional level, an abundant expression of leptin receptors and peripheral T cell activation facilitates leptin signal to metabolically license T cells for activation. In such a way that, leptin links the nutritional status with immunity by regulating the intrinsic metabolism of T cells (Saucillo et al., 2014).

Leptin induces the expression of CD25 and human leukocyte antigen (HLA)-DR on peripheral blood B-lymphocytes and in turn activates JAK2/STAT3 and p38MAPK/ERK 1/2 to produce IL-6, IL-10, and TNF- α (Agrawal et al., 2011). Leptin receptor expression was significantly higher in Tregs compared to CD4+CD25- effector T cells and leptin directly acts on Tregs to inhibit their function and proliferation (De Rosa et al., 2007). The persistence of high systemic leptin levels triggers the mTOR signaling to inhibit Tregs proliferation. Tregs-derived leptin acts in autocrine fashion to maintain their hyporesponsiveness. In *db/db* mice, Tregs show a decreased mTOR activity and increased proliferation (Procaccini et al., 2012). Leptin regulates the survival and proliferation of autoreactive CD4+ T cells by modulating the activity of Bcl-2 and Th1/Th17 cytokines via nutrient/energy-sensing Akt-mTOR pathway (Galgani et al., 2010). In animal models with autoimmunity and infectious diseases, leptin regulates Th1/Th2/Treg balance to control the disease (Procaccini et al., 2012). Acute leptin during infection and inflammation may be a protective module of the host response to inflammation (Sarraf et al., 1997). Leptin induces the proliferation of naive T cells (CD4+CD45RA+) but inhibits memory T cells (CD4+CD45RO+) in mice model (Lord et al., 1998). Leptin facilitates a survival signal to CD4+CD8+ and CD4+CD8- T cells during maturation (Howard et al., 1999). T cells skewing toward Th1 response by leptin seems to be mediated by inducing the synthesis of IL-2, IL-12, and IFN- γ and inhibiting the production of IL-10 and IL-4 (Martín-Romero et al., 2000; Napoleone et al., 2007). The isoform type and quantity of LEPRs expression on immune cells is based on cell type. For example, Ob-Rb expresses on 25% of monocytes and 12% of neutrophils (Zarkesh-Esfahani et al., 2001). A variety of functions of immune cells mediated by leptin is orchestrated by different isoforms of LEPR and CD4+ T cell population alone express three different

isoforms of LEPR (Walduck and Becher, 2012). Therefore, leptin shows differential activity on CD4+ effector T cells and Treg cells at the same time.

LEPTIN INDUCES PHAGOCYTOSIS IN MICROBIAL INFECTIONS

Phagocytosis is a key event executed by certain immune cells to internalize the foreign particles (may be pathogen) inside the cell and subsequent killing. Leptin induces phagocytic activity of macrophages and prevents the apoptosis of a variety of immune cells involved in innate and adaptive immune response by delaying the cleavage of *Bid* and *Bax*, release of cytochrome-c from mitochondria, and activation of both caspase-8 and caspase-3 (Bruno et al., 2005). Upon binding to the Ob-Rb expressed on the cell surface, leptin can induce the phagocytic activity of neutrophils (Fernández-Riejos et al., 2010). Leptin was able to induce the macrophages phagocytic activity caused by *Leishmania major* infection in mouse model (Gainsford et al., 1996) and *in vitro* *L. donovani* infection in human macrophages (THP-1) and peripheral blood mononuclear cells (PBMCs) (Dayakar et al., 2016). Leptin stimulates neutrophils to increase the intracellular reactive oxygen species (ROS) within the phagosomes (Caldefie-Chez et al., 2001; Fernández-Riejos et al., 2010). It activates the phagosomes by inducing actin polymerization and rejuvenating actinomyosine interaction (Attoub et al., 2000), which eventually enhances neutrophilic phagocytosis (Mancuso et al., 2002; Shirshv and Orlova, 2005). During *Klebsiella pneumoniae* infection, leptin knock-out mice exhibited defective phagocytic response, in which, neutrophils have shown decreased expression of CD11b on their surface. With exogenous leptin supply, the CD11b expression was normalized, and CD11b-dependent phagocytosis induction by leptin in neutrophils enabled the animals to recover from *K. pneumoniae* infection (Moore et al., 2003). Leptin induced CD11b expression and phagocytosis in neutrophils during uptake of *Listeria monocytogenes* was mediated by TNF- α produced from monocytes (Tian et al., 2002). In *Escherichia coli* infection, leptin-deficiency impaired the phagocytosis by peritoneal macrophages; adequate supply of leptin inhibited the normal lymphocytes apoptosis by FAS-mediated pathway, and protected the starved mice from the loss of lymphocytes (Merrick et al., 1997). Steroids induced apoptosis in lymphocytes was reversed by leptin administration (Papathanassoglou et al., 2006). *K. pneumoniae* infection has amplified the mortality rate in leptin-deficient mice by impairing bacterial clearance, and an *in vitro* study demonstrated that leptin supplementation reduced this infection by increasing the phagocytic activity of alveolar macrophages. Pre-treatment of peritoneal macrophages of leptin-deficient mice with higher concentrations of murine leptin restored the cysteinyl-leukotriene synthesis, which helped in improving phagocytosis. The systemic administration of leptin by intraperitoneal route in septic *ob/ob* and septic wild-type mice improved the neutrophil phagocytosis of *E. coli* by 21 and 10% respectively compared to untreated *ob/ob* mice (Tschöp et al., 2010).

Leptin induces the phosphorylation of Akt kinase and intracellular ROS production from *L. donovani* infected THP-1 to stimulate the macrophage phagocytic activity (Dayakar et al., 2016). In consistence, similar results were published with sodium-antimony gluconate treatment to *L. donovani* infection, which is a first-line drug to cure visceral leishmaniasis (VL) in the Indian subcontinent (Basu et al., 2006). As mentioned-above in neutrophilic phagocytosis, the intracellular ROS helps in rapid internalization of parasites by the host cells via inducing the fusion of phagosome with lysosome (Gueirard et al., 2008) for oxidative killing (Laufs et al., 2002). Leptin was also shown to promote the host defense in pulmonary bacterial infection of mouse model (Mancuso et al., 2002). These studies support the view that leptin administration could be a novel approach for protection against the bacterial infections, and may prove beneficial to human population susceptible to bacterial pneumonia under certain pathological conditions like HIV infection, malnutrition, and diabetes mellitus (Jubiz et al., 1984; Skerrett et al., 1990; Coffey et al., 1996; Cederholm et al., 2000).

FATE OF LEPTIN IN MICROBIAL INFECTIONS

Generally, leptin-deficiency is associated with enhanced susceptibility to several infections. At the same time, certain infections also caused the downregulation of systemic leptin levels and mimics malnutrition like situation. Fever, diarrhea, malabsorption, low appetite, loss of nitrogen, and nutrients induce the malnutrition state and increase the mortality rate by infections (Müller et al., 2003). A few such infections; bacteria (Table 2A), virus and fungus (Table 2B), and parasite (Table 2C) infections and their pathogenicity in either low systemic leptin or leptin-deficiency and impaired leptin signaling conditions are presented below in detail.

Plasma Leptin Levels and Disease Severity of Pulmonary Infections

Several studies reported that plasma leptin levels are lower in TB patients than in healthy controls. Certain clinical conditions like muscle wasting, inflammation, and decreased energy intake in TB patients results in high severity of disease (van Crevel et al., 2002). Furthermore, leptin levels were higher in female patients with higher body fat mass than in male patients with equal body weights suffering with TB infections (Çakir et al., 1999). Even at the normal physiological conditions, leptin levels (5–10 ng/ml) were two-folds higher in females compared to those of males at equal BMI (Thomas et al., 2000). Leptin-deficient mice with pulmonary TB were deficient in CD4+ and CD8+ T-lymphocytes number and activation. They were unable to generate IFN- γ and DTH responses, the exogenous leptin supply restored the lymphocyte trafficking, IFN- γ production, and granuloma formation successfully, and disease severity was substantially reduced (Wieland et al., 2005). Leptin-deficient mice also exhibited greater susceptibility and prolific lethality

TABLE 2 | Leptin and/or its signaling associated events in multiple microbial infections.

(A) Leptin vs. bacterial infections		
Infection type	Observation	References
<i>Mycobacterium tuberculosis</i> (TB)	<ul style="list-style-type: none"> Low systemic leptin levels During leptin deficiency; Defective granulomas Reduced CD4+ & CD8+ T-cell proliferation & activation Impaired DTH response Depleted IFN-γ levels Increased disease severity 	van Crevel et al., 2002 Wieland et al., 2005
<i>Klebsiella pneumonia</i> (Pneumococcal pneumonia)	During leptin-deficiency; <ul style="list-style-type: none"> High susceptibility Impaired leukotriene synthesis & phagocytosis by neutrophils Low CD11b on neutrophils Impaired bacterial clearance & increased mortality 	Moore et al., 2003 Mancuso et al., 2002
<i>Streptococcus pneumoniae</i> (Pulmonary pneumonia)	During leptin-deficiency; <ul style="list-style-type: none"> Impaired phagocytosis by alveolar macrophages Impaired killing by PMNs High TNF-α, MIP-2, PGE₂ in the lung Failure of host defense system 	Hsu et al., 2007
<i>Clostridium difficile</i> (Colitis)	Q223R (rs1137101) mutation; <ul style="list-style-type: none"> Impaired Stat3 signaling Inadequate inflammation High rate of infection ob-Rb intracellular domain Tyr 1138 Ser mutation; Switch on Stat3/SOCS3 signaling low chemokines production & immune cells recruitment 	Madan et al., 2014
Sepsis (SIRS)	Leptin deficiency; <ul style="list-style-type: none"> Highly fatal CNS leptin signaling induces protective immunity against this infection 	Takahashi et al., 2004 Tschöp et al., 2010
<i>Staphylococcus aureus</i> (Sepsis arthritis)	<ul style="list-style-type: none"> Reduced leptin production Higher susceptibility & IL-6 levels in <i>db/db</i> 	Hultgren and Tarkowski, 2001

(Continued)

TABLE 2 | Continued

(A) Leptin vs. bacterial infections		
<i>Helicobacter pylori</i> (Gastric ulcers)	<ul style="list-style-type: none"> Increased gastric leptin No change in systemic leptin Reduced gastric leptin after cure <i>Db/db</i> exhibited high susceptibility 	Azuma et al., 2001 Khosravi et al., 2015
Bacterial peritonitis	LEPR Q223R mutation in CRH1 domain <ul style="list-style-type: none"> higher susceptibility to infection 	Bracho-Riquelme et al., 2011
<i>Listeria monocytogenes</i>	<ul style="list-style-type: none"> Downregulation of MCP-1 in <i>db/db</i> and <i>ob/ob</i>, and KC mRNA in <i>db/db</i> mice liver 	Ikejima et al., 2005
(B) Leptin vs. virus and fungal infections		
Infection type	Observation	References
HIV (AIDS)	<ul style="list-style-type: none"> Increased expression of LEPRs on monocytes Low systemic leptin levels Leptin inhibited ROS and oxidative burst by HIV+ monocyte Monocytes desensitization & Impaired immunity During anti-retroviral therapy leptin positively correlated with CD4+ T-cells Induced SOCS3 expression Inhibited IFN-α/β JAK/STAT signaling 	Sánchez-Margalet et al., 2002 Estrada et al., 2002 Sánchez-Pozo et al., 2003 Najib and Sánchez-Margalet, 2002 Karp et al., 1998 Azzoni et al., 2010 Matarese et al., 2002 Akhtar et al., 2010
Influenza A/H1N1 Pneumonia	<ul style="list-style-type: none"> Acute raise in pulmonary leptin levels Increased neutrophil survival Increased neutrophilia In obesity, global reduction of LEPRs Reduced viral clearance Impaired CD8+ T-cell memory Induced SOCS3 expression 	Ubags et al., 2014 Morgan et al., 2010 Radigan et al., 2014 Karlsson et al., 2010 Pauli et al., 2008
Adenovirus	<ul style="list-style-type: none"> Induced obesity Increased risk of influenza Decreased leptin & nor-epinephrine Increased appetite & glucose uptake & corticosterone Decreased lipolysis 	Hur et al., 2013

(Continued)

TABLE 2 | Continued

Hepatitis-B & Epstein Barr virus	During obesity / hyperleptinemia; • Induced SOCS3 expression • Inhibited IFN- α / β JAK/STAT signaling	Michaud et al., 2010 Tian et al., 2012
Encephalomyocarditis	• Impaired expression of cardiac adiponectin • Induced expression of TNF- α • Severe inflammatory myocardial damage	Takahashi et al., 2006
Coxsackie virus B4	• Higher susceptibility in <i>db/db</i> animals	Webb et al., 1976
<i>Candida albicans</i> (Fungus)	Leptin receptor-deficiency in obesity; • Impaired immunity During stress; • low systemic leptin levels • High TNF- α levels	Rodríguez-Galán et al., 2010

(C) Leptin vs. intra and extracellular parasite infections

Infection type	Observation	References
<i>Entamoeba histolytica</i> (Amoebiasis)	• Low serum leptin levels in amoebic liver abscess • LEPR Q223R mutation in CRH1 domain; • High disease severity • LEPR E233R mutation; • High susceptibility 2012 • Leptin deficiency; • Intermediate susceptibility • Intensive epithelial denudation • Integral leptin signaling protects via • Sat3 and Erk or Akt pathways • Leptin promotes regeneration & mucin secretion from intestinal epithelium • Inhibits apoptosis & maintains integrity in intestinal epithelium	Alam et al., 2016 Duggal et al., 2011 Vedantam and Viswanathan, 2012 Sukhotnik et al., 2009 El Homsy et al., 2007 Brun et al., 2007
<i>Leishmania major</i> & <i>L. donovani</i>	• Low serum leptin levels • Reduced phagocytosis by macrophage • Leptin induces pErk1/2 & pAkt in macrophages & Phagocytosis • Increased Th1 cytokine response • Induced protective immunity	Dayakar et al., 2016 Gainsford et al., 1996 Shivhare et al., 2015

(Continued)

TABLE 2 | Continued

	in <i>ob/ob</i> liver • Increased IFN γ , IL12, IL1 β • Increased CD8+ T-cell count • Increased IgG2a levels • Decreased IgG1 levels • Increased granuloma • Repaired tissue degeneration • Controlled weight loss • Reduced parasite load • Reduced PD-1 & CTLA-4 expression	Maurya et al., 2016 Dayakar et al., 2017
<i>E. Histolytica</i> & <i>Giardia</i>	• Higher leptin levels • Damage of gut epithelial cells • Activation of mesenteric lymphnodes & adipose tissue • Eosinophilia & extensive tissue invasion & High pathogenicity	Desreumaux et al., 1999 Yahya et al., 2016
<i>Taenia taeniaformis</i>	• Low systemic leptin levels • Anorexia • High PGE2 & Inhibition IL-12 & Th2 immunity • Inhibition of skin Langerhans cells to lymphnodes	Krebs and Kacelnik, 1991 Löhms and Sundström, 2004 Leid and McConnell, 1983
<i>Heligmosomoides bakeri</i>	• Higher serum leptin levels • Acute inflammation • High IL-1 β , TNF- α , and IL-6	Tu et al., 2007 Noah et al., 1994
Malaria	• Higher serum leptin levels	Pulido-Mendez et al., 2002

to pneumonia infection, caused by either *K. pneumonia* or *Streptococcus pneumoniae*. Leptin supply to *ob/ob* animals improved host defense against pneumococcal pneumonia caused by *K. pneumonia* by increased pulmonary bacterial clearance and host survival. Pulmonary bacterial load during *S. pneumonia* infection in leptin-deficient individuals results in the failure of host defense system, which is associated with abundant production of TNF- α , macrophage inflammatory peptide (MIP)-2 and prostaglandin-E₂ (PGE₂) in the lung tissue. The key innate immunity events like phagocytosis by alveolar macrophages and killing by neutrophil polymorphonuclear leukocytes (PMN) were impaired. It results in successive evasion of *S. pneumonia* infection, *in vitro*. However, exogenous leptin has tremendously improved the survival rates in leptin-deficient mice- by inducing substantial clearance of bacteria from pulmonary tissue as well as from blood (bacteraemia). Likewise, *in vitro* *S. pneumonia* infection was controlled by exogenous leptin through inducing reconstitution of alveolar macrophage

phagocytosis and PMN-mediated H_2O_2 production (Hsu et al., 2007).

Role of Leptin in Mucosal Immunity

C. difficile is a leading cause of nosocomial infection, which results in the development of colitis. Earlier studies have reported that Q-to-R mutation at position 223 in the LEPR cytokine receptor homology 1 (CRH1) domain (LEPR Q223R) is associated with increased susceptibility to bacterial peritonitis (Bracho-Riquelme et al., 2011) and to infectious colitis as well as liver abscess caused by *E. histolytica* in humans (Duggal et al., 2011). Similarly, the risk of *C. difficile* infection in humans is higher in LEPR Q223R (rs1137101) model, which is a homozygous allelic mutation that results in impaired STAT3 signaling and increased dissemination of infection. In murine model, the mechanism of susceptibility to *C. difficile* was elucidated as the animals being deficit in functional LEPR and adequate inflammation to clear the infection from the gut lumen. In addition to this, a mutation (Tyr 1138 Ser) in tyrosine 1138 residue located in the intracellular domain of LEP-Rb isoform mediates STAT3/SOCS3 signaling, which results in decreased chemokine production and immune cells recruitment at the site of infection in mucosal gut tissue. Leptin was shown to be protective against *C. difficile* colitis by inducing STAT3 inflammatory pathway, which is impaired in LEPR Q223R mutation (Madan et al., 2014). Similarly, the *db/db* mice exhibited greater susceptibility to *H. pylori* infection. In humans, *H. pylori* infection substantially increased the localized gastric leptin levels but their levels were significantly diminished after cure. However, the systemic circulating leptin levels in serum were not altered during this infection (Azuma et al., 2001). Similarly, in pigs, the enteric *Salmonella typhimurium* challenge did not alter the serum leptin levels (Jenkins et al., 2004). In another study, *H. pylori* infection induced the gut leptin levels in specific pathogen-free mice by interacting with gut microbiome (Khosravi et al., 2015).

Leptin Offers Protection Against Sepsis

Sepsis is another systemic inflammatory response syndrome (SIRS) in certain infection states (Santos-Alvarez et al., 1999). It is responsible for multiple organ failure and high rate of mortality. Leptin deficiency is highly fatal in mice suffering from sepsis due to severe organ damage (Takahashi et al., 2004). Systemic leptin replacement modulated the immune response against sepsis and increased survival in both leptin-deficient and wild-type mice. It has also been reported that endogenous CNS leptin signaling is necessary to induce adequate anti-septic immune response. In sepsis, the leptin infusion via intracerebroventricular route into the CNS of *ob/ob* mice significantly reduced IL-6 levels in serum thereby controlled systemic inflammation and improved survival. Genetic rescue of leptin signaling in the CNS of *db/db* mice improved the survival in sepsis compared to non-rescued *db/db* mice. In humans, three-fold higher leptin levels were reported in the patients' recovered from sepsis compared to that of non-survivors. These observations reveal the neuroendocrine regulation of systemic immunity and therapeutic potential of leptin in infectious disease (Tschöp et al., 2010). Septic arthritis is caused by *Staphylococcus aureus*; leptin production was found

to be downregulated during this infection, in murine model. The *db/db* mice exhibited greater susceptibility to *S. aureus* infection. Though exogenous recombinant leptin supply failed in restoring the basal leptin levels and clearance of bacterial load in these animals, it substantially reduced the severity of septic arthritis by regulating the production of inflammatory cytokine IL-6 (Hultgren and Tarkowski, 2001).

Leptin Offers Resistance to *L. monocytogenes* Infection

L. monocytogenes is an intracellular bacterium, which severely affects immunodeficient individuals and neonates to causing listeriosis, meningitis, and endocarditis (Economou et al., 2000; Portnoy et al., 2002; Chan et al., 2005). "Listeriolysin O" produced by this bacterium inhibits antigen-processing by inducing the lysis of phagosome membrane in macrophages, which results in abundant intracellular growth of bacteria (Carrero et al., 2004; Birmingham et al., 2008). In addition to this, "Listeriolysin O" also cause death in antigen-presenting cells (APCs) by inducing the production of inflammatory mediators (Savill et al., 1993; Carrero and Unanue, 2006) and this bacterial infection leads to the apoptosis in T-lymphocytes (Leib et al., 1996; Zychlinsky and Sansonetti, 1997). The *db/db* and *ob/ob* mice were highly susceptible to this infection and incapable to clear the bacteria from liver. The hepatic infection of *L. monocytogenes* downregulates the expression of chemokines such as monocyte chemoattractant protein (MCP)-1 and KC mRNA in *db/db* mice and MCP-1 in *ob/ob* mice when compared to their heterozygote (*db/m* and *ob/?*) phenotypes. Leptin administration in *ob/ob* mice restored the expression of MCP-1 and offered the resistance to *L. monocytogenes*. On the other hand, insulin treatment in *db/db* mice restored the expression of MCP-1 and KC mRNA and enhanced the rate of infection clearance. The hyperglycaemia in leptin-deficiency impairs the host system to clear the bacteria from liver but leptin therapy may corrected the blood glucose levels by increasing insulin sensitivity and improved host resistance to this bacterial infection (Ikejima et al., 2005).

Leptin Diminishes Oxidative Burst in HIV+ Monocytes

Generally, certain levels of leptin can stimulate the monocytes to produce ROS via activation of membrane-bound NADPH oxidase (Rossi, 1986). Intracellular ROS can act as a second messenger in LEPR signaling of monocytes (Martín-Romero and Sánchez-Margalet, 2001; Sanchez-Margalet and Martin-Romero, 2001) and also maintain acute proinflammatory conditions (Chaudhri and Clark, 1989). It was reported that the HIV infection can also induce ROS production from monocytes and macrophages (Kimura et al., 1993; Trial et al., 1995; Elbim et al., 1999). The ROS production is an indicator of programmed cell-death in monocytes (Um et al., 1996). Interestingly, HIV+ monocytes have increased expression of LEPRs, displaying their hyperactive state (Matarese et al., 2002). However, leptin stimulation of these HIV+ monocytes partially inhibited the production of ROS (Sánchez-Pozo et al., 2003), this could be

either the desensitization of HIV+ monocytes for leptin as observed in other hyper-inflammatory states such as sepsis, in which the monocytes skewed into hypo-inflammatory/anergy state by LPS stimulation (Karp et al., 1998) and results in the attenuation of oxidative burst (Von Knethen and Brüne, 2001) or the consistency of anti-apoptotic function of leptin with the inhibition of oxidative burst in HIV+ monocytes (Najib and Sánchez-Margalet, 2002). The low systemic leptin levels in HIV patients (Estrada et al., 2002) due to reduced adiposity may contribute to immunodeficiency (Kotler et al., 1985). However, during active anti-retroviral therapy, leptin levels were correlated with CD4+ T cells in HIV patients (Matarese et al., 2002).

Leptin Resistance or Impaired Signaling Induces SOCS3 and Susceptibility to Virus Infections

It was demonstrated that the impaired leptin signaling is attributed to defective immunity for influenza A/H1N1 (Morgan et al., 2010) and HIV infections (Azzoni et al., 2010) due to the loss of interdisciplinary regulation among immunologic, metabolic, and neuro-endocrinological aspects. However, an acute induction of pulmonary leptin levels during H1N1 pneumonia in both mice and human models directly increased the neutrophilia and neutrophils survival without inducing any secondary cytokines (Ubags et al., 2014). Global reduction of the LEPRs, results in reduced viral clearance and worse outcomes against influenza A challenge in obese mice. However, these outcomes are not specific to the reduced LEPR in lung epithelial cells or macrophages but may be associated with impaired leptin signaling in non-myeloid populations such as NK and T cells (Radigan et al., 2014). For instance, during influenza virus infection in diet-induced obesity, the CD8+ T cell memory was depleted and pulmonary SOCS3 mRNA expression was induced when compared to infected lean mice (Karlsson et al., 2010). Apart from influenza, other viruses such as hepatitis-B, HIV, and Epstein Barr virus can also induce SOCS3 expression to ensure their survival and evade the host immunity by inhibiting IFN- α/β JAK/STAT signaling (Pauli et al., 2008; Akhtar et al., 2010; Michaud et al., 2010; Tian et al., 2012). IFNs are potent antiviral substances, capable of inducing maturation and activation of DCs, and bridging both innate and adaptive immunity, is in contrast to the function of SOCS3, which typically inhibits T cells proliferation and activation by directly targeting CD28 (Kubo et al., 2003). Altogether, the induced SOCS3 levels either in viral infection or hyperleptinemia state of over-nutrition directing to host immune dysfunction. Therefore, in obesity the potential failure of vaccination, especially against viral infections could be regulated by SOCS3 antagonists. A recent study proposed that the saponins derived from fungal endophytes could be potential inhibitors of leptin and may repair its resistance in obesity, and may modulates immune response in favor of host against multiple diseases (Mouli et al., 2016). On the other hand, adenovirus infection can induce obesity, which is a high risk factor for influenza caused morbidity and mortality. During adenovirus infection induced obesity, the cellular uptake of glucose is induced, and simultaneously lipolysis is reduced

through the stimulation of corticosterone secretion. In addition, this infection may increase the appetite and substantially decrease the levels of nor-epinephrine and leptin, which tends to immune dysfunction (Hur et al., 2013).

During leptin-deficiency, encephalomyocarditis virus infection in mice contributed to the development of severe inflammatory myocardial damage due to impaired expression of cardiac adiponectin and induced expression of TNF- α (Takahashi et al., 2006). Inbred male C57BL/Ks homozygous *db/db* mice exhibited higher susceptibility to Coxsackie virus B4 infection than that of heterozygous normal (*db/+*) and normal (*+/+*) genotypic mice (Webb et al., 1976).

Cyclic-Relationship of Malnutrition With Parasite Infections Regulates Leptin Production

Malnutrition in children is directly linked to the enteric parasite infections, which causes damage to intestinal mucosal epithelial cells by inducing inflammation and ulceration, it eventually leading to multiple pathological conditions like anorexia, indigestion, malabsorption, and nutrient loss (Vermeulen et al., 1998; Saldiva et al., 2002), and responsible to mimic malnutrition. Malnutrition is the hall mark of low systemic leptin levels (Sánchez-Margalet et al., 2003) and gut parasite infections may induce this state. A recent study on Bangladesh population suffering from amoebic liver abscess caused by *E. histolytica*, provides a significant correlation between disease severity and low serum leptin levels to malnutrition (Alam et al., 2016). The reduced systemic leptin levels found in *Taenia taeniaformis* infected mice may be the result of increased hunger rate induced by parasites (Krebs and Kacelnik, 1991; Löhms and Sundström, 2004). This infection also tended to produce lower body mass (anorexia) in animals, which is a symptom of malnutrition. A positive correlation between leptin levels and body mass was consistent in normal animals but such a relationship was absent in infected animals, unveiling the possible effect of the parasite on leptin biosynthesis and production (Löhms et al., 2012). A similar condition was reported on enteric parasitic infections in humans (Yahya et al., 2016). Helminths evolved many strategies to evade host immunity for their endurance (Maizels and Yazdanbakhsh, 2003); a report suggested that the larval stage of *T. taeniaformis* induced PGE₂, which inhibited IL-12 and skewed the host immunity to Th2-type (Leid and McConnell, 1983). As was discussed earlier in *S. pneumonia* infection, the elevated levels of PGE₂ inhibited the infiltration of skin Langerhans cells to the lymph nodes (LNs), which is a crucial step in the initiation of immunity (Maizels and Yazdanbakhsh, 2003).

There are few contradictory reports, which suggest that leptin levels increased during parasitic infection in children (Zaralis et al., 2008). For example, higher serum leptin levels were reported in malaria (Pulido-Mendez et al., 2002) and in gastrointestinal nematode infection by *Heligmosomoides bakeri* (Tu et al., 2007). It is possible that low endogenous leptin levels in children (Howard et al., 1999) might result in short-time increase of leptin levels due to acute inflammation and production of

IL-1 β , TNF- α , and IL-6 caused by the gut infections (Noah et al., 1994). A significant increase in leptin levels was observed during *E. histolytica*, *Strongyloides*, and *Giardia* co-infections. These parasites are reported to cause damage to the gut epithelial cells, which results in the activation of mesenteric LNs and then adjacent adipose tissue to secrete the leptin (Desreumaux et al., 1999). Leptin functions as an eosinophil survival factor in humans (Conus et al., 2005), which plays a key role in the host defense system against gut parasitic infection. The level of eosinophilia indicates the relative severity of the disease due to tissue invasion by the parasites (Park and Bochner, 2010). Co-infection of *E. histolytica* and *Strongyloides* positively correlated with increased leptin suggests it promotes pathogen tissue invasion and pathogenicity. This is however, not found in infections with *Giardia*, *Hymenolepis nana*, and *Oxyuris*, but reappeared with *E. histolytica* and *Giardia* co-infection suggesting that *E. histolytica* is a crucial player of tissue invasion (Yahya et al., 2016).

LEPR Signaling and *E. histolytica* Infection

Enteric leptin plays a crucial role in the immunity to *E. histolytica* (Guo et al., 2011). Apart from this, it promotes regeneration and inhibits apoptosis in intestinal epithelium (Sukhotnik et al., 2009), stimulates mucin secretion (El Homsy et al., 2007) and maintains intestinal epithelium integrity (Brun et al., 2007). Its secretion into the gastric juice regulates digestion and absorption (Morton et al., 1998). Furthermore, intact leptin signaling plays a key role in offering protection against gut parasite infections e.g., *E. Histolytica* caused amoebiasis. However, a mutation (E233R) or polymorphism in LEPR is likely to enhance the susceptibility for *E. Histolytica* infection by four-folds in children, irrespective of their nutritional status. In mice, leptin-deficiency has shown intermediate susceptibility and leptin-receptor deficiency has shown high susceptibility to this amoeboid infection, and mice ceca developed intensive epithelial denudation. An integral leptin signaling in intestinal epithelial cells via STAT3 and Erk or Akt pathways was found to be protective against these amoebic infections, which is governed by non-adipokine action of leptin (Vedantam and Viswanathan, 2012).

Leptin Induces Protective Immunity to Intracellular Parasite Infections

Leishmaniasis is a vector-borne intracellular infectious disease caused by the protozoan *Leishmania* sp., For the first time, we have hypothesized the possible role of leptin in human VL (Dayakar et al., 2011). Thereafter, several studies on the relationship between leptin and disease outcome in leishmaniasis, indicated that exogenous recombinant leptin augmented the host protective immunity with the combination of miltefosine in mouse macrophages (J774.1 cell line) during *in vitro* *L. donovani* infection (Shivahare et al., 2015). We have also—demonstrated that leptin induced the host protective Th1-type cytokine response in human THP-1 macrophages and PBMCs. Leptin was able to maintain the defense against *L. donovani* infection through the classical activation of macrophages by inducing the phosphorylation of Erk1/2 and Akt kinase (Dayakar et al., 2016). In addition, leptin was shown to induce protective

immunity in normal C57BL/6 mice; it reduced the parasite load in visceral organs such as spleen, liver, and bone marrow derived macrophages, induced IgG2a, IFN- γ , IL-12, IL-1 β , and nitric oxide (NO) production. However, leptin failed to restore protective immunity and reduce parasite load in the spleen of *ob/ob* mice but succeeded to reduce the parasite load in liver (Maurya et al., 2016). In malnourished BALB/c mice, leptin induced Th1 immune response and IgG2a class-switching against *L. donovani* challenge. In this study, the fascinating outcome is the serum leptin levels significantly reduced by the parasite infection irrespective of malnutrition i.e., systemic leptin levels were reduced in well-nourished infected animals also (Dayakar et al., 2017). We assume that perturbations in host lipid profile could disturb the host immunity and promote the parasite growth and diffusion inside the lymphoid tissues (Ghosh et al., 2013). It could be a novel mechanism exhibited by the *Leishmania* parasite to evade the host immune defense.

Interaction Between Leptin and *Candida albicans* Infection

Leptin receptor-deficient obese (*fa/fa*) rats show impaired host defense against *C. albicans* infection whereas, in stressed rats this infection caused a prompt reduction in systemic leptin levels and increased TNF- α levels (Rodríguez-Galán et al., 2010). However, it has been suggested that the leptin can activate healing the critical illness in stress-related activities (Bornstein et al., 1998). Leptin regulates the production of endogenous cortisol through hypothalamic-pituitary-adrenal (HPA) axis, which induces stress response, and hematopoiesis.

SCOPE AND CHALLENGES OF LEPTIN IN VACCINES FORMULATION

To the best of our knowledge, several vaccines failed to prove their efficacy in preclinical studies, and the lack of appropriate immuno-adjuvant could be one of the potential reasons. With the advancement of scientific knowledge and innovative technology, it becomes easier to identify and develop novel vaccine or adjuvant tools (Kennedy and Poland, 2011; Poland et al., 2011). The goal of adjuvant is to elicit robust vaccine-specific immune response and immune homeostasis. Leptin is one such molecule, which can restore inflammatory response without eliciting adverse side-effects since it is produced endogenously. For example, a long-term leptin replacement therapy in congenital leptin-deficient children restored the Th1/Th2 cytokine balance and proliferation of lymphocytes, neutrophils, and monocytes (Farooqi et al., 2002). The 7 days of leptin treatment in these children had no effect on body weight loss, though it reduced energy intake (Farooqi et al., 2007). In contrast, the intracerebroventricular route of leptin (1 μ g/day) infusion for 7 days in C57B6/J and *ob/ob* mice substantially reduced the daily intake of food and body weight (Tschöp et al., 2010). The peripheral leptin administration does not affect either food intake or body weight (Bryson, 2000). It acts directly on immune cells. In consistence with this hypothesis, we observed that the subcutaneous route of recombinant leptin (5 μ g/day)

administration into the malnourished BALB/c mice infected by *L. donovani* did not alter the amount of food intake or weight gain; in fact, it controlled the further loss of body weight. In addition, an increased infiltration of CD8+ T cells and their activity was observed in the spleen tissue in terms of Granzyme-A expression and cytotoxic T lymphocyte Antigen (CTLA)-4 and programmed death protein (PD-1) repression (Dayakar et al., 2017). Collectively, our study suggests that leptin can be a potential adjuvant tool in kala-azar vaccination strategies. It was also shown that the peripheral administration of recombinant leptin markedly reduced food intake and body weight in *ob/ob* and diet-induced obese mice without apparent toxicity and had no effect on *db/db* mice (Campfield et al., 1995; Halaas et al., 1995). But these observations in wild-type lean mice are quite lesser and had not reported on alteration in metabolic parameters (Pelleymounter et al., 1995), suggesting clinical perspectives of leptin treatment in weight related complications. However, exogenous leptin therapy may not be beneficial to the obese individuals (Heymsfield et al., 1999) having hyperleptinemia and leptin resistance i.e., impaired leptin signaling due to LEPR deficiency or transport saturation. But the administration of chemical chaperons such as 4-phenylbutyric acid (4-PBA) and tauroursodeoxycholic acid (TUDCA) has reduced the ER stress in diet-induced obesity and increased the leptin sensitivity by ten-folds beside to weight loss during high-fat diet (Ozcan et al., 2009). The clinical investigation on obese and type-2 diabetic phenotypes is required to confirm the therapeutic potential of TUDCA as it known to regulate the weight-loss and leptin/insulin sensitivity (Ozcan et al., 2006), and interact directly with immune cells. The molecular chaperon heat-shock protein 60 (HSP60) may have potential role in the regulation of obesity related chronic ER stress and its expression is correlated with circulatory leptin (Märker et al., 2012). In *in vitro*, leptin stimulates the expression of HSP60 (Bonior et al., 2006), which exerts pro/anti-inflammatory response by interacting with TLR-2 and TLR-4, unveiling the interaction between leptin and chaperons. However, the food and drug administration (FDA) approval of TUDCA for the treatment of primary biliary cirrhosis (Invernizzi et al., 1999) and its inhibitory potential against influenza A viral replication by inducing ER stress (Hassan et al., 2012) are to be controversial for its application in leptin/leptin signaling impaired pathologies. Hence, there is a great scope for active research to identify a specific pharmacotherapy candidate to improve leptin signaling in obesity. Targeting SOCS-3 expression and PTPs activity using appropriate inhibitors and implying ER stress reducing measures could help in reversing leptin insensitivity in obesity.

Studies have shown that immature DCs primed with leptin were licensed to skew the immune response toward Th1-type by upregulating the production of IL-12p70 upon CD40 stimulation. It was also able to induce the activity of autologous CD8+ T cells in terms of perforin and IFN- γ production (Mattioli et al., 2008). The reinfusion of leptin-pulsed autologous DCs into the patients with cancer may induce anti-tumor specific CD8+ T cell response by infiltrating into the LNs. In view of this, there is a scope to develop vaccines against multiple

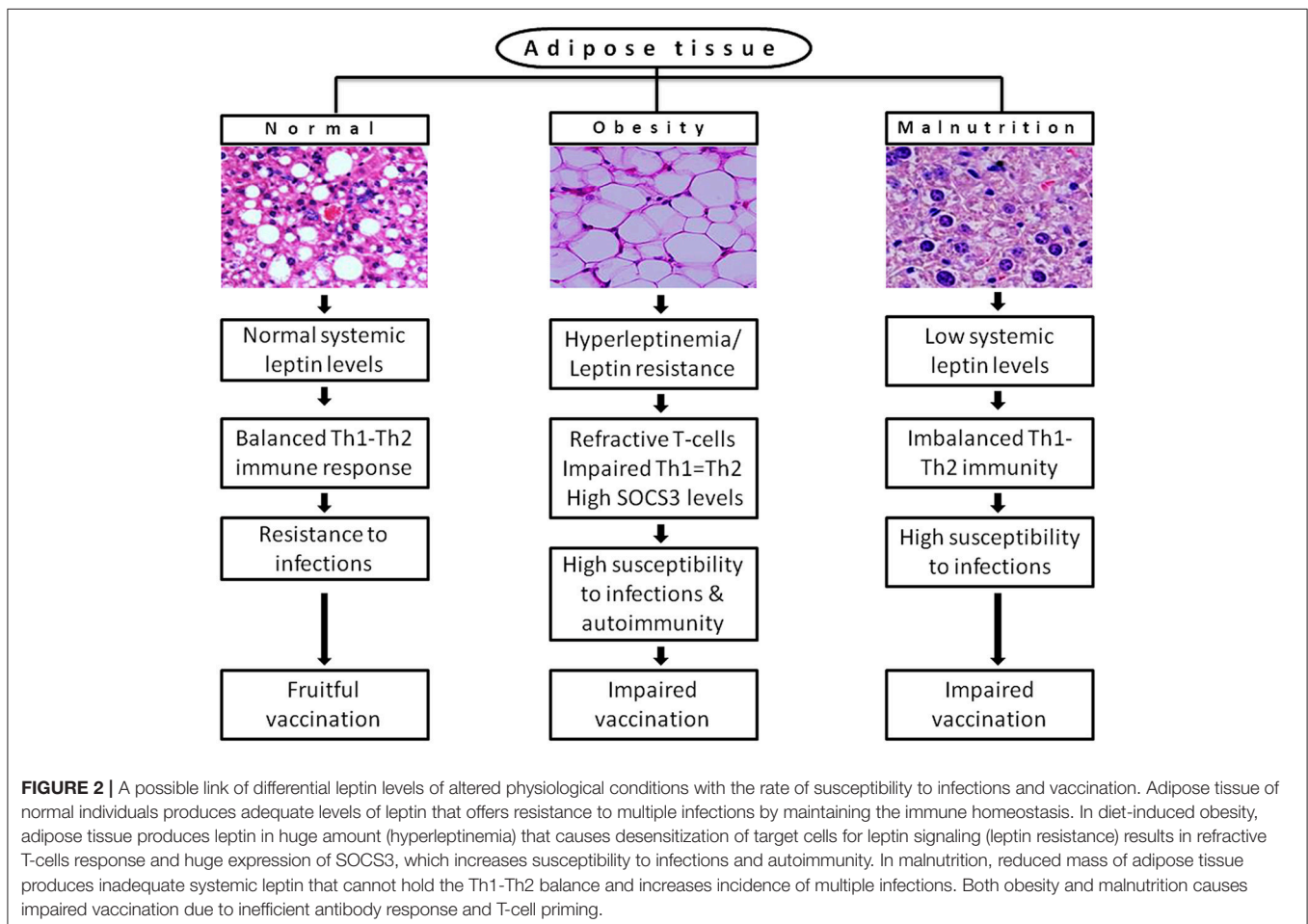
infections e.g., HIV using leptin as an adjuvant in immune cell-based therapy (Martín-Romero et al., 2000; Mattioli et al., 2005). Leptin resistance or desensitization of signaling in obesity (BMI ≥ 30 kg/m²) and over-nutrition impaired antigen-specific IgG response as well as reduced CD69, IFN- γ , and Granzyme-B in CD8+ T cells to influenza vaccination (Sheridan et al., 2012). Similarly, hepatitis-B vaccination failed due to reduced HBsAg specific IgG response (Weber et al., 1985) and tetanus vaccination also failed due to low anti-tetanus IgG and high IL-6 (Eliakim et al., 2006). Overall impaired antibody response may be due to the sharp reduction in B-lymphocytes count, for example in *ob/ob* mice, a firm reduction in pre-B-cells count for 21% and immature B-cells count for 12% was noticed. However, this was further repaired by exogenous leptin supply, unveiling the role of leptin in B-cells generation and activation (Claycombe et al., 2008).

Despite the lack of investigations on leptin-based therapies, the immunostimulatory potential of leptin cannot be neglected in vaccines development, as an adjuvant (White et al., 2013). Certain investigators tried to explore the adjuvant role of leptin in mucosal vaccination against a gram-positive bacterial pneumonia caused by *R. equi* infection in foals and immunodeficient humans (Cauchard et al., 2011). In this study, mice were vaccinated with LL-VapA (a native *Lactococcus lactis* vector expressing virulence-associated protein-A of *R. equi*) alone or with the combination of LL-leptin (a recombinant *L. lactis* strain for leptin production) through an intra-gastric or intranasal route against *R. equi*. However, only the co-immunization (combination of LL-VapA + LL-leptin) was able to produce protective immunity, when it was ingested through gastric route. On the other hand, LL-VapA alone was able protect against bacterial challenge when it was vaccinated through intranasal route but the co-immunization has stimulated the immune response. Similarly, the LEPR-deficient mice were not protected by prophylactic vaccination in spite of mild gastritis and pathogen specific antibody response during *H. pylori* infection (Wehrens et al., 2008), indicating the importance of leptin and its signaling in the generation host protective immune response. Leptin signaling in mucosal epithelium of vaccinated stomach possibly trigger the infiltration of effector CD4+ T cells, neutrophils and macrophages, and reduce CD4+ Treg cells to *H. pylori* challenge. CD4+ T cells produced leptin stimulates their own proliferation by autocrine mechanism as well as epithelial cells to induce protective immune response and suppress Tregs mediated pathogenic response (Walduck and Becher, 2012). Acute systemic inflammation induced by *S. typhi* vaccination in humans doubled the plasma IL-6 levels but it did not affect the leptin levels within 24 h, indicating that leptin is not a key molecule in early systemic inflammation (Ekström et al., 2015).

In conclusion, the current knowledge suggests a finite role of leptin signaling in immunity, but the data is insufficient at clinical standards. It is based on measuring the concentration of systemic leptin levels, which is not a well-defined marker of actual leptin signaling. In addition, the current eating habits and sedentary lifestyle of developed countries and of urban population in developing countries are becoming real hurdles to control the obesity in children and adults. They are the risk factors for

fruitful vaccination attempts to various infections, which emerges in hypo or hyperleptinemia state and in impaired Th1/Th2 balance state shown in **Figure 2**. However, there is an increasing evidence that leptin is a part of immunopathology of certain physiological conditions. For instance, high systemic leptin in mice associated with T cell mediated hepatotoxicity (Faggioni et al., 2000a) liver fibrosis (Leclercq et al., 2002) autoimmune encephalomyelitis (Matarese et al., 2001; Sanna et al., 2003) intestinal inflammation (Siegmond et al., 2002), coronary heart disease (Yudkin et al., 1999), and type-2 diabetes (Pickup et al., 2000; Matarese et al., 2002). In humans, it associated with pancreatitis (Konturek et al., 2002), sepsis and septic shock (Arnalich et al., 1999) suggests that non-physiological excess levels of leptin are toxic to the host system due to excessive proinflammatory cytokine response and inflammation, which causes tissue damage. The strategies following to preserve the number, proliferation and activity of naturally occurring Foxp3+CD4+CD25+ Tregs may help to counteract the excessive inflammation. As the leptin is a negative regulator of Tregs, the neutralization of leptin with monoclonal antibody in Tregs unlocks their hyporesponsiveness or anergic state by the rapid degradation of cyclin dependent kinase inhibitor p27 (p27^{kip1}) and phosphorylation of Erk1/2, and increases IL-2

dependent Foxp3+ Tregs proliferation without altering their suppressive role (De Rosa et al., 2007). This phenomenon may help to protect from autoimmunity but increases susceptibility to intracellular infections. Therefore, the strategic usage of Tregs with the manipulation of leptin signaling may provide a new opportunity to control infectious and autoimmunity disorders. In addition to this, a better understanding the network of underlying mechanisms that connected with the impaired leptin signaling or central vs. peripheral leptin resistance in obesity-related disorders, autoimmunity, and infectious diseases may empower our knowledge toward identifying potential therapeutics to increase the leptin sensitivity as wells as vaccine response to infections. Despite the insulin therapy to improve the cellular uptake of glucose and hyperglycaemia and resulting diabetes in *db/db* individuals, it would be a fascinating discovery if we address a novel strategy to improve leptin signaling in *db/db* cases besides to conventional receptor gene cloning approach in target cells. The lack of functional leptin in *ob/ob* and insufficient leptin in malnutrition or starvation obviously responds to exogenous leptin treatment. However, the route of administration is also critically important. By considering the type of disorder (i.e., metabolic, immunological, endocrine, infectious, and lifestyle) and molecular basis of



pathogenicity, leptin can be targeted as a potential therapeutic molecule as well as an adjuvant tool to improve the vaccines efficiency without affecting anti-inflammatory or autoimmune responses.

Our further goal is to find out the correlation between systemic leptin levels and disease severity of VL by using clinical samples of pre/post-treated and disease relapsed patients from endemic regions of India. Though DCs are potential APCs and produce antileishmanial immune response, the studies on DC-based immunotherapy for VL remains low. Antigen-pulsed DCs in conjugation with Antimonial drug was tried against established murine VL. However, the drug conjugation may repeat the complications of toxicity and resistance. The DC-based therapy alone was tried against cutaneous leishmaniasis (CL) but it was proved inefficient to heal the disease, highlighting the importance of an adjuvant in immunotherapy. Therefore, in future prospective, we proposed to investigate the adjuvant potential of recombinant leptin in DC-based immunotherapy for VL.

REFERENCES

- Agrawal, S., Gollapudi, S., Su, H., and Gupta, S. (2011). Leptin activates human B cells to secrete TNF- α , IL-6, and IL-10 via JAK2/STAT3 and p38MAPK/ERK1/2 signaling pathway. *J. Clin. Immunol.* 31, 472–478. doi: 10.1007/s10875-010-9507-1
- Akhtar, L. N., Qin, H., Muldowney, M. T., Yanagisawa, L. L., Kutsch, O., Clements, J. E., et al. (2010). Suppressor of cytokine signaling 3 inhibits antiviral IFN- β signaling to enhance HIV-1 replication in macrophages. *J. Immunol.* 185, 2393–2404. doi: 10.4049/jimmunol.0903563
- Alam, F., Salam, A., Mahmood, I., Kabir, M., and Chowdhury, S. (2016). Amebic liver abscess is associated with malnutrition and low serum leptin level. *J. Infect. Dis. Ther.* 4:298. doi: 10.4172/2332-0877.1000298
- Arnalich, F., Lopez, J., Codoceo, R., Jim Nez, M., Madero, R., and Montiel, C. (1999). Relationship of plasma leptin to plasma cytokines and human survival in sepsis and septic shock. *J. Infect. Dis.* 180, 908–911. doi: 10.1086/314963
- Attoub, S., Noe, V., Pirola, L., Bruyneel, E., Chastre, E., Mareel, M., et al. (2000). Leptin promotes invasiveness of kidney and colonic epithelial cells via phosphoinositide 3-kinase-, rho-, and rac-dependent signaling pathways. *FASEB J.* 14, 2329–2338. doi: 10.1096/fj.00-0162
- Azuma, T., Suto, H., Ito, Y., Ohtani, M., Dojo, M., Kuriyama, M., et al. (2001). Gastric leptin and *Helicobacter pylori* infection. *Gut* 49, 324–329. doi: 10.1136/gut.49.3.324
- Azzoni, L., Crowther, N. J., Firnhaber, C., Foulkes, A. S., Yin, X., Glencross, D., et al. (2010). Association between HIV replication and serum leptin levels: an observational study of a cohort of HIV-1-infected South African women. *J. Int. AIDS Soc.* 13:33. doi: 10.1186/1758-2652-13-33
- Basu, J. M., Mookerjee, A., Sen, P., Bhaumik, S., Sen, P., Banerjee, S., et al. (2006). Sodium antimony gluconate induces generation of reactive oxygen species and nitric oxide via phosphoinositide 3-kinase and mitogen-activated protein kinase activation in Leishmania donovani-infected macrophages. *Antimicrob. Agents Chemother.* 50, 1788–1797. doi: 10.1128/AAC.50.5.1788-1797.2006
- Baumann, H., Morella, K. K., White, D. W., Dembski, M., Bailon, P. S., Kim, H., et al. (1996). The full-length leptin receptor has signaling capabilities of interleukin 6-type cytokine receptors. *Proc. Natl. Acad. Sci. U.S.A.* 93, 8374–8378. doi: 10.1073/pnas.93.16.8374
- Birmingham, C. L., Canadien, V., Kaniuk, N. A., Steinberg, B. E., Higgins, D. E., and Brumell, J. H. (2008). Listeriolysin O allows *Listeria monocytogenes* replication in macrophage vacuoles. *Nature* 451, 350–354. doi: 10.1038/nature06479

AUTHOR CONTRIBUTIONS

SK: Selection of topic, outline of review to be drafted, analysis of leptin interplay with cytokines in infection and immunity, abstract writing and tables information was drafted and edited the overall review to make it to its final shape, and working with references. DA: Literature gathering, preparation of first draft to be corrected by SK, drawing of figures and discussions on view points of scoping leptin and vaccine formulations, and adding proper references to the contexts given in review. CS: Potential discussion and inputs in drafting leptin role of immunity in leishmania.

ACKNOWLEDGMENTS

We thank Prof. Vadlakonda Lakshminpathi for his critical evaluation and suggestions while constructing the review. Dr. S. S. Mohanraj's kind help is also acknowledged for his help in re-drawing Figure 1.

- Bjorbak, C., Lavery, H. J., Bates, S. H., Olson, R. K., Davis, S. M., Flier, J. S., et al. (2000). SOCS3 mediates feedback inhibition of the leptin receptor via Tyr985. *J. Biol. Chem.* 275, 40649–40657. doi: 10.1074/jbc.M007577200
- Black, R. E., Allen, L. H., Bhutta, Z. A., Caulfield, L. E., De Onis, M., Ezzati, M., et al. (2008). Maternal and child undernutrition: global and regional exposures and health consequences. *Lancet* 371, 243–260. doi: 10.1016/S0140-6736(07)61690-0
- Bonior, J., Jaworek, J., Konturek, S. J., and Pawlik, W. W. (2006). Leptin is the modulator of HSP60 gene expression in AR42J cells. *J. Physiol. Pharmacol.* 57(Suppl. 7), 135–143.
- Bornstein, S. R., Licinio, J., Tauchnitz, R., Engelmann, L., Negrao, A. B., Gold, P., et al. (1998). Plasma leptin levels are increased in survivors of acute sepsis: associated loss of diurnal rhythm, in cortisol and leptin secretion. *J. Clin. Endocrinol. Metab.* 83, 280–283. doi: 10.1210/jcem.83.1.4610
- Bracho-Riquelme, R. L., Loera-Castañeda, V., Torres-Valenzuela, A., Loera-Castañeda, G. A., and Sánchez-Ramírez, J. P. (2011). Leptin and leptin receptor polymorphisms are associated with poor outcome (death) in patients with non-appendicular secondary peritonitis. *Critical Care* 15:R227. doi: 10.1186/cc10467
- Brun, P., Castagliuolo, I., Leo, V. D., Buda, A., Pinzani, M., Palù, G., et al. (2007). Increased intestinal permeability in obese mice: new evidence in the pathogenesis of nonalcoholic steatohepatitis. *Am. J. Physiol. –Gastrointest. Liver Physiol.* 292, G518–G525. doi: 10.1152/ajpgi.00024.2006
- Bruno, A., Conus, S., Schmid, I., and Simon, H.-U. (2005). Apoptotic pathways are inhibited by leptin receptor activation in neutrophils. *J. Immunol.* 174, 8090–8096. doi: 10.4049/jimmunol.174.12.8090
- Bryson, J. M. (2000). The future of leptin and leptin analogues in the treatment of obesity. *Diabetes Obes. Metab.* 2, 83–89. doi: 10.1046/j.1463-1326.2000.00052.x
- Burguera, B., Couce, M. E., Curran, G. L., Jensen, M. D., Lloyd, R. V., Cleary, M. P., et al. (2000). Obesity is associated with a decreased leptin transport across the blood-brain barrier in rats. *Diabetes* 49, 1219–1223. doi: 10.2337/diabetes.49.7.1219
- Cakir, B., Yönm, A., Güler, S., Odabaşı, E., Demirbaş, B., Gürsoy, G., et al. (1999). Relation of leptin and tumor necrosis factor α to body weight changes in patients with pulmonary tuberculosis. *Horm. Res. Paediatr.* 52, 279–283. doi: 10.1159/000023495
- Caldefie-Chezet, F., Poulin, A., Tridon, A., Sion, B., and Vasson, M. (2001). Leptin: a potential regulator of polymorphonuclear neutrophil bactericidal action? *J. Leukoc. Biol.* 69, 414–418. doi: 10.1189/jlb.69.3.414

- Campfield, L. A., Smith, F. J., Guise, Y., Devos, R., and Burn, P. (1995). Recombinant mouse OB protein: evidence for a peripheral signal linking adiposity and central neural networks. *Science* 269, 546–549. doi: 10.1126/science.7624778
- Carrero, J. A., and Unanue, E. R. (2006). Lymphocyte apoptosis as an immune subversion strategy of microbial pathogens. *Trends Immunol.* 27, 497–503. doi: 10.1016/j.it.2006.09.005
- Carrero, J. A., Calderon, B., and Unanue, E. R. (2004). Listeriolysin O from *Listeria monocytogenes* is a lymphocyte apoptogenic molecule. *J. Immunol.* 172, 4866–4874. doi: 10.4049/jimmunol.172.8.4866
- Cauchard, S., Bermudez-Humaran, L., Blugeon, S., Laugier, C., Langella, P., and Cauchard, J. (2011). Mucosal co-immunization of mice with recombinant lactococci secreting VapA antigen and leptin elicits a protective immune response against *Rhodococcus equi* infection. *Vaccine* 30, 95–102. doi: 10.1016/j.vaccine.2011.10.026
- Ceddia, R. (2005). Direct metabolic regulation in skeletal muscle and fat tissue by leptin: implications for glucose and fatty acids homeostasis. *Int. J. Obes.* 29, 1175–1183. doi: 10.1038/sj.jco.0803025
- Cederholm, T., Lindgren, J., and Palmblad, J. (2000). Impaired leukotriene C4 generation in granulocytes from protein-energy malnourished chronically ill elderly. *J. Intern. Med.* 247, 715–722. doi: 10.1046/j.1365-2796.2000.00691.x
- Chan, J. L., Moschos, S. J., Bullen, J., Heist, K., Li, X., Kim, Y. B., et al. (2005). Recombinant methionyl human leptin administration activates signal transducer and activator of transcription 3 signaling in peripheral blood mononuclear cells *in vivo* and regulates soluble tumor necrosis factor- α receptor levels in humans with relative leptin deficiency. *J. Clin. Endocrinol. Metab.* 90, 1625–1631. doi: 10.1210/jc.2004-1823
- Chandra, R. K. (1992). Nutrition and immunity in the elderly. *Nutr. Rev.* 50, 367–371. doi: 10.1111/j.1753-4887.1992.tb02482.x
- Chaudhri, G., and Clark, I. (1989). Reactive oxygen species facilitate the *in vitro* and *in vivo* lipopolysaccharide-induced release of tumor necrosis factor. *J. Immunol.* 143, 1290–1294.
- Claycombe, K., King, L. E., and Fraker, P. J. (2008). A role for leptin in sustaining lymphopoiesis and myelopoiesis. *Proc. Natl. Acad. Sci. U.S.A.* 105, 2017–2021. doi: 10.1073/pnas.0712053105
- Coffey, M. J., Phare, S. M., Kazanjian, P. H., and Peters-Golden, M. (1996). 5-Lipoxygenase metabolism in alveolar macrophages from subjects infected with the human immunodeficiency virus. *J. Immunol.* 157, 393–399.
- Considine, R. V., and Caro, J. F. (1997). Leptin and the regulation of body weight. *Int. J. Biochem. Cell Biol.* 29, 1255–1272. doi: 10.1016/S1357-2725(97)00050-2
- Conus, S., Bruno, A., and Simon, H.-U. (2005). Leptin is an eosinophil survival factor. *J. Allergy Clin. Immunol.* 116, 1228–1234. doi: 10.1016/j.jaci.2005.09.003
- Dayakar, A., Chandrasekaran, S., Veronica, J., and Maurya, R. (2011). Role of leptin in human visceral leishmaniasis? *Med. Hypotheses* 77, 416–418. doi: 10.1016/j.mehy.2011.05.032
- Dayakar, A., Chandrasekaran, S., Veronica, J., and Maurya, R. (2016). Leptin induces the phagocytosis and protective immune response in *Leishmania donovani* infected THP-1 cell line and human PBMCs. *Exp. Parasitol.* 160, 54–59. doi: 10.1016/j.exppara.2015.12.002
- Dayakar, A., Chandrasekaran, S., Veronica, J., Bharadwaja, V., and Maurya, R. (2017). Leptin regulates Granzyme-A, PD-1 and CTLA-4 expression in T cell to control visceral leishmaniasis in BALB/c Mice. *Sci. Rep.* 7:14664. doi: 10.1038/s41598-017-15288-7
- De Rosa, V., Procaccini, C., Cali, G., Pirozzi, G., Fontana, S., Zappacosta, S., et al. (2007). A key role of leptin in the control of regulatory T cell proliferation. *Immunity* 26, 241–255. doi: 10.1016/j.immuni.2007.01.011
- Desreumaux, P., Ernst, O., Geboes, K., Gambiez, L., Berrebi, D., Müller-Alouf, H., et al. (1999). Inflammatory alterations in mesenteric adipose tissue in Crohn's disease. *Gastroenterology* 117, 73–81. doi: 10.1016/S0016-5085(99)70552-4
- Duggal, P., Guo, X., Haque, R., Peterson, K. M., Ricklefs, S., Mondal, D., et al. (2011). A mutation in the leptin receptor is associated with *Entamoeba histolytica* infection in children. *J. Clin. Invest.* 121:1191. doi: 10.1172/JCI45294
- Economou, M., Karyda, S., Kansouzidou, A., and Kavaliotis, J. (2000). *Listeria meningitis* in children: report of two cases. *Infection* 28, 121–123. doi: 10.1007/s150100050061
- Ekström, M., Söderberg, S., and Tornvall, P. (2015). Acute systemic inflammation is unlikely to affect adiponectin and leptin synthesis in humans. *Front. Cardiovasc. Med.* 2:7. doi: 10.3389/fcvm.2015.00007
- El Homs, M., Ducroc, R., Claustre, J., Jourdan, G., Gertler, A., Estienne, M., et al. (2007). Leptin modulates the expression of secreted and membrane-associated mucins in colonic epithelial cells by targeting PKC, PI3K, and MAPK pathways. *Am. J. Physiol. Gastrointest. Liver Physiol.* 293, G365–G373. doi: 10.1152/ajpgi.00091.2007
- Elbim, C., Pillet, S., Prevost, M., Preira, A., Girard, P., Rogine, N., et al. (1999). Redox and activation status of monocytes from human immunodeficiency virus-infected patients: relationship with viral load. *J. Virol.* 73, 4561–4566.
- Eliakim, A., Swindt, C., Zaldivar, F., Casali, P., and Cooper, D. M. (2006). Reduced tetanus antibody titers in overweight children. *Autoimmunity* 39, 137–141. doi: 10.1080/08916930600597326
- Estrada, V., Serrano-Ríos, M., Martínez, L. M., Villar, N., González, L. A., Téllez, M. J., et al. (2002). Leptin and adipose tissue maldistribution in HIV-infected male patients with predominant fat loss treated with antiretroviral therapy. *J. Acquir. Immune Defic. Syndr.* 29, 32–40. doi: 10.1097/00042560-2002101010-00004
- Faggioni, R., Jones-Carson, J., Reed, D. A., Dinarello, C. A., Feingold, K. R., Grunfeld, C., et al. (2000a). Leptin-deficient (ob/ob) mice are protected from T cell-mediated hepatotoxicity: role of tumor necrosis factor α and IL-18. *Proc. Natl. Acad. Sci. U.S.A.* 97, 2367–2372. doi: 10.1073/pnas.040561297
- Faggioni, R., Moser, A., Feingold, K. R., and Grunfeld, C. (2000b). Reduced leptin levels in starvation increase susceptibility to endotoxin shock. *Am. J. Pathol.* 156, 1781–1787. doi: 10.1016/S0002-9440(10)65049-3
- Farooqi, I. S., Bullmore, E., Keogh, J., Gillard, J., O'hahilly, S., and Fletcher, P. C. (2007). Leptin regulates striatal regions and human eating behavior. *Science* 317:1355. doi: 10.1126/science.1144599
- Farooqi, I. S., Matarese, G., Lord, G. M., Keogh, J. M., Lawrence, E., Agwu, C., et al. (2002). Beneficial effects of leptin on obesity, T cell hyporesponsiveness, and neuroendocrine/metabolic dysfunction of human congenital leptin deficiency. *J. Clin. Invest.* 110, 1093–1103. doi: 10.1172/JCI0215693
- Fernández-Riejos, P., Najib, S., Santos-Alvarez, J., Martín-Romero, C., Pérez-Pérez, A., González-Yanes, C., et al. (2010). Role of leptin in the activation of immune cells. *Mediators Inflamm.* 2010:68343. doi: 10.1155/2010/568343
- Gainsford, T., Willson, T. A., Metcalf, D., Handman, E., McFarlane, C., Ng, A., et al. (1996). Leptin can induce proliferation, differentiation, and functional activation of hemopoietic cells. *Proc. Natl. Acad. Sci. U.S.A.* 93, 14564–14568. doi: 10.1073/pnas.93.25.14564
- Galgani, M., Procaccini, C., De Rosa, V., Carbone, F., Chieffo, P., La Cava, A., et al. (2010). Leptin modulates the survival of autoreactive CD4⁺ T cells through the nutrient/energy-sensing mammalian target of rapamycin signaling pathway. *J. Immunol.* 185, 7474–7479. doi: 10.4049/jimmunol.1001674
- Ghosh, J., Bose, M., Roy, S., and Bhattacharyya, S. N. (2013). *Leishmania donovani* targets Dicer1 to downregulate miR-122, lower serum cholesterol, and facilitate murine liver infection. *Cell Host Microbe* 13, 277–288. doi: 10.1016/j.chom.2013.02.005
- Grinspoon, S., Gulick, T., Askari, H., Landt, M., Lee, K., Anderson, E., et al. (1996). Serum leptin levels in women with anorexia nervosa. *J. Clin. Endocrinol. Metab.* 81, 3861–3863.
- Gueirard, P., Laplante, A., Rondeau, C., Milon, G., and Desjardins, M. (2008). Trafficking of *Leishmania donovani* promastigotes in non-lytic compartments in neutrophils enables the subsequent transfer of parasites to macrophages. *Cell Microbiol.* 10, 100–111. doi: 10.1111/j.1462-5822.2007.01018.x
- Guo, X., Roberts, M. R., Becker, S. M., Podd, B., Zhang, Y., Chua, S. C., et al. (2011). Leptin signaling in intestinal epithelium mediates resistance to enteric infection by *Entamoeba histolytica*. *Mucosal Immunol.* 4, 294–303. doi: 10.1038/mi.2010.76
- Halaas, J. L., Gajiwala, K. S., Maffei, M., Cohen, S. L., Chait, B. T., Rabinowitz, D., et al. (1995). Weight-reducing effects of the plasma protein encoded by the obese gene. *Science* 269, 543–546. doi: 10.1126/science.7624777
- Hassan, I. H., Zhang, M. S., Powers, L. S., Shao, J. Q., Baltrusaitis, J., Rutkowski, D. T., et al. (2012). Influenza A viral replication is blocked by inhibition of the inositol-requiring enzyme 1 (IRE1) stress pathway. *J. Biol. Chem.* 287, 4679–4689. doi: 10.1074/jbc.M111.284695
- Heymsfield, S. B., Greenberg, A. S., Fujioka, K., Dixon, R. M., Kushner, R., Hunt, T., et al. (1999). Recombinant leptin for weight loss in obese and lean adults: a randomized, controlled, dose-escalation trial. *JAMA* 282, 1568–1575. doi: 10.1001/jama.282.16.1568
- Hosoi, T., Sasaki, M., Miyahara, T., Hashimoto, C., Matsuo, S., Yoshii, M., et al. (2008). Endoplasmic reticulum stress induces leptin resistance. *Mol. Pharmacol.* 74, 1610–1619. doi: 10.1124/mol.108.050070

- Houseknecht, K., and Portocarrero, C. (1998). Leptin and its receptors: regulators of whole-body energy homeostasis. *Domest. Anim. Endocrinol.* 15, 457–475. doi: 10.1016/S0739-7240(98)00035-6
- Howard, J. K., Lord, G. M., Matarese, G., Vendetti, S., Gbatei, M. A., Ritter, M. A., et al. (1999). Leptin protects mice from starvation-induced lymphoid atrophy and increases thymic cellularity in ob/ob mice. *J. Clin. Invest.* 104:1051. doi: 10.1172/JCI6762
- Hsu, A., Aronoff, D., Phipps, J., Goel, D., and Mancuso, P. (2007). Leptin improves pulmonary bacterial clearance and survival in ob/ob mice during pneumococcal pneumonia. *Clin. Exp. Immunol.* 150, 332–339. doi: 10.1111/j.1365-2249.2007.03491.x
- Huang, L., Wang, Z., and Li, C. (2001). Modulation of circulating leptin levels by its soluble receptor. *J. Biol. Chem.* 276, 6343–6349. doi: 10.1074/jbc.M009795200
- Hultgren, O. H., and Tarkowski, A. (2001). Leptin in septic arthritis: decreased levels during infection and amelioration of disease activity upon its administration. *Arthritis Res. Ther.* 3:389. doi: 10.1186/ar332
- Hur, S. J., Kim, D. H., Chun, S. C., and Lee, S. K. (2013). Effect of adenovirus and influenza virus infection on obesity. *Life Sci.* 93, 531–535. doi: 10.1016/j.lfs.2013.08.016
- Ikejima, S., Sasaki, S., Sashinami, H., Mori, F., Ogawa, Y., Nakamura, T., et al. (2005). Impairment of host resistance to *Listeria monocytogenes* infection in liver of db/db and ob/ob mice. *Diabetes* 54, 182–189. doi: 10.2337/diabetes.54.1.182
- Invernizzi, P., Setchell, K. D., Crosignani, A., Battezzati, P. M., Larghi, A., O'Connell, N. C., et al. (1999). Differences in the metabolism and disposition of ursodeoxycholic acid and of its taurine-conjugated species in patients with primary biliary cirrhosis. *Hepatology* 29, 320–327. doi: 10.1002/hep.510290220
- Jaedick, K. M., Roythorne, A., Padgett, K., Todryk, S., Preshaw, P. M., and Taylor, J. J. (2013). Leptin up-regulates TLR2 in human monocytes. *J. Leukoc. Biol.* 93, 561–571. doi: 10.1189/jlb.1211606
- Jenkins, N. L., Turner, J., Dritz, S., Durham, S., and Minton, J. (2004). Changes in circulating insulin-like growth factor-I, insulin-like growth factor binding proteins, and leptin in weaned pigs infected with *Salmonella enterica* serovar Typhimurium. *Domest. Anim. Endocrinol.* 26, 49–60. doi: 10.1016/j.domaniend.2003.09.001
- Jubiz, W., Draper, R. E., Gale, J., and Nolan, G. (1984). Decreased leukotriene B₄ synthesis by polymorphonuclear leukocytes from male patients with diabetes mellitus. *Prostaglandins Leukotrienes Med.* 14, 305–311. doi: 10.1016/0262-1746(84)90114-8
- Karlsson, E. A., Sheridan, P. A., and Beck, M. A. (2010). Diet-induced obesity in mice reduces the maintenance of influenza-specific CD8⁺ memory T cells. *J. Nutr.* 140, 1691–1697. doi: 10.3945/jn.110.123653
- Karp, C. L., Wysocka, M., Ma, X., Marovich, M., Factor, R. E., Nutman, T., et al. (1998). Potent suppression of IL-12 production from monocytes and dendritic cells during endotoxin tolerance. *strain* 1:18547. doi: 10.1002/(SICI)1521-4141(199810)28:10<18547::AID-IMMU3128>3.0.CO;2-T
- Katona, P., and Katona-Apte, J. (2008). The interaction between nutrition and infection. *Clin. Infect. Dis.* 46, 1582–1588. doi: 10.1086/587658
- Kennedy, R. B., and Poland, G. A. (2011). The top five “game changers” in vaccinology: toward rational and directed vaccine development. *OMICS* 15, 533–537. doi: 10.1089/omi.2011.0012
- Khosravi, Y., Seow, S. W., Amoyo, A. A., Chiow, K. H., Tan, T. L., Wong, W. Y., et al. (2015). *Helicobacter pylori* infection can affect energy modulating hormones and body weight in germ free mice. *Sci. Rep.* 5:8731. doi: 10.1038/srep08731
- Kimura, T., Kameoka, M., and Ikuta, K. (1993). Amplification of superoxide anion generation in phagocytic cells by HIV-1 infection. *FEBS Lett.* 326, 232–236. doi: 10.1016/0014-5793(93)81797-4
- Konturek, P. C., Jaworek, J., Maniatioglou, A., Bonior, J., Meixner, H., Konturek, S. J., et al. (2002). Leptin modulates the inflammatory response in acute pancreatitis. *Digestion* 65, 149–160. doi: 10.1159/000064935
- Kotler, D. P., Wang, J., and Pierson, R. (1985). Body composition studies in patients with the acquired immunodeficiency syndrome. *Am. J. Clin. Nutr.* 42, 1255–1265. doi: 10.1093/ajcn/42.6.1255
- Krebs, D. L., and Hilton, D. J. (2001). SOCS proteins: negative regulators of cytokine signaling. *Stem Cells* 19, 378–387. doi: 10.1634/stemcells.19-5-378
- Krebs, J., and Kacelnik, A. (1991). “Decision-making,” in *Behavioural Ecology: an Evolutionary Approach*, 3rd Edn., eds J. D. Krebs and N. B. Davies (Oxford: Blackwell Scientific Publications), 105–136.
- Kubo, M., Hanada, T., and Yoshimura, A. (2003). Suppressors of cytokine signaling and immunity. *Nat. Immunol.* 4:1169. doi: 10.1038/nri1012
- La Cava, A., and Matarese, G. (2004). The weight of leptin in immunity. *Nat. Rev. Immunol.* 4, 371–379. doi: 10.1038/nri1350
- Laufs, H., Müller, K., Fleischer, J., Reiling, N., Jahnke, N., Jensenius, J. C., et al. (2002). Intracellular survival of *Leishmania major* in neutrophil granulocytes after uptake in the absence of heat-labile serum factors. *Infect. Immun.* 70, 826–835. doi: 10.1128/IAI.70.2.826-835.2002
- Leclercq, I. A., Farrell, G. C., Schriemer, R., and Robertson, G. R. (2002). Leptin is essential for the hepatic fibrogenic response to chronic liver injury. *J. Hepatol.* 37, 206–213. doi: 10.1016/S0168-8278(02)00102-2
- Lee, F. Y., Li, Y., Yang, E. K., Yang, S. Q., Lin, H. Z., Trush, M. A., et al. (1999). Phenotypic abnormalities in macrophages from leptin-deficient, obese mice. *Am. J. Physiol.* 276, C386–C394. doi: 10.1152/ajpcell.1999.276.2.C386
- Lee, G.-H., Proenca, R., Montez, J., Carroll, K., Darvishzadeh, J., Lee, J., et al. (1996). Abnormal splicing of the leptin receptor in diabetic mice. *Nature* 379, 632–635. doi: 10.1038/379632a0
- Leib, S. L., Kim, Y. S., Chow, L. L., Sheldon, R. A., and Tauber, M. G. (1996). Reactive oxygen intermediates contribute to necrotic and apoptotic neuronal injury in an infant rat model of bacterial meningitis due to group B streptococci. *J. Clin. Invest.* 98, 2632–2639. doi: 10.1172/JCI119084
- Leid, R. W., and McConnell, L. (1983). PGE₂ generation and release by the larval stage of the cestode, *Taenia taeniaeformis*. *Prostaglandins Leukotrienes Med.* 11, 317–323. doi: 10.1016/0262-1746(83)90043-4
- Licinio, J., Negrão, A. B., Mantzoros, C., Kaklaman, V., Wong, M.-L., Bongiorno, P. B., et al. (1998). Synchronicity of frequently sampled, 24-h concentrations of circulating leptin, luteinizing hormone, and estradiol in healthy women. *Proc. Natl. Acad. Sci. U.S.A.* 95, 2541–2546. doi: 10.1073/pnas.95.5.2541
- Loffreda, S., Yang, S., Lin, H., Karp, C., Brengman, M., Wang, D., et al. (1998). Leptin regulates proinflammatory immune responses. *FASEB J.* 12, 57–65. doi: 10.1096/fasebj.12.1.57
- Löhms, M., and Sundström, L. F. (2004). Leptin and social environment influence the risk-taking and feeding behaviour of Asian blue quail. *Anim. Behav.* 68, 607–612. doi: 10.1016/j.anbehav.2003.12.019
- Löhms, M., Moalem, S., and Björklund, M. (2012). Leptin, a tool of parasites? *Biol. Lett.* 8, 849–852. doi: 10.1098/rsbl.2012.0385
- Lord, G. M., Matarese, G., Howard, J. K., Baker, R. J., Bloom, S. R., and Lechler, R. I. (1998). Leptin modulates the T-cell immune response and reverses starvation-induced immunosuppression. *Nature* 394, 897–901. doi: 10.1038/29795
- Macia, L., Delacore, M., Abboud, G., Ouk, T. S., Delanoye, A., Verwaerde, C., et al. (2006). Impairment of dendritic cell functionality and steady-state number in obese mice. *J. Immunol.* 177, 5997–6006. doi: 10.4049/jimmunol.177.9.5997
- Madan, R., Guo, X., Naylor, C., Buonomo, E. L., Mackay, D., Noor, Z., et al. (2014). Role of leptin-mediated colonic inflammation in defense against *Clostridium difficile* colitis. *Infect. Immun.* 82, 341–349. doi: 10.1128/IAI.00972-13
- Maizels, R. M., and Yazdanbakhsh, M. (2003). Immune regulation by helminth parasites: cellular and molecular mechanisms. *Nat. Rev. Immunol.* 3, 733–744. doi: 10.1038/nri1183
- Mancuso, P., Gottschalk, A., Phare, S. M., Peters-Golden, M., Lukacs, N. W., and Huffnagle, G. B. (2002). Leptin-deficient mice exhibit impaired host defense in Gram-negative pneumonia. *J. Immunol.* 168, 4018–4024. doi: 10.4049/jimmunol.168.8.4018
- Märker, T., Sell, H., Zillesen, P., Glode, A., Kriebel, J., Ouwens, D. M., et al. (2012). Heat shock protein 60 as a mediator of adipose tissue inflammation and insulin resistance. *Diabetes* 61, 615–625. doi: 10.2337/db10-1574
- Martin-Romero, C., and Sánchez-Margalet, V. (2001). Human leptin activates PI3K and MAPK pathways in human peripheral blood mononuclear cells: possible role of Sam68. *Cell. Immunol.* 212, 83–91. doi: 10.1006/cimm.2001.1851
- Martin-Romero, C., Santos-Alvarez, J., Goberna, R., and Sánchez-Margalet, V. (2000). Human leptin enhances activation and proliferation of human circulating T lymphocytes. *Cell. Immunol.* 199, 15–24. doi: 10.1006/cimm.1999.1594

- Matarese, G., Castelli-Gattinara, G., Cancrini, C., Bernardi, S., Romiti, M., Savarese, C., et al. (2002). Serum leptin and CD4+ T lymphocytes in HIV+ children during highly active antiretroviral therapy. *Clin. Endocrinol.* 57, 643–646. doi: 10.1046/j.1365-2265.2002.01634.x
- Matarese, G., Di Giacomo, A., Sanna, V., Lord, G. M., Howard, J. K., Di Tuoro, A., et al. (2001). Requirement for leptin in the induction and progression of autoimmune encephalomyelitis. *J. Immunol.* 166, 5909–5916. doi: 10.4049/jimmunol.166.10.5909
- Matarese, G., Moschos, S., and Mantzoros, C. S. (2005). Leptin in immunology. *J. Immunol.* 174, 3137–3142. doi: 10.4049/jimmunol.174.6.3137
- Mattioli, B., Straface, E., Matarrese, P., Quaranta, M. G., Giordani, L., Malorni, W., et al. (2008). Leptin as an immunological adjuvant: enhanced migratory and CD8+ T cell stimulatory capacity of human dendritic cells exposed to leptin. *FASEB J.* 22, 2012–2022. doi: 10.1096/fj.07-098095
- Mattioli, B., Straface, E., Quaranta, M. G., Giordani, L., and Viora, M. (2005). Leptin promotes differentiation and survival of human dendritic cells and licenses them for Th1 priming. *J. Immunol.* 174, 6820–6828. doi: 10.4049/jimmunol.174.11.6820
- Maurya, R., Bhattacharya, P., Ismail, N., Dagur, P. K., Joshi, A. B., Razdan, K., et al. (2016). Differential role of leptin as an immunomodulator in controlling visceral leishmaniasis in normal and leptin-deficient mice. *Am. J. Trop. Med. Hyg.* 95, 109–119. doi: 10.4269/ajtmh.15-0804
- Merrick, J. C., Edelson, B. T., Bhardwaj, V., Swanson, P. E., and Unanue, E. R. (1997). Lymphocyte apoptosis during early phase of *Listeria* infection in mice. *Am. J. Pathol.* 151:785.
- Michaud, F., Coulombe, F., Gaudreault, E., Paquet-Bouchard, C., Rola-Pleszczynski, M., and Gosselin, J. (2010). Epstein-Barr virus interferes with the amplification of IFN α secretion by activating suppressor of cytokine signaling 3 in primary human monocytes. *PLoS ONE* 5:e11908. doi: 10.1371/journal.pone.0011908
- Moore, S. I., Huffnagle, G. B., Chen, G.-H., White, E. S., and Mancuso, P. (2003). Leptin modulates neutrophil phagocytosis of *Klebsiella pneumoniae*. *Infect. Immun.* 71, 4182–4185. doi: 10.1128/IAI.71.7.4182-4185.2003
- Morgan, O. W., Bramley, A., Fowlkes, A., Freedman, D. S., Taylor, T. H., Gargiullo, P., et al. (2010). Morbid obesity as a risk factor for hospitalization and death due to 2009 pandemic influenza A (H1N1) disease. *PLoS ONE* 5:e9694. doi: 10.1371/journal.pone.0009694
- Morrison, C. D. (2008). Leptin resistance and the response to positive energy balance. *Physiol. Behav.* 94, 660–663. doi: 10.1016/j.physbeh.2008.04.009
- Morton, N. M., Emilsson, V., Liu, Y.-L., and Cawthorne, M. A. (1998). Leptin action in intestinal cells. *J. Biol. Chem.* 273, 26194–26201. doi: 10.1074/jbc.273.40.26194
- Mouli, K. C., Pragathi, D., Jyothi, U. N., Kumar, V. S., Naik, M. H., Balananda, P., et al. (2016). Leptin inhibitors from fungal endophytes (LIFE)s: will be novel therapeutic drugs for obesity and its associated immune mediated diseases. *Med. Hypotheses* 92, 48–53. doi: 10.1016/j.mehy.2016.04.032
- Müller, O., Garenne, M., Kouyaté, B., and Becher, H. (2003). The association between protein-energy malnutrition, malaria morbidity and all-cause mortality in West African children. *Trop. Med. Int. Health* 8, 507–511. doi: 10.1046/j.1365-3156.2003.01043.x
- Najib, S., and Sánchez-Margalet, V. C. (2002). Human leptin promotes survival of human circulating blood monocytes prone to apoptosis by activation of p42/44 MAPK pathway. *Cell. Immunol.* 220, 143–149. doi: 10.1016/S0008-8749(03)00027-3
- Napoleone, E., Di Santo, A., Amore, C., Baccante, G., Di Febbo, C., Porreca, E., et al. (2007). Leptin induces tissue factor expression in human peripheral blood mononuclear cells: a possible link between obesity and cardiovascular risk? *J. Thromb. Haemostasis* 5, 1462–1468. doi: 10.1111/j.1538-7836.2007.02578.x
- Noah, L., Bosma, N., and Jansen, J. (1994). Mucosal tumor necrosis factor- α , interleukin-1 β , and interleukin-8 production in patients with *Helicobacter pylori*. *Scand. J. Gastroenterol.* 29, 425–429.
- Ozcan, L., Ergin, A. S., Lu, A., Chung, J., Sarkar, S., Nie, D., et al. (2009). Endoplasmic reticulum stress plays a central role in development of leptin resistance. *Cell Metab.* 9, 35–51. doi: 10.1016/j.cmet.2008.12.004
- Ozcan, U., Yilmaz, E., Ozcan, L., Furuhashi, M., Vaillancourt, E., Smith, R. O., et al. (2006). Chemical chaperones reduce ER stress and restore glucose homeostasis in a mouse model of type 2 diabetes. *Science* 313, 1137–1140. doi: 10.1126/science.1128294
- Papathanassoglou, E., El-Haschimi, K., Li, X. C., Matarese, G., Strom, T., and Mantzoros, C. (2006). Leptin receptor expression and signaling in lymphocytes: kinetics during lymphocyte activation, role in lymphocyte survival, and response to high fat diet in mice. *J. Immunol.* 176, 7745–7752. doi: 10.4049/jimmunol.176.12.7745
- Park, Y. M., and Bochner, B. S. (2010). Eosinophil survival and apoptosis in health and disease. *Allergy Asthma Immunol. Res.* 2, 87–101. doi: 10.4168/aaair.2010.2.2.87
- Pauli, E.-K., Schmolke, M., Wolff, T., Viemann, D., Roth, J., Bode, J. G., et al. (2008). Influenza A virus inhibits type I IFN signaling via NF- κ B-dependent induction of SOCS-3 expression. *PLoS Pathog.* 4:e1000196. doi: 10.1371/journal.ppat.1000196
- Pelkeymounter, M. A., Cullen, M. J., Baker, M. B., Hecht, R., Winters, D., Boone, T., et al. (1995). Effects of the obese gene product on body weight regulation in ob/ob mice. *Science* 269, 540–543. doi: 10.1126/science.7624776
- Pickup, J. C., Chusney, G. D., and Mattock, M. B. (2000). The innate immune response and type 2 diabetes: evidence that leptin is associated with a stress-related (acute-phase) reaction. *Clin. Endocrinol.* 52, 107–112. doi: 10.1046/j.1365-2265.2000.00921.x
- Poland, G. A., Kennedy, R. B., and Ovsyannikova, I. G. (2011). Vaccinomics and personalized vaccinology: is science leading us toward a new path of directed vaccine development and discovery? *PLoS Pathog.* 7:e1002344. doi: 10.1371/journal.ppat.1002344
- Portnoy, D. A., Auerbuch, V., and Glomski, I. J. (2002). The cell biology of *Listeria monocytogenes* infection: the intersection of bacterial pathogenesis and cell-mediated immunity. *J. Cell Biol.* 158, 409–414. doi: 10.1083/jcb.200205009
- Procaccini, C., Jirillo, E., and Matarese, G. (2012). Leptin as an immunomodulator. *Mol. Aspects Med.* 33, 35–45. doi: 10.1016/j.mam.2011.10.012
- Pulido-Mendez, M., De Sanctis, J., and Rodríguez-Acosta, A. (2002). Leptin and leptin receptors during malaria infection in mice. *Folia Parasitol.* 49, 249–251. doi: 10.14411/fp.2002.046
- Radigan, K. A., Morales-Nebreda, L., Soberanes, S., Nicholson, T., Nigdelioglu, R., Cho, T., et al. (2014). Impaired clearance of influenza A virus in obese, leptin receptor deficient mice is independent of leptin signaling in the lung epithelium and macrophages. *PLoS ONE* 9:e108138. doi: 10.1371/journal.pone.0108138
- Rodríguez, L., Graniel, J., and Ortiz, R. (2007). Effect of leptin on activation and cytokine synthesis in peripheral blood lymphocytes of malnourished infected children. *Clin. Exp. Immunol.* 148, 478–485. doi: 10.1111/j.1365-2249.2007.03361.x
- Rodríguez-Galán, M. C., Porporatto, C., Sotomayor, C. E., Cano, R., Cejas, H., and Correa, S. G. (2010). Immune-metabolic balance in stressed rats during *Candida albicans* infection. *Stress* 13, 373–383. doi: 10.3109/10253891003667870
- Rossi, F. (1986). The O₂—forming NADPH oxidase of the phagocytes: nature, mechanisms of activation and function. *Biochimica et Biophysica Acta* 853, 65–89. doi: 10.1016/0304-4173(86)90005-4
- Saldiva, S. R., Carvalho, H., Castilho, V., Struchiner, C., and Massad, E. (2002). Malnutrition and susceptibility to enteroparasites: reinfection rates after mass chemotherapy. *Paediatr. Perinat. Epidemiol.* 16, 166–171. doi: 10.1046/j.1365-3016.2002.00402.x
- Sánchez-Margalet, V., and Martín-Romero, C. (2001). Human leptin signaling in human peripheral blood mononuclear cells: activation of the JAK-STAT pathway. *Cell. Immunol.* 211, 30–36. doi: 10.1006/cimm.2001.1815
- Sánchez-Margalet, V., and Najib, S. (1999). p68 Sam is a substrate of the insulin receptor and associates with the SH2 domains of p85 PI3K. *FEBS Lett.* 455, 307–310. doi: 10.1016/S0014-5793(99)00887-X
- Sánchez-Margalet, V., Martín-Romero, C., González-Yanes, C., Goberna, R., Rodríguez-Baño, J., and Muniaín, M. (2002). Leptin receptor (Ob-R) expression is induced in peripheral blood mononuclear cells by *in vitro* activation and *in vivo* in HIV-infected patients. *Clin. Exp. Immunol.* 129, 119–124. doi: 10.1046/j.1365-2249.2002.01900.x
- Sánchez-Margalet, V., Martín-Romero, C., Santos-Alvarez, J., Goberna, R., Najib, S., and Gonzalez-Yanes, C. (2003). Role of leptin as an immunomodulator of blood mononuclear cells: mechanisms of action. *Clin. Exp. Immunol.* 133, 11–19. doi: 10.1046/j.1365-2249.2003.02190.x

- Sánchez-Pozo, C., Rodríguez-Baño, J., Domínguez-Castellano, A., Muniain, M., Goberna, R., and Sánchez-Margalet, V. (2003). Leptin stimulates the oxidative burst in control monocytes but attenuates the oxidative burst in monocytes from HIV-infected patients. *Clin. Exp. Immunol.* 134, 464–469. doi: 10.1111/j.1365-2249.2003.02321.x
- Sanna, V., Di Giacomo, A., La Cava, A., Lechler, R. I., Fontana, S., Zappacosta, S., et al. (2003). Leptin surge precedes onset of autoimmune encephalomyelitis and correlates with development of pathogenic T cell responses. *J. Clin. Invest.* 111, 241–250. doi: 10.1172/JCI200316721
- Santos-Alvarez, J., Goberna, R., and Sánchez-Margalet, V. (1999). Human leptin stimulates proliferation and activation of human circulating monocytes. *Cell. Immunol.* 194, 6–11. doi: 10.1006/cimm.199.9.1490
- Sarraf, P., Frederich, R. C., Turner, E. M., Ma, G., Jaskowski, N. T., Rivet, D. J., et al. (1997). Multiple cytokines and acute inflammation raise mouse leptin levels: potential role in inflammatory anorexia. *J. Exp. Med.* 185, 171–176. doi: 10.1084/jem.185.1.171
- Saucillo, D. C., Gerriets, V. A., Sheng, J., Rathmell, J. C., and Maciver, N. J. (2014). Leptin metabolically licenses T cells for activation to link nutrition and immunity. *J. Immunol.* 192, 136–144. doi: 10.4049/jimmunol.1301158
- Savill, J., Fadok, V., Henson, P., and Haslett, C. (1993). Phagocyte recognition of cells undergoing apoptosis. *Immunol. Today* 14, 131–136. doi: 10.1016/0167-5699(93)90215-7
- Schaible, U. E., and Stefan, H. (2007). Malnutrition and infection: complex mechanisms and global impacts. *PLoS Med.* 4:e115. doi: 10.1371/journal.pmed.0040115
- Sheridan, P. A., Paich, H. A., Handy, J., Karlsson, E. A., Hudgens, M. G., Sammon, A. B., et al. (2012). Obesity is associated with impaired immune response to influenza vaccination in humans. *Int. J. Obes.* 36, 1072–1077. doi: 10.1038/ijo.2011.208
- Shirshov, S., and Orlova, E. (2005). Molecular mechanisms of regulation of functional activity of mononuclear phagocytes by leptin. *Biochemistry* 70, 841–847. doi: 10.1007/s10541-005-0193-1
- Shivhare, R., Ali, W., Vishwakarma, P., Natu, S., Puri, S. K., and Gupta, S. (2015). Leptin augments protective immune responses in murine macrophages and enhances potential of miltefosine against experimental visceral leishmaniasis. *Acta Trop.* 150, 35–41. doi: 10.1016/j.actatropica.2015.06.024
- Siegmund, B., Lehr, H. A., and Fantuzzi, G. (2002). Leptin: a pivotal mediator of intestinal inflammation in mice. *Gastroenterology* 122, 2011–2025. doi: 10.1053/gast.2002.33631
- Skerrett, S. J., Henderson, W. R., and Martin, T. R. (1990). Alveolar macrophage function in rats with severe protein calorie malnutrition. Arachidonic acid metabolism, cytokine release, and antimicrobial activity. *J. Immunol.* 144, 1052–1061.
- Spencer, N., and Daynes, R. A. (1997). IL-12 directly stimulates expression of IL-10 by CD5+ B cells and IL-6 by both CD5+ and CD5-B cells: possible involvement in age-associated cytokine dysregulation. *Int. Immunol.* 9, 745–754. doi: 10.1093/intimm/9.5.745
- St-Pierre, J., and Tremblay, M. L. (2012). Modulation of leptin resistance by protein tyrosine phosphatases. *Cell Metab.* 15, 292–297. doi: 10.1016/j.cmet.2012.02.004
- Sukhotnik, I., Coran, A. G., Mogilner, J. G., Shamian, B., Karry, R., Lieber, M., et al. (2009). Leptin affects intestinal epithelial cell turnover in correlation with leptin receptor expression along the villus-crypt axis after massive small bowel resection in a rat. *Pediatr. Res.* 66, 648–653. doi: 10.1203/PDR.0b013e3181be9f84
- Sung, C. K., Sanchez-Margalet, V., and Goldfine, I. D. (1994). Role of p85 subunit of phosphatidylinositol-3-kinase as an adaptor molecule linking the insulin receptor, p62, and GTPase-activating protein. *J. Biol. Chem.* 269, 12503–12507.
- Takahashi, H., Tsuda, Y., Takeuchi, D., Kobayashi, M., Herndon, D. N., and Suzuki, F. (2004). Influence of systemic inflammatory response syndrome on host resistance against bacterial infections. *Crit. Care Med.* 32, 1879–1885. doi: 10.1097/01.CCM.0000139606.34631.61
- Takahashi, T., Yu, F., Saegusa, S., Sumino, H., Nakahashi, T., Iwai, K., et al. (2006). Impaired expression of cardiac adiponectin in leptin-deficient mice with viral myocarditis. *Int. Heart J.* 47, 107–123. doi: 10.1536/ihj.47.107
- Taleb, S., Herbin, O., Ait-Oufella, H., Verreth, W., Gourdy, P., Barateau, V., et al. (2007). Defective leptin/leptin receptor signaling improves regulatory T cell immune response and protects mice from atherosclerosis. *Arterioscler. Thromb. Vasc. Biol.* 27, 2691–2698. doi: 10.1161/ATVBAHA.107.149567
- Tartaglia, L. A. (1997). The leptin receptor. *J. Biol. Chem.* 272, 6093–6096. doi: 10.1074/jbc.272.10.6093
- Tartaglia, L. A., Dembski, M., Weng, X., Deng, N., Culpepper, J., Devos, R., et al. (1995). Identification and expression cloning of a leptin receptor, OB-R. *Cell* 83, 1263–1271. doi: 10.1016/0092-8674(95)90151-5
- Thomas, T., Burguera, B., Melton, L. J., Atkinson, E. J., O'Fallon, W., Riggs, B. L., et al. (2000). Relationship of serum leptin levels with body composition and sex steroid and insulin levels in men and women. *Metab. Clin. Exp.* 49, 1278–1284. doi: 10.1053/meta.2000.9519
- Tian, Y., Chen, W.-L., Kuo, C.-F., and Ou, J.-H. J. (2012). Viral-load-dependent effects of liver injury and regeneration on hepatitis B virus replication in mice. *J. Virol.* 86, 9599–9605. doi: 10.1128/JVI.01087-12
- Tian, Z., Sun, R., Wei, H., and Gao, B. (2002). Impaired natural killer (NK) cell activity in leptin receptor deficient mice: leptin as a critical regulator in NK cell development and activation. *Biochem. Biophys. Res. Commun.* 298, 297–302. doi: 10.1016/S0006-291X(02)02462-2
- Trial, J., Birdsall, H. H., Hallum, J. A., Crane, M. L., Rodriguez-Barradas, M. C., De Jong, A. L., et al. (1995). Phenotypic and functional changes in peripheral blood monocytes during progression of human immunodeficiency virus infection. Effects of soluble immune complexes, cytokines, subcellular particulates from apoptotic cells, and HIV-1-encoded proteins on monocytes phagocytic function, oxidative burst, transendothelial migration, and cell surface phenotype. *J. Clin. Invest.* 95:1690.
- Tschöp, J., Nogueiras, R., Haas-Lockie, S., Kasten, K. R., Castañeda, T. R., Huber, N., et al. (2010). CNS leptin action modulates immune response and survival in sepsis. *J. Neurosci.* 30, 6036–6047. doi: 10.1523/JNEUROSCI.4875-09.2010
- Tu, T., Koski, K., Wykes, L., and Scott, M. (2007). Re-feeding rapidly restores protection against *Heligmosomoides bakeri* (Nematoda) in protein-deficient mice. *Parasitology* 134, 899–909. doi: 10.1017/S0031182007002314
- Ubags, N. D., Vernooij, J. H., Burg, E., Hayes, C., Bement, J., Dilli, E., et al. (2014). The role of leptin in the development of pulmonary neutrophilia in infection and acute lung injury. *Crit. Care Med.* 42:e143. doi: 10.1097/CCM.0000000000000048
- Um, H.-D., Orenstein, J. M., and Wahl, S. M. (1996). Fas mediates apoptosis in human monocytes by a reactive oxygen intermediate dependent pathway. *J. Immunol.* 156, 3469–3477.
- van Crevel, R., Karyadi, E., Netea, M. G., Verhoef, H., Nelwan, R. H., West, C. E., et al. (2002). Decreased plasma leptin concentrations in tuberculosis patients are associated with wasting and inflammation. *J. Clin. Endocrinol. Metab.* 87, 758–763. doi: 10.1210/jcem.87.2.8228
- Vedantam, G., and Viswanathan, V. K. (2012). Leptin signaling protects the gut from *Entamoeba histolytica* infection. *Gut. Microbes.* 3, 2–3. doi: 10.4161/gmic.19424
- Vermeulen, M., Steyn, N., Nel, H., Ten Brink, R., and Lombard, R. (1998). The prevalence of gastrointestinal helminths and the nutritional status of rural preschool children in Northern Province. *South Afr. Med. J.* 88, 1217–1222.
- Von Knethen, A., and Brüne, B. (2001). Delayed activation of PPAR γ by LPS and IFN- γ attenuates the oxidative burst in macrophages. *FASEB J.* 15, 535–544. doi: 10.1096/fj.00-0187com
- Walduck, A. K., and Becher, D. (2012). Leptin, CD4(+) T(reg) and the prospects for vaccination against *H. pylori* infection. *Front. Immunol.* 3:316. doi: 10.3389/fimmu.2012.00316
- Webb, S. R., Loria, R. M., Madge, G. E., and Kibrick, S. (1976). Susceptibility of mice to group B coxsackie virus is influenced by the diabetic gene. *J. Exp. Med.* 143, 1239–1248. doi: 10.1084/jem.143.5.1239
- Weber, D. J., Rutala, W. A., Samsa, G. P., Santimaw, J. E., and Lemon, S. M. (1985). Obesity as a predictor of poor antibody response to hepatitis B plasma vaccine. *JAMA* 254, 3187–3189. doi: 10.1001/jama.1985.03360220053027
- Wehrens, A., Aebischer, T., Meyer, T. F., and Walduck, A. K. (2008). Leptin receptor signaling is required for vaccine-induced protection against *Helicobacter pylori*. *Helicobacter* 13, 94–102. doi: 10.1111/j.1523-5378.2008.00591.x
- White, S. J., Taylor, M. J., Hurt, R. T., Jensen, M. D., and Poland, G. A. (2013). Leptin-based adjuvants: an innovative approach to improve vaccine response. *Vaccine* 31, 1666–1672. doi: 10.1016/j.vaccine.2013.01.032

- Wieland, C. W., Florquin, S., Chan, E. D., Leemans, J. C., Weijer, S., Verbon, A., et al. (2005). Pulmonary *Mycobacterium tuberculosis* infection in leptin-deficient ob/ob mice. *Int. Immunol.* 17, 1399–1408. doi: 10.1093/intimm/dxh317
 - Woodward, B. (1998). Protein, calories, and immune defenses. *Nutr. Rev.* 56, S84–S92. doi: 10.1111/j.1753-4887.1998.tb01649.x
 - Yahya, R. S., Awad, S. I., Kizilbash, N., El-Baz, H. A., and Atia, G. (2016). Enteric parasites can disturb leptin and adiponectin levels in children. *Arch. Med. Sci.* 14, 101–106. doi: 10.5114/aoms.2016.60707
 - Yudkin, J. S., Yajnik, C. S., Mohamed-Ali, V., and Bulmer, K. (1999). High levels of circulating proinflammatory cytokines and leptin in urban, but not rural, Indians. A potential explanation for increased risk of diabetes and coronary heart disease. *Diabetes Care* 22, 363–364. doi: 10.2337/diacare.22.2.363
 - Zaralis, K., Tolcamp, B. J., Houdijk, J. G., Wylie, A. R., and Kyriazakis, I. (2008). Consequences of protein supplementation for anorexia, expression of immunity and plasma leptin concentrations in parasitized ewes of two breeds. *Br. J. Nutr.* 101, 499–509. doi: 10.1017/S000711450802401X
 - Zarkesh-Esfahani, H., Pockley, G., Metcalfe, R. A., Bidlingmaier, M., Wu, Z., Ajami, A., et al. (2001). High-dose leptin activates human leukocytes via receptor expression on monocytes. *J. Immunol.* 167, 4593–4599. doi: 10.4049/jimmunol.167.8.4593
 - Zhang, F., Basinski, M. B., Beals, J. M., Briggs, S. L., Churgay, L. M., Clawson, D. K., et al. (1997). Crystal structure of the obese protein Ieptin-E100. *Nature* 387, 206–209. doi: 10.1038/387206a0
 - Zhang, Y., Proenca, R., Maffei, M., Barone, M., Leopold, L., and Friedman, J. M. (1994). Positional cloning of the mouse obese gene and its human homologue. *Nature* 372, 425–432. doi: 10.1038/372425a0
 - Zychlinsky, A., and Sansonetti, P. (1997). Perspectives series: host/pathogen interactions. Apoptosis in bacterial pathogenesis. *J. Clin. Invest.* 100, 493–495. doi: 10.1172/JCI119557
- Conflict of Interest Statement:** The authors declare that the research was conducted in the absence of any commercial or financial relationships that could be construed as a potential conflict of interest.
- Copyright © 2018 Alti, Sambamurthy and Kalangi. This is an open-access article distributed under the terms of the Creative Commons Attribution License (CC BY). The use, distribution or reproduction in other forums is permitted, provided the original author(s) and the copyright owner are credited and that the original publication in this journal is cited, in accordance with accepted academic practice. No use, distribution or reproduction is permitted which does not comply with these terms.



The *in Vitro* Antigenicity of *Plasmodium vivax* Rhoptry Neck Protein 2 (PvRON2) B- and T-Epitopes Selected by HLA-DRB1 Binding Profile

Carolina López^{1,2}, Yoelis Yepes-Pérez^{1,3}, Diana Díaz-Arévalo^{1,4}, Manuel E. Patarroyo^{1,5} and Manuel A. Patarroyo^{1,6*}

¹ Molecular Biology and Immunology Department, Fundación Instituto de Inmunología de Colombia, Bogotá, Colombia, ² PhD Program in Biomedical and Biological Sciences, Universidad del Rosario, Bogotá, Colombia, ³ MSc Program in Microbiology, Universidad Nacional de Colombia, Bogotá, Colombia, ⁴ Faculty of Agricultural Sciences, Universidad de Ciencias Aplicadas y Ambientales, Bogotá, Colombia, ⁵ School of Medicine, Universidad Nacional de Colombia, Bogotá, Colombia, ⁶ Basic Sciences Department, School of Medicine and Health Sciences, Universidad del Rosario, Bogotá, Colombia

OPEN ACCESS

Edited by:

Jorge Enrique Gómez Marín,
University of Quindío, Colombia

Reviewed by:

Pedro Ismael Da Silva Junior,
Instituto Butantan, Brazil
Sara Maria Robledo,
Universidad de Antioquia, Colombia

*Correspondence:

Manuel A. Patarroyo
mapatarr.fidic@gmail.com

Received: 18 December 2017

Accepted: 24 April 2018

Published: 15 May 2018

Citation:

López C, Yepes-Pérez Y, Díaz-Arévalo D, Patarroyo ME and Patarroyo MA (2018) The *in Vitro* Antigenicity of *Plasmodium vivax* Rhoptry Neck Protein 2 (PvRON2) B- and T-Epitopes Selected by HLA-DRB1 Binding Profile. *Front. Cell. Infect. Microbiol.* 8:156. doi: 10.3389/fcimb.2018.00156

Malaria caused by *Plasmodium vivax* is a neglected disease which is responsible for the highest morbidity in both Americas and Asia. Despite continuous public health efforts to prevent malarial infection, an effective antimalarial vaccine is still urgently needed. *P. vivax* vaccine development involves analyzing naturally-infected patients' immune response to the specific proteins involved in red blood cell invasion. The *P. vivax* rhoptry neck protein 2 (PvRON2) is a highly conserved protein which is expressed in late schizont rhoptries; it interacts directly with AMA-1 and might be involved in moving-junction formation. Bioinformatics approaches were used here to select B- and T-cell epitopes. Eleven high-affinity binding peptides were selected using the NetMHCIIpan-3.0 *in silico* prediction tool; their *in vitro* binding to HLA-DRB1*0401, HLA-DRB1*0701, HLA-DRB1*1101 or HLA-DRB1*1302 was experimentally assessed. Four peptides (39152 (HLA-DRB1*04 and 11), 39047 (HLA-DRB1*07), 39154 (HLA-DRB1*13) and universal peptide 39153) evoked a naturally-acquired T-cell immune response in *P. vivax*-exposed individuals from two endemic areas in Colombia. All four peptides had an SI greater than 2 in proliferation assays; however, only peptides 39154 and 39153 had significant differences compared to the control group. Peptide 39047 was able to significantly stimulate TNF and IL-10 production while 39154 stimulated TNF production. Allele-specific peptides (but not the universal one) were able to stimulate IL-6 production; however, none induced IFN- γ production. The Bepipred 1.0 tool was used for selecting four B-cell epitopes *in silico* regarding humoral response. Peptide 39041 was the only one recognized by *P. vivax*-exposed individuals' sera and had significant differences concerning IgG subclasses; an IgG2 > IgG4 profile was observed for this peptide, agreeing with a protection-inducing role against *P. falciparum* and *P. vivax* as previously described for antigens such as RESA

and MSP2. The bioinformatics results and *in vitro* evaluation reported here highlighted two T-cell epitopes (39047 and 39154) being recognized by memory cells and a B-cell epitope (39041) identified by *P. vivax*-exposed individuals' sera which could be used as potential candidates when designing a subunit-based vaccine.

Keywords: *Plasmodium vivax*, PvRON2, HLA-DRB1 typing, antigenicity, synthetic peptide, epitope, cellular and humoral response

BACKGROUND

Malaria is one of the most important public health problems in tropical and subtropical regions worldwide. Nearly 3.3 billion people globally are at risk of contracting the disease; 214 million new cases appeared and 438,000 deaths occurred in 2015. Malaria is caused by parasites from the phylum Apicomplexa, genus *Plasmodium*. *Plasmodium vivax* is the second most prevalent known species and has the greatest geographical distribution as it can develop in its vector at lower temperatures and survive at higher altitudes. It also has a latent form known as hypnozoite; this remains in the hepatocytes, enabling parasite survival in a host for a long time (Mueller et al., 2009; Guerra et al., 2010; WHO, 2016).

Although malarial cases in Latin America decreased during the last decade, a rise in cases reported from Venezuela and Colombia has been reported in 2015 and 2016 (PAHO/WHO, 2017), Colombia being listed as the fourth regarding incidence during 2015 (i.e., 10% of malarial events) (WHO, 2016). A passive surveillance study of malarial transmission in Colombia between 2011 and 2013 showed that 50.7% of cases were caused by *P. vivax*, 48.9% by *P. falciparum* and 0.4% mixed infection (Arévalo-Herrera et al., 2015). A severe malaria study on Colombia's Pacific coast showed that *P. vivax* induced acute anemia in children and *P. falciparum* patients had high renal and hepatic damage rates (Arévalo-Herrera et al., 2017).

Since *P. vivax* has wide-scale global distribution, some strategies used to combat malaria involve using insecticide-impregnated mosquito nets and drugs such as sulphadoxine-pyrimethamine, artemisinin, and chloroquine (WHO, 2016); despite such efforts, vector insecticide resistance and parasite resistance to anti-malarial drug has increased during recent years (Rieckmann et al., 1989; Fairhurst and Dondorp, 2016). Administering anti-malarial drugs, together with developing an effective antimalarial vaccine, is considered a relevant control strategy for preventing and eradicating malaria (WHO, 2016).

More than 50 proteins have been described to date as being involved in malarial parasite's red blood cell (RBC) invasion; most have been identified at molecular level and characterized immunologically in *P. falciparum* (Bozdech et al., 2003; Cowman and Crabb, 2006). Conversely, studying *P. vivax* proteins involved in host invasion has been difficult, mainly due to technical restrictions such as the lack of a continuous *in vitro* parasite culture, leading to inadequate study of parasite biology (Udomsangpetch et al., 2008; Mueller et al., 2009).

Parasites from the phylum Apicomplexa have specialized organelles such as rhoptries which contain a large amount of proteins involved in host cell invasion (Counihan et al., 2013). Six *P. vivax* rhoptry neck proteins have been identified to date: Pv34, PvRON1, PvRON2, PvRON4, PvRALP and PvRON5 (Mongui et al., 2009; Arévalo-Pinzón et al., 2011, 2013, 2015; Moreno-Perez et al., 2011; Cheng et al., 2015). They have been described as possible targets for blocking *P. vivax* invasion of RBC (Mongui et al., 2009).

P. vivax rhoptry neck protein 2 (PvRON2) is 2,204 amino acids (aa) long and is expressed in late schizont rhoptries (Arévalo-Pinzón et al., 2011). It is a highly conserved protein which is secreted by specialized organelles and forms part of the complex of proteins called RONs. This protein, like its orthologs in *T. gondii* (TgRON2) and *P. falciparum* (PfRON2) interacts directly with the AMA-1 protein. The RON complex is involved in forming the moving junction (MJ) (electro dense ring-shaped structure) which allows parasite entry to a host cell (Aikawa et al., 1978; Lamarque et al., 2011). RON2's crucial role during merozoite (Mrz) invasion of erythrocytes, moving junction (MJ) formation and subsequent parasitophorous vacuole (PV) formation (Cao et al., 2009; Collins et al., 2009; Srinivasan et al., 2011) makes it a good vaccine candidate. Moreover, Srinivasan *et al.* have shown that vaccination with the PfAMA1-RON2L complex induce protection in *Aotus* monkeys, mediated by high neutralizing

Abbreviations: aa, amino acids; AMA, apical membrane antigen; APC, antigen presenting cell; BSA, bovine serum albumin; CBA, Cytometric Bead Array; CFSE, carboxyfluorescein diacetate N-succinimidyl ester; CPD, citrate phosphate dextrose; DAPI, 4', 6-diamidino-2-phenylindole dihydrochloride; DNA, deoxyribonucleic acid; DBP, Duffy binding protein; ELISA, enzyme-linked immunosorbent assay; FITC, fluorescein isothiocyanate; GAMA, GPI-anchored micronemal antigen; gDNA, genomic deoxyribonucleic acid; GPI, glycosylphosphatidylinositol; HA, hemagglutinin antigen; HABPs, high activity binding peptides; HLA, human leucocyte antigen; HPLC, high-performance liquid chromatography; IEDB, immune epitope database; IFA, indirect immunofluorescence assays; IFN- γ , interferon gamma; IgG, immunoglobulin G; IL, interleukin; MHC, major histocompatibility complex; MJ, moving junction; Mrz, merozoites; MSP, merozoite surface protein; NGS, next generation

sequencing; NK, natural killer; NKT, natural killer T-cells; OD, optical density; *P. falciparum*, *Plasmodium falciparum*; *P. vivax*, *Plasmodium vivax*; PBMC, peripheral blood mononuclear cells; PBS, phosphate buffered saline; PBST, PBS-0.05% Tween 20; pg, picograms; PHA, phytohemagglutinin; pNPP, p-nitrophenylphosphate; pRBC, parasite red blood cells; PV, parasitophorous vacuole; RALP, rhoptry-associated leucine (Leu) zipper-like protein; RBC, red blood cells; RON, rhoptry neck proteins; RPMI, roswell park memorial institute; RT, room temperature; SE, standard error; SEM, standard error of the mean; SI, stimulation index; *T. gondii*, *Toxoplasma gondii*; TBS, tris-buffered saline; TBSA, TBS-1% BSA; TCR, T-lymphocyte receptor; Th1, T helper 1; Th2, T helper 2; TMB, 3,3',5,5'-tetramethylbenzidine; TNF, tumor necrosis factor; TRAg, tryptophan-rich antigen; TT, tetanus toxoid; VDR, vitamin D3 receptor; μ M, micromolar.

antibody titers that prevent the invasion of RBC (Srinivasan et al., 2017).

The development of bioinformatics tools during the last few decades has enabled predicting vaccine candidates based on peptide binding affinity for major histocompatibility complex (MHC) class I or class II (Sturniolo et al., 1999; Nielsen and Lund, 2009; Wang et al., 2010; Zhang et al., 2012; Andreatta et al., 2015). The immune system's function is to recognize and differentiate between self and non-self-antigens so as to trigger cellular and/or humoral immune responses. MHC class II proteins (HLA-II in humans) are expressed on antigen presenting cells' (APC) surface (i.e., macrophages, dendritic cells and B-lymphocytes). These recognize extracellular antigens and can bind 13- to 18-aa-long peptides. One of the main difficulties in designing a vaccine is the high HLA polymorphism, especially from HLA-DRB1, this being the most polymorphic locus. Antigen binding capability varies from one allele to another, increasing or reducing affinity and driving immune responses. Selecting peptides as good vaccine candidates relies on their ability to be recognized by HLA-DRB1 alleles to ensure a protection-inducing immune response (Stern and Calvo-Calle, 2009). T-cells can trigger stronger immune responses after their APC recognition, depending on the peptides bound to MHC receptors (Blum et al., 2013).

Antigen-antibody interaction plays an essential role in humoral immune responses against pathogens. Bioinformatics tools are extremely useful for identifying antigenic determinants or B-cell epitopes when designing vaccines (Bergmann-Leitner et al., 2013; Panda and Mahapatra, 2017). Predicting linear B-cell epitopes (contiguous aa in a protein sequence) is based on several methods for determining aa physicochemical properties, such as solvent accessibility, hydrophilicity and flexibility (El-Manzalawy et al., 2017; Solihah et al., 2017).

This paper describes naturally-acquired T-cell and antibody immune responses to PvRON2 in *P. vivax*-exposed individuals from two of Colombia's endemic areas (Córdoba and Chocó), in the search for vaccine candidates. Eleven high-affinity epitopes were selected by NetMHCIIpan-3.0 (Andreatta et al., 2015) *in silico* prediction and their *in vitro* binding to at least one of HLA-DRB1*0401, HLA-DRB1*0701, HLA-DRB1*1101 and HLA-DRB1*1302 was assessed by competition assays. The Bepipred 1.0 tool was used for selecting four B-cell epitopes *in silico*. A good immune response was observed against two T-cell and one B-cell epitopes; further studies aimed at testing these peptides as components of a subunit vaccine against *P. vivax* are thus recommended.

MATERIALS AND METHODS

In Silico B-Cell and T-Cell Epitope High Binding Prediction

The PvRON2 aa sequence (PlasmoDB database code: PVX_117880) was used for predicting T-cell epitopes having high binding affinity for the HLA-DRB1 alleles most frequently occurring in endemic areas worldwide (HLA-DRB1*0401, HLA-DRB1*0701, HLA-DRB1*1101, and HLA-DRB1*1302) (Marsh et al., 1999). NetMHCIIpan-3.0 (Andreatta et al., 2015)

was used for predicting these epitopes and confirmed by IEDB (Sturniolo et al., 1999; Nielsen and Lund, 2009; Wang et al., 2010) and TEPITOPE software (Zhang et al., 2012). Three epitopes per HLA-DRB1 were selected for *in vitro* analysis according to highest predicted binding values (Table 1).

Bepipred 1.0 (Larsen et al., 2006) and Antheprot 2000 V6.0 (Deléage et al., 2001) were used for predicting B-cell epitopes. Four epitopes were chosen as they agreed with average high Parker antigenicity, hydrophilicity and solvent accessibility values obtained with Antheprot software, and the high values obtained with the Bepipred tool (0.35 default threshold and 75% specificity); such peptides were further used for analyzing humoral responses *in vitro* (Table 2).

Synthetic Peptides

Peptides selected *in silico* were purchased from Twenty First Century Biochemicals Inc. (260 Cedar Hill Street Marlboro, MA 01752 USA) and characterized by matrix-assisted laser desorption/ionization time-of-flight mass spectrometry (MALDI-TOF MS). The biotinylated peptides used as control for HLA peptide binding in competition assays were synthesized using sulfo-NHS-LC-Biotin (Pierce Chemical, Rockford).

HLA-DR Molecules Purification

HLA-DRB1* molecules were purified from human HLA-DRB1*0401 (IHW09025), HLA-DRB1*0701 (IHW09051), HLA-DRB1*1101 (IHW09043) and HLA-DRB1*1302 (IHW09055) homozygous lymphoblastoid B-cell lines (International Histocompatibility Working Group) and cultured in RPMI-1640 (Gibco) with 10% FBS (Gibco), at 37°C in a 5% CO₂ atmosphere. The purification was carried out as previously described by Vargas et al. (2003), briefly 5×10^9 cells were lysed at 1×10^8 cell/mL final density in lysis buffer with 10 µg/mL protease inhibitors [antipain, pepstatin A, soybean trypsin, leupeptin, and chymostatin (SIGMA-ALDRICH)]. The lysate was mixed with Protein A-Sepharose CL-4B beads (GE Healthcare) linked to mAb L243 (ATCC HB-55; anti-DR was purified by affinity chromatography using Protein A-Sepharose CL-4B beads) overnight, HLA-DRB1* molecules were obtained by affinity chromatography. HLA-DRB1 protein purity was confirmed by native SDS-PAGE (12%) and Western-blot; positive aliquots' concentration was determined by the Micro BCA protein assay kit (Thermo Scientific); HLA-DRB1 proteins were stored at -80°C until use.

In Vitro Peptide-Binding Assays and IC50 Values

Peptide binding competition assays were performed to test PvRON2 high-affinity binding peptides selected by *in silico* analysis using NetMHCIIpan 3.0 software. Selected unlabeled peptides competed with biotinylated control peptide in binding to HLA-DRB1*. The biotinylated peptides used were haemagglutinin antigen HA₃₀₆₋₃₁₈ (PKYVKQNTLKLAT) for HLA-DRB1*04 and HLA-DRB1*11 (Hammer et al., 1994; Saravia et al., 2008) and tetanus toxoid (TT) (QYIKANSKFIGITE) for HLA-DRB1*07 and HLA-DRB1*13 (Doolan et al., 2000).

TABLE 1 | T-epitopes selected *in silico* and PvRON2 *in vitro* binding.

Peptide code	Sequence	CoreF	HLA-DRB1* allele	NetMHCIIpan 3.0 (%Rank)	Binding percentage*	IC50 μ M*	IC50 ratio
39147	LKPFYSLETMLMANS	FYSLETMLM	DRB1*0401	0.3	92.6	4.6	0.2
			DRB1*0701	2.5	83.2	26.0	1.1
			DRB1*1101	10.0	79.3	23.0	4.8
			DRB1*1302	34.0	63.0	79.0	10.6
39148	NVRKFFLNDVSSIRH	FFLNDVSSI	DRB1*0401	1.0	83.0	11.9	0.6
			DRB1*0701	5.0	79.9	39.7	1.7
			DRB1*1101	19.0	73.8	83.4	17.5
			DRB1*1302	1.4	94.2	7.4	1.0
39149	DKSFISEANSFRNEE	FISEANSFR	DRB1*0401	3.5	85.8	26.3	1.4
			DRB1*0701	17.0	42.8	ND	ND
			DRB1*1101	26.0	36.5	ND	ND
			DRB1*1302	24.0	33.5	ND	ND
39150	QTAFRKFFKKIISLG	FFKKIISLG FRKFFKKII	DRB1*0401	17.0	83.6	33.7	1.7
			DRB1*0701	6.5	67.2	51.8	2.2
			DRB1*1101	1.2	87.6	83.4	17.5
			DRB1*1302	48.0	7.7	ND	ND
39151	KLKYIFKRRKTMKKK	FKRRKTMKK YIFKRRKTM	DRB1*0401	37.0	65.3	40.0	2.1
			DRB1*0701	6.0	36.0	ND	ND
			DRB1*1101	0.1	78.5	51.1	10.7
			DRB1*1302	27.0	13.1	ND	ND
39152	LFYVNLFIMSSLSRK	LFIMSSLSR FIMSSLSRK	DRB1*0401	3.0	65.8	2.8	0.1
			DRB1*0701	2.0	11.0	ND	ND
			DRB1*1101	1.4	91.8	1.9	0.4
			DRB1*1302	27.0	94.7	8.0	1.1
39153	MKLLQHIPANLLENI	LLQHIPANLL	DRB1*0401	0.5	61.2	57.0	2.9
			DRB1*0701	0.1	85.4	7.5	0.3
			DRB1*1101	6.5	72.7	52.1	10.9
			DRB1*1302	0.1	91.9	10.7	1.4
39154	LKFIVRGNNLKFLLNN	IVRGNNLKF FIVRGNNLK IVRGNNLKF	DRB1*0401	11.0	22.2	ND	ND
			DRB1*0701	4.5	43.7	ND	ND
			DRB1*1101	3.0	24.9	ND	ND
			DRB1*1302	0.2	90.1	6.5	0.9
39046	NYEYIASSSNIYLM	YIASSSNIY YIASSSNI	DRB1*0401	0.8	91.8	28.4	1.5
			DRB1*0701	0.3	91.5	23.3	1.0
			DRB1*1101	13.0	82.9	120.0	25.2
			DRB1*1302	0.2	92.8	29.6	4.0
39047	RGPVNYHFSNYMNL	VNYHFSNYM YHFSNYMNL VNYHFSNYM	DRB1*0401	16.0	59.8	54.5	2.8
			DRB1*0701	10.0	90.4	6.0	0.3
			DRB1*1101	37.0	0.0	ND	ND
			DRB1*1302	13.0	37.8	ND	ND
39048	TPIIVKYDNTTHAKNR	IIVKYDNTHA	DRB1*0401	12.0	90.7	11.9	0.6
			DRB1*0701	41.0	10.5	ND	ND
			DRB1*1101	24.0	16.8	ND	ND
			DRB1*1302	8.5	3.3	ND	ND

Peptide code and sequence are shown; core and %rank according to NetMHCIIpan 3.0 predicted HLA-DRB alleles and values. Binding assays and IC50 values were obtained from the methodology for all peptides. IC50 was assessed for peptides having $\geq 50\%$ binding, IC50 values were expressed as ratios (IC50 peptide/IC50 control peptide), and good binders were considered when their ratio was ≤ 10 . Specific peptides were selected as those having the lowest ratio value for each allele and a universal peptide had to have the lowest mean ratio value.

Data from this study; ND means that a peptide had less than 50% binding so that its IC50 value was not evaluated. %Rank values were considered as follows: weak binders rank ≤ 10 and strong binders ≤ 2 . IC50 values were calculated for each control peptide with each DRB1 allele, the controls HA-DRB1*0401 IC50 = 19.44 μ M; TT-DRB1*0701 IC50 = 23.37 μ M; HA-DRB1*1101 IC50 = 4.77 μ M; TT-DRB1*1302 IC50 = 7.46 μ M. Peptides having a IC50 ratio ≤ 10 were considered good binders.

TABLE 2 | Humoral response to PvRON2 B-cell epitopes.

B epitope code	Amino acid sequence	Average response
39041	YGRTRNKRYMHRNPGEKYKG	0.159 (SE = 0.026)
39042	KLQQEQNELNEEKERQRQEN	0.104 (SE = 0.016)
39043	QEQQEEEDNDPNPNSKKNKG	0.142 (SE = 0.018)
39044	EKIRKQEEEEERINNQRRA	0.094 (SE = 0.015)
PvGAMA-CT	434–749 aa	0.475 (SE = 0.071)

IgG absorbance readings for individuals exposed to natural *P. vivax* infection from endemic areas of Colombia. B-cell epitope code, aa sequences, control protein and average response (OD) are shown. SE, standard error.

HLA-DR molecules (0.1 μ M) were incubated for 24 h with 5 μ M biotinylated HA or TT peptides and a 50-fold excess of unlabeled peptide (250 μ M). The mix was incubated for 2 h in Maxisorb NUNC-immune modules (Thermo Scientific) covered with anti-DR. The complex was incubated with alkaline phosphatase streptavidin (Vector Labs) and as substrate alkaline phosphatase yellow (pNPP) liquid substrate (Sigma-Aldrich). Optical density (OD) was determined at 405 nm using a Multiskan GO (Thermo Scientific, Waltham, Massachusetts, USA) ELISA reader. Inhibition was calculated as a percentage, by using the following formula:

$$100 * \left[1 - \left(\frac{\Delta OD \text{ in the presence of competitor}}{\Delta OD \text{ in the absence of competitor}} \right) \right]$$

IC50 values (50% concentration inhibition) were determined for peptides able to inhibit high-affinity control peptide binding to a particular HLA-DR by more than 50% (Saravia et al., 2008). The peptides and control peptides were tested in 5–250 μ M serial dilutions for the competition assays; Mathematica (version 10.1) software (Wolfram Research, Inc., Mathematica, Champaign, IL 2015) was used for calculating IC50 values, using two-phase exponential decay. IC50 values were calculated as a relative value using the following formula:

$$1 - \left[\frac{(\Delta OD \text{ in the presence of competitor})}{(\Delta OD \text{ in the absence of competitor})} \right]$$

Study Population

Peripheral blood was obtained from 79 people living in the Colombian departments of Chocó and Córdoba (known *P. vivax* malaria endemic areas, having the highest case incidence) who had suffered previous episodes of malaria. Inclusion criteria consisted of being over 18 years-old, residing in a *P. vivax*-endemic area, having had 1 or more episodes of *P. vivax* malaria (the last one 6 months beforehand) and having received suitable treatment for the disease. Although a stronger immune response would have been expected in acutely-infected *P. vivax* individuals, the construction of study groups required a prior HLA typing and thus, a second sample had to be taken from individuals matching the alleles of interest to assess antigenicity. Taking this into account, the antigenicity sample was taken from people that had suffered *P. vivax* malaria at

least 6 months earlier. A control group of 50 individuals was selected; this consisted of healthy adults residing in Bogotá, Colombia, who had never lived in malaria-endemic areas and who had never experienced malarial infection. This study was performed according to the legal framework for research in Colombia and Ministry of Health's Resolution 8430 of 1993. The patients had the least risk, all data were kept confidential and were rigorously protected. The samples were collected after all individuals signed an informed consent form; all procedures were evaluated and approved by FIDIC's ethics committee.

HLA-DRB1 Typing

Genomic DNA (gDNA) from 300 μ L peripheral blood samples was extracted using a Wizard Genomic DNA Purification Kit (Promega Corporation, Madison, USA), following the manufacturer's instructions. gDNA was used for high resolution HLA-DRB1 typing by Histogenetics (Ossining, NY, USA) through Next Generation Sequencing (NGS) technology using Illumina MiSeq.

PBMC Isolation

Twenty-nine people carrying HLA-DRB1 typing for HLA-DRB1*04, HLA-DRB1*07, HLA-DRB1*11 and HLA-DRB1*13 alleles were selected from *P. vivax* endemic areas of Colombia's Córdoba and Chocó departments. Eight people carrying the same HLA-DRB1* alleles from a non-endemic area formed the control group. About 40 mL peripheral blood was collected in citrate phosphate dextrose (CPD) tubes and 6 mL peripheral blood in BD vacutainer serum collection tubes (BD Vacutainer Oakville, ON). Thick blood smears were used for confirming samples negative for malaria. Peripheral blood mononuclear cells (PBMC) were isolated by Ficoll-Paque PLUS (GE Healthcare) gradient centrifugation. Briefly, the buffy coat was resuspended in RPMI 1640 (Gibco) and separated by Ficoll, spinning at 1,000 g for 30 min at room temperature (RT). Mononuclear cells were collected, washed and spun at 800 g for 10 min, twice. Cell viability was evaluated by trypan blue exclusion test and cells were counted in a Neubauer chamber.

T-Cell Proliferation

Briefly, 2×10^5 PBMC were cultured in 200 μ L RPMI-1640 (Gibco), 2 mM glutamine, 1 mM sodium pyruvate, 2 g/L sodium bicarbonate, 100 μ g/mL streptomycin and 100 U/mL penicillin (all Gibco) and 10% heat-inactivated autologous plasma in 96-well round-bottomed plates (Costar, Corning Incorporated). Proliferation activity was evaluated by flow cytometry using carboxyfluorescein diacetate *N*-succinimidyl ester (CFSE, 5 μ M) (CellTrace CFSE cell proliferation kit, Molecular Probes, Eugene, Oregon, USA) reduction in replicating cells.

The cells were left without stimulation (unstimulated control) or were stimulated by co-culture with synthetic peptides (10 μ g/mL) or 2% mitogen phytohemagglutinin (PHA) (Sigma) or 5 μ g/mL *P. vivax* lysate as positive controls. Pv12 low binding peptide was selected (39115) by binding assay and used as negative control (manuscript in preparation). The 96-well plates

were incubated in 5% CO₂ at 37°C for 5 days; 100 µL culture supernatant was then collected per well and stored at –80°C until analysis for cytokine production. Duplicate assays were carried out.

The CD4-Pacific Blue-stained cell stimulation index was calculated by proliferative cells' relative percentage loss of carboxyfluorescein succinimidyl ester (CFSE) in the presence of antigen, divided by percentage relative CFSE loss for proliferative cells without antigen (Racanelli et al., 2011). Data was averaged for each antigen and for both exposed individuals and control groups. SI ≥ 2 was taken as antigen-specific positive proliferation. A Pacific Blue-labeled mouse anti-human CD4 (RPA-T4 clone) antibody (BD Biosciences), was used for CFSE-cell cluster measure. The samples were then read on a FACS Canto II flow cytometer; FlowJo software (v7.6.5, Ashland, Oregon, USA) was used for analyzing the results.

Cytokine Secretion

IFN-γ, TNF, IL-10, and IL-6 levels in lymphocyte culture supernatant were determined with a BD CBA Human Th1/Th2 Cytokine Kit II (San Jose, CA, USA), following the manufacturer's instructions. Supernatants were read on a FACS Canto II flow cytometer; FCAP Array software (v3.0.1) was used for analyzing the results. Results were expressed in pg/mL for each cytokine; data were compared between unstimulated and stimulated PBMC supernatant culture. Two standard deviations higher than that for control group were taken as positive antigen-specific production.

Indirect Immunofluorescence Assays (IFA)

IFA followed that previously described by Moreno-Pérez et al. (2013) with some modifications. Briefly, blood samples from individuals having active *P. vivax* infection were spun at 1,750 g for 12 min at RT. Both plasma and buffy coat were recovered and parasite red blood cells (pRBC) were washed with saline solution. pRBC were passed through a 60% Percoll gradient and spun at 1,750 g for 20 min. *P. vivax*-pRBC were diluted until 5–7 schizonts per field and confirmed by acridine orange. Twenty µL of diluted pRBC were placed into multitest microscope slide wells (Tekdon Incorporated) and incubated for 30 min. The supernatant was then removed, and microscopic slides left overnight (ON) at room temperature (RT) to air dry. The slides were then blocked for 30 min at RT with tris-buffered saline (TBS) 1% bovine serum albumin (TBSA) solution and washed three times. The serum samples from 30 exposed individuals and 8 sera from the control group were diluted in TBSA at 1:50 dilution and incubated for 1 h in a humid chamber. Reactivity was observed by fluorescence microscopy using anti-human IgG-FITC antibody (Sigma-Aldrich) diluted 1:50 in TBSA for 45 min in a humid chamber. The parasite nuclei were stained with 4', 6-diamidino-2-phenylindole dihydrochloride (DAPI) (0.25 µg/mL) for 5 min at RT and washed twice with 0.05% TBS-Tween 20 and three washes with TBS to remove excess reagent. The slides were visualized on an Olympus BX51 fluorescence microscope, using 100X oil immersion objective; DP2-BSW software (v2.2 Olympus Corporation) was then used to take

images and ImageJ 1.51n software (National Institutes of Health, USA) for merging images.

Enzyme-Linked Immunosorbent (ELISA) and Subclass IgG Assays

Total IgG antibodies were measured in serum from exposed individuals and control group. Maxisorb NUNC-immune modules (Thermo Scientific) were coated with 1 µg of each epitope and of rPvGAMA (10 µg/mL) (Baquero et al., 2017) in phosphate-buffered saline (PBS), pH 7.2, and incubated ON at 4°C. The immune modules were washed three times with PBS-0.05% Tween 20 solution (PBST) the next day and then blocked with 2.5% (wt/vol) non-fat powdered milk in PBST solution for 1 h at RT. Serum at 1:100 dilution was incubated for 2 h (100 µL per well) in duplicate. Secondary antibody horseradish peroxidase-conjugated goat anti-human IgG (Vector labs) was added at 1:10,000 dilution in blocked solution and incubated for 1 h at RT. TMB 2-Component Microwell Peroxidase Substrate (Sera-Care) was added at 100 µL/well to detect monoclonal antibody binding. The reaction was stopped by adding an equal volume of 1M phosphoric acid (H₃PO₄); OD was measured at 450 nm using a Multiskan GO (Thermo Scientific, Waltham, Massachusetts, USA) ELISA reader. Cut-off value was determined as negative control serum samples' mean plus two standard deviations; IgG subclasses were determined for positive total IgG serum.

The ELISA protocol described above was followed to evaluate IgG subclasses with minor modifications, as follows: 3% (wt/vol) bovine serum albumin (BSA, Sigma) in PBST was used as blocking agent/solution and serum at 1:100 dilution was incubated for 2 h in duplicate. A 1:1,000 dilution of monoclonal anti-human IgG1-biotin antibody produced in mouse (clone 8c/6-39), 1:15,000 monoclonal anti-human IgG2-biotin antibody produced in mouse (clone HP-6014), 1:40,000 monoclonal anti-human IgG3-biotin antibody produced in mouse (clone HP-6050) and 1:60,000 anti-human IgG4-biotin antibody, mouse monoclonal (clone HP-6025) (Sigma Aldrich) were used. ImmunoPure streptavidin, horseradish peroxidase conjugate (Thermo Scientific), at 1:5,000, dilution, was used as secondary antibody and TMB 2-Component Microwell peroxidase as substrate. The reaction was stopped by adding an equal volume of 1M phosphoric acid (H₃PO₄). OD was measured at 450 nm, using a Multiskan GO ELISA reader (Thermo Scientific, Waltham, Massachusetts, USA).

Statistical Analysis

GraphPad Prism software (version 5.0, San Diego, CA, USA) was used for analysis and constructing graphs. A Mann-Whitney test was used for comparing two groups regarding non-parametric data and Kruskal-Wallis test (with Dunn's multiple comparison post-test) for comparing more than two groups. Student's *t*-test was used for comparing two groups of data having a normal distribution. A 95% confidence interval was used. *p* ≤ 0.05 was considered significant. Significance level has been highlighted on all graphs by asterisks, as follows: **p* < 0.05; ***p* < 0.005, and ****p* < 0.0005.

RESULTS

T-Epitope Selection According *in Vitro* Binding Profile

Table 1 gives PvRON2 antigenic epitope prediction results. Eleven epitopes were selected *in silico* for HLA-DRB1*04, *07, *11, and *13 alleles (3 epitopes for each allele and 2 epitopes for the *07 allele). These epitopes were evaluated *in vitro* for their ability to bind all alleles of interest; those having greater than 50% binding were carefully chosen as high-binding peptides (Figure 1).

In vitro results showed that 10/11 (90.9%) peptides bound to the HLA-DRB1*04 allele (73.45% mean binding), being the most promiscuous allele studied; 7/10 (70%) peptides bound to HLA-DRB1*11 (64.47% mean binding); 6/11 (54.5%) of the peptides bound to HLA-DRB1*07 (58.33% mean binding) and HLA-DRB1*13 (56.55% mean binding). Four of the eleven peptides bound to all alleles studied here and were thus considered universal epitopes (39046, 39147, 39148, and 39153). Experimental binding assays and *in silico* binding predictions agreed in a 70.45% for the alleles studied (Table 1).

The IC₅₀ value was calculated for all high-binding peptides to select the ones displaying higher affinity. Different peptide

concentrations (μM) were used and the point at which 50% of the control peptide was displaced was thus calculated. IC₅₀ μM value was calculated using a second order exponential decay function (Figure 2). IC₅₀ assays demonstrated that epitope 39152 had the lowest IC₅₀ ratio for HLA-DRB1*04 (0.15) and HLA-DRB1*11 (0.4), so it was thus selected as a good epitope for both alleles. Epitope 39047 (0.26) was selected as specific epitope for HLA-DRB1*07 and epitope 39154 (0.88) for HLA-DRB1*13. Of the four universal epitopes, peptide 39153 had the lowest IC₅₀ mean value (Table 1, Figure 2). The selected epitopes were screened for antigenicity according to their HLA-DRB1* binding profile in previously typed patients.

Evaluating T-Cell Response Against Selected Epitopes

The people in the study had to have resided in the area for at least the last 5 years (average 29 years) and have had 1 or multiple episodes of *P. vivax* malaria, the last episodes dated between 2011 and 2015. It is well known that a naturally-acquired response requires a long period of time and multiple exposures to the parasite (Wipasa et al., 2002). HLA-DRB1* allele distribution for the 79 people here typed is shown in the Supplementary Table 1.

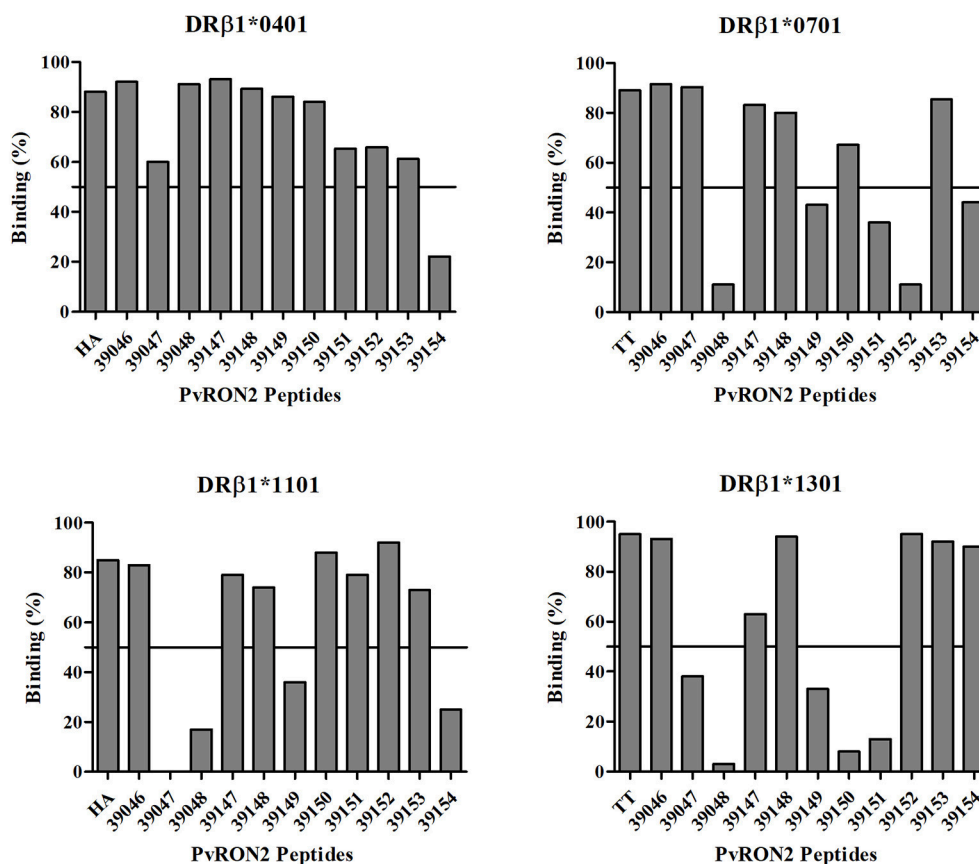


FIGURE 1 | PvRON2 peptides *in vitro* binding to purified HLA-DRB1* molecules. A cut-off line is shown at 50% binding, used for selecting high-binding peptides for further evaluation of IC₅₀ value. Each plot shows percentage epitope binding to HLA-DRB1* in this study and that for their control peptide.

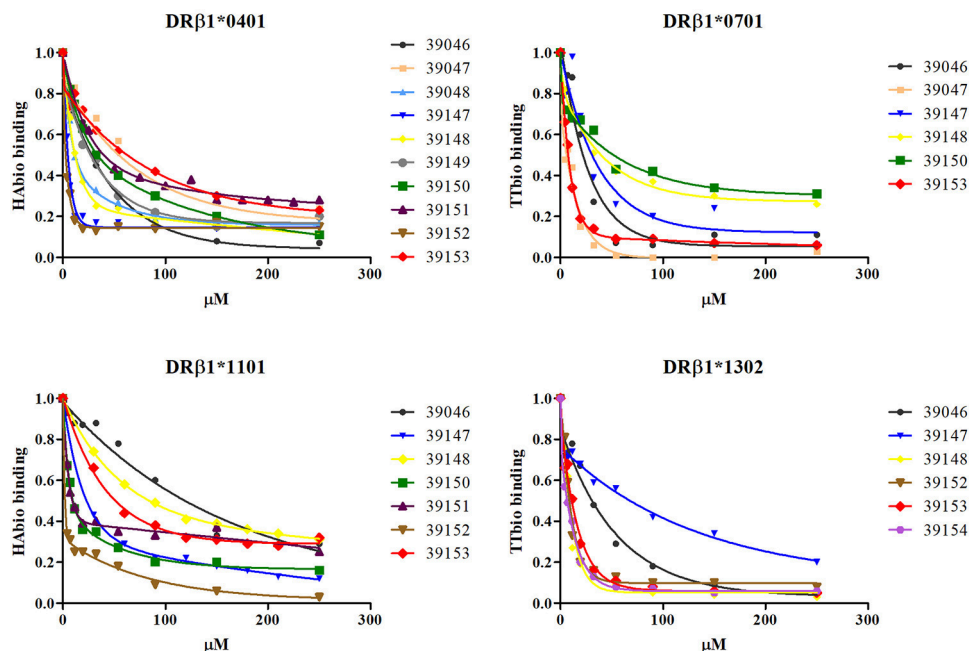


FIGURE 2 | *In vitro* assays for calculating a PvRON2 peptide's IC₅₀ value. Different epitope concentrations were evaluated for calculating the value at which control peptide was displaced by 50% (using a second order exponential decay function). Each point under the curve represents evaluated epitope concentration-dependent control peptide (μM) binding.

Among the alleles of interest, HLA-DRB1*04 had a frequency of 12.66%, HLA-DRB1*07 a frequency of 12.03%, HLA-DRB1*11 a frequency of 8.23% and HLA-DRB1*13 a frequency of 9.49%.

PBMC from individuals exposed to *P. vivax* infection (and control group) were stimulated with 10 μg/mL PvRON2 peptides and incubated for 5 days to evaluate proliferative response. Both universal epitope 39153 and DRB1* allele-specific peptides induced proliferation (≥ 2 Stimulation Index) in individuals from endemic areas, whereas there was no proliferation regarding specific peptides for each allele or parasite lysate in the control group (Table 3 and Supplementary Table 2). There were statistically significant differences for universal epitope 39153 ($p = 0.0075$), DRB1*13-specific peptide 39154 ($p = 0.0387$) and DRB1*07-specific peptide 39047 ($p = 0.0260$) between the group of exposed individuals and the control group. This response to the different antigens used in the lymphoproliferation assay, was compared with a Kruskal-Wallis test (with a Dunn's multiple comparison post-test), where no statistically significant differences were found in response to the different peptides.

Low-binding control peptide 39115 showed the lowest proliferative response (SI = 2.018) and was significantly different regarding the control group ($p = 0.0289$). *P. vivax* lysate also induced a greater proliferative response in exposed individuals, despite no statistically significant differences were observed when compared to the control group (Figure 3). However, peptide 39115 induced T cell proliferation in 7 of the 29 exposed individuals, despite no binding to HLA-DRB1* was either predicted or observed *in vitro*. Considering that this peptide is a T epitope from the Pv12 protein as shown by the

lymphoproliferation assays, further analyses to assess whether it is being presented by other class II molecules such as HLA-DP or HLA-DQ are worth carrying out.

P. vivax lysate also induced a greater proliferative response in exposed individuals; however, no statistically significant differences were observed when compared to control group (Figure 3). The mean SI = 12.47 ± 1.636 SE is for exposed individuals and mean SI = 5.45 ± 1.138 SE for the control group. Despite the SI values of PMBCs stimulated with PHA were significantly higher between exposed individuals and control group ($p = 0.0103$), 96.6% of exposed individuals and the 100% of control group responded to PHA (data not shown).

PvRON2 Epitope-Dependent Cytokine Secretion

IFN- γ , TNF (Th1 profile) and IL-10, IL-6 (Th2 profile) production in culture supernatant was quantitatively measured after stimulating PBMCs with peptides selected for HLA-DRB1* by binding assays. *P. vivax*-lysate and PHA were used as positive controls and unstimulated PBMCs as a baseline. Statistical analysis between unstimulated and stimulated PBMCs from exposed individuals showed that IFN- γ was only significant after stimulation with *P. vivax*-lysate ($p = 0.0001$). TNF production was significantly different for peptides 39047 ($p = 0.01$), 39154 ($p = 0.04$) and *P. vivax*-lysate ($p = 0.0001$). IL-10 had higher production with peptide 39047 ($p = 0.001$) and *P. vivax*-lysate ($p = 0.0001$). IL-6 responses were significantly greater to peptides 39047 ($p = 0.01$), 39152 ($p = 0.0025$), 39154 ($p = 0.002$) and *P. vivax*-lysate ($p = 0.0001$) (Figure 4). Cytokine levels were

TABLE 3 | A summary of PBMC proliferative response to PvRON2 T-cell epitopes.

Antigen	HLA-DRB1*	Average response (SI)		p-value
		Exposed individuals	Control group	
39153	Universal epitope	3.354 (SE 0.578)	0.935 (SE 0.282)	0.0075**
39152	DRB1*04 DRB1*11	3.052 (SE 1.09)	1.004 (SE 0.198)	0.1751
39047	DRB1*07	3.108 (SE 0.737)	1.156 (SE 0.267)	0.0260*
39154	DRB1*13	3.697 (SE 1.17)	0.888 (SE 0.327)	0.0387*
39115	Low-binding control peptide	2.018 (SE 0.347)	0.87 (SE 0.231)	0.0289*
Parasite lysate	Positive control	3.664 (SE 0.607)	1.474 (SE 0.255)	0.0735

Data regarding individuals exposed to *P. vivax* infection and control group. (SI, stimulation index; SE, standard error). Mann-Whitney's test and Student's t-test p-values were determined for exposed individuals compared to control group. * $p < 0.05$, ** $p < 0.005$.

compared with the Kruskal-Wallis test (with a Dunn's multiple comparison post-test) between 39115 and all other peptides in exposed individuals, a significantly higher TNF and IL-6 production was observed for peptide 39154 ($p < 0.0001$).

Control group data was also analyzed; significant differences were found for IFN- γ production after PBMCs had been stimulated with peptides 39047 ($p = 0.002$), 39154 ($p = 0.0006$) and *P. vivax*-lysate ($p = 0.0006$). IL-6 production was greater after being stimulated with peptides 39152 ($p = 0.0006$), 39047 ($p = 0.002$), 39154 ($p = 0.01$) and *P. vivax*-lysate ($p = 0.0001$). This suggests that naïve T-cells and/or other innate cells, such as macrophages, natural killer (NK), natural killer T-cells (NKT) and non-cytotoxic innate lymphoid cells recognized peptides and lysate and produced cytokines (Artis and Spits, 2015) (Supplementary Figure 1).

Cytokine levels were compared between exposed individuals and control group, significant differences being found regarding TNF production for epitope 39153 ($p = 0.0127$). Significant differences were found for epitope 39047 ($p = 0.005$) and 39152 epitope ($p = 0.010$) IL-6 production (Figure 5).

Detecting Antibodies Against *P. vivax*-Infected RBC by IFA

Naturally-acquired anti-malarial antibodies were detected using Multitest slides (MP Biomedicals) coated with parasitized RBC. The thirty exposed patients' sera reacted against *P. vivax* but the control group's sera did not. Supplementary Figure 2 shows the fluorescence pattern obtained with these sera.

An Analysis of PvRON2 B-Epitope Humoral Immune Response in *P. vivax*-Exposed Individuals

Antibody response against four *in silico* selected PvRON2 B-epitopes was evaluated in sera from 30 individuals exposed to natural *P. vivax* infection (Figure 6, Table 2). The highest number of seropositive samples was for the 39041-epitope (6/30, 20% of samples), followed by 39042 and 39043 (3/30, 10% of samples) and 39044 (2/30, 6.6% of samples). Peptides 39041 and 39043 showed the highest mean response (0.1598 and 0.1422, respectively), and significant differences were observed regarding 39044 which had the lowest mean response (0.0949)

out of all four peptides. The Kruskal-Wallis test (with Dunn's multiple comparison post-test) was used for statistical analysis, there were significant differences regarding epitope response ($p = 0.003$). Although there were no statistically significant differences between exposed individuals and control group, there was a tendency for a greater response in the first group (data not shown). rPvGAMA was used as positive control, 70% of samples being seropositive (21/30 samples); significant differences with control group were observed ($p = 0.0004$) (Supplementary Figure 3).

The ELISA results were analyzed by endemic area, showing an evident tendency for a greater response in the samples from the Chocó department compared to the Córdoba department (Figure 7). The Mann-Whitney test gave a significantly higher response for peptides 39041 ($p = 0.0135$), 39042 ($p = 0.0171$), 39043 ($p = 0.0007$) and 39044 ($p = 0.0492$) in *P. vivax*-exposed individuals. Samples from Colombia's Chocó ($n = 13$) and Córdoba ($n = 17$) departments. From these samples, six reacted positively to at least one PvRON2 B-epitope, where 83% ($n = 5$) of the samples were from Chocó's department. Positive sera reacted to the four peptides, 83% were from samples from the Chocó department. Although 39041, 39042, and 39044 peptides had no significant differences between exposed individuals from the Chocó and control group, 39043 had a significantly higher response ($p = 0.0186$). Differences between endemic areas were only observed in response to PvRON2 B-cell epitopes since there were no significant differences between both areas regarding PvGAMA ($p = 0.4265$), as it was expected to occur when a whole recombinant protein is used as antigen (several epitopes present within it, could be differentially recognized by exposed individuals, and a similar overall response was thus detected). Seropositive samples were selected for evaluating IgG subclasses.

The Prevalence of IgG Subclass Response Against PvRON2 B-Epitopes in Individuals Exposed to Natural *P. vivax* Infection

Seropositive samples from exposed individuals recognizing B-epitopes were selected for IgG subclass evaluation. Of the four peptides evaluated, only 39041 had significant differences between IgG subclasses ($p = 0.0004$) while there were no

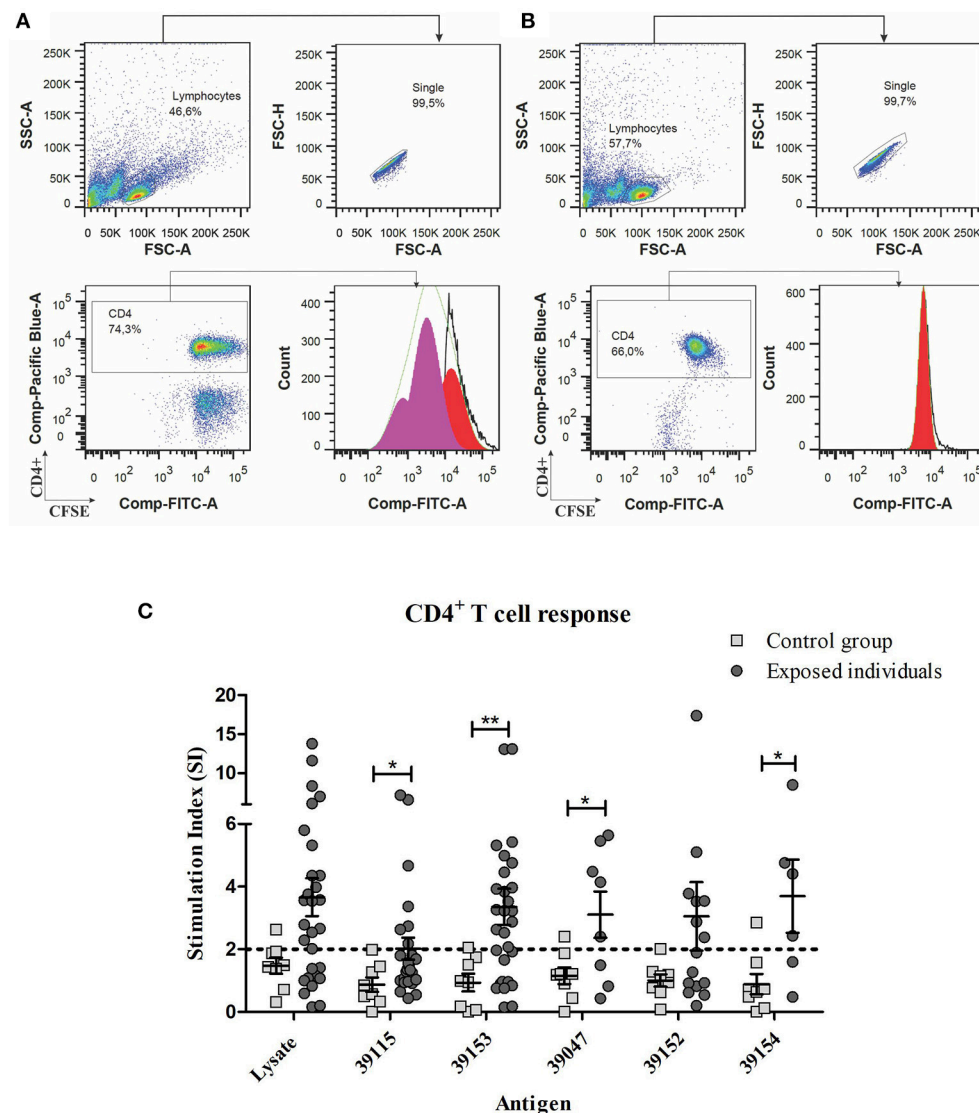


FIGURE 3 | Gating strategy for the proliferation assays and PBMC proliferative response to *Pv*RON2 epitopes from individuals exposed to *P. vivax* infection compared to control group. **(A)** *P. vivax*-exposed individuals' PBMC stimulated with universal peptide (39153). **(B)** Non-stimulated *P. vivax* exposed individuals' PBMCs. **(A,B)** Upper left plot, selected lymphocyte population (SSC-A vs. FSC-A), upper right plot selection of single cells from lymphocyte population (FSC-H vs. FSC-A). The lower left-hand plot shows gated CFSE label lymphocytes (Comp-FITC-A) for analyzing CD4+ T-cells (Comp-Pacific Blue-A). Lower right-hand plot shows CD4+ lymphocyte proliferation analyzed by FlowJo software (v7.6.5, Ashland, Oregon, USA) using 7 peaks or cell generations. **(C)** Mann-Whitney and Student's *t*-tests were used for assessing statistically significant differences between exposed individuals and control group. Universal peptide 39153 ($n = 29$), DRB1*04 and DRB1*11 peptide 39152 ($n = 15$), DRB1*07-specific peptide 39047 ($n = 8$), DRB1*13-specific peptide 39154 ($n = 6$), low-binding control peptide 39115 ($n = 29$) and *P. vivax* lysate ($n = 29$) responses are shown. The CD4+ cells were labeled with Pacific Blue mouse anti-human CD4 (RPA-T4 clone) antibody. Statistically significant differences ($p \leq 0.05$) are shown and data represents the means \pm SEM for all values. * $p < 0.05$ and ** $p < 0.005$.

significant differences for the other peptides. 39041 had clear IgG2 predominance regarding other subclasses, having statistically significant differences with IgG1 and IgG4 (the latter having the lowest mean response) (Figure 8).

DISCUSSION

Developing countries desperately need strategies aimed at preventing malaria (especially that caused by *P. vivax*), such as approaches for developing specific drugs and protective vaccines

which are currently unavailable. Although there are *P. vivax* vaccines in phases I and IIa (López et al., 2017), they have not induced sterile protection (Bennett et al., 2016). Developing a *P. vivax* vaccine requires studies analyzing naturally-infected patients' immune response regarding proteins involved in erythrocyte invasion. Several *P. vivax* vaccine candidates' binding regions have been characterized to date, such as reticulocyte binding proteins (RBPs) (Urquiza et al., 2002), the Duffy binding protein (DBP) (Ocampo et al., 2002), the *P. vivax* GPI-anchored micronemal antigen (PvGAMA) (Baquero et al., 2017), some

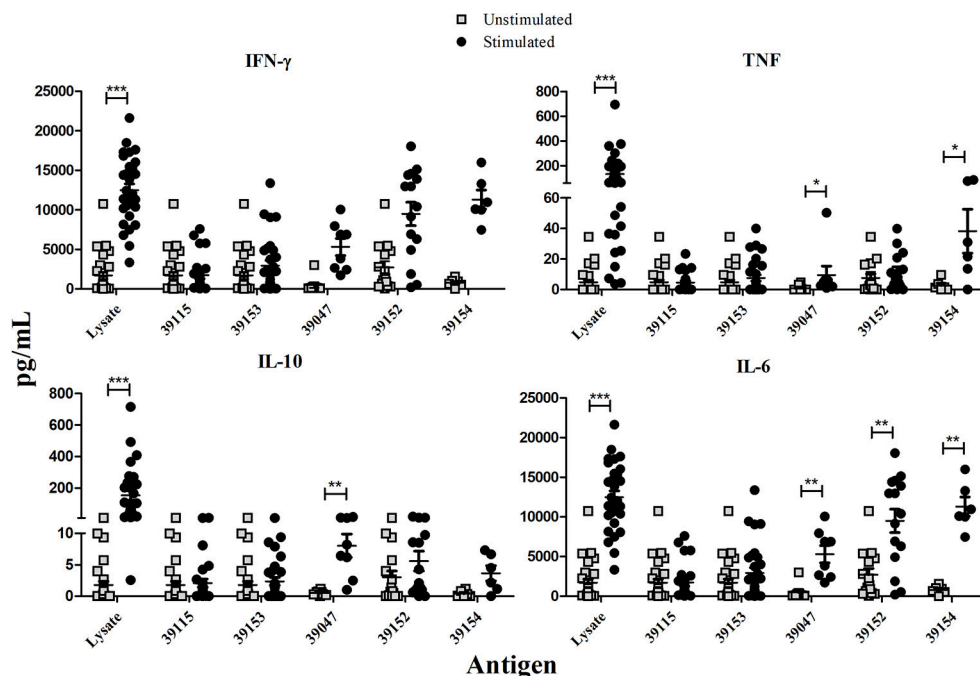


FIGURE 4 | Exposed individuals' supernatant culture *in vitro* cytokine production. Individual data shows the mean value of non-stimulated and PBMCs stimulated with universal epitope (39153), specific epitopes 39047, 39152, and 39154, and *P. vivax* lysate. IFN- γ , TNF, IL-10, and IL-6 levels were measured by CBA kit; cytokine concentration is expressed in pg/mL. Statistically significant differences ($p \leq 0.05$) are shown and data represents the means \pm SEM for all values. * $p < 0.05$, ** $p < 0.005$ and *** $p < 0.0005$.

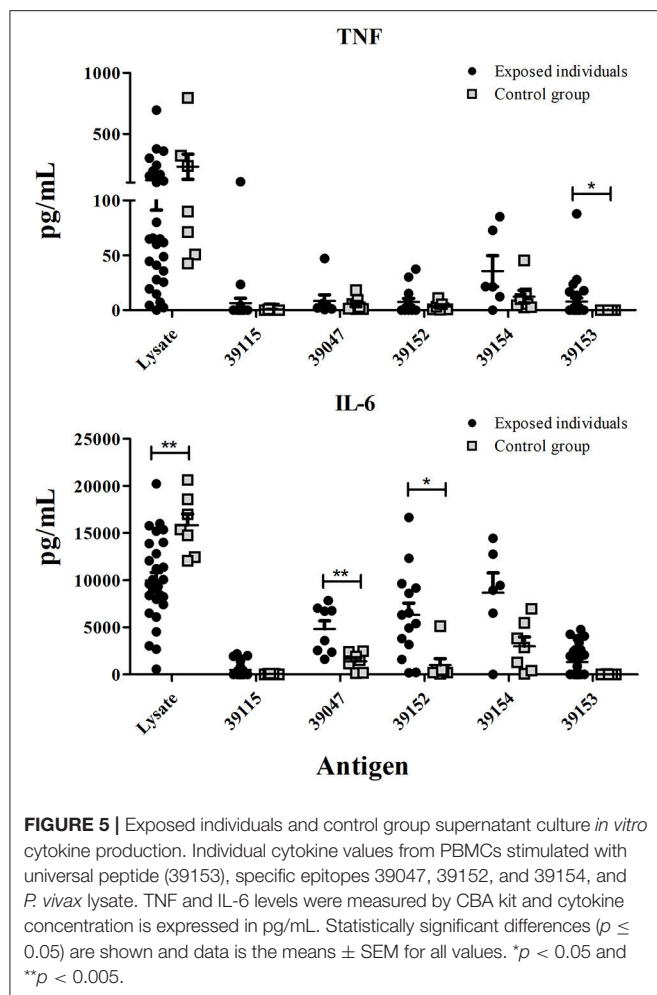
proteins from the tryptophan-rich antigen (PvTRAg) family (Zeeshan et al., 2014), merozoite surface protein-1 (PvMSP-1) (Rodríguez et al., 2002) and apical membrane antigen-1 (AMA-1) (Arévalo-Pinzón et al., 2017). Important mediators in AMA-1 erythrocyte binding have also been identified, such as rhoptry neck proteins (RONs), including PvRON5 (Arévalo-Pinzón et al., 2015), PvRON4 (Arévalo-Pinzón et al., 2013) and PvRON2 (Arévalo-Pinzón et al., 2011). RONs have been strongly associated with MJ formation, thereby helping parasite entry into erythrocytes; RON2 is a vaccine candidate since anti-AMA1 and anti-RON2 antibodies can block erythrocyte invasion (Arévalo-Pinzón et al., 2011; Lamarque et al., 2011; Srinivasan et al., 2011; Tyler et al., 2011; Vulliez-Le Normand et al., 2017).

The data presented here has described naturally-acquired T-cell immune responses to PvRON2 high-affinity binding-MHC-II DRB1* peptides in *P. vivax*-exposed individuals from two endemic areas of Colombia. Certain requirements are involved in protection-inducing vaccine design; for example, the proper antigen presentation by MHC-II and MHC-I molecules to T-cell receptors, so as to induce strong immune responses. MHC class II and I molecules are critical in host-pathogen interactions as they determine host immune response quality. High-affinity peptide-MHCII-TCR binding time or peptide-MHCII complex amount is critical for mounting protective T-cell responses (Blum et al., 2013; Tubo et al., 2013). Post-genomic era bioinformatics tools and reverse vaccinology approaches have drawn scientists' attention, since an individual antigen can be screened from one or several microorganisms and the highest affinity epitopes

be determined from these might induce protective immune responses (Sette and Rappuoli, 2010).

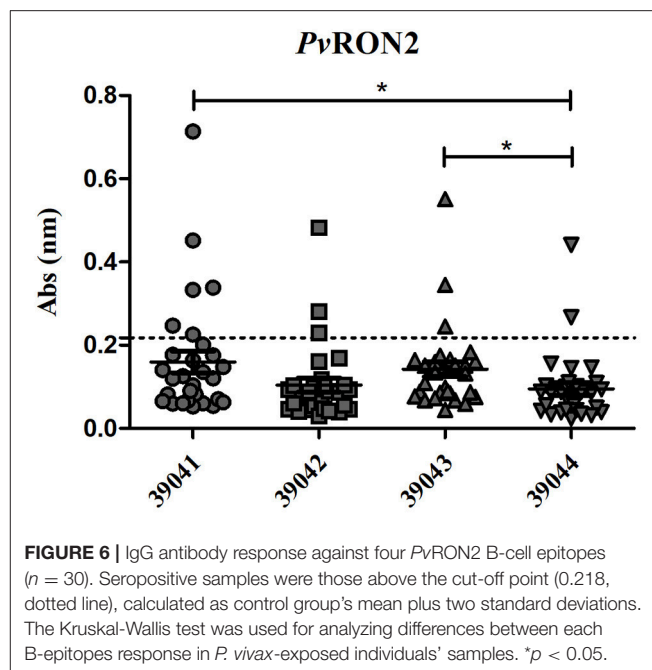
This study has analyzed the PvRON2 sequence aa to determine high-binding HLA-DRB1* T-cell epitopes *in silico*. NetMHCIIpan 3.0 (Andreatta et al., 2015) predicted eleven high-affinity HLA-DRB1* epitopes where at least one epitope bound to one HLA-DRB1* molecule; this was confirmed by *in vitro* competition assays using biotin-control peptides. However, some predicted epitopes have not bound to HLA-DRB1*, according to other studies (Bergmann-Leitner et al., 2013), while HLA-DRB1*04 bound to 10/11 peptides here. A previous study has shown a strong naturally-acquired humoral response in HLA-DRB1*04 people living in the Brazilian Amazon against 5/9 recombinant *P. vivax* proteins (Lima-Junior et al., 2012). HLA-DRB1*04 is one of the most frequently occurring alleles in Colombian Amerindian groups, accompanied by DR2 (DRB1*1602), DR6 (DRB1*1402) and DR8 (DRB1*0802). The patients' blood samples used in this study were mostly taken from Amerindians from Córdoba and Chocó. Tule (5 HLA-DRB1*04 alleles) is the main Amerindian population in Córdoba and the Waunana (4 HLA-DRB1*04 alleles) in the Chocó region, having more diverse DRB1 alleles than other groups (Trachtenberg et al., 1996).

Previous studies had suggested that some alleles' over dominance in a population could be due to the spread of advantageous alleles (positive selection) after pathogen-driven selection. This has been shown by Hill et al., in a study of West African alleles (HLA-DRB1*1302-DQB1*0501) which were not



present in other racial groups and were associated with protection against severe malaria, i.e., directional selection (Hill et al., 1991).

Several factors (e.g., parasite evasion mechanisms and immune molecule polymorphism) can affect protection-inducing immune responses to malarial parasites and, consequently, malaria vaccine development. Parasite evasion mechanisms include immunodominant antigen polymorphism, antigenic variation and diversion, epitope masking and the smoke-screen strategy. *P. vivax* and *P. ovale* have additional escape mechanisms which are mediated by long-lasting hypnozoites, as well as using different erythrocyte invasion pathways (Rénia and Goh, 2016). MHC Class I and II have enormous allele polymorphism and aa sequence variation in the peptide binding region, thereby enabling peptides to bind to different alleles (Blum et al., 2013). Such variability hampers a single epitope-based vaccine against *Plasmodium* parasites being developed; however, *in silico* analysis of T- and B-cell epitopes could be useful for identifying vaccine candidates represented by different epitopes which could provide coverage of the whole target population. The exposed patients studied here were grouped according to their HLA-DRB1* to cover the most frequently occurring alleles in the endemic population worldwide, such as HLA-DRB1*04, HLA-DRB1*07, HLA-DRB1*11, and HLA-DRB1*13. Cell-mediated immune



responses were investigated based on MHC class II peptide binding specificity and humoral immune responses by detecting antibody levels against linear B-cell epitopes.

Antibodies against *P. vivax* blood-stage proteins are important elements for blocking RBC invasion (Wipasa et al., 2002); such antibodies thus play an important role in identifying and validating *P. vivax* vaccine candidates (Soares et al., 1999; Lima-Junior et al., 2008; Storti-Melo et al., 2012; Changrob et al., 2017; Rodrigues-Da-Silva et al., 2017). We confirmed the presence of naturally-acquired humoral responses against four PvRON2 B-epitopes which were recognized by IgG antibodies and subclasses. Low individual PvRON2 B-epitope responder frequency was observed (20% 39041, 10% 39042, 6.6% 39043 and 39044); such low responses have previously been reported for other blood-stage antigens such as PvMSP8. A loss of mean response to a target protein has been observed as time has elapsed when average response has been about ten times greater to recombinant protein than linear epitopes in acute-infection patients (Cheng et al., 2017). This has been associated with short-lived antibodies, due to short-lasting memory responses or parasite-induced B-cell dysregulation (Rénia and Goh, 2016) and parasite genetic variations or in exposed populations.

Antibody response differences against PvRON2 B-cell epitopes between exposed individuals from Chocó (83%) and Córdoba (17%), could be attributed to several factors, including the level of parasitemia and the number of episodes (Druilhe and Pérignon, 1994). The last 3 SIVIGILA reports (2015–2017), showed a higher incidence of *P. vivax* infection in Chocó regarding Córdoba (Instituto-Nacional-De-Salud, 2017). Other intrinsic factors from the responders such as their HLA, sex, age, psychological stress, nutrition and other infectious diseases could also be involved in such differences (Van Loveren et al., 2001).

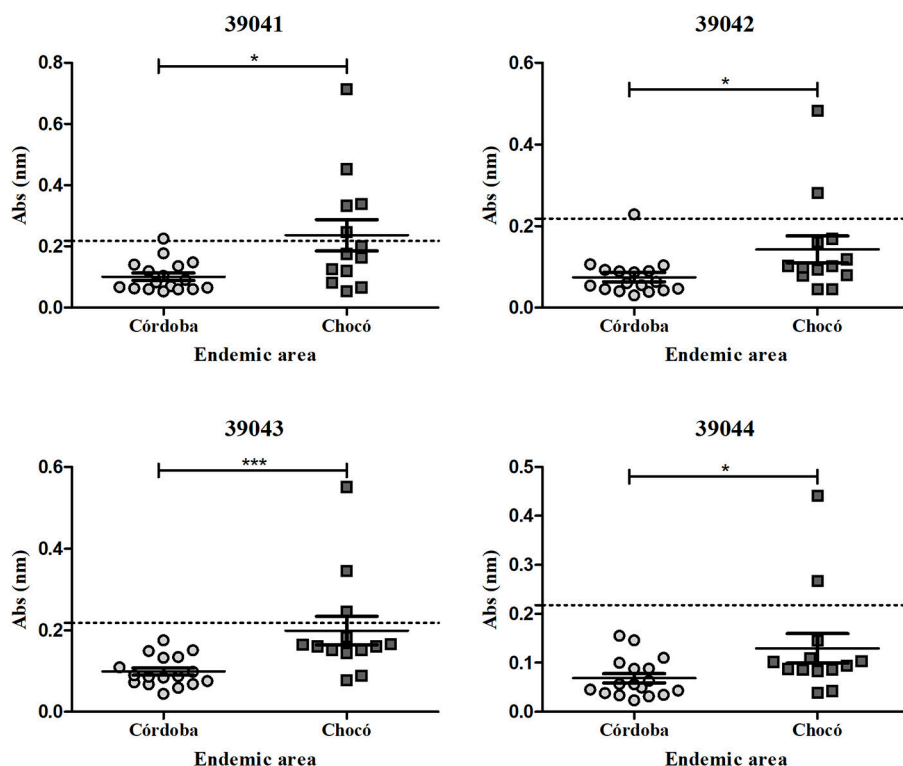


FIGURE 7 | IgG antibody response to PvRON2 B epitopes by endemic area. Significant differences (calculated by Mann-Whitney test) between samples from Colombia's Chocó ($n = 13$) and Córdoba ($n = 17$) departments are shown. The dashed line indicates the cut-off point for seropositive samples. * $p < 0.05$ and *** $p < 0.0005$.

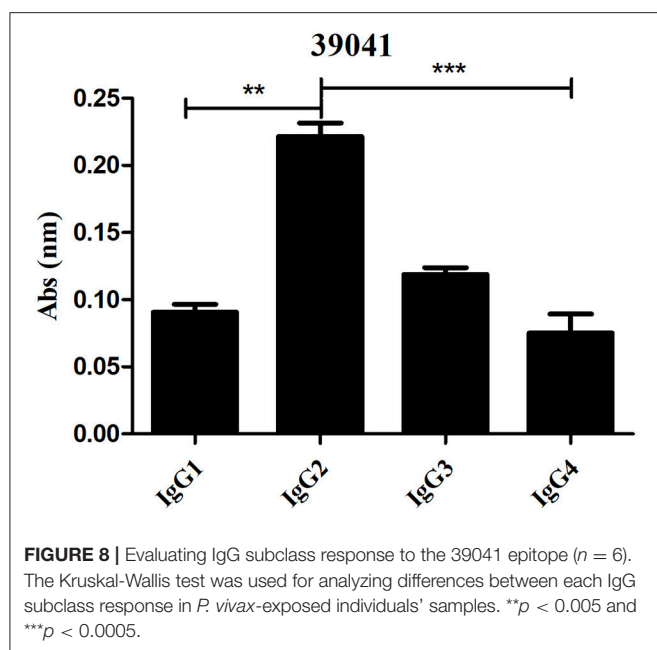
Two of the selected B-epitopes (39042 and 39044) were located on an α -helical coiled motif protein and other studies have shown that selected *in silico* peptides related to these motifs have been recognized by naturally-acquired antibodies and have been immunogenic in mice (Villard et al., 2007; Arévalo-Pinzón et al., 2011); however, 39042 (10%) and 39044 (6.6%) epitopes had the lowest recognition values in our study. 39041 had significant differences in the IgG subclasses analyzed; IgG2 predominated while low IgG4 and IgG1 levels were observed. A predominant IgG2 response and low IgG4 reactivity in previous studies has been associated with *P. falciparum* infection resistance and clearance, IgG2/IgG4 relationship being associated with a protective role (Aucan et al., 2000). Similar results have been found in PvMSP8 studies recording IgG2 non-cytophilic antibody predominance which has been associated with resistance to *P. vivax* malaria (Cheng et al., 2017). 39041 has been seen to be immunogenic in mice (Arévalo-Pinzón et al., 2011) and its potentially protective role makes this peptide a pivotal PvRON2 epitope for inclusion in a subunit-based vaccine.

It has been thought that antibodies would be enough to protect against malaria and that T-cells do not play an important role during the erythrocyte stage. Advances in immunology-related knowledge have demonstrated that B-cells must be activated by CD4+ T-helper cells to prompt good humoral responses, thereby inducing cytokine, memory cell and antibody production

(Batista and Harwood, 2009; Tubo et al., 2013; Yuseff et al., 2013). The role of exposed patients' T-cell response against PvRON2 high-affinity binding peptides was studied in cytokine proliferation and production assays. Only exposed individuals' PBMC cultures showed proliferation induced by universal and specific binding peptides, suggesting that PvRON2 induced memory T-cells against high-affinity peptides. However, Th1 and Th2 cytokine responses were low, except for IL-6. Low cytokine responses/production have been observed in other studies; Silva-Flannery et al., found that immunization with monomeric peptide did not result in peptide-specific IFN- γ -secreting cell expansion and was not protective. They also reported that the monomeric peptide was less taken up by antigen-presenting cells and was not going through the phagolysosome (Silva-Flannery et al., 2009).

Cytokine production by unexposed individuals' PBMCs against PvRON2 synthetic peptides may have been due to dendritic or macrophages cells priming naïve T-cells and inducing effector T-cell cytokine production; nevertheless, secretion was very low for some of them.

Unlike the other cytokines tested here, IL6 was highly secreted by exposed patients' PBMCs; this was not surprising, since one of IL6's multi-functions is to stimulate hybridoma and plasmacytoma cell growth and help antibody production (Matsuda et al., 1988). IL6, together with IL12 and VDR, have been associated with reduced parasitemia, its severity and



gametocytemia clearance in *P. vivax*-exposed individuals (Sortica et al., 2014). *P. vivax* lysate-induced cytokine responses in unexposed individuals' PBMCs could be explained by innate immune cell cytokine production, i.e., macrophages, dendritic cells, NK, NKT and naïve T-cells which become effector cells (Stevenson and Riley, 2004). High cytokine induction in healthy individuals compared to *P. vivax*-exposed individuals might be related to a parasite evasion mechanism for inhibiting effective immune responses able to eliminate the parasite (Rénia and Goh, 2016). Nonetheless, the healthy individuals had not been exposed to *P. vivax* since immunofluorescence assays did not show their antibodies' reactivity to the parasite.

Taken together, the *in silico* T-cell and B-cell epitope selection results highlighted two T-cell epitopes (39047 and 39154) and one B-cell epitope (39041) as promising vaccine candidates. Despite the significant differences observed in immune responses evoked in the exposed individuals compared to the control group, overall the responses were relatively low. All selected peptides were conserved among the 11 *P. vivax* strains which may also explain such low immune responses. This has been demonstrated in *P. falciparum* studies where conserved high activity binding peptides (HABPs) were poorly antigenic and poorly immunogenic (Patiño et al., 1997; Lougovskoi et al., 1999; Ocampo et al., 2000; Parra et al., 2000; Hensmann et al., 2004). It should be stressed that caution must be taken, since using these 3 promising peptides in a multi-epitope vaccine in their unmodified state would probably mean that they could induce low immunogenicity and not provide long-lasting protection; however, proven approaches have shown that modifying their critical residues should induce a strong and long-lasting protection-inducing immune response (Patarroyo et al., 2010).

HABPs have been seen to be *P. falciparum* vaccine candidates during the last two decades (Rodríguez et al., 2008); however,

they must be modified to make them antigenic and protection-inducing by replacing critical aa with others having the same mass but different polarity (Cifuentes et al., 2008; Patarroyo et al., 2011). Such HABPs can only be used in a tailor-made vaccine targeting a specific HLA-DRB1* endemic population; however, a universal protection-inducing vaccine will require studying other peptides which can bind to other HLA-DRB1* alleles. Future studies should be carried out using modified peptides aimed at assessing immunogenicity and protection-inducing ability in the *Aotus* experimental model to confirm their suitability as *P. vivax* vaccine candidates. Likewise, additional peptides should be included to cover all parasite stages, aiming at a 100% protection-inducing, multistage, multi-epitope, minimal subunit-based vaccine.

AUTHOR CONTRIBUTIONS

CL: designed and performed the experiments, analyzed the data, drafted the manuscript. YY-P: designed and performed the experiments, analyzed the data, drafted the manuscript, designed the figures. DD-A: drafted the manuscript. MEP: critical suggestions regarding the manuscript. MAP: conceiving the work and drafting all versions of the manuscript. All authors have revised the manuscript and approved the version to be submitted.

FUNDING

This work was financed by the Departamento Administrativo de Ciencia, Tecnología e Innovación (COLCIENCIAS) through grant RC # 0309-2013. CL received support from Colciencias within the framework of the Convocatoria Nacional para Estudios de Doctorado en Colombia (call for candidates # 6172).

ACKNOWLEDGMENTS

We would like to thank all the people from Bahía Solano (Chocó) and Tierra Alta (Córdoba) who participated in this study, as well as all the people from healthcare institutions who coordinated sample collection, especially the Centro Médico Cubis in Bahía Solano, Chocó. We would like to thank Jason Garry for translating the manuscript, Natalia Hincapié-Escobar for her technical support, Alejandro Giraldo Escobar for his support with the native community, the Immunotoxicology group (UNAL) for their experimental support, Carlos Fernando Suárez for his critical suggestions and Luis Alfredo Baquero for donating rPvGAMA.

SUPPLEMENTARY MATERIAL

The Supplementary Material for this article can be found online at: <https://www.frontiersin.org/articles/10.3389/fcimb.2018.00156/full#supplementary-material>

Supplementary Figure 1 | Control group supernatant culture *in vitro* cytokine production. Data individual show the mean value of unstimulated and stimulated PBMC (n = 8) with universal epitope (39153), specific epitopes (39047, 39152,

and 39154) and *P. vivax* lysate. IFN- γ , TNF, IL-10, and IL-6 levels were measured by CBA kit and cytokine concentration is expressed in pg/mL. Statistically significant differences ($p \leq 0.05$) are shown and data is the means \pm SEM of all values.

Supplementary Figure 2 | Immunofluorescence patterns for exposed individuals from Colombia's *P. vivax*-endemic areas and the control group. The upper panels show one Bahía Solano's exposed individual serum recognition of pRBC. Nuclei were stained with DAPI, the parasite with anti-parasite FITC and then, both were merged. The bottom panels show serum from one non-exposed individual.

REFERENCES

- Aikawa, M., Miller, L. H., Johnson, J., and Rabbege, J. (1978). Erythrocyte entry by malarial parasites. A moving junction between erythrocyte and parasite. *J. Cell Biol.* 77, 72–82. doi: 10.1083/jcb.77.1.72
- Andreatta, M., Karosiene, E., Rasmussen, M., Stryhn, A., Buus, S., and Nielsen, M. (2015). Accurate pan-specific prediction of peptide-MHC class II binding affinity with improved binding core identification. *Immunogenetics* 67, 641–650. doi: 10.1007/s00251-015-0873-y
- Arévalo-Herrera, M., Lopez-Perez, M., Medina, L., Moreno, A., Gutierrez, J. B., and Herrera, S. (2015). Clinical profile of *Plasmodium falciparum* and *Plasmodium vivax* infections in low and unstable malaria transmission settings of Colombia. *Malar. J.* 14:154. doi: 10.1186/s12936-015-0678-3
- Arévalo-Herrera, M., Rengifo, L., Lopez-Perez, M., Arce-Plata, M. I., García, J., and Herrera, S. (2017). Complicated malaria in children and adults from three settings of the Colombian Pacific Coast: a prospective study. *PLoS ONE* 12:e0185435. doi: 10.1371/journal.pone.0185435
- Arévalo-Pinzón, G., Bermúdez, M., Curtidor, H., and Patarroyo, M. A. (2015). The *Plasmodium vivax* rhoptry neck protein 5 is expressed in the apical pole of *Plasmodium vivax* VCG-1 strain schizonts and binds to human reticulocytes. *Malar. J.* 14:1. doi: 10.1186/s12936-015-0619-1
- Arévalo-Pinzón, G., Bermúdez, M., Hernández, D., Curtidor, H., and Patarroyo, M. A. (2017). *Plasmodium vivax* ligand-receptor interaction: PvAMA-1 domain I contains the minimal regions for specific interaction with CD71+ reticulocytes. *Sci. Rep.* 7:9616. doi: 10.1038/s41598-017-10025-6
- Arévalo-Pinzón, G., Curtidor, H., Abril, J., and Patarroyo, M. A. (2013). Annotation and characterization of the *Plasmodium vivax* rhoptry neck protein 4 (Pv RON4). *Malar. J.* 12:356. doi: 10.1186/1475-2875-12-356
- Arévalo-Pinzón, G., Curtidor, H., Patiño, L. C., and Patarroyo, M. A. (2011). PvRON2, a new *Plasmodium vivax* rhoptry neck antigen. *Malar. J.* 10:60. doi: 10.1186/1475-2875-10-60
- Artis, D., and Spits, H. (2015). The biology of innate lymphoid cells. *Nature* 517, 293–301. doi: 10.1038/nature14189
- Aucan, C., Traoré, Y., Tall, F., Nacro, B., Traoré-Leroux, T., Fumoux, F., et al. (2000). High immunoglobulin G2 (IgG2) and low IgG4 levels are associated with human resistance to *Plasmodium falciparum* malaria. *Infect. Immun.* 68, 1252–1258. doi: 10.1128/IAI.68.3.1252-1258.2000
- Baquero, L. A., Moreno-Pérez, D. A., Garzón-Ospina, D., Forero-Rodríguez, J., Ortiz-Suárez, H. D., and Patarroyo, M. A. (2017). PvGAMA reticulocyte binding activity: predicting conserved functional regions by natural selection analysis. *Parasit. Vectors* 10:251. doi: 10.1186/s13071-017-2183-8
- Batista, F. D., and Harwood, N. E. (2009). The who, how and where of antigen presentation to B cells. *Nat. Rev. Immunol.* 9, 15–27. doi: 10.1038/nri2454
- Bennett, J. W., Yadava, A., Tosh, D., Sattabongkot, J., Komisar, J., Ware, L. A., et al. (2016). Phase 1/2a trial of Plasmodium vivax malaria vaccine candidate VMP001/AS01B in malaria-naïve adults: safety, immunogenicity, and efficacy. *PLoS Negl. Trop. Dis.* 10:e0004423. doi: 10.1371/journal.pntd.0004423
- Bergmann-Leitner, E. S., Chaudhury, S., Steers, N. J., Sabato, M., Delvecchio, V., Wallqvist, A. S., et al. (2013). Computational and experimental validation of B and T-cell epitopes of the *in vivo* immune response to a novel malarial antigen. *PLoS ONE* 8:e71610. doi: 10.1371/journal.pone.0071610
- Blum, J. S., Wearsch, P. A., and Cresswell, P. (2013). Pathways of antigen processing. *Ann. Rev. Immunol.* 31, 443–473. doi: 10.1146/annurev-immunol-032712-095910
- Supplementary Figure 3 |** IgG antibody response against PvGAMA control recombinant protein. Significant differences (calculated by Mann-Whitney test) are shown between samples from exposed individuals and control. The dashed line indicates the cut-off point for seropositive samples.
- Supplementary Table 1 |** Exposed-individuals' HLA-DRB1* allele frequency
- Supplementary Table 2 |** Non-exposed individuals' lymphoproliferation assay using PvRON2 peptides.
- Bozdech, Z., Llinás, M., Pulliam, B. L., Wong, E. D., Zhu, J., and Derisi, J. L. (2003). The transcriptome of the intraerythrocytic developmental cycle of *Plasmodium falciparum*. *PLoS Biol.* 1:e5. doi: 10.1371/journal.pbio.0000005
- Cao, J., Kaneko, O., Thongkukiatkul, A., Tachibana, M., Otsuki, H., Gao, Q., et al. (2009). Rhoptry neck protein RON2 forms a complex with microneme protein AMA1 in *Plasmodium falciparum* merozoites. *Parasitol. Int.* 58, 29–35. doi: 10.1016/j.parint.2008.09.005
- Changrob, S., Han, J. H., Ha, K. S., Park, W. S., Hong, S. H., Chootong, P., et al. (2017). Immunogenicity of glycosylphosphatidylinositol-anchored micronemal antigen in natural *Plasmodium vivax* exposure. *Malar. J.* 16:348. doi: 10.1186/s12936-017-1967-9
- Cheng, Y., Lu, F., Lee, S. K., Kong, D. H., Ha, K. S., Wang, B., et al. (2015). Characterization of *Plasmodium vivax* early transcribed membrane protein 11.2 and exported protein 1. *PLoS ONE* 10:e0127500. doi: 10.1371/journal.pone.0127500
- Cheng, Y., Wang, B., Changrob, S., Han, J. H., Sattabongkot, J., Ha, K. S., et al. (2017). Naturally acquired humoral and cellular immune responses to *Plasmodium vivax* merozoite surface protein 8 in patients with *P. vivax* infection. *Malar. J.* 16:211. doi: 10.1186/s12936-017-1837-5
- Cifuentes, G., Bermúdez, A., Rodríguez, R., Patarroyo, M. A., and Patarroyo, M. E. (2008). Shifting the polarity of some critical residues in malarial peptides' binding to host cells is a key factor in breaking conserved antigens' code of silence. *Med. Chem.* 4, 278–292. doi: 10.2174/157340608784325160
- Collins, C. R., Withers-Martinez, C., Hackett, F., and Blackman, M. J. (2009). An inhibitory antibody blocks interactions between components of the malarial invasion machinery. *PLoS Pathog.* 5:e1000273. doi: 10.1371/journal.ppat.1000273
- Counihan, N. A., Kalanon, M., Coppel, R. L., and De Koning-Ward, T. F. (2013). Plasmodium rhoptry proteins: why order is important. *Trends Parasitol.* 29, 228–236. doi: 10.1016/j.pt.2013.03.003
- Cowman, A. F., and Crabb, B. S. (2006). Invasion of red blood cells by malaria parasites. *Cell* 124, 755–766. doi: 10.1016/j.cell.2006.02.006
- Deléage, G., Combet, C., Blanchet, C., and Geourjon, C. (2001). ANTHEPROT: an integrated protein sequence analysis software with client/server capabilities. *Comput. Biol. Med.* 31, 259–267. doi: 10.1016/S0010-4825(01)00008-7
- Doolan, D. L., Southwood, S., Chesnut, R., Appella, E., Gomez, E., Richards, A., et al. (2000). HLA-DR-promiscuous T cell epitopes from *Plasmodium falciparum* pre-erythrocytic-stage antigens restricted by multiple HLA class II alleles. *J. Immunol.* 165, 1123–1137. doi: 10.4049/jimmunol.165.2.1123
- Druihlhe, P., and Pérignon, J. L. (1994). Mechanisms of defense against *P. falciparum* asexual blood stages in humans. *Immunol. Lett.* 41, 115–120. doi: 10.1016/0165-2478(94)90118-X
- El-Manzalawy, Y., Dobbs, D., and Honavar, V. G. (2017). *in silico* prediction of linear B-cell epitopes on proteins. *Methods Mol. Biol.* 1484, 255–264. doi: 10.1007/978-1-4939-6406-2_17
- Fairhurst, R. M., and Dondorp, A. M. (2016). Artemisinin-resistant *Plasmodium falciparum* malaria. *Microbiol. Spectr.* 4. doi: 10.1128/microbiolspec.EI10-0013-2016
- Guerra, C. A., Howes, R. E., Patil, A. P., Gething, P. W., Van Boeckel, T. P., Temperley, W. H., et al. (2010). The international limits and population at risk of *Plasmodium vivax* transmission in 2009. *PLoS Negl. Trop. Dis.* 4:e774. doi: 10.1371/journal.pntd.0000774
- Guevara Patiño J.A., Holder, A. A., McBride, J. S., and Blackman, M. J. (1997). Antibodies that inhibit malaria merozoite surface protein-1 processing and

- erythrocyte invasion are blocked by naturally acquired human antibodies. *J. Exp. Med.* 186, 1689–1699. doi: 10.1084/jem.186.10.1689
- Hammer, J., Bono, E., Gallazzi, F., Belunis, C., Nagy, Z., and Sinigaglia, F. (1994). Precise prediction of major histocompatibility complex class II-peptide interaction based on peptide side chain scanning. *J. Exp. Med.* 180, 2353–2358. doi: 10.1084/jem.180.6.2353
- Hensmann, M., Li, C., Moss, C., Lindo, V., Greer, F., Watts, C., et al. (2004). Disulfide bonds in merozoite surface protein 1 of the malaria parasite impede efficient antigen processing and affect the *in vivo* antibody response. *Eur. J. Immunol.* 34, 639–648. doi: 10.1002/eji.200324514
- Hill, A. V., Allsopp, C. E., Kwiatkowski, D., Anstey, N. M., Twumasi, P., Rowe, P. A., et al. (1991). Common west African HLA antigens are associated with protection from severe malaria. *Nature* 352, 595–600. doi: 10.1038/352595a0
- Instituto-Nacional-De-Salud (2017). *Boletín Epidemiológico Semanal-SIVIGILA*. Bogotá, DC: Instituto-Nacional-De-Salud.
- Lamarque, M., Besteiro, S., Papoin, J., Roques, M., Vulliez-Le Normand, B., Morlon-Guyot, J., et al. (2011). The RON2-AMA1 interaction is a critical step in moving junction-dependent invasion by apicomplexan parasites. *PLoS Pathog.* 7:e1001276. doi: 10.1371/journal.ppat.1001276
- Larsen, J. E., Lund, O., and Nielsen, M. (2006). Improved method for predicting linear B-cell epitopes. *Immunome Res.* 2:2. doi: 10.1186/1745-7580-2-2
- Lima-Junior, J. C., Rodrigues-Da-Silva, R. N., Banic, D. M., Jiang, J., Singh, B., Fabrício-Silva, G. M., et al. (2012). Influence of HLA-DRB1 and HLA-DQB1 alleles on IgG antibody response to the P. vivax MSP-1, MSP-3 α and MSP-9 in individuals from Brazilian endemic area. *PLoS ONE* 7:e36419. doi: 10.1371/journal.pone.0036419
- Lima-Junior, J. C., Tran, T. M., Meyer, E. V., Singh, B., De-Simone, S. G., Santos, F., et al. (2008). Naturally acquired humoral and cellular immune responses to *Plasmodium vivax* merozoite surface protein 9 in Northwestern Amazon individuals. *Vaccine* 26, 6645–6654. doi: 10.1016/j.vaccine.2008.09.029
- López, C., Yepes-Pérez, Y., Hincapié-Escobar, N., Díaz-Arévalo, D., and Patarroyo, M. A. (2017). What is known about the immune response induced by *Plasmodium vivax* malaria vaccine candidates? *Front. Immunol.* 8:126. doi: 10.3389/fimmu.2017.00126
- Lougovskoi, A. A., Okoyeh, N. J., and Chauhan, V. S. (1999). Mice immunised with synthetic peptide from N-terminal conserved region of merozoite surface antigen-2 of human malaria parasite *Plasmodium falciparum* can control infection induced by *Plasmodium yoelii* yoelii 265BY strain. *Vaccine* 18, 920–930. doi: 10.1016/S0264-410X(99)00330-8
- Marsh, S. G., Parham, P., and Barber, L. D. (1999). *The HLA Factsbook*. San Diego, CA: Academic Press.
- Matsuda, T., Hirano, T., and Kishimoto, T. (1988). Establishment of an interleukin 6 (IL 6)/B cell stimulatory factor 2-dependent cell line and preparation of anti-IL 6 monoclonal antibodies. *Eur. J. Immunol.* 18, 951–956. doi: 10.1002/eji.1830180618
- Mongui, A., Angel, D. I., Gallego, G., Reyes, C., Martinez, P., Guhl, F., et al. (2009). Characterization and antigenicity of the promising vaccine candidate *Plasmodium vivax* 34kDa rhoptry antigen (Pv34). *Vaccine* 28, 415–421. doi: 10.1016/j.vaccine.2009.10.034
- Moreno-Pérez, D. A., Areiza-Rojas, R., Flórez-Buitrago, X., Silva, Y., Patarroyo, M. E., and Patarroyo, M. A. (2013). The GPI-anchored 6-Cys protein Pv12 is present in detergent-resistant microdomains of *Plasmodium vivax* blood stage schizonts. *Protist* 164, 37–48. doi: 10.1016/j.protis.2012.03.001
- Moreno-Perez, D. A., Montenegro, M., Patarroyo, M. E., and Patarroyo, M. A. (2011). Identification, characterization and antigenicity of the *Plasmodium vivax* rhoptry neck protein 1 (Pv RON1). *Malar. J.* 10:1. doi: 10.1186/1475-2875-10-314
- Mueller, I., Galinski, M. R., Baird, J. K., Carlton, J. M., Kochar, D. K., Alonso, P. L., et al. (2009). Key gaps in the knowledge of *Plasmodium vivax*, a neglected human malaria parasite. *Lancet Infect. Dis.* 9, 555–566. doi: 10.1016/S1473-3099(09)70177-X
- Nielsen, M., and Lund, O. (2009). NN-align. An artificial neural network-based alignment algorithm for MHC class II peptide binding prediction. *BMC Bioinformatics* 10:296. doi: 10.1186/1471-2105-10-296
- Ocampo, M., Urquiza, M., Guzmán, F., Rodríguez, L.E., Suarez, J., Curtidor, H., et al. (2000). Two MSA 2 peptides that bind to human red blood cells are relevant to *Plasmodium falciparum* merozoite invasion. *Chem. Biol. Drug Design* 55, 216–223. doi: 10.1034/j.1399-3011.2000.00174.x
- Ocampo, M., Vera, R., Eduardo Rodríguez, L., Curtidor, H., Urquiza, M., Suarez, J., et al. (2002). *Plasmodium vivax* Duffy binding protein peptides specifically bind to reticulocytes. *Peptides* 23, 13–22. doi: 10.1016/S0196-9781(01)00574-5
- Panda, S. K., and Mahapatra, R. K. (2017). *In-silico* screening, identification and validation of a novel vaccine candidate in the fight against *Plasmodium falciparum*. *Parasitol. Res.* 116, 1293–1305. doi: 10.1007/s00436-017-5408-z
- Parra, M., Hui, G., Johnson, A. H., Berzofsky, J. A., Roberts, T., Quakyi, I. A., et al. (2000). Characterization of conserved T- and B-cell epitopes in *Plasmodium falciparum* major merozoite surface protein 1. *Infect. Immun.* 68, 2685–2691. doi: 10.1128/IAI.68.5.2685-2691.2000
- Patarroyo, M. A., Bermúdez, A., López, C., Yepes, G., and Patarroyo, M. E. (2010). 3D analysis of the TCR/pMHCII complex formation in monkeys vaccinated with the first peptide inducing sterilizing immunity against human malaria. *PLoS ONE* 5:e9771. doi: 10.1371/journal.pone.0009771
- Patarroyo, M. E., Bermúdez, A., and Patarroyo, M. A. (2011). Structural and immunological principles leading to chemically synthesized, multiantigenic, multistage, minimal subunit-based vaccine development. *Chem. Rev.* 111, 3459–3507. doi: 10.1021/cr100223m
- PAHO/WHO (2017). *Epidemiological Alert Increase in Cases of Malaria*. The Pan American Health Organization [Online]. Available online at: <http://www.paho.org>
- Racanelli, V., Brunetti, C., De Re, V., Caggiari, L., De Zorzi, M., Leone, P., et al. (2011). Antibody Vh repertoire differences between resolving and chronically evolving hepatitis C virus infections. *PLoS ONE* 6:e25606. doi: 10.1371/journal.pone.0025606
- Rénia, L., and Goh, Y. S. (2016). Malaria parasites: the great escape. *Front. Immunol.* 7:463. doi: 10.3389/fimmu.2016.00463
- Rieckmann, K., Davis, D., and Hutton, D. (1989). *Plasmodium vivax* resistance to chloroquine? *Lancet* 334, 1183–1184.
- Rodrigues-Da-Silva, R. N., Soares, I. F., Lopez-Camacho, C., Martins Da Silva, J. H., Perce-Da-Silva, D. S., Têva, A., et al. (2017). *Plasmodium vivax* cell-traversal protein for ookinets and sporozoites: naturally acquired humoral immune response and B-cell epitope mapping in Brazilian amazon inhabitants. *Front. Immunol.* 8:77. doi: 10.3389/fimmu.2017.00077
- Rodríguez, L. E., Curtidor, H., Urquiza, M., Cifuentes, G., Reyes, C., and Patarroyo, M. E. (2008). Intimate molecular interactions of *P. falciparum* merozoite proteins involved in invasion of red blood cells and their implications for vaccine design. *Chem. Rev.* 108, 3656–3705. doi: 10.1021/cr068407v
- Rodríguez, L. E., Urquiza, M., Ocampo, M., Curtidor, H., Suárez, J., García, J., et al. (2002). *Plasmodium vivax* MSP-1 peptides have high specific binding activity to human reticulocytes. *Vaccine* 20, 1331–1339. doi: 10.1016/S0264-410X(01)00472-8
- Saravia, C., Martínez, P., Granados, D. S., Lopez, C., Reyes, C., and Patarroyo, M. A. (2008). Identification and evaluation of universal epitopes in *Plasmodium vivax* Duffy binding protein. *Biochem. Biophys. Res. Commun.* 377, 1279–1283. doi: 10.1016/j.bbrc.2008.10.153
- Sette, A., and Rappuoli, R. (2010). Reverse vaccinology: developing vaccines in the era of genomics. *Immunity* 33, 530–541. doi: 10.1016/j.immuni.2010.09.017
- Silva-Flannery, L. M., Cabrera-Mora, M., Dickherber, M., and Moreno, A. (2009). Polymeric linear peptide chimeric vaccine-induced antimalaria immunity is associated with enhanced *in vitro* antigen loading. *Infect. Immun.* 77, 1798–1806. doi: 10.1128/IAI.00470-08
- Soares, I. S., Da Cunha, M. G., Silva, M. N., Souza, J. M., Del Portillo, H. A., and Rodrigues, M. M. (1999). Longevity of naturally acquired antibody responses to the N- and C-terminal regions of *Plasmodium vivax* merozoite surface protein 1. *Am. J. Trop. Med. Hyg.* 60, 357–363. doi: 10.4269/ajtmh.1999.60.357
- Solihah, B., Winarko, E., Hartati, S., and Wibowo, M. E. (2017). “A systematic review: B-cell conformational epitope prediction from epitope characteristics view,” in *2017 3rd International Conference on Science and Technology-Computer (ICST)* (Yogyakarta: IEEE), 93–98.
- Sortica, V. A., Cunha, M. G., Ohnishi, M. D., Souza, J. M., Ribeiro-Dos-Santos, Â. K., Santos, S. E., et al. (2014). Role of IL6, IL12B and VDR gene polymorphisms in *Plasmodium vivax* malaria severity, parasitemia and gametocytemia levels in an Amazonian Brazilian population. *Cytokine* 65, 42–47. doi: 10.1016/j.cyto.2013.09.014
- Srinivasan, P., Baldeviano, G. C., Miura, K., Diouf, A., Ventocilla, J. A., Leiva, K. P., et al. (2017). A malaria vaccine protects Aotus monkeys

- against virulent *Plasmodium falciparum* infection. *NPJ Vaccines* 2:14. doi: 10.1038/s41541-017-0015-7
- Srinivasan, P., Beatty, W. L., Diouf, A., Herrera, R., Ambroggio, X., Moch, J. K., et al. (2011). Binding of Plasmodium merozoite proteins RON2 and AMA1 triggers commitment to invasion. *Proc. Natl. Acad. Sci. U.S.A.* 108, 13275–13280. doi: 10.1073/pnas.1110303108
- Stern, L. J., and Calvo-Calle, J. M. (2009). HLA-DR: molecular insights and vaccine design. *Curr. Pharmaceut. Design* 15, 3249–3261. doi: 10.2174/138161209789105171
- Stevenson, M. M., and Riley, E. M. (2004). Innate immunity to malaria. *Nat. Rev. Immunol.* 4, 169–180. doi: 10.1038/nri1311
- Storti-Melo, L. M., Da Costa, D. R., Souza-Neiras, W. C., Cassiano, G. C., Couto, V. S., Póvoa, M. M., et al. (2012). Influence of HLA-DRB-1 alleles on the production of antibody against CSP, MSP-1, AMA-1, and DBP in Brazilian individuals naturally infected with *Plasmodium vivax*. *Acta Trop.* 121, 152–155. doi: 10.1016/j.actatropica.2011.10.009
- Sturniolo, T., Bono, E., Ding, J., Radrizzani, L., Tuereci, O., Sahin, U., et al. (1999). Generation of tissue-specific and promiscuous HLA ligand databases using DNA microarrays and virtual HLA class II matrices. *Nat. Biotechnol.* 17, 555–561. doi: 10.1038/9858
- Trachtenberg, E., Keyeux, G., Bernal, J., Rhodas, M., and Erlich, H. (1996). Results of expedition humana. *HLA* 48, 174–181. doi: 10.1111/j.1399-0039.1996.tb02625.x
- Tubo, N. J., Pagán, A. J., Taylor, J. J., Nelson, R. W., Linehan, J. L., Ertelt, J. M., et al. (2013). Single naive CD4+ T cells from a diverse repertoire produce different effector cell types during infection. *Cell* 153, 785–796. doi: 10.1016/j.cell.2013.04.007
- Tyler, J. S., Treeck, M., and Boothroyd, J. C. (2011). Focus on the ringleader: the role of AMA1 in apicomplexan invasion and replication. *Trends Parasitol.* 27, 410–420. doi: 10.1016/j.pt.2011.04.002
- Udomsangpet, R., Kaneko, O., Chotivanich, K., and Sattabongkot, J. (2008). Cultivation of plasmodium vivax. *Trends Parasitol.* 24, 85–88. doi: 10.1016/j.pt.2007.09.010
- Urquiza, M., Patarroyo, M. A., MariV., Ocampo, M., Suarez, J., Lopez, R. et al. (2002). Identification and polymorphism of *Plasmodium vivax* RBP-1 peptides which bind specifically to reticulocytes. *Peptides* 23, 2265–2277. doi: 10.1016/S0196-9781(02)00267-X
- Van Loveren, H., Van Amsterdam, J. G., Vandebriel, R. J., Kimman, T. G., Rümke, H. C., Steerenberg, P. S., et al. (2001). Vaccine-induced antibody responses as parameters of the influence of endogenous and environmental factors. *Environ. Health Perspect.* 109, 757–764. doi: 10.1289/ehp.01109757
- Vargas, L. E., Parra, C. A., Salazar, L. M., Guzmán, F., Pinto, M., and Patarroyo, M. E. (2003). MHC allele-specific binding of a malaria peptide makes it become promiscuous on fitting a glycine residue into pocket 6. *Biochem. Biophys. Res. Commun.* 307, 148–156. doi: 10.1016/S0006-291X(03)01129-X
- Villard, V., Agak, G. W., Frank, G., Jafarshad, A., Servis, C., Nébié, I., et al. (2007). Rapid identification of malaria vaccine candidates based on alpha-helical coiled coil protein motif. *PLoS ONE* 2:e645. doi: 10.1371/journal.pone.0000645
- Vulliez-Le Normand, B., Saul, F. A., Hoos, S., Faber, B. W., and Bentley, G. A. (2017). Cross-reactivity between apical membrane antigen 1 and rhoptry neck protein 2 in *P. vivax* and *P. falciparum*: a structural and binding study. *PLoS ONE* 12:e0183198. doi: 10.1371/journal.pone.0183198
- Wang, P., Sidney, J., Kim, Y., Sette, A., Lund, O., Nielsen, M., et al. (2010). Peptide binding predictions for HLA DR, DP and DQ molecules. *BMC Bioinformatics* 11:568. doi: 10.1186/1471-2105-11-568
- WHO (2016). *World Malaria Report 2016*. Geneva: World Health Organization.
- Wipasa, J., Elliott, S., Xu, H., and Good, M. F. (2002). Immunity to asexual blood stage malaria and vaccine approaches. *Immunol. Cell Biol.* 80, 401–414. doi: 10.1046/j.1440-1711.2002.01107.x
- Yuseff, M.-I., Pierobon, P., Reversat, A., and Lennon-Duménil, A.-M. (2013). How B cells capture, process and present antigens: a crucial role for cell polarity. *Nat. Rev. Immunol.* 13, 475–486. doi: 10.1038/nri3469
- Zeeshan, M., Tyagi, R. K., Tyagi, K., Alam, M. S., and Sharma, Y. D. (2014). Host-parasite interaction: selective Pv-fam-a family proteins of *Plasmodium vivax* bind to a restricted number of human erythrocyte receptors. *J. Infect. Dis.* 211, 1111–1120. doi: 10.1093/infdis/jiu558
- Zhang, L., Chen, Y., Wong, H.-S., Zhou, S., Mamitsuka, H., and Zhu, S. (2012). TEPITOPEpan: extending TEPITOPE for peptide binding prediction covering over 700 HLA-DR molecules. *PLoS ONE* 7:e30483. doi: 10.1371/journal.pone.0030483

Conflict of Interest Statement: The authors declare that the research was conducted in the absence of any commercial or financial relationships that could be construed as a potential conflict of interest.

Copyright © 2018 López, Yepes-Pérez, Díaz-Arévalo, Patarroyo and Patarroyo. This is an open-access article distributed under the terms of the Creative Commons Attribution License (CC BY). The use, distribution or reproduction in other forums is permitted, provided the original author(s) and the copyright owner are credited and that the original publication in this journal is cited, in accordance with accepted academic practice. No use, distribution or reproduction is permitted which does not comply with these terms.



Chitosan Microsphere Used as an Effective System to Deliver a Linked Antigenic Peptides Vaccine Protect Mice Against Acute and Chronic Toxoplasmosis

Jingjing Guo[†], Xiahui Sun[†], Huiquan Yin, Ting Wang, Yan Li, Chunxue Zhou, Huaiyu Zhou, Shenyi He* and Hua Cong*

Department of Human Parasitology, Shandong University, School of Medicine, Jinan, China

OPEN ACCESS

Edited by:

Kamal El Bissati,
University of Chicago, United States

Reviewed by:

Fiona Luisa Henriquez,
University of the West of Scotland,
United Kingdom
Hetron Mweemba Munang'andu,
Norwegian University of Life Sciences,
Norway

*Correspondence:

Shenyi He
shenyihe@sdu.edu.cn
Hua Cong
conghua@sdu.edu.cn

[†]These authors have contributed
equally to this work.

Received: 24 January 2018

Accepted: 30 April 2018

Published: 23 May 2018

Citation:

Guo J, Sun X, Yin H, Wang T, Li Y, Zhou C, Zhou H, He S and Cong H (2018) Chitosan Microsphere Used as an Effective System to Deliver a Linked Antigenic Peptides Vaccine Protect Mice Against Acute and Chronic Toxoplasmosis. *Front. Cell. Infect. Microbiol.* 8:163. doi: 10.3389/fcimb.2018.00163

Multiple antigenic peptide (MAP) vaccines have advantages over traditional *Toxoplasma gondii* vaccines, but are more susceptible to enzymatic degradation. As an effective delivery system, chitosan microspheres (CS) can overcome this obstacle and act as a natural adjuvant to promote T helper 1 (Th1) cellular immune responses. In this study, we use chitosan microparticles to deliver multiple antigenic epitopes from GRA10 (G10E), containing three dominant epitopes. When G10E was entrapped within chitosan microparticles (G10E-CS), adequate peptides for eliciting immune response were loaded in the microsphere core and this complex released G10E peptides stably. The efficiency of G10E-CS was detected both *in vitro*, via cell culture, and through *in vivo* mouse immunization. *In vitro*, G10E-CS activated Dendritic Cells (DC) and T lymphocytes by upregulating the secretion of costimulatory molecules (CD40 and CD86). *In vivo*, Th1 biased cellular and humoral immune responses were activated in mice vaccinated with G10E-CS, accompanied by significantly increased production of IFN- γ , IL-2, and IgG, and decreases in IL-4, IL-10, and IgG1. Immunization with G10E-CS conferred significant protection with prolonged survival in mice model of acute toxoplasmosis and statistically significant decreases in cyst burden in murine chronic toxoplasmosis. The results from this study indicate that chitosan microspheres used as an effective system to deliver a linked antigenic peptides is a promising strategy for the development of efficient vaccine against *T. gondii*.

Keywords: *Toxoplasma gondii*, chitosan microspheres, peptides, epitopes, vaccine

INTRODUCTION

Toxoplasma gondii is an important medical pathogen that infects approximately 30% of the global population. Generally, toxoplasmosis is asymptomatic in immune-competent hosts, however, it can result in severe symptoms in immunocompromised individuals due to cerebral cyst reactivation. Another potentially fatal presentation is vertical transmission in the fetus, which can result in encephalitis, neonatal malformations, or spontaneous abortion (Blader et al., 2015; Dimier-Poisson et al., 2015). Current drug treatment cannot control this disease completely because of the inability

of drugs to kill bradyzoites (Henriquez et al., 2010). Therefore, the advantages of a preemptive vaccine for preventing toxoplasmosis are obvious (Innes, 2010). Traditional vaccine development strategies against *T. gondii* mainly focused on subunit and DNA vaccines. Their use raises several issues, since subunit vaccines have poor stability and may cause undesired immune responses (Skwarczynski and Toth, 2014), and DNA vaccines have the theoretical risk of genomic integration into host cells (Kofler et al., 2004).

Peptide-based vaccines could overcome these weaknesses. They use minimal antigenic epitopes to induce desired immune responses, and are less likely to trigger allergic or autoimmune responses (Skwarczynski and Toth, 2016). In recent years, there has been increasing interest in the study of peptide-based vaccines (Dudek et al., 2010). *T. gondii* is an intracellular parasite with a complex life cycle, so synthetic multiple antigenic peptide (MAP) vaccines containing different epitopes may prove a highly efficacious strategy in the development of *T. gondii* vaccines (Henriquez et al., 2010).

Successful *T. gondii* infection requires active invasion and the formation of the parasitophorous vacuole (PV) (Braun et al., 2008). Dense granules are secretory organelles involved in maturation and modification of both the PV and its membrane (PVM) (Nam, 2009). Dense granule proteins (GRAs) are major components of the vacuole surrounding tachyzoites and encysted bradyzoites, and are related to host-parasite interactions and immune responses (Cesbron-Delauw and Capron, 1993). Dense granule protein 10 (GRA10) which is released into the PV shortly after invasion and then localizes to the PVM (Ahn et al., 2005), is essential for parasite growth with potential immunogenic capability. Researchers found that there is severe inhibition of *T. gondii* growth in human fibroblasts cells when GRA10 is knocked out (Witola et al., 2014). Of note, immunogenic peptides from GRA10 in a vaccine formulation have not been previously explored.

However, peptides are very susceptible to enzymatic degradation. Thus, a delivery system is needed to protect protease-sensitive epitopes from degradation (van Riet et al., 2014; Skwarczynski and Toth, 2016). Recently, microparticles as a delivery system to load antigens has emerged as one of the most promising strategies to induce a strong immune response (Kwon et al., 2005; Reddy et al., 2007). In this way, the peptides are delivered by microspheres, thereby inducing enhanced recognition by the immune system compared with naked easy degradation peptides (van der Lubben et al., 2001). Thus far, many types of microparticles have been tested, and chitosan has attracted particular interest. Chitosan is the deacetylated form of chitin, a naturally occurring and abundantly available biocompatible polysaccharide (Shrestha et al., 2014). Chitosan microspheres have many advantages over traditional vaccine microsphere formulations with starch, gelatin, or albumin. They are easy to load with peptides, thereby circumventing protein denaturation (Lin et al., 2013). Compared to other biodegradable polymers, chitosan is the only one that has a cationic (Bernkop-Schnürch and Dünnhaupt, 2012) and mucoadhesive character, increasing residual time at the site of absorption, therefore prolonging the release time of protein

antigens (Agnihotri et al., 2004). When chitosan degrades, the amino sugars produced are nontoxic and easily removable from the body without causing side reactions (Wang et al., 2016). More importantly, chitosan is a demonstrated natural adjuvant to promote dendritic cell (DC) activation and T helper 1 (Th1) cellular-associated immune responses via cGAS-STING signaling pathway (Carroll et al., 2016; Riteau and Sher, 2016). Collectively, as an attractive carrier and adjuvant, chitosan has been used extensively in vaccine applications (Islam and Ferro, 2016).

Herein, we present a novel attempt to combine highly immunogenic MAP from GRA10 with chitosan microspheres in the design of a vaccine against *T. gondii*. In this study, three dominant epitopes from GRA10 were screened from nine potential epitopes and were used to synthesize the MAP of GRA10 (G10E). The release efficiency of these chitosan microparticles containing the MAP of GRA10 (G10E-CS) was detected in terms of peptide loading and releasing efficiency. As an adjuvant, the capacity of chitosan to activate dendritic cells and T lymphocytes was tested *in vitro*. Furthermore, the protective effect of G10E-CS vaccination on acute and chronic toxoplasmosis murine models was evaluated. This study aims to make a contribution to peptides vaccines against *T. gondii* by exploring chitosan microspheres, an effective delivery system, to enhance MAP vaccine immunogenicity.

MATERIALS AND METHODS

Animals

Female 6–8-weeks-old BALB/c and C57BL/6 mice were purchased from Shandong University Laboratory Animal Centre (Jinan, China) and housed in SPF conditions. All the mice were housed 5 per cage under pathogen-free conditions and were adequately supplied with sterilized water and food.

Ethical Approval

Experiments were carried out in accordance with animal ethics approved by the Institutional Animal Care and Use Committee of Shandong University under Contract LL201602044. Humane endpoints were chosen to terminate the pain or distress of experimental animals via euthanasia.

Parasite

Tachyzoites of the high-virulence RH strain (type I) (Howe and Sibley, 1995) of *T. gondii* were propagated in human foreskin fibroblast (HFF) cells in Dulbecco's modified Eagle's medium (DMEM) (Sigma-Aldrich, USA) supplemented with 10% fetal bovine serum (FBS) (Clark Biosciences, USA) as previously described (Shen and Sibley, 2014). Pru (Prugniald) strain (type II), a low-virulence strain of *T. gondii*, (Saeij et al., 2005) was a kind gift from Professor Xingquan Zhu at Lanzhou Veterinary Research Institute, China. The cysts of the type II Pru strain were maintained in Kunming mice by oral passage of infectious cysts in mice as previously described (Zhou et al., 2016).

Screening of Candidate Epitopes From GRA10

The PROTEAN subroutine in the DNASTAR software package was used to predict the B cell epitopes of GRA10 (TGME49_268900, ToxoDB) as described previously (Wang et al., 2014). Three B cell candidate epitopes, GRA10_{192–215} (P1), GRA10_{221–244} (P2), and GRA10_{310–332} (P3), were selected with good hydrophilicity, high conformational flexibility, surface accessibility and strong antigenicity.

To predict the CD8⁺ and CD4⁺ T cell epitopes of GRA10, the complete amino acid sequence of the protein was analyzed using consensus algorithms available at the Immune Epitope Database and Analysis Resource (IEDB, <http://www.iedb.org/>) as described previously (Cong et al., 2010). GRA10_{49–57} (P4), GRA10_{161–169} (P5), and GRA10_{300–308} (P6) were chosen based on their predicted binding affinity to MHC I supertype molecules (those with a percentile rank lower than 10 were selected; Moutafsi et al., 2006). GRA10_{80–94} (P7), GRA10_{170–184} (P8), and GRA10_{180–194} (P9) were chosen based on their predicted binding affinity to MHC II (Wang et al., 2008). The peptides (P1–P9) sequences are shown in **Table 1** and were synthesized (>95% purity) by Synpeptide Co., Ltd. (Shanghai, China) and stored at –80°C.

ELISA analysis of serum samples from *T. gondii* infected mice was used to screen three GRA10 B cell epitopes as previously described (Cardona et al., 2009). IgG OD value was recorded as the absorbance at 450 nm detected by a Thermo Scientific Multiskan FC Microplate Photometer (Thermo Scientific, USA). Meanwhile, lymphocyte proliferation assays of infected mice were used to screen GRA10 CD8⁺ T cell epitopes and CD4⁺ T cell epitopes as previously described (Wallace et al., 2008).

Construction of Multiple Antigenic Peptide (MAP) of GRA10 (G10E)

T. gondii GRA10 MAP (G10E) was designed by linking the selected epitopes with the spacer sequence Gly-Ser (**Figure 1**) and

TABLE 1 | Candidates of B cell or T cell epitopes predicted from GRA10 of *T. gondii*.

Type	Epitope	Sequence
B cell epitope ^a	GRA10 _{192–215}	TQSPPESSRKRRRSGKKRGKRVS(P1)
	GRA10 _{221–244}	GSGLTPSDEPVDGCDRVREEAERE(P2)
	GRA10 _{310–332}	GDKNDTDTTQNKDTGSTQSQRAN(P3)
CD8 ⁺ T cell epitope ^b	GRA10 _{49–57}	LPKKGVPVG(P4)
	GRA10 _{161–169}	LGYCALLPL(P5)
	GRA10 _{300–308}	VPPVLKISR(P6)
CD4 ⁺ T cell epitope ^c	GRA10 _{80–94}	SGFSLSSGSGSVWE(P7)
	GRA10 _{170–184}	LTEEQFRHRRRLQKR(P8)
	GRA10 _{180–194}	RLQKRAMVLCGYTQS(P9)

^aThree B cell candidate epitopes, GRA10_{192–215} (P1), GRA10_{221–244} (P2), and GRA10_{310–332} (P3) with good hydrophilicity, high conformational flexibility, surface accessibility and strong antigenicity, were selected via DNASTAR software.

^{b,c}CD8⁺ and CD4⁺ T cell epitopes of GRA10 were analyzed using consensus algorithms available at the Immune Epitope Database and Analysis Resource (IEDB, <http://www.iedb.org/>).

then synthesized by Synpeptide Co., Ltd. (Shanghai, China) and stored at –80°C.

Preparation of Chitosan Microspheres Loaded With G10E (G10E-CS)

Chitosan microspheres loaded with G10E were prepared by emulsion crosslinking method as previously described (Jose et al., 2013; Pichayakorn and Boonme, 2013) with minor modifications. Briefly, chitosan solution (3% w/w) was prepared by dissolving chitosan in 2% aqueous glacial acetic acid as aqueous phase. G10E peptides were mixed in this solution. Oil phase was paraffin oil containing 5% Span80. The aqueous phase was gradually added into the oil phase and continuously mixed at 1,000 rpm for 2 h to form water-in-oil (w/o) emulsion. Subsequently, genipin was added into the mixture and mixed further for 2 h. The obtained microspheres were then separated by centrifugation at 3,000 rpm and the sediment was washed thrice with petroleum ether, isopropanol and deionized water and finally dried using a freeze dryer (CHRIST ALPHA 1-4 LSC, Germany) (**Figure 1**).

G10E-CS microspheres were characterized for morphological shape by a scanning electron microscope (JSM6610LV SEM, JEOL Ltd., Japan) as previously described (Wang et al., 2005). The samples were dusted on an adhesive carbon tape and coated with a thin layer of gold. Samples were then imaged at magnification of 15,000. The particle size and zeta potential of chitosan microspheres was determined by dynamic light scattering on a Zetasizer NanoZS (Malvern, UK). Measurements were carried out in triplicate.

Loading Capacity and Encapsulation Efficiency

1–5 mg/ml G10E peptides were mixed with 3% (w/v) chitosan microspheres and crosslinked by genipin as above described. The suspension was centrifuged (3,000 rpm for 30 min) to collect the supernatant. Then, the non-bound G10E concentration in the supernatant was determined by Protein Quantitative Reagent Kit-BCA Method (Beyotime, China) (Wang et al., 2016). Loading capacity (LC) and encapsulation efficiency (EE) in chitosan microspheres were determined by applying the following equations:

$$\text{Loading capacity (\%LC)} = \frac{(\text{total amount G10E}) - (\text{free G10E})}{\text{weight of microparticles}} \times 100\%$$

$$\text{Encapsulation efficiency (\%EE)} = \frac{(\text{total amount G10E}) - (\text{free G10E})}{\text{total G10E}} \times 100\%$$

Evaluation of Release Characteristics of G10E in Vitro

G10E release from chitosan microparticles *in vitro* was determined in PBS (pH 7.4) as previously described (Skop et al., 2013) with minor modifications. Genipin-crosslinked G10E-CS microspheres and G10E peptides were dispersed in PBS (pH 7.4) at 37°C under mild shaking (100 rpm). At specific time

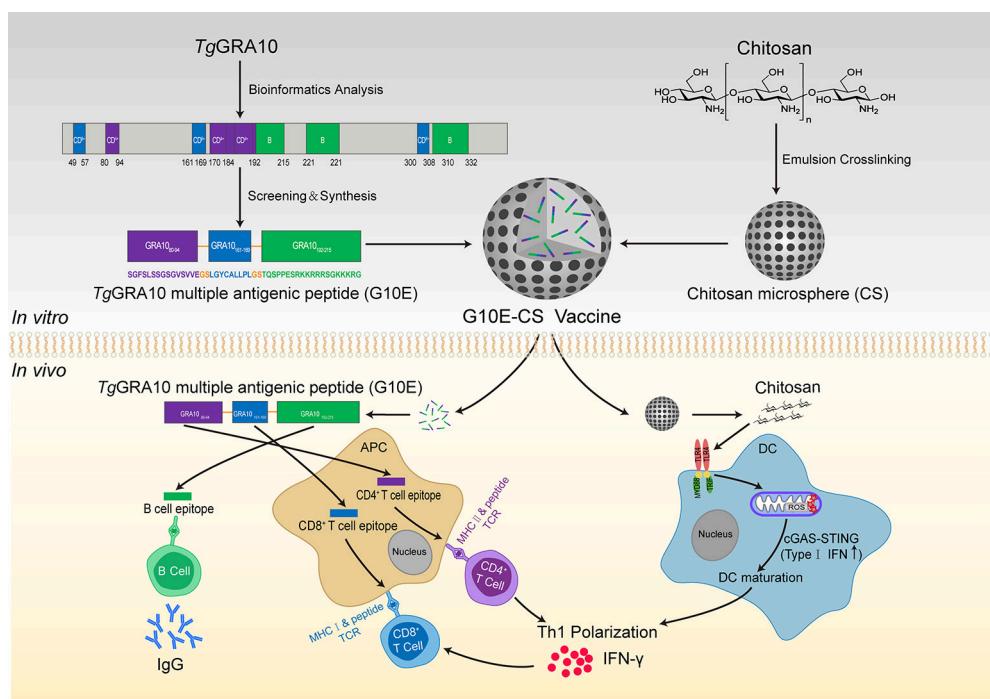


FIGURE 1 | Construction of *T. gondii* G10E-CS vaccine and potential immune mechanism involved in vaccination with G10E-CS *in vivo*. In this study, dominant B cell, CD8⁺ and CD4⁺ T cell epitopes from GRA10 protein of *T. gondii* were selected by bioinformatics and immunological analysis. Then the G10E-CS microsphere vaccine formed by three dominant epitopes and linked by sequence GS was loaded onto chitosan microspheres by emulsion cross-linking method. When BALB/c mice were immunized with G10E-CS, the G10E peptides released from the microspheres induced specific humoral and cellular response. At the same time, chitosan as an attractive adjuvant could induce activation of dendritic cells (DCs) via cGAS-STING signaling pathway and then promote T helper 1 (Th1) cellular immune responses.

intervals, 250 μ l of the supernatant containing the released G10E was taken by centrifugation and stored at -20°C in tubes. The chitosan microspheres that settled at the bottom of the tube were resuspended in PBS (pH 7.4) after each collection. After the last time point, the protein concentration of all the collected G10E was analyzed using the Protein Quantitative Reagent Kit-BCA Method.

The degradation of released G10E was analyzed by gel electrophoresis. Briefly, G10E-CS microspheres were dispersed in PBS (pH 7.4) using a shaking air bath (37°C , 100 rpm) for 15 d. After centrifuging (5,000 rpm, 20 min), the microsphere precipitate at the bottom of the tube was collected to be analyzed by gel electrophoresis.

The Expression of Costimulatory Molecules on the Surface of Stimulated Dendritic Cells

Bone-marrow derived dendritic cells (DCs) were prepared as previously described (Molavi et al., 2010). Briefly, C57BL/6 mice were euthanized, intact femurs were removed, and purified of surrounding muscle tissue. The bones were washed with sterile PBS, the bone marrow cells were harvested by repeated flushing with RPMI 1640 using a syringe with a 0.45 mm diameter needle. To derive conventional DCs, bone marrow cells (2×10^6 cells/ml) were cultured for 7 days in 6-well plate (Corning Inc.,

USA) in RPMI 1640 medium (Hyclone, USA) supplemented with 10% FBS (Hyclone, USA), 50 μM penicillin and streptomycin, and 20 ng/ml GM-CSF and IL-4 (Sigma-Aldrich, USA). Half of the medium was replaced with fresh complete medium on day 3 and 5. At day 7, non-adherent cells were harvested and ready for use as mature DCs.

To analyse costimulatory molecule expression, dendritic cells (2×10^6 cells/ml) were seeded in 96-well plate (Corning Inc., USA) in the same medium as described above (including GM-CSF and IL-4) and cultured with CpG (4 $\mu\text{g}/\text{mL}$), CS, G10E or G10E-CS (10 $\mu\text{g}/\text{mL}$ each) for 48 h. CpG, a TLR agonist that generally enhances CD40 and CD86 surface expression, served as a positive control. Cell suspension was subsequently stained with 0.3 $\mu\text{g}/\text{mL}$ of anti-CD11c, 1.25 $\mu\text{g}/\text{mL}$ of anti-CD86 and 2.5 $\mu\text{g}/\text{mL}$ of anti-CD40 antibody (BD Biosciences, USA) (Carroll et al., 2016). Samples were detected by Cytotflex S Flow Cytometer (Beckman Coulter, USA) and the data were analyzed by CytExpert software.

Activation of Dendritic Cells and Lymphocyte *in Vitro* Induced by G10E-CS Microspheres

Dendritic cells (DCs) were plated at 2×10^5 cells per well and stimulated as described above. At the same time, lymphocytes isolated from the spleen of C57BL/6 mice were plated in 96-well

plates, at a density of 2×10^6 cells/ml, in 100 μ L RPMI-1640 medium supplemented with 10% FBS, 50 μ M penicillin and streptomycin. Then, induced DCs were cocultured with these T cells (1:10 ratio) for 72 h (Höpken et al., 2005), and lymphocyte proliferation was measured by CCK-8 assay. In the meantime, supernatants of mixed cells were assayed for IL-2 and IFN- γ using a commercial ELISA Kit (R&D Systems, USA) following the procedure recommended by the manufacturer.

Cytotoxicity of G10E-CS Microspheres

The cytotoxicity of the G10E-CS microspheres *in vitro* was evaluated by CCK-8 assay (Dojindo, Japan) conducted on the aforementioned dendritic cells (DCs) and T lymphocytes as previously described (Shrestha et al., 2014). Briefly, these cells were added to 96-well plates of 2×10^6 cells/ml at 100 μ L per well and incubated overnight. The culture medium was then replaced by serum-free medium with different concentrations (125, 250 μ g/mL and 500 μ g/mL) of G10E-CS microspheres and incubated for 48 and 72 h at 37°C. Ten micro liters CCK-8 was added to the wells and the absorbance of the solution was measured at 450 nm in a Thermo Scientific Multiskan FC Microplate Photometer (Thermo Scientific, USA). Cell viability (%) was defined as the OD ratio in test group relative to controls. All experiments were carried out five times.

Immunization and Challenge Infection in Mice

BALB/c mice were randomly divided into four groups ($n = 23$ per group) and were immunized thrice via intramuscular injection at 2-week intervals with G10E (100 μ g), G10E-CS microspheres containing 100 μ g of G10E (667 μ g) (LC = 15%) or empty CS microsphere (667 μ g) (Zhou et al., 2007; Jose et al., 2012). Mice that received 100 μ L PBS were used as non-immunized control.

Two weeks after the last immunization, the protection of G10E-CS microspheres against acute and chronic *T. gondii* infection was investigated as previously described (Wang J. L. et al., 2017). Ten mice per immunized group were infected intraperitoneally with a lethal dose of RH strain (1×10^3 tachyzoites). The challenged mice were monitored over a period of 21 days and observed daily for mortality.

At the same time, 10 mice per group were challenged orally with a sublethal dose of cysts (30 cysts) of the PRU strain (type II) to evaluate the effect of vaccination in mice with chronic toxoplasmosis. All surviving mice were euthanized at 45 days after challenge. Brains were collected and homogenized in 1 ml PBS. The number of cysts per brain was confirmed by counting eight 10 μ L samples of each cerebral homogenate under an optical microscope.

Detection of Total IgG and Antibody Isotypes in Vaccinated Mice

Serum samples were collected from the mice by retro-orbital bleeding at 0, 2, 4, and 6 weeks after immunization. Standard ELISA assay was used to determine the levels of *T. gondii*-specific IgG, IgG1 and IgG2a antibodies in the serum samples as previously described (Tang et al., 2016). Briefly, 96-well plates were coated with the 100 μ L (10 μ g/mL) G10E peptides in 50 mM carbonate-bicarbonate buffer (pH 9.6) and were incubated at

4°C overnight. After washing three times with PBS plus 0.05% Tween 20 (PBST), the coated plates were blocked with 1% low fat milk in PBST for 1 h at 37°C. The mouse serum was diluted in PBS (1:25) and incubated at 37°C for 1 h. Then plates were washed, and anti-mouse-IgG, IgG1 or IgG2a HRP-conjugated antibodies (Sigma-Aldrich, USA) were added to each well. Peroxidase activity was revealed by 10 mg/ml 3, 3', 5, 5'-tetramethylbenzidine (TMB, Sigma-Aldrich, USA) and stopped by adding 50 μ L of 2 M H₂SO₄. The results were recorded as the absorbance at 450 nm and detected by a Thermo Scientific Multiskan FC Microplate Photometer (Thermo Scientific, USA). For each serum sample the assay was done in triplicate and average values were calculated.

Lymphocyte Proliferation Assay

Two weeks after the last immunization, three mice per group were euthanized to obtain single splenocyte suspensions as described previously (Luo et al., 2017). After erythrocytes were lysed, the splenocytes were adjusted to a concentration of 2×10^6 cells/ml in RPMI-1640 medium with 10% FBS and plated in 96-well plates in presence of the G10E peptides (10 μ g/mL). Plates were incubated for 72 h at 37°C. Lymphocyte proliferative activity was measured by a Cell Counting Kit-8 (CCK-8, Dojindo; Japan) according to manufacturer's instructions. The absorbance was detected at 450 nm and the stimulation index (SI) was calculated.

Flow Cytometry Analysis of T Cell Subsets and Cytokine Production

The percentages of CD4⁺ and CD8⁺ T lymphocytes subsets and the production of cytokine in the splenocytes of immunized mice were determined using flow cytometry techniques as described previously (Zhang et al., 2015b; Wang S. et al., 2017). Briefly, splenocytes (2×10^6 cells/ml) of vaccinated mice were stimulated with G10E peptides (10 μ g/mL) for 72 h. Then the suspensions were stained with anti-mouse CD3-APC, anti-mouse CD4-FITC and anti-mouse CD8-PE (eBiosciences, USA) for 30 min at 4°C in the dark.

Splenocytes (2×10^6 cells/ml) were also stimulated with G10E peptides for 72 h in the presence of Cell Stimulation Cocktail (eBiosciences, USA) containing Phorbol myristate acetate (PMA, 20 ng/ml), Ionomycin (2 μ g/ml), Brefeldin A (1 μ g/ml), and Monensin (1 μ g/ml) to inhibit the secretion of cytokine into the extracellular space. The cells were fixed using an Intracellular Fixation & Permeabilization Buffer Set Kit in accordance with the manufacturer's protocol (eBiosciences, USA) and then stained directly with anti-mouse CD4-FITC, anti-mouse CD8-PE, anti-mouse IL-2 (APC), anti-mouse IFN- γ (PerCP-Cyanine 5.5), anti-mouse IL-4 (APC), and anti-mouse IL-10 (PerCP-Cyanine 5.5) (eBiosciences, USA) for 30 min at 4°C. All these cell population were analyzed by Cytotflex S Flow Cytometer (Beckman Coulter, USA) and the data were analyzed by CytExpert software.

Statistical Analysis

Statistical analysis was carried out using SPSS19.0 (SPSS Inc., Chicago, IL, USA) and GraphPad Prism 7.0 (GraphPad Software Inc., San Diego, USA). Differences between groups were analyzed

using one-way ANOVA analysis. Student's *t*-test was used for comparison between levels of IgG1 and IgG2a isotypes. Survival percentage was analyzed by the Kaplan-Meier test and survival curves were compared using the Log-rank test. Data are expressed as means \pm SD. Values of *p* < 0.05 were considered statistically significant.

RESULTS

Epitopes Screened From TgGRA10 and Construction of Multiple Antigenic Peptide

The peptide sequences of candidate epitopes from GRA10 showing high affinity in the prediction algorithm in Table 1 were further tested in mice. The IgG test showed that all the B cell

epitopes from GRA10 could recognize the IgG in the serum of BALB/c mice infected by *T. gondii*, in which GRA10_{192–215} (P1) was demonstrated to induce highest level of IgG (Figure 2Aa). Lymphocyte proliferation testing showed that GRA10_{161–169} (P5) and GRA10_{80–94} (P7) stimulated the highest level of proliferation of lymphocytes in infected mice (Figure 2Ab).

Thus, GRA10_{192–215} (P1), GRA10_{161–169} (P5), and GRA10_{80–94} (P7) were chosen to construct the MAP G10E with linker GS (Figure 1). Mice immunized with P1(B cell epitope), P5(CD4⁺ T cell epitope), P7(CD8⁺ T cell epitope) or G10E were tested for B cell antibody level and T cell proliferation ability. The results showed that significant enhanced B cell and T cell immune responses were achieved in G10E vaccinated group (Figures 2Ba,b).

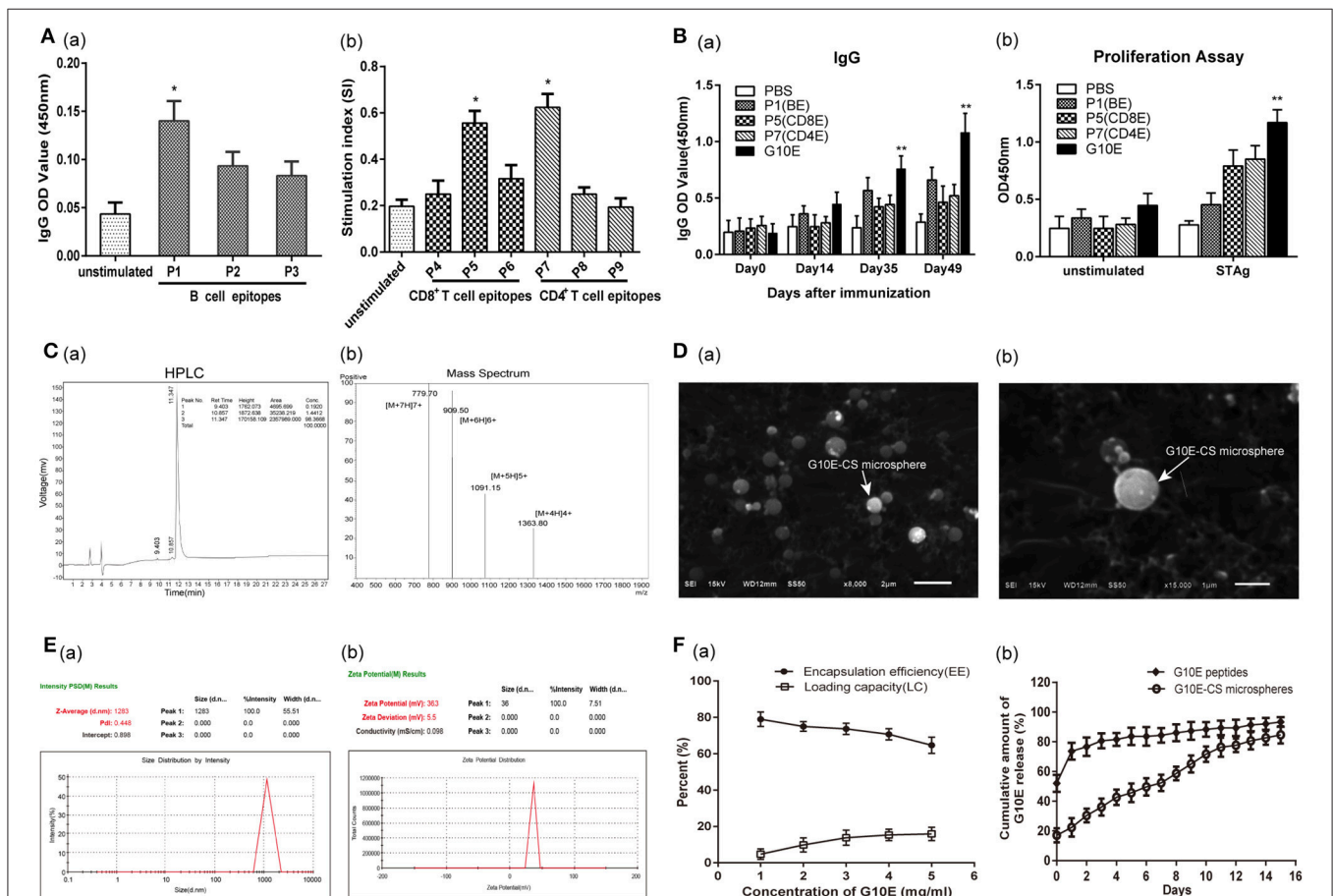


FIGURE 2 | Screening of dominant epitopes from GRA10 and characteristic of G10E-CS. **(A)** Screening of the dominant B cell epitopes **(a)** and T cell epitopes **(b)** from TgGRA10. Positive serum samples from *T. gondii* infected mice were used to screen dominant B cell epitopes by ELISA analysis. Lymphocyte proliferation test was used to identify dominant CD8⁺ T and CD4⁺ T cell epitopes from spleen cells of infected mice by CCK-8 assay. P1(TQSPSPESRKKRRRSRGKKRGRKRSV)(B cell epitope), P5(LGYCALLPL)(CD8⁺ T cell epitope) and P7(SGFSLSSGSGVSVVE)(CD4⁺ T cell epitope) were selected to construct the multiple antigenic peptide (MAP) of *T. gondii* GRA10 (G10E). Values represent mean \pm SD (*n* = 5). **p* < 0.05. **(B)** Immunogenicity of P1, P5, P7 and G10E peptides. Mice immunized with P1(B cell epitope), P5(CD4⁺ T cell epitope), P7(CD8⁺ T cell epitope) or G10E (P5-P7-P1) were tested for B cell antibody **(a)** and T cell proliferation ability **(b)**. ***p* < 0.01. **(C)** The purity of G10E peptides detected by high performance liquid chromatography (HPLC) **(a)** and the molecular weight of G10E peptides analyzed by electrospray ionization mass spectrometry (ESI-MS) **(b)**. **(D)** Scanning electron microscopy (SEM) images of G10E-CS microspheres prepared by emulsion crosslinking method. G10E-CS microspheres were then imaged at magnification of $\times 15,000$ (bar represents 1 μ m). **(E)** The diameter **(a)** and zeta of G10E-CS **(b)** microparticles was detected by Malvern particle size potentiometer. **(F)** Loading capacity (%LC) and encapsulation efficiency (%EE) of G10E-CS microspheres amongst 1–5 mg/ml concentration of total G10E peptides **(a)**. Release profile of G10E peptides from free G10E peptides and crosslinked chitosan microparticles (G10E-CS) *in vitro* over a 15-day period **(b)**. The amount of G10E in the supernatant was measured using BCA assay. Values represent mean \pm SD (*n* = 3).

Physical Characterization and Release of Chitosan Microspheres Loaded With G10E

Chitosan microspheres loaded with G10E peptides (G10E-CS) were prepared by emulsion cross-linking method. The purity of G10E was 98.4% detected by high performance liquid chromatography (HPLC) (Figure 2Ca), and its molecular weight was 5450.9 daltons, analyzed by electrospray ionization mass spectrometry (ESI-MS) (Figure 2Cb). The morphology of G10E-CS microspheres formed using 3% chitosan was spherical in shape with a smooth surface, as observed by scanning electron microscopy (SEM) (Figure 2D). The average diameter of G10E-CS microparticles was 1283 nm with the low dpi detected by Malvern particle size potentiometer, suggesting that G10E-CS were uniform in size (Figure 2Ea).

The zeta potential of the CS microspheres was positive 37.1 ± 5.2 mV while the G10E peptides was negative 31.7 ± 9.1 mV (Table S1). After loading G10E into chitosan microspheres, the G10E-CS's zeta potential were positive 36.0 ± 5.48 mV (Figure 2Eb). Size and zeta analysis of G10E-CS formulations confirmed that G10E was completely loaded into the core of the CS microspheres, and not simply adherent to their surfaces.

The loading capacity and encapsulation efficiency of the chitosan microparticles were analyzed. When the concentration of G10E reached 4 mg/ml, a high encapsulation efficiency (EE) of 71% was achieved, and the peptide loading was almost saturated (15.3%). Therefore, 4 mg/ml G10E peptides were selected as the optimal concentration (Figure 2Fa).

We further evaluated the release of the entrapped G10E peptides from the chitosan microparticles. The crosslinked G10E-CS microspheres showed the more favorable and steady release profile (Figure 2Fb). Only 22.4% of the total encapsulated G10E peptides were released within the first day and slowly released 2.4–6.9% peptides daily over the next 14 days. While G10E peptides released 80% in the first 2 days in the freedom style. This was further supported by PAGE and SDS-PAGE analysis of released G10E (Figure S1).

G10E-CS Microspheres Induce the Activation of Dendritic Cells and Lymphocyte *in Vitro*

In order to determine if chitosan can induce dendritic cells (DC) activation *in vitro*, the expression of the co-stimulatory molecules CD40 and CD86 was detected by flow cytometry in stimulated DCs. Dramatic upregulation of CD40 and CD86 in DCs was observed after incubation with G10E-CS, G10E, CS, CpG (positive control) compared to PBS groups ($p < 0.05$; Figure 3A). G10E-CS microspheres achieved the highest level of the co-stimulatory molecules in dendritic cells ($p < 0.01$).

We further confirmed that CD86 and CD40 could provide activate lymphocytes. Hence, we assessed T cell proliferation and cytokines levels in supernatant of C57BL/6 mice lymphocytes after coculture with the above stimulated DC cells *in vitro*. As shown in Figure 3B, stimulated DCs provided more efficient co-stimulation of T cell proliferation, especially for G10E-CS stimulated cells ($p < 0.01$).

Supernatants of lymphocytes cocultured with the DCs showed that the CpG, G10E-CS, G10E microparticles could induce substantial production of IFN- γ and IL-2 compared to other groups ($p < 0.05$). The level of IFN- γ induced by G10E-CS microspheres ($p < 0.01$) was particularly noteworthy (Figure 3C).

Further, we studied the cytotoxic activity and biocompatibility of G10E-CS. Using CCK-8 assay, the viability of dendritic cells and T cells was analyzed by exposing them to different concentrations of G10E-CS (125, 250, and 500 μ g/ml) for different incubation times (48 or 72 h). For DCs and lymphocytes, the results demonstrated that all the G10E-CS microspheres showed cell viabilities higher than 90% of the negative control (Figure 3D). Hence, G10E-CS microspheres were suggested to be safe for the mouse vaccine.

G10E-CS Induced Robust *T. gondii* Specific Humoral Immune Responses

Specific IgG in the sera of mice vaccinated intramuscularly with G10E-CS, G10E, CS, was measured every 2 weeks. A dramatically higher level of total IgG was observed in the sera of mice immunized with G10E-CS and G10E after the third immunization, in contrast to the other groups. G10E-CS immunized mice had the highest level of *T. gondii* specific IgG ($p < 0.05$) (Figure 4A).

Furthermore, the level of specific IgG1 and IgG2a sub-classes against G10E peptides was measured. As shown in Figure 4B, significant production of IgG2a and IgG1 was observed in the sera of mice immunized with G10E-CS ($p < 0.01$) compared with G10E group. These results indicated that mice immunized with G10E-CS microspheres generated Th1 polarize immune response with more IgG2a than IgG1.

G10E-CS Induced Robust *T. gondii* Specific Cellular Immune Response

Antigen-specific proliferative responses of lymphocytes from immunized mice were detected by CCK-8 2 weeks after the third immunization and represented by the SI value as illustrated in Figure 5A. The level of lymphocyte proliferation in the mice immunized with G10E-CS ($p < 0.01$) and G10E ($p < 0.05$) was significantly higher than those of other groups. This result indicated that the T lymphocytes proliferation of mice vaccinated with G10E-CS was successfully stimulated.

To determine CD8⁺ or CD4⁺ T cells numbers after vaccination, the percentages of CD4⁺ and CD8⁺ T lymphocytes subsets in the spleen of immunized mice were evaluated by flow cytometry analysis. As shown in Figures 5Ba,b, the percentages of CD8⁺ and CD4⁺ T cells were both increased in mice immunized with G10E-CS and G10E compared to other groups ($p < 0.05$). G10E-CS-immunized mice also had the highest ratio of CD8⁺/CD4⁺ ($p < 0.05$). G10E-CS microspheres, therefore, could elicit more activation of CD8⁺ and CD4⁺ T cells in immunized mice than other vaccine formulations.

The production of cytokines in splenocytes supernatants of immunized mice was evaluated by Flow Cytometry. Significantly higher levels of IFN- γ and IL-2 were secreted by lymphocytes of

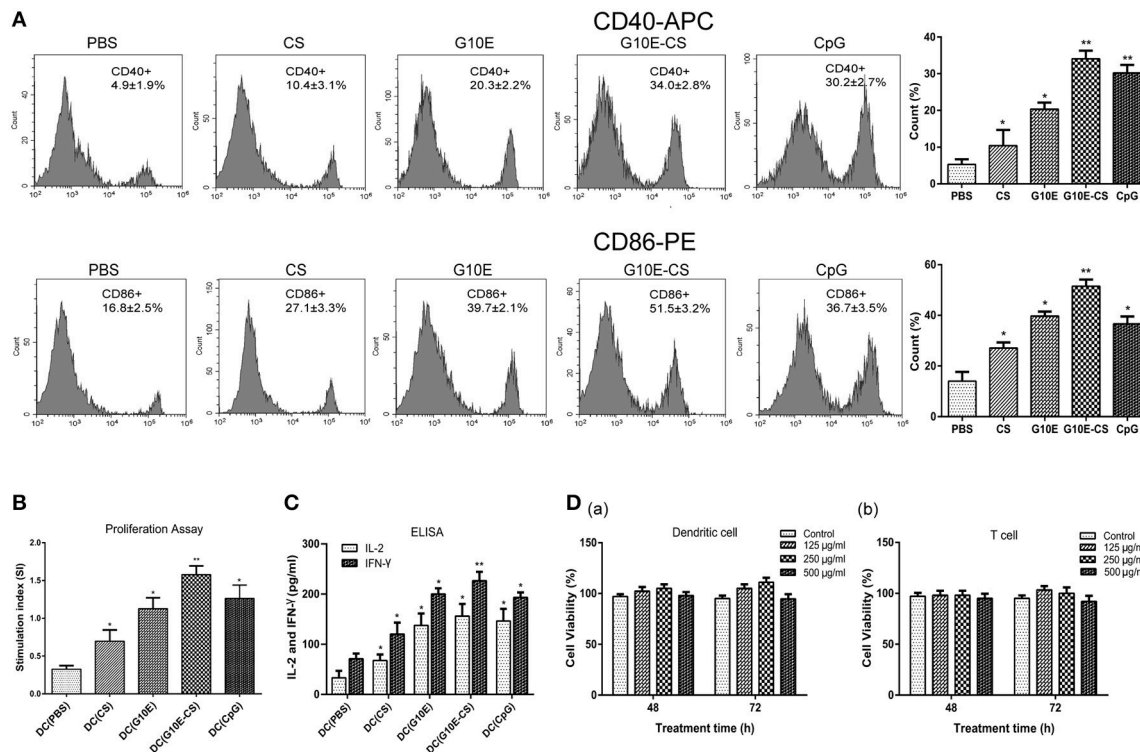


FIGURE 3 | G10E-CS induce the activation of dendritic cells and lymphocyte *in vitro*. **(A)** The expression of the co-stimulatory molecules CD40 and CD86 on the surface of stimulated dendritic cells (DCs). DCs of C57BL/6 mice were incubated with G10E-CS, G10E, CS, CpG, or PBS for 48 h and the expression of CD40 and CD86 were detected by flow cytometry. Values represent mean \pm SD ($n = 5$). * $p < 0.05$, ** $p < 0.01$. **(B)** The analysis of T lymphocyte proliferation induced by stimulated DC cells. DCs of C57BL/6 mice were incubated with CpG, G10E-CS, CS, G10E, or PBS for 48 h and then they were cocultured with lymphocyte from C57BL/6 mice for 72 h. The lymphocyte proliferation was measured by CCK-8 assay. **(C)** The expression of cytokines (IFN- γ , IL-2) in the supernatant of lymphocytes induced by the stimulated DC cells. The supernatants of mixed cells were assayed for IL-2 and IFN- γ using ELISA assay. Data represent mean \pm SD representative of three independent experiments. * $p < 0.05$, ** $p < 0.01$. **(D)** Cytotoxicity of G10E-CS microparticles on dendritic cells (DCs) **(a)** and T cells **(b)**. DCs and T cells were incubated with different concentrations (125, 250, and 500 μ g/ml) of G10E-CS microsphere for different incubation times (48 and 72 h) and cytotoxicity of G10E-CS was assessed by CCK-8 assay (mean \pm SD, $n = 5$).

the G10E-CS ($p < 0.01$) and G10E ($p < 0.05$) immunized mice compared to that of CS and PBS (Figures 5Ca,b). Interestingly, spleen cells from mice immunized with G10E-CS produced more IL-10 and IL-4 compared to other groups ($p < 0.05$; Figures 5Da,b).

G10E-CS Immunization Against Acute and Chronic Toxoplasmosis

In order to evaluate if G10E-CS could confer effective protection against *T. gondii* acute and chronic infection, immunized mice were challenged with RH tachyzoites, 10 mice per group were challenge with 1×10^3 RH tachyzoites 2 weeks after the last immunization. The survival curves of immunized mice challenged with 1×10^3 RH tachyzoites 2 weeks after the last immunization were illustrated in Figure 6A. All mice vaccinated with PBS, G10E, or CS succumbed within 10 days of infection. In contrast, a significantly prolonged survival time (21 days) was observed in mice vaccinated with G10E-CS microspheres compared to other groups ($p < 0.01$). While only 3 days survival extension when mice immunized with only G10E without CS (10 days) compared to control group ($p > 0.05$).

The efficacy of this vaccine formulation in the context of chronic infection with *T. gondii* was also evaluated by challenging the immunized mice with 30 cysts of the PRU strain orally. On day 45 post challenge, as shown in Figure 6B, G10E-CS immunized mice had fewer cysts (882 ± 194 cysts) in brain than G10E (1852 ± 245 cysts), CS (1966 ± 183 cysts) and PBS (2091 ± 215 cysts) treated mice ($p < 0.01$). This result suggests that the G10-CS microsphere vaccine could significantly reduce the cyst form in mice chronically infected with *T. gondii*.

DISCUSSION

In this study, we first screened and constructed a MAP encoding three dominant B, CD8 $^+$ and CD4 $^+$ cell epitopes from *T. gondii* GRA10 (G10E). Chitosan microspheres were loaded with adequate G10E in an effort to protect the peptides from enzymatic degradation and release the G10E peptides stably. This complex was referred to as G10E-CS. *In vitro*, G10E-CS microspheres induced DC maturation and T cell activation with enhanced expression of costimulatory molecules (CD40 and CD86). *In vivo*, significantly prolonged survival and

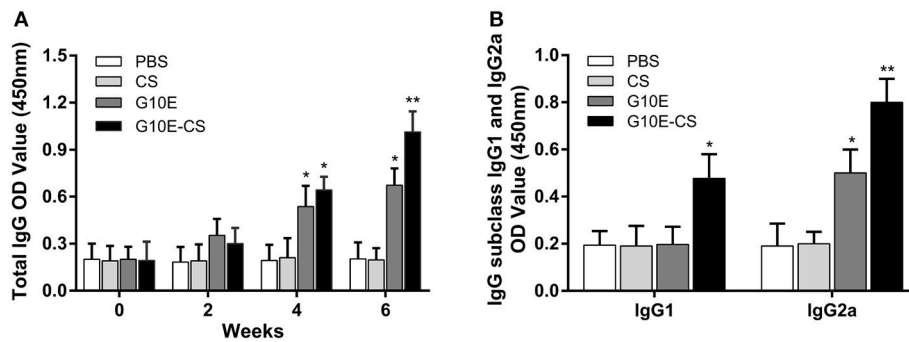


FIGURE 4 | Humoral immune response induced in BALB/C mice after vaccination with G10E-CS. **(A)** Detection of total anti-*GRA10* IgG antibody in the sera of immunized BALB/C mice. The mice were immunized intramuscular injection three times at 2 weeks interval with G10E, CS, G10E-CS, or PBS. Sera were collected from mice by retro-orbital bleeding at 0, 2, 4, and 6 weeks after immunization. The levels of *T. gondii*-specific IgG antibody in the sera of samples was used to determine by ELISA assay. **(B)** Detection of IgG subclass IgG1 and IgG2a antibodies in the sera of the immunized mice. Sera were collected at 2 weeks after the last vaccination. The level of IgG1 and IgG2a antibodies were measured by ELISA. Results are expressed as the mean of OD450 \pm SD ($n = 15$) and are representative of at least three independent experiments. * $p < 0.05$, ** $p < 0.01$.

decreased brain cyst burden were observed in mice vaccinated with G10E-CS, accompanied by strong humoral and cellular responses.

To control outbreaks of toxoplasmosis, caused by this intracellular protozoan parasite with its complex life cycle, the MAP vaccine, containing multiple epitopes, has many advantages over traditional vaccines (Henriquez et al., 2010; Skwarczynski and Toth, 2016). Currently, individual B (Darcy et al., 1992), CD4⁺ T (Grover et al., 2012), CD8⁺ T (Blanchard et al., 2008) cell epitopes have been able to induce partially protective immune responses against toxoplasmosis, and MAP vaccines are more likely to confer more robust protection (Bastos et al., 2016). GRA proteins of *T. gondii*, major components of both tachyzoites and bradyzoites, are related to host-parasite interaction and immune response. Dense granule protein 10 (GRA10) is essential for parasite growth with potential immunogenic capability, and it had not been studied as a candidate vaccine antigen prior to the work presented herein. In this study, we used bioinformatics and immunological methods to select nine B cell or T cell mimotopes of GRA10. Among them, three strongest immunogenic B and T cell epitopes, namely B cell epitope (TQSPPE SRKKRRRS GKKKRGKRSV), CD8⁺ T cell epitope (LGYCALLPL), and CD4⁺ T cell epitope (SGFSLSSGSGVSVVE), were selected to construct the MAP, G10E. Peptide-based vaccines have some weaknesses. For example, they are poor immunogens, in and of themselves, and very susceptible to enzymatic degradation. Therefore, they need the assistance of an effective delivery system (Salvador et al., 2011; Skwarczynski and Toth, 2016).

Recently, a variety of delivery systems have been used for the formulation of peptide vaccines against *T. gondii*. Of particular interest, usage of nano- and micro-particles for vaccine delivery has rapidly become popular (Skwarczynski and Toth, 2016). Poly(lactide-co-glycolide) (PLG) has been tested as safe delivery systems to encapsulate recombinant SAG1 protein (Chuang et al., 2013) or rhoptry proteins (ROP18 and

ROP38) (Xu et al., 2015) as controlled-release microparticle vaccines. Nanosized carriers have also been used to deliver parasite antigens to immune competent cells. Assembled GRA7-derived HLA-B*0702-restricted epitopes into nanospheres (SAPN) (El Bissati et al., 2014) or loaded *T. gondii* extracts protein in porous nanoparticles (DGNP) (Dimier-Poisson et al., 2015) have been developed. All these delivery systems could protect protein epitopes against enzymatic degradation, and microspheres can sustain the stable release of antigen. Chitosan has particular advantages because easily assumes a spherical conformation, and is positively charged. It has been widely studied for vaccine delivery systems to increase the response to immunization with protein antigens, DNA plasmids, and bacterial derived toxins (Arca et al., 2009; Chua et al., 2012). There is comparatively little assessment of the utility of chitosan-based microparticles as vaccine carriers for peptides.

In our study, G10E-CS microspheres prepared by emulsion cross-linking were spherical in shape and had uniform diameter around 1,283nm. Size and zeta analysis of G10E-CS formulations confirmed that G10E was completely loaded into the core of the CS microspheres, and not simply adherent to their surfaces. These properties ensured no obvious degradation of G10E peptides during loading and release processes. This was further supported by PAGE analysis of released G10E. As a cationic polymer, chitosan can bind strongly to cell surfaces with a predominantly negative charge, thereby increasing residence time and releasing peptides in a sustained fashion in targeted cells (Koppolu et al., 2014). In this study, we observed a slow-release effect of G10E-CS microspheres. It is worth noting that nano- or micro-particles used in vaccines are often limited by their toxicity and the difficulty with which they are manufactured (Zhang et al., 2015a). These effects have been observed with chitosan microspheres in the past. Glutaraldehyde, the traditional cross-linking agent used in the production process of CS microparticles may be built into the vaccine carrier and show cell cytotoxicity (Agnihotri et al., 2004).

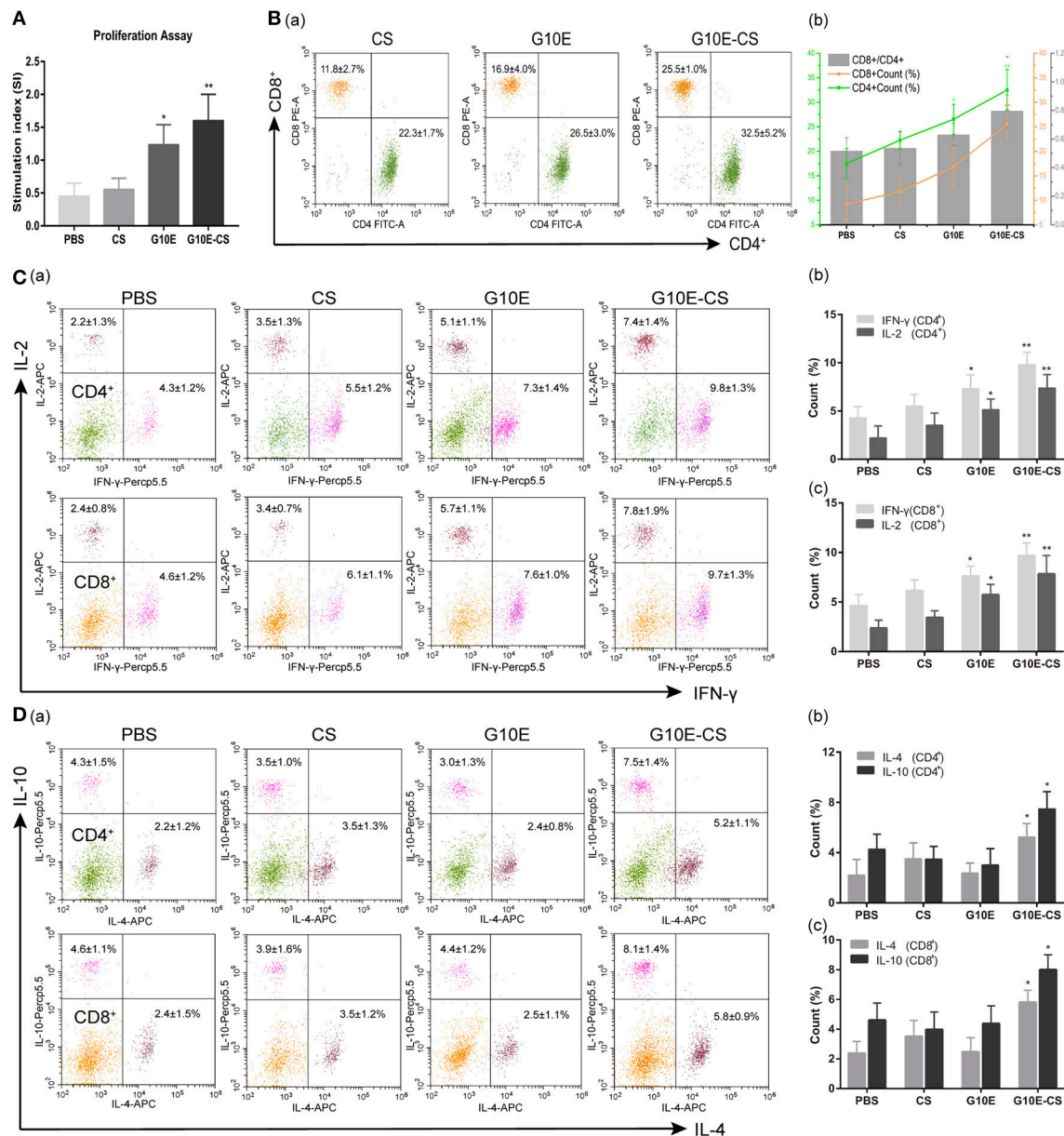


FIGURE 5 | Cellular immune response induced in BALB/C mice after vaccination with G10E-CS. BALB/c mice were immunized with G10E-CS, CS, G10E, or PBS three times at 2-week intervals. Then splenocytes were harvested from three mice per group 2 weeks after the final immunization. Cellular immune responses were analyzed after stimulation with G10E peptides (10 μ g/ml) for 72 h. **(A)** The lymphocyte proliferative response in immunized mice was measured by CCK-8 assay. The absorbance was detected at 450 nm and the stimulation index (SI) was calculated. **(B)** The percentages of T lymphocyte subsets **(a)** and ratio of CD8⁺/CD4⁺ **(b)** in immunized mice. The G10E stimulated splenocytes were stained with anti-mouse CD3-APC, anti-mouse CD4-FITC and anti-mouse CD8-PE for 30 min and cell population was analyzed by flow cytometry. **(C,D)** The production of cytokines (IFN- γ , IL-2) **(C)** and cytokines (IL-4, IL-10) **(D)** in the immunized mice. The splenocytes were stimulated with G10E peptides for 72 h in the presence of Cell Stimulation Cocktail to inhibit the secretion of cytokine into the extracellular and were fixed using an Intracellular Fixation & Permeabilization Buffer Set Kit. After stained with anti-mouse CD8-FITC, anti-mouse IL-2 (APC), anti-mouse IFN- γ (PerCP-Cyanine 5.5), anti-mouse IL-4 (APC) and anti-mouse IL-10 (PerCP-Cyanine5.5) for 30 min, the cells population was analyzed by flow cytometry. Data represent the mean \pm SD and splenocytes from three mice in each group were tested individually. * $p < 0.05$, ** $p < 0.01$.

To overcome this problem, we replaced glutaraldehyde with genipin, an aglucone of geniposide extracted from gardenia fruits and used in traditional Chinese medicine with demonstrated low cell cytotoxicity (Lin et al., 2013). Moreover, its low

crosslinking speed with chitosan could avoid the occurrence of agglomeration (Jin et al., 2004). This difference led to the more uniform particle size observed herein. As expected, all concentrations of G10E-CS microspheres studied showed

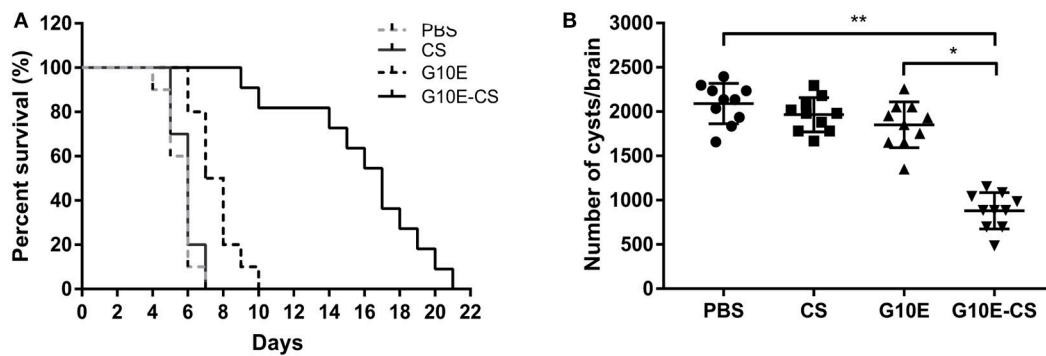


FIGURE 6 | Protection of G10E-CS immunized mice against acute and chronic *Toxoplasma gondii* infection. **(A)** Survival rate of vaccinated mice after lethal RH strain tachyzoites challenge. Two weeks after the final immunization, 10 mice per group were intraperitoneally infected with 1×10^3 tachyzoites of RH strain and observed daily for mortality. **(B)** The cyst number in the brain of mice after sublethal PRU strain cyst challenge. 10 mice per group were challenged orally with a sublethal dose of cysts (30 cysts) of the PRU strain (type II). Cyst load was counted from whole brain homogenates of mice 45 days after challenge. Data are representative results of three independent experiments and are represented as the means \pm SD. * $p < 0.05$, ** $p < 0.01$.

almost no cytotoxicity, a direct result of the choices of molecules with studies supporting good biocompatibility and low cytotoxicity.

Generally, immune responses mediated by $CD4^+$ Th1 cell, especially the cytotoxic T lymphocyte (CTL) response, can directly suppress the growth of dividing tachyzoites and reactivation of the cysts of *T. gondii* (Ching et al., 2016). Thus, activation of T cells and production of Th1 cytokines are pivotal for the control of the parasite (Wang J. L. et al., 2017). Given the effective delivery system of the chitosan (CS) microspheres, the MAP (G10E) were stably released, inducing a strong cell-mediated immune response. In this study, we observed that T lymphocyte proliferation in mice immunized with G10E-CS microspheres was significantly higher than other groups. Meanwhile, percentages of $CD8^+$ and $CD4^+$ T lymphocyte were both increased dramatically in this group, together with the highest ratio of $CD8^+/CD4^+$ T cells. The ability of G10E-CS microspheres to stimulate T lymphocytes proliferation and differentiation was similar to that noted in a previous study (Xu et al., 2015), which encapsulated *T. gondii* ROP38/18 into PLG microparticles. The $CD8^+$ T lymphocyte subset is important in responding to *T. gondii* infection and the helper $CD4^+$ T subgroup appears to cooperate in the control of chronic infection by producing IFN- γ and redundant $CD8^+$ T cells (Caetano et al., 2006).

IFN- γ plays a major role in protecting the infected host against *T. gondii* infection. Its secretion is directly proportional to the mortality rate of infected mice, because it can inhibit tachyzoite propagation during the early stages of infection by activating phagocytes such as macrophages, provide the appropriate cytokine environment (Innes et al., 2009; Sonaimuthu et al., 2016). IL-2 is essential for the development of cytotoxic $CD8^+$ lymphocytes (Sa et al., 2013). As expected, we found that mice injected with G10E-CS generate the highest levels of IFN- γ and IL-2 in all immunized mice. Thus, we speculate that G10E-CS induces a stronger cell-mediated immune response than G10E

due to enhanced delivery via the CS delivery system, and the response is stronger than CS alone due to the immunogenicity of the MAP, G10E. IFN- γ and IL-2 are critical for coordinating protective immunity against *T. gondii* (Luo et al., 2017). Many nano- and micro-particle vaccine formulations against *T. gondii* have observed similar results (Chuang and Yang, 2014; El Bissati et al., 2014; Dimier-Poisson et al., 2015; Xu et al., 2015).

Previous studies have also indicated a key role for vesicle size in determining the Th1/Th2 bias of the resulting immune response. Vaccination using influenza A antigen entrapped in the larger bilosome formulation (980 nm) resulted in a more biased Th1 response as measured by antigen-specific IgG2a serum levels and splenocyte IFN- γ production than vaccination using the smaller bilosomes (250 nm) (Mann et al., 2009). In this study, the size of G10E-CS microparticles was about 1,000 nm which result in Th1 bias immune response.

Th2-related IL-4 and IL-10 possess the antagonistic effect to IFN- γ (Bessieres et al., 1997), making this observation compelling. Interestingly, we also found spleen cells from mice immunized with G10E-CS produced slightly more IL-4, IL-10 than other groups. It has found that the early mortality of infected mice in the acute phase of toxoplasmosis is caused by severe inflammatory effects and lethal immunopathology provoked by IFN- γ , rather than parasitic infection itself (Ching et al., 2016). Even it has been recognized that a protective immune response against *T. gondii* infection requires a Th1 predominance response (Kumar et al., 1998; Meira et al., 2014). Th2-related cytokines play a vital role in downregulating this short-term deleterious inflammatory effect and reduce fatality following *T. gondii* infection (Neyer et al., 1997; Pinzan et al., 2015). Our findings are consistent with this conclusion. It is worth mentioning that GRA10 is found to translocate into the host cell nucleus and interact with signal transducers and promote activation of transcription factor 6 (STAT6). STAT6 plays a central role in the activation of the IL-4 response, triggering the expression of anti-apoptotic factors. In sum,

mice immunized with G10E-CS have induced a combined Th1/Th2 immune response, skewed predominantly toward a Th1 response.

The critical role of antibody in immunity against *T. gondii* has long been recognized (Correa et al., 2007). Antigen-specific antibody can inhibit the tachyzoite directly and impair attachment to host cells (Sayles et al., 2000). In the present study, the increased production of total IgG, IgG2a and IgG1 were all observed in the sera of mice immunized with G10E-CS microspheres. As IgG1 is Th2 related and IgG2a is associated with Th1-driven immunity (Germann et al., 1995; Wang S. et al., 2017), our data supports the idea that G10E-CS microspheres generated Th1 polarize immune response with more IgG2a than IgG1.

Although there are some effective nano- or micro-particles vaccines against *T. gondii*, almost no delivery system can simultaneously act as a good adjuvant. A potent adjuvant required for *T. gondii* vaccines is able to elicit a Th1-type immune response (Verma and Khanna, 2013). It is exciting to find that chitosan can also serve as an attractive candidate adjuvant to induce dendritic cells (DCs) activation and, thereby, promote Th1 cellular immune responses (Riteau and Sher, 2016). In particular, internalized chitosan induces mitochondrial stress and increase reactive oxygen species (ROS) production, which act as a trigger for cGAS-STING pathway (Carroll et al., 2016). This pathway could mediate the production of IFN- γ , responsible for triggering the activation of DCs and T helper type 1 (Th1) immunity responses (Dubensky et al., 2013). DC activation is characterized by elevated surface expression of costimulatory molecules CD40 and CD86 (Reis e Sousa, 2006). The costimulatory molecules also have a key role in regulating T cell proliferation, cytokine production and generation of CTL (Chen and Flies, 2013). In our study, we found that bone-marrow-derived DCs exposed to G10E-CS microspheres *in vitro* showed drastically increased expression of CD40 and CD86. G10E-CS stimulated DCs could both induce efficient costimulation of T cell proliferation and substantial production of IFN- γ and IL-2. Therefore, G10E-CS microspheres could induce DC maturation and T cell activation *in vitro* by upregulating the expression of costimulatory molecules.

The survival rate of vaccinated mice against *T. gondii* challenge is considered the most direct way to assess a candidate vaccine (Zheng et al., 2017). In the present study, we found that mice vaccinated with G10E-CS microspheres have significantly prolonged survival time (21 days) against lethal challenge with the virulent RH strain of *T. gondii*. In contrast, mice immunized with PBS, G10E, or CS had all succumbed within 10 days after infection. Evaluation of the ability of G10E-CS to protect against chronic infection was also of interest. After challenging with a sublethal dose of cysts of the PRU strain, cyst burden in mice vaccinated with G10E-CS was greatly decreased (57.8% reduction) compared to the other groups. These results, taken together, proved that our G10E-CS microsphere vaccine

was able to protect against both acute and chronic *T. gondii* infection.

In summary, in this study, G10E-CS microspheres have triggered a strong, mixed Th1/Th2 cellular and humoral immune response in immunized mice. At the same time, CS as a potent adjuvant, has also enhanced cellular immunity by eliciting Th1-type immune responses. Therefore, the humoral and cellular immune responses induced by G10E-CS microspheres were interrelated and synergistic in strengthening protection against *T. gondii*. Our results proved that chitosan microparticles loaded with MAPs could be a promising approach to vaccine development against *T. gondii*.

A limitation of this study was that the loading capacity (LC%) of the chitosan microsphere was low (15.3%). This may be due to liquid paraffin on the surface of the microspheres, which was hard to clean completely, potentially affecting the peptides contact with the microspheres. Interestingly, this loading capacity was slightly higher than that observed with chitosan-based microspheres loaded with other protein (Li et al., 2017). It will be necessary to increase the loading capacity to improve the protection efficiency of G10E-CS vaccine. Therefore, other optimized published methods for manufacturing protein-loaded chitosan particles can be used in future research.

AUTHORS CONTRIBUTIONS

HC and HY designed experiments. HY, JG, TW, and XS performed experiments and analyzed data. JG and HY wrote the manuscript. HC and YL revised the manuscript. CZ, HZ, and SH provided advice for experiment. All authors read and approved the final manuscript.

ACKNOWLEDGMENTS

This study was supported by grants from the development Project of Shandong Province (Grant No. 2016GSF201201), Shandong Natural Science Foundation Project (Grant No. ZR2017MH043 and ZR2016HM74) and the National Natural Science Foundation Project of China (Grant No. 81171604).

SUPPLEMENTARY MATERIAL

The Supplementary Material for this article can be found online at: <https://www.frontiersin.org/articles/10.3389/fcimb.2018.00163/full#supplementary-material>

Figure S1 | The release of G10E peptides was analyzed by PAGE (A) and SDS-PAGE (B). G10E-CS microspheres were dispersed in PBS (pH 7.4) using a shaking air bath (37°C, 100 rpm) for 15 d. After centrifuging (5,000 rpm, 20 min), the microspheres precipitation at the bottom of the tube was collected to be analyzed by non-denaturing gel electrophoresis (PAGE) and denaturing gel electrophoresis (SDS-PAGE).

Table S1 | Size and zeta potential of G10E-CS, CS and G10E. Size and zeta potential of chitosan microspheres loaded with G10E peptides (G10E-CS), chitosan microspheres (CS) and free G10E peptides.

REFERENCES

- Agnihotri, S. A., Mallikarjuna, N. N., and Aminabhavi, T. M. (2004). Recent advances on chitosan-based micro- and nanoparticles in drug delivery. *J. Adv. Release* 100, 5–28. doi: 10.1016/j.jconrel.2004.08.010
- Ahn, H. J., Kim, S., and Nam, H. W. (2005). Host cell binding Of Gra10, a novel, constitutively secreted dense granular protein from *Toxoplasma gondii*. *Biochem. Biophys. Res. Commun.* 331, 614–620. doi: 10.1016/j.bbrc.2005.03.218
- Arca, H. C., Günbeyaz, M., and Senel, S. (2009). Chitosan-based systems for the delivery of vaccine antigens. *Expert Rev. Vaccines* 8, 937–953. doi: 10.1586/erv.09.47
- Bastos, L. M., Macêdo, A. G., Silva, M. V., Santiago, F. M., Ramos, E. L., Santos, F. A., et al. (2016). *Toxoplasma gondii*-derived synthetic peptides containing B- and T-cell epitopes from Gra2 protein are able to enhance mice survival in a model of experimental toxoplasmosis. *Front. Cell. Infect. Microbiol.* 6:59. doi: 10.3389/fcimb.2016.00059
- Bernkop-Schnürch, A., and Dünhaupt, S. (2012). Chitosan-based drug delivery systems. *Eur. J. Pharm. Biopharm.* 81, 463–469. doi: 10.1016/j.ejpb.2012.04.007
- Bessieres, M. H., Swierczynski, B., Cassaing, S., Miedouge, M., Olle, P., Seguela, J. P., et al. (1997). Role of Ifn-Gamma, Tnf- α , Il4 and Il10 In the regulation of experimental *Toxoplasma gondii* infection. *J. Eukaryot. Microbiol.* 44, 87s. doi: 10.1111/j.1550-7408.1997.tb05800.x
- Blader, I. J., Coleman, B. I., Chen, C. T., and Gubbels, M. J. (2015). Lytic cycle of *Toxoplasma gondii*: 15 years later. *Annu. Rev. Microbiol.* 69, 463–485. doi: 10.1146/annurev-micro-091014-104100
- Blanchard, N., Gonzalez, F., Schaeffer, M., Joncker, N. T., Cheng, T., Shastri, A. J., et al. (2008). Immunodominant, protective response to the parasite *Toxoplasma gondii* requires antigen processing in the endoplasmic reticulum. *Nat. Immunol.* 9, 937–944. doi: 10.1038/ni.1629
- Braun, L., Travier, L., Kieffer, S., Musset, K., Garin, J., Mercier, C., et al. (2008). Purification of *Toxoplasma* dense granule proteins reveals that they are in complexes throughout the secretory pathway. *Mol. Biochem. Parasitol.* 157, 13–21. doi: 10.1016/j.molbiopara.2007.09.002
- Caetano, B. C., Bruña-Romero, O., Fux, B., Mendes, E. A., Penido, M. L., and Gazzinelli, R. T. (2006). Vaccination with replication-deficient recombinant adenoviruses encoding the main surface antigens of *Toxoplasma gondii* induces immune response and protection against infection in mice. *Hum. Gene Ther.* 17, 415–426. doi: 10.1089/hum.2006.17.415
- Cardona, N., De-La-Torre, A., Siachoque, H., Patarroyo, M. A., and Gomez-Marin, J. E. (2009). *Toxoplasma gondii*: P30 peptides recognition pattern in human toxoplasmosis. *Exp. Parasitol.* 123, 199–202. doi: 10.1016/j.exppara.2009.06.017
- Carroll, E. C., Jin, L., Mori, A., Muñoz-Wolf, N., Oleszycka, E., Hbt, M., et al. (2016). The Vaccine adjuvant chitosan promotes cellular immunity via DNA sensor Cgas-Sting-dependent induction of type I interferons. *Immunity* 44, 597–608. doi: 10.1016/j.immuni.2016.02.004
- Cesbron-Delauw, M. F., and Capron, A. (1993). Excreted/secreted antigens of *Toxoplasma gondii*—their origin and role in the host-parasite interaction. *Res. Immunol.* 144, 41–44. doi: 10.1016/S0923-2494(05)80096-3
- Chen, L., and Flies, D. B. (2013). Molecular mechanisms of T cell co-stimulation and co-inhibition. *Nat. Rev. Immunol.* 13, 227–242. doi: 10.1038/nri3405
- Ching, X. T., Fong, M. Y., and Lau, Y. L. (2016). Evaluation of immunoprotection conferred by the subunit vaccines Of Gra2 and Gra5 against acute toxoplasmosis in Balb/C mice. *Front. Microbiol.* 7:609. doi: 10.3389/fmicb.2016.00609
- Chua, B. Y., Al, K. M., Zeng, W., Mainwaring, D., and Jackson, D. C. (2012). Chitosan microparticles and nanoparticles as biocompatible delivery vehicles for peptide and protein-based immunocontraceptive vaccines. *Mol. Pharm.* 9, 81–90. doi: 10.1021/mp200264m
- Chuang, S. C., and Yang, C. D. (2014). Sustained release of recombinant surface antigen 2 (Rsa2) from Poly(Lactide-Co-Glycolide) microparticles extends protective cell-mediated immunity against *Toxoplasma gondii* in mice. *Parasitology* 141, 1657–1666. doi: 10.1017/S0031182014000997
- Chuang, S. C., Ko, J. C., Chen, C. P., Du, J. T., and Yang, C. D. (2013). Induction of long-lasting protective immunity against *Toxoplasma gondii* in Balb/C Mice by recombinant surface antigen 1 protein encapsulated in poly (Lactide-Co-Glycolide) microparticles. *Parasit. Vectors* 6:34. doi: 10.1186/1756-3305-6-34
- Cong, H., Mui, E. J., Witola, W. H., Sidney, J., Alexander, J., Sette, A., et al. (2010). Human immunome, bioinformatic analyses using Hla supermotifs and the parasite genome, binding assays, studies of human T cell responses, and immunization of Hla-A*1101 transgenic mice including novel adjuvants provide a foundation For Hla-A03 Restricted Cd8+T cell epitope based, adjuvanted vaccine protective against *Toxoplasma gondii*. *Immunome Res.* 6:12. doi: 10.1186/1745-7580-6-12
- Correa, D., Cañedo-Solares, I., Ortiz-Alegria, L. B., Caballero-Ortega, H., and Rico-Torres, C. P. (2007). Congenital and acquired toxoplasmosis: diversity and role of antibodies in different compartments of the host. *Parasite Immunol.* 29, 651–660. doi: 10.1111/j.1365-3024.2007.00982.x
- Darcy, F., Maes, P., Gras-Masse, H., Auriault, C., Bossus, M., Deslee, D., et al. (1992). Protection of mice and nude rats against toxoplasmosis by a multiple antigenic peptide construction derived from *Toxoplasma gondii* P30 antigen. *J. Immunol.* 149, 3636–3641.
- Dimier-Poisson, I., Carpentier, R., N'guyen, T. T., Dahmani, F., Ducournau, C., and Betbeder, D. (2015). Porous nanoparticles as delivery system of complex antigens for an effective vaccine against acute and chronic *Toxoplasma gondii* infection. *Biomaterials* 50, 164–175. doi: 10.1016/j.biomaterials.2015.01.056
- Dubensky, T. W., Kanne, D. B., and Leong, M. L. (2013). Rationale, progress and development of vaccines utilizing sting-activating cyclic dinucleotide adjuvants. *Ther. Adv. Vaccines* 1, 131–143. doi: 10.1177/2051013613501988
- Dudek, N. L., Perlmutter, P., Aguilar, M. I., Croft, N. P., and Purcell, A. W. (2010). Epitope discovery and their use in peptide based vaccines. *Curr. Pharm. Des.* 16, 3149–3157. doi: 10.2174/138161210793292447
- El Bissati, B. K., Zhou, Y., Dasgupta, D., Cobb, D., Dubey, J. P., Burkhard, P., et al. (2014). Effectiveness of a novel immunogenic nanoparticle platform for toxoplasma peptide vaccine in hla transgenic mice. *Vaccine* 32, 3243–3248. doi: 10.1016/j.vaccine.2014.03.092
- Germann, T., Bongartz, M., Dlugonska, H., Hess, H., Schmitt, E., Kolbe, L., et al. (1995). Interleukin-12 profoundly up-regulates the synthesis of antigen-specific complement-fixing IgG2a, IgG2b and IgG3 antibody subclasses *in vivo*. *Eur. J. Immunol.* 25, 823–829. doi: 10.1002/eji.1830250329
- Grover, H. S., Blanchard, N., Gonzalez, F., Chan, S., Robey, E. A., and Shastri, N. (2012). The *Toxoplasma gondii* peptide as15 elicits Cd4 T cells that can control parasite burden. *Infect. Immun.* 80, 3279–3288. doi: 10.1128/IAI.00425-12
- Henriquez, F. L., Woods, S., Cong, H., McLeod, R., and Roberts, C. W. (2010). Immunogenetics of *Toxoplasma gondii* informs vaccine design. *Trends Parasitol.* 26, 550–555. doi: 10.1016/j.pt.2010.06.004
- Höpken, U. E., Lehmann, I., Droese, J., Lipp, M., Schüler, T., and Rehm, A. (2005). The ratio between dendritic cells and t cells determines the outcome of their encounter: proliferation versus deletion. *Eur. J. Immunol.* 35, 2851–2863. doi: 10.1002/eji.200526298
- Howe, D. K., and Sibley, L. D. (1995). *Toxoplasma gondii* comprises three clonal lineages: correlation of parasite genotype with human disease. *J. Infect. Dis.* 172, 1561–1566. doi: 10.1093/infdis/172.6.1561
- Innes, E. A. (2010). Vaccination against toxoplasma gondii: an increasing priority for collaborative research. *Expert Rev. Vaccines* 9, 1117–1119. doi: 10.1586/erv.10.113
- Innes, E. A., Bartley, P. M., Buxton, D., and Katzer, F. (2009). Ovine toxoplasmosis. *Parasitology* 136, 1887–1894. doi: 10.1017/S0031182009991636
- Islam, N., and Ferro, V. (2016). Recent advances in chitosan-based nanoparticulate pulmonary drug delivery. *Nanoscale* 8, 14341–14358. doi: 10.1039/C6NR03256G
- Jin, J., Song, M., and Hourston, D. J. (2004). Novel chitosan-based films cross-linked by genipin with improved physical properties. *Biomacromolecules* 5, 162–168. doi: 10.1021/bm034286m
- Jose, S., Fanguero, J. F., Smitha, J., Cinu, T. A., Chacko, A. J., Premaletha, K., et al. (2012). Cross-linked chitosan microspheres for oral delivery of insulin: taguchi design and *in vivo* testing. *Colloids Surf. B Biointerfaces* 92, 175–179. doi: 10.1016/j.colsurfb.2011.11.040
- Jose, S., Fanguero, J. F., Smitha, J., Cinu, T. A., Chacko, A. J., Premaletha, K., et al. (2013). Predictive modeling of insulin release profile from cross-linked chitosan microspheres. *Eur. J. Med. Chem.* 60, 249–253. doi: 10.1016/j.ejmech.2012.12.011
- Kofler, R. M., Aberle, J. H., Aberle, S. W., Allison, S. L., Heinz, F. X., and Mandl, C. W. (2004). Mimicking live flavivirus immunization with a noninfectious RNA vaccine. *Proc. Natl. Acad. Sci. U.S.A.* 101, 1951–1956. doi: 10.1073/pnas.0307145101

- Koppolu, B. P., Smith, S. G., Ravindranathan, S., Jayanthi, S., Suresh, K. T. K., and Zaharoff, D. A. (2014). Controlling chitosan-based encapsulation for protein and vaccine delivery. *Biomaterials* 35, 4382–4389. doi: 10.1016/j.biomaterials.2014.01.078
- Kumar, A., Angel, J. B., Daftarian, M. P., Parato, K., Cameron, W. D., Filion, L., et al. (1998). Differential production of IL-10 by T cells and monocytes of HIV-infected individuals: association of IL-10 Production With CD28-mediated immune responsiveness. *Clin. Exp. Immunol.* 114, 78–86. doi: 10.1046/j.1365-2249.1998.00689.x
- Kwon, Y. J., James, E., Shastri, N., and Fréchet, J. M. (2005). *In vivo* targeting of dendritic cells for activation of cellular immunity using vaccine carriers based on PH-responsive microparticles. *Proc. Natl. Acad. Sci. U.S.A.* 102, 18264–18268. doi: 10.1073/pnas.0509541102
- Li, L., Yang, L., Li, M., and Zhang, L. (2017). A cell-penetrating peptide mediated chitosan nanocarriers for improving intestinal insulin delivery. *Carbohydr. Polym.* 174, 182–189. doi: 10.1016/j.carbpol.2017.06.061
- Lin, Y. H., Tsai, S. C., Lai, C. H., Lee, C. H., He, Z. S., and Tseng, G. C. (2013). Genipin-cross-linked fucose-chitosan/heparin nanoparticles for the eradication of *Helicobacter pylori*. *Biomaterials* 34, 4466–4479. doi: 10.1016/j.biomaterials.2013.02.028
- Luo, F., Zheng, L., Hu, Y., Liu, S., Wang, Y., Xiong, Z., et al. (2017). Induction of protective immunity against *Toxoplasma gondii* In mice by nucleoside triphosphate hydrolase-II (Ntpase-II) self-amplifying RNA vaccine encapsulated in lipid nanoparticle (LNP). *Front. Microbiol.* 8:605. doi: 10.3389/fmicb.2017.00605
- Mann, J. F., Shakir, E., Carter, K. C., Mullen, A. B., Alexander, J., and Ferro, V. A. (2009). Lipid vesicle size of an oral influenza vaccine delivery vehicle influences the Th1/Th2 bias in the immune response and protection against infection. *Vaccine* 27, 3643–3649. doi: 10.1016/j.vaccine.2009.03.040
- Meira, C. S., Pereira-Chiocola, V. L., Vidal, J. E., De Mattos, C. C., Motoie, G., Costa-Silva, T. A., et al. (2014). Cerebral and ocular toxoplasmosis related With *Ifn- γ* , *Tnf- α* , and IL-10 levels. *Front. Microbiol.* 5:492. doi: 10.3389/fmicb.2014.00492
- Molavi, O., Mahmud, A., Hamdy, S., Hung, R. W., Lai, R., Samuel, J., et al. (2010). Development of a poly(D,L-Lactic-Co-Glycolic Acid) nanoparticle formulation of Stat3 inhibitor JSI-124: implication for cancer immunotherapy. *Mol. Pharm.* 7, 364–374. doi: 10.1021/mp900145
- Moutafsi, M., Peters, B., Pasquetto, V., Tschärke, D. C., Sidney, J., Bui, H. H., et al. (2006). A consensus epitope prediction approach identifies the breadth of murine T(Cd8+)-cell responses to vaccinia virus. *Nat. Biotechnol.* 24, 817–819. doi: 10.1038/nbt1215
- Nam, H. W. (2009). Gra proteins of *Toxoplasma gondii*: maintenance of host-parasite interactions across the parasitophorous vacuolar membrane. *Korean J. Parasitol.* 47(Suppl.), S29–S37. doi: 10.3347/kjp.2009.47.S.S29
- Neyer, L. E., Grunig, G., Fort, M., Remington, J. S., Rennick, D., and Hunter, C. A. (1997). Role of interleukin-10 in regulation of T-cell-dependent and T-cell-independent mechanisms of resistance to *Toxoplasma gondii*. *Infect. Immun.* 65, 1675–1682.
- Pichayakorn, W., and Boonme, P. (2013). Evaluation of cross-linked chitosan microparticles containing metronidazole for periodontitis treatment. *Mater. Sci. Eng. C Mater. Biol. Appl.* 33, 1197–1202. doi: 10.1016/j.msec.2012.12.010
- Pinzan, C. F., Sardinha-Silva, A., Almeida, F., Lai, L., Lopes, C. D., Lourenço, E. V., et al. (2015). Vaccination with recombinant microneme proteins confers protection against experimental toxoplasmosis in mice. *PLoS ONE* 10:E0143087. doi: 10.1371/journal.pone.0143087
- Reddy, S. T., Van Der Vlies, A. J., Simeoni, E., Angeli, V., Randolph, G. J., O'Neil, C. P., et al. (2007). Exploiting lymphatic transport and complement activation in nanoparticle vaccines. *Nat. Biotechnol.* 25, 1159–1164. doi: 10.1038/nbt1332
- Reis e Sousa C. (2006). Dendritic cells in a mature age. *Nat. Rev. Immunol.* 6, 476–483. doi: 10.1038/nri1845
- Riteau, N., and Sher, A. (2016). Chitosan: An adjuvant with an unanticipated sting. *Immunity* 44, 522–524. doi: 10.1016/j.immuni.2016.03.002
- Sa, Q., Woodward, J., and Suzuki, Y. (2013). IL-2 produced By Cd8+ immune T cells can augment their IFN- γ production independently from their proliferation in the secondary response to an intracellular pathogen. *J. Immunol.* 190, 2199–2207. doi: 10.4049/jimmunol.1202256
- Saeij, J. P., Boyle, J. P., and Boothroyd, J. C. (2005). Differences among the three major strains of *Toxoplasma gondii* and their specific interactions with the infected host. *Trends Parasitol.* 21, 476–481. doi: 10.1016/j.pt.2005.08.001
- Salvador, A., Igartua, M., Hernández, R. M., and Pedraz, J. L. (2011). An overview on the field of micro- and nanotechnologies for synthetic peptide-based vaccines. *J. Drug Deliv.* 2011:181646. doi: 10.1155/2011/181646
- Sayles, P. C., Gibson, G. W., and Johnson, L. L. (2000). B cells are essential for vaccination-induced resistance to virulent *Toxoplasma gondii*. *Infect. Immun.* 68, 1026–1033. doi: 10.1128/IAI.68.3.1026-1033.2000
- Shen, B., and Sibley, L. D. (2014). *Toxoplasma* aldolase is required for metabolism but dispensable for host-cell invasion. *Proc. Natl. Acad. Sci. U.S.A.* 111, 3567–3572. doi: 10.1073/pnas.1315156111
- Shrestha, N., Shahbazi, M. A., Araújo, F., Zhang, H., Mäkilä, E. M., Kauppila, J., et al. (2014). Chitosan-modified porous silicon microparticles for enhanced permeability of insulin across intestinal cell monolayers. *Biomaterials* 35, 7172–7179. doi: 10.1016/j.biomaterials.2014.04.104
- Skop, N. B., Calderon, F., Levison, S. W., Gandhi, C. D., and Cho, C. H. (2013). Heparin crosslinked chitosan microspheres for the delivery of neural stem cells and growth factors for central nervous system repair. *Acta Biomater.* 9, 6834–6843. doi: 10.1016/j.actbio.2013.02.043
- Skwarczynski, M., and Toth, I. (2014). Recent advances in peptide-based subunit nanovaccines. *Nanomedicine* 9, 2657–2669. doi: 10.2217/nnm.14.187
- Skwarczynski, M., and Toth, I. (2016). Peptide-based synthetic vaccines. *Chem. Sci.* 7, 842–854. doi: 10.1039/c5sc03892h
- Sonaimuthu, P., Ching, X. T., Fong, M. Y., Kalyanasundaram, R., and Lau, Y. L. (2016). Induction of protective immunity against toxoplasmosis in Balb/C mice vaccinated with *Toxoplasma gondii* Rhopty-1. *Front. Microbiol.* 7:808. doi: 10.3389/fmicb.2016.00808
- Tang, X., Yin, G., Qin, M., Tao, G., Suo, J., Liu, X., et al. (2016). Transgenic eimeria tenella as a vaccine vehicle: expressing Tgsag1 elicits protective immunity against *Toxoplasma gondii* infections in chickens and mice. *Sci. Rep.* 6:29379. doi: 10.1038/srep29379
- van der Lubben, I. M., Verhoeve, J. C., Van Aelst, A. C., Borchard, G., and Junginger, H. E. (2001). Chitosan microparticles for oral vaccination: preparation, characterization and preliminary *in vivo* uptake studies in murine peyer's patches. *Biomaterials* 22, 687–694. doi: 10.1016/S0142-9612(00)00231-3
- van Riet, E., Ainai, A., Suzuki, T., Kersten, G., and Hasegawa, H. (2014). Combating infectious diseases; nanotechnology as a platform for rational vaccine design. *Adv. Drug Deliv. Rev.* 74, 28–34. doi: 10.1016/j.addr.2014.05.011
- Verma, R., and Khanna, P. (2013). Development of *Toxoplasma gondii* vaccine: a global challenge. *Hum. Vaccine Immunother.* 9, 291–293. doi: 10.4161/hv.22474
- Wallace, P. K., Tario, J. D., Fisher, J. L., Wallace, S. S., Ernststoff, M. S., and Muirhead, K. A. (2008). Tracking antigen-driven responses by flow cytometry: monitoring proliferation by dye dilution. *Cytometry A* 73, 1019–1034. doi: 10.1002/cyto.a.20619
- Wang, J. L., Elsheikha, H. M., Zhu, W. N., Chen, K., Li, T. T., Yue, D. M., et al. (2017). Immunization with *Toxoplasma gondii* Gra17 deletion mutant induces partial protection and survival in challenged mice. *Front. Immunol.* 8:730. doi: 10.3389/fimmu.2017.00730
- Wang, J., Xu, M., Cheng, X., Kong, M., Liu, Y., Feng, C., et al. (2016). Positive/negative surface charge of chitosan based nanogels and its potential influence on oral insulin delivery. *Carbohydr. Polym.* 136, 867–874. doi: 10.1016/j.carbpol.2015.09.103
- Wang, L. Y., Ma, G. H., and Su, Z. G. (2005). Preparation of uniform sized chitosan microspheres by membrane emulsification technique and application as a carrier of protein drug. *J. Control. Release* 106, 62–75. doi: 10.1016/j.jconrel.2005.04.005
- Wang, P., Sidney, J., Dow, C., Mothé, B., Sette, A., and Peters, B. (2008). A systematic assessment of MHC class II peptide binding predictions and evaluation of a consensus approach. *Plos Comput. Biol.* 4:E1000048. doi: 10.1371/journal.pcbi.1000048
- Wang, S., Zhang, Z., Wang, Y., Gadahi, J. A., Xu, L., Yan, R., et al. (2017). *Toxoplasma gondii* elongation factor 1- α (Tgef-1 α) is a novel vaccine candidate antigen against toxoplasmosis. *Front. Microbiol.* 8:168. doi: 10.3389/fmicb.2017.00168
- Wang, Y., Wang, G., Ou, J., Yin, H., and Zhang, D. (2014). Analyzing and identifying novel B cell epitopes within *Toxoplasma gondii* Gra4. *Parasit. Vectors* 7:474. doi: 10.1186/s13071-014-0474-x

- Witola, W. H., Bauman, B., Mchugh, M., and Matthews, K. (2014). Silencing of Gra10 protein expression inhibits toxoplasma gondii intracellular growth and development. *Parasitol. Int.* 63, 651–658. doi: 10.1016/j.parint.2014.05.001
- Xu, Y., Zhang, N. Z., Wang, M., Dong, H., Feng, S. Y., Guo, H. C., et al. (2015). A Long-lasting protective immunity against chronic toxoplasmosis in mice induced by recombinant rhoptry proteins encapsulated in poly (Lactide-Co-Glycolide) microparticles. *Parasitol. Res.* 114, 4195–4203. doi: 10.1007/s00436-015-4652-3
- Zhang, N. Z., Wang, M., Xu, Y., Petersen, E., and Zhu, X. Q. (2015a). Recent advances in developing vaccines against *Toxoplasma gondii*: an update. *Expert. Rev. Vaccines* 14, 1609–1621. doi: 10.1586/14760584.2015.1098539
- Zhang, N. Z., Xu, Y., Wang, M., Petersen, E., Chen, J., Huang, S. Y., et al. (2015b). Protective efficacy of two novel DNA vaccines expressing *Toxoplasma gondii* Rhomboid 4 and Rhomboid 5 proteins against acute and chronic toxoplasmosis in mice. *Expert. Rev. Vaccines* 14, 1289–1297. doi: 10.1586/14760584.2015.1061938
- Zheng, B., Ding, J., Chen, X., Yu, H., Lou, D., Tong, Q., et al. (2017). Immuno-efficacy OF A *T. gondii* secreted protein with an altered thrombospondin repeat (Tgspatr) as a novel DNA vaccine candidate against acute toxoplasmosis in Balb/C mice. *Front. Microbiol.* 8:216. doi: 10.3389/fmicb.2017.00216
- Zhou, C. X., Zhou, D. H., Elsheikha, H. M., Zhao, Y., Suo, X., and Zhu, X. Q. (2016). Metabolomic profiling of mice serum during toxoplasmosis progression using liquid chromatography-mass spectrometry. *Sci. Rep.* 6:19557. doi: 10.1038/srep19557
- Zhou, X., Liu, B., Yu, X., Zha, X., Zhang, X., Chen, Y., et al. (2007). Controlled release of PEI/DNA complexes from mannose-bearing chitosan microspheres as a potent delivery system to enhance immune response to HBV DNA vaccine. *J. Control. Release* 121, 200–207. doi: 10.1016/j.jconrel.2007.05.018

Conflict of Interest Statement: The authors declare that the research was conducted in the absence of any commercial or financial relationships that could be construed as a potential conflict of interest.

Copyright © 2018 Guo, Sun, Yin, Wang, Li, Zhou, Zhou, He and Cong. This is an open-access article distributed under the terms of the Creative Commons Attribution License (CC BY). The use, distribution or reproduction in other forums is permitted, provided the original author(s) and the copyright owner are credited and that the original publication in this journal is cited, in accordance with accepted academic practice. No use, distribution or reproduction is permitted which does not comply with these terms.

Advantages of publishing in Frontiers



OPEN ACCESS

Articles are free to read
for greatest visibility
and readership



FAST PUBLICATION

Around 90 days
from submission
to decision



HIGH QUALITY PEER-REVIEW

Rigorous, collaborative,
and constructive
peer-review



TRANSPARENT PEER-REVIEW

Editors and reviewers
acknowledged by name
on published articles

Frontiers

Avenue du Tribunal-Fédéral 34
1005 Lausanne | Switzerland

Visit us: www.frontiersin.org

Contact us: info@frontiersin.org | +41 21 510 17 00



REPRODUCIBILITY OF RESEARCH

Support open data
and methods to enhance
research reproducibility



DIGITAL PUBLISHING

Articles designed
for optimal readership
across devices



FOLLOW US

@frontiersin



IMPACT METRICS

Advanced article metrics
track visibility across
digital media



EXTENSIVE PROMOTION

Marketing
and promotion
of impactful research



LOOP RESEARCH NETWORK

Our network
increases your
article's readership